

Assessing the Status and Trends of Spring Chinook Habitat in the Upper Grande Ronde River and Catherine Creek: Annual Report 2016

publication date: April 30, 2017

Authors: Dale A. McCullough, Seth White, Casey Justice, Lauren Burns, Denise Kelsey, and David Graves



Technical Report

17-03

Columbia River Inter-Tribal Fish Commission

700 NE Multnomah St, Ste 1200, Portland OR 97232 • (503)238-0667 • www.critfc.org

Funding for this work came from the Columbia Basin Fish Accords (2008-2018), a ten-year tribal/federal partnership between the Bonneville Power Administration, Bureau of Reclamation, Columbia River Inter-Tribal Fish Commission, The Confederated Tribes of the Umatilla Indian Reservation, The Confederated Tribes of the Warm Springs Reservation of Oregon, US Army Corps of Engineers, and The Confederated Tribes and Bands of the Yakama Nation.

Assessing the Status and Trends of Spring Chinook Habitat in the Upper Grande Ronde River and Catherine Creek

BPA Project # 2009-004-00

Report covers work performed under BPA contract #(s) 71725

Report was completed under BPA contract #(s) 71725

Report covers work performed from: January 2016 – December 2016

Dale A. McCullough, Seth White, Casey Justice, Lauren Burns, Denise Kelsey, and David Graves

Columbia River Inter-Tribal Fish Commission (CRITFC), Portland, OR 97232

Report Created April 2017

This report was funded by the Bonneville Power Administration (BPA), U.S. Department of Energy, as part of BPA's program to protect, mitigate, and enhance fish and wildlife affected by the development and operation of hydroelectric facilities on the Columbia River and its tributaries. The views in this report are the author's and do not necessarily represent the views of BPA.

Table of Contents

Executive Summary	3
Introduction	11
Stream Habitat	15
CHaMP Data Collection	15
Stream Temperature Modeling.....	24
Historical Ecology for Setting Restoration Targets.....	25
Cold-water Refuges	26
Comparison of Regional Water Temperature Models.....	82
Mapping Restoration Intensity	87
RTK Survey of CHaMP Benchmarks.....	96
Low Flow Analysis	114
Peak Flow Analysis	155
Toxic Chemicals in the Environment.....	208
Stream Biota.....	253
Fish-Habitat Relationships.....	253
Redd / Stream Gradient Analysis	261
Influence of Water Temperature on Spawning Success	265
Development of Food Web Metrics.....	286
Benthic and Drift Macroinvertebrates	333
Dissemination of Project Findings.....	364
Appendix 1 – Life Cycle Model	366

Executive Summary

Background and Objectives

The Columbia River Inter-Tribal Fish Commission (CRITFC) is conducting a fish habitat monitoring program in the Upper Grande Ronde River and Catherine Creek basins designed to evaluate the effectiveness of aggregate restoration actions in improving freshwater habitat conditions and viability of salmonids listed under the Endangered Species Act. Critical uncertainties for fisheries managers in the Columbia Basin are whether habitat restoration actions will yield a net improvement in basin-wide habitat quality, and whether expected improvements in fish production can be brought about by improvements in the quality and quantity of salmon habitat. The primary objectives of this project are to: 1) Assess current status and trends in fish habitat characteristics considered to be key limiting factors (particularly water temperature, pool habitats, streamflow, and fine sediment) to viability of spring Chinook Salmon populations; 2) Evaluate effectiveness of aggregate stream restoration actions aimed at improving key limiting habitat factors; and 3) Develop a life cycle model to link biotic responses of spring Chinook populations to projected changes in stream habitat conditions.

Life Cycle Model as an Organizing Concept

One of the central components of this project is a spring Chinook life cycle model which provides a means to integrate habitat monitoring efforts with recovery planning. The life cycle model is a tool to simulate fish population trends in relation to projected habitat conditions, and to examine the relative benefits of habitat improvements on fish population recovery potential. The fundamental basis of the model is that intrinsic watershed factors (such as geology, climate, or valley morphology) interact with human actions (such as forest harvest, cattle grazing, or stream restoration) to affect processes that drive known limiting factors (e.g., flow, temperature, pool area, etc.), and therefore fish survival via both density-dependent and density-independent processes. This conceptual model represents the general structure of our research program.

The life history model is comprised of several interacting subcomponents that are built independently, each of which provides critical information about the interaction between landscape characteristics, instream habitat conditions, and fish response. Some of these subcomponents include modeling stream temperature from local riparian and geomorphic conditions, linking key limiting habitat characteristics (e.g., water temperature, fine sediment, pool abundance, and large woody debris) to fish abundance and productivity, estimating food base and growth potential for salmonids from stream macroinvertebrate data and habitat characteristics, evaluating habitat characteristics and fish use of cold-water refuges, and evaluating the vulnerability of sites to low and high streamflows. Though these components are described here as providing inputs to the life cycle model, each component is a valid research project in its own right that is likely to yield interesting scientific insights and practical applications for conservation.

Progress and Key Findings from Individual Project Components

Stream Habitat Conditions

- Continued collection and QA/QC of stream habitat condition data using the Columbia Habitat Monitoring Program (CHaMP) methodology. Conducted 26 surveys within the spring Chinook salmon extent in 2016, totaling 150 surveys at 63 sites since 2011.
- Summaries of five key habitat metrics revealed that, across spatial extents, there exists large variability within the two more heavily disturbed watersheds (Upper Grande Ronde and Catherine Creek) compared with the Minam River watershed.
- Continued monitoring of stream temperature at 71 sites across three watersheds.

Stream Temperature Modeling

- We used a deterministic water temperature model to investigate potential thermal benefits of riparian reforestation and channel narrowing to Chinook Salmon populations in the Upper Grande Ronde River and Catherine Creek basins.
- A combination of riparian restoration and channel narrowing was predicted to reduce peak summer water temperatures by 6.5 °C on average in the Upper Grande Ronde River and 3.0 °C in Catherine Creek, translating to predicted increases in Chinook Salmon parr abundance of 590% and 67% respectively.
- Although projected climate change impacts on water temperature for the 2080s time period were substantial (i.e., median increase of 2.7 °C in the Upper Grande Ronde and 1.5 °C in Catherine Creek), we predicted that basin-wide restoration of riparian vegetation and channel width could offset these impacts, reducing peak summer water temperatures by about 3.5 °C in the Upper Grande Ronde and 1.8 °C in Catherine Creek.

Historical Ecology for Setting Restoration Targets

- General Land Office (GLO) survey field notes from the 19th century helped demonstrate that in two watersheds severely impacted by Euro-American land use, stream channel widths—a metric representing habitat simplification—increased in accordance with a geomorphic stream classification. Conversely, we did not detect significant change in stream widths in an adjacent, wilderness stream with minimal land use impact.
- Using a mechanistic water temperature model (Heat Source), we predicted that the combination of stream width and riparian restoration could decrease average summer water temperatures 6.6 °C in Upper Grande Ronde and 3.0 °C in Catherine Creek.
- The above restoration scenarios translate into substantial changes in the percentage of stream network habitable to salmon and steelhead migration (from 29% to 79%) and to core juvenile rearing (from 13% to 36%).
- Land use legacies leave an important footprint on the present landscape and are critical for understanding historic habitat-forming processes as a necessary first step towards restoration.

Cold-water Refuges

- We used forward-looking infrared (FLIR) imagery combined with field surveys to describe the distribution, physical habitat characteristics, and fish use of cold-water refuges in the Upper Grande Ronde River basin.
- Cold-water refuges were widespread across the basin, totaling 17,945 m² of refuge habitat. Refuges were 5.8 °C cooler on average than the ambient main channel, but other habitat conditions such as depth, velocity, and fish cover were generally poor.

- We predicted that cold-water refuges could support a maximum capacity of approximately 14,891 juvenile Chinook Salmon, and 1,980 juvenile steelhead. This amounts to approximately 10 % of the total Chinook Salmon summer parr capacity in Upper Grande Ronde basin.
- These results provide managers with a baseline understanding of the distribution, habitat characteristics, and fish production potential of cold-water refuges in the Upper Grande Ronde Basin which can be used to aid in fish management decisions and direct future restoration actions.

Comparison of Regional Water Temperature Models

- We evaluated the effectiveness of two regional stream temperature models to fill in gaps in measured CHaMP stream temperature data and provide predictions of water temperature in unsampled locations.
- We compared modeled stream temperatures from the Northwest Stream Temperature model (NorWeST) and the South Fork Research, INC. Stream Temperature model (SFR) to measured CHaMP stream temperatures for a subset of study years (2011 – 2013).
- Each of the stream temperature models showed a tendency to overestimate temperatures when compared to measured temperatures. However, the NorWeST model explained a considerably larger proportion of variation in measured water temperature ($R^2 = 0.784$) compared with the SFR model ($R^2 = 0.505$) and would therefore be our best option for filling in gaps in data.

Mapping Restoration Intensity

- We conducted a landscape-scale analysis of large woody debris (LWD) additions drawing from an ArcGIS Personal Geodatabase that we compiled, documenting nearly 4500 sites where restoration work was implemented between 1986 and 2014 in the upper Grande Ronde River subbasin.
- We re-analyzed published literature of LWD retention rates over time and developed a LWD retention curve; most LWD was either decaying or being transported from restoration sites after roughly 40 years.
- Using the above LWD retention curve, we predicted the LWD frequencies added across the entire river network from past restoration work and compared that amount to LWD frequencies observed at CHaMP sites. LWD added during restoration projects was positively correlated with observed LWD frequencies, explaining 27% of the variation.
- These results indicate that (a) a large portion of LWD along the river network comes from restoration work (as opposed to natural LWD recruitment) and (b) a landscape perspective is necessary for understanding restoration effectiveness.

RTK Survey of CHaMP Benchmarks

- We used real time kinematic (RTK) satellite navigation equipment to obtain high-accuracy benchmark coordinates at a subset of CHaMP sites in the Upper Grande Ronde River and Catherine Creek basins during summer of 2016.
- These high-accuracy benchmark coordinates were used to transform the CHaMP topographic data collected between 2011 and 2016 to conform more closely with the true stream channel and landscape topography.
- The results from this work serve two primary functions: 1) CHaMP data that have been transformed using RTK benchmark coordinates can be merged with spatial data collected by other agencies in the basin, thereby increasing our ability to accurately describe status and trends in stream habitat conditions, and 2) High accuracy topographic data at CHaMP sites

ensures that analysis of geomorphic change over time can continue into the future even if CHaMP benchmarks are lost or compromised.

Analysis of Low Flows and Implications for Spring Chinook

- The models of streamflow made by Watershed Sciences, Inc. (WSI) for purposes of water temperature modeling produced estimates of flows every 100 m for the entire stream network for every day in the summer period modeled for 2010. These modeled estimates relied upon the CRITFC measurements made at a point in time as well as USGS gage data. The measurements on specific days made by CRITFC matched closely with estimates made by WSI for those same days and locations.
- Low flow statistics (D_5 , D_{10} , D_{25} , D_{50} , and D_{95}) available from USGS in their StreamStats modeling (<https://water.usgs.gov/osw/streamstats/ssonline.html>) using their Version 3 State Applications were computed for many selected locations within the Upper Grande Ronde basin, including several annual CHaMP sites.
- For the upper sites in the UGR, the flow duration values were about D_{33} to D_{38} (33 – 38 % exceedance probability). However, on a longitudinal trajectory down the mainstem, the flow duration probabilities changed gradually so that flows measured near the gage near Perry were found to be extremely rare low flows, virtually never seen under the pristine watershed conditions modeled in StreamStats. This indicates that streamflow declines from naturally occurring levels (i.e., levels that would have been observed in an unmanaged basin) in a downstream direction. This might be due to a combination of factors: (1) increased evaporation from the stream surface area under greatly increased W/D ratios combined with elevated water temperatures that are due to increased solar radiation interception, and (2) water withdrawal or diversion.
- The differences between measured flows at a site and the flows that would be expected to occur under natural conditions indicate the amount of water removed from the stream by the mechanisms described. This amount of water could potentially be restored to the stream with better land use practices and by narrowing of the channel to reduce wetted width. Improvements in streamflow would improve conditions for adult and juvenile Chinook through water temperature reductions. In addition, the presence of increased wetted volume and increased water velocity that would occur under more concentrated flow in a narrowed channel would likely produce greater food supplies, provide greater transport of food past salmon feeding stations, and better growth rates at the lower temperatures that would result.
- Evaluations of the annual streamflows at selected CHaMP sites made here suggest that there is a logical means to mapping out August streamflows on a stream network basis for purposes of rolling up estimates of annual carrying capacity each year.

Analysis of Peak Flows and Implications for Spring Chinook

- Timing of peak flow events in relation to the timing of life stage events is capable of influencing survival at either the incubation stage via scouring or the post-emergence stage (downstream displacement of juveniles to the lower Grande Ronde valley) where mortality would be high during summer juvenile rearing stages.
- It is possible that the magnitude of biological impact of an annual peak flow is a function of (a) a single annual peak flow per year, (b) a peak monthly flow where the peak has a timing corresponding to either incubation or early juvenile emergence, (c) a summation of monthly flows, (d) a count of flows that are greater in magnitude than a certain statistical flow level (e.g., the 99th percentile high flow). We evaluated for the period of years in which CHaMP surveys were done how these indices would vary and create a physical basis for a biological trend.

- Unit stream power was used as a predictor of apparent juvenile survival. This survival index was the ratio of density (numbers/m) of total juvenile Chinook observed in snorkel surveys in one year to the redd density (number of redds/km) observed in the previous year. It was hypothesized that a high unit stream power generated from a single annual peak flow occurring in May-June in the key spawning zone of the UGR would result in an impact on juvenile survival (or displacement downstream) in proportion to its magnitude. Such a relationship between unit stream power and juvenile survival index seems apparent using data only for the upper two CHaMP sites (i.e., dsgn4-000009 and CBW05583-099818). This relationship becomes degraded with inclusion of additional sites downstream. This suggests that additional factors such as total number of redds upstream of each site that generate juveniles and channel complexity or LWD abundance, factors that could provide shelter for juveniles in peak flows, are influential in determining juvenile survival (or resistance to downstream displacement).
- It is the intent of this initial exploration of peak flows that a linkage might be found between annual peak flows and annual variations in juvenile or smolt numbers reaching Lower Granite Dam or an index of survival at this life stage. This report considers a variety of indices of peak flows and compares what these might look like among streams in the Upper Grande Ronde River and Catherine Creek.

Toxic Chemicals in the Environment

- The application of pesticides, herbicides, and fumigants to timberlands and croplands has the potential to be a significant hidden source of mortality of aquatic macroinvertebrates that constitute the food base of the salmonid community. These toxic substances can cause direct mortality of salmonids or provide sublethal impacts to growth rates, reproductive rates, behavior, migration, predator avoidance, etc. that can cause population impairment in a life cycle context and threaten the ability to restore the population.
- In addition to the lethal or sublethal impacts of individual toxics, the fact that there are as many as 482 pesticides, herbicides, and fungicides used in the US and their interactions or synergistic or additive effects are largely unknown or poorly studied makes the potential for impact to the aquatic populations of great concern. Across the US, one or more pesticides were found in 90% of streams on agricultural, urban, or mixed-use land. A study by Gilliom et al. (2006) showed that in 83 streams sampled in agricultural areas, 57% had one or more pesticides present in levels exceeding aquatic-life benchmarks. Chlorpyrifos exceeded benchmarks in 21% of these streams, while atrazine exceeded benchmarks in 18%.
- The USGS provides a website that indicates modeled concentrations in rivers of a wide variety of toxics that are applied on watersheds based on knowledge of amounts applied, timing, types of crops present, and ability of the toxic chemical to migrate through soil or air to streams.
- NOAA (2008) reviewed the known biological literature on impacts of chlorpyrifos, diazinon, and malathion. A wide range of impacts to fish and aquatic macroinvertebrates was described. Among the findings were that four prey species eaten by salmonids had acute toxicity levels of 0.1-50 $\mu\text{g/l}$. LC50 values on a wide range of aquatic macroinvertebrates were less than 1 $\mu\text{g/l}$ (EPA 2003, as cited by NOAA 2008). Diazinon, another organophosphorus pesticide, can cause mortality in macroinvertebrates at concentrations as low as 0.06 $\mu\text{g/l}$, growth impairment at concentrations of 0.8 $\mu\text{g/l}$, and impaired reproduction at concentrations of 0.1-10 $\mu\text{g/l}$, depending upon species and study.
- USGS data show that expected concentrations of chlorpyrifos in Catherine Creek downstream of Little Creek ranged from 0.002 to 0.01 $\mu\text{g/l}$. A 21-day maximum moving average of chlorpyrifos estimated for applications made in 2012 in Catherine Creek provided a 5-25% chance that the

chronic macroinvertebrate standard of 0.04 *ug/l* would be exceeded. Higher application rates would be likely to create greater concentrations than those estimated for 2012.

- Although the threat of significant limitation of spring Chinook recovery via direct impact to the fish or their prey base from individual pesticides or herbicides appears to be primarily just at or below the levels known to begin causing measurable impacts, there are several reasons to have concern about these toxic substances in the environment. There are many toxics having similar modes of biological impact that could easily work synergistically or additively to heighten the level of mortality. Variations in the extent of planting of crops that typically are subject to applications of these pesticides can cause unpredictable changes in timing of spread of these toxics in the environment. Weather patterns, such as timing of summer precipitation, can cause intense periods of movement of toxics into surface waters. The chemical degradates of primary forms of pesticides and herbicides can be far more toxic than the primary chemical itself. High water temperatures can increase the lethality of any toxic chemical and the combined action of pesticides and herbicides together with other conventional environmental limiting factors that have increased stress levels on listed fish populations are capable of severely restricting recovery potential.

Fish-Habitat Relationships

- CRITFC continued monitoring of Salmon and steelhead densities by completing our second visit to each of three rotating panel sites and sixth visit to annual CHaMP sites.
- Reach-scale juvenile Chinook Salmon densities per linear stream distance declined from 2011-2016 in the Upper Grande Ronde River and potentially in Catherine Creek, though fish densities in the latter population were highly variable. Juvenile Chinook densities in the Minam River were as high or higher than other watersheds, especially in 2015.
- Structural equation modeling (SEM) of fish-habitat relationships—after accounting for position in the watershed—revealed that large woody debris had both direct and indirect effects on juvenile Chinook Salmon densities. LWD had a positive direct effect, potentially through refuge or providing nutrient-rich substrate for biological production. LWD had a positive indirect effect through the association of pools, which were also positively associated with higher fish densities.
- SEM could provide a means for estimate juvenile spring Chinook Salmon rearing density, and provides a flexible model framework for predicting fish responses to site-specific restoration activities and landscape-level processes.

Redd / Stream Gradient Analysis

- We assessed the stream gradient of Chinook redd locations sampled between 2009 and 2016.
- Using binned redd groupings, largest groupings (387 of 842) occurred at locations with mean gradients between 0.51 and 1.00%, with the next largest grouping (281 of 842) occurring where mean gradients were between 1.00 and 1.51%. Very few redds (43 of 842) occurred in locations where mean gradients exceeded 2%. The mean stream gradient for all redds was 1.09%.
- The results indicate a strong preference for spawning habitat based on stream gradient.

Influence of Water Temperature on Spawning Success

- Salmon carcass recovery data from seven populations of spring- and summer-run Chinook Salmon in the Grande Ronde and Imnaha River basins were used to evaluate the relationship between summer water temperature and spawning success (the complement of pre-spawn mortality).
- Despite a high degree of spatial and temporal variability in estimates of spawning success, our analysis revealed a significant negative effect of water temperature on the probability of spawning success.
- These results add to a substantial body of evidence linking high water temperature to reduced spawning success in Pacific Northwest salmon populations and highlight the need for continued habitat restoration or other management actions to improve temperature conditions for fish in temperature-impaired watersheds.

Development of Food Web Metrics from Benthic Macroinvertebrate Data

- Benthic macroinvertebrates (BMIs) are collected in numerous fish-habitat monitoring programs throughout the Pacific Northwest, yet these data are typically used to generate indices of biotic integrity for describing water quality or sensitivity of BMI assemblages to environmental stressors such as water temperature and sediment load. However the same BMI data can be used to describe the quality of food resources for stream-dwelling fish.
- We present methods for two independent approaches: (1) metrics based on a topological food web perspective, requiring the compilation of resource-consumer pairings from literature review and laboratory observations; and (2) metrics based on availability of prey items to the drift, which extends an existing model requiring compilation of various life history and ecological traits of individual BMI taxa.

Benthic and Drift Macroinvertebrates

- Benthic and drift macroinvertebrate samples were collected in all CHaMP sites from 2011-2016.
- Benthic samples provide a means of identifying water quality and channel conditions, such as water temperature, water chemistry, and fine sediment impacts on macroinvertebrate community composition. Factors that influence benthic macroinvertebrate community composition are expected to, in turn, influence the potential for drift macroinvertebrate community composition.
- Drift density (numbers/m³, biomass/m³) and composition were hypothesized as being related to the density (numbers/m², biomass/m²) of taxa in the benthos. This analysis was conducted at the insect order level. More refined evaluation at the family, genus, or species level is needed to adequately understand this relationship.
- Benthic biomass of five principal insect orders vary with position on the mainstem continuum. Plecoptera decline in biomass in a downstream direction in the Upper Grande Ronde River. This river increases significantly in water temperature over the continuum expressed in samples collected in 2016. Trichoptera appear to increase in a downstream direction. Diptera and Coleoptera are relatively stable along this path, but Ephemeroptera are not present in significant biomass and appear to be extinguished toward the downstream end of this series.
- Catherine Creek mainstem provides a much different environmental gradient to that in the Upper Grande Ronde. Plecoptera becomes much greater in abundance with distance downstream. Diptera is present in greater biomass than in the UGR and increases downstream. Ephemeroptera was present in greater biomass upstream, but remains as a more significant component of the community at all sites along its continuum. Water temperatures are not as warm toward the downstream end of this continuum as in the UGR. Trichoptera were a

significant component by biomass in all sites and appeared to increase toward the lower extent of this continuum. Future analyses should explore whether this trajectory is characterized by greater presence of filter feeding Trichoptera.

- Benthic data collected from CHaMP sites in 2016 revealed that metrics that can effectively show environmental trends (longitudinally and at a site over time) include Total Score, O/E (0.5), weighted area inference for water temperature and fine sediment, water temperature sensitive and tolerant taxa, fine sediment sensitive and tolerant taxa, and weighted area inverse method for estimating fine sediment percentage.
- Total Scores for benthic samples taken along the Catherine Creek and UGR mainstems increased with elevation. Regressions of Total Score on elevation were parallel for both mainstem continua, but scores at the same elevation for the UGR were significantly lower than those for Catherine Creek.

Life Cycle Model

- We contracted with Pete McHugh of Eco Logical Research in 2016 to develop a life cycle model (LCM) for spring Chinook Salmon populations in the Catherine Creek (CC) and Upper Grande Ronde River (UGR) watersheds, and to assess the effects of several different habitat restoration treatments, varying in specificity, on the performance of model populations.
- Overall, the base model parameterization appeared to accurately capture both the stage-specific (i.e., freshwater vs. marine) and total life cycle productivity of spring Chinook salmon in Catherine Creek, and predicted abundance of natural-origin fish reaching CC were well within recent average values.
- The 'PNV' and 'WidPNV' scenarios, which assume maximum cooling of stream temperatures in the absence of climate change effects, showed the greatest response, with an approximate 30-40% increase in spawner abundance. On the other hand, 'doing nothing' vegetation/restoration wise in the face of the anticipated effects of climate change on conditions in CC (scenario 'Clim') translated into a 30% reduction in spawner abundance.
- Finally, a scenario testing the effects of ceasing all supplementation efforts after 20 years (all other inputs set to 'Curr' values), illustrated that natural origin Chinook extinction was a virtual certainty under current freshwater and marine capacity/productivity assumptions in the absence of hatchery support.

Conclusions

Significant progress has been made over the last eight years in collection of high quality stream habitat and biotic data as well as development of analytical tools needed to quantify status and trends in habitat conditions and fish populations and to evaluate effectiveness of aggregate restoration activities. CHaMP habitat surveys, fish snorkel surveys and benthic macroinvertebrate sampling have been conducted at 139 unique sites throughout the spring Chinook Salmon distribution area in the upper Grande Ronde, Catherine Creek, and Minam River, providing highly precise and spatially referenced data for a large suite of stream habitat and biotic factors. Because fluvial and riparian processes that create fish habitat generally operate over a relatively long time frame (i.e., decades), we don't feel it would be appropriate or informative at this time to quantify long-term trends in fish habitat conditions. However, the data needed to develop important fish-habitat relationships, habitat-land use relationships, and to parameterize a life cycle model to make projections in fish response to habitat change are now available, and as demonstrated in this report, have been applied successfully to make great strides towards meeting our project objectives.

Introduction

The Columbia River Inter-Tribal Fish Commission is conducting a fish habitat monitoring program in the Upper Grande Ronde River and Catherine Creek basins designed to evaluate the effectiveness of aggregate restoration actions in improving freshwater habitat conditions and viability of ESA-listed spring Chinook Salmon populations. A critical uncertainty for fisheries managers in the Columbia Basin involves determining whether freshwater habitat restoration actions will yield a net improvement in basin-wide habitat quality such that remaining man-caused survival impairments elsewhere during the life cycle can be compensated. Through the Columbia Basin Fish Accords, Bonneville Power Administration funds this project and has an interest in determining whether expected improvements in salmon habitat and, thereby, fish production can be brought about by improvements in the quality and quantity of salmon habitat.

Habitat restoration in the Upper Grande Ronde River basin and Catherine Creek basin is being conducted by agencies such as the U.S. Forest Service (e.g., Upper Grande Ronde mine tailings restoration, where channel damage was done by historic dredge mining of the streambed), the Umatilla Tribe (e.g., McCoy Creek Meadows restoration, where natural river meanders are being restored to a channelized stream), the Oregon Department of Fish and Wildlife, and the Grande Ronde Model Watershed (e.g., stream channel reconfiguration, riparian fencing and planting, and improvement of irrigation diversions). The U.S. Bureau of Reclamation is also conducting studies of water use and availability in Catherine Creek watershed and may implement projects based on their findings.

There have been many studies conducted in recent years examining the current condition of fish habitat in all the subbasins of the Columbia River. Some of the most common impediments to survival of salmon tend to be high water temperatures, increased concentrations of fine sediment in spawning gravel, loss of riparian vegetation, channelization, loss of large woody debris in the channel, loss of large pools for adult fish holding and juvenile rearing, and summertime depletion of streamflows in the channel. Added to these concerns caused by human influence is climate change, which can lead to changes in the timing of runoff from snowmelt, increased summer air temperatures, and change in the seasonal distribution of precipitation.

We are attempting to monitor habitat factors that have been identified by previous studies as key limiting factors. Our monitoring plan includes measurement of: water temperature, streambed substrate composition and fine sediment concentrations, streamflow, water chemistry, riparian condition, stream channel morphology (including spawning habitat and large pool distribution), large woody debris, benthic macroinvertebrates (diversity and density, which indicate long-term water quality), drifting macroinvertebrates (indicating fish food availability), and fish snorkeling (indicating relative abundance of salmonids and qualitative indices of abundance of non-salmonids). Habitat surveys are conducted in 25 sites per year distributed throughout the currently used spring Chinook Salmon spawning and rearing habitat in the Upper Grande Ronde and Catherine Creek basins following methods developed by the Columbia Habitat Monitoring Program (CHaMP; <https://www.champmonitoring.org/>). In addition, CRITFC funded ODFW to conduct CHaMP surveys in

the Minam River in 2014 and 2015 to provide a set of monitoring sites to act as an unmanaged reference for more heavily disturbed, managed sites in the Upper Grande Ronde and Catherine Creek.

As a means to integrate habitat monitoring efforts with recovery planning, CRITFC is developing a life cycle model. The life cycle model is being designed as a tool to simulate population trends in relation to projected environmental conditions, and to examine the relative benefits of habitat improvements on population recovery potential. Initially, a prototype model was developed which includes all Chinook Salmon populations in the Grande Ronde/Imnaha Major Population Group (MPG) of the Snake River Evolutionarily Significant Unit (ESU), which consists of the Grande Ronde River, Catherine Creek, Lostine/Wallowa, Minam, Wenaha, and Imnaha. That model focused on empirical validation of the survival of outmigrating juveniles and returning adults, with particular focus on the environmental and operational variables that influence survival through the hydro system and ocean. This prototype model provides a strong empirical basis for further refinements of the life cycle model to include effects of freshwater habitat conditions on productivity and abundance of rearing juvenile salmonids.

Future refinement of the life cycle model and the research needed to parameterize the model are guided by a basic conceptual model framework (Figure 1). The fundamental basis of the model is that intrinsic watershed factors (such as geology, climate, or valley morphology) interact with human actions (such as forest harvest, cattle grazing, or stream restoration) to affect processes that drive known limiting factors (e.g., flow, temperature, pool area, etc.), and therefore fish survival via both density-dependent and density-independent processes. Current and future habitat conditions can act as predictors of relative change in survival at different life history stages, and therefore affect recovery potential.

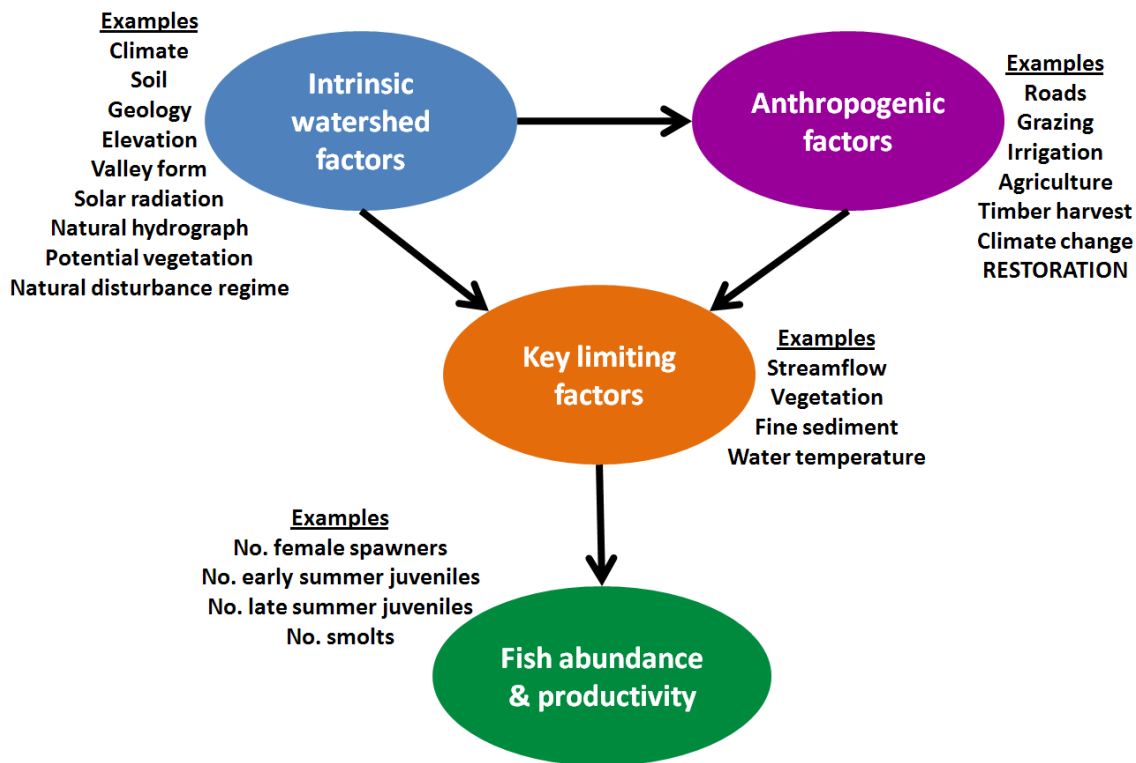


Figure 1. Conceptual framework for relating fish abundance and productivity to watershed characteristics and limiting factors. Direction of arrows indicates direction of influence.

The Upper Grande Ronde/Catherine Creek life cycle model for spring Chinook Salmon (Figure 2) is comprised of several interacting subcomponents that are built independently, each of which provides critical information about the interaction between landscape characteristics, instream habitat conditions, and fish response. Individual subcomponents of the life cycle model, and of our research program, include modeling stream temperature from local riparian and geomorphic conditions; a water temperature model that links summer water temperature metrics to summer juvenile survival; a potential natural vegetation map for estimating stream shade; rates of restoration project addition of large woody debris; macroinvertebrate inputs for estimating the food base and growth potential for drift-feeding salmonids; and a low flow model permitting evaluation of site vulnerability to climatic variations in precipitation, snow melt timing, and air temperature variations. Though these components are described here as potentially providing inputs to the life cycle model, each model is a valid research project in its own right that is likely to yield interesting scientific insights and practical applications for conservation.

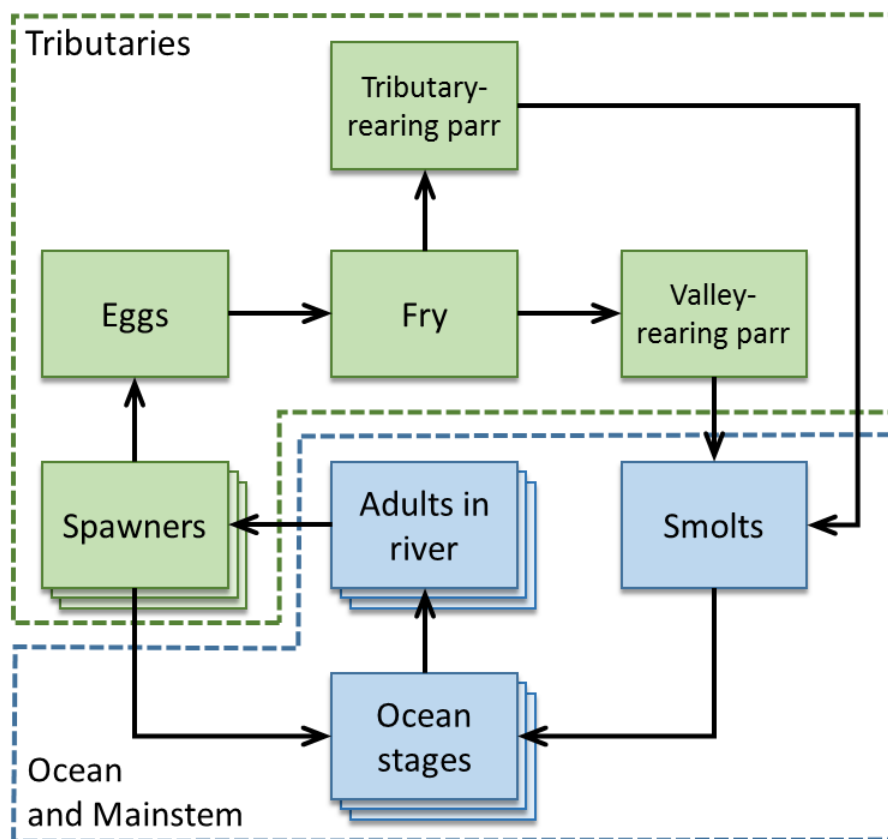


Figure 2. Conceptual diagram of the life cycle model (LCM) framework used to assess restoration scenarios in Catherine Creek. Stacked boxes represent life stages for which multiple ages exist and are tracked accordingly. In our LCM, parr can ‘choose’ to migrate downstream and overwinter in the Grande Ronde Valley (‘Valley’) or remain in the upper mainstem and tributaries of Catherine Creek (‘Tributary’). Otherwise, the LCM’s smolts are enumerated at Lower Granite Dam (LGD), where ‘ocean stages’ begin and are modeled via LGD-to-LGD smolt-to-adult return rates. Fish-habitat modeling described in this report provides capacity estimates for spawner and parr freshwater life stages.

The primary objectives of this project are to: 1) Assess current status and trends in fish habitat characteristics considered to be key limiting factors (particularly water temperature, pool habitats, streamflow, and fine sediment) to viability of spring Chinook Salmon populations; 2) Evaluate effectiveness of aggregate stream restoration actions aimed at improving key limiting habitat factors; 3) Develop a life cycle model to link biotic responses of spring Chinook populations to projected changes in stream habitat conditions.

Stream Habitat

CHaMP Data Collection

Methods

In 2016 we continued to implement the Columbia Habitat Monitoring Program (CHaMP) protocol and sampled 26 sites in the upper Grande Ronde and Catherine Creeks basins. When combined with CHaMP sites surveyed by the Confederated Tribes of the Umatilla Indian Reservation (CTUIR) and ODFW, including the Minam basin, a total of 158 unique sites (427 site visits) have been surveyed in the Grande Ronde basin. CHaMP is designed as a Columbia River basin-wide habitat status and trends monitoring program built around a single protocol with a programmatic approach to data collection and management. CHaMP will result in the collection and analysis of systematic habitat status and trends information that will be used to assess basin-wide habitat conditions and characterize stream responses to watershed restoration and/or management actions. A detailed description of the CHaMP protocol is provided at <http://www.monitoringmethods.org/Protocol/Details/806>).

Survey sites were randomly selected using the Generalized Random Tessellation Stratified (GRTS) survey design (Stevens and Olsen 2004), and were distributed with equal probability across all wadable portions of the stream network that were classified as current or historic spawning and rearing areas for spring Chinook Salmon (Figure 3). The spring Chinook distribution area was modified from maps produced by ODFW, StreamNet (StreamNet 2009), the Grande Ronde Subbasin plan (Nowak 2004), and the NOAA's Interior Columbia Basin Technical Recovery Team (ICTRT), and is described in more detail in McCullough *et al.* (2012).

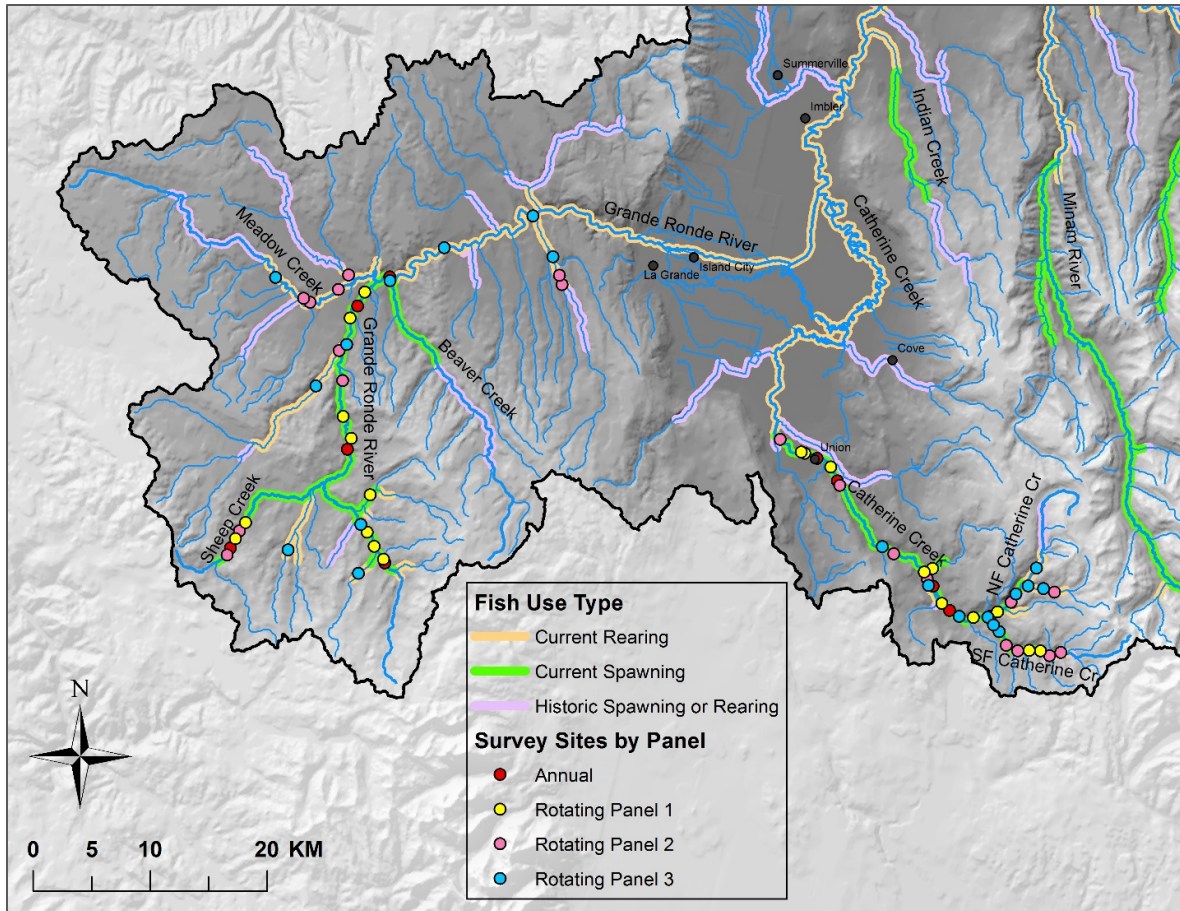


Figure 3. Sample design showing the distribution of CRITFC habitat survey sites in the upper Grande Ronde River and Catherine Creek basins.

We used a 3-year rotating panel design (Table 1) with the intention of achieving a good balance between power to describe current status (i.e., accurate description of spatial variation across the entire sampling extent) and power to detect trends over time. This temporal design includes 5 annual sites and 10 rotating panel sites in the upper Grande Ronde and Catherine Creek basins. Annual sites are surveyed every year and rotating panel sites are surveyed every 3 years. A total of 30 sites are surveyed each year, with a total sample size of 70 unique sites after 3 years. Note that 5 of the 30 sites within CRITFCs target sample frame are surveyed by ODFW each year. The 2016 field season was the sixth year of implementing the protocol in the upper Grande Ronde watershed. This year's surveys were the sixth visit to annual sites and the first revisit to panel 3 sites since the start of the program in 2011.

Dissimilarly to the previous three monitoring seasons, CHaMP data were not collected in the Minam River watershed. These data, which were collected in collaboration with the Oregon Department of Fish and Wildlife since 2013, were selected as suitable reference site locations that could be used as a comparison to the two more significantly disturbed watersheds (i.e. Catherine Creek and Upper Grande Ronde River watersheds).

Table 1. Rotating panel design for CHaMP sites in the Grande Ronde River and Catherine Creek watersheds. Note that 5 of the 30 sites in our survey design are sampled by ODFW each year.

Panel	Year								
	2011	2012	2013	2014	2015	2016	2017	2018	2019
Grande Ronde Chinook									
Annual Panel	5	5	5	5	5	5	5	5	5
Rotating Panel 1	10			10			10		
Rotating Panel 2		10			10			10	
Rotating Panel 3			10			10			10
Catherine Creek Chinook									
Annual Panel	5	5	5	5	5	5	5	5	5
Rotating Panel 1	10			10			10		
Rotating Panel 2		10			10			10	
Rotating Panel 3			10			10			10
Total Annual Samples	30	30	30	30	30	30	30	30	30
Total Unique Samples	70								

A large number of stream habitat variables were measured at each site, generating over 100 metrics describing the condition of the stream. Most of the variables measured were chosen because they are directly related to salmonid fish growth and/or survival or because they provide critical information used to describe ecological processes in the stream or broader landscape that may be indirectly related to fish productivity. The measurements were collected using a combination of traditional habitat data collection methods along with use of technical survey equipment (e.g., Total Stations) that allows for the development of detailed topographic maps of the stream channel. A complete list of metrics generated by CHaMP surveys is available at <https://www.champmonitoring.org/>.

Topographic data are composed of deliberately placed coded points and lines in the stream channel and floodplain that are used to illustrate inflection points in the channel bedform such as pools, the toes and tops of banks, and the thalweg (the location with the highest streamflow) along with important features such as the edge of water, bankfull elevations, and channel unit boundaries (Figure 4, a.). Depending on the channel length and complexity, crews capture between 700 and 1500 points in order to accurately represent a stream reach. The raw data were imported into ArcGIS and processed to create digital elevation models (DEM), channel unit delineations, and water depth maps (Figure 4, b. - d.). These data were evaluated for quality control during the initial processing that occurs directly after the survey. After the field season is completed, the output products from each survey were processed through the River Bathymetry Toolkit (RBT) to derive metrics that are potentially important to fish, such as residual pool depth. After the RBT metrics were created, a second round of quality control analysis is performed to ensure the accuracy of the topographic data. These data were then made available to the public on the program's website (www.champmonitoring.org).

These detailed surveys will become increasingly powerful as the CHaMP program progresses because these surveys can be repeated and overlaid to inform topographic change over time. We have just completed the sixth year of the nine year study design and have started the process of revisiting panel

sites. At the end of the nine year period we will have a minimum of three visits at each site and will be able to quantify the degree of channel and habitat change over time at individual sites and start to look at patterns of channel erosion and aggradation across the watershed.

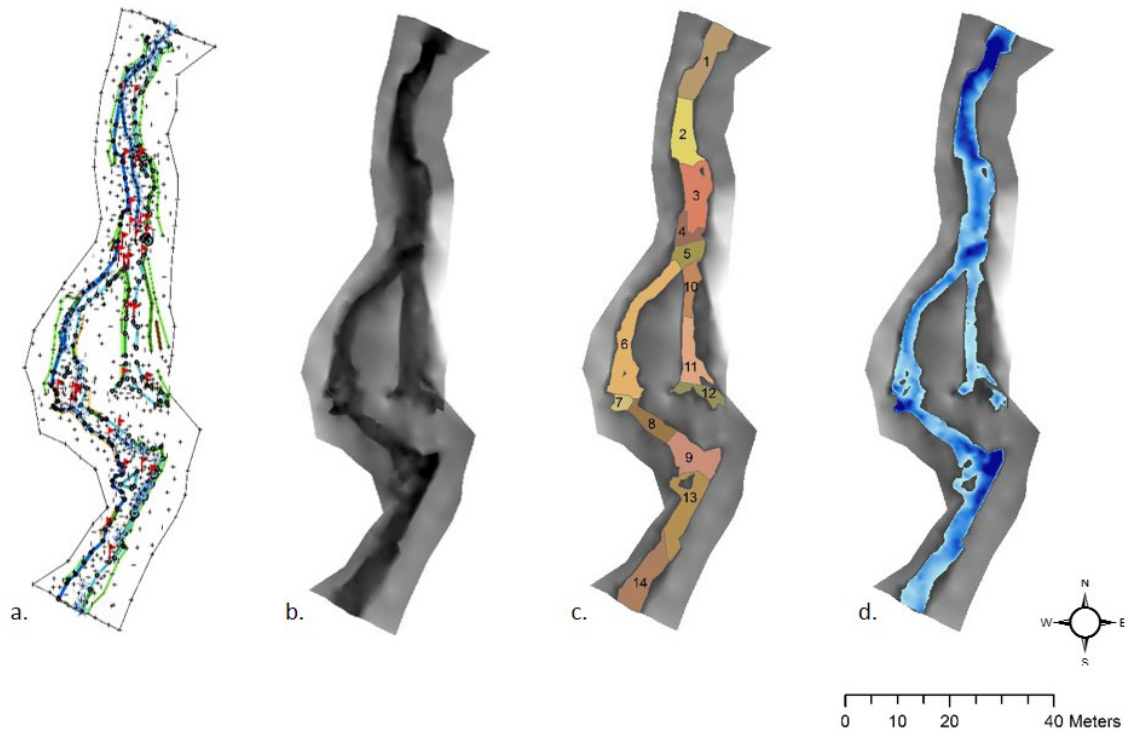


Figure 4. Example of topographic data surveyed conducted on Sheep Creek, site CBW05583-490810 using the CHaMP protocol and a Total Station. The panel depict a) the raw point and line data as surveyed in the field, b) the digital elevation model (DEM), c) channel units overlaid on the DEM, and d) the water depth map produced by analysis at each CHaMP site.

Selected habitat metrics important for Chinook Salmon at various life history stages (percentage area pools, total fish cover, large woody debris frequency, average august water temperature, and maximum 7-day average maximum water temperature) were summarized for all sites across all years by Chinook population group (upper Grande Ronde, Catherine Creek, and Minam), by biologically significant reaches (BSRs), and population stratification within each of the three population groupings (lower, middle, upper). BSR boundaries correspond approximately to the HUC6 watershed boundaries, but were aggregated or modified to better represent significant breaks in physical channel morphology (e.g., tributary junctions or major changes in valley confinement), land ownership, or fish use. BSRs were developed by local experts associated with the Federal Columbia River Power System (FCRPS) Biological Opinion expert panel and restoration implementation group (i.e., Atlas Group) for use in planning and implementing stream restoration actions. Chinook population group classifications are based on the historic and current range extents and are further refined by their location (lower, middle, upper) within each grouping (Figure 5).

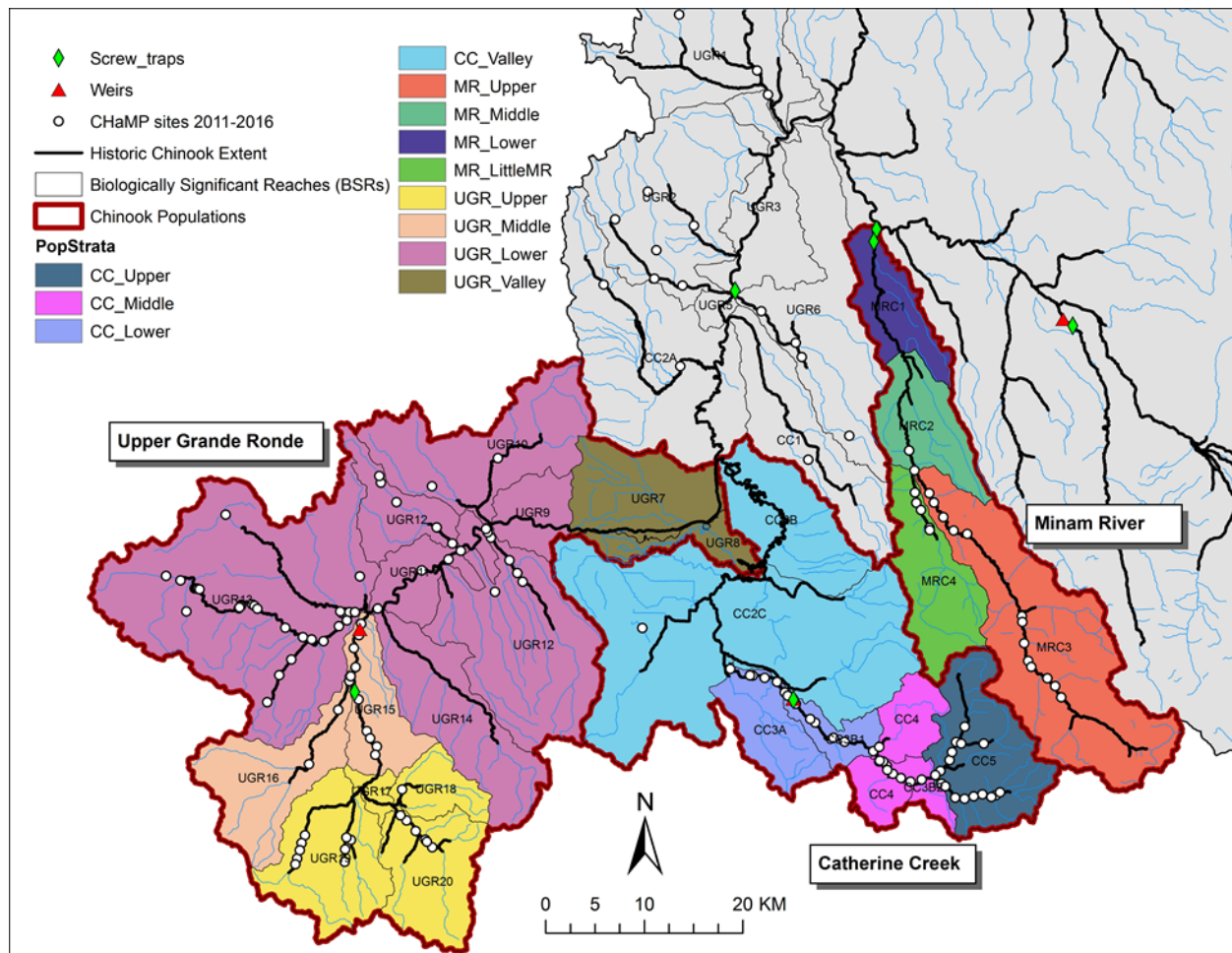


Figure 5. Map showing the spring Chinook population boundaries, CRITFC population strata, and biologically significant reaches (BSR) within the CRITFC study area.

In addition to topographic and habitat characteristics, temperature metrics were calculated. Year round temperature records were collected at all CHaMP sites in the three focal watersheds using Hobo Tidbit and Pro V2 data loggers following the Water Temperature Probe Installation Protocol (<https://www.monitoringmethods.org/Method/Details/846>). Sites were visited once in spring and once in fall to download the data and to assess the condition of the temperature loggers. In addition to the sites monitored through the CHaMP protocol, CRITFC has temperature loggers deployed at 12 other locations in the Catherine Creek and upper Grande Ronde watersheds. These loggers filled in areas where temperature data were not sufficiently captured by the CHaMP program and often are located up- and downstream of significant tributary junctions. The data validation and storage for non-CHaMP sites was conducted by CRITFC staff. The data was validated and summary statistics were calculated to match those metrics derived from the CHaMP data. This database will continue to be updated each year as more temperature data are collected in the field.

Temperature metrics were based on a “summer period” as defined by CHaMP, which is between July 15th and Aug 31st. This timeframe is crucial due to the potentially detrimental influences of high temperatures on salmonids. For every consecutive 7-day period within this 48-day period, rolling

averages of maximum temperatures were calculated (7dAM). The number of 7dAM periods where the average maximum temperature exceeds 12°, 13°, 16°, 18°, 20°, and 22°C was evaluated at every site. These water temperature standards were designated based on beneficial uses by various salmonid life history stages as defined by the Oregon Department of Environmental Quality (Sturdevant 2008). Additionally, the average daily temperature, maximum daily temperature, and the maximum 7-day rolling average of maximum temperature (Max7dAM) are reported over the same summer time period. Monthly statistics, average and maximum temperatures, were also calculated. We have reported on the Max7dAM and Average August temperatures as they are used regionally to summarize stream temperatures and would allow for the most direct crossover between monitoring programs.

In future analyses we plan to extrapolate fish density estimates to include un-sampled portions of the watershed by using the combination of the BSR regions and Chinook population group. Using GRTS we can compute population estimates based on population stratification and then calculate BSR-wide estimates based on the proportional stream length of each classification type. We can use the classification to more accurately extrapolate population metrics to BSR reaches where we have few or no CHaMP sites based on stream type.

Results and Discussion

A summary of five important CHaMP habitat metrics including total fish cover (m²), wetted large woody debris (LWD) frequency (count/100 m), percentage slow water, average August temperature (°C), and the maximum 7-day running average maximum temperature (Max7dAM, °C) within each Chinook population group, population stratification, and Biologically Significant Reaches (BSR) is provided (Table 2). These data include sites sampled by both CRITFC and ODFW within the Chinook habitat extent, which encompassed 130 unique sites (n). Data at each site were averaged across all years, 2011-2016, and then average values and standard deviations were summarized across the various spatial units.

The five habitat metrics for the instream habitat supporting the three ICTRT populations (Catherine Creek, Minam River, and Upper Grande Ronde) reveal important variations at scales of the entire population-specific basin, the component BSRs, and population strata (groupings of BSRs that comprise a longitudinal series of mainstem and associated tributary habitats). With each of the physical habitat metrics summarized at the basin scale, the Upper Grande Ronde had the higher values compared to the Minam except for percentage slow water. The Upper Grande Ronde had average August water temperatures and Max7dAM values that were higher in the upstream and downstream extent of the BSR series than expressed in Catherine Creek. At the population strata scale, Catherine Creek water temperatures were lower in the upper stratum, but at the lower stratum Catherine Creek water temperatures were higher than for the Upper Grande Ronde. This may be attributable to the influence of relatively cooler tributaries to the lower section of the UGR mainstem (e.g., Five Points Creek, Beaver Creek, and upper McCoy Creek). It was surprising that at the ICTRT population spatial scale, the Minam River was intermediate between Catherine Creek and the Upper Grande Ronde in total fish cover (%) and lower than both streams in LWD frequency. At the BSR scale, the UGR had some BSRs with lower LWD frequency than was found in the Minam River or the UGR as average values found at the ICTRT population scale.

The finer spatial resolution of the BSRs highlights particular portions of the two subbasins where extreme temperatures are detrimental to Chinook Salmon. Four of the 5 Catherine Creek BSRs exceed the ODEQ beneficial use threshold for juvenile salmonid rearing of 18°C 7dAM for a minimum of one 7-day period, based on the Max7dAM. Additionally, of these four BSRs, two exceeded the 20°C threshold set for migration corridors for adult salmon for a minimum of a 7-day period. In the Grande Ronde subbasin six of the 7 BSRs exceeded the juvenile rearing threshold and 7 exceeded the adult migration 7dAM temperature. The maximum temperature exceedance based on the Max7dAM metric occurred at BSR UGR11, showing average temperatures across the study period exceeding 27 °C. By breaking the subbasins down into smaller spatial extents we can identify areas of particular risk to Chinook Salmon and focus restoration efforts within particular reaches.

In future modeling efforts we plan to use GRTS to summarize data by population stratification and then use distinct river segments in each BSR to roll-up metrics based on the proportion of each class in a BSR. This will allow us to downscale our GRTS estimates from the whole watershed scale to a finer resolution (e.g., BSR) while leveraging knowledge of habitat data for known historic and current Chinook population ranges. The continued exploration of the trends across spatial extents will further our understanding of how habitat metrics are changing within drainages. We hope to explore how this method may improve our estimates and extrapolation of habitat variables and fish populations.

Table 2. Summary statistics for five habitat variables measured at all CHaMP sites across the Upper Grande Ronde River, Catherine Creek, and the Minam River. Values for each site were averaged over all survey years, 2011-2016 and then summarized based on three different spatial extents: Interior Columbia Technical Recovery Team (ICTRT) populations, biologically significant reaches (BSR), and population strata (PopStrata). For each habitat variable, mean, standard deviation (SD), and the number of sites that had data values (n) are recorded.

Spatial Extent	Total Fish Cover			LWD Frequency (count/100 m)			% Slow Water			Average August Temperature (°C)			Max7dAM (°C)		
ICTRT Populations	<i>Mean</i>	<i>SD</i>	<i>n</i>	<i>Mean</i>	<i>SD</i>	<i>n</i>	<i>Mean</i>	<i>SD</i>	<i>n</i>	<i>Mean</i>	<i>SD</i>	<i>n</i>	<i>Mean</i>	<i>SD</i>	<i>n</i>
Catherine Creek	9.52	5.54	40	13.36	10.28	40	21.37	9.92	40	14.07	2.48	37	18.37	2.99	37
Minam River	10.41	3.87	16	9.82	7.44	16	26.55	14.69	16	12.6	1.02	11	15.86	1.50	11
Upper Grande Ronde River	13.99	12.26	53	15.90	17.57	54	26.21	15.22	53	15.49	2.29	49	21.72	3.82	50
Biologically Significant Reach	<i>Mean</i>	<i>SD</i>	<i>n</i>	<i>Mean</i>	<i>SD</i>	<i>n</i>	<i>Mean</i>	<i>SD</i>	<i>n</i>	<i>Mean</i>	<i>SD</i>	<i>n</i>	<i>Mean</i>	<i>SD</i>	<i>n</i>
CC3A	5.87	3.43	4	7.58	7.26	4	32.67	8.32	4	17.31	0.51	4	21.68	0.54	4
CC3B1	8.05	3.21	9	12.82	10.49	9	20.86	8.63	9	16.87	0.99	8	21.62	1.18	8
CC3B2	7.12	3.18	7	12.39	6.04	7	24.57	12.89	7	14.23	0.72	7	19.13	1.06	7
CC4	20.36	8.34	3	20.45	6.52	3	27.05	8.51	17	14.66	0.07	3	18.97	1.44	3
CC5	10.24	4.42	17	14.16	11.74	17	16.66	5.69	3	11.52	0.86	15	15.28	1.23	15
MRC3	8.83	3.36	10	9.28	8.31	10	30.53	13.76	10	12.62	0.99	6	15.96	1.15	6
MRC4	13.04	3.18	6	10.71	5.60	6	19.91	13.77	6	12.58	1.05	5	15.74	1.82	5
UGR11	6.67	2.20	5	0.55	0.55	5	11.26	8.13	5	19.80	1.21	5	27.12	1.47	5
UGR12	14.85	14.28	7	6.72	5.54	7	15.41	3.89	7	16.43	0.90	5	23.40	1.69	6
UGR13	16.98	12.36	12	20.35	17.21	13	29.54	12.08	12	15.08	2.10	13	20.85	4.05	13
UGR15	7.37	4.25	9	8.05	6.03	9	17.27	8.36	9	17.15	0.47	8	24.46	1.19	8
UGR16	6.95	2.31	4	4.91	1.78	4	16.46	0.93	4	16.33	0.79	3	24.45	0.89	3
UGR19	21.13	17.16	8	18.78	8.33	8	46.47	18.57	8	13.79	1.06	7	20.05	1.89	7
UGR20	13.32	7.30	6	40.21	29.16	6	31.57	15.67	6	15.54	0.68	6	17.51	1.17	6
Population Strata	<i>Mean</i>	<i>SD</i>	<i>n</i>	<i>Mean</i>	<i>SD</i>	<i>n</i>	<i>Mean</i>	<i>SD</i>	<i>n</i>	<i>Mean</i>	<i>SD</i>	<i>n</i>	<i>Mean</i>	<i>SD</i>	<i>n</i>
CC_Lower	7.38	3.43	13	11.21	9.91	13	24.49	10.13	13	17.01	0.89	12	21.64	1.02	12
CC_Middle	11.09	8.05	10	14.81	7.21	10	25.31	11.80	10	14.36	0.63	10	19.08	1.12	10
CC_Upper	10.24	4.42	17	14.16	11.74	17	16.66	5.69	17	11.52	0.86	15	15.28	1.44	15
MR_LittleMR	13.04	3.18	6	10.71	5.60	6	19.91	13.77	6	12.58	1.5	5	15.74	1.82	5
MR_Upper	8.83	3.36	10	9.28	8.31	10	30.53	13.76	10	12.62	0.99	6	15.96	1.15	6
UGR_Lower	14.71	12.50	25	14.43	16.08	26	24.17	12.36	25	15.78	2.30	24	21.93	3.97	25
UGR_Middle	7.23	3.74	13	7.07	5.31	13	17.01	6.93	13	16.91	0.69	11	24.46	1.12	11
UGR_Upper	17.44	13.99	15	28.67	22.11	15	41.21	18.68	15	13.11	1.14	14	18.64	2.15	14

References

McCullough, D.A., C. Justice, S. White, R. Sharma, D. Kelsey, D. Graves, N. Tursich, L. Hill, T. Lewis, R. Lessard, and H. Franzoni. 2012. Monitoring Recovery Trends in Key Spring Chinook Habitat Variables and Validation of Population Viability Indicators, 1/1/2011 - 12/31/2011, Annual Report, 2009-004-00, 802 p.

Nowak, M.C. 2004. Grande Ronde Subbasin Plan. Prepared for Northwest Power and Conservation Council. 491 p.

Stevens, D.L., and A.R. Olsen. 2004. Spatially balanced sampling of natural resources. *Journal of the American Statistical Association* 99, no. 465: 262–278.

StreamNet GIS Data (2003). Metadata for Pacific Northwest coho salmon fish distribution spatial data set. Portland (OR) : StreamNet, May 2003. [31 Jan 2005]. URL: <http://www.streamnet.org/onlinedata/GISData.html>

Stream Temperature Modeling

The following abstract summarizes the manuscript by Justice et al. (2017) titled “Can stream and riparian restoration offset climate change impacts to salmon populations”. Please see <http://www.sciencedirect.com/science/article/pii/S0301479716309793> for further details.

Abstract

Understanding how stream temperature responds to restoration of riparian vegetation and channel morphology in context of future climate change is critical for prioritizing restoration actions and recovering imperiled salmon populations. We used a deterministic water temperature model to investigate potential thermal benefits of riparian reforestation and channel narrowing to Chinook Salmon populations in the Upper Grande Ronde River and Catherine Creek basins in Northeast Oregon, USA. A legacy of intensive land use practices in these basins has significantly reduced streamside vegetation and increased channel width across most of the stream network, resulting in water temperatures that far exceed the optimal range for salmon growth and survival. By combining restoration scenarios with climate change projections, we were able to evaluate whether future climate impacts could be offset by restoration actions. A combination of riparian restoration and channel narrowing was predicted to reduce peak summer water temperatures by 6.5 °C on average in the Upper Grande Ronde River and 3.0 °C in Catherine Creek in the absence of other perturbations. These results translated to increases in Chinook Salmon parr abundance of 590 % and 67 % respectively. Although projected climate change impacts on water temperature for the 2080s time period were substantial (i.e., median increase of 2.7 °C in the Upper Grande Ronde and 1.5 °C in Catherine Creek), we predicted that basin-wide restoration of riparian vegetation and channel width could offset these impacts, reducing peak summer water temperatures by about 3.5 °C in the Upper Grande Ronde and 1.8 °C in Catherine Creek. These results underscore the potential for riparian and stream channel restoration to mitigate climate change impacts to threatened salmon populations in the Pacific Northwest.

References

Justice, C., S. M. White, D. A. McCullough, D. S. Graves, and M. R. Blanchard. 2017. Can stream and riparian restoration offset climate change impacts to salmon populations? *Journal of Environmental Management* 188:212–227.

Historical Ecology for Setting Restoration Targets

Abstract

The following abstract summarizes the manuscript by White et al. (2017). Please see <https://www.elementascience.org/articles/10.1525/elementa.192/> for further details.

Land use legacies can have a discernible influence in present-day watersheds and should be accounted for when designing conservation strategies for riverine aquatic life. We describe the environmental history of three watersheds within the Grande Ronde subbasin of the Columbia River using General Land Office survey field notes from the 19th century. In the two watersheds severely impacted by Euro-American land use, stream channel widths—a metric representing habitat simplification—increased from an average historical width of 16.8 m to an average present width of 20.8 m in large streams; 4.3 m to 5.5 m in small, confined or partly confined streams; and 3.5 m to 6.5 m in small, laterally unconfined streams. Conversely, we did not detect significant change in stream widths in an adjacent, wilderness stream with minimal human impact. Using a mechanistic water temperature model and restoration scenarios based on the historical condition, we predicted that stream restoration in the impacted watersheds could notably decrease average water temperatures—especially when channel narrowing is coupled with riparian restoration—up to a 6.6°C reduction in the upper Grande Ronde River and 3.0°C in Catherine Creek. These reductions in water temperature translated to substantial changes in the percentage of stream network habitable to salmon and steelhead migration (from 29% in the present condition to 79% in the fully restored scenario) and to core juvenile rearing (from 13% in the present condition to 36% in the fully restored scenario). We conclude that land use legacies leave an important footprint on the present landscape and are critical for understanding historic habitat-forming processes as a necessary first step towards restoration.

References

White, SM, C Justice, DA Kelsey, DA McCullough, T Smith. 2017. Legacies of Stream Channel Modification Revealed Using General Land Office Surveys, with Implications for Water Temperature and Aquatic Life. *Elem Sci Anth* 5(3):1-18. doi:10.1525/elementa.192.

Cold-water Refuges

Full Title: Habitat Characteristics and Fish Use of Cold-water Refuges in the Upper Grande Ronde River

Casey Justice, Dale McCullough, Seth White

Columbia River Inter-Tribal Fish Commission (CRITFC)

April 2017

Abstract

Cold-water refuges in streams can provide critical rearing and holding habitat for fishes and other aquatic taxa, particularly in streams with stressful summer water temperatures. We used forward looking infrared (FLIR) imagery combined with field surveys to describe the distribution, physical habitat characteristics, and fish use of cold-water refuges in the Upper Grande Ronde River basin in Northeast Oregon. Cold-water refuges were widespread throughout the Chinook-bearing portions of the Upper Grande Ronde basin, with refuge surface area totaling 17,945 m². Refuges were 5.8 °C cooler on average than the ambient water temperature, with temperature differences between ambient and refuges reaching as high as 12.7 °C. Despite having significantly cooler water temperatures, habitat conditions in cold-water refuges were generally poor, with the majority of refuges having shallow depths, very low water velocity, relatively little shade and cover for fish, and moderate to high levels of fine sediment. We predicted that cold-water refuges could support a maximum of 14,891 Chinook Salmon summer parr, and 1,980 juvenile steelhead. This represents approximately 10 % of the total estimated Chinook Salmon parr capacity for the Upper Grande Ronde Spring Chinook population. If we consider only refuges that were connected to the main channel (i.e., had refuge crest depths > 0.05 m) and contained salmonids, the predicted refuge capacity for Chinook parr and juvenile steelhead was 8,431 and 1,628, respectively. This equates to 5.6 % of the total Chinook Salmon parr capacity. These results provide managers with a baseline understanding of the distribution, habitat characteristics, and fish production potential of cold-water refuges in the Upper Grande Ronde Basin which can be used to aid in fish management decisions and direct future restoration actions including the preservation, enhancement, and creation of new cold-water refuges.

Acknowledgements

We thank multiple people for their contributions to field data collection including Les Naylor and Dave Mack from the Confederated Tribes of the Umatilla Indian Reservation (CTUIR), Nancy Platt, and Monica Blanchard. We also thank Joe Ebersole from the Environmental Protection Agency (EPA), Ted Sedell and Jim Ruzycki from Oregon Department of Fish and Wildlife (ODFW), and Les Naylor for help with project planning, landowner access, and protocol development. We'd also like to acknowledge Brian Kasper and other staff at Quantum Spatial for collecting the forward looking infrared (FLIR) data. Funding for this project was provided by the Bonneville Power Administration as part of the Columbia Basin Fish Accords Agreement (Project # 2009-004-00).

Introduction

High water temperature is an important habitat factor limiting abundance, productivity and spatial distribution of cold-water fish species in many streams across the Pacific Northwest (Beechie et al. 2013). In the Upper Grande Ronde River basin in Northeast Oregon, approximately 86 % of the stream network currently exceeds the 18 °C temperature standard designated for protection of salmon and trout migration and rearing (Justice et al. 2017). Cold-water refuges can help mediate the effects of warm water temperatures on fish by providing discrete zones of cool water rearing or holding habitat during periods of thermal stress (Torgersen et al. 1999, Ebersole et al. 2003, Sutton et al. 2007, Tate et al. 2007).

We used a combination of remotely-sensed forward looking infrared (FLIR) imagery and field surveys to evaluate the spatial distribution, physical characteristics, and fish use of cold-water refuges in the Upper Grande Ronde River basin. In addition, we used habitat suitability criteria to predict the carrying capacity of juvenile Chinook Salmon and steelhead in refuges to evaluate the potential contribution of refuge habitats to the overall population. This baseline understanding of cold-water refuge habitats could serve as a planning tool for restoration practitioners seeking to enhance or protect currently existing cold-water refuges and could be used in combination with ongoing fish and habitat monitoring and population modeling activities to address how refuge size, connectivity, or frequency influence salmon populations.

Methods

Remote Sensing Data Processing

We used FLIR data collected in 2010 (Watershed Sciences 2010) to delineate potential cold-water refuges within the current and historic Chinook Salmon distribution area in the Upper Grande Ronde River (upstream of the Catherine Creek confluence; Figure 6). We defined cold-water refuges as spatially-continuous patches of water with temperatures at least 2 °C less than the ambient water temperature (Kurylyk et al. 2014), less than 25 °C, and a surface area of at least 1 m². Refuge boundaries were delineated manually using ArcGIS for all stream reaches where ambient water temperatures exceeded a maximum weekly maximum temperature (MWMT) of 18 °C as determined from Heat Source temperature simulations calibrated to 2010 climate and hydrologic conditions (Watershed Sciences 2012). MWMT was defined as the maximum seven day running average of the daily maximum

temperature. Cold-water refuges in portions of the stream network where ambient temperatures were below 18 °C were not delineated because they were assumed to provide minimal thermal benefits to Chinook Salmon and steelhead.

Refuges were classified into two size categories including channel unit-scale and segment-scale following the guidelines outlined in Torgersen et al. (2012). Channel unit-scale refuges are at the scale of geomorphic channel units such as pools and riffles and are generally less than 0.5 km in length and include features such as small tributary confluence plumes, lateral seeps, and cold alcoves. Segment-scale refuges typically have lengths in the order of 0.5–1 km in small streams and 5-10 km in large rivers often occur at large tributary confluences and where bounded alluvial valleys force cooler subsurface water upward into the surface water.

Qualifying refuges were classified by refuge type using the classification system described in Dugdale et al. (2013) and references cited therein. Refuge type was based on refuge geomorphology, refuge forming processes, and source of cold water (Table 3). Refuge types included: tributary confluence plume, lateral seep, springbrook, cold side channel, cold alcove, hyporheic upwelling, and wall-base channel. Refuge locations and descriptive information delineated from the FLIR data were then loaded to a GPS-enabled electronic data logger (iPad) along with aerial imagery to aid in navigation to refuge sites for field validation.

Field Data Collection

During summer of 2015, we conducted field surveys at a subset of the refuges that were delineated from the FLIR data to characterize physical habitat conditions, obtain more detailed water temperature measurements, and evaluate fish use using the protocol described in Appendix B of McCullough et al. (2016). These surveys were conducted during the period of summer base flow and maximum annual stream temperature (July 1 – August 31), when cold-water refuges are most important to fish and when contrast between refuge and ambient temperatures was maximized. In addition, surveys were conducted during the warmest time of day (1100 – 1800) to maximize the probability of detecting thermal refuges and to minimize the effect of temporal variation on refuge measurements.

No attempt was made to randomize the selection of refuges for inclusion in the field validation survey because many of the refuges were located on private land with limited access. Instead, we surveyed as many refuges as possible with priority given to refuges located in the mainstem Grande Ronde River and the lower ends of tributaries within the current Chinook use area. In addition, field surveys were focused on channel unit-scale refuges rather than segment-scale refuges because channel unit-scale refuges represented the majority of the cold-water refuge habitat present in the Upper Grande Ronde River.

After navigating to a potential refuge, we cautiously approached the refuge site and visually scanned the water using polarized glasses for fish prior to conducting any habitat measurements. If fish were observed using the refuge, we recorded the species present prior to making any other measurements at the site. When necessary, we used an underwater view scope to distinguish salmonids from other fish species. Next, we used a digital temperature probe (Atkins 35200-K, accuracy 0.1 °C) mounted to a telescoping pole to determine if the water temperature in the refuge met the criteria of being at least

2°C lower than the ambient temperature and ≤ 25 °C. Refuge boundaries were assessed by sweeping the probe from side to side within five centimeters from the stream bottom. Ambient water temperature was measured in the mainstem channel just upstream of the refuge mixing zone. After delineating the refuge boundaries, we visually estimated the surface area of the refuge to determine if it met the minimum size criteria of ≥ 1 m². Additionally, we used the temperature probe to investigate other areas in the near vicinity of the original refuge (< 200 m) that had similar geomorphic characteristics to other cold-water refuges (e.g., alcoves, small side channels, downstream edges of large gravel bars, and deep pools), but that were not detected in the FLIR data.

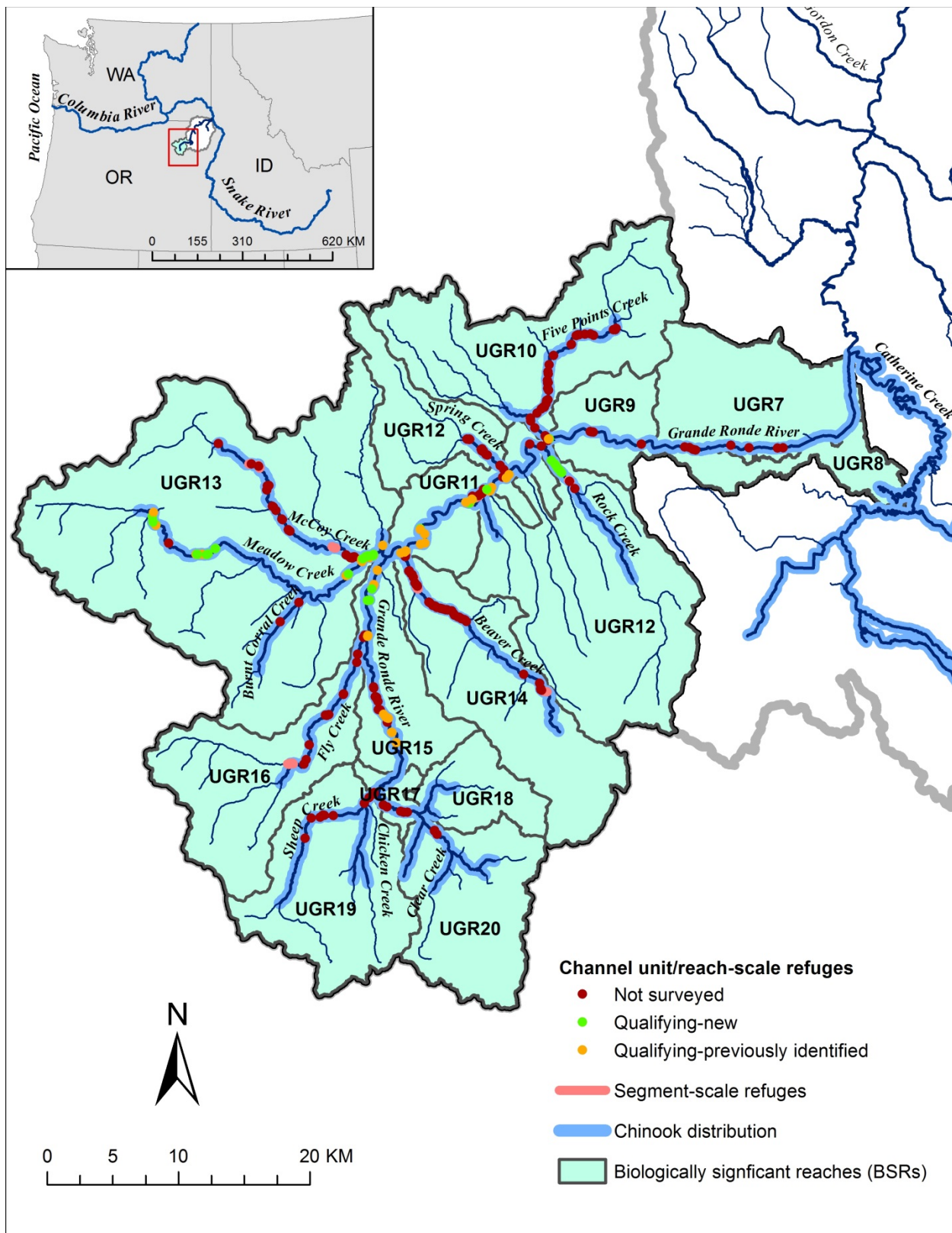
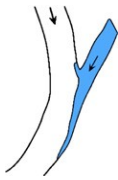
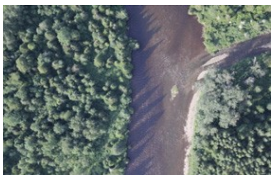
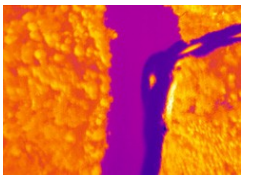
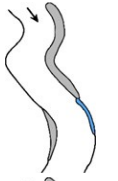
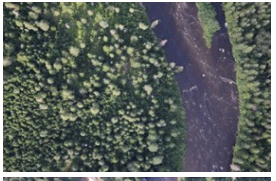
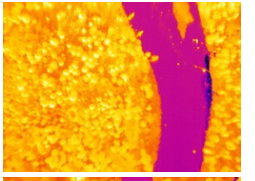

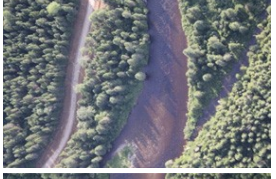
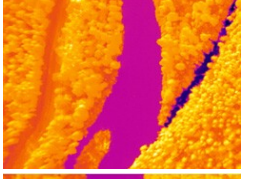
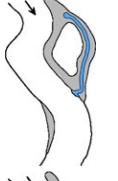
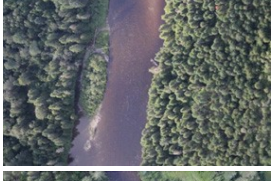
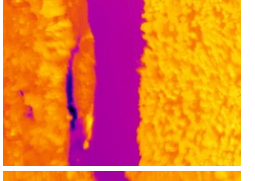
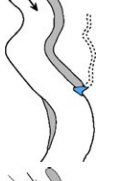
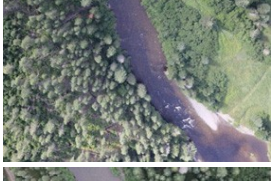
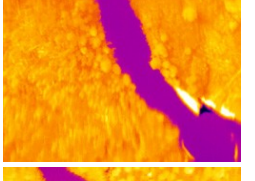


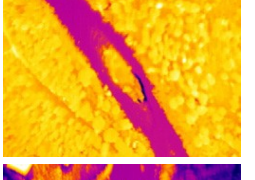
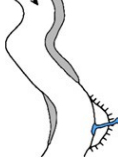

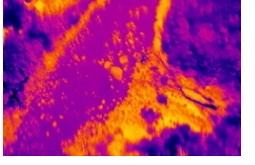


Figure 6. Study area in the Upper Grande Ronde River basin in northeast Oregon showing the location of cold-water refuges identified from Forward Looking Infrared (FLIR) in 2010 and subsequent field surveys in 2015.

Table 3. Descriptions and examples of cold-water refuge types (Dugdale *et al.* 2013).

Thermal refuge	Description	Schematic	Optical image example	TIR image example
Tributary confluence plume	Thermal plumes created prior to mixing where a cold tributary discharges into the main (warmer) river channel.			
Lateral seep	Elongated bank side filaments of cold water inflow observed when the active river channel intersects zones of groundwater flow (often in steep terraces or valleys).			
Springbrook	Cold-water channels flowing from springs, marshland or depressions adjacent to the channel; often associated with abandoned channels. Also includes springs within the main channel.			
Cold side channel	Cold secondary channels flowing in ephemeral flood pathways and normally completely wetted only during periods of high flow.			
Cold alcove	Zones of cold water found at the downstream edge of a bar and often associated with emergence of an abandoned channel or formed when groundwater pathways converge and accumulate in a backwater.			
Hyporheic upwelling	Resurgence of hyporheic flow from the streambed found at the downstream ends of gravel bars, mid-channel islands or in sequence with pool-riffle bedforms.			
Wall-base channel	Runoff-fed channels emerging from terraces or steep valley walls and then flowing over the immediate floodplain into the river channel.			

Potential refuges were assigned a refuge status based on whether or not they met the specified temperature and size criteria, and whether they were previously identified from FLIR data or newly observed in 2015. Refuge status designations included: (1) Qualifying-previously identified – Cold-water refuges that were previously identified from the FLIR data and met the temperature and size criteria; (2) Qualifying-new – Cold-water refuges that were newly identified in the field (i.e., were not present in FLIR data) and met the temperature and size criteria; (3) Non-qualifying – Potential refuges that were delineated from the FLIR data but did not meet the temperature and size criteria when surveyed in the field. These “false positives” may have resulted from thermal anomalies in the FLIR data resulting from shadows or moist vegetation, or from changes in channel morphology, discharge, or groundwater inputs that occurred after the FLIR data was collected; and (4) Not Surveyed – Potential cold-water refuges that were previously identified from the FLIR data but were not surveyed in the field because access was denied by landowners or because there was insufficient time to complete the surveys.

We measured a suite of physical habitat characteristics at each refuge included surface area, mean and max water depth, water velocity (not moving, slow ($> 0 - 0.1$ m/s), moderate to fast ($> 0.1 - 1.1$ m/s), or very fast (> 1.1 m/s)), mean bottom and surface water temperature, min water temperature, refuge crest depth, distance to the main channel, substrate composition, solar access percentage (i.e., percentage of solar radiation reaching the water surface), and fish cover (i.e., percentage by area containing boulders, aquatic vegetation, overhanging vegetation, woody debris, artificial structures, and undercut banks). The refuge crest was defined as the shallowest lateral cross section of the streambed within the wetted flow path connecting the refuge to the main channel. The refuge crest depth was measured at the deepest point along the refuge crest cross section. If the flow path was not continuously wetted, the refuge crest depth was recorded as zero. Further details on survey methods are provided in Appendix B of McCullough et al. (2016).

In addition to instantaneous temperature measurements taken at each refuge, we also deployed water temperature loggers (Onset Hobo Tidbit loggers) in 15 randomly selected refuges and in paired ambient mainstem locations to measure hourly water temperatures throughout the summer sampling period. Loggers within each refuge were placed at the stream bottom in a location representing the approximate mean temperature. Loggers in the main channel were placed upstream of the refuge mixing zone in a well-mixed location.

Data Analysis

We computed basic summary statistics of habitat conditions and fish use within the 99 qualifying cold-water refuges that were surveyed in 2015. In addition, we calculated a suite of temperature metrics for the 15 paired refuge and ambient sites where continuous temperature loggers were deployed including *AvgDailyMax* (average of the daily maximum temperatures), *AvgDailyMin* (average of the daily minimum temperatures), *AvgDailyAvg* (average of the daily average temperatures), *AvgDailyRange* (average of the daily range), *MWMT* (maximum weekly maximum temperature), *PctDaysOver18* (percentage of days when the daily maximum exceeded 18 °C), *PctDaysOver20* (percentage of days when the daily maximum exceeded 20 °C), and *PctDaysOver25* (percentage of days when the daily maximum exceeded 25 °C). The hourly temperature data was limited to a common time frame (July 23 – August 30) prior to calculating temperature metrics to ensure valid comparability across all sites. We

then used a paired t-test to evaluate whether temperature metrics in refuges were statistically different from ambient locations.

We calculated weighted usable area (WUA) for both Chinook Salmon and steelhead in refuges using methods similar to those used in the Physical Habitat Simulation System (PHABSIM) as described in Milhous et al. (1989) and later updated in USGS (2001). Briefly, this method utilizes habitat suitability index (HSI) curves for each fish species, life stage, and habitat variable of interest to quantify the amount of stream habitat that falls within a suitable range for each fish species. HSI curves are simple rating curves that range from zero to one, with one representing habitat conditions that are 100 % suitable and zero representing unsuitable conditions. Ideally, these suitability curves are developed using detailed field observations of micro-habitat fish use across a range of habitat conditions within the study stream of interest. However, in the absence of such data, literature-based curves from similar streams are commonly used (Bovee et al. 1998, Maret et al. 2006). Suitability index values for each habitat variable of interest are then combined into a single composite suitability index (CSI) by computing the geometric mean of the individual suitability index values ($CSI = (SI_{depth} \times SI_{velocity} \times SI_n)^{1/n}$). Finally, WUA is computed by multiplying the CSI by the total stream surface area.

Predictions of WUA in each cold-water refuge were based on suitability curves for water depth, velocity, and water temperature. We used water depth and velocity HSI curves for juvenile Chinook Salmon and steelhead developed from field studies conducted in the Pacific Northwest and Idaho as reported in Maret et al. (2006) (Figure 7 and Figure 8). We developed a water temperature HSI curve for juvenile Chinook salmon using empirical fish abundance estimates and water temperature data collected in the Upper Grande Ronde basin as described in Justice et al. (2017). Similarly, we used the water temperature/survival relationship for rainbow trout described in Bear et al. (2007) to develop a temperature HSI curve for juvenile steelhead (Figure 9). Although dissolved oxygen (DO) was not measured during our field surveys, we attempted to account for the effect of DO on suitability of refuge habitat for salmonids by applying a DO scalar based on data from Ebersole et al. (2003). Ebersole et al. (2003) found that 91 % of cold-water refuges surveyed in the Upper Grande Ronde Basin had suitable DO levels (i.e., DO > 3 ppm). Thus, we multiplied all WUA estimates by 0.91 to account for potential negative effect of low DO on habitat suitability.

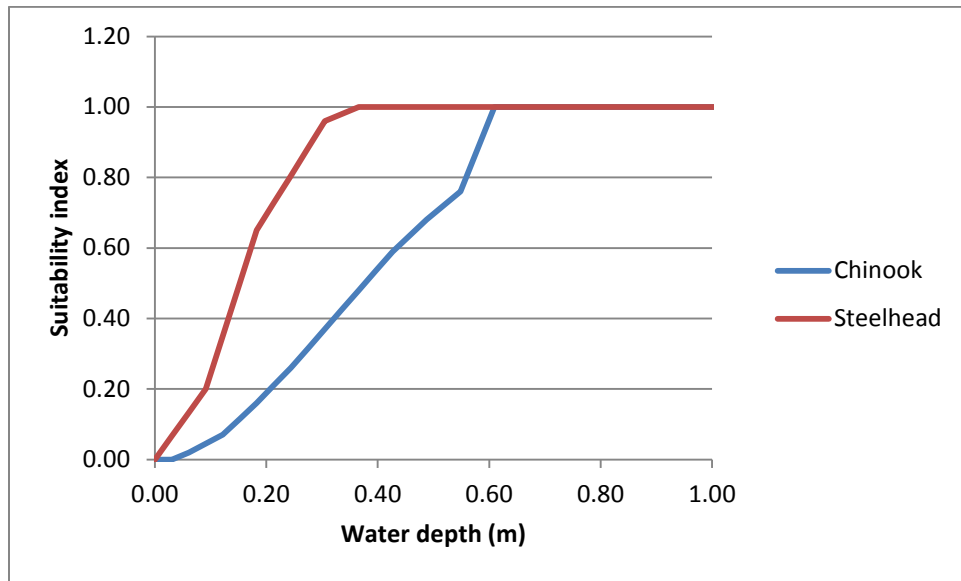


Figure 7. Water depth suitability index curves for juvenile Chinook Salmon and steelhead from Maret et al. (2006).

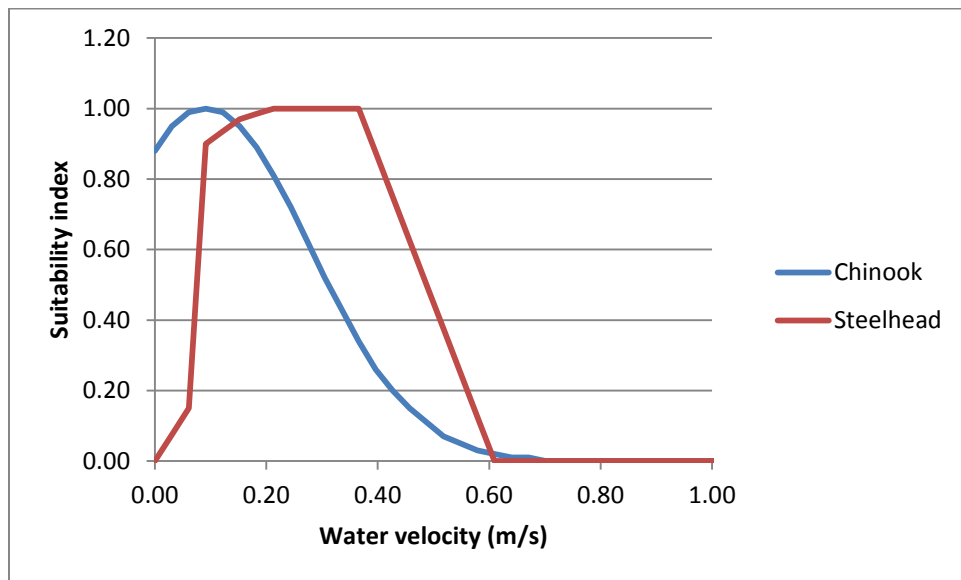


Figure 8. Water velocity suitability index curves for juvenile Chinook Salmon and steelhead from Maret et al. (2006).

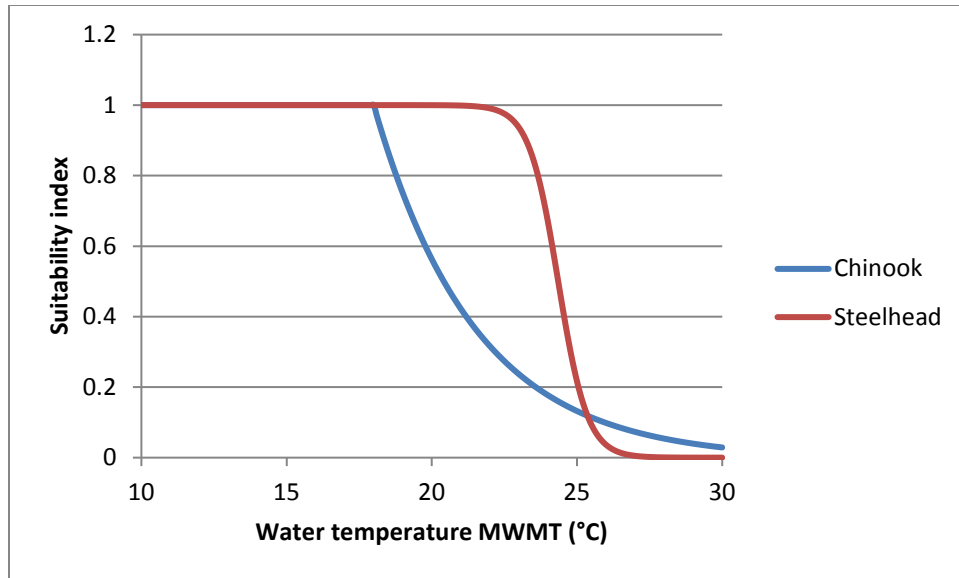


Figure 9. Water temperature suitability index curves for juvenile Chinook Salmon and steelhead from Justice et al. (2017) (Chinook) and Bear et al. (2007) (steelhead).

Field surveys were conducted for a relatively small subsample of the total number of cold-water refuges identified from the FLIR data. To estimate the total amount of refuge habitat present within the entire Upper Grande Ronde Chinook population area, we needed to account for potential refuge habitat that was not surveyed in the field. Specifically, we needed to estimate two things: 1) the area of unsurveyed refuge habitat identified from FLIR that was qualifying (i.e., met the minimum size and temperature criteria described above; termed “unsurveyed qualifying-previously identified”); and 2) the area of qualifying unsurveyed refuge habitat that was new (i.e., unsurveyed refuges that were newly created since 2010 or were not measurable in the 2010 FLIR data; termed “unsurveyed qualifying-new”). To calculate the first, we multiplied the total area of unsurveyed refuges identified from FLIR by the fraction of surveyed refuges identified from FLIR that were qualifying (0.59). To calculate the second, we multiplied the total area of unsurveyed refuges identified from FLIR by the ratio of new to previously-identified refuges (0.37). Finally, total qualifying refuge area was calculated by summing the surface area of surveyed qualifying refuges, unsurveyed qualifying-previously identified refuges, and unsurveyed qualifying-new refuges.

We used a similar method to estimate WUA for Chinook and steelhead in unsurveyed refuges. Specifically, WUA in unsurveyed refuges was calculated by multiplying the fraction of WUA in surveyed qualifying refuges out of the total surveyed qualifying refuge area by the estimated total unsurveyed qualifying refuge area. Thus, we assumed that the proportion of qualifying refuge habitat that was usable for fish would remain constant for the refuge habitat that was not surveyed in the field. Finally, we calculated total WUA by summing the WUA in surveyed and unsurveyed refuges.

We predicted rearing capacity of juvenile Chinook Salmon and steelhead within cold-water refuges by multiplying WUA in each refuge by the 95th percentile of the fish density values computed from channel unit-scale snorkel survey data collected in the Upper Grande Ronde River between 2011 and 2015 (data

downloaded from the ODFW/CRITFC snorkel database on March 10, 2016; data distributed by Chris Horn, ODFW, La Grande Fish Research). Fish density values for Chinook Salmon and steelhead used to estimate capacity were 1.6 and 1.1 fish/m² respectively.

To understand the potential contribution of cold-water refuges to the overall Chinook Salmon population in terms of fish capacity, we calculated the percentage of the total fish capacity for the population that came from refuges. To do this, we first estimated total population-level Chinook Salmon summer parr capacity using a Beverton-Holt stock recruitment function fit to the spawner and summer parr data estimated by ODFW (Brian Jonasson, La Grande Fish Research, distributed on Feb 2, 2016; Figure 10). These data included brood years 1992-1993, 2006, 2008-2013. Missing brood years were due to insufficient sample size required to estimate summer parr abundance. A detailed description of sampling and estimation methods for spawner abundance is provided in Feldhaus et al. (2017), while summer parr abundance estimation methods are described in Jonasson et al. (2015). To estimate the percentage of Chinook Salmon parr capacity from refuges, we simply divided the estimated parr capacity in refuges by the total population capacity and multiplied by 100. No attempt was made to estimate the percentage of juvenile steelhead capacity from refuges because data on total steelhead spawner and summer juvenile abundance were not available.

Despite meeting the temperature and size criteria to qualify as a cold-water refuge, many of the refuges we observed in the field were completely isolated from the main channel (i.e., refuges were not connected by flowing water to the main channel) and did not contain salmonids. It's likely that these isolated refuges would provide a less meaningful contribution to the overall population because fish residing in isolated refuges may have a reduced ability to avoid predators and access food resources in the main channel (Brewitt et al. 2017), and because dissolved oxygen concentrations in isolated refuges may be lower due to the lack of surface flow inputs. To account for this, and to provide a more conservative and probably more accurate assessment of the overall contribution of refuge habitat to the salmonid populations, we also calculated total refuge area, WUA, and parr capacity for only those refuges that contained salmonids and that had a refuge crest depth greater than 0.05 m, a depth we assumed represented a significant barrier to movement of juvenile and adult salmonids. Owing to their much larger size and apparent accessibility to salmonids as determined from evaluation of the FLIR data, we assumed that all segment-scale refuges met these criteria of having salmonids present and crest depths > 0.05 m.

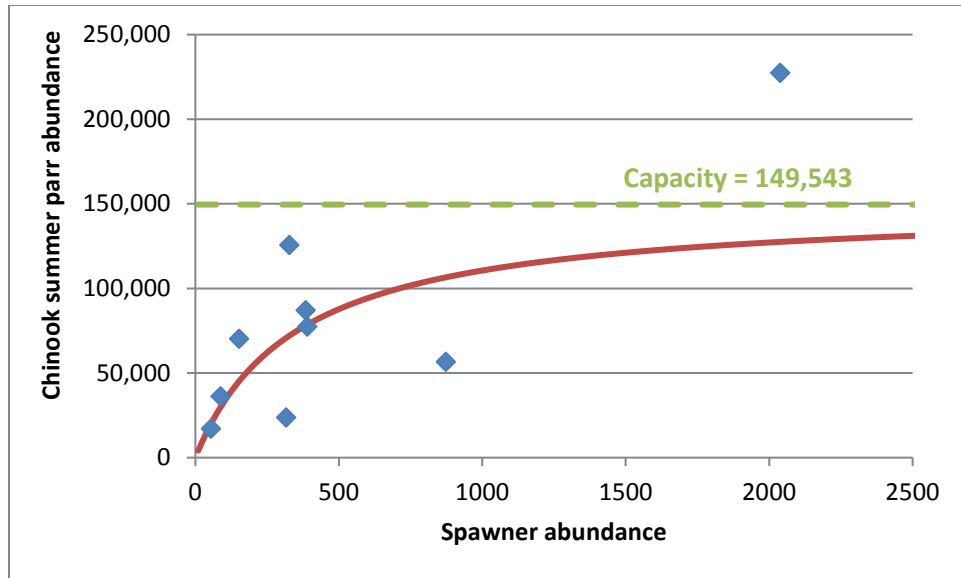


Figure 10. Relationship between spawner abundance and Chinook Salmon summer parr abundance in the Upper Grande Ronde River, brood years 1992-2013. The red line represents a Beverton-Holt curve fit to the data, and the green dashed line represents the estimated parr capacity as determined from the Beverton-Holt function.

Results and Discussion

A total of 322 channel unit-scale and 10 segment-scale cold-water refuges were identified in the Upper Grande Ronde basin using the 2010 FLIR data, totaling 18,357 m² of potential refuge habitat (Table 4). Of these, 97 refuges were surveyed in the field during the summer of 2015, with 48 determined to be non-qualifying and 49 qualifying. An additional 50 new refuges were surveyed in 2015 that were not present in the 2010 FLIR data.

Of the 99 qualifying cold-water refuges that were surveyed in the field, the majority (56.5 % by area) were classified as cold side channels (Table 5). Springbrooks were the second most common refuge type in terms of refuge area (12.3 %), followed closely by tributary confluence plumes (11.8 %). Lateral seeps represented the smallest percentage of total surveyed refuge area (3.8 %). The percentage of WUA for juvenile Chinook Salmon by refuge type closely followed the percentages by surface area (Table 5). However, the WUA results for juvenile steelhead showed a significant divergence from the aerial percentage of available refuge habitat (Table 5). For example, tributary confluence plumes represented the highest WUA for steelhead (55.8 %), but this refuge type represented only 11.8 % of the available refuge habitat. The disproportionately high WUA for steelhead in tributary confluence plumes is likely the result of higher water velocities in these refuge types (Table 6), and steelhead's corresponding preference for higher velocity habitats (Figure 8). Examples of the different refuge types surveyed in the field including photographs and descriptive information are provided in Appendix 1.

Salmonids were present in approximately 61.6 % (by area) of the cold-water refuges that were surveyed (Table 7). Approximately 24.9 % of the refuges did not have salmonids present, and salmonid presence could not be determined in the remaining 13.5 % due to poor visibility. As expected, weighted usable area for Chinook Salmon and steelhead was highest in cold-water refuges with salmonids present. For example, refuges with salmonids present accounted for approximately 60 % of the Chinook WUA and 89.4 % of the steelhead WUA (Table 7). Similarly, refuges that contained Chinook Salmon only accounted for the largest percentage of WUA for Chinook (34.1 % of the total WUA), while refuges that contained steelhead accounted for the largest percentage of WUA for steelhead (63.1 %). These intuitive results lend some credibility to the habitat suitability index curves that were used to predict WUA.

Table 4. Number and surface area (m²) of cold-water refuges identified from Forward Looking Infrared (FLIR) and field surveys in the Upper Grande Ronde River basin by refuge scale (channel unit or segment)

Refuge status	Count	Area (m ²)	Percentage	
			By count	By area
Channel unit-scale refuges				
Non-qualifying	48	2132	12.9	17.4
Not surveyed	225	5038	60.5	41.2
Qualifying-new	50	1922	13.4	15.7
Qualifying-previously identified	49	3132	13.2	25.6
Subtotal	372	12224	100.0	100.0
Segment-scale refuges				
Not surveyed	10	8055		
Total	382	20279		

Table 5. Surface area and weighted usable area (WUA) of channel unit-scale cold-water refuges surveyed in the field in 2015 by refuge type.

Refuge type	Count	Area (m ²)	Percentage		Chinook		Steelhead	
			By count	By area	WUA	%	WUA	%
Cold alcove	11	338	11.1	6.7	174	6.6	52	10.4
Cold side channel	41	2858	41.4	56.5	1427	54.0	32	6.3
Hyporheic upwelling	17	445	17.2	8.8	289	10.9	65	13.0
Lateral seep	14	191	14.1	3.8	44	1.7	29	5.8
Springbrook	3	624	3.0	12.3	456	17.2	44	8.7
Tributary confluence plume	13	598	13.1	11.8	253	9.6	281	55.8
Total	99	5054	100.0	100.0	2643	100.0	503	100.0

Table 6. Mean depth, velocity, and temperature in channel unit-scale cold-water refuges by refuge type.

Refuge Type	Count	Mean refuge depth (m)	Mean refuge velocity (m/s)	Mean refuge bottom temperature (°C)
Cold alcove	11	0.30	0.014	19.2
Cold side channel	41	0.27	0.002	17.4
Hyporheic upwelling	17	0.35	0.012	17.0
Lateral seep	14	0.12	0.018	16.9
Springbrook	3	0.31	0.033	12.8
Tributary confluence plume	13	0.20	0.108	17.5
Total	99	0.26	0.022	17.4

Table 7. Salmonid presence/absence in channel unit-scale cold-water refuges.

Salmonids present	Count	Area (m ²)	Percentage		Chinook		Steelhead	
			By count	By area	WUA	%	WUA	%
No	42	1258	42.4	24.9	638	24.1	26	5.2
Unknown	17	681	17.2	13.5	421	15.9	27	5.5
Yes	40	3115	40.4	61.6	1584	60.0	449	89.4
Chinook only	13	1489	13.1	29.5	900	34.1	119	23.7
Steelhead only	21	974	21.2	19.3	468	17.7	317	63.1
Chinook & Steelhead	4	581	4.0	11.5	187	7.1	13	2.5
Unknown	2	71	2.0	1.4	29	1.1	0	0.0
Total	99	5054	100.0	100.0	2643	100.0	503	100.0

Mean refuge bottom temperatures ranged from 9.7 to 23.3 °C (mean = 17.4 °C), while adjacent ambient temperatures ranged from 16.2 to 29.1 °C (mean = 23.2 °C) (Table 8). On average, refuges were 5.8 °C cooler than the ambient water temperature, with temperature differences between ambient and refuges reaching as high as 12.7 °C. This is a significant difference in terms of salmonid temperature tolerance limits. For example, in portions of the Grande Ronde River where temperatures reach 25 °C, the approximate upper incipient lethal limit for Chinook Salmon, cold-water refuges may have temperatures in the 19-20 °C range, and in some cases much cooler. While temperatures in this range are not optimal for salmonid rearing, they could potentially allow fish to survive through the warmest periods of the summer.

Vertical stratification of water temperatures within refuges (i.e., the difference between the surface and bottom water temperature) was generally low, but was quite high in some rare instances. The mean vertical temperature difference (surface – bottom) ranged from 0 to 10.7 °C (mean = 1.4 °C; Table 8) and tended to be highest in cold alcoves and lowest in springbrooks. The majority of refuges (75 %) had vertical temperature differences less than 1.9 °C.

A comparison of hourly water temperatures from July 23 to August 30 measured in 15 cold-water refuges and adjacent ambient mainstem sites showed consistently lower water temperatures in refuges compared with ambient locations (Figures 6 and 7). With the exception of the average daily minimum,

all temperature metrics computed from the hourly temperature measurements were significantly lower in refuges compared with ambient mainstem locations ($p < 0.001$; Table 9). In addition, the daily temperature range in refuges varied considerably across sites. For example, water temperatures in some refuges were almost constant throughout the measurement period, with daily ranges as low as 0.1 °C (Figure 12, 119), while daily ranges were considerably higher (up to 7 °C) at other refuges. The magnitude of variation in hourly refuge temperatures at refuges did not appear to be consistently related to refuge type (i.e., cold alcove, cold side channel, tributary confluence plume).

With the exception of having cooler water temperatures than the ambient mainstem channel, physical habitat conditions for salmonids were generally poor among the 99 cold-water refuges surveyed in 2015. The majority of refuges (75 %) had water depths less than 0.3 meters (Table 8). According to the depth suitability curve from Maret et al. (2006) (Figure 7), a depth of 0.3 m is suboptimal for rearing juvenile Chinook Salmon, while depths above 0.6 meters are preferred. Similarly, water velocities in refuges were very low, averaging 0 m/s, with the majority of refuges (75 %) having velocities below 0.1 m/s. Slow flowing water is most problematic for juvenile steelhead according to the velocity suitability index curves from Maret et al. (2006) (Figure 8), although flowing water is critically important for most riverine fish species and stream ecosystems in general because it delivers food resources and nutrients from upstream, increases dissolved oxygen levels, and controls the distribution of substrate particles on the stream bottom, among other things.

Refuge crest depth, which indicates the minimum depth that fish would encounter along the flow path between the refuge and the main channel, ranged from 0 to 0.5 m (mean = 0.1 m). Approximately 68 % of the surveyed refuges had refuge crest depths < 0.05 m, and 31 % of refuges had a crest depth of 0, meaning they were completely isolated from the main channel. While some fish may be able to survive for limited periods of time in isolated refuge habitats, the lack of connectivity to the main channel presents a host of challenges for salmonids including limited ability to access food resources in the main channel (Brewitt et al. 2017), reduced dissolved oxygen concentration, and reduced ability to avoid predators.

Fine sediment (< 2 mm) concentrations on the stream bottom was moderate to high in cold-water refuges, with fine sediment levels averaging 37 % and ranging as high as 100 % (Table 8). In a study of fine sediment impacts on rearing juvenile salmonids in a northern California river, Suttle et al. (2004) found that increasing concentrations of fine sediment impaired growth and survival of juvenile steelhead trout and reduced macroinvertebrate prey availability. In addition, they found no threshold level of fine sediment below which fine-sediment had no effect on salmonid growth and survival. Fine sediment concentrations tended to be highest in isolated refuges with little or no streamflow and lowest in refuges that were in or directly adjacent to the main channel, such as tributary confluence plumes.

Table 8. Physical habitat characteristics measured at 99 channel unit-scale cold-water refuges in the Upper Grande Ronde River basin during the summer of 2015.

Habitat metric	min	max	mean	Percentile		
				25 th	50 th	75 th
Refuge surface area (m ²)	1.9	502.0	51.0	9.2	23.8	49.9
Mean refuge depth (m)	0.0	0.9	0.3	0.1	0.2	0.3
Max refuge depth (m)	0.1	1.1	0.4	0.3	0.4	0.5
Mean water velocity (m/s)	0.0	0.3	0.0	0.0	0.0	0.1
Mean refuge bottom temperature (°C)	9.7	23.3	17.4	15.6	17.1	19.3
Mean refuge surface temperature (°C)	9.8	25.3	18.7	16.3	18.8	21.5
Mean refuge vertical temp. diff. (°C) (surface - bottom)	0.0	10.7	1.4	0.2	0.9	1.9
Min refuge temperature (°C)	10.0	22.3	15.5	13.4	15.5	17.4
Ambient temperature (°C)	16.2	29.1	23.2	21.2	23.4	25.3
Mean temp. diff. (ambient - mean refuge bottom)	0.8	12.7	5.8	3.8	5.5	7.3
Max temp. diff. (ambient - min refuge)	2.1	15.4	7.7	5.2	7.1	9.8
Refuge crest depth (m)	0.0	0.5	0.1	0.0	0.1	0.1
Distance to main channel (m)	0.0	100.0	11.9	0.0	1.0	9.5
Sand and fines < 2 mm (%)	0.0	100.0	37.3	15.0	30.0	60.0
Solar access (%)	12.0	100.0	66.5	45.5	72.0	91.0
Total fish cover (%)	0.0	125.0	53.8	20.8	50.2	85.0
Boulders (%)	0.0	30.0	3.0	0.0	0.0	5.0
Aquatic vegetation (%)	0.0	100.0	34.7	0.0	15.0	72.5
Overhanging vegetation (%)	0.0	75.0	7.4	0.0	5.0	10.0
Woody debris (%)	0.0	65.0	6.7	0.0	0.0	5.0
Artificial structures (%)	0.0	5.0	0.1	0.0	0.0	0.0
Undercut banks (%)	0.0	43.7	1.8	0.0	0.0	0.5

Table 9. Summary statistics of hourly temperature data collected between July 23 and August 30, 2015 at 15 paired refuge and ambient river locations.

Metric	Ambient			Refuge			Difference (Ambient - Refuge)		
	Min	Max	Avg.	Min	Max	Avg.	Avg.	t Stat	p-value
<i>AvgDailyMax</i>	21.4	25.5	24.0	11.5	21.1	16.9	7.1	13.0	1.6E-09
<i>AvgDailyMin</i>	12.4	15.5	13.8	9.3	15.7	13.2	0.7	1.8	0.09*
<i>AvgDailyAvg</i>	16.9	20.2	18.7	11.4	17.4	14.9	3.7	9.0	1.6E-07
<i>AvgDailyRange</i>	8.5	11.6	10.2	0.1	7.0	3.7	6.5	14.3	4.7E-10
<i>MWMT</i>	23.5	28.4	26.5	11.8	22.3	18.0	8.5	13.4	1.1E-09
<i>PctDaysOver18</i>	94.9	100.0	97.3	0.0	97.4	44.8	52.5	4.9	1.1E-04
<i>PctDaysOver20</i>	79.5	97.4	92.5	0.0	84.6	16.8	75.7	12.2	3.8E-09
<i>PctDaysOver25</i>	2.6	64.1	39.5	0.0	0.0	0.0	39.5	7.1	2.6E-06

* Based on two-tailed critical t value; all other tests based on one-tailed critical t value.

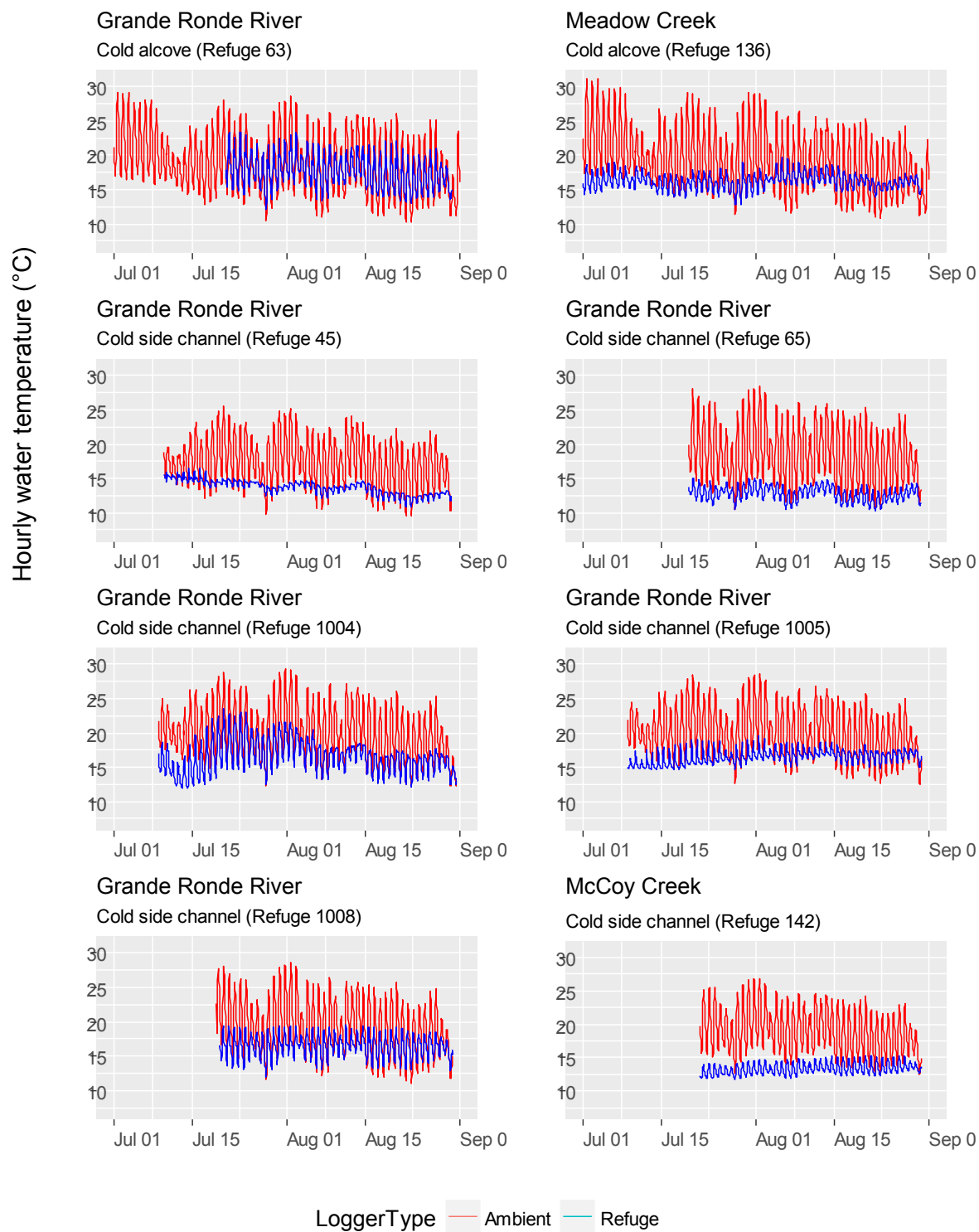


Figure 11. Hourly water temperature in 15 cold-water refuges and adjacent ambient mainstem sites in the Upper Grande Ronde River basin.

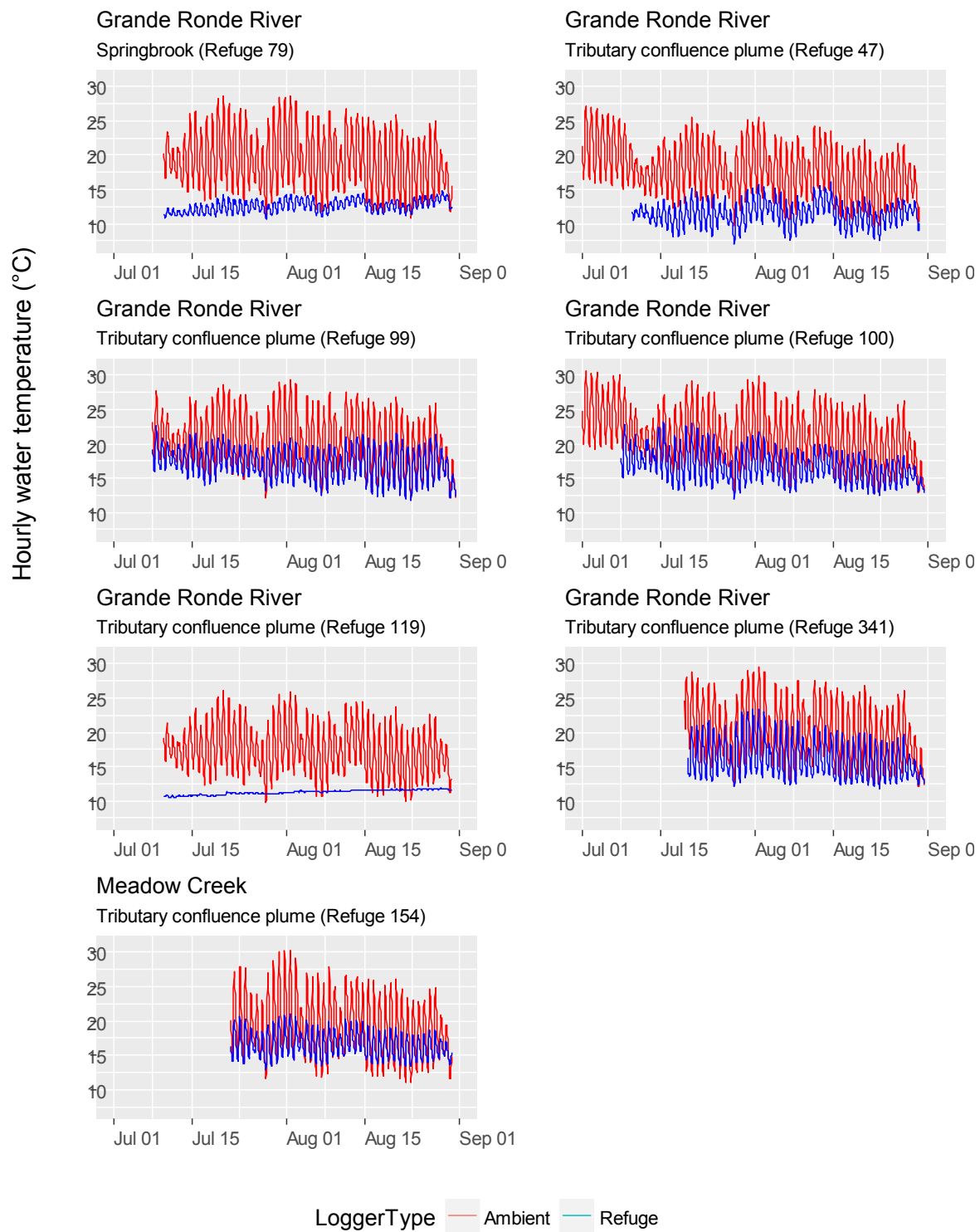


Figure 12. Hourly water temperature in 15 cold-water refuges and adjacent ambient mainstem sites in the Upper Grande Ronde River basin.

Solar access, or the percentage of solar radiation that reached the stream surface, ranged from 12 to 100 % (mean = 66.5 %) (Table 8). The complement of solar access is effective shade (i.e., effective shade = 100 – solar access). Thus, cold-water refuges averaged only 33.5 % shade, which is low compared with the more densely forested upper portions of the Grande Ronde River basin where effective shade typically ranged from 50-75 % (Watershed Sciences 2012). Higher levels of shade at refuge locations would be desirable to improve and maintain thermal benefits to fish, provide cover from avian predators, and provide a source of terrestrial invertebrate prey to fish.

Total fish cover in cold-water refuges ranged from 0 to 125 % (mean = 53.8 %) (Table 8). Values exceeding 100 % were due to overlapping cover elements (e.g., woody debris overlapped by overhanging vegetation). While an average cover value of 53.8 % sounds pretty good from a fish's perspective, the vast majority of this cover was attributed to aquatic vegetation (i.e., 34.7 % of the total cover). In some cases, aquatic vegetation provides useful cover to fish. However, in many cases, aquatic vegetation is largely composed of filamentous algae and other types of blue-green algae, which are often an indicator of impaired river conditions including low stream flow, high amounts of solar radiation, and in some cases, high nutrient inputs. If we consider only those cover elements that are most beneficial to juvenile salmonids (i.e., boulders, overhanging vegetation, woody debris, and undercut banks), then fish cover in refuges would average approximately 18.9 %. While not insignificant, this level of cover could be improved at refuges in order to provide additional shade and cover from predators.

Cold-water refuge area across the entire Upper Grande Ronde Chinook distribution area totaled 17,945 m², of which 9,890 (55 %) came from channel unit-scale refuges and 8,055 m² (45 %) came from segment-scale refuges (Table 10). Weighted usable area (WUA) for juvenile Chinook Salmon in refuges was estimated at 9,384 m², with the majority (55 %) coming from channel unit-scale refuges. Steelhead WUA totaled 1,785 m², with 55 % coming from channel unit-scale refuges. We estimated that channel unit- and segment-scale refuges combined could support a maximum capacity of 14,891 Chinook Salmon parr and 1,980 juvenile steelhead. The considerably higher predicted capacity for Chinook Salmon compared with steelhead in refuges was due primarily to very slow water velocities in most refuges and steelhead's comparatively lower preference for low-velocity habitat (Figure 8). Chinook Salmon capacity in refuges represented approximately 10 % of the total estimated Chinook Salmon parr capacity for the Upper Grande Ronde population, with 5.5 % coming from channel unit-scale refuges, and 4.5 % coming from segment-scale refuges.

Total area of cold-water refuges with salmonids present and having refuge crest depths > 0.05 m was estimated at 10,552 m² (Table 10). Chinook Salmon and steelhead WUA in these refuges totaled 5,313 and 1,468 m², respectively. Predicted Chinook parr capacity in these refuges was 8,431, while juvenile steelhead capacity totaled 1,628. Overall, these non-isolated refuge habitats accounted for approximately 5.6 % of the total Chinook Salmon parr capacity in the Upper Grande Ronde basin.

Cold-water refuge habitat was most abundant in biologically significant reach (BSR) UGR13 (Meadow Creek; Table 11), which contained approximately 4,747 m² of total refuge habitat, 2,675 m² of WUA for Chinook, and 480 m² of WUA for steelhead. Reaches UGR11 (mainstem Grande Ronde River between

Meadow Creek and Five Points Creek), and UGR16 (Fly Creek) contained the second and third most refuge habitat, with refuge area totaling 3,916 and 3,023 m², respectively. Reaches UGR14 (Beaver Creek) and UGR12 (Rock Creek and Spring Creek) also contained a substantial amount of cold-water refuge habitat (total refuge area = 2,932 and 1,507 m², respectively). These top five BSRs were predicted to contribute approximately 9 % of the total Chinook Salmon parr capacity for the Upper Grande Ronde basin. Detailed maps showing the locations of cold-water refuges within each of the Upper Grande Ronde BSRs is provided in Appendix 2.

After filtering out refuges that didn't contain salmonids and had refuge crest depths < 0.05 m, UGR16 was estimated to contain the largest amount of cold-water refuge habitat among all of the Upper Grande Ronde BSRs (total refuge area = 2,751 m²; Table 10). Reaches UGR13 and UGR14 (Beaver Creek) contained the next highest refuge area (total refuge area = 2,384 and 2,271 m², respectively), followed by UGR11 (refuge area = 1,656 m²) and UGR12 (refuge area = 924 m²). These five BSRs contributed to approximately 5.4 % of the total Chinook Salmon parr capacity.

All supporting data referenced in this report is available upon request from CRITFC including FLIR data, ArcGIS files showing delineated cold-water refuge boundaries and midpoint locations, field survey data, and analysis files. In addition, we've provided basic information for all qualifying refuges such as refuge ID, type, status, and location in Appendix 3.

Table 10. Total refuge area, weighted usable area (WUA) and capacity for Chinook Salmon parr and juvenile steelhead in refuges, and percentage of total Chinook parr capacity from refuges for channel unit-scale refuges, segment-scale refuges, and all refuges combined. Results are shown for all qualifying refuges and for refuges limited to those with salmonids present and having refuge crest depth > 0.05m.

Refuge area and fish capacity estimates	Channel unit-scale refuges	Segment-scale refuges	All Refuges
<i>All qualifying refuges</i>			
Total refuge area (m ²)	9890	8055	17945
WUA Chinook (m ²)	5172	4212	9384
WUA steelhead (m ²)	984	801	1785
Chinook parr capacity	8207	6684	14891
Steelhead juvenile capacity	1091	889	1980
Percentage of total population Chinook parr capacity	5.5	4.5	10.0
<i>Refuges with salmonids present and refuge crest depth > 0.05 m</i>			
Total refuge area (m ²)	2497	8055	10552
WUA Chinook (m ²)	1101	4212	5313
WUA steelhead (m ²)	667	801	1468
Chinook parr capacity	1747	6684	8431
Steelhead juvenile capacity	739	889	1628
Percentage of total population Chinook parr capacity	1.2	4.5	5.6

Note: All segment-scale refuges were assumed to have salmonids present and refuge crest depths > 0.05 m.

Table 11. Total refuge area, weighted usable area (WUA) and capacity for Chinook Salmon parr and juvenile steelhead in refuges, and percentage of total Chinook parr capacity from refuges grouped by biologically significant reach (BSR). Results are shown for all qualifying refuges and for refuges limited to those with salmonids present and having refuge crest depth > 0.05m.

BSR	Refuge area (m ²)	WUA Chinook (m ²)	WUA Steelhead (m ²)	Chinook parr capacity	Steelhead parr capacity	% of total Chinook capacity
<i>All qualifying refuges</i>						
UGR13	4747	2675	480	4244	532	2.8
UGR11	3916	1919	367	3046	408	2.0
UGR16	3023	1574	307	2497	340	1.7
UGR14	2932	1533	288	2433	320	1.6
UGR12	1507	810	121	1285	134	0.9
UGR10	716	374	71	594	79	0.4
UGR15	467	182	85	288	95	0.2
UGR9	285	134	31	213	34	0.1
UGR7	151	79	15	126	17	0.1
UGR19	121	64	12	101	13	0.1
UGR17	66	34	7	55	7	0.0
UGR20	12	6	1	10	1	0.0
Total	17945	9384	1785	14891	1980	10.0
<i>Refuges with salmonids present and refuge crest depth > 0.05 m</i>						
UGR16	2751	1432	287	2273	318	1.5
UGR13	2384	1205	338	1912	375	1.3
UGR14	2271	1170	261	1857	290	1.2
UGR11	1656	793	316	1258	351	0.8
UGR12	924	480	105	762	117	0.5
UGR15	203	86	66	137	73	0.1
UGR10	181	80	48	126	54	0.1
UGR9	94	29	23	45	25	0.0
UGR7	38	17	10	27	11	0.0
UGR19	31	14	8	21	9	0.0
UGR17	17	7	4	12	5	0.0
UGR20	3	1	1	2	1	0.0
Total	10552	5313	1468	8431	1628	5.6

Note: Data were sorted in descending order by Chinook parr capacity to aid in interpretation of the results.

Summary

This study provides a baseline summary of the quantity, spatial distribution, physical habitat conditions, and fish use of cold-water refuges in the Upper Grande Ronde River basin. Overall, we found that cold-water refuges were widespread throughout the Upper Grande Ronde River Chinook Salmon distribution area, with BSRs UGR13 (Meadow Creek), UGR11 (mainstem Grande Ronde River between Meadow Creek and Five Points Creek), and UGR16 (Fly Creek) containing the largest surface area of refuge habitat. Of the various refuge types, cold side channels were by far the most abundant. Despite having significantly cooler water temperatures than the ambient mainstem river, habitat conditions in cold-water refuges were generally poor, with the majority of refuges having shallow depths, very low water velocity, relatively little shade and cover for fish, and moderate to high levels of fine sediment. In addition, only 41 % of the total predicted cold-water refuge area contained salmonids and had refuge crest depths > 0.05 m, indicating that a large proportion of the refuges were isolated from the main channel during base flow conditions when water temperatures were at their peak. These isolated refuges could prevent fish from accessing much needed food resources in the main channel (Brewitt et al. 2017), and could exacerbate problems with predation and low dissolved oxygen. However, this study was conducted in 2015, when streamflow was at historically low levels throughout the Pacific Northwest region. It's likely that the quantity and connectivity of refuge habitats would change substantially under different baseflow conditions (Dugdale et al. 2013) and in response to restoration actions and natural channel change. As such, additional FLIR and field validation surveys in different flow years could be informative for improving our understanding of the distribution and frequency of cold-water refuge habitats in the Grande Ronde basin.

We predicted that cold-water refuges could support a maximum of 14,891 Chinook Salmon summer parr, and 1,980 juvenile steelhead. This represents approximately 10 % of the total estimated Chinook Salmon parr capacity for the Upper Grande Ronde Spring Chinook population. If we consider only refuges that were connected to the main channel (i.e., had refuge crest depths > 0.05 m) and contained salmonids, the predicted refuge capacity for Chinook parr and juvenile steelhead was 8,431 and 1,628, respectively. This equates to 5.6 % of the total Chinook Salmon parr capacity. These capacity estimates represent a model-based prediction of potential fish abundance in refuges based largely on literature-derived habitat suitability curves. These estimates could be improved in the future by obtaining empirical estimates of fish abundance in cold-water refuges, and/or by developing habitat suitability curves using in-basin empirical data. That said, these results represent a reasonable estimate of fish capacity in refuges using the best available data, and highlight the important contribution of cold-water refuges to the overall salmon and steelhead populations in the Upper Grande Ronde basin.

The relatively poor habitat conditions in cold-water refuges as well as their limited connectivity to the main channel indicate the need and opportunity for land owners and natural resource managers to improve these vital refuge habitats. Increasing riparian vegetation cover at refuge sites would be a cost-effective way to enhance the thermal benefits of cold-water refuges for fish, increase cover from avian predators, and possibly improve food resources for fish by increasing inputs of allochthonous organic matter and terrestrial invertebrates. Vegetation enhancement could also stabilize streambanks at refuge sites and potentially reduce fine sediment inputs to the stream channel. Many refuge habitats could also

benefit from addition of large woody debris (LWD) and other instream cover elements for fish. While the connectivity or size of refuges could be directly improved by restoration practitioners using heavy machinery or other means (Kurylyk et al. 2014), such actions have the potential to disrupt hyporheic flow paths and other geomorphic process that created the refuges in the first place. As such, direct manipulation of cold-water refuge connectivity should be implemented with careful consideration of the geomorphic context and hyporheic/groundwater dynamics at the refuge. Alternatively, a more broad-scale holistic approach to stream restoration which focusses on improving floodplain and hyporheic connectivity and fostering healthy riparian ecosystems throughout the stream network, should provide more abundant and more flow-connected refugia over the long term.

Given the threat that climate change and associated warming of rivers poses to fish populations in the Pacific Northwest (Beechie et al. 2013) and across North America (Lynch et al. 2016), cold-water refugia will play an increasingly important role in preserving the viability of threatened fish populations. These results provide managers with a baseline understanding of the spatial distribution, physical habitat characteristics, and potential fish use of cold-water refuges in the Upper Grande Ronde Basin than can be used to help direct future restoration priorities and other research questions.

References

- Bear, E. A., T. E. McMahon, and A. V. Zale. 2007. Comparative Thermal Requirements of Westslope Cutthroat Trout and Rainbow Trout: Implications for Species Interactions and Development of Thermal Protection Standards. *Transactions of the American Fisheries Society* 136(4):1113–1121.
- Beechie, T., H. Imaki, J. Greene, A. Wade, H. Wu, G. Pess, P. Roni, J. Kimball, J. Stanford, P. Kiffney, and N. Mantua. 2013. Restoring salmon habitat for a changing climate. *River Research and Applications* 29: 939-960.
- Bovee, K. D., B. L. Lamb, C. B. Stalnaker, J. Taylor, and J. Henriksen. 1998. Stream habitat analysis using the instream flow incremental methodology. Page 131. U.S. Geological Survey, Biological Resources Division Information and Technology Report USGS/BRD-1998-0004.
- Brewitt, K. S., E. M. Danner, and J. W. Moore. 2017. Hot eats and cool creeks: juvenile Pacific salmonids use mainstem prey while in thermal refuges. *Canadian Journal of Fisheries and Aquatic Sciences*.
- Dugdale, S. J., N. E. Bergeron, and A. St-Hilaire. 2013. Temporal variability of thermal refuges and water temperature patterns in an Atlantic salmon river. *Remote Sensing of Environment* 136:358–373.
- Ebersole, J. L., W. J. Liss, and C. A. Frissell. 2003. Thermal heterogeneity, stream channel morphology, and salmonid abundance in northeastern Oregon streams. *Canadian Journal of Fisheries and Aquatic Sciences* 60:1266–1280.
- Feldhaus, J. W., T. L. Hoffnagle, D. L. Eddy, and K. N. Ressel. 2017. Lower Snake River compensation plan: Oregon spring Chinook Salmon evaluation studies 2014 annual progress report. Page 68. Oregon Department of Fish and Wildlife, Salem, OR.
- Jonasson, B. ., E. Sedell, S. K. Banks, A. B. Garner, C. Horn, K. L. Bliesner, J. W. Dowdy, F. W. Drake, S. D. Favrot, J. M. Hay, N. A. McConnell, J. P. Ophoff, B. C. Power, J. R. Ruzycski, and R. W. Carmichael. 2015. Investigations into the life history of naturally produced spring Chinook Salmon and summer steelhead in the Grande Ronde River Subbasin. Page 88. Oregon Department of Fish and Wildlife, Annual Report 2014 BPA Project # 1992-026-04, La Grande, OR.
- Justice, C., S. M. White, D. A. McCullough, D. S. Graves, and M. R. Blanchard. 2017. Can stream and riparian restoration offset climate change impacts to salmon populations? *Journal of Environmental Management* 188:212–227.
- Kurylyk, B. L., K. T. B. MacQuarrie, T. Linnansaari, R. A. Cunjak, and R. A. Curry. 2014. Preserving, augmenting, and creating cold-water thermal refugia in rivers: concepts derived from research on the Miramichi River, New Brunswick (Canada). *Ecohydrology* 8(6):1095–1108.
- Lynch, A. J., B. J. E. Myers, C. Chu, L. A. Eby, J. A. Falke, R. P. Kovach, T. J. Krabbenhoft, T. J. Kwak, J. Lyons, C. P. Paukert, and J. E. Whitney. 2016. Climate Change Effects on North American Inland Fish Populations and Assemblages. *Fisheries* 41(7):346–361.

- Maret, T. R., J. E. Hortness, and D. S. Ott. 2006. Instream flow characterization of upper Salmon River Basin streams, central Idaho, 2005. Page 110. U.S. Geological Survey, Department of the Interior, 2006–5230.
- McCullough, D. A., S. White, C. Justice, M. Blanchard, R. Lessard, D. Kelsey, D. Graves, and J. Nowinski. 2016. Assessing the status and trends of spring Chinook habitat in the Upper Grande Ronde River and Catherine Creek. Page 123. Columbia River Inter-Tribal Fish Commission, BPA Project # 2009-004-00, Portland, OR.
- Milhous, R. T., M. A. Updike, and D. M. Schneider. 1989. Physical habitat simulation system reference manual: version II. Page 403. U.S. Fish and Wildlife Service, Volume 89, Issue 16, Washington, DC.
- Suttle, K. B., M. E. Power, J. M. Levine, and C. McNeely. 2004. How fine sediment in riverbeds impairs growth and survival of juvenile salmonids. *Ecological Applications* 14(4):969–974.
- Sutton, R. J., M. L. Deas, S. K. Tanaka, T. Soto, and R. A. Corum. 2007. Salmonid observations at a Klamath River thermal refuge under various hydrological and meteorological conditions. *River Research and Applications* 23(7):775–785.
- Tate, K. W., D. L. Lancaster, and D. F. Lile. 2007. Assessment of thermal stratification within stream pools as a mechanism to provide refugia for native trout in hot, arid rangelands. *Environmental Monitoring and Assessment* 124(1-3):289–300.
- Torgersen, C. E., D. M. Price, H. W. Li, and B. A. McIntosh. 1999. Multiscale thermal refugia and stream habitat associations of chinook salmon in northeastern Oregon. *Ecological Applications* 9(1):301–319.
- Torgersen, C. E., J. L. Ebersole, and D. M. Keenan. 2012. Primer for identifying cold-water refuges to protect and restore thermal diversity in riverine landscapes. U.S. Environmental Protection Agency, Seattle, Washington. 78 p.
- USGS (U.S. Geological Survey). 2001. PHABSIM for Windows: User’s manual and exercises. Page 288. U.S. Department of Interior, U.S. Geological Survey, Midcontinent Ecological Science Center, Open File Report 01-340.
- Watershed Sciences, Inc.. 2010. Airborne thermal infrared remote sensing, Upper Grande Ronde River Basin, Oregon. Prepared for the Columbia River Inter-Tribal Fish Commission. Watershed Sciences, Inc., Corvallis, OR.
- Watershed Sciences, Inc.. 2012. Upper Grande Ronde River Basin stream temperature model expansion. Prepared for the Columbia River Inter-Tribal Fish Commission. Watershed Sciences, Inc., Portland, Oregon.

Appendix 1 – Examples of Refuge Types

Cold Alcoves

Grande Ronde River (refuge 65):

Refuge temp = 18.6 °C, ambient temp = 26.5 °C, significant Chinook use, slow flowing water, dense aquatic vegetation, good connection to main channel.



Grande Ronde River (refuge 1039):

Refuge temp = 20.8 °C, ambient temp = 25.1 °C, salmonid use unknown, slow flowing water, very low fish cover, good connection to main channel.



Meadow Creek (refuge 1015):

Refuge temp = 14.6 °C, ambient temp = 26.2 °C, few non-salmonids present, non-flowing water, dense aquatic vegetation, good connection to main channel.



Meadow Creek (refuge 130):

Refuge temp = 20.2 °C, ambient temp = 26 °C, several steelhead present, non-flowing water, low fish cover, good connection to main channel.



Figure A1 - 1. Examples of cold alcove refuges in the Upper Grande Ronde River basin, 2015.

Cold Side Channels

Grande Ronde River (refuge 1008):

Refuge temp = 18.7 °C, ambient temp = 21 °C, abundant Chinook, descent woody debris cover, flowing water, good gravel/cobble substrate, shallow connection to main channel.



Grande Ronde River (refuge 86):

Refuge temp = 22.9 °C, ambient temp = 27.8 °C, a few non-salmonids present, non-flowing water, dense algae cover, poor connection to main channel.



Meadow Creek (refuge 1013):

Refuge temp = 20.6 °C, ambient temp = 26.7 °C, few steelhead present, shallow depth, poor cover, non-flowing water, good connection to main channel.



McCoy Creek (refuge 1027):

Refuge temp = 17.6 °C, ambient temp = 24.4 °C, salmonid presence unknown, mostly pikeminnow, non-flowing water, dense algae cover, descent connection main channel.



Figure A1 - 2. Examples of cold side channel refuges in the Upper Grande Ronde River basin, 2015.

Hyporheic Upwellings

Fly Creek (refuge 123):

Refuge temp = 16.3 °C, ambient temp = 24.5 °C, few unknown salmonids present, non-flowing water, good fish cover, poor connection to main channel.



McCoy Creek (refuge 1030):

Refuge temp = 21.3 °C, ambient temp = 23.7 °C, salmonid presence unknown, dominated by pikeminnow, slow-flowing water, low fish cover, in main channel.



Meadow Creek (refuge 1034):

Refuge temp = 17.3 °C, ambient temp = 22.5 °C, steelhead present, low fish cover, slow-flowing water, in main channel.



Rock Creek (refuge 1040):

Refuge temp = 15.9 °C, ambient temp = 20.2 °C, steelhead present, non-flowing water, minimal cover, in main channel.



Figure A1 - 3. Examples of hyporheic upwelling refuges in the Upper Grande Ronde River basin, 2015.

Lateral Seeps

Grande Ronde River (refuge 39):

Refuge temp = 15.4 °C, ambient temp = 21.7 °C, one Chinook present, non-flowing water, low/moderate fish cover, poor connection to main channel.



Grande Ronde River (refuge 46):

Refuge temp = 16.4 °C, ambient temp = 21.3 °C, no fish present, very shallow, non-flowing water, low fish cover, descent connection to main channel.



Grande Ronde River (refuge 75):

Refuge temp = 21.7 °C, ambient temp = 26 °C, abundant Chinook, slow-moving water, moderate cover from grasses and aquatic veg, narrow patch along main channel margin.



Grande Ronde River (refuge 96):

Refuge temp = 23.3 °C, ambient temp = 28.9 °C, school of 30-40 steelhead present, slow-flowing water, dense algae cover, narrow patch along main channel margin.



Figure A1 - 4. Examples of lateral seep refuges in the Upper Grande Ronde River basin, 2015.

Springbrooks

Grande Ronde River (refuge 79):

Refuge temp = 14.3 °C, ambient temp = 18.8 °C, Chinook present but mostly pikeminnow, non-flowing water, muddy substrate, dense algae cover, poor connection to main channel.



Meadow Creek (refuge 126):

Refuge temp = 9.7 °C, ambient temp = 20.4 °C, steelhead present, very shallow, slow-flowing water, good overhanging veg cover, good connection to main channel.



Meadow Creek (refuge 149):

Refuge temp = 14.3 °C, ambient temp = 23.3 °C, Chinook present in low numbers, slow-moving water, dense algae cover, good connection to main channel at lower end.



Figure A1 - 5. Examples of springbrook refuges in the Upper Grande Ronde River basin, 2015.

Tributary Confluence Plumes

Unnamed tributary confluence with Grande Ronde River (refuge 47):

Refuge temp = 11.7 °C, ambient temp = 21.0 °C, abundant Chinook, slow-moving water, good fish cover, good connection to main channel, great example of ideal refuge habitat



Beaver Creek confluence with Grande Ronde River (refuge 73):

Refuge temp = 23.1 °C, ambient temp = 25.4 °C, no fish present, moderate velocity water, low fish cover, minimal thermal refuge.



Spring Creek confluence with Grande Ronde River (refuge 99):

Refuge temp = 21.8 °C, ambient temp = 27.9 °C, steelhead present, slow-flowing water, minimal fish cover.



Dark Canyon Creek confluence with Meadow Creek (refuge 154):

Refuge temp = 19.6 °C, ambient temp = 25.4 °C, abundant Chinook and steelhead, some cover from boulders.



Figure A1 - 6. Examples of tributary confluence plume refuges in the Upper Grande Ronde River basin, 2015.

Appendix 2 – Maps of Refuges by Biologically Significant Reach (BSR)

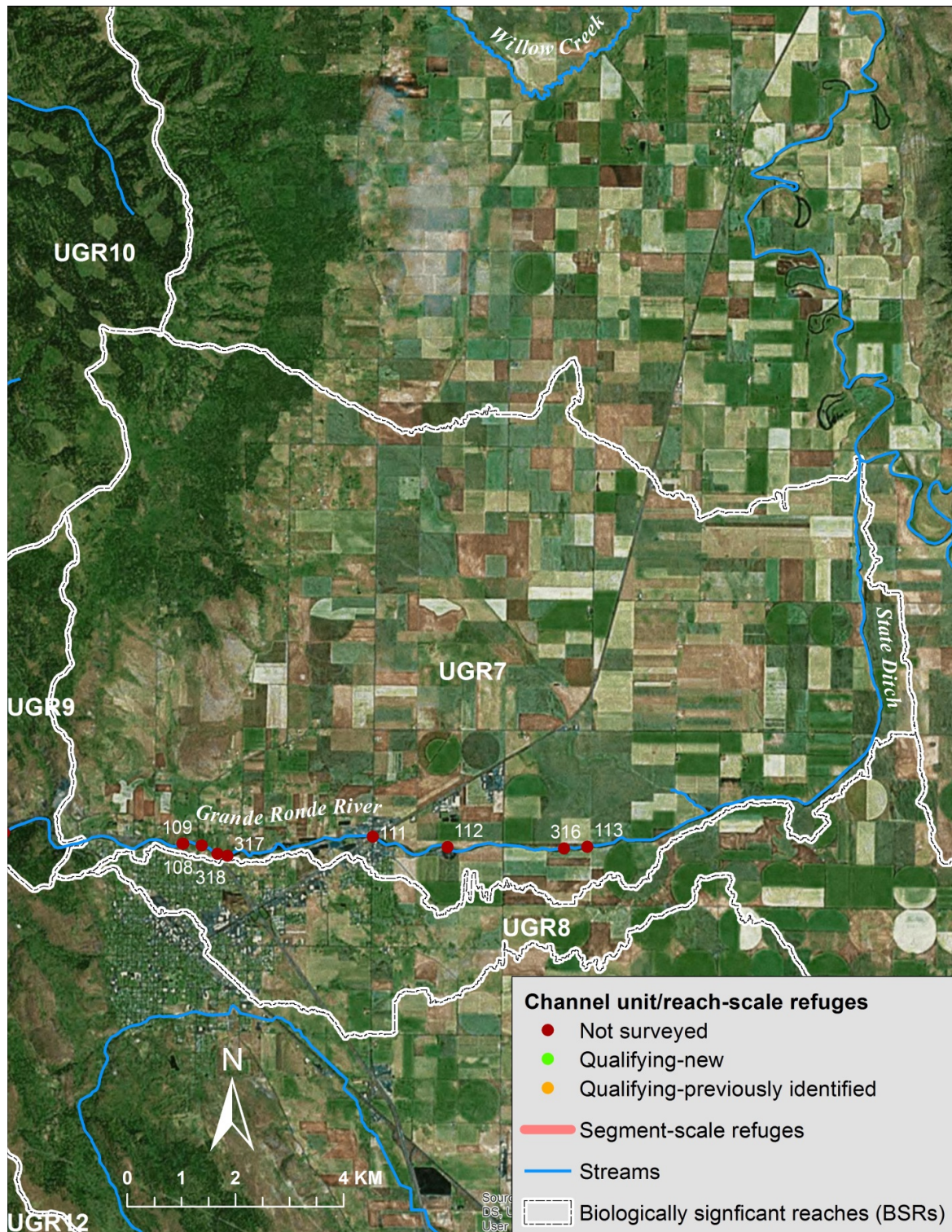


Figure A2 - 1. Map of cold-water refuges identified in biologically significant reach (BSR) UGR7.

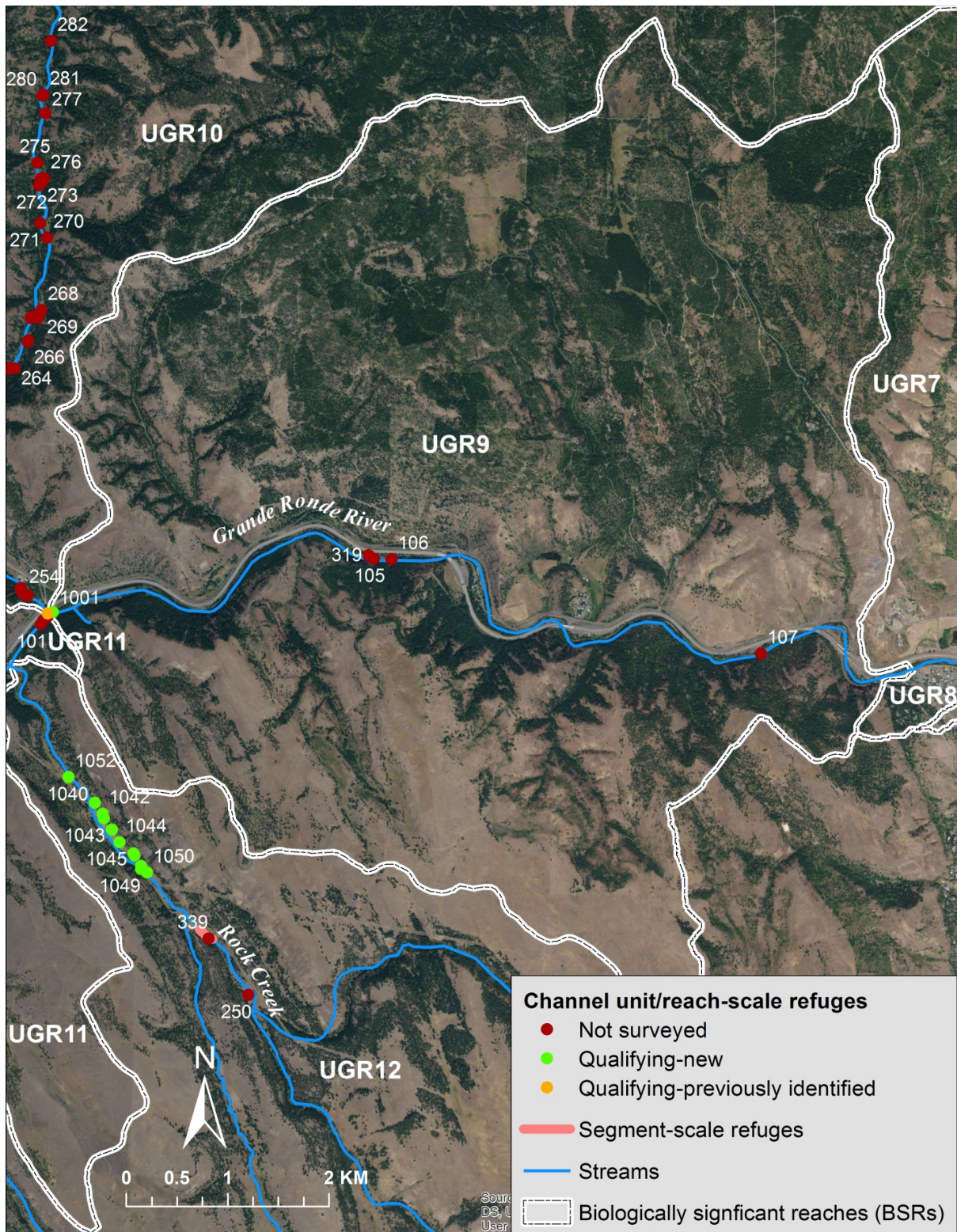


Figure A2 - 2. Map of cold-water refuges identified in biologically significant reach (BSR) UGR9.

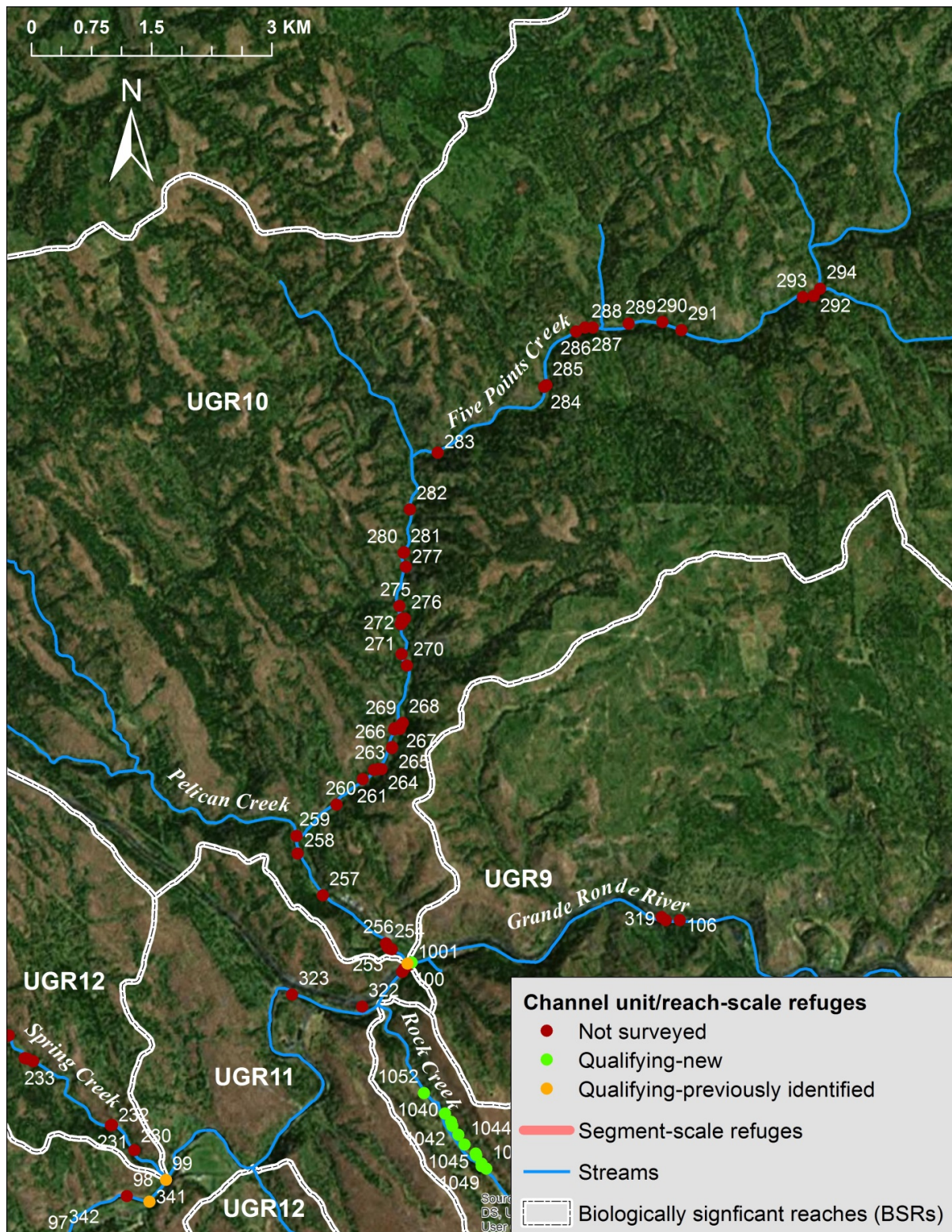


Figure A2 - 3. Map of cold-water refuges identified in biologically significant reach (BSR) UGR10.

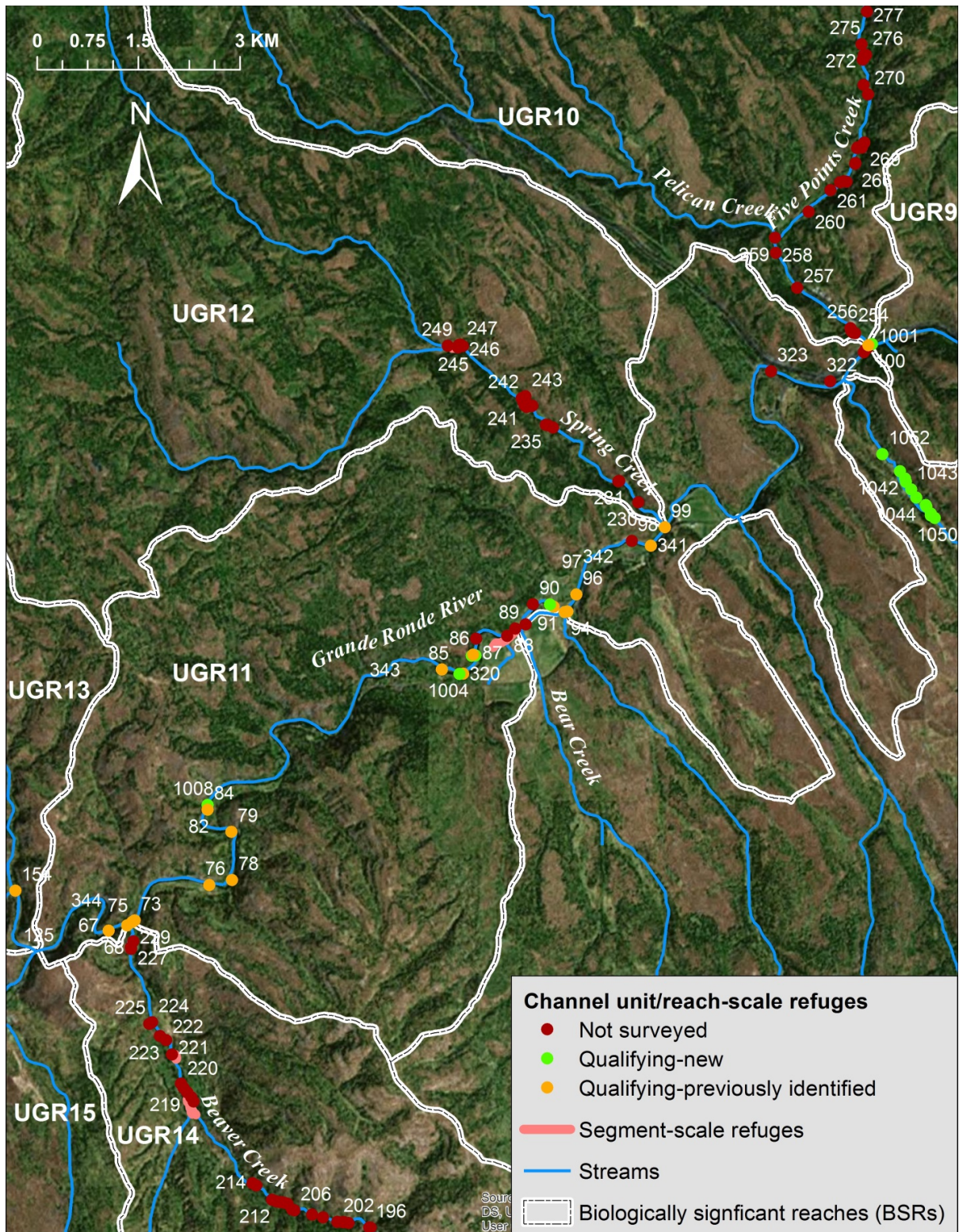


Figure A2 - 4. Map of cold-water refuges identified in biologically significant reach (BSR) UGR11.

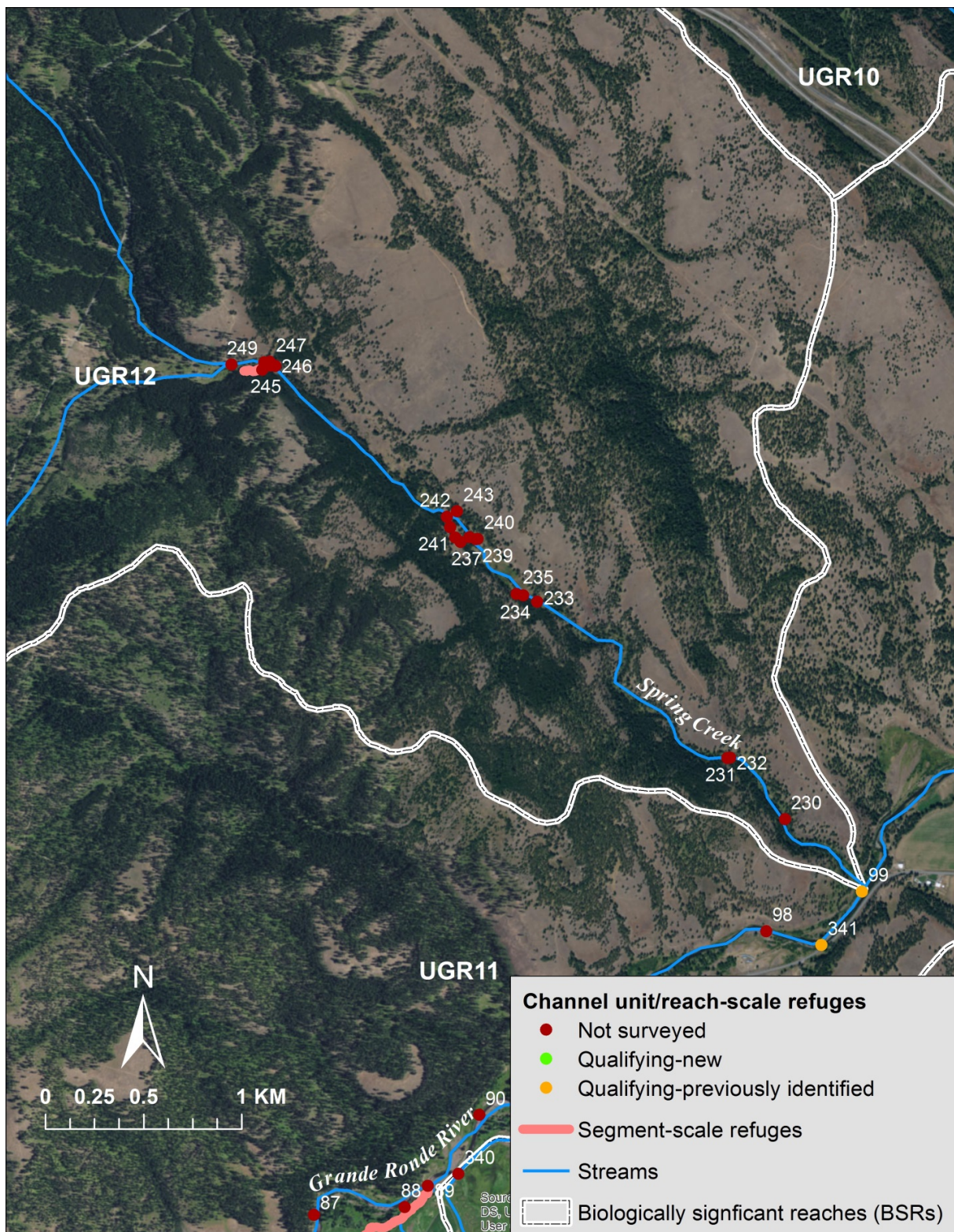


Figure A2 - 5. Map of cold-water refuges identified in biologically significant reach (BSR) UGR12 (Spring Creek).

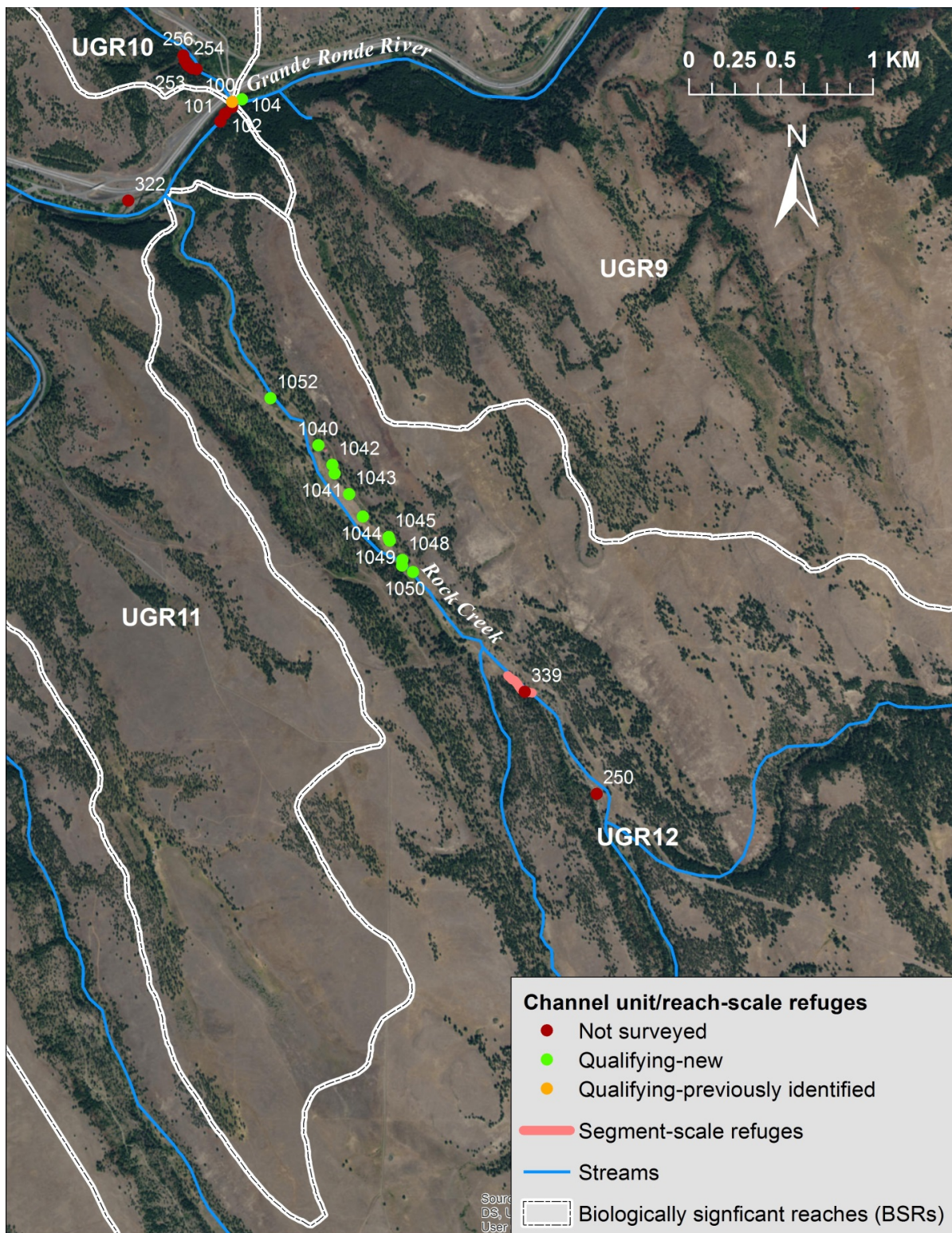


Figure A2 - 6. Map of cold-water refuges identified in biologically significant reach (BSR) UGR12 (Rock Creek).

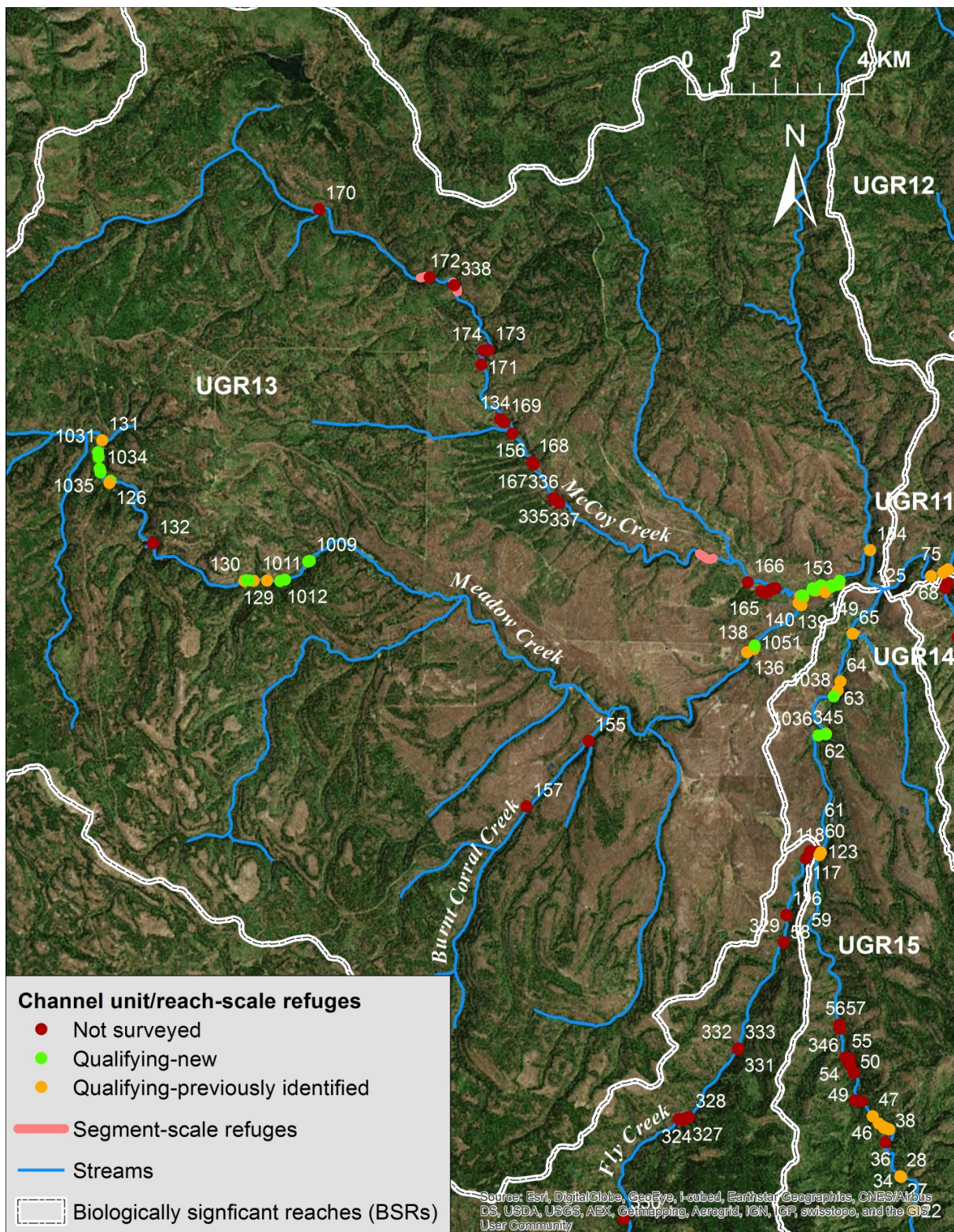


Figure A2 - 7. Map of cold-water refuges identified in biologically significant reach (BSR) UGR13.

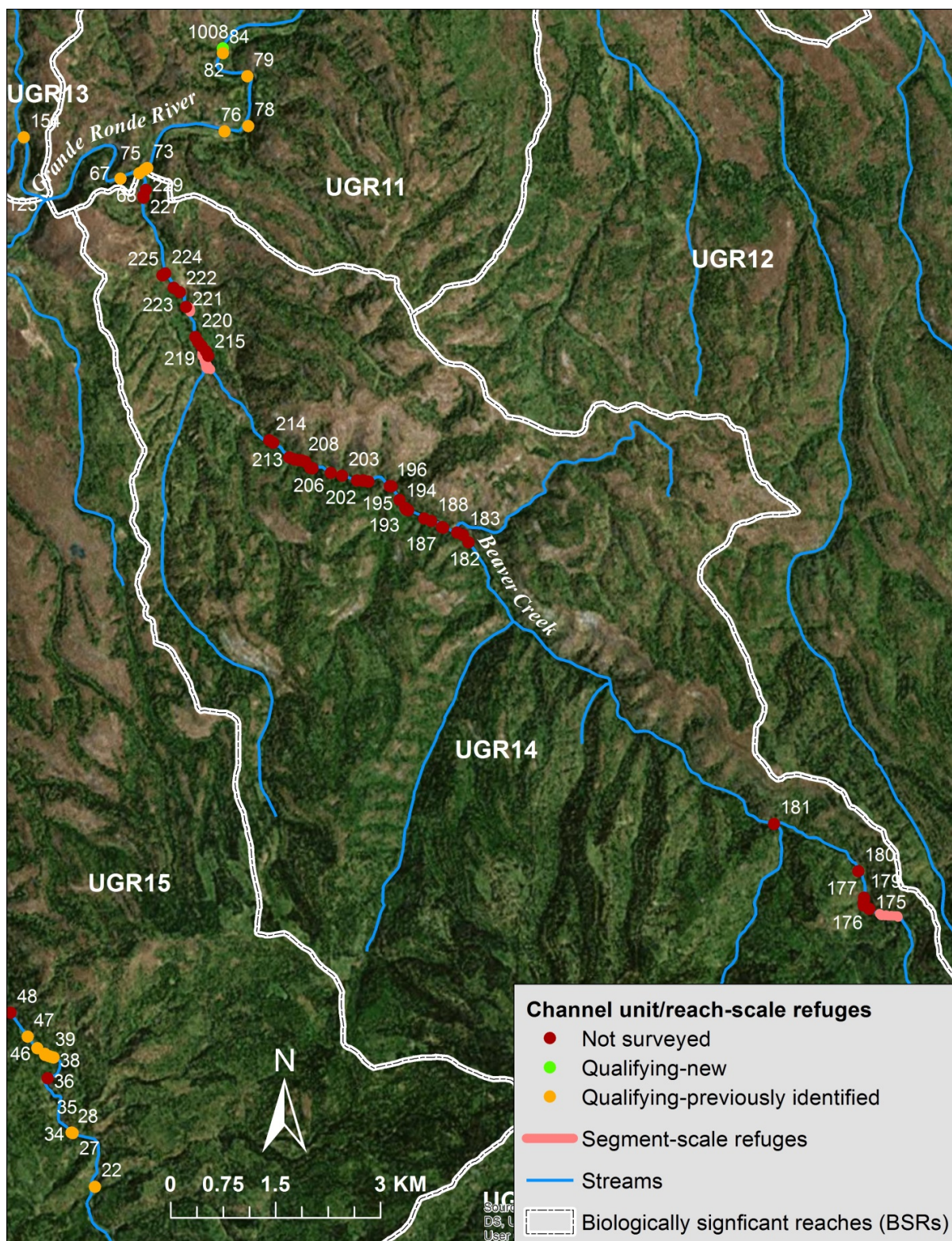


Figure A2 - 8. Map of cold-water refuges identified in biologically significant reach (BSR) UGR14.

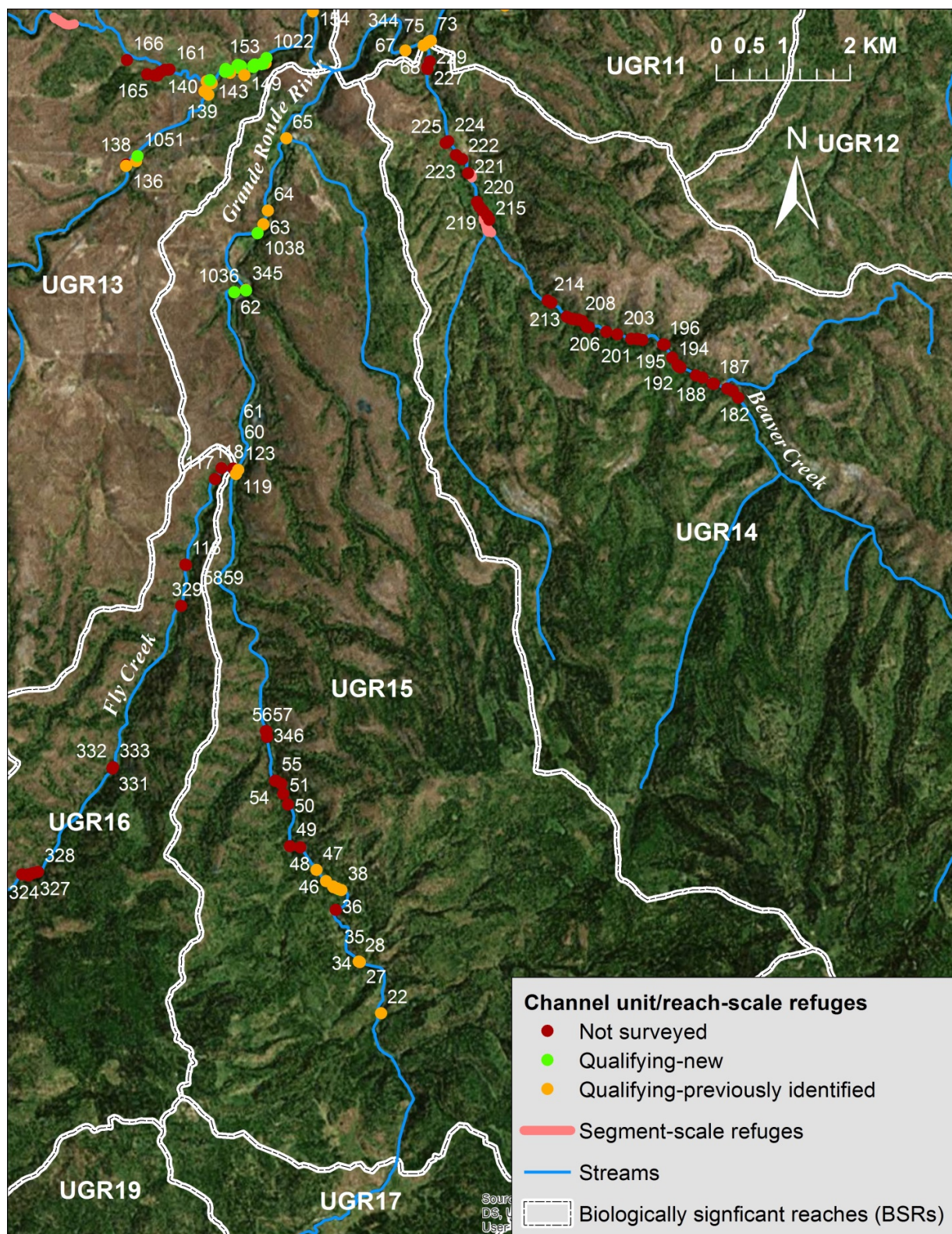


Figure A2 - 9. Map of cold-water refuges identified in biologically significant reach (BSR) UGR15.

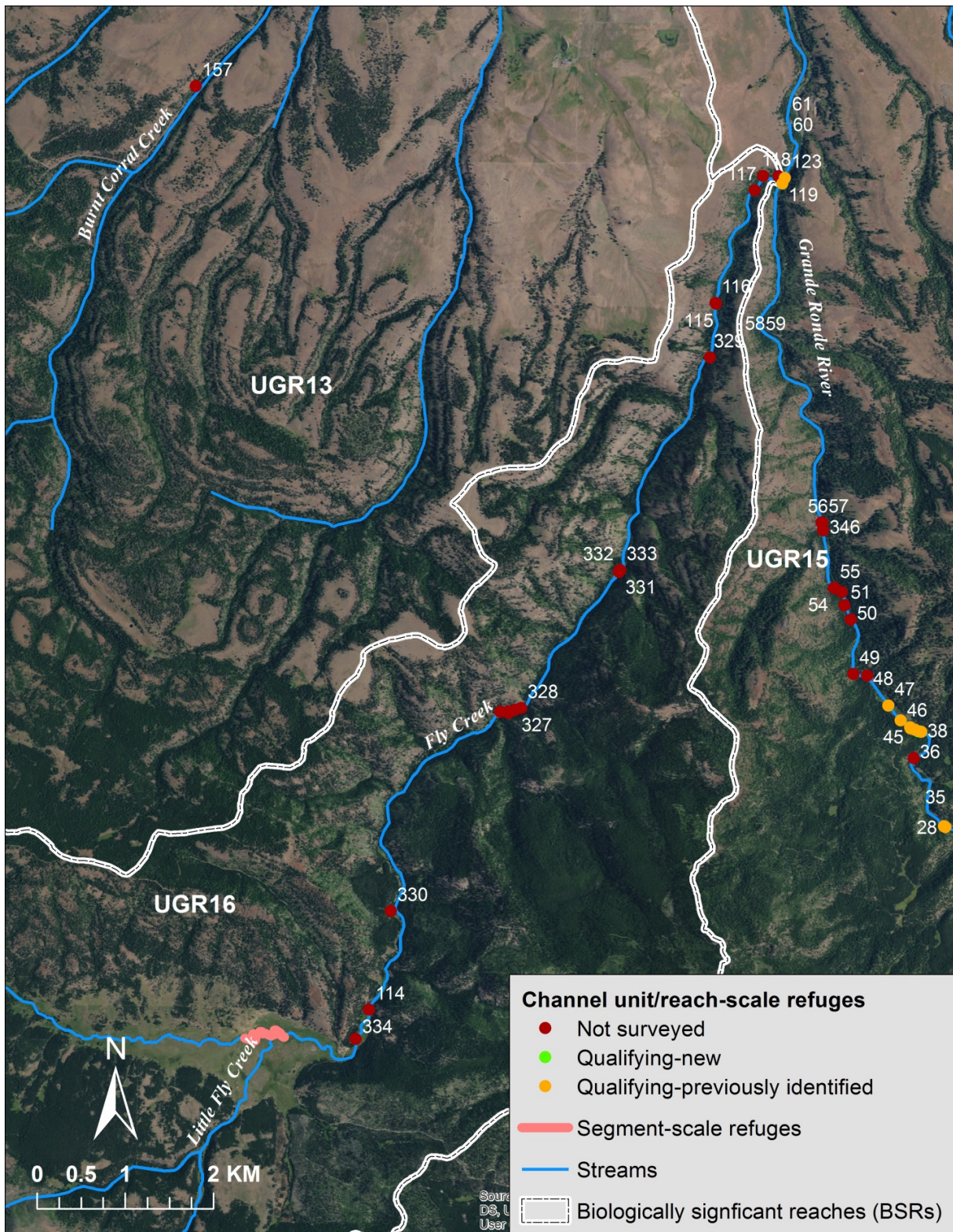


Figure A2 - 10. Map of cold-water refuges identified in biologically significant reach (BSR) UGR16.

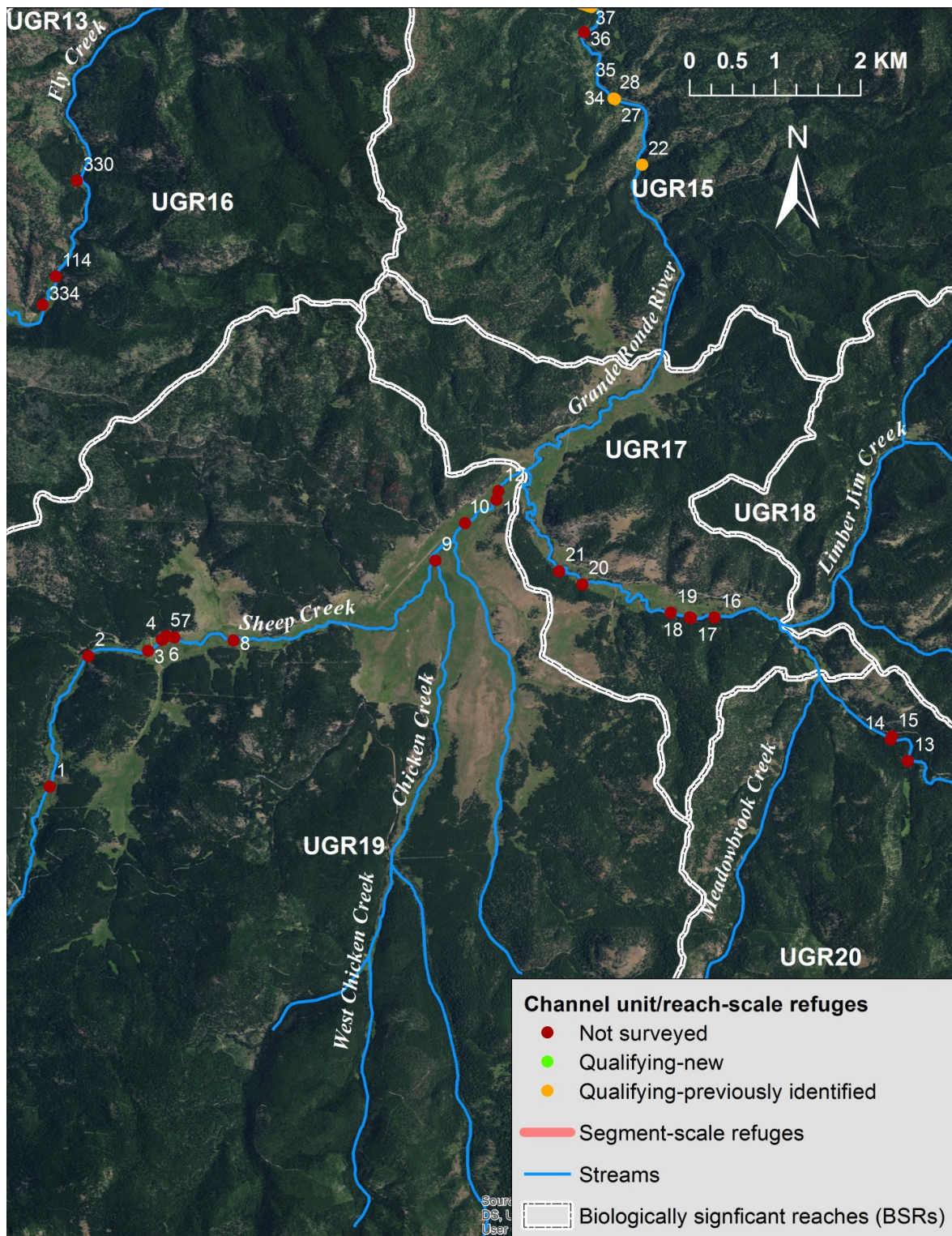


Figure A2 - 11. Map of cold-water refuges identified in biologically significant reaches (BSRs) UGR17-UGR20.

Appendix 3 – Table of Refuge Locations

Table A3 - 1. Type, status, and location of cold-water refuges identified from forward looking infrared (FLIR) and field surveys in the Upper Grande Ronde River basin, 2015.

Refuge ID	Refuge type	Refuge status	Stream name	BSR	UTM Easting	UTM Northing
1	Cold alcove	Not surveyed	Sheep Creek	UGR19	385712.5411	4991801.58
2	Tributary confluence plume	Not surveyed	Sheep Creek	UGR19	386166.0867	4993332.121
3	Hyporheic upwelling	Not surveyed	Sheep Creek	UGR19	386861.6562	4993393.918
4	Hyporheic upwelling	Not surveyed	Sheep Creek	UGR19	387022.8683	4993523.602
5	Lateral seep	Not surveyed	Sheep Creek	UGR19	387080.9262	4993564.162
6	Hyporheic upwelling	Not surveyed	Sheep Creek	UGR19	387032.7277	4993525.374
7	Hyporheic upwelling	Not surveyed	Sheep Creek	UGR19	387170.8769	4993550.709
8	Hyporheic upwelling	Not surveyed	Sheep Creek	UGR19	387863.0604	4993515.607
9	Hyporheic upwelling	Not surveyed	Sheep Creek	UGR19	390226.3395	4994450.812
10	Hyporheic upwelling	Not surveyed	Sheep Creek	UGR19	390571.5628	4994889.124
11	Hyporheic upwelling	Not surveyed	Sheep Creek	UGR19	390939.3155	4995160.399
12	upwelling	Not surveyed	Sheep Creek	UGR19	390963.8844	4995261.351
13	Cold alcove	Not surveyed	Grande Ronde River	UGR20	395756.8896	4992103.565
14	Cold side channel	Not surveyed	Grande Ronde River	UGR20	395555.7905	4992357.387
15	Cold side channel	Not surveyed	Grande Ronde River	UGR20	395567.8642	4992389.458
16	Cold side channel	Not surveyed	Grande Ronde River	UGR17	393493.4416	4993782.666
17	Cold side channel	Not surveyed	Grande Ronde River	UGR17	393215.9666	4993776.391
18	Hyporheic upwelling	Not surveyed	Grande Ronde River	UGR17	393199.8058	4993781.901
19	Cold side channel	Not surveyed	Grande Ronde River	UGR17	392978.9544	4993839.522
20	Lateral seep	Not surveyed	Grande Ronde River	UGR17	391947.2416	4994171.749

Refuge						
ID	Refuge type	Refuge status	Stream name	BSR	UTM Easting	UTM Northing
21	Hyporheic upwelling	Not surveyed	Grande Ronde River	UGR17	391674.0547	4994325.994
22	Tributary confluence plume	Qualifying- previously identified	Unnamed	UGR15	392644.5554	4999083.514
27	Lateral seep	Qualifying- previously identified	Grande Ronde River	UGR15	392327.2271	4999850.623
28	Lateral seep	Qualifying- previously identified	Grande Ronde River	UGR15	392309.831	4999858.919
36	Unknown	Not surveyed	Grande Ronde River	UGR15	391967.6506	5000634.232
38	Lateral seep	Qualifying- previously identified	Grande Ronde River	UGR15	392052.574	5000930.947
39	Lateral seep	Qualifying- previously identified	Grande Ronde River	UGR15	391982.2079	5000954.368
42	Cold side channel	Qualifying- previously identified	Grande Ronde River	UGR15	391932.9331	5000969.652
45	Cold side channel	Qualifying- previously identified	Grande Ronde River	UGR15	391926.1661	5000983.213
46	Lateral seep	Qualifying- previously identified	Grande Ronde River	UGR15	391819.7421	5001063.811
47	Tributary confluence plume	Qualifying- previously identified	Grande Ronde River	UGR15	391680.2528	5001229.316
48	Cold side channel	Not surveyed	Grande Ronde River	UGR15	391437.4875	5001571.534
49	Cold side channel	Not surveyed	Grande Ronde River	UGR15	391282.2781	5001588.416
50	Lateral seep	Not surveyed	Grande Ronde River	UGR15	391253.5382	5002208.865
51	Unknown	Not surveyed	Grande Ronde River	UGR15	391179.347	5002369.704
52	Lateral seep	Not surveyed	Grande Ronde River	UGR15	391152.1362	5002519.885
53	Lateral seep	Not surveyed	Grande Ronde River	UGR15	391072.9667	5002564.7

Refuge ID	Refuge type	Refuge status	Stream name	BSR	UTM Easting	UTM Northing
54	Lateral seep	Not surveyed	Grande Ronde River	UGR15	391068.287	5002566.828
55	Lateral seep	Not surveyed	Grande Ronde River	UGR15	391059.9955	5002567.593
56	Unknown	Not surveyed	Grande Ronde River	UGR15	390919.0182	5003309.774
57	Lateral seep	Not surveyed	Grande Ronde River	UGR15	390928.1607	5003309.341
62	Lateral seep	Qualifying- previously identified	Grande Ronde River	UGR15	390447.0852	5009883.036
63	Cold alcove	Qualifying- previously identified	Grande Ronde River	UGR15	390885.2815	5010903.153
64	Lateral seep	Qualifying- previously identified	Grande Ronde River	UGR15	390948.4481	5011106.534
65	Cold alcove	Qualifying- previously identified	Grande Ronde River	UGR15	391224.5877	5012191.918
68	Lateral seep	Qualifying- previously identified	Grande Ronde River	UGR11	393008.0188	5013502.781
73	Tributary confluence plume	Qualifying- previously identified	Beaver Creek	UGR11	393391.9178	5013652.985
74	Cold side channel	Qualifying- previously identified	Grande Ronde River	UGR14	393280.0338	5013579.307
75	Lateral seep	Qualifying- previously identified	Grande Ronde River	UGR11	393353.8889	5013631.401
76	Cold side channel	Qualifying- previously identified	Grande Ronde River	UGR11	394496.8947	5014178.963
78	Cold side channel	Qualifying- previously identified	Grande Ronde River	UGR11	394834.7125	5014252.234
79	Springbrook	Qualifying- previously identified	Grande Ronde River	UGR11	394824.6124	5014965.813

Refuge ID	Refuge type	Refuge status	Stream name	BSR	UTM Easting	UTM Northing
84	Cold side channel	Qualifying- previously identified	Grande Ronde River	UGR11	394473.9365	5015295.025
85	Cold side channel	Qualifying- previously identified	Grande Ronde River	UGR11	397942.9022	5017372.504
86	Cold side channel	Qualifying- previously identified	Grande Ronde River	UGR11	398404.9692	5017593.079
87	Lateral seep	Not surveyed	Grande Ronde River	UGR11	398447.3894	5017828.985
88	Lateral seep	Not surveyed	Grande Ronde River	UGR11	398909.8387	5017868.872
89	Tributary confluence plume	Not surveyed	Grande Ronde River	UGR11	399028.6438	5017978.451
90	Lateral seep	Not surveyed	Grande Ronde River	UGR11	399290.5694	5018339.659
91	Lateral seep	Qualifying- previously identified	Grande Ronde River	UGR11	399595.3578	5018300.226
93	Tributary confluence plume	Qualifying- previously identified	Grande Ronde River	UGR11	399801.0031	5018229.954
94	isolated pool	Qualifying- previously identified	Jordan Creek	UGR12	399757.5573	5018224.532
96	Lateral seep	Qualifying- previously identified	Grande Ronde River	UGR11	399931.7234	5018483.238
98	Cold alcove	Not surveyed	Grande Ronde River	UGR11	400753.5747	5019277.834
99	Tributary confluence plume	Qualifying- previously identified	Grande Ronde River	UGR11	401242.5622	5019480.469
100	Tributary confluence plume	Qualifying- previously identified	Grande Ronde River	UGR11	404256.0864	5022178.697
101	Cold side channel	Not surveyed	Grande Ronde River	UGR11	404191.3977	5022071.681
102	Cold side channel	Not surveyed	Grande Ronde River	UGR11	404216.3111	5022111.925
103	Cold side channel	Not surveyed	Grande Ronde River	UGR11	404256.1224	5022149.53

Refuge						
ID	Refuge type	Refuge status	Stream name	BSR	UTM Easting	UTM Northing
105	Cold side channel	Not surveyed	Grande Ronde River	UGR9	407481.1048	5022720.176
106	Cold side channel	Not surveyed	Grande Ronde River	UGR9	407656.2117	5022716.874
107	Cold side channel	Not surveyed	Grande Ronde River	UGR9	411306.1711	5021783.865
108	Cold side channel	Not surveyed	Grande Ronde River	UGR7	414606.9868	5021572.475
109	Cold side channel	Not surveyed	Grande Ronde River	UGR7	414621.4382	5021573.597
110	Cold alcove	Not surveyed	Grande Ronde River	UGR7	414966.9678	5021544.109
111	Cold side channel	Not surveyed	Grande Ronde River	UGR7	418132.919	5021705.266
112	Cold side channel	Not surveyed	Grande Ronde River	UGR7	419516.259	5021510.786
113	Lateral seep	Not surveyed	Grande Ronde River	UGR7	422107.6225	5021519.322
114	Cold alcove	Not surveyed	Fly Creek	UGR16	385783.6143	4997774.963
115	Lateral seep	Not surveyed	Fly Creek	UGR16	389723.0499	5005795.067
116	Lateral seep	Not surveyed	Fly Creek	UGR16	389716.2281	5005806.439
117	Lateral seep	Not surveyed	Fly Creek	UGR16	390161.2607	5007084.992
118	Lateral seep	Not surveyed	Fly Creek	UGR16	390255.2723	5007247.824
119	Tributary confluence plume	Qualifying- previously identified	Grande Ronde River	UGR16	390474.4139	5007162.01
120	Hyporheic upwelling	Not surveyed	Fly Creek	UGR16	390430.9321	5007243.153
121	Hyporheic upwelling	Not surveyed	Fly Creek	UGR16	390449.0202	5007225.441
122	Hyporheic upwelling	Not surveyed	Fly Creek	UGR16	390473.1465	5007202.55
123	Hyporheic upwelling	Qualifying- previously identified	Fly Creek	UGR15	390505.3291	5007223.705
126	Springbrook	Qualifying- previously identified	Meadow Creek	UGR13	374338.4943	5015619.393
128	Cold side channel	Qualifying- previously identified	Meadow Creek	UGR13	377918.2706	5013399.259

Refuge ID	Refuge type	Refuge status	Stream name	BSR	UTM Easting	UTM Northing
129	Cold side channel	Qualifying- previously identified	Meadow Creek	UGR13	377612.089	5013394.062
130	Cold alcove	Qualifying- previously identified	Meadow Creek	UGR13	377406.5203	5013396.931
131	Tributary confluence plume	Qualifying- previously identified	Smith Creek	UGR13	374175.5891	5016587.521
132	Tributary confluence plume	Not surveyed	Meadow Creek	UGR13	375321.9873	5014244.854
134	Springbrook	Not surveyed	McCoy Creek	UGR13	383215.4459	5017068.892
135	Cold side channel	Not surveyed	McCoy Creek	UGR13	383281.624	5017014.368
136	Cold alcove	Qualifying- previously identified	Meadow Creek	UGR13	388827.9323	5011776.614
137	Cold alcove	Not surveyed	Meadow Creek	UGR13	388833.1363	5011795.559
138	Cold side channel	Qualifying- previously identified	Meadow Creek	UGR13	388979.3172	5011846.411
139	Cold alcove	Qualifying- previously identified	Meadow Creek	UGR13	390059.4946	5012841.911
140	Cold alcove	Qualifying- previously identified	Meadow Creek	UGR13	389998.7555	5012891.862
142	Cold side channel	Qualifying- previously identified	McCoy Creek	UGR13	390033.8914	5013044.049
143	Cold side channel	Qualifying- previously identified	Meadow Creek	UGR13	390107.1352	5013013.772
145	Cold side channel	Qualifying- previously identified	Meadow Creek	UGR13	390386.9605	5013170.606
149	Springbrook	Qualifying- previously identified	Meadow Creek	UGR13	390598.4392	5013137.942
153	Cold side channel	Qualifying- previously identified	Meadow Creek	UGR13	390916.6266	5013317.916

Refuge						
ID	Refuge type	Refuge status	Stream name	BSR	UTM Easting	UTM Northing
154	Tributary confluence plume	Qualifying- previously identified	Meadow Creek	UGR13	391624.0032	5014092.523
155	Tributary confluence plume	Not surveyed	Burnt Corral Creek	UGR13	385227.9724	5009752.172
156	Cold side channel	Not surveyed	McCoy Creek	UGR13	383496.9074	5016740.194
157	Unknown	Not surveyed	Burnt Corral Creek	UGR13	383814.1905	5008270.013
158	Lateral seep	Not surveyed	McCoy Creek	UGR13	389341.7715	5013183.462
159	Hyporheic upwelling	Not surveyed	McCoy Creek	UGR13	389405.4081	5013216.322
160	Hyporheic upwelling	Not surveyed	McCoy Creek	UGR13	389451.3106	5013215.562
161	Hyporheic upwelling	Not surveyed	McCoy Creek	UGR13	389478.7198	5013221.487
162	Hyporheic upwelling	Not surveyed	McCoy Creek	UGR13	389298.8751	5013131.697
163	Hyporheic upwelling	Not surveyed	McCoy Creek	UGR13	389277.6717	5013127.998
164	Hyporheic upwelling	Not surveyed	McCoy Creek	UGR13	389255.9003	5013130.282
165	Hyporheic upwelling	Not surveyed	McCoy Creek	UGR13	389144.3344	5013150.489
166	Hyporheic upwelling	Not surveyed	McCoy Creek	UGR13	388839.4874	5013362.887
167	Springbrook	Not surveyed	McCoy Creek	UGR13	383979.558	5016033.37
168	Springbrook	Not surveyed	McCoy Creek	UGR13	383938.9588	5016091.843
169	Cold side channel	Not surveyed	McCoy Creek	UGR13	383311.3715	5016997.809
170	Tributary confluence plume	Not surveyed	McCoy Creek	UGR13	379103.7577	5021839.113
171	Cold side channel	Not surveyed	McCoy Creek	UGR13	382788.3882	5018307.74
172	Springbrook	Not surveyed	McCoy Creek	UGR13	381617.4744	5020290.244
173	Tributary confluence plume	Not surveyed	McCoy Creek	UGR13	382956.8288	5018636.301
174	Cold side channel	Not surveyed	McCoy Creek	UGR13	382831.7681	5018623.232
175	Cold alcove	Not surveyed	Beaver Creek	UGR14	403721.6044	5003055.333
176	Cold side channel	Not surveyed	Beaver Creek	UGR14	403643.4902	5003103.847
177	Cold side channel	Not surveyed	Beaver Creek	UGR14	403642.5925	5003145.877
178	Cold side channel	Not surveyed	Beaver Creek	UGR14	403648.6662	5003167.853
179	Cold alcove	Not surveyed	Beaver Creek	UGR14	403647.3223	5003217.404
180	Lateral seep	Not surveyed	Beaver Creek	UGR14	403565.0557	5003594.495
181	Tributary confluence plume	Not surveyed	Beaver Creek	UGR14	402358.648	5004273.31

Refuge						
ID	Refuge type	Refuge status	Stream name	BSR	UTM Easting	UTM Northing
182	Cold alcove	Not surveyed	Beaver Creek	UGR14	397992.0684	5008301.355
183	Cold alcove	Not surveyed	Beaver Creek	UGR14	397909.4167	5008403.779
184	Cold side channel	Not surveyed	Beaver Creek	UGR14	397826.9374	5008441.545
185	Cold side channel	Not surveyed	Beaver Creek	UGR14	397629.089	5008510.601
186	Cold side channel	Not surveyed	Beaver Creek	UGR14	397622.5485	5008512.477
187	Cold side channel	Not surveyed	Beaver Creek	UGR14	397606.8851	5008518.234
188	Cold side channel	Not surveyed	Beaver Creek	UGR14	397456.4871	5008603.848
189	Cold alcove	Not surveyed	Beaver Creek	UGR14	397356.369	5008639.738
190	Cold side channel	Not surveyed	Beaver Creek	UGR14	397126.298	5008757.626
191	Cold side channel	Not surveyed	Beaver Creek	UGR14	397112.4443	5008763.72
192	Cold side channel	Not surveyed	Beaver Creek	UGR14	397097.304	5008772.282
193	Cold side channel	Not surveyed	Beaver Creek	UGR14	397084.4616	5008788.438
194	Cold side channel	Not surveyed	Beaver Creek	UGR14	397000.7029	5008905.612
195	Cold side channel	Not surveyed	Beaver Creek	UGR14	396886.3737	5009098.322
196	Cold side channel	Not surveyed	Beaver Creek	UGR14	396865.6023	5009103.447
197	Cold alcove	Not surveyed	Beaver Creek	UGR14	396557.9119	5009169.982
198	Cold alcove	Not surveyed	Beaver Creek	UGR14	396494.7025	5009181.082
199	Lateral seep	Not surveyed	Beaver Creek	UGR14	396487.1624	5009183.214
200	Lateral seep	Not surveyed	Beaver Creek	UGR14	396475.7978	5009182.679
201	Lateral seep	Not surveyed	Beaver Creek	UGR14	396481.5345	5009182.654
202	Lateral seep	Not surveyed	Beaver Creek	UGR14	396391.6825	5009184.6
Hyporheic						
203	upwelling	Not surveyed	Beaver Creek	UGR14	396180.8743	5009252.067
204	Cold side channel	Not surveyed	Beaver Creek	UGR14	396019.9701	5009291.372
205	Cold side channel	Not surveyed	Beaver Creek	UGR14	395724.5375	5009366.51
206	Cold side channel	Not surveyed	Beaver Creek	UGR14	395756.9296	5009356.39
207	Cold side channel	Not surveyed	Beaver Creek	UGR14	395654.4624	5009454.388
208	Cold alcove	Not surveyed	Beaver Creek	UGR14	395605.7894	5009468.886
209	Cold alcove	Not surveyed	Beaver Creek	UGR14	395574.1251	5009474.668
210	Cold side channel	Not surveyed	Beaver Creek	UGR14	395538.7021	5009480.41
211	Cold side channel	Not surveyed	Beaver Creek	UGR14	395494.0227	5009488
212	Cold side channel	Not surveyed	Beaver Creek	UGR14	395424.8617	5009515.2
213	Cold side channel	Not surveyed	Beaver Creek	UGR14	395193.5471	5009724.528
214	Cold alcove	Not surveyed	Beaver Creek	UGR14	395137.8551	5009759.445
215	Cold side channel	Not surveyed	Beaver Creek	UGR14	394262.9782	5010968.462
216	Cold side channel	Not surveyed	Beaver Creek	UGR14	394232.9606	5011031.087
Hyporheic						
217	upwelling	Not surveyed	Beaver Creek	UGR14	394174.1222	5011102.762
218	Cold alcove	Not surveyed	Beaver Creek	UGR14	394165.9544	5011110.699
219	Cold side channel	Not surveyed	Beaver Creek	UGR14	394114.9239	5011171.36
220	Cold side channel	Not surveyed	Beaver Creek	UGR14	394079.2709	5011235.738
221	Cold side channel	Not surveyed	Beaver Creek	UGR14	393945.4824	5011666.83

Refuge						
ID	Refuge type	Refuge status	Stream name	BSR	UTM Easting	UTM Northing
222	Cold alcove	Not surveyed	Beaver Creek	UGR14	393856.8527	5011876.899
223	Lateral seep	Not surveyed	Beaver Creek	UGR14	393768.5365	5011938.882
224	Cold alcove	Not surveyed	Beaver Creek	UGR14	393650.1083	5012144.868
225	Springbrook	Not surveyed	Beaver Creek	UGR14	393610.3179	5012118.277
226	Cold side channel	Not surveyed	Beaver Creek	UGR14	393337.3749	5013243.231
227	Cold side channel	Not surveyed	Beaver Creek	UGR14	393340.6177	5013229.277
228	Cold side channel	Not surveyed	Beaver Creek	UGR14	393334.6134	5013252.128
229	Cold side channel	Not surveyed	Beaver Creek	UGR14	393372.493	5013341.432
230	Cold alcove	Not surveyed	Spring Creek	UGR12	400849.0265	5019848.646
231	Cold side channel	Not surveyed	Spring Creek	UGR12	400556.1377	5020161.691
232	Cold side channel	Not surveyed	Spring Creek	UGR12	400569.609	5020163.274
233	Lateral seep	Not surveyed	Spring Creek	UGR12	399586.2576	5020958.24
234	Lateral seep	Not surveyed	Spring Creek	UGR12	399513.882	5020991.939
235	Cold alcove	Not surveyed	Spring Creek	UGR12	399480.3117	5020999.391
236	Hyporheic upwelling	Not surveyed	Spring Creek	UGR12	399168.5067	5021286.3
237	Hyporheic upwelling	Not surveyed	Spring Creek	UGR12	399194.6961	5021263.663
238	Hyporheic upwelling	Not surveyed	Spring Creek	UGR12	399240.7803	5021288.166
239	Hyporheic upwelling	Not surveyed	Spring Creek	UGR12	399273.8597	5021278.289
240	Hyporheic upwelling	Not surveyed	Spring Creek	UGR12	399282.374	5021279.921
241	Springbrook	Not surveyed	Spring Creek	UGR12	399142.7456	5021339.08
242	Hyporheic upwelling	Not surveyed	Spring Creek	UGR12	399125.0879	5021392.475
243	Hyporheic upwelling	Not surveyed	Spring Creek	UGR12	399176.1207	5021420.822
244	Hyporheic upwelling	Not surveyed	Spring Creek	UGR12	398228.084	5022163.659
245	Hyporheic upwelling	Not surveyed	Spring Creek	UGR12	398183.1207	5022143.162
246	Hyporheic upwelling	Not surveyed	Spring Creek	UGR12	398250.1193	5022163.518
247	Hyporheic upwelling	Not surveyed	Spring Creek	UGR12	398220.7246	5022183.658
248	Hyporheic upwelling	Not surveyed	Spring Creek	UGR12	398193.1177	5022182.048
249	Hyporheic upwelling	Not surveyed	Spring Creek	UGR12	398026.8453	5022169.678

Refuge						
ID	Refuge type	Refuge status	Stream name	BSR	UTM Easting	UTM Northing
	Hyporheic					
250	upwelling	Not surveyed	Rock Creek	UGR12	406240.1106	5018409.706
251	Lateral seep	Not surveyed	Five Points Creek	UGR10	404061.9798	5022356.52
252	Cold side channel	Not surveyed	Five Points Creek	UGR10	404037.8612	5022361.265
253	Cold side channel	Not surveyed	Five Points Creek	UGR10	404018.739	5022374.703
254	Cold side channel	Not surveyed	Five Points Creek	UGR10	404011.9237	5022380.475
255	Cold side channel	Not surveyed	Five Points Creek	UGR10	403998.2828	5022404.298
256	Lateral seep	Not surveyed	Five Points Creek	UGR10	403989.5453	5022430.634
257	Springbrook	Not surveyed	Five Points Creek	UGR10	403200.8975	5023030.013
258	Cold side channel	Not surveyed	Five Points Creek	UGR10	402885.0389	5023547.958
	Tributary					
259	confluence plume	Not surveyed	Pelican Creek	UGR10	402872.9506	5023769.862
260	Lateral seep	Not surveyed	Five Points Creek	UGR10	403370.5991	5024158.478
	Hyporheic					
261	upwelling	Not surveyed	Five Points Creek	UGR10	403697.0918	5024476.866
	Hyporheic					
262	upwelling	Not surveyed	Five Points Creek	UGR10	403839.022	5024593.857
263	Cold alcove	Not surveyed	Five Points Creek	UGR10	403890.9403	5024604.286
264	Springbrook	Not surveyed	Five Points Creek	UGR10	403933.3984	5024602.055
265	Lateral seep	Not surveyed	Five Points Creek	UGR10	404065.3556	5024879.248
266	Lateral seep	Not surveyed	Five Points Creek	UGR10	404060.9778	5024864.301
267	Springbrook	Not surveyed	Five Points Creek	UGR10	404161.6185	5025105.395
268	Lateral seep	Not surveyed	Five Points Creek	UGR10	404196.3355	5025179.81
269	Lateral seep	Not surveyed	Five Points Creek	UGR10	404186.7884	5025164.04
270	Lateral seep	Not surveyed	Five Points Creek	UGR10	404251.4479	5025893.558
	Hyporheic					
271	upwelling	Not surveyed	Five Points Creek	UGR10	404184.2417	5026037.629
272	Cold side channel	Not surveyed	Five Points Creek	UGR10	404174.1101	5026410.917
273	Cold side channel	Not surveyed	Five Points Creek	UGR10	404190.6862	5026430.329
274	Cold side channel	Not surveyed	Five Points Creek	UGR10	404189.7338	5026476.779
275	Cold alcove	Not surveyed	Five Points Creek	UGR10	404156.9006	5026635.939
276	Cold alcove	Not surveyed	Five Points Creek	UGR10	404223.8869	5026480.138
277	Cold alcove	Not surveyed	Five Points Creek	UGR10	404234.5506	5027125.024
278	Cold side channel	Not surveyed	Five Points Creek	UGR10	404098.1415	5025111.083
279	Cold side channel	Not surveyed	Five Points Creek	UGR10	404089.1816	5025099.478
280	Cold alcove	Not surveyed	Five Points Creek	UGR10	404206.906	5027299.782
281	Cold alcove	Not surveyed	Five Points Creek	UGR10	404214.1257	5027307.383
282	Cold alcove	Not surveyed	Five Points Creek	UGR10	404289.0732	5027839.411
283	Cold alcove	Not surveyed	Five Points Creek	UGR10	404635.1915	5028548.151
284	Cold side channel	Not surveyed	Five Points Creek	UGR10	405963.2456	5029368.049
285	Cold side channel	Not surveyed	Five Points Creek	UGR10	405989.6462	5029390.825
286	Cold side channel	Not surveyed	Five Points Creek	UGR10	406362.5974	5030061.217

Refuge						
ID	Refuge type	Refuge status	Stream name	BSR	UTM Easting	UTM Northing
287	Cold side channel	Not surveyed	Five Points Creek	UGR10	406473.114	5030107.845
288	Cold side channel	Not surveyed	Five Points Creek	UGR10	406571.2677	5030109.191
289	Cold alcove	Not surveyed	Five Points Creek	UGR10	407016.5148	5030156.131
290	Cold side channel	Not surveyed	Five Points Creek	UGR10	407438.9402	5030178.856
291	Cold side channel	Not surveyed	Five Points Creek	UGR10	407677.1978	5030079.106
292	Springbrook	Not surveyed	Five Points Creek	UGR10	409328.0088	5030502.103
293	Cold side channel	Not surveyed	Five Points Creek	UGR10	409192.3225	5030488.349
294	Tributary	Not surveyed	Grande Ronde	UGR10	409406.8499	5030594.035
	confluence plume		River			
316	Cold alcove	Not surveyed	Grande Ronde	UGR7	421675.2506	5021488.921
			River			
317	Lateral seep	Not surveyed	Grande Ronde	UGR7	415443.3682	5021349.436
			River			
318	Lateral seep	Not surveyed	Grande Ronde	UGR7	415257.6429	5021387.161
			River			
319	Cold alcove	Not surveyed	Grande Ronde	UGR9	407428.6935	5022755.221
			River			
320	Cold side channel	Qualifying- previously identified	Grande Ronde	UGR11	398256.9238	5017310.99
			River			
322	Cold side channel	Not surveyed	Grande Ronde	UGR11	403690.0532	5021640.098
			River			
323	Cold side channel	Not surveyed	Grande Ronde	UGR11	402815.1056	5021790.602
324	Cold side channel	Not surveyed	River	UGR11	402815.1056	5021790.602
325	Hyporheic	Not surveyed	Fly Creek	UGR16	387368.4895	5001146.454
	upwelling		Fly Creek			
326	Tributary	Not surveyed	Fly Creek	UGR16	387364.9245	5001162.642
	confluence plume		Fly Creek			
327	Cold side channel	Not surveyed	Fly Creek	UGR16	387270.4623	5001162.24
328	Cold side channel	Not surveyed	Fly Creek	UGR16	387441.3665	5001183.711
329	Lateral seep	Not surveyed	Fly Creek	UGR16	387509.6778	5001202.486
330	Lateral seep	Not surveyed	Fly Creek	UGR16	389653.253	5005186.42
331	Springbrook	Not surveyed	Fly Creek	UGR16	386031.2352	4998897.064
332	Lateral seep	Not surveyed	Fly Creek	UGR16	388622.1335	5002748.396
333	Lateral seep	Not surveyed	Fly Creek	UGR16	388626.3553	5002767.761
334	Lateral seep	Not surveyed	Fly Creek	UGR16	388633.7435	5002770.626
335	Lateral seep	Not surveyed	Fly Creek	UGR16	385630.2979	4997442.415
336	Cold side channel	Not surveyed	McCoy Creek	UGR13	384443.5102	5015242.745
337	Cold side channel	Not surveyed	McCoy Creek	UGR13	384428.3938	5015271.587
338	Cold side channel	Not surveyed	McCoy Creek	UGR13	384561.5688	5015161.981
339	Springbrook	Not surveyed	McCoy Creek	UGR13	382176.596	5020110.825
339	Springbrook	Not surveyed	Rock Creek	UGR12	405848.2547	5018965.683

Refuge ID	Refuge type	Refuge status	Stream name	BSR	UTM Easting	UTM Northing
340	Tributary confluence plume	Not surveyed	Grande Ronde River	UGR12	399182.9926	5018038.701
341	Tributary confluence plume	Qualifying- previously identified	Grande Ronde River	UGR11	401035.2418	5019207.024
345	Tributary confluence plume	Qualifying- previously identified	Warm Springs Creek	UGR15	390619.4438	5009920.173
346	Tributary confluence plume	Not surveyed	Grande Ronde River	UGR15	390938.2566	5003222.661
1001	Lateral seep	Qualifying- new	Grande Ronde River	UGR9	404308.7923	5022192.343
1004	Cold side channel	Qualifying- new	Grande Ronde River	UGR11	398202.7561	5017307.417
1005	Cold side channel	Qualifying- new	Grande Ronde River	UGR11	398385.8502	5017574.496
1006	Cold side channel	Qualifying- new	Grande Ronde River	UGR11	398437.6814	5017579.219
1007	Cold side channel	Qualifying- new	Grande Ronde River	UGR15	392018.9063	5000939.298
1008	Cold side channel	Qualifying- new	Grande Ronde River	UGR11	394471.9677	5015365.066
1009	Cold side channel	Qualifying- new	Meadow Creek	UGR13	378888.1469	5013841.819
1010	Cold side channel	Qualifying- new	Meadow Creek	UGR13	378851.0426	5013830.305
1011	Cold side channel	Qualifying- new	Meadow Creek	UGR13	378327.5022	5013416.936
1012	Cold side channel	Qualifying- new	Meadow Creek	UGR13	378220.2505	5013390.105
1013	Cold side channel	Qualifying- new	Meadow Creek	UGR13	377458.6006	5013411.48
1014	Cold alcove	Qualifying- new	Meadow Creek	UGR13	377507.1984	5013408.317
1015	Cold alcove	Qualifying- new	Meadow Creek	UGR13	390083.9502	5013061.515
1016	Cold side channel	Qualifying- new	Meadow Creek	UGR13	390307.9199	5013187.867
1017	Cold alcove	Qualifying- new	Meadow Creek	UGR13	390319.8243	5013227.221
1018	Cold alcove	Qualifying- new	Meadow Creek	UGR13	390361.084	5013203.503

Refuge ID	Refuge type	Refuge status	Stream name	BSR	UTM Easting	UTM Northing
1019	Cold side channel	Qualifying-new	Meadow Creek	UGR13	390852.9008	5013299.457
1020	Cold side channel	Qualifying-new	Meadow Creek	UGR13	390860.7251	5013307.212
1021	Cold side channel	Qualifying-new	Meadow Creek	UGR13	390876.3005	5013304.832
1022	Cold side channel	Qualifying-new	Meadow Creek	UGR13	390927.7336	5013393.178
1023	Cold side channel	Qualifying-new	Meadow Creek	UGR13	390752.9191	5013294.626
1024	Cold side channel	Qualifying-new	Meadow Creek	UGR13	390734.0039	5013280.84
1025	Cold side channel	Qualifying-new	Meadow Creek	UGR13	390733.1934	5013256.628
1026	Hyporheic upwelling	Qualifying-new	McCoy Creek	UGR13	390549.0713	5013269.146
1027	Cold side channel	Qualifying-new	McCoy Creek	UGR13	390530.9282	5013272.793
1028	Cold side channel	Qualifying-new	McCoy Creek	UGR13	390505.5513	5013289.235
1029	Cold side channel	Qualifying-new	McCoy Creek	UGR13	390497.3577	5013287.376
1030	Hyporheic upwelling	Qualifying-new	McCoy Creek	UGR13	390515.9451	5013241.382
1031	Lateral seep	Qualifying-new	Meadow Creek	UGR13	374077.3967	5016312.969
1032	Cold side channel	Qualifying-new	Meadow Creek	UGR13	374087.7384	5016205.96
1033	Tributary confluence plume	Qualifying-new	Meadow Creek	UGR13	374362.2934	5015664.153
1034	Hyporheic upwelling	Qualifying-new	Meadow Creek	UGR13	374135.7636	5015859.925
1035	Hyporheic upwelling	Qualifying-new	Meadow Creek	UGR13	374117.1375	5015937.091
1036	Lateral seep	Qualifying-new	Grande Ronde River	UGR15	390446.4172	5009885.27
1037	Tributary confluence plume	Qualifying-new	Warm Springs Creek	UGR15	390621.8345	5009908.575
1038	Cold side channel	Qualifying-new	Grande Ronde River	UGR15	390796.0576	5010768.674
1039	Cold alcove	Qualifying-new	Grande Ronde River	UGR11	399540.614	5018333.766

Refuge						
ID	Refuge type	Refuge status	Stream name	BSR	UTM Easting	UTM Northing
1040	Hyporheic upwelling	Qualifying-new	Rock Creek	UGR12	404725.2556	5020308.128
1041	Hyporheic upwelling	Qualifying-new	Rock Creek	UGR12	404813.69	5020153.673
1042	Hyporheic upwelling	Qualifying-new	Rock Creek	UGR12	404801.7872	5020201.189
1043	Hyporheic upwelling	Qualifying-new	Rock Creek	UGR12	404892.0255	5020041.373
1044	Hyporheic upwelling	Qualifying-new	Rock Creek	UGR12	404967.9357	5019918.777
1045	Hyporheic upwelling	Qualifying-new	Rock Creek	UGR12	405107.3705	5019808.562
1046	Hyporheic upwelling	Qualifying-new	Rock Creek	UGR12	405114.1298	5019788.903
1047	Hyporheic upwelling	Qualifying-new	Rock Creek	UGR12	405110.6351	5019796.29
1048	Hyporheic upwelling	Qualifying-new	Rock Creek	UGR12	405181.602	5019683.327
1049	Hyporheic upwelling	Qualifying-new	Rock Creek	UGR12	405180.8347	5019653.114
1050	Hyporheic upwelling	Qualifying-new	Rock Creek	UGR12	405239.652	5019618.34
1051	Cold side channel	Qualifying-new	Meadow Creek	UGR13	388999.8062	5011922.618
1052	Cold side channel	Qualifying-new	Rock Creek	UGR12	404464.5102	5020563.421

Comparison of Regional Water Temperature Models

Introduction

Water temperature is an important characteristic that is used to understand the relationship between stream habitat environmental factors that affect the distribution, growth, survival, and production of salmonids (Bouwes et al. 2011). As such, in-stream water temperature is a metric that has been collected under the CHaMP monitoring protocol from 2011 through 2016. Using hourly logged stream temperature data at each of the monitoring locations, and extrapolating between survey sites, a basin wide estimate of the daily and seasonal stream temperatures can be achieved. However, CHaMP's rotating panel sampling design, equipment malfunction, and logger loss lead to numerous missing values in the stream temperature dataset which pose issues concerning the accuracy of already extrapolated data between survey sites and years.

Previous CRITFC analyses have used the Northwest Stream Temperature model (NorWeST) to fill in gaps of missing stream temperature data. However, continued analysis and modeling of stream temperatures as a result of the CHaMP program has led to the development of another regional model created by South Fork Research, Inc. (SFR). As additional stream temperature models became available, we evaluated which model or combination of models would yield the best relationship between measured and modeled stream temperature. We compared two existing water temperature models: 1) NorWeST and 2) SFR Stream Temperature Model.

Methods

Year round temperature records were collected at all CHaMP sites using Hobo Tidbit and Pro V2 data loggers following the Water Temperature Probe Installation Protocol starting in 2011 (<https://www.monitoringmethods.org/Method/Details/846>). Sites were visited once in spring and once in fall to download the data and to assess the condition of the temperature loggers. Monthly average and maximum temperatures were calculated for the "summer period" (July 15th through Aug 31st) as defined by CHaMP, and these data were used by both the NorWeST and SFR models for parameterization. For each of the models we were interested in average August stream temperature. Focusing on the Upper Grande Ronde, Catherine Creek, and the Minam watersheds, we obtained average August water temperatures from CHaMP loggers (www.champmonitoring.org) and the NorWeST database, and average August 8 day water temperatures from the SFR model. For each of the stream temperature models these data were subset to only include comparable years between the two stream temperature models (2011 – 2013).

The NorWeST model uses a spatial statistical network with a set of 12 possible covariates and the CHaMP logger data as the model inputs for predict historic and future water temperatures under future climate scenarios (Isaak et al. 2011). The modeled data were estimated for nodes distributed throughout the stream networks at 1-km intervals. Concerning years 2012 and 2013, water temperatures were estimated based on elevation-adjusted air temperature data and 2011 CHaMP data and not from temperature logger data for 2012 and 2013 directly.

NorWeST covariates:

- | | |
|--|-----------------------------------|
| 1) Air temperature August (C) | 7) Stream slope % |
| 2) Stream discharge August (m ³ /s) | 8) Mean annual precipitation (mm) |
| 3) Elevation (m) | 9) Base flow index (BFI) |
| 4) Latitude (m) | 10) Glacier % of catchment area |
| 5) Canopy % | 11) Lake % of catchment area |
| 6) Cumulative drainage area (km sq.) | 12) Tailwater (0/1) |

The SFR model uses confluence-to-confluence approach with a three model inputs to calculate 8-day mean, min, and max annual stream temperature to create temperature estimates throughout the Interior Columbia River Basin, excepting the Minam River (ICRB; McNyset et al. 2015). Here, 8-day mean stream temperature values were extracted using corresponding August Julian day (day range 209 through 241).

SFR covariates:

- 1) Land surface temperature (LST) from MODIS
- 2) Julian day
- 3) Elevation (m)

Each of the stream temperature models output spatially referenced stream temperature data. Using these data and a geographic information system (GIS) we constrained our target temperature data from each of the models on the basis of a 1:1 relationship to the 138 survey sites between the UGR and Minam watersheds (i.e. for each survey site there was exactly one modeled stream temperature from each of the modeled results). These relationships were established by spatial proximity, whereby modeled nodes or temperature values within a distance of each site were selected. To ensure accuracy the remaining points were manually validated and edited where necessary to acquire the 1:1 relationship for each of the modeled results. The spatially joined data from GIS were exported and merged by survey site and survey date.

We used a linear model approach, where predicted basin water temperatures for each model were regressed against measured CHaMP water temperature across all monitoring sites in the study basin (Figure 13 (NorWeST); Figure 14 (SFR)). Model selection was validated using AIC and root mean square error (RMSE) for both the NorWeST and SFR models.

Results and Discussion

Across all of the CHaMP study sites median average August stream temperatures ranged from 8.8 °C to 20.5 °C for the NorWeST model, 10.2 °C to 18.0 °C for the SFR model, and 9.8 °C to 21.7 °C for the CHaMP loggers (Table 12). Between years of modeled stream temperature, the warmest temperatures were observed in 2012.

Table 12. Summary statistics for the two stream temperature modeled results and measured CHaMP data.

Year	NorWeST Avg. August Modeled Temp (°C)				SFR Avg. 8D August Modeled Temp (°C)				CHaMP Max7dAM Avg. August Temp (°C)			
	median	min	max	SD	median	min	max	SD	median	min	max	SD
2010									12.4	11.3	13.5	1.6
2011	14.8	8.8	20.1	2.4	14.7	10.2	18.0	2.2	14.6	10.1	19.1	2.7
2012	15.3	9.3	20.5	2.4	15.3	11.6	17.9	1.7	15.0	9.8	19.4	2.5
2013	14.7	8.7	19.9	2.4	14.4	10.3	17.2	2.1	14.7	11.2	20.7	2.3
2014					15.3	12.0	17.2	1.6	14.4	10.5	21.7	2.6
2015					14.8	10.8	17.4	1.7	14.5	10.2	19.7	2.4

Predicted basin water temperatures for each model were regressed against measured CHaMP water temperature across all monitoring sites in the study basin (Figure 13 (NorWeST); Figure 14 (SFR)). Root mean square error (RMSE) for the two models were 1.16 °C for NorWeST and 1.83 °C for SFR; the lower RMSE model result for the NorWeST model of the SFR model indicates better model accuracy.

In both cases, there was a positive significant relationship between CHaMP and modeled temperature data. Each of the models slightly overestimated the CHaMP temperatures (Table 12). While not apparent in Table 1, the stronger linear model fit produced by the NorWeST model explained 27% more ($R^2 = 0.784$) of the variation within the data than the SFR model fit (Figure 2; $R^2 = 0.505$)

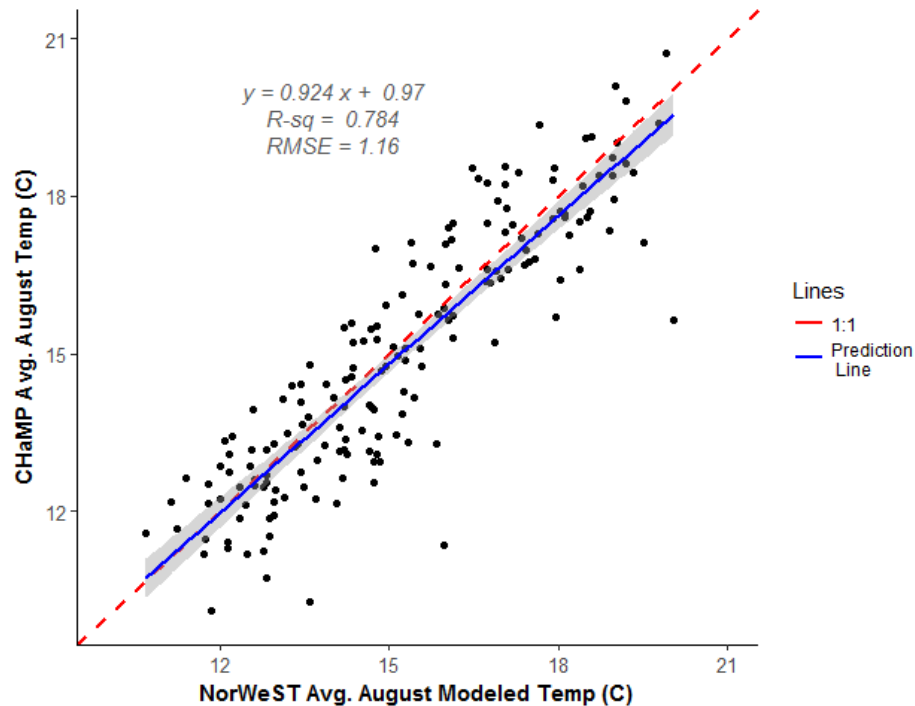


Figure 13. CHaMP average August temperatures (2011 – 2013) regressed against NorWeST average August water temperatures for matching years.

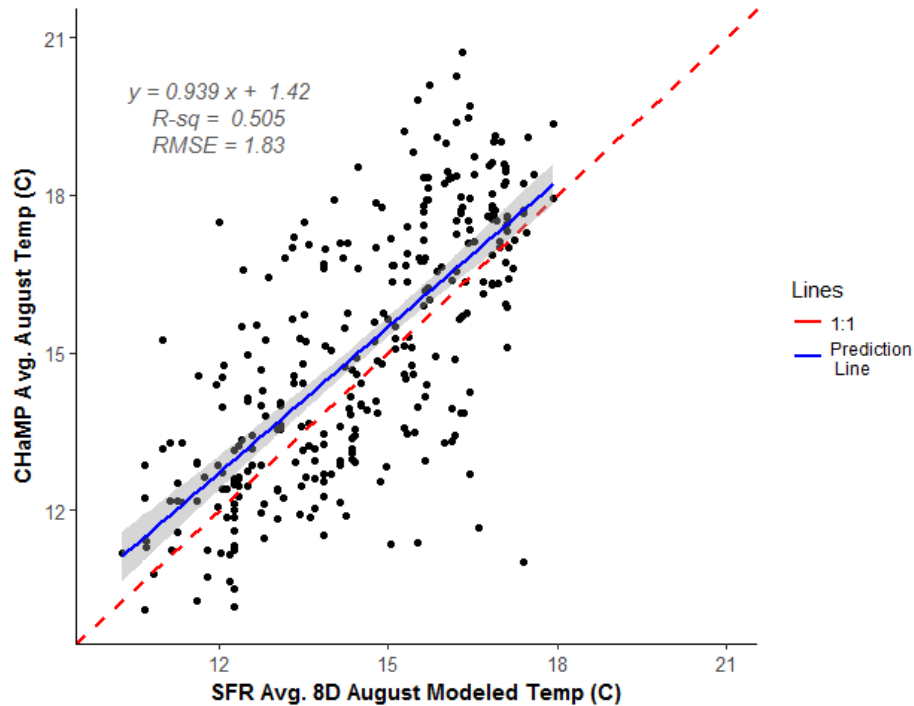


Figure 14. CHaMP average August temperatures (2011 – 2013) regressed against SFR average 8D August water temperatures for matching years.

Models were evaluated primarily using Akaike’s Information Criterion (AIC). For each of the two evaluated stream temperature models (NorWeST and SFR) the combination of explanatory variables that provided the best-fitting model varied. The best-fitting model for the NorWeST data included the covariate of year in addition to the modeled NorWeST average August modeled temperature as an explanatory variable ($R^2 = 0.815$, $\Delta AIC = 0$). For the SFR model, the best-fitting model included only the modeled SFR average 8D August modeled temperature as an explanatory variable ($R^2 = 0.49$, $\Delta AIC = 0$).

We selected the NorWeST model as the best candidate to fill gaps in the current CHaMP temperature dataset based on goodness of fit, explained variance, and RMSE. The comprehensive list of possible covariates used in the NorWeST model compared to the SFR model likely played a large role in more accurately predicting stream temperatures within the Upper Grande Ronde Basin (UGRB). Though the SFR model is not suitable for our needs within the UGRB because of the seasonal temperature and hydrologic variability that occurs there, in other parts of the ICRB the SFR model more accurately reflects measured stream temperatures. Unlike the NorWeST model, the SFR model has the added benefit that temperatures are modeled outside of average August, making seasonal analyses possible.

References

- Bouwes, N., Moberg, J., Weber, N., Bouwes, B., Beasley, C., Bennett, S., Hill, A.C., Jordan, C.E., Miller, R., Nelle, P. and Polino, M., 2011. Scientific protocol for salmonid habitat surveys within the Columbia Habitat Monitoring Program. Prepared by the Integrated Status and Effectiveness Monitoring Program and published by Terraqua, Inc., Wauconda, Washington. Inc., Wauconda, WA.
- Isaak, D.J., Wenger, S.J., Peterson, E.E., Ver Hoef, J.M., Hostetler, S., Luce, C.H., Dunham, J.B., Kershner, J., Roper, B.B., Nagel, D. and Horan, D., 2011. NorWeST: an interagency stream temperature database and model for the Northwest United States. US Fish and Wildlife Service, Great Northern Landscape Conservation Cooperative Grant. Project website: [www. fs. fed. us/rm/boise/AWAE/projects/NorWeST. html](http://www.fs.fed.us/rm/boise/AWAE/projects/NorWeST.html).
- McNyset, K.M., Volk, C.J. and Jordan, C.E., 2015. Developing an Effective Model for Predicting Spatially and Temporally Continuous Stream Temperatures from Remotely Sensed Land Surface Temperatures. *Water*, 7(12), pp.6827-6846.

Mapping Restoration Intensity

Introduction

With the decline of endangered salmon populations in the Columbia basin and uncertainty associated with the extent that tributary restoration actions can significantly help recover populations, it is important to evaluate the influence of habitat restoration on fish habitat at appropriate spatial and temporal scales. Evaluating stream restoration projects at tributary and watershed scales, as opposed to the common practice of evaluating restoration effectiveness at individual restoration sites, can offer insights into habitat actions required to address limiting factors for freshwater salmon production.

In 2015 we finalized work on compiling restoration project data for the upper Grande Ronde River watershed (McCullough et al. 2015). While the restoration database reports several types of activities (e.g., channel reconstruction, riparian planting and fencing, fish passage improvements, etc.), in 2016 we investigated an application of large woody debris (LWD) additions. For this portion of the project, our overarching question was: do previous LWD additions explain the observed quantity of LWD along the river network? If so, this would indicate that natural LWD recruitment rates alone are not enough to support the currently observed LWD frequencies in the upper Grande Ronde River and Catherine Creek.

Methods

From a variety of sources (Table 13), nearly 4500 project sites were listed as separate records, displaying available project information per site available from data sources. Project activities were categorized into actions and sub-categories (e.g., action: enhancing instream complexity, sub-category: large woody debris addition). Data on restoration activities was first stored in an MS Excel spreadsheet, which provided the flexibility to modify data input and create new data when new types of information were encountered in restoration project descriptions. After all known sources of information were collected and the information or created data underwent quality control and quality assurance procedures, a geodatabase was created to convert and store the data for future use. We used an ArcGIS Personal Geodatabase, which uses MS Access as the database structure. This allowed us to create spatial data on site locations and to create stand-alone attribute tables of hierarchical data groupings (e.g., information on restoration projects, which are composed of multiple work sites; or information on individual work sites, which comprise individual projects). The ArcGIS database structure can be joined to the spatial data for mapping or analysis. Because the data are stored in a relational MS Access database, queries and reports can be initiated using the Access features of the database. Detailed metadata tables were also created.

Table 13. Data sources for restoration project information in the upper Grande Ronde River Subbasin. Values for total number of unique work sites indicate number of restoration work sites reported by a specific source that were not already reported by another source.

Agency	Source	Data Archive	Year Range	Total Number Of Unique Work Sites
Oregon Watershed Enhancement Board	oregonexplorer.info	Oregon Watershed Restoration Inventory	1992-2013	3837
Grande Ronde Model Watershed	Mason Bailie & grmw.org/projectdb	Grande Ronde Model Watershed Project Database	1987-2013	348
National Oceanic and Atmospheric Administration	Monica Diaz	Pacific Northwest Salmon Habitat Project Database	1986-2012	174
Oregon Department of Fish and Wildlife Grande Ronde Watershed District	Winston Morton	Grande Ronde Fish Habitat Database	1985-2012	32
Bureau of Land Management, Vale District	blm.gov/or/gis/data.php	Interagency Restoration Database	1993-2014	20
The Confederated Tribes of the Umatilla Indian Reservation	Les Naylor	CTUIR Fish Accord Habitat Projects, Limiting Factors and Accomplishments 2008-2014 project information spreadsheets	2008-2014	13
The Freshwater Trust, Flow Restoration for Northeast Oregon	Aaron Maxwell	Freshwater Trust Accomplishments Reports	2013-2014	10
U.S. Forest Service, Wallowa-Whitman National Forest	Kayla Morinaga & Joe Platz	2010-2012 La Grande Ranger District Aquatics Program Accomplishment Reports & Wallowa-Whitman National Forest La Grande Ranger District Restoration Projects within the Grande Ronde River Watersheds (2008-2014) & (1988-2008) project information spreadsheets	1988-2014	8
Bonneville Power Administration	cbfish.org	Taurus Database	1984-2014	6
National Oceanic and Atmospheric Administration	map.critfc.org/flexviewers/pcsrfttribal	Pacific Coastal Salmon Recovery Fund	2005-2011	1
Total Work Sites			1984-2014	4449

To address the question of whether previous LWD additions explain the observed quantity of LWD along the river network, we needed to (1) find a common unit of measurement for LWD in the restoration database, since practitioners reported metrics in several inconsistent ways (e.g., miles of LWD added, number of LWD pieces, or number of LWD structures); (2) extrapolate the common metric to all sites reporting LWD additions; (3) account for the loss of LWD over time from degradation or downstream transport; and (4) establish an empirical relationship between the amount of LWD added over time with the amount of LWD observed at or near CHaMP sites.

We first needed to establish a metric that could act as a common denominator among several metrics. Among the 163 LWD projects in the database, the most commonly reported metric was miles treated with LWD (MIsLWD). In cases where the miles treated with LWD was unknown, we extrapolated using the relationship between maximum extent of restoration project (MaxMIs) and miles treated with LWD: $MIsLWD = 0.21 + 0.85 \times MaxMIs$ ($R^2 = 0.75$, $p\text{-value} < 0.001$, $n = 96$). We converted MIsLWD to number of pieces of LWD (NLgPcs) based on a linear relationship between co-occurrences between metrics, with intercept set to zero: $NLgPcs = MIsLWD \times 196.09$ ($R^2 = 0.83$, $p\text{-value} < 0.001$, $n = 12$).

Next, because our restoration database documented projects as early as 1986, we needed to estimate the rate at which LWD would be retained over several decades. We used data from a literature review (Philip Roni et al. 2015) tabulating the number of retained vs. unretained pieces of LWD from individual restoration projects across a range of years. After removing several studies that defined functional LWD as anything other than “retained,” a total of 12 instances were used in a logistic regression (GLM) with quasibinomial errors. After applying extrapolations of LWD additions to restoration sites and the decay function for wood retained over time, we compared the amount of LWD added by restoration practitioners to the observed LWD at CHaMP sites using linear regression.

Results and Discussion

A GIS map of restoration projects provides the opportunity for analyzing the distribution of restoration activity throughout the watershed in relation to other landscape features such as ecoregions, topography, and landowner type. To demonstrate the scope of restoration work conducted across the landscape from 1986-2014, we mapped all 705 restoration projects excluding those reporting only invasive plant treatments (Figure 15). Regardless of land owner type, restoration work was extensive across all fish-bearing streams in the Upper Grande Ronde and Catherine Creek. With the exception of a few isolated headwater sections, restoration work of one type or another was ubiquitous.

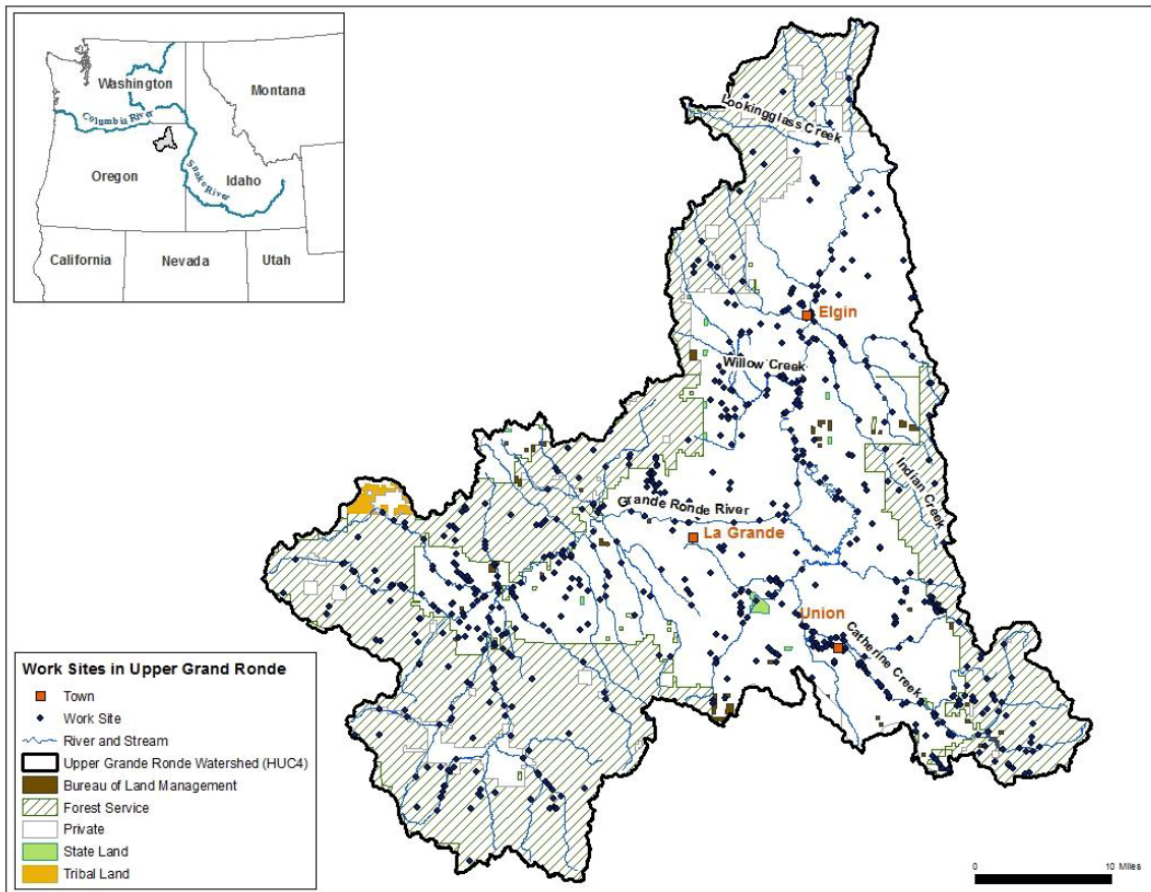


Figure 15. Map of the 705 restoration work sites completed in the upper Grande Ronde River sub-basin between 1986 and 2014. Invasive plant treatments are excluded from map.

For nearly all restoration activity types, there is little consistency among the metrics reported (Table 14). For example, out of 27 water lease/purchase projects, 10 reported the amount (in cubic feet per second) of water rights acquired, 8 reported acres of land pertaining to the water acquisition, and 8 reported the dates of instream acquisition. Out of 36 boulder addition projects, 36 reported miles of boulders added, 2 reported acres of boulders, 5 reported number of boulder structures, and 11 reported number of boulders, with some overlap among metrics. An effort by regional partners to establish consistent metrics for restoration projects would greatly assist a programmatic approach to restoration assessment.

Table 14. Number of restoration projects and work sites by action and sub-category, and the number of times each project has an associated metric measurement reported (labeled No. Instances Metric Reported). The total number of work sites and projects are less than the sums of No. of Work Sites and No. Projects columns because multiple restoration activities were conducted at several projects.

Action	Sub-Category	No. Projects	No. of Work Sites	Metric	No. Instances Metric Reported by Project
Fish Passage	Diversion Screening	17	17	Cubic Feet per Second Diverted	15
				Number of Passage Improvements	3
	Removal of Barriers	67	84	Miles Unblocked Stream	34
				Number of Passage Improvements	59
Instream Structures	Large Woody Debris Additions	127	160	Miles Large Woody Debris	96
				Log Weirs (# Installed)	9
				Acres Large Woody Debris	8
				Number Logs Pieces	31
				Number Logjam Structures	25
	Bank Stabilization	78	97	Miles Streambank Stabilization	68
				Acres Streambank Stabilization	8
				Jetties, Barbs (Number of)	15
				Rock Weirs, Cross Veins (Number of)	15
	Boulder Addition	36	46	Miles Boulders	25
				Acres Boulders	2
				Number Boulder Structures	5
				Boulders (Number of)	11
	Beaver Activity Observed	1	1		0
	Engineered Pools	8	9	Number Pools Created	4
	Modification/Removal of Bank Armoring	0	0		0
	Nutrient Addition	0	0		0
Off-Channel / Floodplain	Levee Set-Back or Removal	13	13	Acres Riparian Habitat Created	1
				Miles of Dike Removal or Modification Riparian	2
	Floodplain Reconnection or Creation	36	36	Miles Floodplain Restored	16
				Acres Floodplain Restored	15
	Remeandering	28	39	Acres Channel Reconfiguration	2
				Miles Channel Reconfiguration	16
				Miles Main Channel Created	9
	Side-Channel/Alcove Construction	15	22	Acres Side Channel Created	1
				Miles Side Channel Created	8
				Backwater Alcoves in Feet	4
				New Spring/Tributary Channels in Feet	2
	Thermal Refugia	1	1		0
	Wetland Restoration	19	25	Acres Wetland Habitat Restored	11
Riparian Improvement	Installed Fencing	189	227	Stream Miles Fenced	151
				Planting Miles Fenced	6

Action	Sub-Category	No. Projects	No. of Work Sites	Metric	No. Instances Metric Reported by Project	
	Planting	180	215	Upland Miles Fenced	4	
				Average Buffer Width Fencing	4	
				Riparian Acres Protected by Fencing	144	
				Upland Acres Protected by Fencing	16	
				Acres Wetland Habitat Protected by Fencing	2	
				X-Fencing (Number of)	19	
				Number Plants Planted	25	
				Riparian Miles Planted and/or Seeded	123	
				Acres Riparian Planted and/or Seeded	99	
				Upland Miles Planted and/or Seeded	5	
	Acres Upland Planted and/or Seeded	17				
	Wetland Acres Planted and Seeded	4				
	Seeding in Pounds	18				
	Sedge/Rush Mats in Feet	5				
	Invasive Plant Removal	17	3762	Miles Upland Invasive Control	0	
				Miles Riparian Invasive Control	12	
				Acres Riparian Invasive Control	11	
				Acres Upland Invasive Control	8	
	Sediment Reduction / Addition	Road Decommissioning	54	73	Feet Average Buffer Width Road Obliteration	3
					Miles of Trail/Road Recontoured/Removed	45
Miles Trail/Road Recontoured/Removed Upland Acres Road Obliterated					8	
Improving Agricultural/Forestry Practices		77	109	Acres Improved Agriculture	57	
Spawning Gravel Addition		5	5	Miles Treated Spawning Gravel	2	
Acquisition & Protection	Land Acquisition, Lease, or Easement	54	56	Acres of Acquisition, Lease, or Easement	31	
				Stream Miles of Acquisition, Lease, or Easement	32	
				Years out Acquisition, Lease, or Easement	2	
				Flow Augmentation	Water Lease or Purchase	27
Acres of Acquisition, Lease, or Easement Pertaining to Water Lease or Purchase	8					
Instream Dates	8					
Irrigation Improvements	12	15	Acres Improved Irrigation		1	
Mitigate Point Source Impacts	4	4	Miles Toxic Cleanup		1	
			Acres Toxic Cleanup	1		
		546	4449	Site Length	380	
		546	4449	Site Acres	316	

Our attempt to establish an empirical relationship between LWD added in restoration projects and LWD observed at CHaMP sites revealed several insights. In our re-analysis of studies reviewed by (Philip Roni et al. 2015), we established that LWD is retained at sites for approximately 40 years (Figure 16, $p < 0.001$, residual deviance = 162.89 on 10 *d.f.*), and therefore expectations of benefit from restoration for fish should account for this retention rate. This finding is in contrast to the predictions by (P. Roni et al. 2002), who suggested the duration of LWD effectiveness would range from 5-20 years. Our model of LWD retention predicts that after 20 years, approximately 60% of LWD would be retained at a site. The relationship we established between restoration project and age was used to estimate the amount of LWD remaining from past restoration activities across the entire river network and adjacent to individual CHaMP sites.

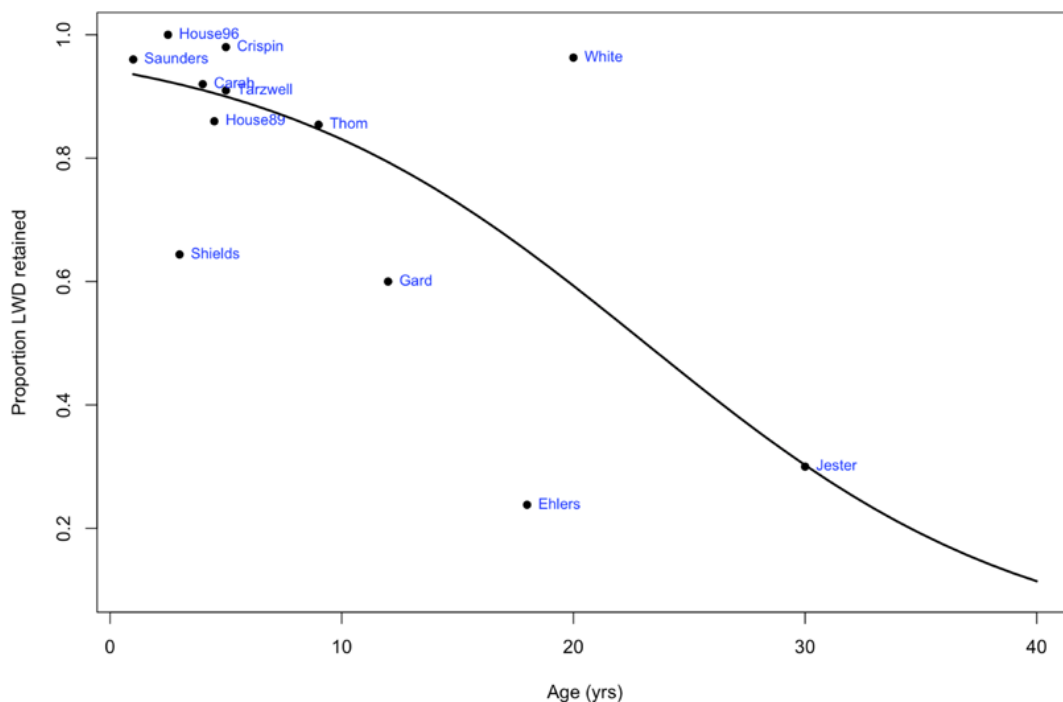


Figure 16. Relationship between proportion of LWD retained and age in years from 12 studies reviewed in Roni et al. (2015) (logistic regression $p < 0.001$, residual deviance = 162.89 on 10 *d.f.*).

We established a relationship between LWD added through restoration projects and LWD measured at CHaMP sites (Figure 17). Linear regression revealed the relationship was significant, and that LWD additions explained 27% of the variation in LWD frequencies at CHaMP sites: $LWD_{CHaMP} = 22.53 + 0.88 \times LWD_{Restoration}$ ($R^2 = 0.27$, $p\text{-value} < 0.001$, $n = 37$). Without this understanding that roughly a quarter of all LWD observed along the river network is attributable to past restoration actions, models attempting to explain the relationship between LWD and factors associated with natural wood recruitment alone (e.g., riparian canopy density) would be ignoring a major source of variability.

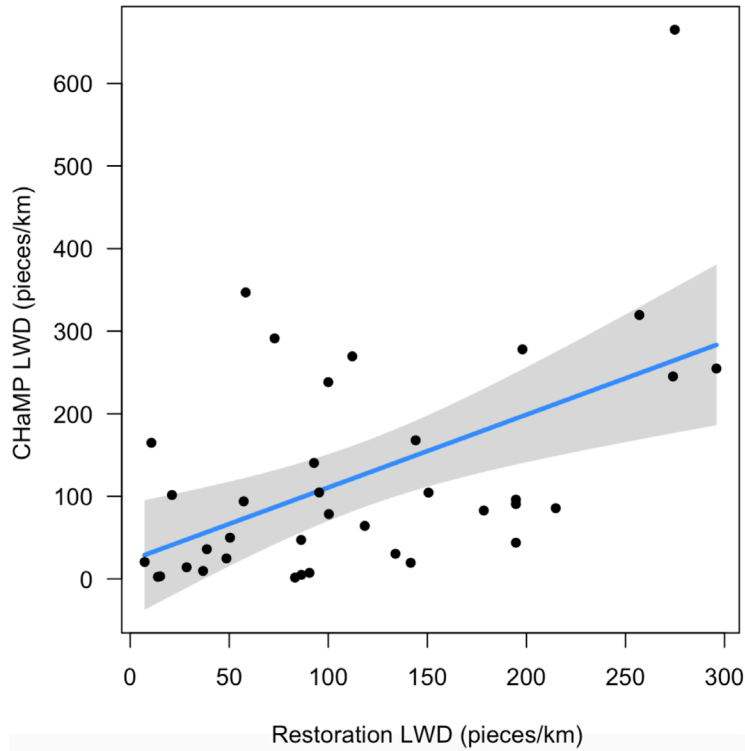


Figure 17. Relationship between CHaMP LWD and restoration LWD (linear regression $R^2 = 0.27$, p -value < 0.001, $n = 37$).

Our work compiling restoration activities from various sources across several decades (Table 13) and throughout the entire Upper Grande Ronde watershed (Figure 15) demonstrates that site-specific assessments of restoration may not be adequate if the desired outcome is describing restoration across the riverscape. Site-specific assessments using a before-after-treatment-control (BACI) design, for example, ignore the extensive history of restoration in the basin and fail to acknowledge a landscape perspective of restoration effectiveness monitoring.

References

- McCullough, D.A., S.M White, C. Justice, M. Blanchard, R. Lessard, D. Kelsey, D. Graves, and J. Nowinski. 2015. Assessing the Status and Trends of Spring Chinook Habitat in the Upper Grande Ronde River and Catherine Creek. Annual Report to Bonneville Power Administration. Portland, OR: Columbia River Inter-Tribal Fish Commission.
- Roni, P., T.J. Beechie, R.E. Bilby, F.E. Leonetti, M.M. Pollock, and G.R. Pess. 2002. A Review of Stream Restoration Techniques and a Hierarchical Strategy for Prioritizing Restoration in Pacific Northwest Watersheds. *North American Journal of Fisheries Management* 22 (1): 1–20. doi:10.1577/1548-8675(2002)022<0001:AROSRT>2.0.CO;2.
- Roni, Philip, Tim Beechie, George Pess, Karrie Hanson, and Bror Jonsson. 2015. Wood Placement in River Restoration: Fact, Fiction, and Future Direction. *Canadian Journal of Fisheries and Aquatic Sciences* 72 (3): 466–78. doi:10.1139/cjfas-2014-0344.

RTK Survey of CHaMP Benchmarks

Benchmarks are semi-permanent survey markers used in the Columbia Habitat Monitoring Program (CHaMP) to establish the coordinate system at each survey site. By re-occupying site benchmarks during a survey, surveyors are able to measure precise changes in stream channel topography over time. However, because the benchmark coordinates were originally established using a handheld global positioning system (GPS) with a high degree of error (5-15 m), topographic survey data from CHaMP can't be merged with other high-accuracy spatial data such as Light Detection and Ranging (LiDAR), forward looking infrared (FLIR) imagery, geo-rectified aerial photos, and stream and floodplain surveys collected by other agencies in the basin. In addition, if CHaMP benchmarks are lost or compromised, surveyors are unable to re-occupy the original coordinate system, and thereby lose the ability to measure changes in channel topography over time. To address these issues, we used real time kinematic (RTK) satellite navigation equipment (Topcon Hiper II and V, Sokkia GCX2) to obtain high-accuracy geographic coordinates at benchmarks located at a subset of CHaMP sites in the Upper Grande Ronde River and Catherine Creek basins during summer of 2016. These high-accuracy benchmark coordinates were then used to transform the CHaMP topographic data collected between 2011 and 2016 to conform more closely with the true stream channel and landscape topography. The results from this work serve two primary functions: 1) CHaMP data that has been transformed using RTK benchmark coordinates can be merged with spatial data collected by other agencies in the basin, thereby increasing our ability to accurately describe status and trends in stream habitat conditions, and 2) High accuracy topographic data at CHaMP sites ensures that analysis of geomorphic change over time can continue into the future even if CHaMP benchmarks are lost or compromised.

We used a variety of different strategies for RTK setup and surveying depending on the site layout and degree of topographic obstructions and tree cover. Ideally, the RTK base station was set up over a known point (i.e., a survey marker that had been previously established by professional survey crews) that was located at a high point with good exposure to open sky and good radio connectivity to the benchmarks at one or more CHaMP sites. Base station coordinates for RTK surveys were usually based on a static GPS process in which GPS location data at the base were continuously collected for a period of at least 15 minutes (rapid static) and ideally longer than two hours (static). Raw static files were then post-processed using the Online Positioning User Service (OPUS) website (<https://www.ngs.noaa.gov/OPUS/>) to obtain high-accuracy National Spatial Reference System (NSRS) coordinates. In some cases, we used control points from previous professional topographic surveys to serve as base station occupation points for the RTK survey. Control files were obtained from the Confederated Tribes of the Umatilla Indian Reservation (CTUIR) and Anderson Perry and Associates (Allen Childs, CTUIR, personal communication), and LiDAR reports by Watershed Sciences (Watershed Sciences 2007(a), 2007(b), 2009(a), 2009(b), 2009(c), 2013). All coordinates were translated to Universal Transverse Mercator (UTM) format (Datum NAD1983 (2011), Geoid NAVD88 GEOID12B) for consistency with CHaMP data.

After establishing the base location with the RTK, CHaMP benchmark locations were surveyed using either the RTK rover, or a Total Station (Topcon ES), depending on radio connectivity and satellite

coverage. All benchmark locations were surveyed in accordance with the CHaMP accuracy guidelines (i.e., horizontal error ≤ 0.03 , vertical error ≤ 0.015).

A total of 45 base points were surveyed using the static GPS procedure and were subsequently corrected using OPUS (Table 15). Base point processing times (i.e., duration of static data collection) ranged from 18 minutes to 5 hours 6 minutes (mean = 1 hour 49 minutes). Latitude accuracy at base points ranged from 0.002 to 0.066 m (mean = 0.008 m), while longitude accuracy ranged from 0.003 to 0.125 m (mean = 0.013 m). Accuracy of orthometric heights (elevation) ranged from 0.015 to 0.250 m (mean = 0.046 m).

We surveyed a total of 221 benchmarks distributed across 61 CHaMP sites (Table 16). In addition, multiple topographic check points were surveyed with the RTK rover to verify survey accuracy relative to available LiDAR data.

Transformation of CHaMP topographic data using RTK-generated benchmark coordinates was successfully completed at 51 of the 158 CHaMP sites in the Grande Ronde Basin (Table 17). This included transformation of 121 unique site visits (i.e., site and year combinations). Some sites that were surveyed with RTK could not be transformed because fewer than two of the original CHaMP benchmarks were present at the site. An example of the transformed water surface boundary compared with the original water surface boundary at site CBW05583-071770 on the Upper Grande Ronde River is provided in Figure 18. A detailed description of the transformation procedures is provided in Appendix 1.

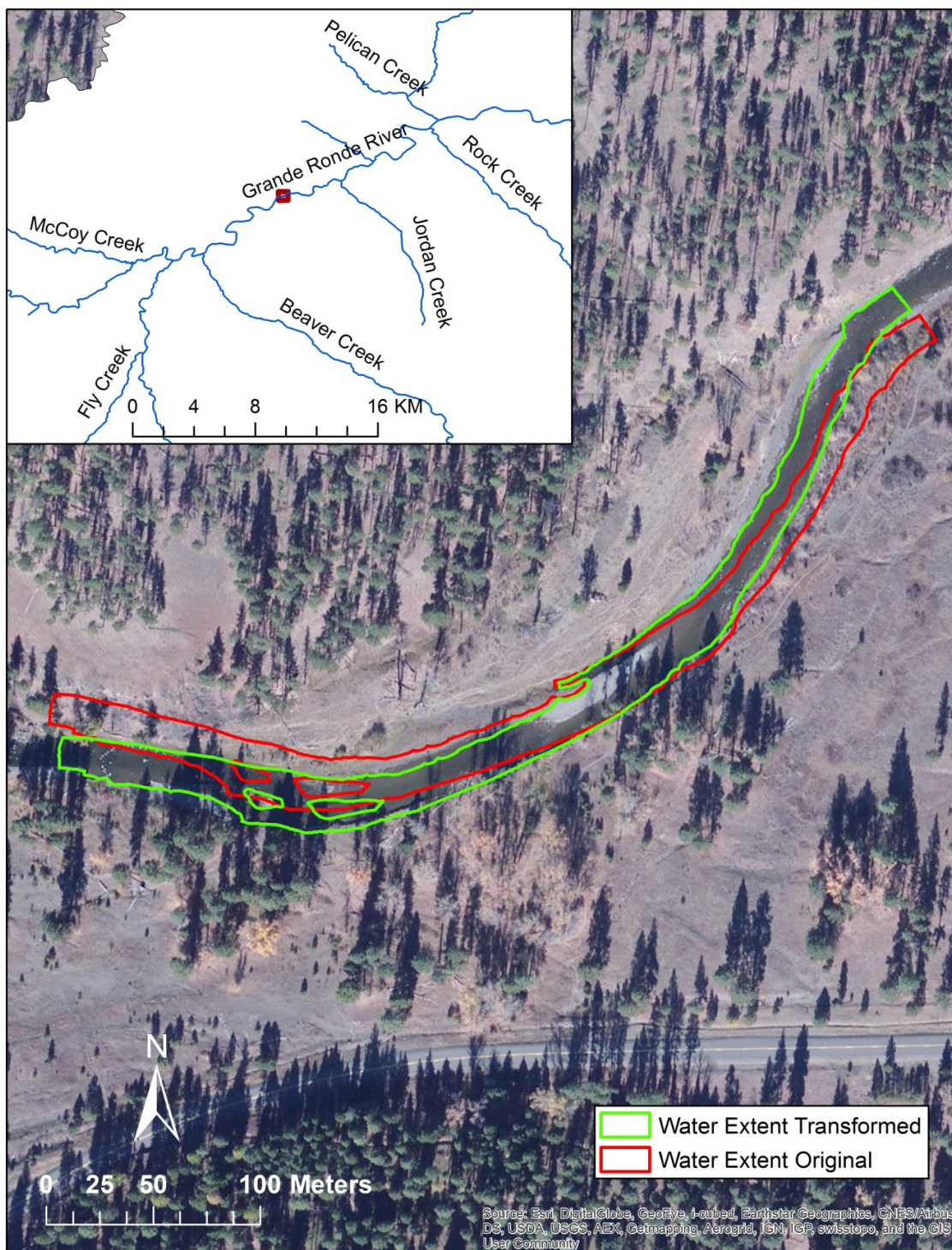


Figure 18. Example of the surveyed water extent at site CBW05583-071770 on the Upper Grande Ronde River using the original coordinate system (red boundary) compared with the RTK-transformed coordinate system (green boundary). Note that the transformed boundary is a much closer match to the aerial basemap imagery.

Table 15. Base station locations used for real time kinematic (RTK) surveys in the Upper Grande Ronde Basin.

Base point	OPUS duration	Solution type	UTM Northing	UTM Easting	Elevation (m)
2007	0.057025463	rapid static	5019578.7	401821.116	936.44
2010	0.199305556	static	5008137.948	392371.259	1229.589
2011	0.180902778	static	5001236.339	390156.35	1563.762
2012	0.1	static	5010700.44	388125.605	1098.35
2020	0.186805556	static	5011526.162	389475.814	1064.212
2021	0.047407407	rapid static	5021476.361	402944.702	925.581
2022	0.018125	rapid static	4993728.526	389232.558	1270.326
2024	0.085416667	static	5017195.212	399040.22	948.004
3003	0.1	static	4990546.049	397472.727	1405.033
3005	0.0665625	rapid static	5018972.212	400413.87	934.824
3024	0.041712963	rapid static	5002474.972	437041.829	917.482
3152	0.085416667	static	5014044.391	392869.993	1014.029
3225	0.0665625	rapid static	5018972.212	400413.871	934.825
5050	0.2125	static	5009009.661	388985.47	1111.563
5058	0.01431713	rapid static	5006256.742	389940.277	1082.116
5060	0.017164352	rapid static	5004036.593	390904.853	1110.711
5068	0.020277778	rapid static	5000489.772	392016.08	1172.22
5089	0.125347222	static	4991036.618	389702.229	1311.812
5100	0.059791667	rapid static	4997886.744	444119.335	1014.668
5106	0.016064815	rapid static	4997818.6	444071.209	1015.593
5107	0.089236111	static	4998147.575	443699.07	1007.53
5130	0.056736111	rapid static	4996784.605	445184.003	1038.003
5135	0.012662037	rapid static	4997564.124	444498.448	1023.032
5138	0.090277778	static	4996400.519	446006.252	1052.372
5152	0.017731481	rapid static	4992617.913	395215.168	1312.625
5154	0.021608796	rapid static	4995374.316	395291.665	1328.73
5158	0.098611111	static	5003778.026	435391.898	890.361
5165	0.024571759	rapid static	5000083.596	440268.839	958.587
5168	0.023368056	rapid static	4997547.126	385686.311	1311.717
5174	0.037800926	rapid static	4988314.619	384637.194	1369.615
5179	0.041724537	rapid static	4989492.328	398446.337	1413.066
5196	0.1625	static	4989149.653	384915.868	1354.272
5216	0.098611111	static	5006797.363	430662.367	839.178
5226	0.109027778	static	5000508.584	438753.226	941.33
5239	0.084027778	static	4996116.718	446809.974	1067.312
5246	0.088194444	static	5006570.09	432175.909	852.205
5256	0.048738426	rapid static	4996376.193	448138.313	1095.11
5261	0.06587963	rapid static	4997365.189	450037.91	1150.137
5268	0.055902778	rapid static	4998314.309	450850.831	1196.272
5273	0.084027778	static	5005240.741	434150.075	873.062
5285	0.138541667	static	4999130.456	450981.36	1301.118
5299	0.090972222	static	4996520.407	449080.444	1114.331

5305	0.066724537	rapid static	4997109.953	444498.296	1034.14
3002_stk	0.027013889	rapid static	4989634.404	398215.186	1409.318
CRITFC_HOUSE	0.097222222	static	5018324.561	415342.253	842.22

Table 16. Real time kinematic (RTK) surveyed control points and topographic check points (code = “ck”) collected in the Upper Grande Ronde and Catherine Creek basins during summer, 2016. CHaMP site names are provided in the Code field along with the original benchmark number.

Name	UTM Northing (m)	UTM Easting (m)	Elevation (m)	Code
5001	5018753.995	400010.861	937.311	dsgn4-000205_2
5002	5018845.175	400014.619	936.399	MOCK000075-BM604
5003	5018931.144	400074.477	935.646	dsgn4-000205_404
5004	5018778.524	400048.005	936.4	mock2012_000075_603
5005	5018748.759	400062.037	938.047	dsgn4-000005-301
5006	5019324.772	401187.398	932.018	420954_2
5007	5019254.105	401128.652	933.249	420954_1
5008	5019329.223	401121.367	931.626	420954_403
5009	5017205.749	397185.116	954.545	071770_301
5010	5017153.904	396971.105	955.344	071770_303
5011	5017359.024	396945.263	986.317	071770_302
5012	5017282.636	396954.254	954.705	MOCK2012_000029_BM609
5013	5017278.855	396986.655	954.462	MOCK2012_000029_BM607
5014	5017243.488	397010.732	955.309	MOCK2012_000029_BM606
5015	5017225.391	397001.453	955.159	MOCK2012_000029_BM608
5016	5013701.018	392862.795	993.838	dsgn4-000245_1
5017	5013731.16	392864.403	995.696	dsgn4-000245_401
5018	5013679.163	392811.021	997.069	dsgn4-000245_301
5019	5013631.535	392922.465	1022.695	dsgn4-000245_302
5020	5021507.665	403662.81	912.882	109658_603
5021	5021560.7	403837.639	920.147	109658_301
5022	5021673.966	403739.91	915.766	109658_302
5023	5011797.556	388863.863	1035.544	514874_201
5024	5011717.08	388827.021	1036.401	514874_202
5025	5011655.372	388895.979	1036.734	514874_203
5026	5012420.485	389605.285	1034.256	252730_609
5027	5012430.29	389621.537	1033.798	252730_608
5028	5012436.323	389643.565	1031.796	252730_1
5029	5012385.077	389640.959	1028.707	252730_607
5030	5012387.301	389667.522	1028.208	252730_502
5031	5012374.516	389625.222	1028.572	252730_3
5032	5013156.308	389369.781	1028.299	015162_202
5033	5013221.581	389381.436	1028.074	015162_201
5034	5013168.698	389314.324	1028.185	015162_203
5035	5013201.107	390535.702	1018.833	000213_403
5036	5013233.682	390611.858	1018.242	000213_302
5037	5013138.329	390615.987	1018.91	000213_1

Name	UTM Northing (m)	UTM Easting (m)	Elevation (m)	Code
5038	5011977.157	391183.099	1012.105	269114_1
5039	5011871.438	391184.016	1013.885	269114_401
5040	5011908.878	391170.512	1013.097	269114_2
5041	5010911.704	390905.796	1022.584	dsgn4-000202_1
5042	5010928.886	390851.441	1020.951	dsgn4-000202_301
5043	5010866.5	390806.816	1021.546	dsgn4-000202_302
5044	5010840.819	390782.997	1028.042	dsgn4-000202_2
5045	5010810.469	390812.17	1022.635	dsgn4-000202_3
5046	5009623.578	390363.638	1038.385	457530_401
5047	5009513.673	390347.285	1037.076	457530_2
5048	5009406.452	390394.86	1038.228	457530_3
5049	5009576.804	390398.677	1037.006	457530_1
5050	5009009.661	388985.47	1111.563	CRITFC_CTRL_AL_CAP
5051	5007501.03	390657.531	1053.937	031546_303
5052	5007605.201	390659.547	1053.363	031546_302
5053	5007661.136	390608.669	1052.89	031546_301
5054	5007451.411	390670.136	1057.497	ck
5055	5006742.75	390025.695	1082.294	506682_201
5056	5006710.209	390017.149	1083.475	506682_203
5057	5006713.416	390056.439	1072.149	506682_202
5058	5006256.772	389940.279	1082.139	092986_2
5059	5006220.99	389920.427	1082.777	092986_3
5060	5004036.609	390904.858	1110.734	486202_202
5061	5001119.372	391868.31	1160.009	235322_3
5062	5001150.411	391839.369	1159.911	ck
5063	5001193.68	391786.969	1159.172	ck
5064	5001156.925	391747.202	1157.016	235322_401
5065	5001168.038	391730.437	1156.581	ck
5066	5001199.812	391722.85	1156.901	235322_1
5067	5001137.824	391716.135	1159.093	235322_402
5068	5000489.784	392016.07	1172.244	370490_301
5069	5000500.143	392027.273	1171.167	ck
5070	5000342.339	392165.166	1173.217	ck
5071	5000487.09	392022.088	1172.295	370490_601
5072	4999651.723	392715.049	1184.828	321338_3
5073	4999590.942	392676.494	1192.456	321338_2
5074	4999576.803	392752.862	1191.831	321338_401
5075	4999539.162	392733.34	1188.13	ck
5076	4999592.703	392735.342	1187.111	ck
5077	4998655.072	392560.318	1205.184	000277_202
5079	4998752.091	392579.041	1205.035	ck
5080	4998803.705	392584.975	1204.404	ck
5081	5010285.365	387032.524	1055.577	285498_204
5082	5010318.016	387192.885	1054.737	285498_203

Name	UTM Northing (m)	UTM Easting (m)	Elevation (m)	Code
5083	5010363.233	387269.199	1067.981	285498_202
5084	5010301.931	387280.365	1054.566	285498_201
5085	5010458.697	386095.617	1068.581	498490_201
5086	5010488.269	386068.636	1069.325	498490_203
5087	5010510.343	386097.907	1070.989	498490_202
5088	5000408.371	392178.785	1182.581	370490_303
5089	4991036.618	389702.229	1311.812	CRITFC_CTRL_AL_CAP
5090	4990380.263	389589.562	1324.183	000006_1
5091	4990404.486	389605.944	1323.974	000006_2
5092	4990381.895	389626.395	1324.159	000006_3
5093	4990354.94	389615.463	1324.758	ck
5094	4990402.982	389614.271	1323.934	ck
5095	4989150.812	389500.1	1357.772	294202_303
5096	4989152.281	389469.102	1358.494	294202_302
5097	4989193.631	389487.893	1356.217	294202_301
5098	4987975.333	389428.469	1402.864	CRITFC_CTRL_PL_CAP
5099	4987913.57	389484.646	1424.877	CRITFC_CTRL_PL_CAP
5101	4997932.58	444094.721	1014.483	dsgn4-000010_402
5102	4997848.828	444126.808	1015.18	dsgn4-000010_301
5103	4997885.113	444194.067	1016.914	dsgn4-000010_1
5104	4997913.235	444187.048	1015.955	dsgn4-000010_601
5105	4997924.105	444184.677	1016.015	dsgn4-000010_3
5108	4998104.555	443698.144	1008.162	CRITFC_CTRL_AL_CAP
5109	4998109.527	443666.149	1007.679	ORW03446-071176_301
5111	4998032.445	443670.259	1009.067	ORW03446-071176_303
5112	4998062.408	443608.268	1015.826	ORW03446-071176_302
5114	4998210.053	443797.821	1007.547	CBW05583-417962_203
5115	4998221.738	443766.104	1007.262	CBW05583-417962_201
5116	4998242.917	443783.797	1006.644	CBW05583-417962_202
5122	5001968.909	437209.531	915.262	CBW05583-491690_503
5123	5002028.532	437188.365	914.76	CBW05583-491690_501
5124	5001990.531	437125.141	915.348	CBW05583-491690_502
5126	4997647.57	444503.795	1032.803	CBW05583-325034_301
5128	4997580.175	444558.298	1036.757	CBW05583-325034_303
5131	4996796.859	445192.758	1038.328	CBW05583-456106_402
5132	4996798.607	445189.619	1038.418	CBW05583-456106_2
5135	4996857.572	445103.26	1036.158	CBW05583-456106_401
5136	4996886.18	445147.072	1037.13	CBW05583-456106_1
5136_0	4997561.687	444475.579	1022.446	CBW05583-325034_302
5137	4996809.74	445235.543	1038.353	CBW05583-456106_3
5142	4989964.284	397834.506	1404.999	dsgn4-000009_203
5143	4989991.976	397761.624	1404.323	dsgn4-000009_1
5145	4989991.013	397782.871	1404.005	dsgn4-000009_BOS
5146	4990000.173	397812.236	1405.008	dsgn4-000009_302

Name	UTM Northing (m)	UTM Easting (m)	Elevation (m)	Code
5147	4990216.725	397709.102	1405.227	CBW05583-280042_401
5148	4990164.838	397672.633	1402.465	CBW05583-280042_3
5149	4990115.933	397638.078	1404.293	CBW05583-280042_1
5152	4992617.913	395215.168	1312.625	CRITFC_CTRL_AL_CAP
5155	4995403.531	395320.686	1327.201	CBW05583-108010_2
5156	4995313.314	395353.764	1327.068	CBW05583-108010_402
5157	4995290.954	395296.232	1324.633	CBW05583-108010_BOS
5160	5004005.118	435383.134	889.304	CBW05583-278698_303
5161	5003887.521	435308.342	889.274	CBW05583-278698_302
5162	5002451.27	436717.621	908.193	CBW05583-147626_301
5163	5002596.435	436806.007	908.193	CBW05583-147626_303
5164	5002549.018	436880.371	909.525	CBW05583-147626_302
5165	5000083.596	440268.839	958.587	ORW03446-137980_202
5166	5000056.89	440301.663	959.117	ORW03446-137980_203
5169	4997757.286	385832.757	1319.256	dsgn4-000094_3
5170	4997797.414	385791.546	1308.896	dsgn4-000094_504
5171	4997809.566	385735.14	1313.304	dsgn4-000094_2
5172	4997858.042	385803.744	1308.848	dsgn4-000094_1
5175	4988331.567	384624.615	1369.573	CRITFC_CTRL_AL_CAP
5177	4988224.068	384581.333	1371.789	CBW05583-228666_3
5180	4989440.305	398352.563	1411.799	CBW05583-099818_301
5181	4989479.923	398396.391	1413.21	CBW05583-099818_303
5182	4989436.412	398429.396	1415.316	CBW05583-099818_302
5183	4990187.176	397605.735	1404.926	CBW05583-280042_402
5184	4992646.391	395151.238	1311.371	CBW05583-468458_303
5185	4992621.116	395131.438	1310.144	CBW05583-468458_302
5186	4992645.319	395113.306	1309.61	CBW05583-468458_301
5187	4995328.346	395282.268	1326.883	CBW05583-108010_3
5188	4995282.806	395285.27	1324.45	CBW05583-108010_401
5189	4990152.487	390128.903	1333.594	ORW03446-159368_202
5190	4990102.815	390085.779	1333.948	ORW03446-159368_504
5191	4990138.266	390086.657	1333.446	ORW03446-159368_501
5192	4990113.616	390131.947	1334.065	ORW03446-159368_203
5197	4989140.967	384917.359	1354.436	CBW05583-490810_401
5199	4989088.131	384912.4	1356.055	CBW05583-490810_2
5200	4989106.054	384878.558	1355.472	CBW05583-490810_1
5201	4989852.279	385055.07	1343.783	CBW05583-335162_201
5202	4989870.651	385017.574	1343.799	CBW05583-335162_203
5203	4989878.266	385015.419	1343.685	CBW05583-335162_501
5204	4989884.478	385050.59	1343.737	CBW05583-335162_202
5205	4990624.172	385379.11	1333.113	CBW05583-138554_3
5206	4990639.42	385427.964	1332.697	CBW05583-138554_2
5207	4990673.749	385416.723	1331.961	CBW05583-138554_1
5208	4990700.602	385431.737	1331.516	CBW05583-138554_401

Name	UTM Northing (m)	UTM Easting (m)	Elevation (m)	Code
5209	4998654.997	392558.109	1205.463	dsgn4-000277_602
5210	4998772.425	392530.264	1202.448	dsgn4-000277_1
5211	4998735.738	392577.791	1205.131	dsgn4-000277_3
5212	5000333.887	392047.831	1173.234	CBW05583-370490_302
5214	5004023.535	390866.831	1111.373	CBW05583-486202_203
5215	5004007.488	390898.724	1113.926	CBW05583-486202_201
5217	5006881.158	430587.741	838.559	CBW05583-430250_401
5218	5006904.057	430602.042	838.818	CBW05583-430250_3
5219	5006871.392	430561.962	838.338	CBW05583-430250_1
5220	5006937.467	430621.585	839.414	CBW05583-430250_2
5223	5006788.16	430934.156	840.979	CBW045583-217258_2
5224	5006797.645	430903.507	840.012	CBW045583-217258_401
5225	5006824.037	430881.569	840.076	CBW045583-217258_1
5227	5000564.917	439052.455	964.466	CBW05583-311466_301
5228	5000556.769	439118.136	956.858	CBW05583-311466_302
5229	5000595.923	439198.647	962.432	CBW05583-311466_305
5232	5000508.185	439064.952	942.956	CBW05583-311466_303
5233	5000522.923	439151.646	944.793	CBW05583-311466_304
5234	5000045.626	440248.472	958.504	CRITFC_CTRL_AL_CAP
5235	5000072.733	440179.504	963.173	ORW03446-137980_201
5236	4996423.716	445933.333	1055.341	CBW05583-527786_3
5237	4996393.983	445924.011	1050.962	CBW05583-527786_2
5238	4996407.2	445898.682	1050.475	CBW05583-527786_1
5242	4996106.683	446825.066	1067.701	CBW05583-036266_301
5244	4996058.303	446811.078	1089.013	CBW05583-036266_302
5245	4996095.255	446882.977	1068.226	CBW05583-036266_303
5247	5006598.791	432122.902	851.457	dsgn4-000204_301
5251	5006598.811	432116.384	851.352	dsgn4-000204_203
5252	5006613.594	432134.857	850.747	dsgn4-000204_2
5253	5006612.262	432096.813	850.103	dsgn4-000204_201
5255	5006595.282	432075.059	850.428	dsgn4-000204_302
5257	4996366.632	448118.311	1094.829	CBW05583-368042_1
5259	4996388.875	448170.83	1095.138	CBW05583-368042_3
5260	4996339.106	448165.224	1095.288	CBW05583-368042_2
5264	4997214.023	449929.756	1145.384	CBW05583-138666_2
5265	4997210.232	449903.342	1144.436	CBW05583-138666_3
5267	4997182.283	449903.7	1143.276	CBW05583-138666_1
5269	4998305.515	450867.41	1195.536	CBW05583-531882_501
5271	4998318.748	450895.033	1196.038	CBW05583-531882_203
5272	4998283.585	450894.054	1195.562	CBW05583-531882_202
5274	5004737.603	434475.167	878.67	CBW05583-340318_202
5275	5004691.718	434482.97	878.95	CBW05583-340318_203
5276	5004718.348	434428.151	878.167	CBW05583-340318_201
5277	5005021.408	434120.531	889.341	CBW05583-405674_302

Name	UTM Northing (m)	UTM Easting (m)	Elevation (m)	Code
5278	5005072.777	434110.451	874.482	CBW05583-405674_3
5279	5005128.157	434111.509	873.552	CBW05583-405674_401
5280	5005116.141	434092.956	874.377	CBW05583-405674_2
5281	5005092.738	434160.869	873.65	CBW05583-405674_301
5282	5005229.17	434149.347	873.016	LIDAR_CK
5283	5005199.839	434150.239	873.216	LIDAR_CK
5284	5005156.116	434151.641	873.525	LIDAR_CK
5290	4999093.791	451147.715	1228.864	CBW05583-253354_304
5291	4999121.355	451115.474	1230.273	CBW05583-253354_301
5292	4999132.46	451192.488	1244.409	CBW05583-253354_302
5295	5000214.444	451601.091	1284.775	dsgn4-000168_2
5296	5000203.82	451569.179	1283.835	dsgn4-000168_501
5297	5000189.277	451577.758	1283.583	dsgn4-000168_204
5298	5000180.471	451606.306	1284.771	dsgn4-000168_3
5302	4996749.703	449361.02	1136.487	dsgn4-000001_302
5303	4996714.888	449375.199	1123.034	dsgn4-000001_1
5304	4996776.545	449404.579	1136.152	dsgn4-000001_203
5308	4997206.798	444485.276	1027.973	CBW05583-062890_1
5309	4997169.13	444542.135	1030.832	CBW05583-062890_3
5310	4997219.504	444531.789	1026.535	CBW05583-062890_2
5311	4999088.649	443131.668	993.818	CBW05583-090282_2
5312	4999067.148	443143.232	994.064	CBW05583-090282_1
5313	4999065.176	443144.736	994.717	CBW05583-090282_401
5314	4999069.903	443182.895	994.026	CBW05583-090282_3
5315	4999088.622	443130.147	992.742	CBW05583-090282_402

Table 17. List of CHaMP visits that were successfully transformed using RTK-generated benchmark coordinates.

Organization	Site	Year	Transformation notes
CRITFC	CBW05583-015162	2012	done, used corrected gdb, checked all layers
CRITFC	CBW05583-015162	2015	done, used corrected gdb, checked all layers
CRITFC	CBW05583-031546	2013	done, used corrected gdb, checked all layers
CRITFC	CBW05583-031546	2016	done, used corrected gdb, checked all layers
CRITFC	CBW05583-036266	2013	done, used corrected gdb, checked all layers
CRITFC	CBW05583-036266	2016	done, used corrected gdb, checked all layers
CRITFC	CBW05583-071770	2013	done, used corrected gdb, checked all layers, redid wetted centerline and cross section
CRITFC	CBW05583-071770	2016	done, used corrected gdb, checked all layers
CRITFC	CBW05583-099818	2013	done, used corrected gdb, checked all layers
CRITFC	CBW05583-099818	2016	done, used corrected gdb, checked all layers
CRITFC	CBW05583-108010	2011	done, used corrected gdb, checked all layers, redid wetted centerline and crosssections, didn't actually publish with GIS
CRITFC	CBW05583-108010	2014	done, used corrected gdb, checked all layers
CRITFC	CBW05583-109658	2013	done, used corrected gdb, checked all layers
CRITFC	CBW05583-109658	2016	done, used corrected gdb, checked all layers
CRITFC	CBW05583-138554	2011	done, used corrected gdb, checked all layers, redid wetted/bankfull CL and crosssection
CRITFC	CBW05583-138554	2014	done, used corrected gdb, checked all layers
CRITFC	CBW05583-138666	2011	done, used corrected gdb, checked all layers
CRITFC	CBW05583-138666	2014	done, used corrected gdb, checked all layers
CRITFC	CBW05583-217258	2011	done, used corrected gdb, checked all layers, redid channel units
CRITFC	CBW05583-217258	2014	done, used corrected gdb, checked all layers, fixed cross section ends
CRITFC	CBW05583-235322	2011	done, used corrected gdb, checked all layers
CRITFC	CBW05583-235322	2014	done, used corrected gdb, checked all layers, fixed cross section ends
CRITFC	CBW05583-253354	2013	done, had to redo cross section (missing) but also had to redo wetted/bankfull extent and centerline
CRITFC	CBW05583-253354	2016	done, used corrected gdb, checked all layers
CRITFC	CBW05583-269114	2011	done, used corrected gdb, checked all layers, redid channel units and bf centerline and crosssections
CRITFC	CBW05583-269114	2014	done, used corrected gdb, checked all layers, fixed wetted, centerline, cross section
CRITFC	CBW05583-278698	2013	done, used corrected gdb, checked all layers

Organization	Site	Year	Transformation notes
CRITFC	CBW05583-278698	2016	done, had to redo topo survey because no benchmarks in gdb, checked all layers
CRITFC	CBW05583-280042	2011	done, used corrected gdb, checked all layers, couldn't actually publish
CRITFC	CBW05583-280042	2014	done, used corrected gdb, checked all layers, fixed cross section ends
CRITFC	CBW05583-285498	2012	done, used corrected gdb, checked all layers, redid water extent, centerline, and crosssection
CRITFC	CBW05583-285498	2015	done, used corrected gdb, checked all layers
CRITFC	CBW05583-294202	2013	done, found gdb on external harddrive, checked all layers
CRITFC	CBW05583-294202	2016	done, did not use corrected gdb, checked all layers
CRITFC	CBW05583-311466	2013	done, had to redo cross section (missing) but also had to redo wetted/bankfull extent and centerline
CRITFC	CBW05583-311466	2016	done, used corrected gdb, checked all layers
CRITFC	CBW05583-321338	2011	done, used corrected gdb, checked all layers, couldn't actually publish
CRITFC	CBW05583-321338	2014	done, used corrected gdb, checked all layers, fixed cross section ends
CRITFC	CBW05583-325034	2013	done, had to redo cross section (missing) but also had to redo wetted/bankfull extent and centerline
CRITFC	CBW05583-325034	2016	done, used corrected gdb, checked all layers
CRITFC	CBW05583-335162	2012	done, used corrected gdb, checked all layers
CRITFC	CBW05583-335162	2015	done, used corrected gdb, checked all layers
CRITFC	CBW05583-340138	2012	done, used corrected gdb, checked all layers
CRITFC	CBW05583-340138	2015	done, used corrected gdb, checked all layers
CRITFC	CBW05583-368042	2011	done, used corrected gdb, checked all layers, redid bf centerline and cross sections, within the gdb it says 268042 - just a typo I think
CRITFC	CBW05583-368042	2014	done, used corrected gdb, checked all layers, fixed cross section ends
CRITFC	CBW05583-370490	2013	done, used corrected gdb, checked all layers
CRITFC	CBW05583-370490	2016	done, used corrected gdb, checked all layers
CRITFC	CBW05583-405674	2011	done, used corrected gdb, checked all layers
CRITFC	CBW05583-405674	2012	done, used corrected gdb, checked all layers
CRITFC	CBW05583-405674	2013	done, had to redo cross section (missing) but also had to redo wetted/bankfull extent and centerline
CRITFC	CBW05583-405674	2014	done, used corrected gdb, checked all layers, fixed cross section ends
CRITFC	CBW05583-405674	2015	done, used corrected gdb, checked all layers

Organization	Site	Year	Transformation notes
CRITFC	CBW05583-405674	2016	done, used corrected gdb, checked all layers
CRITFC	CBW05583-417962	2012	done, used corrected gdb, corrected bankfull centerline and crosssection
CRITFC	CBW05583-417962	2015	done, used corrected gdb, checked all layers
CRITFC	CBW05583-430250	2011	done, used corrected gdb, checked all layers, redid bf centerline and cross section
CRITFC	CBW05583-430250	2014	done, used corrected gdb, checked all layers, fixed cross section ends
CRITFC	CBW05583-456106	2011	done, used corrected gdb, checked all layers, redid wetted extent, centerline, and cross section
CRITFC	CBW05583-456106	2014	done, used corrected gdb, checked all layers, fixed cross section ends
CRITFC	CBW05583-457530	2014	done, used corrected gdb, checked all layers
CRITFC	CBW05583-468458	2013	done, had to redo cross section (missing) but also had to redo wetted/bankfull extent and centerline
CRITFC	CBW05583-468458	2016	done, used corrected gdb, looks much better than original tin, checked all layers
CRITFC	CBW05583-490810	2011	done, used corrected gdb, checked all layers, redid wetted extent, centerline, and cross section
CRITFC	CBW05583-490810	2014	done, used corrected gdb, checked all layers, fixed cross section ends
CRITFC	CBW05583-491690	2015	done, used corrected gdb, checked all layers
CRITFC	CBW05583-491690	2016	done, used corrected gdb, checked all layers
CRITFC	CBW05583-498490	2012	done, used corrected gdb, checked all layers
CRITFC	CBW05583-498490	2015	done, used corrected gdb, checked all layers
CRITFC	CBW05583-506682	2012	done, used corrected gdb, checked all layers, redid bankfull extent, centerline, and crosssection
CRITFC	CBW05583-506682	2015	done, used corrected gdb, checked all layers
CRITFC	CBW05583-514874	2012	done, used corrected gdb, checked all layers, redid wetted centerline, crosssections
CRITFC	CBW05583-514874	2015	done, used corrected gdb, checked all layers
CRITFC	CBW05583-531882	2012	done, used corrected gdb, checked all layers
CRITFC	CBW05583-531882	2015	done, used corrected gdb, checked all layers
CRITFC	dsgn4-000010	2011	done, used corrected gdb, checked all layers, wasn't actually able to publish
CRITFC	dsgn4-000010	2012	done, used corrected gdb, checked all layers, redid water extent, centerline, and crosssection
CRITFC	dsgn4-000010	2013	done, had to redo cross section (missing) but also had to redo wetted/bankfull extent and centerline

Organization	Site	Year	Transformation notes
CRITFC	dsgn4-000010	2014	done, used corrected gdb, checked all layers, redid bf cross section
CRITFC	dsgn4-000010	2015	done, used corrected gdb, checked all layers
CRITFC	dsgn4-000010	2016	done, used corrected gdb, checked all layers
CRITFC	dsgn4-000202	2011	done, used corrected gdb, checked all layers
CRITFC	dsgn4-000202	2012	done, used corrected gdb, checked all layers, redid wetted/bankful centerline and crosssection
CRITFC	dsgn4-000202	2013	done, had to redo cross section (missing) but also had to redo wetted/bankfull extent and centerline
CRITFC	dsgn4-000202	2014	done, used corrected gdb, checked all layers, redid bf centerline/cross sections
CRITFC	dsgn4-000202	2015	done, used corrected gdb, checked all layers
CRITFC	dsgn4-000202	2016	done, used corrected gdb, checked all layers
CRITFC	dsgn4-000277	2011	done, used corrected gdb, checked all layers, redid bankful extent, centerline, and cross sections
CRITFC	dsgn4-000277	2012	done, used corrected gdb, checked all layers
CRITFC	dsgn4-000277	2013	done, had to redo cross section (missing) but also had to redo wetted/bankfull extent and centerline
CRITFC	dsgn4-000277	2014	done, used corrected gdb, checked all layers
CRITFC	dsgn4-000277	2015	done, used corrected gdb, checked all layers
CRITFC	dsgn4-000277	2016	done, used corrected gdb, checked all layers
CRITFC	ORW03446-071176	2013	done, had to redo cross section (missing) but also had to redo wetted/bankfull extent and centerline
CRITFC	ORW03446-071176	2016	done, used corrected gdb, checked all layers
CRITFC	ORW03446-137980	2012	done, used corrected gdb, checked all layers
CRITFC	ORW03446-137980	2015	done, used corrected gdb, checked all layers
ODFW	CBW05583-062890	2013	done, used corrected gdb, checked all layers
ODFW	CBW05583-062890	2016	done, used corrected gdb, checked all layers
ODFW	CBW05583-090282	2011	done, used corrected gdb, checked all layers, didn't actually publish
ODFW	CBW05583-090282	2014	done, used corrected gdb, checked all layers
ODFW	CBW05583-092986	2011	done, used corrected gdb, checked all layers
ODFW	CBW05583-092986	2014	done, used corrected gdb, checked all layers, no job file
ODFW	CBW05583-147626	2013	done, used corrected gdb, checked all layers
ODFW	CBW05583-252730	2011	done, used corrected gdb, checked all layers
ODFW	CBW05583-252730	2012	done, used corrected gdb, checked all layers
ODFW	CBW05583-252730	2013	done, used corrected gdb, checked all layers, redid wetted/bankful polygon, cl, and crosssections
ODFW	CBW05583-252730	2015	done, used corrected gdb, checked all layers

Organization	Site	Year	Transformation notes
ODFW	CBW05583-252730	2016	done, used corrected gdb, checked all layers
ODFW	CBW05583-420954	2011	done, used corrected gdb, checked all layers
ODFW	CBW05583-420954	2014	done, used corrected gdb, checked all layers, didn't actually publish
ODFW	CBW05583-486202	2012	done, used corrected gdb, checked all layers, redid wetted cl and crosssections and channel units
ODFW	CBW05583-486202	2015	done, used corrected gdb, checked all layers
ODFW	dsgn4-000006	2016	done, used corrected gdb, checked all layers
ODFW	dsgn4-000094	2011	done, used corrected gdb, checked all layers
ODFW	dsgn4-000094	2012	done, used corrected gdb, checked all layers
ODFW	dsgn4-000094	2013	done, used corrected gdb, checked all layers, redid wetted/bankful polygon, cl, and crosssections
ODFW	dsgn4-000094	2015	done, used corrected gdb, checked all layers, did both 45 and 161
ODFW	dsgn4-000094	2016	done, used corrected gdb, checked all layers
ODFW	ORW03446-159368	2012	done, used corrected gdb, checked all layers
ODFW	ORW03446-159368	2015	done, used corrected gdb, checked all layers

References

- Watershed Sciences. 2007(a). LiDAR remote sensing data collection: Grande Ronde River valley, Oregon. Page 24. Watershed Sciences, Inc., Portland, OR.
- Watershed Sciences. 2007(b). LiDAR and true-color orthophotographs airborne data acquisition and processing: Grande Ronde and Lemhi River basins. Page 34. Watershed Sciences, Inc., Portland, OR.
- Watershed Sciences. 2009(a). LiDAR airborne data acquisition and processing: Upper Grande Ronde River, OR. Page 20. Watershed Sciences, Inc., Portland, OR.
- Watershed Sciences. 2009(b). LiDAR and true-color orthophotographs airborne data acquisition and processing: Grande Ronde basin, OR. Page 22. Watershed Sciences, Inc., Corvallis, OR.
- Watershed Sciences. 2009(c). LiDAR data collection phase Grande Ronde River basin. Page 25. Watershed Sciences, Inc., Portland, OR.
- Watershed Sciences. 2013. Grande Ronde technical data report - delivery 2. Page 27. Watershed Sciences, Inc., Corvallis, OR.

Appendix 1. CHaMP Topographic Data Transformation Procedures

Transformation procedures written by Danielle Grundy, January 2017.

Prepare Files and Tools

Make sure you download the old CHaMP Transformation tool found here <http://ctt.joewheaton.org/> and have the *CHaMP_Retransformation_Tools* toolbox.

Download the Tin and the corrected geodatabase for the site you are going to retransform from cm.org. Unzip the files to an easily navigable folder with the site name that has no spaces in the file path. This is easiest when using the C drive.

Generate a channel unit CSV file from the CHaMP Workbench and save it in the same folder: Navigate to the appropriate year and site within Workbench, right-click and choose *Generate a channel unit CSV file* from the drop-down list.

Now you are ready to retransform.

Prepare Survey: Open ArcMap. Once open do not open the existing survey. I found if you *prepare the survey* first ArcMap is more stable. Navigate to the *CHaMP_Retransformation_Tools* toolbox with ArcCatalog. I also found using ArcCatalog was more stable than using ArcToolbox. Expand *Retransformation Workflow* and double click *Prepare survey for Re-transformation*. Add the geodatabase and TIN. This will make a new geodatabase with Transformation added at the end of the name. Once completed, open the newly created survey with the label transformation.

Transform: Open up the old CHaMP transformation tool. Choose UTM Zone 11 (NAD83) for your coordinate system and the transformation row will automatically populate. Add the coordinates and elevation to all three benchmarks. If you only have two benchmarks then just recopy one of your existing benchmarks into the third row. The tool will not move forward unless you have three benchmarks. Finally, add your geodatabase into the output workspace then click *Select Inputs*. On the next screen make sure the labels for each benchmark are correct. Pick which benchmarks you want as your hinge and bearing. Don't agonize over this since you can change this on the next screen too. Click *Proceed to Transformation*. On the next screen, you can preview the residual errors with each set of benchmarks, and if you upload imagery with the *Add Data* tool you can compare the transformation to the imagery. Basically, you want to have the lowest residual error possible. With the RTK coordinates, the residual error is generally below 5 cm and always below 10 cm. If there is high residual error between the hinge and bearing benchmarks than something is wrong and do not retransform. The third benchmark, which you are not using to transform, can have high error especially if you had to make up coordinates for it. Click that you visually verified the transformation and checked residual errors and *Save to file and Exit*. **Make sure to record which benchmarks you use as your hinge and bearing so you can use the same transformation repeatedly.**

Reconstruct TIN: Next, navigate back to the *CHaMP_Retransformation_Tools* with ArcCatalog and expand *Stand Alone Utilities*. Click on the *reconstruct TIN*. Navigate to the projected folder under the Transformation geodatabase. Add in the TINNode, TINAREA, and TINLINE. Under *output TIN* navigate to the site folder and add TIN_Transformed2 for the name. Hit okay. **NOTE:** At times when the *Reconstruct TIN* is opened up it can crash ArcMap. If this happens reopen up ArcMap, and to reopen the transformed geodatabase you have to copy a DEM over to it using ArcCatalog. It will not open otherwise. Use whatever DEM you like just remember to delete it once you have reopened the geodatabase. Run the *Reconstruct TIN* tool. It generally works the second time around.

Clean UP GDB: Under Table of Contents remove all layers except for the TIN_transformed2. At this point, I usually like to compare the old tin with the new tin and the imagery to ensure that the re-projection is better than the old. It generally is better. If not, I don't know what to do since I have not come across that. If it all looks good, proceed to the next step. Navigate to your newly transformed geodatabase with ArcCatalog and expand it. Change the name of MapImages and SurveyInfo to MapImages2 and SurveyInfo2, respectively. Then, navigate back to the *CHaMP_Retransformation_Tools* with ArcCatalog, and under *Re-Transformation Workflow* click on *Clean up GDB after Re-transformation*. Add in the transformed geodatabase and original geodatabase and click okay.

Yay, you are done with the retransformation! Erase the original TIN and the tin_transformed2 from the site folder. Keep the tin_transformed TIN which was generated by the last tool. Use this to generate a DEM and process the rest of the survey like normal with the CHaMP Workflow manager. You will have to regenerate all rasters. Generally, the other layers are kept intact and are present. Double check those layers to ensure they are accurate and represent the site.

Low Flow Analysis

Full Title: Analysis of Low Flows in the Upper Grande Ronde River Basin and Implications for Spring Chinook Carrying Capacity

Introduction

Juvenile salmon viability is a function of productivity, abundance, spatial structure, and diversity (McElhaney et al. 2000). Juvenile spring Chinook Salmon carrying capacity is generally thought to be a function of a variety of habitat quality variables. Water temperature is a habitat variable that sets a physiologically-based foundation for the ability of any stream reach to support salmonid juveniles. Control on juvenile abundance is imposed via a variety of means. Juveniles are eliminated from a stream reach progressively by direct thermal mortality when water temperatures increase above approximately 23°C. A temperature metric that is generally useful as an index to this threshold is the 7-day rolling average of the daily maximum temperature (7-DADM). Below this threshold, control of abundance via temperature is brought about by a combination of effects: (1) ability of a fish to feed at a rate and acquire sufficient high quality food from the drift component of the macroinvertebrate community of the reach so that bioenergetic demands are met—i.e., so that somatic growth exceeds metabolism, (2) behavioral preferences for thermal regimes, (3) physical ability of the fish to migrate to express its thermal preferences, (4) ability of a fish to compete for food with other species that may be more adapted to the water temperature, (5) ability of the fish to avoid predation under the water temperature regime (6) cumulative stress from a variety of factors, such as disease, lack of cover, competitive interactions, etc.

Modeling fish population growth rate with a Beverton-Holt model involves definition of two parameters: productivity and carrying capacity. Temperature defines the area of suitable habitat for Chinook juveniles and the potential abundance of those juveniles in a given reach owing to a combination of acute and chronic (long-term, single or multi-factor, cumulative) mortality effects. A potential carrying capacity is set by the current thermal regime. This thermal regime is defined by the current riparian condition in the stream-adjacent zone, the riparian zone upstream of the reach, and the riparian zone condition for the entire upstream stream network in the watershed for the ESA-listed population. This thermal regime is also defined by the existing hyporheic interaction with the floodplain and the climate regime (current annual air temperature and precipitation patterns). The air temperature and climate regimes interacting with the riparian condition (shading) and channel structure (hyporheic interaction) determine the realized water temperature regime for the stream and reach. On top of this thermal regime framework rests the additional current habitat conditions that more narrowly define the carrying capacity. Pool area (qualifying depth of 0.8 m) and frequency, large woody debris (LWD) volume by habitat type or pieces or volume per 100 m, substrate composition, water quality (alkalinity, conductivity), thalweg depth diversity, and fine sediment are some of the key factors that determine the realized capacity for the reach. Thalweg depth diversity is one index that can represent habitat heterogeneity. This is a relatively intuitive concept for a variety of biological effects. For example, it would seem to relate to the ability of juveniles to shelter in low velocity microhabitat and feed in neighboring higher velocity habitat. This should also provide microhabitats uniquely suitable for a wide

range of sizes of salmonids. In addition to the thalweg depth diversity, inter-annual variation in mean depths of various channel unit types would indicate variation in suitable habitat area for salmonids. This inter-annual variation describes a low flow regime for a reach that defines inter-annual variation in rearing capacity. Juvenile rearing capacity has typically been attributed to depth and low and high velocity thresholds, plus substrate size minimum thresholds with instream flow modeling. The spatial distribution and area of habitat meeting depth (D), velocity (V), and substrate size thresholds can be calculated with HSI (Habitat Suitability Index) models.

Given the annual streamflow characteristics and associated climatic conditions (e.g., initiation of snowmelt, Julian date for initiation of baseflow, annual variation in winter precipitation), and the current channel morphology that is the result of a history of peak streamflows and land uses (e.g., riparian harvest, livestock grazing in the streamside zone, road building adjacent to stream channels, historical splash-damming of the river, trends in LWD, and basin-wide sediment delivery), the annual summer streamflows in stream channels will create predictable patterns of depth and velocity that set juvenile carrying capacity and potential spawning habitat.

If it is known what the discharge is at a channel cross-section at one point in time during the summer from CHaMP surveys at study sites, the flows at other times during the summer could be modeled. That is, if the discharge at a CHaMP site on July 15 in year 201x is $0.5 \text{ m}^3/\text{s}$, for example, and we can estimate what the discharge would be on August 15 (date of peak spawning) of that year, the topographic survey of the channel could be used with the estimated discharge to predict the wetted area by channel unit. Summer discharge at CHaMP sites can be extrapolated from the time of survey to another time in summer if we know the relationship between streamflows at the CHaMP site and a downstream gage. The following analysis of summer low flows is an exploration of the relationship between summer flow at CHaMP sites and the USGS gages, the potential that localized water use creates deviations in this relationship, and the ability to identify a median flow for August and variation in summer flows. The RBT (River Bathymetry Toolkit) could adjust the stage height to create the predicted discharge, thereby calculating the wetted area. The hydraulic model would allow mapping of the depth and velocity contours so that change in spawnable area and rearing area can be computed. These metrics would be good indicators of capacity (spawning and rearing capacity).

Methods

Walters et al. (2013) were able to relate 19 years of juvenile survival data to streamflow and temperature. They found that spring streamflow and summer water temperature were key variables in modeling juvenile Chinook survival and that survival was cut in half when streamflow was diverted. In addition, climate change caused additional reductions in carrying capacity from those related to streamflow and water temperature.

Walters et al. (2016 Appendix) used the USGS StreamStats tool to calculate natural streamflows (i.e., without the influence of diversions or other anthropogenic uses). Walters et al. (2016 Appendix) stated that StreamStats does not account for groundwater inputs, so differences between gaged streamflow and StreamStats streamflows can be partially attributable to groundwater effects.

In the Upper Grande Ronde, we assume that variation in the gaged flow for August relative to the median long-term August flow from StreamStats is attributable to variations in upstream level of irrigation and other out-of-stream water uses (diversion, groundwater pumping from hydrologically connected streamside areas, agricultural watering) and annual variations in winter precipitation inputs and runoff timing.

StreamStats (USGS 2016) was run on a variety of locations in the Upper Grande Ronde, including sites along the mainstem and the mouths of major tributaries. Sites along the mainstem were selected to represent the watershed upstream of major tributaries. StreamStats provides basin characteristics (e.g., drainage area, mean annual precipitation, mean elevation, etc.) as well as streamflow characteristics for any point on the stream network. Median (i.e., D_{50}) August streamflows computed using StreamStats for each selected site were plotted on a sketch of the basic stream network. In addition, streamflows that were measured during CRITFC field surveys during either CHaMP field work (2011-2015) or in work conducted to enable water temperature model development in 2010 were plotted and tabulated to show the relationship to StreamStats natural flow estimates. In addition, the streamflow model developed by Watershed Sciences, Inc. from CRITFC's 2010 flow measurements provided flow estimates for each 100-m interval on the mainstem and all major tributaries. These values were also contrasted with StreamStats natural flow values. This was useful because numerous stream nodes were unable to be accessed on the Vey Meadows Ranch due to landowner denial and remote sensing by FLIR allowed temperature profiles to bridge inaccessible zones of the stream network.

Results and Discussion

The upper zone of the Upper Grande Ronde River basin (i.e., upstream of Meadow Creek) was selected as a test site for evaluating the relationship between streamflows measured in 2010 and the long-term USGS gage near Perry and also the streamflow statistics for low flows calculated in StreamStats. Figure 19 (Justice et al. 2016) displays the river kilometer designations throughout the stream network for this upper zone of the Grande Ronde. These river kilometer positions represent nodes on the stream network where major tributaries enter the mainstem and also points on major tributaries where other tributaries enter. These were nodes where various in-channel streamflow measurements were made in 2010 by CRITFC and also where StreamStats calculations were performed using USGS online tools.

The upper zone of the Upper Grande Ronde River runs from approximately CHaMP site dsgn4-000277 upstream to the mine tailings area on the mainstem and up Sheep, Chicken, and Limber Jim Creeks (Figure 20). Between August 12 and August 19, 2010, streamflow measurements were taken to enable development of a water temperature model.

Measured streamflows above and below nodes on the stream network appear to be additive, confirming the quality of discharge measurements made. Also, there was often slight decreases or increases in flow along the mainstem, indicating either “losing” reaches or additions from lateral groundwater flow or small tributary entry. For example, at CHaMP site dsgn4-000009 on the mainstem, the streamflow measured on August 19, 2010 was $0.308 \text{ m}^3/\text{s}$ (Figure 2). Limber Jim Creek added $0.066 \text{ m}^3/\text{s}$ (measured on August 14); Clear Creek mouth added $0.05 \text{ m}^3/\text{s}$ above dsgn4-000009 (or 16% of the

flow in the mainstem) (August 19). Sheep Creek, measured at CBW05583-138554 was 0.0824 m³/s (August 12). Chicken Creek added 0.050 m³/s to the lower end of Sheep Creek. These flows total 0.556 m³/s. The flow at dsgn4-000277 was 0.607 m³/s. A flow of only 0.101 m³/s was unaccounted for. This flow could enter the mainstem from lateral seepage from the floodplain from the upper end of Sheep Creek to its mouth and from the upper end of the mainstem Grande Ronde to its confluence with Sheep Creek and downstream through the canyon to dsgn4-000277. This is a small flow increment attributable to drainage from the floodplain. Meadowbrook Creek is the only tributary in this zone of a significant drainage area, but it was not measured because it enters on inaccessible private property and contributes extremely little flow.

Watershed Sciences, Inc. developed a Heat Source water temperature model for CRITFC based on streamflows measured by CRITFC at strategically placed nodes. Accumulation of drainage area with distance downstream, the streamflows measured at nodes, and flows at nearby gages were used to extrapolate flows to ungaged points on the stream network, spaced at 100-m intervals. Streamflows were measured over a relatively short period of time (August 12-19, 2010) so that flows could be related to water temperatures measured by Hobo temperature loggers scattered around the network at the same nodes where flows were measured. Streamflows estimated for August 14, 2010 in the Heat Source model were based on streamflows measured from August 12-19, 2010 and adjusted according to the nearest streamflow gages. Flows for August 14, 2010 in the upper portion of the Grande Ronde are displayed in Figure 21. This date was selected to represent a mid-point in August, which one of the two warmest months and is at the start of the spring Chinook spawning period. It also provides the basis for making contrasts between flows at gages for that date and StreamStats statistics for August as a whole.

At dsgn4-000009 on the upper part of the mainstem Grande Ronde, the streamflow on August 14, 2010 was 0.393 m³/s, as modeled by Heat Source in the process of calculating hourly water temperatures for the summer 2010 period (Figure 21). The flow at the mouth of Limber Jim Creek was 0.076 m³/s. The streamflow at the upper end of Sheep Creek (CBW05583-138554) was 0.088 m³/s and Chicken Creek added 0.055 m³/s. The flow on the mainstem Grande Ronde at dsgn4-000277 was 0.624 m³/s. The sum of these four sources was 0.612 m³/s, which allows for only 0.012 m³/s to accumulate from lateral contribution from the floodplain. The streamflows calculated in Heat Source modeling at these nodes for August 14 compare very closely to those measured on other days in the period from August 12-19 (Figure 20).

StreamStats (USGS) D₅₀ low flow statistics for August are displayed on the same stream network of the upper end of the Upper Grande Ronde (Figure 22). For example at dsgn4-000009 on the UGR mainstem, the D₅₀ August statistic is 0.239 m³/s. Sheep Creek mainstem at Chicken Creek mouth is 0.071 m³/s, while the mouth of Chicken Creek is 0.061 m³/s. Sheep Creek mouth, at the confluence with the UGR is 0.140 m³/s. The confluence of Sheep Creek and the UGR produces a joint D₅₀ flow of 0.559 m³/s. Downstream a short distance to dsgn4-000277, the D₅₀ streamflow there is 0.569 m³/s. At this same CHaMP site, the actual modeled (by WSI) streamflow from measurements made in 2010 in the field from August 12-19 was 0.624 m³/s, a value nearly identical to the D₅₀ value. The streamflow modeled for upper Sheep Creek at CBW05583-138554 was 0.088 m³/s, while the D₅₀ flow from StreamStats was 0.071 m³/s. The modeled flow of the UGR at the confluence with Sheep was 0.477 m³/s, while the D₅₀

flow for August was $0.419 \text{ m}^3/\text{s}$. These and other comparisons indicate that the mid-August streamflows for 2010 (Figure 20 and Figure 21) were very similar to D_{50} August streamflows computed in StreamStats (Figure 22). This means that the August 2010 streamflows represent near median streamflows that are based on a long flow record for many CHaMP sites toward the upper portion of the basin.

Because it was assumed that the upstream part of the Upper Grande Ronde watershed would be more homogeneous geologically, have minimal water withdrawals for farming downstream to Meadow Creek, and have a more homogeneous climate, we examined streamflow statistics for that watershed first. Given that measured streamflows on August 2010 were very similar to the D_{50} streamflows from StreamStats in this portion of the watershed, it was decided to extend this comparison to the larger watershed downstream to the USGS gage near Perry. A regression of the streamflows at the USGS gage near Perry (Figure 23) on the mainstem Grande Ronde (13318960) against the streamflows at the gage below Clear Creek (13317850) for years 1997-2016, where data from 1999 were missing for gage 13317850, revealed a very high correspondence between the two gages ($n = 19$, $R^2 = 0.864$, $P < 0.001$). This implies that if there is an ability to link D_{50} August flows to flows measured in 2010 in the upper portion of the basin, this relationship may hold for the entire basin downstream to the gage near Perry.

Extending the comparison of the August streamflows downstream from Meadow Creek to the USGS gage near Perry, we found that the streamflow of the mainstem Grande Ronde above Beaver Creek (at CHaMP site dsgn4-000245) was $0.742 \text{ m}^3/\text{s}$ (Figure 24). The D_{50} streamflow for August at this same location was estimated to be $0.977 \text{ m}^3/\text{s}$ (Figure 25). The measured streamflow at Hilgard State Park on August 17, 2010 was $0.831 \text{ m}^3/\text{s}$ and the streamflow upstream of Five Points Creek on the mainstem Grande Ronde was $0.761 \text{ m}^3/\text{s}$ (Figure 24). However, the D_{50} flow for the mainstem Grande Ronde upstream of Five Points Creek was $1.625 \text{ m}^3/\text{s}$.

The streamflow at the Grande Ronde mainstem gage (13317850) below Clear Creek on August 14, 2010 was $0.396 \text{ m}^3/\text{s}$, while the flow at the gage (13318960) near Perry on August 14, 2010 was $1.109 \text{ m}^3/\text{s}$. Flows at the gage near Perry varied from $1.331 \text{ m}^3/\text{s}$ to $0.793 \text{ m}^3/\text{s}$ between August 12 and August 19 (the time period when flows were measured in 2010 to create the temperature model. Flows declined daily from August 12 through August 18. Because the D_{50} flow above Five Points Creek (i.e., only 2.9 km upstream of the gage near Perry) was $1.625 \text{ m}^3/\text{s}$ and all the other measured streamflows upstream of Meadow Creek closely matched their corresponding D_{50} flows (i.e., natural flows without water withdrawal), it seemed possible that the discrepancy between the D_{50} flow ($1.634 \text{ m}^3/\text{s}$) near Perry and its August 14 flow ($1.019 \text{ m}^3/\text{s}$) or the mean flow for August 12-19 ($0.984 \text{ m}^3/\text{s}$) represents the amount of water extracted from the stream. This difference in flow is $0.62\text{-}0.65 \text{ m}^3/\text{s}$, based on the flow values above. It would be instructive to apply the water withdrawal database available from Oregon Water Resources Department (<https://www.oregon.gov/owrd/Pages/wr/index.aspx>; water rights database) to try to calculate what the total water withdrawal upstream of the gage near Perry would be. It appears that this effect arises downstream of Meadow Creek most significantly.

For the period August 1-31, 2010, the average daily streamflow near Perry was $0.928 \text{ m}^3/\text{s}$, while the median was $0.906 \text{ m}^3/\text{s}$. The minimum and maximum for August of this year ranged from 0.566 to $1.359 \text{ m}^3/\text{s}$ (Table 18). The streamflow for August 15 was very similar to the mean for the month.

The measured streamflow above Beaver Creek on August 18, 2010 was $0.742 \text{ m}^3/\text{s}$ and the flow in Beaver Creek at the mouth on August 24, 2010 was $0.110 \text{ m}^3/\text{s}$. These flows combined would nearly approximate the August flow of the Grande Ronde below Beaver Creek, or $0.852 \text{ m}^3/\text{s}$ (Figure 24). The streamflow measured downstream on August 18 above Spring Creek was $0.844 \text{ m}^3/\text{s}$. This indicates that the streamflow declined slightly over a distance of 13.2 km between Beaver Creek and Spring Creek. This section includes several small tributaries, including Bear Creek and Jordan Creek. There is significant farming with sprinkler irrigation over this span of stream. Streamflow declined slightly more downstream from Spring Creek to Hilgard State Park, where it reached $0.831 \text{ m}^3/\text{s}$ (August 17), and further to $0.761 \text{ m}^3/\text{s}$ upstream of Five Points Creek (August 17). The combined streamflows of the Grande Ronde above Five Points and Five Points at its mouth (measured by CRITFC) totaled $0.802 \text{ m}^3/\text{s}$. The streamflow measured at the gage near Perry on August 17 and 18 was $0.793 \text{ m}^3/\text{s}$.

It appears that the streamflows measured in the Grande Ronde basin near Perry (USGS gage 13318960) during mid-August 2010 reflect something less than the D_{50} August flow values. The D_{50} streamflow for August is $1.634 \text{ m}^3/\text{s}$ (Table 19). The D_{95} value is 1.169 and the D_5 flow is $3.285 \text{ m}^3/\text{s}$. The measured streamflow at the gage at Perry on August 14, 2010 was $1.109 \text{ m}^3/\text{s}$ (Table 3), which is lower than the D_{95} value. The flow at the gage on August 17 and 18 was $0.793 \text{ m}^3/\text{s}$, which was even lower than D_{95} . A comparison of August 14 streamflows for years from 2010 to 2016 reveals a range from 0.510 to $1.246 \text{ m}^3/\text{s}$ (Table 20). This lends further credibility to identifying the August 2010 flows as something lower than D_{50} values. It also suggests that very low streamflows recorded in 2015 and 2016 (i.e., 0.453 and $0.510 \text{ m}^3/\text{s}$, respectively), which are far less than the August D_{95} value, represent anthropogenically influenced flow values. Also, because the measured August streamflows at sites in the upper portion of the UGR are fairly close to D_{50} values and they become lower than the D_{95} value downstream near Perry, it appears that a steady water withdrawal from combined uses occurs with distance downstream. It will need to be assessed whether the extreme low flows experienced in 2015 and 2016 are significantly influenced by lower than normal mean annual precipitation and advanced timing of snowmelt, or whether water withdrawal is also very great during these years in the summer season.

Given the high level of correspondence between the mean annual August streamflows from the two long-term USGS gages on the UGR (UGR near Perry or 13318960 and UGR downstream of Clear Creek, or 13317850) (Figure 22), and the relatively short travel times from the headwaters to the gage at Perry, one might think that on a daily basis the streamflows measured at various CHaMP sites might exhibit consistent proportions of the flows at the gages near Perry and downstream of Clear Creek. It is often assumed that flows measured at a long-term gage such as the UGR near Perry can be used to estimate the flows at points upstream in proportion to the size of the watershed at unmeasured points upstream. However, discrepancies in the percentages of flows at the gage near Perry for CHaMP sites in a downstream series could show increasing amounts of water withdrawal or evaporation. Evidence of this effect would impose considerations for how to make this adjustment for summer months having significant irrigation or evaporation.

CHaMP site dsgn4-000009 (RK 91.3; Table 20) appears to have very consistent streamflows from 2010 through 2015 for miscellaneous measurements made from June 30 to August 19 (Table 22). Even though streamflows during this summer period at dsgn4-000009 varied by a factor of 5.1 from 2010 through

2015, its percentages of streamflow near Perry ranged only from 21.8% to 34.0% even though the Perry gage was 62.1 km downstream and there were intervening points of water withdrawal, while the percentage of streamflow below Clear Creek (i.e., 2.7 km downstream, Table 22) ranged from 69.5 to 86.4%. If flows at dsgn4-000009 in the headwaters are not affected by water withdrawal, but the flows near Perry are subject to variable amounts of withdrawal as well as naturally varying climatic conditions (i.e., high and low water years), then one would expect variations in the percentage that dsgn4-000009 flows comprise of those near Perry. Given the sources of variation, it is surprising that these percentages are so stable from 2010-2015 at dsgn4-000009.

CHaMP site dsgn4-000277 had miscellaneous streamflows recorded from 2010-2015 over the period July 15 through September 1. These measured flows represented only one value per year except for 2011 in which seven streamflows were measured. Flows varied during this period by a factor of 3.0. The percentages of streamflow near Perry ranged only from 26.1% to 76.6%, while the percentage of streamflow below Clear Creek (i.e., 4.7 km upstream; Table 23) ranged from 105.9 to 171.0%. Even within a single year (2011), the dsgn4-000277 site varied in percentage that its daily streamflow between August 11 and September 1 comprised of the Perry gage and the gage below Clear Creek. Percentages of the flow near Perry in this 2-week period in 2011 varied from 60.0 to 82.7%. The percentage of flow at the gage below Clear Creek ranged from 134.2 to 171.0%. Flows at this CHaMP site ranged from 0.585 to 0.820 m³/s, while the flows near Perry ranged from 0.765 to 1.331 m³/s and those below Clear Creek ranged from 0.368 to 0.595 m³/s for those days. If the average current velocity is 0.25 m/s from dsgn4-000277 to the gage near Perry (54.7 km distance), it would require 2.53 days for water to travel this distance. In 2011, it appeared that there was as much as about 15% change in streamflow at the Perry gage in any 3-day period from August 11-September 1. Direction of change in streamflows was not always parallel either. From August 24 to 28, 2011 streamflows increased at dsgn4-000277, but they consistently declined near Perry as measured at the USGS gage. This behavior of flows with time as well as the distance required for water to move from one CHaMP site to a nearby gage appears to create variation in the percentage that flows on a single day at a CHaMP site comprise of a gage in the same basin on the same day. It may be that monthly averages provide a more consistent basis for comparison.

Further down the Grande Ronde mainstem is annual CHaMP site dsgn4-000202 (Table 24). The flows at this site (RK 58.4) ranged from 44.0 to 54.8% of the flows near Perry for measurements made in years 2011-2015 for miscellaneous dates between July 19 and September 7. These percentages were relatively stable over the years in which CHaMP monitoring was done, despite the fact that this CHaMP site is 29.2 km from the gage near Perry. The gage below Clear Creek is nearly equidistant upstream (30.2 km), but the percentages of streamflow varied from 91.3 to 142.2% of the gage values.

A short distance downstream at dsgn4-000245 (above Beaver Creek) for miscellaneous streamflow measurements made between July 28 and August 28 over the years 2010-2015 (Table 25), the percentages of streamflow at the gage near Perry fluctuated from 41.3 to 93.6%. It is unlikely that this fluctuation compared to the more stable relationship between dsgn4-000202 and the Perry gage is due to any water withdrawal made between the two CHaMP sites.

It is possible that streamflows in late July are still affected significantly by timing of snowmelt so that there is variation in the percentage snowmelt contribution versus groundwater. If this is true it could lead to some amount of annual variation in the source of streamflow on a given date in July from year to year as snowpack and melt timing varies. Flows at the gage below Clear Creek would likely be more heavily influenced by snowmelt in late July or early August than flows near Perry. The D_{50} streamflow near Perry is a flow based on estimated natural conditions without the effect of water withdrawal and is $1.634 \text{ m}^3/\text{s}$ (Table 19). The D_{95} near Perry is $1.169 \text{ m}^3/\text{s}$. Taking all individual streamflow measurements from this USGS gage for 1997-2016 for August and calculating the 50th and 95th percentile flows results in flow values of 0.743 and $0.398 \text{ m}^3/\text{s}$, respectively (Table 26), corresponding to the percentile definitions in Risley et al. (2008). If the mean August flow is calculated on an annual basis for this same period of years and percentiles are calculated from this set of 20 data points, 50th and 95th percentile values (D_{50} and D_{95} for Risley et al.) are also estimated as 0.675 and $0.435 \text{ m}^3/\text{s}$. The fact that there is such a large discrepancy between the D_{50} value calculated from StreamStats for the gage site near Perry and the actual calculated value from mean daily flows at the gage for all August periods for 1997-2016 shows that there is a significant amount of water that is lost from the stream by either evapotranspiration or diversion and irrigation.

CHaMP annual site dsgn4-000205 is located at RM 41.0) (Table 21). Streamflows were measured there between July 14 and August 21 over the years from 2010 through 2015 (Table 27). During this summer period, the miscellaneous streamflows spanned the range 0.400 to $1.347 \text{ m}^3/\text{s}$ while streamflows at the Perry gage ranged from 0.510 to $2.973 \text{ m}^3/\text{s}$. The flows at this CHaMP site were computed as a percentage of flows near Perry gage (1331896) (RK 29.2) and the USGS gage below Clear Creek (13317850) (RK 88.6). There is a distance of 51.1 km between site dsgn4-000205 and the USGS gage below Clear Creek and 11.0 km between this site and the downstream gage near Perry. Based on the miscellaneous streamflow measurements made from 2010-2015 in the July-August period, the flows at dsgn4-000205 comprised from 71.0 to 106.4% of the flows of the gage near Perry, and were 150.4% to 280.0% of the flows below Clear Creek.

Basin characteristics were compiled using StreamStats for various annual CHaMP sites and other strategic sites selected in 2010 for measuring streamflows and water temperatures (Table 28). Drainage areas varied among these sites from 46.36 to 1753.42 km^2 in area. Drainage density (km/km^2) gave a slight indication of being higher at greater mean basin elevations, but overall, drainage density varied only from 0.416 to $0.640 \text{ km}/\text{km}^2$. Mean annual precipitation was higher with mean basin elevation. At mean basin elevations above 1700 m , mean annual precipitation varied from 795.0 to 861.1 mm . Likewise mean annual maximum air temperature was lower above 1700 m mean basin elevation (i.e., range from 9.89 - 10.72°C) than at the elevations from 1319.8 to 1700 (i.e., range from 11.11 - 12.44°C). The same relationship held true for mean maximum January air temperature, where air temperatures ranged from -0.67 to -1.28°C above 1700 m , and from 0.11 to 1.00 below 1700 m . Meadow Creek appeared to be anomalous among these watersheds by having the highest mean annual maximum air temperature (12.44°C) and the highest mean maximum January air temperature (1.00°C). It also had the lowest mean basin elevation. The relatively low mean basin elevation and high air temperatures probably result in earlier snowmelt in this basin. Other basins not included in Table 28, such as Spring

Creek, Rock Creek, and Five Points Creek should be contrasted with these others as a means to explain variations in summer streamflows.

Streamflow statistics were compiled for many of the same CHaMP sites and other strategically selected sites throughout the Upper Grande Ronde basin (Table 29). Median August streamflows (D_{50}) streamflows (m^3/s) were tabulated from StreamStats for these sites and were converted to a standardized form by dividing by drainage area (km^2). Plots of these standardized D_{50} streamflows vs. mean basin elevation (m) and mean annual precipitation (mm) yielded statistically significant regressions (Figure 26 and Figure 27). The StreamStats method used by USGS (Risley et al. 2008) predicts streamflows from regressions based on basin characteristics such as annual minimum air temperature, annual maximum air temperature, drainage area, drainage density, mean elevation, percent impervious area, January minimum air temperature, January maximum air temperature, mean slope mean annual precipitation, basin relief, soil capacity, soil permeability, maximum elevation, and maximum slope. However, the low flow frequency statistics (D_5 - D_{50}) for August in the Upper Grande Ronde (Region 6 in Risley et al. 2008) are computed from drainage area, mean annual precipitation, and maximum elevation. D_{95} is computed from drainage area, mean annual precipitation, minimum elevation, and drainage density.

Median August streamflows (D_{50} , m^3/s) were compiled from StreamStats flow frequency statistics for a set of annual CHaMP sites and the Upper Grande Ronde River near the Perry gage (Table 30). Drainage areas of the watersheds draining to each of the CHaMP sites were computed from the basin characteristics function in StreamStats. The D_{50} of each CHaMP site was divided by the D_{50} computed for the Grande Ronde River near Perry. Also, average streamflow for each CHaMP site averaged for all miscellaneous summer season flow measurements (primarily July-August) were divided by the average of concurrent flow measurements at the Perry gage for the same days when CHaMP surveys were made. These two sets of flows relativized to flows at Perry were plotted against watershed area (km^2) (Figure 28). The sites selected to contrast with the flow near Perry (RK 29.2) were arrayed along the mainstem Grande Ronde between RK 53.8 and RK 91.3. The plots based on D_{50} flows and average flows (2010-2015 for summer season miscellaneous data in July-August) were very similar. The plot of D_{50} values against watershed area shows that the method used by USGS to compute this statistic ends up providing a linear fit to the estimates from their multiple regression, which is based on various basin characteristics that include drainage area as one of 3 or 4 characteristics. The linear nature of this plot indicates that it is reasonable to project flows at points upstream based on their proportional size of their watersheds in relation to the watershed upstream of Perry gage. The plot based on multi-year averages of flows on CHaMP survey dates as a proportion of the average of flows at Perry for the same set of survey dates as for CHaMP sites also yielded a linear relationship that generally supports the proportional relationship of flows at a site to the gage near Perry. However, the difference in slope may be due to the influence of progressive water loss with distance downstream. This could cause the relative proportion of the flow near Perry being greater toward the headwaters and decline toward the gage.

Given the evaluation of streamflow measurements from CHaMP sites and estimation of whether the flow in any individual year is a D_{50} flow or occurs at higher or lower frequency, the StreamStats values for D_5 - D_{95} (m^3/s) were plotted against their frequencies for several example annual CHaMP sites.

Starting with an annual site in the headwaters on the UGR mainstem at dsgn4-000009, this yielded a near-straight line regression ($y = -0.0042x + 0.4487$) (Figure 29). If the UGR were still in pristine condition, it would be possible to measure a flow in August at any point along the UGR mainstem and use the regression of streamflow vs. flow frequency from StreamStats to estimate for that flow what the flow frequency would be. Under current conditions, with a dense road system and other widespread land uses, the measured August flow would likely be lower than historic under similar climatic conditions, so it would tend to be more similar to an August low flow with a lower frequency of occurrence (i.e., a greater percentage of all low flows under pristine conditions are higher than that measured flow under current watershed conditions).

The measured streamflow on August 19, 2010 by CRITFC at dsgn4-000009 was $0.308 \text{ m}^3/\text{s}$. This streamflow equates to a $D_{33.5}$ value using the regression in Figure 29. WSI used the CRITFC streamflow data and streamflow data from available long-term gages in the basin to model the daily streamflows for every 100 m throughout the stream network for which water temperatures were modeled using Heat Source. The WSI modeled August 15, 2010 streamflow for dsgn4-000009 was $0.346 \text{ m}^3/\text{s}$ (Table 31). This flow equates to a $D_{24.45}$ flow instead of D_{50} (Figure 30). The actual measured flow of $0.308 \text{ m}^3/\text{s}$ at this site is estimated to be an August $D_{33.5}$ flow, or a flow for which 33.5% of values are higher. That is, under historic conditions at that point in the stream network, that flow in August would rank as a higher than median flow for all years in which average August flows are observed.

The same procedure was conducted on CHaMP site dsgn4-000277 (RK 83.9). This site had a large number of its streamflow measurements made from 2010-2015 in August (Table 32). Plotting the streamflows (m^3/s) derived from StreamStats for July, August, and September against the frequencies of these flows (Figure 31) yielded an equation for August below: $y = -0.267 \ln(x) + 1.5813$ ($R^2 = 0.9854$), where y is streamflow (m^3/s) and x is the flow frequency from StreamStats, which would indicate the frequency of natural flows free of anthropogenic impact. This equation can be used to solve for flow frequency (x) when a flow value (y) is to be evaluated.

The August 18, 2010 flow frequency value at dsgn4-000277 (RK 83.9) was 38.44% (i.e., $D_{38.44}$) (Figure 33). This computed frequency value was similar to the value ($D_{33.5}$) computed for the August flow at dsgn4-000009 (RK 91.3). With such similarity in flow frequency values at sites spanning 7.4 km of the mainstem Upper Grande Ronde, it might be assumed that flows at all sites across that spatial range could be adjusted to the same flow frequency for those specific locations. So with annual measurements of streamflow at CHaMP sites dsgn4-000009 and dsgn4-000277, if we determine how that flow corresponds to August flow distributions, we can determine the frequency of these flows based on StreamStats values for these sites. Then, if there are rotating panel CHaMP sites between these annual sites that are not measured in any given year, but we have topographic surveys of these sites, it would be possible to assume that those sites had flows corresponding to the same flow frequency. A regression of streamflow vs. flow frequency would yield the flow for each site for the year in question. Knowing the August streamflow for each rotating panel site, we can then use RBT to calculate the wetted area and amounts of the various channel unit types, assuming that topographic channel characteristics have not changed substantially from the most recent survey.

Despite the similarity in flow frequency for sites upstream of RK 83.9, the Grande Ronde River at Perry had a CRITFC-measured flow of $0.802 \text{ m}^3/\text{s}$ on August 17, 2010 (i.e., $0.761 \text{ m}^3/\text{s}$ on the UGR below Five Points plus $0.041 \text{ m}^3/\text{s}$ at Five Points Creek mouth). The D_{50} flow from StreamStats is $1.634 \text{ m}^3/\text{s}$ and the D_{95} flow is $1.17 \text{ m}^3/\text{s}$. This means that an August measured flow of $0.802 \text{ m}^3/\text{s}$ occurs naturally at a frequency that is far less than 5% of the time (i.e., 95% of all values would be higher than that if watershed conditions were pristine). Flow on August 2010 was most likely significantly reduced by human land uses. If climatic conditions are such that August flows at CHaMP sites high in the watershed are approximately D_{33} , but flows near Perry are $D_{>95}$, it would mean that the low flows near Perry are not attributable to normal climatic variation.

In order to explore further at what point on the mainstem Grande Ronde the August flow frequencies change, flows at the annual site at dsgn4-000245 (RK 53.8) were evaluated in a similar manner as for dsgn4-000277. Streamflows were measured for this site every year from 2010-2015 and most values were in August or late July (Table 33). StreamStats flow frequencies for unmanaged watershed conditions at this site were computed and the flows corresponding to each frequency were plotted (Figure 32). Flows in August and September were very similar for each frequency. This makes it very acceptable to use the August equation to relate streamflow and flow frequency for both August and September. However, flows in July were considerably higher at each frequency value. We have assumed in this report that flows on July 28-31 would be still very close to August flows. Typically, flows decline throughout July each year, making it a dynamic month. Because the August-September time period is used for spawning by spring Chinook in the basin and the low flows at this time create conditions that could produce critical variations in rearing capacity, it would be best to use flows measured in these months for the purposes of estimating concurrent flows for all CHaMP sites throughout the basin. In order to roll up carrying capacity at a basin level, it should be done for a critical point in time having stable flows (e.g., August-September when adults are spawning). At this time period juvenile rearing may reach a bottleneck dictated by carrying capacity. The use of RBT to model wetted volume or other metric related to carrying capacity could form the basis for rolling up carrying capacity from all surveyed CHaMP sites in the basin. Otherwise, this roll-up in a given year would be based only on the annual sites and those rotating sites measured in that year.

The equation for August flow frequencies at dsgn4-000245 ($y = -0.448 \ln(x) + 2.7202$, where x is frequency for monthly streamflows and y is streamflow (m^3/s)) allows one to compute long-term flow frequencies for the flows measured in August over the period 2010-2015 at this site (Table 33, Figure 31). On August 18, 2010 a streamflow of $0.742 \text{ m}^3/\text{s}$ was measured. This corresponds to an August flow frequency (unmanaged watershed flow over the long term) of 82.73% (i.e., a $D_{82.73}$ flow). This means that 82.73% of all August streamflows would be greater than this flow. In other words, it is a very low flow.

For August 2010 the flow measurements made by CRITFC, compared against the August flow statistics from StreamStats reveals that they vary longitudinally from a value of about D_{33} to D_{38} between RK 91.4 and 83.9, then decline to D_{83} at RK 53.8, and decline further to $D_{>95}$ at RK 29.3. Because flows at each site diverge increasingly from the frequencies predicted from StreamStats modeling with distance downstream, one can assume that anthropogenic impacts increase downstream to produce this

divergence from natural conditions. It is possible that these conditions expressed by flow frequencies vary somewhat daily with changes in magnitude of irrigation. There are also expected variations from year to year that depend upon climatic variations in annual precipitation levels, air temperatures, timing of snowmelt, and evaporation rates. Annual variations created by this combination of climatic and land use effects can produce large variations in carrying capacity. With relatively low levels of habitat seeding by adult spring Chinook spawners, the lowest levels of carrying capacity produced may still not limit population response, but this question remains to be answered. At the very least, the lower than natural levels of streamflow create worse than normal water temperature patterns. Restoration of natural streamflows also is indicated as a significant solution for improving carrying capacity toward potential levels. This can involve both an increase in habitable volume or area and a decrease in water temperatures. Currently, the water temperature modeling done via work in Justice et al. (2016) and White et al. (2016) deals with only restoration of natural levels of riparian vegetation (shade) and channel widths. Restoration of streamflows would provide a significant benefit to improvement in spring Chinook population viability by expansion of suitable habitat.

The longitudinal pattern of flow frequency changes at sites along the mainstem Grande Ronde River is shown in Table 29. For selected annual CHaMP sites and the Grande Ronde near Perry, spanning a range from RK 91.3 to RK 29.2, the streamflows found in the WSI Grande Ronde River mainstem spreadsheet were compiled for August 15, 2010 (Table 31). CRITFC measured flows during this period in August and on this basis, WSI modeled the flows for the entire Grande Ronde stream network. The August D_{50} values were also computed for the selected sites from StreamStats (Table 29 and Table 31). WSI streamflow values for August 15, 2010 at the selected annual sites were then plotted vs. D_{50} streamflows for those sites (Figure 30). The resulting regression was highly significant (Figure 30). The point in the mainstem where a streamflow of approximately $0.4 \text{ m}^3/\text{s}$ was found corresponded to a D_{50} of $0.4 \text{ m}^3/\text{s}$. However, the Grande Ronde near Perry (RK 29.2) had a streamflow of only $1.153 \text{ m}^3/\text{s}$ when the D_{50} was $1.634 \text{ m}^3/\text{s}$. That is, beyond RK 85.0, there was a linear shift producing an increasingly lower streamflow compared to the D_{50} flow. This is likely due to cumulative water extractions in the watershed with distance along the mainstem.

An ability to estimate annual changes in carrying capacity or long-term trends in carrying capacity would improve our ability to model life cycle dynamics based on CHaMP habitat and water quality data. At this time there have been CHaMP surveys conducted in summers of 2011 through 2016. At annual sites, surveys conducted in any given year may have been done in late June, or in July, August, or September. With the scope of analysis done here, we have favored data from those years in which surveys were conducted in either very late July, or August and very early September to make calculations easier and more reliable. CHaMP site dsgn4-000245 had many of its annual surveys done on dates fitting these criteria. Wetted volume, a metric from the CHaMP survey, is one that is a good candidate for expressing variations in carrying capacity. Using only CHaMP data, a plot of wetted volume (m^3) against streamflow (m^3/s) reveals a linear relationship ($y = 1043.4x + 1375.6$, $R^2 = 0.9083$, $n = 6$). August 2015 was a very low flow month over the time span 2011-2016. It also produced a very low wetted volume. September 2016 was also a very low flow year and had slightly lower wetted volume. Year 2011 was a high flow year and had the highest wetted volume. CRITFC measured streamflow in 2010, but since no ChaMP

surveys were made then we have no data on wetted volume for that year. Year 2011 had nearly twice as high an August flow as in 2010 (Table 25), so it is likely that wetted volume was lower in that year.

The wetted volume calculated from a selected year's CHaMP surveys were also plotted against flow frequencies (%), where these flow frequencies were predicted from the regression of StreamStats-based August streamflows on flow frequency (Figure 31). When measured streamflows (i.e., measured in a CHaMP survey) are lower than StreamStats flows for a site at the D_{95} frequency level, one could say that the frequency of occurrence is $D_{>95}$. However, using the regression equation yields values that go beyond the range for which the regression is valid, generating values higher than 100%. However, plotting these values provides a representation of the ability of a calculated flow frequency to predict wetted volume. This plot was made for data for annual site dsgn4-000245. The flows on August 2, 2011 were the highest measured flows for the period 2011-2016 (Figure 33). They also had a flow frequency similar to a relatively high summer low flow that would be expected under pristine conditions (Figure 34). However, the extreme low measured flows in 2015 and 2016 were representative of flows occurring naturally under pristine conditions very close to 0% of the time (i.e., $D_{>95}$).

Annual CHaMP site dsgn4-000205 had surveys conducted in August or near August in all years between 2011 and 2016, except for 2015 (Figure 35). A plot of wetted volume (m^3) against streamflow (m^3/s) for these years produced a linear regression ($y = 700.52x + 1637.3$, $R^2 = 0.9714$). The slope of this line is similar to that for annual site dsgn4-000245. At each of these sites, using the regression plots, a flow of about $0.5 m^3/s$ produces a wetted volume of about $1900 m^3$; a flow of about $1.4 m^3/s$ produces a wetted volume of about 2700 to $2800 m^3$. However, the wetted volume at dsgn4-000277 for a flow of $0.5 m^3/s$ was about $800 m^3$ and the maximum flow recorded for this period was about $0.8 m^3/s$ (Figure 36). Site dsgn4-000277 is at RK 83.9, while dsgn4-000245 and dsgn4-000205 are at RK 53.8 and RK 40.2, respectively. In the case of the site at RK 83.9, a flow of $0.5 m^3/s$ produced a wetted volume of $800 m^3$, and for the two sites at RK 53.8 and RK 40.2, a wetted volume of about $1900 m^3$ was produced.

For a constant streamflow of $0.5 m^3/s$ to produce different wetted volumes, there must be differences in the channels. This could be brought about by one channel having a lower gradient than the others. Also, average water velocities might vary among sites. Also, site wetted lengths were different, so a standardization was required. These observations led to a consideration of differences among sites in width (W) and depth (D) and wetted volume per meter.

Gradient, wetted site length, average wetted width based on cross sections calculated from GIS tools, and average wetted W/D were nearly indistinguishable among the sample dates on which these topographic surveys were made at these annual sites. For this reason, a comparison among these three sites was made using averages of the six values obtained from annual surveys between 2011 and 2016 (Figure 35). On the basis of average wetted CHaMP site data for the three example sites found at RK 83.9, RK 53.8, and RK 40.2 in a downstream direction, it was found that stream gradient declined from 0.01 to 0.005 to 0.003 with progress downstream. Average wetted volume for these same six years of samples went from $364.49 m^3$ in the headwaters to $617.29 m^3$ downstream. Because these sites had different lengths, volumes were standardized by dividing by size length. Average wetted volume divided by wetted site length changed from 2.195 in the headwaters to about 3.1 in the downstream two sites.

Average wetted width was a metric provided in the data download from champmonitoring.org. Average wetted width increased in a downstream direction from 13.77 to 15.70 to 19.98 m. Average wetted W/D was another metric provided in the output from CHaMP topographic analysis. These values were extremely high in the site at RK 40.2 (i.e., 107.69). This indicates a highly degraded condition. The upstream two sites were more similar to one another and were only slightly less large (average of about 80). Average wetted depth (D) was then calculated by dividing W by W/D. These average depths were all similar and ranged from 0.167 to 0.201.

Similar calculations were also done to assess width (W), depth (D), and velocity (V) at these same three annual CHaMP sites based on the wetted metrics obtained from CHaMP topographic analysis for the years in which streamflow was closest to 0.50 m³/s. For sites at RK 83.99, RK 53.8, and RK 40.2 these dates were August 12, 2014, July 30, 2012, and August 21, 2012 (Figure 36). Data available from CHaMP topographic analysis by download were average wetted width and average wetted W/D. Again the W/D at the lowest downstream site was very large (113.50) indicating a highly degraded channel. The two upstream channels also had W/D values indicative of degraded conditions, but were somewhat less.

By use of W and W/D for the dates on which streamflows near 0.50 m³/s were observed, D was calculated. Average wetted depths (D) for the three sites ranged from 0.147 m at the upstream site to 0.201 m and the intermediate site and was 0.171 m at the lowest site. Average wetted width (W) and average wetted depth (D) were multiplied together to calculate average wetted cross-section. With a streamflow of about 0.50 m³/s on these survey dates, the average stream water velocity (V) was calculated by dividing the streamflow by the cross-sectional area. Velocity was highest (0.26 m/s) in the headwater site and declined in a downstream direction. Velocities were very similar (about 0.15 m/s) in the two downstream sites.

The upstream site at RK 83.9 (dsgn4-000277) had the smallest average wetted volume/wetted site length (m³/m), the smallest average wetted width and smallest averaged wetted depth, but the largest stream gradient and average water velocity on sample dates having nearly 0.50 m³/s streamflow.

Summary

1. Streamflow measurements were made by CRITFC monitoring staff in 2010 across the upper Grande Ronde and Catherine Creek basins for purposes of developing a water temperature model. These measurements were all made in close time proximity (August 12-19) so that flow variations from day to day would be minimized.
2. Considering only the upper Grande Ronde for evaluation purposes, it was found that streamflow measurements evaluated on a stream network basis were accurately made. Measurements made near the USGS gage near Perry were nearly identical to the value reported by USGS. Also, measurements in confluent tributaries matched the flows in the mainstem below the confluence. The series of measurements made longitudinally varied in logical progressions where moderate gains or losses were observed downstream that revealed interactions with the floodplain or contributing streams.

3. The models of streamflow made by Watershed Sciences, Inc. (WSI) for purposes of water temperature modeling produced estimates of flows every 100 m for the entire stream network for every day in the summer period modeled for 2010. These modeled estimates relied upon the CRITFC measurements made at a point in time as well as USGS gage data. The measurements on specific days made by CRITFC matched closely with estimates made by WSI for those same days and locations.
4. Many of the sites measured in 2010 became annual CHaMP sites that were surveyed each year under the CHaMP program from 2011-2016.
5. Low flow statistics available from USGS in their StreamStats modeling (<https://water.usgs.gov/osw/streamstats/ssonline.html>) using their Version 3 State Applications were computed for many selected locations within the Upper Grande Ronde basin, including several annual CHaMP sites. Flow duration statistics (D_5 , D_{10} , D_{25} , D_{50} , and D_{95}) were computed for these locations in the stream network using StreamStats. Risley et al. (2008) stated that the D_5 flow duration is a high flow with a 5 percent exceedance probability. That is, for all days in the flow record, only 5% of all flows are higher than this. A D_{95} value is a low flow where 95% of the values are higher than this. StreamStats tabulates the flow duration statistics by month. Because adult spring Chinook spawning occurs in August and September in the Grande Ronde and because juvenile spring Chinook rearing in these months represents a critical limiting factor due to high water temperatures, the influence of streamflow duration in August was targeted.
6. There is a high correlation between August streamflows at the USGS gage near Perry and the gage below Clear Creek based on August gage data from 1997-2016 (1999 data were missing).
7. In 2010 the streamflows measured toward the headwaters of the Upper Grande Ronde when compared to the August D_{50} values (median August flows) were slightly less. After plotting the D_5 , D_{10} , D_{25} , D_{50} , and D_{95} streamflows vs. the percentage probability values (i.e., 5, 10, 25, 50, and 95), the regression produced for any stream site provides a means to calculate the probability value that corresponds to the measured streamflow in August at the site. For the upper sites in the UGR, the flow duration values were about D_{33} to D_{38} . However, on a longitudinal trajectory down the mainstem, the flow duration probabilities changed gradually so that flows measured near the gage near Perry were found to be extremely rare low flows, virtually never seen under the pristine watershed conditions modeled in StreamStats. This indicates that streamflow decline from naturally occurring levels (i.e., levels that would have been observed in an unmanaged basin) in a downstream direction. This might be due to a combination of factors: (1) increased evaporation from the stream surface area under greatly increased W/D ratios combined with elevated water temperatures that are due to increased solar radiation interception, and (2) water withdrawal or diversion. Natural variation also causes annual changes in August streamflows due to cycles of air temperature, humidity, and wind speed, as well as cycles of snow accumulation water equivalent and melt timing.

8. At the selected annual CHaMP sites there is variation from year to year for measurements made in the August period in the percentage that a measured streamflow at a representative cross-section comprises of the USGS gage flows near Perry and below Clear Creek. This could be due to the unpredictability of water diversions or use (e.g., livestock watering) during August that occur between the CHaMP site and the gages. Another cause for variation is the number of days required for water to flow from a site to a gage or a gage to a site. This can be significant because, for example, on a single date in August (i.e., August 14), streamflows at the USGS gage near Perry varied from 0.585 to 0.820 m³/s over a period from August 11, 2010 to September 1, 2010. With streamflow varying daily at the Perry gage and with 2 or more days required for water to flow from a CHaMP site to the gage, the correspondence between flows on the same data at the CHaMP site and the gage can vary.
9. Despite the probabilities of variations due to flow travel time, calculations of the percentages that daily flow at a CHaMP site comprise of the flow at the USGS gages are relatively consistent from year to year (based on 2011-2016).
10. D₅₀ streamflows calculated at a series of study sites along the UGR mainstem that are standardized by drainage area (m³/s/km²) and plotted against mean basin elevation produce a significant regression. Similarly, a significant regression is produced when these standardized streamflows (representing August median values) are plotted against mean annual precipitation. The modeling of D₅₀ by Risley et al. (2008) is based on drainage area, mean annual precipitation, and maximum elevation. Although maximum elevation was used in the streamflow statistics model by Risley et al. (2008), mean elevation and the standardized D₅₀ flow produce a very significant regression. Under conditions of climate change, the mean annual precipitation for a basin might decrease but presumably the relationship between precipitation and elevation would remain the same.
11. CHaMP data collected in surveys made at annual sites indicates for samples collected in the August or near August period that the wetted volume at a site increases with streamflow. For example at dsgn4-000245 as streamflow increases from 0.236 to 1.410 m³/s, wetted volume in the channel increases from 1452 to 2827 m³. This indicates that variations in flows that occurred between 2011 and 2016 produced large variations in wetted volume that could possibly be considered to be shifts in juvenile carrying capacity. Shifts in adult carrying capacity would be expressed better as a change in pool volume as a portion of the total wetted volume. The flows in 2015 and 2016 were extremely low at this site at RK 53.8. When contrasted with the natural August streamflow duration statistics for that site, the probabilities of experiencing flows that low were very low. These exceptionally low flows are likely due to a combination of water uses and evaporation.
12. The differences between measured flows at a site and the flows that would be expected to occur under natural conditions indicates the amount of water removed from the stream by the mechanisms described. This amount of water could potentially be restored to the stream with better land use practices and by narrowing of the channel to reduce wetted width.

Improvements in streamflow would improve conditions for adult and juvenile Chinook through water temperature reductions. In addition, the presence of increased wetted volume and increased water velocity that would occur under more concentrated flow in a narrowed channel would likely produce greater food supplies, provide greater transport of food past salmon feeding stations, and better growth rates at the lower temperatures that would result.

13. Evaluations of the annual streamflows at selected CHaMP sites made here suggest that there is a logical means to mapping out August streamflows on a stream network basis for purposes of rolling up estimates of annual carrying capacity each year. This design would work as follows.
 - a. Conduct CHaMP sampling along the mainstem UGR at the annual and rotating panel sites assigned for that year. In particular, measure streamflow and survey channel and wetted feature topography with the Total Station. Acquire the metrics of wetted volume, wetted W, wetted W/D, etc. for each site.
 - b. Calculate the streamflow probability for each site each year by reference to the regression of each site's streamflow duration frequency vs. probabilities.
 - c. If the sites in a longitudinal series from upstream to downstream are comprised by Annual Site A, Rotating Panel 1 Site B, Rotating Panel 2 Site C, and Annual Site D, for example, the only samples available for this portion of the stream in the year where Rotating Panel 1 sites are sampled would be Annual Site A, Rotating Panel 1 Site B, and Annual Site D. If we determine the flow frequency for Annual Site A and Rotating Panel 1 Site B which are in the headwaters and not affected by water withdrawals, they will probably have very similar flow frequencies by reference to StreamStats flow statistics.
 - d. If we then determine the flow frequency for Rotating Panel 1 Site B, and Annual Site D and find that the frequencies change in the downstream direction so that the flow frequency shifts toward that of a more extreme low flow (e.g., made a transition from a flow frequency of D_{40} to D_{50} between the two sites), then it could be assumed that the flow duration at Rotating Panel 2 Site C would be intermediate. This might be estimated by interpolation based on distance between the points.
 - e. This process can be continued for all Rotating Panel 2 and Rotating Panel 3 sites so that actual streamflows could be estimated for August-September periods when no CHaMP surveys were done in those years. With estimated and measured streamflows for each CHaMP site (all annual and rotating panel sites), the RBT (River Bathymetry Toolkit) could be used to predict wetted channel and wetted volume, or other characteristics related to carrying capacity for each site. These estimates of carrying capacity could then be rolled up to a basin scale. Rollups made only on the basis of the much more limited set of CHaMP sited measured in any given year would be less statistically meaningful.

Figures

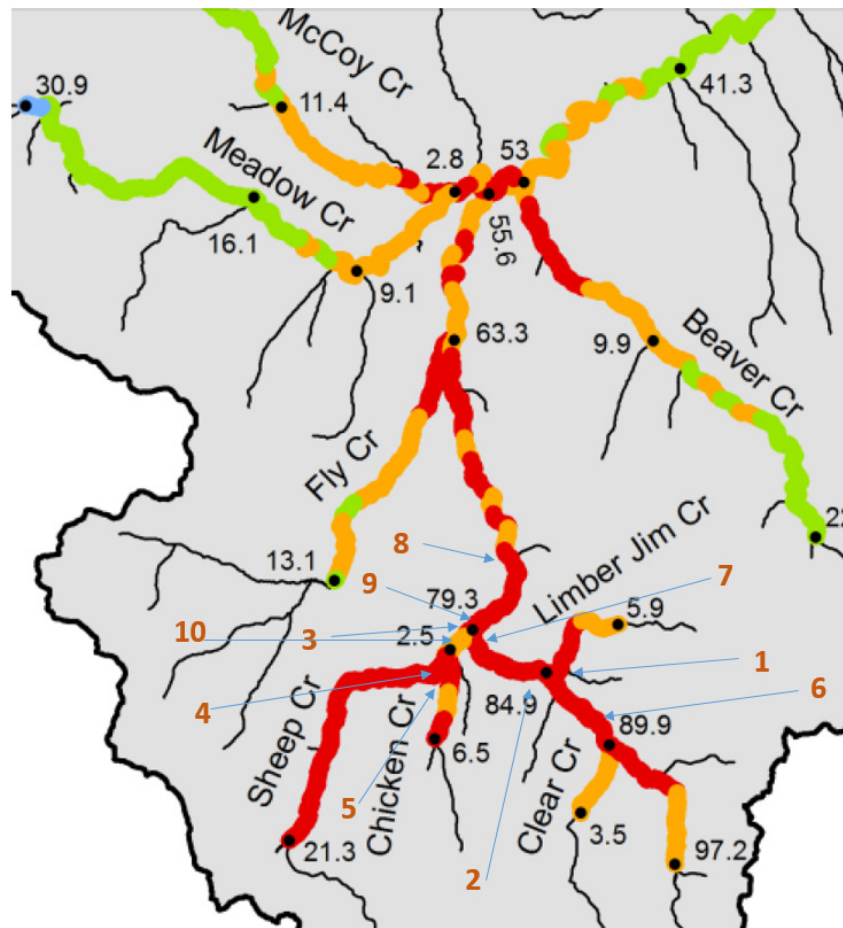


Figure 19. The upper zone of the Upper Grande Ronde basin, with the mainstem and major tributaries that were modeled for water temperature using Heat Source. Number in red indicate points on the stream network where StreamStats analysis of streamflow statistics and basin characteristics were calculated. Numbers in black indicate the river kilometer for the mainstem and tributaries. Base figure taken from Justice et al. (2016).

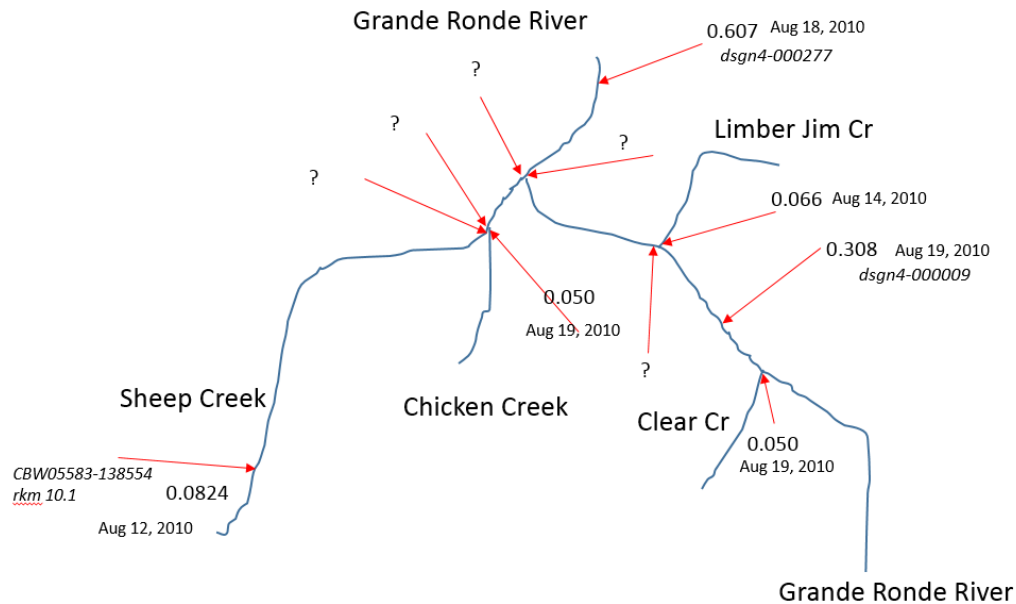


Figure 20. Streamflow measurements made by CRITFC on August 12-19, 2010 for select points on the Upper Grande Ronde stream network (from the dsgn4-000277 CHaMP site on the mainstem to the headwaters). Values are instantaneous flow measurements (m³/s) made during the day.

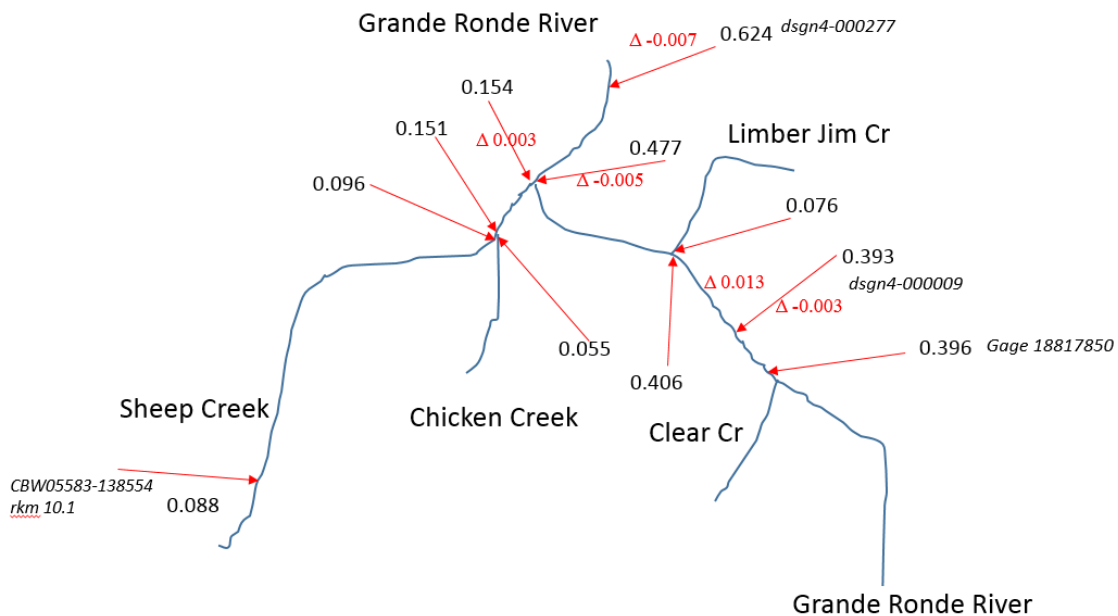


Figure 21. Streamflows modeled by Watershed Sciences, Inc. (WSI) from the extensive network of streamflow measurements made by CRITFC on August 12-19, 2010 for select points on the Upper Grande Ronde stream network. Values are estimates of mean daily flow (m³/s). All WSI values are those estimated for August 14, 2010.

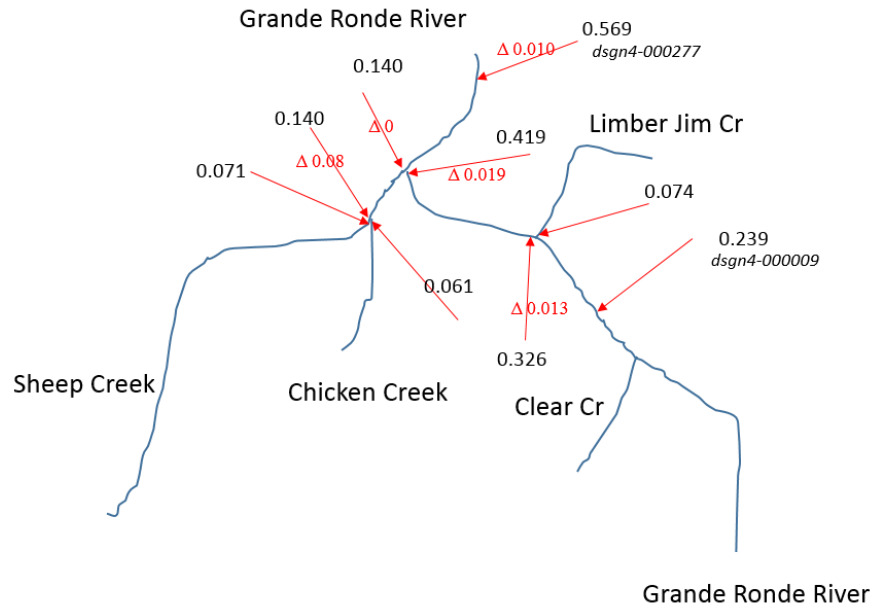


Figure 22. StreamStats (USGS) low flow statistics for select points on the Upper Grande Ronde stream network. Values are the D₅₀ or median low flow (m³/s) for August for all years of record.

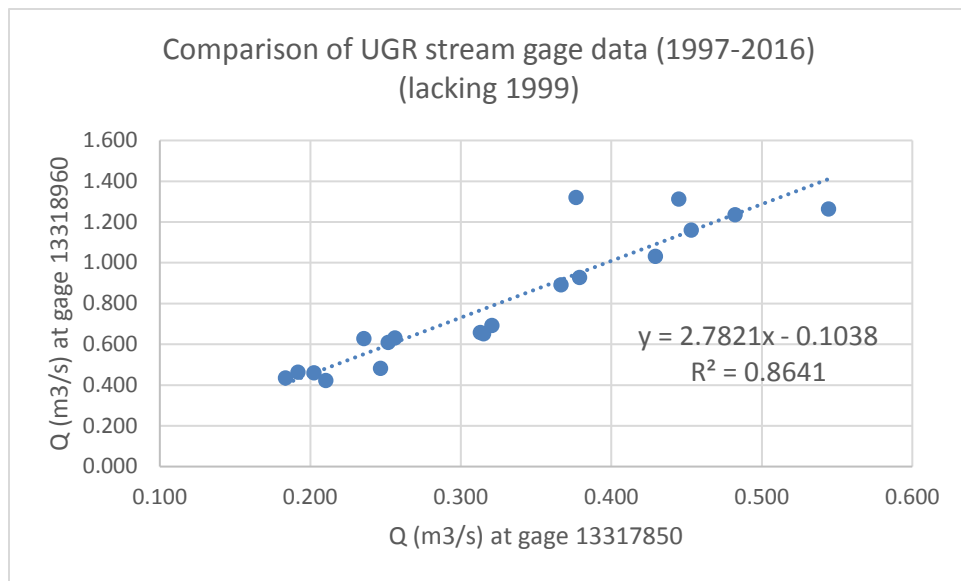


Figure 23. Regression of mean August flows at the USGS gage near Perry (13318960) against mean August flows at the Grande Ronde below Clear Creek, near Starkey, Oregon (13317850) for years 1997-2016, where data from 1999 were missing for gage 13317850.

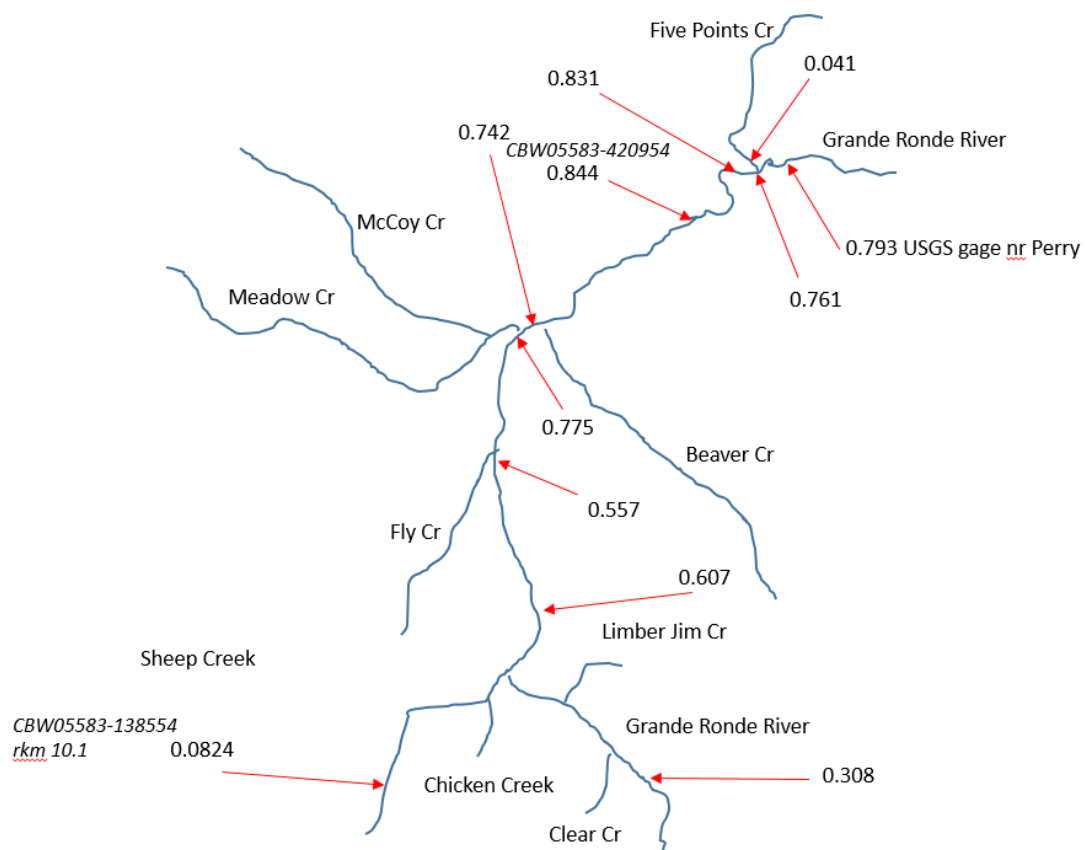


Figure 24. Streamflow measurements made by CRITFC on August 12-19, 2010 for select points on the Upper Grande Ronde stream network from Five Points Creek to the headwaters. Values are instantaneous flow measurements (m^3/s) made during the day. The flow measured by USGS at gage 13318960 on August 17-18 was included as a contrast to CRITFC measurements.

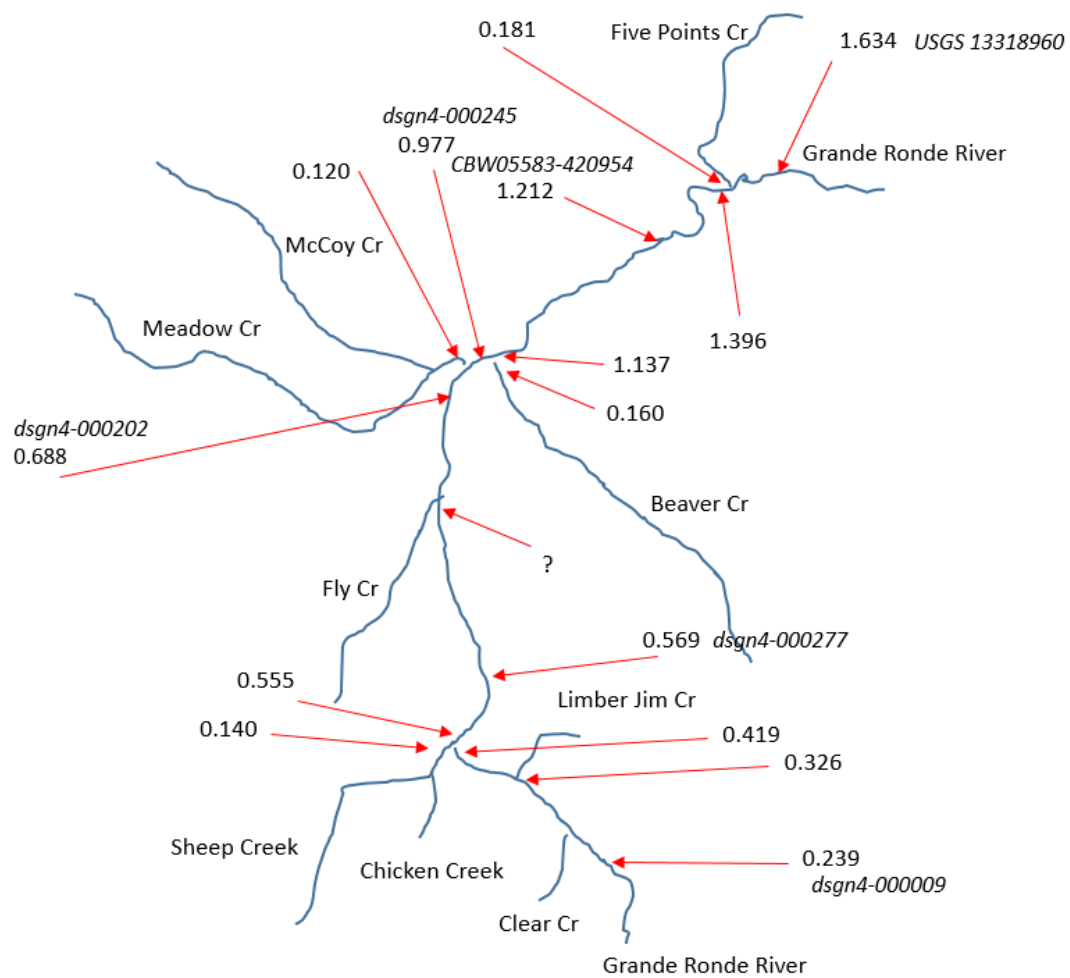


Figure 25. Streamflow statistics (D₅₀) generated by StreamStats (USGS 2016) for August during the period of record for select points on the Upper Grande Ronde stream network (USGS gage 13318960 near Perry to the headwaters). Values are in m³/s.

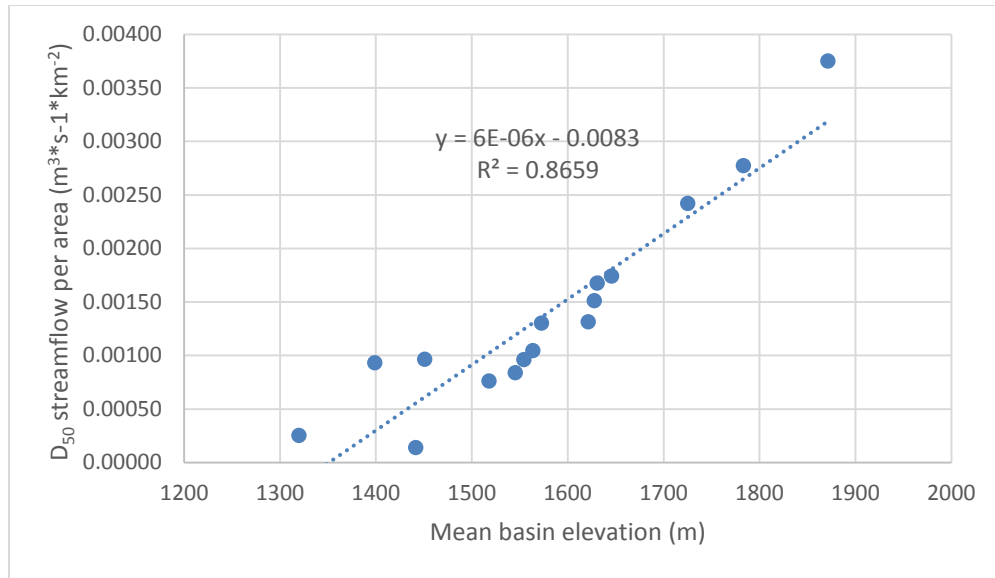


Figure 26. The relationship between D_{50} streamflow standardized by area and watershed elevation at its mouth for selected stream sites in the Upper Grande Ronde basin. See Table 30 for a list of sites.

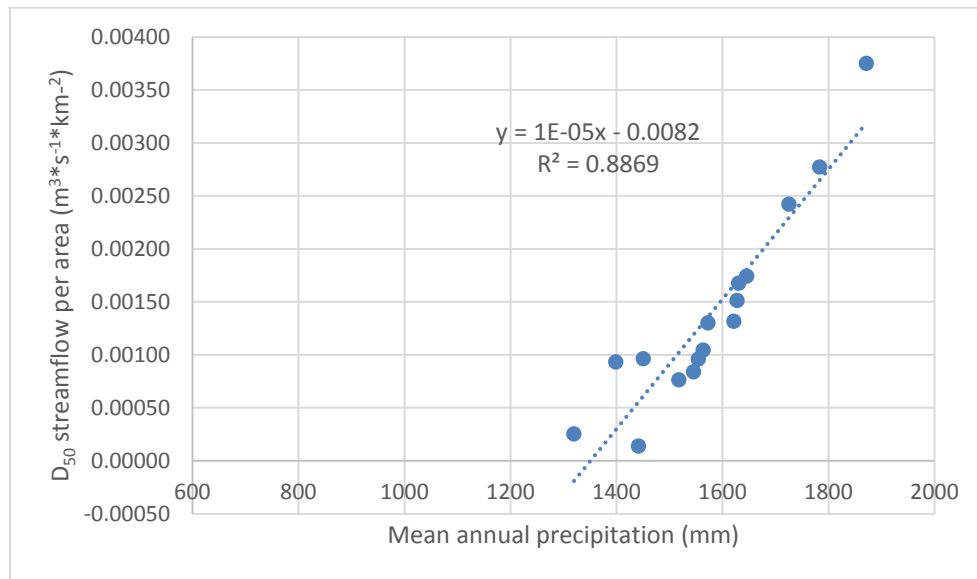


Figure 27. The relationship between D_{50} streamflow standardized by area and mean annual precipitation by watershed for selected stream sites in the Upper Grande Ronde basin. See Table 28 for a list of sites.

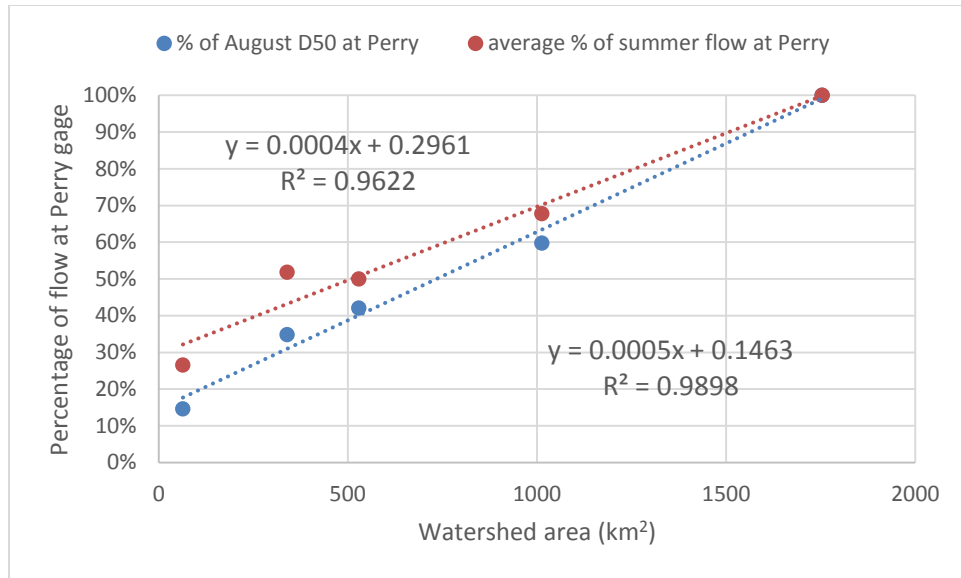


Figure 28. Relationship of percentage of streamflow at the Perry gage for selected “annual” CHaMP sites to watershed area. Note: Percentages based on D_{50} streamflows for August were computed by dividing the D_{50} August streamflow at selected “annual” CHaMP sites by the D_{50} August streamflow for the UGR at the Perry USGS gage site (13318960). The percentage of flows at the Perry gage were computed by dividing the average of streamflows made at selected CHaMP sites for random summer days that primarily are drawn from the July-August period by the streamflows reported for the USGS gage 13318960 for that same set of days spanning the years 2011-2015.

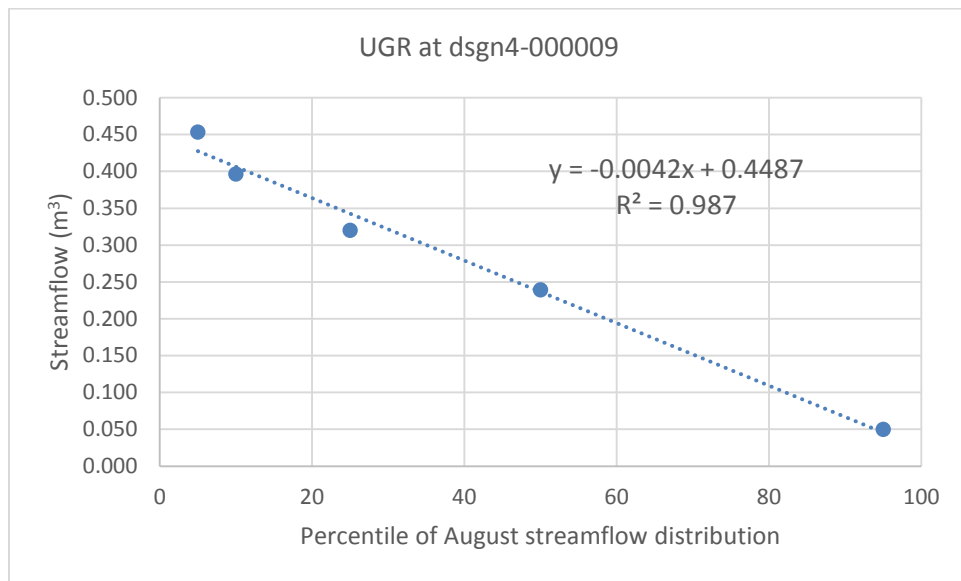


Figure 29. StreamStats values for D_5 , D_{10} , D_{25} , D_{50} , and D_{95} August streamflows for CHaMP site dsgn4-000009.

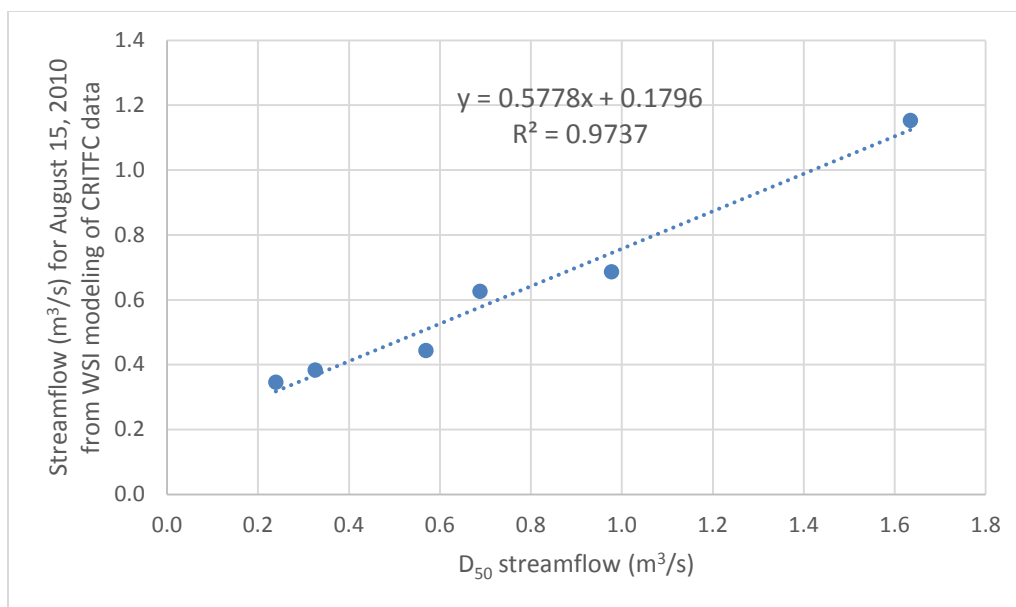


Figure 30. Relationship between streamflow for August 15, 2010 estimated by Watershed Sciences, Inc. based on streamflow data collected from August 12 to August 19 by CRITFC vs. D_{50} streamflow from StreamStats for a set of selected CHaMP sites. This plot is based on selected CHaMP annual sites and the USGS gage site near Perry. See Table 30 for a list of those sites. Data plotted for the USGS gage site near Perry is the streamflow measured by the gage on August 15, 2010 and the D_{50} value from StreamStats for the gage site.

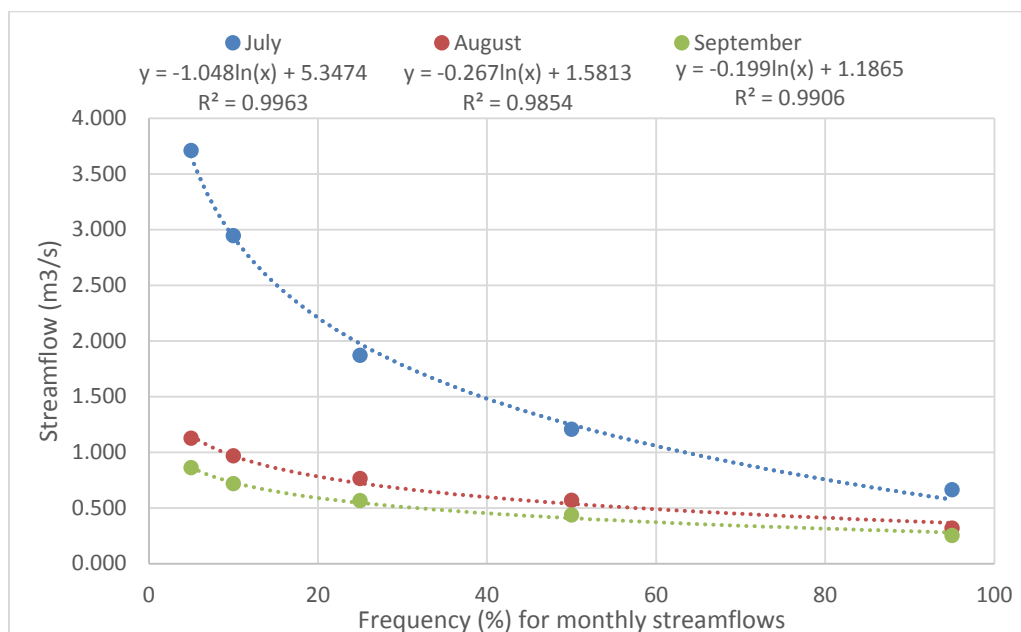


Figure 31. StreamStats values for D_5 , D_{10} , D_{25} , D_{50} , and D_{95} July, August, and September streamflows for CHaMP site dsgn4-000277 (RK 83.9).

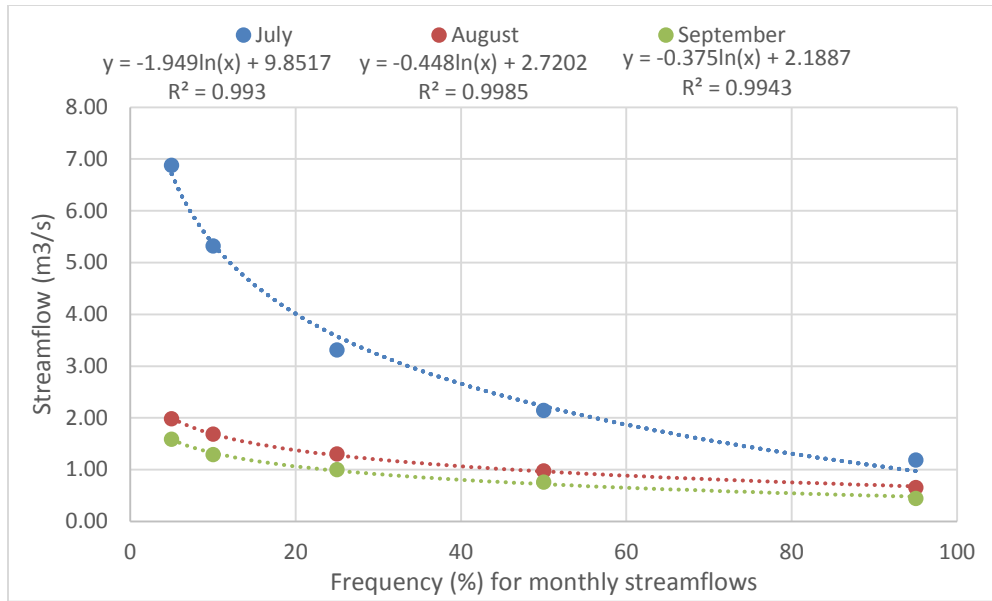


Figure 32. StreamStats values for D₅, D₁₀, D₂₅, D₅₀, and D₉₅ July, August, and September streamflows for CHaMP site dsgn4-000245 (RK 53.8).

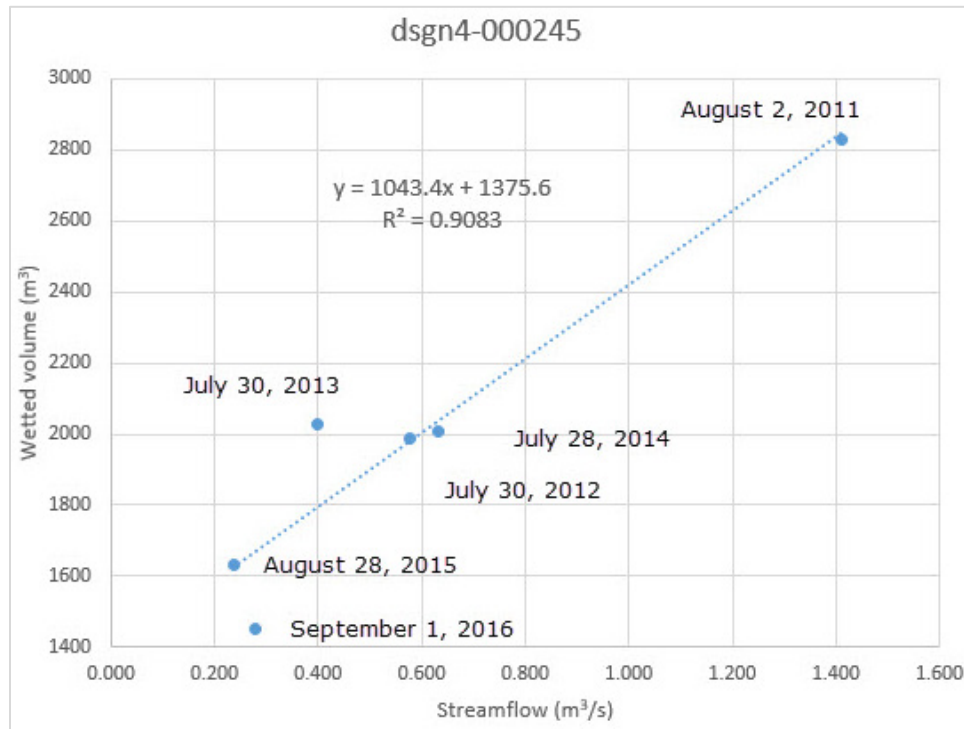


Figure 33. Prediction of wetted volume (m³) from measured streamflow (m³/s) at CHaMP site dsgn4-000245 for years where surveys were taken in August or close to August.

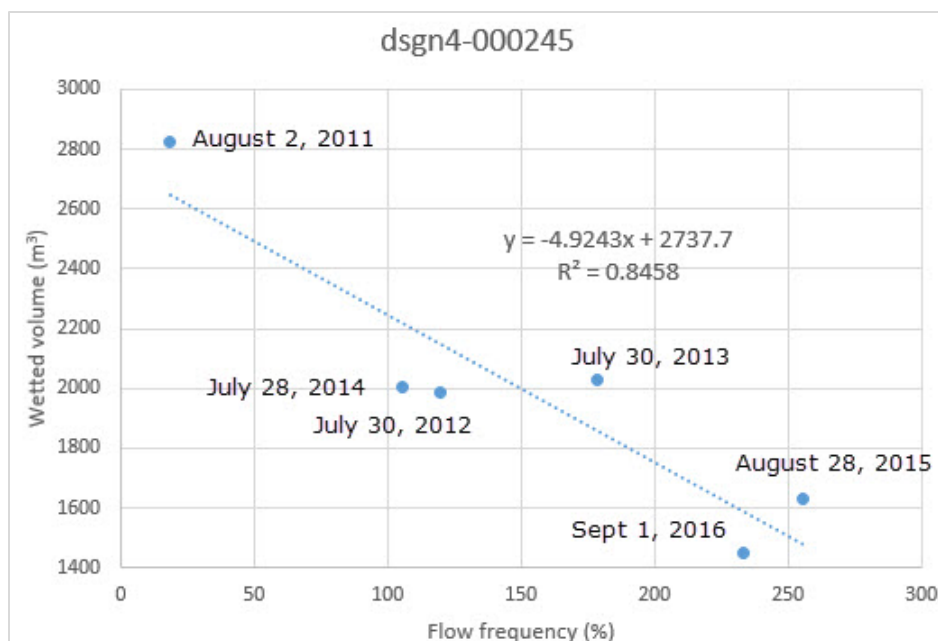


Figure 34. Relationship between wetted volume (m^3) in CHaMP site dsgn4-000245 and the estimated flow frequency (%) for the dates on which flows were measured at the site. Flow frequencies were estimated from the regression of StreamStats streamflow (m^3/s) on flow frequency (%) values (i.e., D_5 , D_{10} , D_{25} , D_{50} , and D_{95} , see Risley et al. 2008) for August.

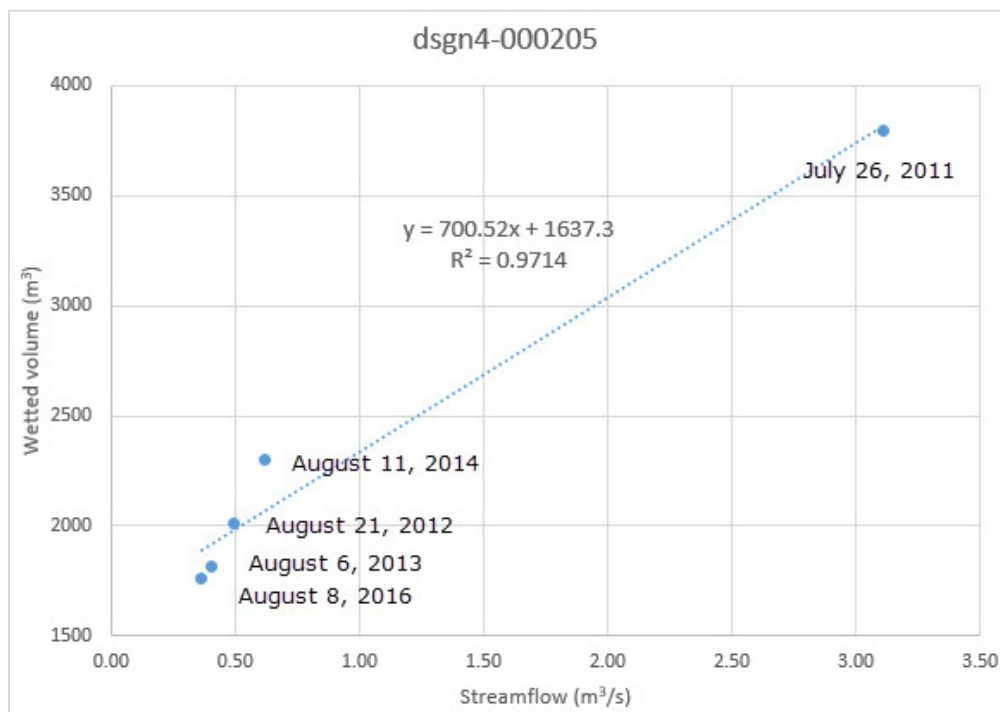


Figure 35. Prediction of wetted volume (m^3) from measured streamflow (m^3/s) at CHaMP site dsgn4-000205 for years where surveys were taken in August or close to August.

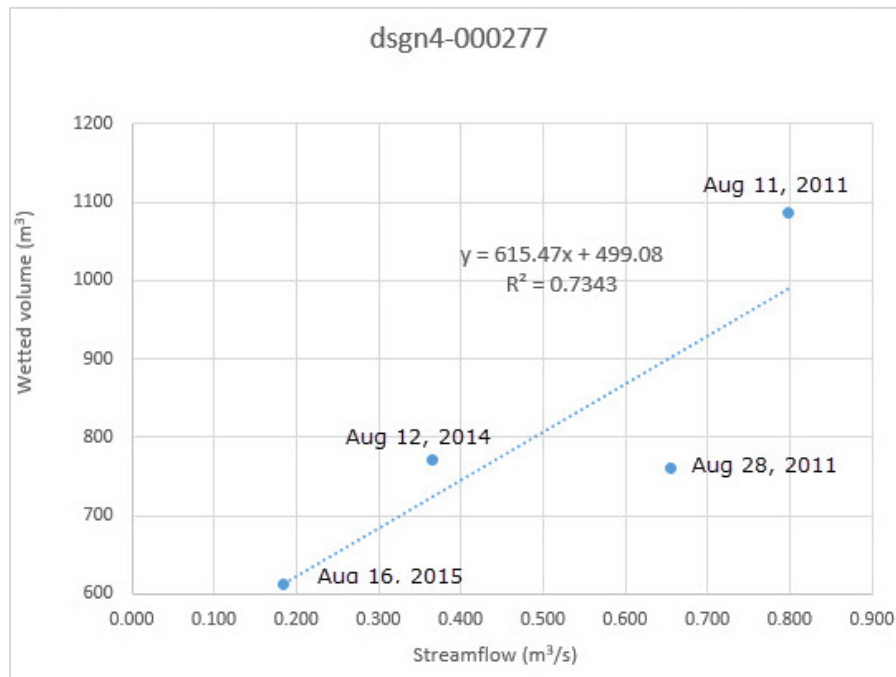


Figure 36. Prediction of wetted volume (m³) from measured streamflow (m³/s) at CHaMP site dsgn4-000277 for years where surveys were taken in August or close to August.

Tables

Table 18. Streamflow statistics for the period August 1-31, 2010 at USGS gage 13318960 on the Grande Ronde River near Perry.

Statistics for August 1-31, 2010 streamflow	m ³ /s
Mean	0.928
Standard error	0.047
Median	0.906
Standard deviation	0.259
Min	0.566
Max	1.359
Streamflow on August 15, 2010	0.934

Table 19. Streamflow statistics for August in the Upper Grande Ronde River mainstem and major tributaries. The D50 August streamflow (m³/s) represents the median August flow for the period of record. The D95 August flow is the flow that is exceeded 95% of all days in August.

Stream	D ₅	D ₁₀	D ₂₅	D ₅₀	D ₉₅
	m ³ /s				
Chicken Creek-mouth	0.123	0.106	0.084	0.061	0.028
Sheep Cr above Chicken Cr	0.142	0.122	0.097	0.071	0.075
Limber Jim Creek mouth	0.143	0.124	0.100	0.074	0.049
Meadow Creek	0.233	0.199	0.155	0.119	0.197
Sheep below confluence with Chicken	0.280	0.241	0.190	0.140	0.115
Sheep Cr. mouth	0.280	0.240	0.189	0.140	0.114
Beaver Creek	0.314	0.272	0.216	0.163	0.082
UGR at dsgn4-000009	0.453	0.396	0.320	0.239	0.050
UGR mainstem above Limber Jim Creek mouth	0.629	0.547	0.439	0.326	0.099
UGR mainstem above Sheep Creek mouth	0.807	0.702	0.561	0.419	0.163

GR below confluence of Sheep and UGR	1.090	0.940	0.742	0.555	0.323
GR at dsgn4- 000277	1.124	0.968	0.765	0.569	0.317
dsgn4-000245	1.985	1.685	1.305	0.977	0.654
Grande Ronde above Spring Creek	0.340	0.294	0.235	0.181	0.135
Grande Ronde above Five Points	2.823	2.396	1.849	1.396	0.926
Grande Ronde near Perry- 13318960	3.285	2.786	2.155	1.634	1.169
Grande Ronde at dsgn4-000202	1.376	1.178	0.920	0.688	0.385

Table 20. Streamflow values (m³/s) at the Grande Ronde River USGS gage near Perry (13318960) for August 14 from 2010-2016.

Date	Mean daily flow (m ³ /s)
8/14/2010	1.019
8/14/2011	1.218
8/14/2012	0.566
8/14/2013	0.680
8/14/2014	1.246
8/14/2015	0.453
8/14/2016	0.510

Table 21. Location (river km, or RK) of various annual CHaMP monitoring sites and other points on the mainstem Upper Grande Ronde used for streamflow measurement.

Sites	River km
dsgn4-000009	91.3
USGS gage 13317850	88.6
Limber Jim mouth	84.9
dsgn4-000277	83.9
Sheep Cr. mouth	79.3
dsgn4-000202	58.4
Meadow Cr. mouth	55.6
dsgn4-000245	53.8
dsgn4-000205	41.0
Five Points mouth	32.1
USGS gage nr Perry 13318960	29.2

Table 22. Comparison of the streamflows at CHaMP site dsgn4-000009 (RM 88.5) to the Grande Ronde River USGS gage near Perry (13318960) and Grande Ronde below Clear Creek (13317850) for all dates on which CHaMP streamflow measurements were taken at this “annual” site.

Date	dsgn4-000009 (m ³ /s)	USGS gage 13318960 near Perry (m ³ /s)	USGS gage 13317850 below Clear Cr. (m ³ /s)	% of streamflow near Perry	% of streamflow below Clear Cr.
August 19, 2010	0.308	0.9061	0.368	34.0%	83.7%
July 20, 2011	1.189	4.559	1.586	26.1%	74.9%
July 16, 2012	0.451	2.067	0.538	21.8%	83.8%
August 1, 2012	0.269	0.850	0.311	31.6%	86.4%
July 11, 2013	0.355	1.444	0.510	24.5%	69.5%
June 30, 2014	1.220	5.069	1.586	24.1%	76.9%
July 7, 2015	0.216	0.906	0.340	23.9%	63.6%

Table 23. Comparison of streamflows at CHaMP site dsgn4-000277 (RM 83.9) against the streamflows at the USGS gage near Perry (13318960) and Grande Ronde below Clear Creek (13317850) for all dates on which CHaMP streamflow measurements were taken at this “annual” site..

Date	dsgn4-000277 (m ³ /s)	USGS gage 13318960 near Perry (m ³ /s)	USGS gage 13317850 below Clear Cr. (m ³ /s)	% of streamflow near Perry	% of streamflow below Clear Cr.
August 18, 2010	0.607	0.793	0.396	76.6%	153.3%
August 11, 2011	0.799	1.331	0.595	60.0%	134.2%
August 16, 2011	0.820	1.189	0.481	68.9%	170.5%
August 21, 2011	0.727	0.991	0.425	73.3%	171.0%
August 24, 2011	0.595	0.878	0.396	67.7%	150.1%
August 27, 2011	0.608	0.850	0.396	71.6%	153.5%
August 28, 2011	0.656	0.793	0.396	82.7%	165.7%
September 1, 2011	0.585	0.765	0.368	76.4%	158.8%
August 9, 2012	0.273	0.680	0.258	40.2%	105.9%
July 15, 2013	0.561	2.152	0.425	26.1%	132.1%
August 12, 2014	0.366	0.736	0.340	49.7%	107.5%
August 16, 2015	0.185	0.396	0.210	46.6%	88.0%

Table 24. Comparison of the streamflows at CHaMP site dsgn4-000202 (RM 52.8) to the Grande Ronde River USGS gage near Perry (13318960) and Grande Ronde below Clear Creek (13317850) for all dates on which CHaMP streamflow measurements were taken at this “annual” site.

Date	dsgn4-000202 (m ³ /s)	USGS gage 13318960 near Perry (m ³ /s)	USGS gage 13317850 below Clear Cr. (m ³ /s)	% of streamflow near Perry	% of streamflow below Clear Cr.
July 25, 2011	1.691	3.087	1.189	54.8%	142.2%
August 6, 2012	0.324	0.736	0.272	44.0%	119.2%
July 19, 2013	0.482	0.963	0.396	50.1%	121.8%
July 26, 2013	0.284	0.595	0.311	47.8%	91.3%
September 7, 2014	0.308	0.623	0.244	49.4%	126.1%
August 3, 2015	0.224	0.425	0.215	52.7%	104.1%

Table 25. Comparison of streamflows at CHaMP site dsgn4-000245 (RM 52.4) against the streamflows at the USGS gage near Perry (13318960) and Grande Ronde below Clear Creek (13317850) for all dates on which CHaMP streamflow measurements were taken at this “annual” site..

Date	dsgn4-000245 (m ³ /s)	USGS gage 13318960 near Perry (m ³ /s)	USGS gage 13317850 below Clear Cr. (m ³ /s)	% of streamflow near Perry	% of streamflow below Clear Cr.
August 18, 2010	0.742	0.793	0.396	93.6%	187.4%
August 2, 2011	1.410	2.067	0.934	68.2%	151.0%
July 30, 2012	0.576	0.934	0.311	61.6%	185.2%
July 30, 2013	0.398	0.510	0.283	78.1%	140.7%
July 28, 2014	0.632	1.529	0.425	41.3%	148.6%
August 28, 2015	0.236	0.368	0.210	64.2%	112.6%

Table 26. Percentile ranking of streamflows from the USGS stream gage near Perry for the period 1997-2016. Data for this period is based on approved values through 9/30/2014 and provisional values from October 1, 2014 to October 14, 2016. Percentiles of streamflow were calculated both from all August mean daily flow values for the period of record and also from the mean annual August flows for the same period of record. The 50th and 5th percentile flows correspond in concept to the D₅₀ and D₉₅ flows from StreamStats.

Percentile ranking based on daily August streamflow (m ³ /s) (1997-2016)	
50 th percentile flow	0.743
5 th percentile flow	0.398
Percentile ranking based on mean August streamflow (m ³ /s) (1997-2016)	
50 th percentile flow	0.675
5 th percentile flow	0.435

Table 27. Comparison of the streamflows at CHaMP site dsgn4-000205 (RM 40.2) to the Grande Ronde River USGS gage near Perry (13318960) and Grande Ronde below Clear Creek (13317850) for all dates on which CHaMP streamflow measurements were taken at this “annual” site.

Date	dsgn4-000205 (m ³ /s)	USGS gage 13318960 near Perry (m ³ /s)	USGS gage 13317850 below Clear Cr. (m ³ /s)	% of streamflow near Perry	% of streamflow below Clear Cr.
August 18, 2010	0.844	0.793	0.396	106.4%	213.1%
July 26, 2011	3.109	2.973	1.133	104.6%	274.4%
August 21, 2012	0.495	0.623	0.227	79.5%	218.1%
August 6, 2013	0.400	0.510	0.266	78.4%	150.4%
August 11, 2014	0.621	0.708	0.340	87.7%	182.6%
July 14, 2015	1.347	1.897	0.481	71.0%	280.0%

Table 28. Compilation of selected basin characteristics for various Upper Grande Ronde River and tributary sites.

Stream	Drainage area (km ²)	Drainage density (km/km ²)	Mean annual precip (mm)	Mean annual max air T (°C)	Mean max Jan air T (°C)	Min basin elev (m)	Mean basin elev (m)
UGR near Perry	1753.42	0.559	673.1	12.22	0.61	893.1	1399.0
UGR at dsgn4-000202	528.35	0.416	701.0	11.56	0.11	1021.0	1572.8
Meadow Cr	468.79	0.565	624.8	12.44	1.00	999.7	1319.8
UGR at dsgn4-000277	339.29	0.541	739.1	11.28	-0.22	1204.0	1630.7
UGR below confluence of UGR and Sheep	318.57	0.534	744.2	11.22	-0.28	1261.0	1645.9
UGR above Sheep Cr. mouth	173.01	0.565	795.0	10.72	-0.67	1249.7	1725.2
Beaver Cr	155.92	0.572	731.5	11.44	-0.11	990.6	1563.6
Sheep Cr. mouth	145.56	0.497	685.8	11.78	0.17	1249.7	1554.5
Fly Cr.	128.46	0.497	640.1	11.89	0.50	1146.0	1517.9
UGR above Limber Jim mouth	117.59	0.590	812.8	10.44	-0.89	1286.3	1783.1
Sheep Cr. above Chicken Cr.	84.43	0.447	675.6	11.78	0.22	1258.8	1545.3
UGR at dsgn4-000009	63.71	0.640	861.1	9.89	-1.28	1405.1	1871.5
Limber Jim mouth	48.95	0.485	772.2	11.11	-0.33	1286.3	1627.6
Chicken Cr	46.36	0.522	713.7	11.44	-0.11	1258.8	1621.5

Table 29. Relationship between drainage area at selected points in the Upper Grande Ronde basin and D₅₀ streamflow statistics, watershed elevation at its mouth, and mean annual precipitation.

Stream	Drainage area (km ²)	D ₅₀ (m ³ /s)	D ₅₀ streamflow per area (m ³ *s-1/km ²)	Min basin elev (m)	Mean basin elev (m)	Mean annual precip (mm)
UGR near Perry	1753.42	1.634	0.00093	893.1	1399.0	673.1
UGR above Spring Creek	1289.81	0.181	0.00014	929.6	1441.7	665.5
UGR above Beaver Cr (dsgn4-000245)	1012.69	0.977	0.00096	993.6	1450.8	662.9
UGR at dsgn4-000202	528.35	0.688	0.00130	1021.0	1572.8	701.0
Meadow Cr	468.79	0.119	0.00025	999.7	1319.8	624.8
UGR at dsgn4-000277	339.29	0.569	0.00168	1204.0	1630.7	739.1
UGR below confluence of UGR and Sheep	318.57	0.555	0.00174	1261.0	1645.9	744.2
UGR above Sheep Cr. mouth	173.01	0.419	0.00242	1249.7	1725.2	795.0
Beaver Cr	155.92	0.163	0.00105	990.6	1563.6	731.5
Sheep Cr. mouth	145.56	0.140	0.00096	1249.7	1554.5	685.8
Fly Cr.	128.46	0.098	0.00076	1146.0	1517.9	640.1
UGR above Limber Jim mouth	117.59	0.326	0.00277	1286.3	1783.1	812.8
Sheep Cr. above Chicken Cr.	84.43	0.071	0.00084	1258.8	1545.3	675.6
UGR at dsgn4-000009	63.71	0.239	0.00375	1405.1	1871.5	861.1
Limber Jim mouth	48.95	0.074	0.00151	1286.3	1627.6	772.2
Chicken Cr	46.36	0.061	0.00132	1261.0	1621.5	713.7

Table 30. Relationship between drainage area for selected “annual” CHaMP stream sites in the Upper Grande Ronde basin and streamflows at those sites as a percentage of D₅₀ flows at the Perry site and as a percentage of flows in the summer at the UGR gage at Perry (13318960). Note: Percentages based on D₅₀ streamflows for August were computed by dividing the D₅₀ August streamflow at selected “annual” CHaMP sites by the D₅₀ August streamflow for the UGR at the Perry USGS gage site (13318960). The percentage of flows at the Perry gage were computed by dividing the average of streamflows made at selected CHaMP sites for random summer days that primarily are drawn from the July-August period by the streamflows reported for the USGS gage 13318960 for that same set of days spanning the years 2011-2015.

Sites on Upper Grande Ronde	Drainage area (km ²)	D ₅₀ (m ³ /s)	% of flow at Perry based on D ₅₀	% of flow at Perry based on annual measurements
UGR near Perry	1753.42	1.634	1.000	1.000
UGR above Beaver Cr (dsgn4-000245)	1012.69	0.977	0.598	0.678
UGR at dsgn4-000202	528.35	0.688	0.421	0.500
UGR at dsgn4-000277	339.29	0.569	0.348	0.518
UGR at dsgn4-000009	63.71	0.239	0.146	0.266

Table 31. Flow frequency values for August flows measured in CHaMP surveys at site dsgn4-000245 (RK 53.8). Values were computed from the equation derived from plotting StreamStats values for August in Figure 32.

Date	Streamflow (m ³ /s)	Flow frequency (%)
August 18, 2010	0.742	82.73
August 2, 2011	1.410	18.63
July 30, 2012	0.576	119.85
July 30, 2013	0.398	178.26
July 28, 2014	0.632	105.86
August 28, 2015	0.236	255.70

Table 32. Flow frequency values for August flows measured in CHaMP surveys at site dsgn4-000277 (RK 83.9). Values were computed from the equation derived from plotting StreamStats values for August in Figure 31.

Date	Flow (m ³ /s)	D value (%)
August 18, 2010	0.607	38.44
August 11, 2011	0.799	18.76
August 16, 2011	0.820	17.31
August 21, 2011	0.727	24.56
August 24, 2011	0.595	40.28
August 27, 2011	0.608	38.29
August 28, 2011	0.656	31.98
August 9, 2012	0.273	134.19
August 12, 2014	0.366	94.93
August 16, 2015	0.185	186.93

Table 33. Modeled WSI streamflow values for August 15, 2010 for selected annual sites and the Grande Ronde near Perry USGS site contrasted with D₅₀ values computed by StreamStats.

Stream	Drainage area (km ²)	D ₅₀ (m ³ /s)	August 15, 2010 streamflow (WSI; m ³ /s)	River km
UGR at dsgn4-000009	63.71	0.239	0.346	91.3
UGR above Limber Jim mouth	117.59	0.326	0.384	85.0
GR at dsgn4-000277	339.29	0.569	0.444	83.9
UGR at dsgn4-000202	528.35	0.688	0.626	58.4
GR above Beaver Cr (dsgn4-000245)	1012.69	0.977	0.686	53.8
GR near Perry	1753.42	1.634	1.153	29.2

Table 34. Average channel conditions for years 2011-2016 that may be used to explain the differences in wetted volume at a fixed streamflow.

Annual CHaMP site	dsgn4-000205	dsgn4-000245	dsgn4-000277
Location on mainstem	RK 40.2	RK 53.8	RK 83.9
Gradient (decimal)	0.003	0.005	0.010
Average wetted volume (m ³)	617.29	612.03	364.49
Average wetted volume /wetted site length (m ³ /m)	3.078	3.104	2.195
Average wetted width (m)	19.98	15.70	13.77
Average wetted W/D	107.69	78.19	82.37
Average wetted D, calc from avg W and W/D	0.186	0.201	0.167

Table 35. Average channel conditions for three selected annual CHaMP sites surveyed on a mid-summer date in the period 2011-2016 that had a wetted volume closest to 0.5 m³/s.

CHaMP annual site	dsgn4-000205	dsgn4-000245	dsgn4-000277
Location on mainstem	RK 40.2	RK 53.8	RK 83.9
Sample date with flow closest to 0.50 m ³ /s	August 21, 2012	July 30, 2012	August 12, 2014
Average wetted width (m)	19.37	16	13.03
Average wetted W/D	113.50	79.55	88.92
Average wetted D, calc from avg W and W/D	0.171	0.201	0.147
Avg wetted cross-sectional area on date closest to flow of 0.50 m ³ /s	3.31	3.22	1.91
Wetted volume on date closest to flow of 0.50 m ³ /s	2010.5	1989.4	772.0
Streamflow (m ³ /s)--example within range experienced	0.500	0.500	0.500
Average V at flow of 0.5 m ³ /s based on avg W and avg D above (m/s)	0.151	0.155	0.262

References

- Collings, M.R. 1974. Generalization of spawning and rearing discharges for several Pacific salmon species in western Washington. U.S. Geological Survey, Open-file Report (for the WDF). Tacoma, Washington. 39 p.
- Collings, M.R., R.W. Smith, and G.T. Higgins. 1972. The hydrology of four streams in western Washington as related to several Pacific salmon species. U.S. Geological Survey, Water-Supply Paper 1968. 109 p.
- Collings, M.R., and Hill, G.W. 1973. Hydrology of ten streams in western Washington as related to several Pacific salmon species. U.S. Geological Survey Water-Resources Investigations 11-73, 149 p.
- Gippel, C.J. and M.J. Stewardson. 1998. Use of wetted perimeter in defining minimum environmental flows. *Regulated Rivers: Research & Management* 14:53-67.
- Guay, J.C., D. Boisclair, M. Leclerc, and M. Lapointe. 2003. Assessment of the transferability of biological habitat models for Atlantic salmon parr (*Salmo salar*). *Can. J. Fish. Aqu. Sci.* 60(11):1398-1408.
- Kelly, V.J. and White, S. 2016. A method for characterizing late-season low-flow regime in the upper Grand Ronde River Basin, Oregon. U.S. Geological Survey Scientific Investigations Report 2016-5041, 41 p., <http://pubs.usgs.gov/ofr/2016/5041/>
- McElhaney, P., M. H. Ruckelshaus, M. J. Ford, T. C. Wainwright, and E. P. Bjorkstedt. 2000. Viable salmonid populations and the recovery of evolutionarily significant units. NOAA Technical Memo NMFS-NWFSC-42. U.S. Department of Commerce. 156 pp.
- OWRD. 2016. Water rights. Oregon Water Resources Department. https://www.oregon.gov/owrd/Pages/wr/index.aspx#Access_Water_Right_Data_and_Maps
- Rantz, S.E. 1964. Stream hydrology related to the optimum discharge for king salmon spawning on the northern California Coast Ranges. U.S. Geol. Surv. Water-Supply Pap. 1779(AA), 16pp.
- Risley, J.C., A. Stonewall, and T. Haluska. 2008. Estimating flow-duration and low-flow frequency statistics for unregulated streams in Oregon. U.S. Geological Survey Scientific Investigations Report 08-5126, 23 p.
- USGS. 2016. StreamStats Version 3.0. http://streamstatsags.cr.usgs.gov/v3_beta/viewer.htm?stabbr=OR.

Walters, A.W., Krista K. Bartz, Michelle M. McClure. 2013. Interactive Effects of Water Diversion and Climate Change for Juvenile Chinook Salmon in the Lemhi River Basin (U.S.A.). Conservation Biology 27(6): 1179-1189.

Walters, A.W., Krista K. Bartz, Michelle M. McClure. 2013. Interactive Effects of Water Diversion and Climate Change for Juvenile Chinook Salmon in the Lemhi River Basin (U.S.A.). Conservation Biology 27(6): 1179-1189. Appendix S-1. Streamflow and temperature estimates for scenarios in the survival and capacity analyses.

Files included in analysis

MetricAndCovariates-Access-20150911.xlsx

17_Grande_Ronde_Hyd_Flow-dm.xlsx

11-Sheep_Creek_Hyd_Flow.xlsx

10_Chicken_Creek_Hyd_Flow.xlsx

Grande Ronde River-near Perry-13318960.xlsx

USGS 13317850-Grande Ronde below Clear Creek.xlsx

Flow_measurements_2010.xlsm

StreamStats-low flow estimation basins.pptx

Low flow input points-dm.pptx

Risley-2009-USGS-low flow statistics-tables.xls

MetricVisitInformationMasterDB_20170206.xlsx

Peak Flow Analysis

Full Title: Analysis of Peak Flows in the Upper Grande Ronde River Basin and Implications for Spring Chinook Carrying Capacity

Introduction

Spring Chinook Salmon viability is a function of productivity, abundance, spatial structure, and diversity (McElhaney et al. 2000). Juvenile spring Chinook Salmon carrying capacity and survival are generally thought to be a function of a variety of habitat quality variables. For purposes of creating a simple habitat-based life cycle model, CRITFC has adopted a model framework that is based on a limited number of habitat variables: (1) summer water temperature (from CHaMP, NorWeST (USFS 2017)), (2) fine sediment (McNeil core measurements from 2011-2013; McCullough et al. 2015), (3) pool frequency analysis based on Oregon Land Survey data (White et al. 2017), McIntosh's (1994) monitoring in the Grande Ronde, and the McIntosh et al. (1994, 2000) comparison of 1940s NOAA surveys with 1990s re-surveys, (4) adult pre-spawning mortality based on Justice's (see this annual report) analysis of spawning success vs. water temperature exposure in several rivers in the Grande Ronde basin and the Imnaha River, (5) food availability for juvenile salmon based on White's (in-progress) SEM-based analysis of macroinvertebrate community trait characteristics relative to habitat conditions, (6) smolt survival, which is a function of fish length, which is based upon Justice et al.'s (2014) statistical relationship developed between smolt length and water temperature, (7) and spawnable habitat area, which will be estimated by use of HSI modeling with topographic surveys, streamflow estimates, and the River Bathymetry Toolkit, which allows the wetted stream channel to be delineated by adjustment of stage height.

CRITFC already produced a life cycle model for six populations of spring Chinook of the Grande Ronde basin (McCullough et al. 2015). This model is an empirically-based model reliant on Beverton-Holt computations with adult spawners and juvenile outmigrants as input data. We are currently expanding this effort to develop a model based on functional relationships between adult and juvenile survival and abundance and key habitat factors, such as those described above.

Although this new life cycle modeling approach is intended to be simple at the outset to facilitate development and testing, it is obvious that there are numerous opportunities for survival to be influenced by additional variables that are not well represented by the key variables selected. For example, water temperature is a key variable linked to juvenile distribution and survival. It is highly related to riparian cover as well as drainage area and elevation. Water temperature during the summer rearing and spawning season is also responsive to changes in streamflow. Streamflow annual variations can be attributed to annual amount of precipitation and especially depth of snowpack, but also timing of snowmelt, which is linked to seasonality of air temperature trends. These factors influence both the magnitude and timing of peak flow events as well as the annual variations in low flow events. Timing of peak flow events in relation to the timing of life stage events is capable of influencing survival at either the incubation stage via scouring or the post-emergence stage (downstream displacement of juveniles

to the lower Grande Ronde valley) where mortality would be high during summer juvenile rearing stages.

The purpose of this exploration of peak flows in the Upper Grande Ronde River and Catherine Creek is to determine whether (1) gaging station data exist for the time frame involved in our CHaMP monitoring program (i.e., 2011-2016), (2) indices can be created that might reflect the potential impact of peak flows to spring Chinook life stage survivals, (3) data can be extrapolated from a gage to other ungaged locations in the basin, (4) peak flows are implicated in mortality or displacement of juveniles produced from their parent spawners, (5) redd densities are linked to substrate composition of riffles and channel gradient.

Methods

Stream gaging stations are available in the Upper Grande Ronde River and in Catherine Creek on either the mainstem or on tributaries (Table 36). Many of these gaging stations are discontinued or do not have records that overlap the years in which CHaMP surveys were made. Others have very short periods of record, making them unsuitable for development of useful flow statistics. Gaging stations on tributaries, such as Meadow Creek below Dark Canyon Creek (13318210), Five Points Creek at Hilgard (13318920), or North Fork Catherine Creek near Medical Springs (13319900) are still active and have several years of record that could provide interesting comparisons with flows measured on the mainstem (Table 36). However, for purposes of this peak flow analysis, we used gaging stations on the mainstem Upper Grande Ronde River (13317850 and 13318960) and Catherine Creek (13320000 and 13320300).

Of the four gages mentioned in the Upper Grande Ronde and Catherine Creek that will be the focus of this work, only gage 13320000 (Catherine Cr NR Union, OR) is a USGS gage. Data for this gage can be obtained at USGS (2017a).

The other three gages are all gages maintained by Oregon Water Resources Department (OWRD). OWRD gages tend to begin operation in the early 1990s at a time when many USGS gages were being discontinued. OWRD streamflow data, either average daily flows, peak flows, flow duration curves, or instantaneous flows (i.e., every 15 minutes for the recent two-year period) were obtained from OWRD (2017a).

Miscellaneous peak flow data were obtained directly from OWRD by contacting Richard Marvin (richard.k.marvin@oregon.gov). Questions about obtaining regional peak flow regression data were resolved by contacting Kenneth Stahr (kenneth.l.stahr@oregon.gov). Advice on methods for analyzing peak flows using the USGS (2017b) website and means of predicting peak flows were gained by contacting John Risley (jrisley@usgs.gov).

Regional regression equations were obtained using data from OWRD (2017b) derived from their peak discharge estimation mapping tool. This website was used by entering latitude and longitude of either CHaMP sites or sites of stream gages so that return period (years) could be estimated from peak flows at the gages. For CHaMP sites near the gage in the upper extent of the Upper Grande Ronde where

drainage area does not vary significantly among gages, we were able to extrapolate annual peaks with confidence from those measured at the gage to CHaMP sites upstream and downstream that are within the key spawning areas. These regional peak flow frequency estimations were based on equations similar to those available in Cooper (2006) for Region 3 (i.e., the hydrological region that encompasses the Upper Grande Ronde River basin). Those from OWRD made use of basin characteristics available from USGS's (2017c) StreamStats tool. Peak flows were associated with basin characteristics so that they could be used to predict return periods. We plotted peak flow vs. return period to derive a regression equation. This equation was then used to predict return periods (years) at the gaged site for a set of annual of peak flows. Because an OWRD gage (13317850, Grande Ronde bl Clear Creek) was near the CHaMP sites in the upper end of the mainstem, a direct peak flow analysis based on annual peak flows was conducted. This analysis was provided courtesy of John Risley (USGS) in Portland. Data input consisted of 20 years of streamflow peak records captured between 1993 and 2016. Data points for years 1998-2000 and 2006 were missing. Data were converted to Watstore format and entered into the PeakFQ program, which computed the peak flow frequencies using standard Bulletin 17B defaults and the 17B generalized skew for the gage site.

Stream power and unit stream power were calculated using equations provided in Wikipedia.com.

$$\Omega = \rho g Q S$$

where, Ω is the stream power, ρ is the density of water (1000 kg/m^3), g is acceleration due to gravity (9.8 m/s^2), Q is discharge (m^3/s), and S is the channel slope.

$$\omega = \rho g Q S / b$$

where, ω is the unit stream power, and b is the width of the channel. From summertime CHaMP surveys only bankfull channel width (BFW) was able to be measured. It was assumed in this analysis that average site BFW is equal to peak flow wetted width at all peak flows experienced from 2011-2016.

Peak flows at each of the ten CHaMP sites at the uppermost portion of the UGR mainstem were estimated from peak flow measurements made at OWRD gage site 13317850. The 20 annual peak flow values available for this site were used to compute peak flow frequencies. The peak flows estimated by this USGS procedure were plotted against return period and regression equations computed. The regression equation was used to calculate the return period for each annual peak flow recorded from 2011-2016 at the gage site. From this return period an appropriate "area coefficient" was assigned to the peak flow for each year (see Cooper 2006).

Peak flows were then calculated for each of the 10 CHaMP sites in the UGR, where 4 sites were upstream of the gage (13317850), 2 were downstream of the gage but upstream of the confluence with Sheep Creek, and 4 were downstream of the Sheep Creek confluence on the mainstem UGR. Peak flows were estimated at these ungaged sites by assuming that the return interval would be the same as for the gaged site.

The equation used to predict peak flows upstream or downstream of this gage was (see Cooper 2006):

$$Q_u = Q_g (A_u/A_g)^a$$

where,

Q_u = the estimated discharge for the ungaged watershed,

Q_g = the discharge from the log-Pearson Type III distribution fitted to the annual series of peak discharges at the gaging station,

A_u = the area of the ungaged watershed,

A_g = the area of the gaged watershed, and

a = the exponent termed the area coefficient that would be specific for a hydrologic region (i.e., Region 3, which encompasses the UGR) and a return period.

Area coefficients used in this analysis were selected to match the return period of the peak flow for each year (Table 37).

Peak flows were then predicted by this method for each of the 10 CHaMP sites for each year from 2011-2016. Stream power and unit stream power were calculated from these peak flows, the channel gradient, and the mean BFW for each site. Total juvenile Chinook counts obtained from snorkeling each CHaMP site in year (x) were associated with redd counts for a 1-km reach measured upstream from the bottom-of-site at each CHaMP site for year $(x-1)$. That is redd counts tallied from multiple surveys in August-September of year $(x-1)$ were then subject to a peak flow that tended to occur in May-June of year (x) . Juveniles observed by snorkeling in year (x) were then related to the redds from the previous year to demonstrate the influence of stream power or unit stream power of the intervening peak flow. An index of juvenile survival (or displacement downstream) was computed as total number per m of juvenile Chinook in each CHaMP site divided by number of redds per km tallied for the 1-km reach upstream of the bottom-of-site for each of the 10 CHaMP sites.

For purposes of calculating peak flow frequencies by application of traditional USGS methodology, it is necessary to have true peak flow values obtained from instantaneous flow measurements. In the Upper Grande Ronde such values are obtained from measurements recorded every 15 minutes. OWRD reports the annual true peak flows for each gage in Oregon, but for the most recent years it was necessary to derive these from provisional, instantaneous flow records or by contacting OWRD. In this report these peak flow values will be termed “true peak flows.” Because average daily flows are easier to obtain, we also derived maximum annual average daily flows that we term simply “peak flows.” While this may not be technically appropriate, it saves verbiage in this report.

Results and Discussion

Orientation to the Upper Grande Ronde River and Catherine Creek Basins

For purposes of estimating peak flows in the Upper Grande Ronde River and Catherine Creek, two stream flow gages are key to this estimation for relating to spawning and summer rearing areas (USGS 13320000 Catherine Creek nr Union and OWRD 13317850 Grande Ronde River bl Clear Creek). Both

gages are currently in operation and are able to provide data relevant to the CHaMP monitoring years (2011-2016). The Catherine Creek gage has 88 complete water years from 1911 to 2014, while the GR gage below Clear Creek has 17 complete years from 1992-2012. Years from end dates expressed above were filled in using provisional flow records. Gage 13317850 covers a drainage area of 39.00 mi² as listed by OWRD and gage 13320000 has a drainage area of 103.00 mi², as listed by OWRD.

Gage 13319900 on the NF Catherine Creek has also been active since 1992, but has only 2 years with peak flow records, so was not useful in this analysis. The Upper Grande Ronde River OWRD gage 13318960 near Perry has a drainage area of 678 mi² according to OWRD. This gage has been in operation since 1996 and has 18 years of peak flow records up to 2014. USGS gage 13319000 (Grande Ronde at La Grande, Oregon) is discontinued, but has 80 years of flow records dating from 1903 to 1989. This gage provides a good basis for developing peak flow frequency data for the region and can be compared with the gage very nearby at 13318960.

Examination of Peak Flows and Flow Patterns at the Gages

For the Upper Grande Ronde River, the lower basin's peak flows at 13318960 will be compared to the upper basin's peak flows at 13317850 in the middle of the spawning zone. Annual maximum daily average streamflows (termed "peak flows" here) over the period 1996-2016 occurred in 1997, 2011, and 2014 at the UGR site near Perry (13318960; Figure 37). Peak flows in 2010 were also relatively high. Peak flows in the period 1998-2009 were relatively stable. The annual peak flow in 1997 arrived in January and was part of a historic flood that affected the entire Pacific Northwest. The peak flow in 2011 was nearly as great and occurred at the initial year of CHaMP surveys.

For the UGR gage below Clear Creek (13317850), based on data from 1993-2016 (missing data for 1998-2000) the peak flow occurred in 1993. Years 2010 and 2011 had the next highest annual peak flows (Figure 38). In the years covered by CHaMP surveys (2011-2016), peak annual flows were highest in 2011, lowest in 2015, and were low to moderate contrasted with the overall performance in the period 1993-2016.

A plot of the average daily flows for the Grande Ronde mainstem near Perry (13318960) with Catherine Creek near Union (13320000) (Figure 39) shows that streamflow varies by a little more than two orders of magnitude in the UGR mainstem, but not quite two orders in Catherine Creek near Union. We deliberately omitted use of data from Catherine Creek at Union because of the major impact of summer water withdrawals that affect this gage. Minimum flows are typically lower in the UGR than in Catherine Creek. Peak flows are always higher in the UGR near Perry than in Catherine Creek. These flows are not standardized by drainage area.

Average daily streamflows for the Upper Grande Ronde gage near Perry (13318960) vs Catherine Creek gage 1332000 plotted for the period 11/1/1998-10/13/2016 was relatively linear, but also shows a large degree of scatter (Figure 40). The drainage area for the gage near Perry on the UGR is 1753.4 km² while the drainage area for the Catherine Creek gage is 266.8 km². Despite the significant amount of scatter in this relationship, the regression is highly significant ($P < 0.001$, $n=6557$). However, the difference in size of these drainages and different basin characteristics make the daily correspondence in flows poor.

Gage 13320000 on Catherine Creek (266.8 km²) and gage 13317850 (101.01 km²) on the Grande Ronde River are much closer in drainage area. The elevations at the gages are also more comparable to one another (944.9 m vs. 1371.6 m). This resulted in a much closer relationship between mean daily flow values over a multi-year period (Figure 41). This probably is indicative of a greater similarity in timing of snowmelt.

Examination of Average Monthly and Maximum Monthly Streamflows

Timing of average monthly and maximum monthly streamflows in the UGR mainstem changes considerably with position in the watershed. The UGR below Clear Creek (13317850) has average monthly flows that are much more consistent than they are downstream near Perry. The mean flow was highest in June in 2011 and next highest in May of 1993 (Figure 42). In 1997, the year of the extreme floods in the Pacific Northwest, May had the next highest mean monthly flow. In all years except 2010 and 2011, May had the highest average flows. In 2010 and 2011, highest average monthly flows occurred in June. In most of the other months between 1993 and 2016 (data missing for 1998-2000), average monthly flows were low and stable.

A plot of average monthly streamflows for 1997-2016 for the Upper Grande Ronde gage site near Perry (13318960; Figure 43) reveals that the May 2011 average flows were highest within this period of years. It is interesting that the extreme peak flows of January 1997 produced an average January flow that was not particularly high. This reveals a problem in using mean monthly flow or maximum mean monthly flow alone as a biologically significant index. April average flows were frequently the highest average monthly flows in many years or were exceeded only by May average flows at this site. January and February average flows were relatively low in all years. March flows were highest for this period of years in 2004 and 2014. June average flows were relatively high only in 2008, 2010, and 2011, but were exceeded by the flows in May in 2008 and 2011.

A plot of maximum monthly streamflow (m³/s) for January-June for 1993-2016 (missing data from 1998-2000) at gage 13317850 (GR below Clear Creek; Figure 44) reveals interesting monthly patterns. In 1993 the May peak flow was the highest value achieved for this January-June period from 1993-2016. The next highest flows in order were June 2010, May 2011, and May 1997. In 2011, monthly peak flows were nearly identical in both May and June. In 2012 the peak flow occurred in April, with May and June having the next highest monthly peak flows. For this site, it appears to be typical for May peaks to be highest in every year and June peaks to be next highest. January, February, and March peak flows were typically low, as expressed in data from 1993-2016.

A matching analysis was done of the maximum monthly streamflow (m³/s) for January-December for 1993-2016 (missing data from October-December 1996, and 1997-1998) at gage 13320000 (Catherine Creek near Union, Oregon) (Figure 45). Catherine Creek near Union has annual peak flow values that are approximately three times greater than the UGR below Clear Creek. However, in terms of timing of monthly peak flows, the two sites behave in a very similar manner. The May 1993 peak in the UGR was the highest peak in a period from 1993 to 2016. For a nearly comparable period of years in Catherine Creek, its highest peak occurred in June of 2010. In the years since 2000, the UGR below Clear Creek had its highest five annual monthly peaks in May of 2006, 2008, 2009, 2011, and June 2010. The highest five

peaks in Catherine Creek near Union occurred on May 2006, 2008, 2011, June 2010, and April 2012. In both streams, the annual peak monthly flow occurred in May predominantly, but also in June and April. Both streams had the lowest annual monthly peak flows in 2015. This was also the year of lowest low flows during the years of CHaMP surveys.

There is a relationship between the peak streamflows for May and June for the years from 1993-2016 (missing years 1998-2000) at OWRD site 13317850 (Figure 46 and Figure 47). This reveals that in years with very low May peak flows, the June peak flows are also low. And conversely, when May peak flows are high, the June peak flows are also high. Biologically, this implies that in any year in the upper extent of the UGR mainstem, when high peak flows occur in May, the fish will also experience high flows in June. The previous graph showing all months from January through June for the upper extent of the UGR indicates that there is no year having higher peak flows in January-March than occur in April-June. The same is not true for the UGR near Perry where peak flows can occur in January, February, or March that are higher than those that primarily occur in either May, June, or April. The higher occurrence of peak flows earlier in the year toward the lower part of the UGR mainstem means that the occurrence of scouring flows may kill incubating eggs, while the peaks that occur from April-June may displace juveniles downstream. If they are displaced far downstream and are not able to redistribute upstream into thermally suitable habitat, these displaced individuals will become delayed mortalities.

Shifting focus to the Upper Grande Ronde gage site near Perry (13318960) (Figure 48), we see that a plot of monthly maximum streamflows for 1997-2016 reveals that the May 2011 maximum flow was second highest within this period of years. Peak flow in 1997 (an extreme high flow year) was somewhat greater than in 2011. In March 2014, maximum peak flow was lower than the May 2011 flow but was higher than the peaks that occurred in other months of 2014; the next lower peak came in January 2011. In 2011 peak flows in order from high to low occurred in May, January, April, and March. In most years, the peak flows near Perry occurred in April. In the 20 years from 1997-2016, the highest monthly peak flows occurred this many times respectively by month: January, 1; February, 2; March, 4; April, 7; May, 5; and June, 1 in the UGR near Perry.

For the UGR below Clear Creek (i.e., the upper portion of the mainstem), peak monthly streamflows occur predominantly in May and June. Adding all mean daily streamflow values (m^3/s) for all days per month (Figure 49) may provide an index to the period of strongest biological impact to the juvenile populations inhabiting this stream zone. These sums of mean daily streamflows reveal that in 2011, June had the greatest total. The next greatest total monthly flow in this period occurred in May 1993. May 1997 also had a relatively highly total monthly flow. Year 1997 was remarkable due to the extremely high peak in January and other peaks throughout the January-June period, including a high value in May. Consequently, water year 1997 included several high peaks in winter that could have caused mortality from scour, but also high spring peaks that could also have displaced juveniles. Aside from that year, biological impacts in the upper portion of the UGR were primarily a function of May and June peaks or cumulative monthly flows as shown in Figure 49.

Long-Term Trends

The long-term trends (1912-2016) in peak annual streamflow (based on a daily flow series) for Catherine Creek at the gage near Union (13320000; Figure 50) reveal a variation from approximately 7 to 43 m³/s in peak flows. Since 2010 peak streamflows declined significantly. However, the apparent long-term negative trends do not appear to be statistically significant ($R^2=0.0054$, $P=0.48$, $n=89$). This gage has the longest period of record in the basin and is important for that reason in evaluating the presence of long-term trends in peaks.

Development of Statistical Expressions of Peak Flows to Explain Biological Response

Above, we offered the possibility that biological impact magnitudes could be indexed by cumulative monthly flows. However, this method may somewhat discount the impact of peak values within the month if a month is constituted by stable but moderately high flows. That is, high cumulative total monthly flows could occur with stable but moderate flows. Alternatively, cumulating only days that exceed certain physical or statistical thresholds during the month could provide a good index to cumulative biologic impact. While a sum of average daily flows by month may reveal the magnitude of impact to a Chinook juvenile population inhabiting positions within the UGR, the magnitude of these impacts may be more attuned to peaks exceeding thresholds. The 99th percentile streamflow (a value higher than 99% of all values for the entire period of record) was selected as a potential biological threshold that could indicate ability to scour incubating eggs or displace juveniles downstream, depending upon which month in the year the thresholds were exceeded.

In 2011, a high flow year, there were 26 days that had streamflows greater than or equal to the 99th percentile value flow on the GR below Clear Creek, and 21 days on the UGR near Perry (Figure 51). Percentiles were based on the entire period of record for average daily flows. These two sites responded similarly in 2011. In 2008, 2009, and 2014, peak flows exceeding the 99th percentile flow were less frequent. On Catherine Creek, in 2006, 2008 and 2011, peak flows occurred on several days each year, with 2011 having 15 occurrences that exceeded the 99th percentile flow on Catherine Creek near Union (Figure 52). The other Catherine Creek site at Union paralleled the response of the site upstream.

In the upper portion of the UGR (i.e., UGR below Clear Creek), there were 23 days in June 2011 having flows exceeding the 99th percentile value (Figure 53). In 1993 and 2008, there were 16 and 9 days, respectively, having peak flows \geq 99% value. Totals of May and June number of days with peak flows \geq 99% levels, where total counts were \geq 10, occurred in 1993, 1997, 2008, and 2011. Despite 2010 having high peak flows as revealed in other charts, it did not have a high cumulative number of days with peaks above this threshold level.

By adding the flows (average daily flow) for all days per year in the period January-June that exceeded the 99th percentile value, the idea is that an index of amount of work done on the streambed might be calculated. With this method used to compare the years 2001-2016 for gages 13318960 and 13317850 on the UGR (Figure 54), it was found that the greatest cumulative peak flow levels occurred in 2011 at both gages. Cumulative peak flows in 2008, 2009 and 2010 were also relatively high for this 16-year period as measured at each gage. In 2006 and 2014, cumulative peak flows were high at the UGR near Perry, and were mirrored by peak flow totals below Clear Creek. In 2002 and 2004 peak flows at the

UGR near Perry were relatively high while peak flow totals below Clear Creek did not respond at all. This might reflect very uniform rates of snowmelt in those years, and higher rates affecting the lower mainstem. For Catherine Creek, January-June 2011 had the greatest cumulative peak flow totals, like for the Grande Ronde sites (Figure 55). Peak flow totals were also substantial, but smaller, in 2006, 2008 and 2009.

The frequency of flows exceeding certain thresholds can be visualized by viewing an annual flow duration curve based on long-term flow records. A plot of the annual flow duration curve for the Grande Ronde mainstem below Clear Creek (gage 13317850) is presented in Figure 56. Data were obtained from OWRD (2017a). This curve shows that 45% of all flow values (i.e., between flow durations of 40-95%) are between 0.18 and 0.45 m³/s at this site. This site also has 5% of all daily flows above 4.1 m³/s. When the month of May is considered alone, its flow duration curve has 5% of all daily flows exceeding 8.3 m³/s (Figure 57).

Monthly flow duration statistics are available from OWRD for the Grande Ronde below Clear Creek (gage 13317850). Data were obtained from OWRD (2017a). For May in all years incorporated in the rating, 90% of the time flows were greater than about 1.8 m³/s and in June, 90% of the time flows were greater than about 1 m³/s (Figure 57). These flow duration curves merge at 5% duration, where in each month 5% of the time flows were greater than the same value (approximately 8 m³/s). The April flow duration curve was distinctly lower than those for May and June. In 5% of the time, April flows were greater than 3.7 m³/s, and 90% of the time April flows are greater than 0.43 m³/s. Surprisingly, July streamflows are also very distinct and are next highest. For 5% of the time July flows are greater than 1.9 m³/s and 90% of the time they are greater than 0.34 m³/s. March flows have a moderate and distinct occurrence in the 5-30% flow duration range, but all other monthly flow duration curves are very similar to one another.

At gage 13317850 the median flow duration values by month ranked from high to low are May (3.37 m³/s, June (2.44 m³/s), April (1.16 m³/s), July (0.62 m³/s), and the remaining months (0.27-0.37 m³/s) (Figure 57).

A plot of the annual flow duration curve for the Grande Ronde mainstem near Perry (gage 13318960) was also made from data obtained from OWRD (2017a) (Figure 58). This curve shows that 55% of all flow values (i.e., between flow durations of 40-95%) are between 0.57 and 5.2 m³/s at this site. This site also has 5% of all daily flows above 45.9 m³/s. When the months of April and May are considered independently, their flow duration curves have 5% of all daily flows exceeding 70 m³/s (Figure 59).

Monthly flow duration statistics are available from OWRD (2017a) for the Grande Ronde near Perry (gage 13318960). For April and May the flow duration curves are very similar. These curves converge for flows of 5-30% (Figure 59). The 5% duration flow for both April and May is about 70 m³/s. The March duration curve is very similar in values from approximately 5% to 50% duration. The February and June flow duration curves are nearly identical from 20% to 95%, but June has 5% duration of flows greater than 47.6 m³/s. The January flow duration curve is distinctly lower than that of February and June. The median flow duration values by month, ranked from high to low are April (29.7 m³/s), May, June (21.5

m³/s), February (7.2 m³/s), January (3.8 m³/s), December, July (1.8 m³/s), November, October, August, and September (0.65 m³/s). August and September are months in which Chinook spawning is ending and are the lowest flows as recorded at this position within the UGR basin. These flows are most likely significantly influenced by water use within the basin. The significant difference in flow duration curves between the UGR near Perry and the UGR below Clear Creek highlights the difficulty of providing conditions suitable for spawning farther downstream than currently is the predominant condition. For greater illumination on the potential flows that were available to spawners historically far downstream (i.e., upstream of Perry), one would have to evaluate the low flow duration curves available from USGS. See the low flow document in this annual report.

The gage on the Grande Ronde mainstem near Perry is the furthest downstream currently operating mainstem gage that is above the city of La Grande, Oregon, while the gage on Catherine Creek mainstem near Union, Oregon is the furthest downstream gage not influenced significantly by irrigation water withdrawals. A regression of mean annual flows from the gage on Catherine Creek (13320000) plotted against the mean annual flows on the Upper Grande Ronde (13318960) were significantly related ($Y = 0.204x + 1.2301$, $R^2 = 0.8573$) (Figure 60).

Plotting the peak annual streamflows on the Catherine Creek gage near Union (13320000) vs the peak annual streamflow at the mainstem gage on the Upper Grande Ronde near Perry (13318960) reveals a high level correspondence, similar to that expressed in terms of mean annual streamflow. This regression equation is $Y = 0.2447x + 2.0583$, $R^2 = 0.8127$ (Figure 61).

Although the Catherine Creek gage at Union, Oregon has significant impact from irrigation diversions upstream of town and is unsuitable for recording low flows that are reflective of inherent basin characteristics, it is suitable for registering peak flows that occur prior to irrigation season. To demonstrate this, the annual peak streamflows of the two Catherine Creek mainstem gages (13320000 and 1320300) were regressed (Figure 62). This relationship is expressed by the equation $Y = 1.108x - 1.2395$ ($R^2 = 0.9779$), where X = peak annual streamflow at gage 13320000 and Y = peak annual streamflow at gage 1320300.

The streamflow gages in the Upper Grande Ronde and Catherine Creek that are currently operating and have a significant number of years of data were used to contrast the hydrologic differences among the years during which CHaMP surveys were conducted. During these years, adult redd counts were collected during August-September of each year by ODFW, followed by juvenile snorkel counts made by CRITFC staff in the following year in late June-mid-September. The intervening May-June period provided peak flows in the upper portion of the UGR that may be strong enough to displace or kill juveniles rearing at the CHaMP sites. Annual patterns of peak flows for the years during which CHaMP surveys were made have been evaluated in this report in terms of magnitude of annual peak flows (i.e., maximum annual average daily flow), monthly cumulative flows for May and June, and cumulative number of days per year (January-June) with peak flows greater than or equal to the 99th percentile value of average daily flow for the entire period of record available.

In addition to what has been termed annual peak flow here, the true peak flows were also used to compute stream power and unit stream power. This required first using the USGS program PeakFQ to calculate flow frequencies from the gage nearest the spawning area in the Upper Grande Ronde (i.e., OWRD gage 13317850). This program yielded data that were then plotted to show the relationship between annual peak flow (cfs) and return period (years) (Figure 63 and Figure 64). At gage 13317850 (below Clear Creek) the true peak flow in 2011 was 464 cfs. Using equation $Y = 0.3715 e^{0.0074X}$, we calculated that the return period was 11.51 years. This is contrasted with 3.38 years based on the general regional peak flow regression plotted from data obtained from OWRD (2017b). At gage 13318960 (near Perry), the regional regression equation predicts a 2011 true peak flow of 7600 cfs (reached on May 16) equates to a return period of 20.17 years. The comparison of these two data sources suggests that the true peak flow frequencies observed at the two Grande Ronde gages in 2011 were very similar. Also, the regional regression equation from OWRD (2017b) data does not seem to apply well to a watershed as small as that at OWRD gage 13317850. The USGS program PeakFQ appeared to perform much better as a predictive tool with the annual peak flow data to estimate flow frequencies.

Assuming that the return period for peak flows experienced within the Upper Grande Ronde would be the same at each of the 10 CHaMP sites in the uppermost portion of the mainstem each year, we applied the formula from Cooper (2006) with its area coefficient that is dependent upon the value of the annual true peak flow return period to estimate the peak flow for each CHaMP site among the 10 sites clustered around OWRD gage 13317850 (Table 37; Figure 65). For each of the CHaMP sites, site and basin characteristics were compiled to facilitate making estimates of peak streamflow, stream power, and unit stream power at each site based on peak flows measured at the nearby gage site (Table 38). Estimates of the true peak flow at each CHaMP site for the period 2011-2016 provide a means to use a single annual true peak flow at each site (Table 39) to calculate the highest annual stream power and unit stream power values (Table 40). These values were then used as a predictive tool to relate to an index of juvenile survival (snorkel count of juveniles/m divided by redds per km upstream of the bottom of site counted in the previous year) (Table 41).

The bulk of the Chinook spawning in the Upper Grande Ronde basin based on surveys made by ODFW occurs upstream of CHaMP site CBW05583-235322, and extends through the meandering section on Vey Ranch upstream to the mine tailings reach which is found on USFS lands. Site CBW05583-099818 is the upstream CHaMP site located in this reach. OWRD gage 13317850 is located at a point on the UGR mainstem where the drainage area is 102.56 km² (Table 38). There are four CHaMP sites upstream of this gage and two downstream of the gage, but are upstream of the confluence with Sheep Creek. The drainage areas of these CHaMP sites range from 60.3% to 102.4% of the drainage area at the gage itself. Cooper (2006) suggests that gage data are most directly applicable to ungaged sites above or below the gage when the drainage area of the ungaged site is between 50 and 150% of the gage's drainage area. These six CHaMP sites meet this criterion. There are four additional CHaMP sites found downstream of the Sheep Creek confluence. The relative drainage areas for these sites range from 330.1% to 351.2% of that at the OWRD gage. While this is not ideal for extrapolation of the peak flow data from the gage to these downstream ungaged sites, we did so nonetheless.

Biological Response to Peak Flows

The clearest expression of a relationship between juvenile survival (or displacement) index can be found at CHaMP site dsgn4-000009 (an annual site). This site does not have extensive length of spawning habitat above it so the ability of displaced juveniles to be replenished by downstream movement of surviving juveniles from upstream is more limited. For CHaMP site dsgn4-000009, the relationship between juvenile Chinook survival index vs. unit stream power plotted was well described by a linear regression ($Y = -0.0001X + 0.9978$, $R^2 = 0.7262$), based on data for years 2011-2016 (Figure 66). This site is downstream from site CBW05583-099818. This site is considered to be a classic spawning site with relatively low gradient (0.75%), cold water, and suitable size substrate ($D_{50} = 39$ mm, $D_{84} = 89$ mm). Note: this graph is based on use of true annual peak flow to calculate unit stream power. Essentially the same regression was derived by using maximum annual average daily flow instead of true peak flow. This equation was $Y = -0.0001X + 0.9767$, $R^2 = 0.764$.

Juvenile Chinook survival index vs. unit stream power was also plotted for CHaMP sites dsgn4-000009 and CBW05583-099818. Site CBW05583-099818 is a rotating panel 3 site, so provides juvenile data for 2013 and 2016. These two CHaMP sites were the most upstream sites on the Upper Grande Ronde mainstem. Consequently, they are influenced least by zones of very high redd densities that could provide a source of high juvenile numbers to downstream CHaMP sites even in years when very high peak flows might be expected to move a high proportion of juveniles downstream. The 8 data points for these two sites produce a regression $Y = 2.456 e^{-0.0005X}$, $R^2 = 0.8176$ (Figure 67) or a linear regression of the form $ASI = 1265 - 0.19 USP$, $R^2 = 0.61$, $P = 0.021$ (Figure 68). The linear regression was derived from a statistical analysis that considered the strongest relationships between apparent juvenile survival index and annual peak flow, channel gradient, stream power, and unit stream power (White pers. comm.).

The uppermost ten CHaMP sites on the UGR were snorkeled from 2011-2016 at times that depended upon whether they were annual or rotating panel sites. Survival index is number of juvenile Chinook per meter observed in year x divided by number of Chinook adult redds per km upstream of the bottom of CHaMP site observed in year $x-1$. Survival index was plotted against unit stream power for these sites where both juvenile and adult redd count data pairs were available (Figure 69). However, this chart deletes the data points for CBW05583-148970 (2014) and dsgn4-000277 (2011) that appeared to be outliers. This regression is expressed by the equation $Y = 20.443 x^{-0.442}$, $R^2 = 0.1854$. Identification of points by site revealed that for some sites, the slope of the regression of juvenile survival vs. unit stream power was not consistent with the overall slope created by the entire set of points. The weaker regression resulting from using the full set of data points for all sites indicates that apparent juvenile survival is a more complex function of more factors than simply unit stream power when the spatial scale is expanded.

Linkage of Spawning Distribution to Channel Gradient and Substrate Composition

A multiple regression was run with gradient as the dependent variable and two substrate categories (sub D_{50} and sub D_{84}) as the independent variables. The multiple regression between gradient and these substrate size variables was highly significant. This implies that substrate size would be a very good

indicator of gradient. The multiple regression equation was: $Y = 0.2162 - 0.0329 (\text{SubD}_{50}) + 0.0208 (\text{SubD}_{84})$; $R^2 = 0.8345$, $n = 10$, $P = 0.0018$. Also, given that a large extent of critical spawning area is found within Vey Ranch, which is unavailable for surveying due to landowner denial, prediction of potential spawning densities in this area might accurately be made using channel gradient because it is intimately linked to substrate composition. Substrate composition and channel gradient are highly predictive of spawning potential.

In addition to the multiple regression, each substrate size metric was regressed independently on channel gradient for the 10 CHaMP sites at the uppermost end of the UGR mainstem. Substrate D_{50} particle size was related to channel gradient (%) by the regression equation $Y = 19.488 X + 31.225$, $R^2 = 0.5318$ (Figure 70). Also, substrate D_{84} particle size (mm) was related to channel gradient (%) by the regression equation $Y = 71.083 X + 52.031$, $R^2 = 0.7534$ (Figure 71).

The GIS feature class *ODFW_ReddsSurveys* was added to an ArcGIS project file and layer *AllRedds_09_16* (files in CRITFC geodatabase) was used to depict the spatial location of redds surveyed by ODFW. CHaMP survey extent polygons were used to map the bottom and top of site for the 10 uppermost CHaMP sites on the Upper Grande Ronde mainstem. Counts made of redds from 2009-2016 were cumulated, converted to redds per km and plotted against CHaMP site channel gradient (%). This regression is expressed by the equation $Y = 276.67 e^{-1.453X}$ ($R^2 = 0.7727$) (Figure 72). This regression indicates that the maximum redd densities are associated with channel gradients of about 0.5%. Redd densities decline to about zero at gradients greater than about 4.5%. More intense investigation of this relationship with the abundant data available should be able to make this expression more accurate.

It can be questioned what the ability may be to use data on maximum annual daily average flow instead of true annual peak flows to calculate annual maximum stream power or unit stream power values. If the absolute value of stream power is critical, for example as a means of predicting ability to move bed particles of a certain size, then true peak flow is important. However, if the stream power calculation is a means to contrast peak or maximum flows among years to examine the relationship between peak flows and a juvenile Chinook survival index, then it appears not to be important. There is a very close relationship between true peak and the peak annual mean daily flow at both the OWRD gage near Perry (13318960) (Figure 73) and the OWRD gage below Clear Creek (13317850) (Figure 74).

The uppermost 10 CHaMP sites were selected to evaluate the influence of peak flows, channel gradient, and substrate composition on redd distribution and an apparent survival index of juvenile Chinook. Stream power and unit stream power are derived from a combination of terms such as peak streamflow (m^3/s), channel gradient, and bankfull width. Gradient is tightly linked to substrate composition in riffles, which provides the basic template within which spawning substrate is selected by salmon. The ability of juvenile fish to resist being killed or displaced downstream during peak flows is likely related to stream power indices and gradient, but is also likely related to other channel characteristics, such as fish cover, large woody debris, and streambank overhang area. Streambank overhang would not be well-represented in CHaMP data because it is measured as a summertime metric rather than one found at peak flow.

These 10 CHaMP sites can be visually reviewed to help understand the distribution of spawners in relation to channel characteristics (Figure 75 to Figure 84). Among the 10 sites selected for evaluation of impact of peak flows, site CBW05583-280042 (Figure 82) has the highest redd density (196.2 redds/km). It also had a channel gradient of 0.61%. The D_{50} was 58 mm and D_{84} was 94 mm in riffles. In our past collection of McNeil core samples from pool tails and from spawning patches found as inclusions within riffles, a particle diameter of 11-90 mm was selected as the range for D_{50} for optimal spawning gravel (Justice et al. 2012). The range of water depths for identification of spawning patches was 0.15 to 0.40 m and the range of water velocities was 0.10 to 1.10 m/s (Justice et al. 2012). It is clear from Figure 45 that all these conditions would be ideal at this site. In addition, water temperatures during the spawning and rearing periods are very favorable at this site. On the other extreme among these 10 CHaMP sites at the upper zone on the mainstem Grande Ronde, the D_{50} particle size is 125 mm at site CBW05583-206314 (Figure 80) and the redd density was 0.0 redds/km. Gradient was also highest for the overall site length at 4.78%. Even with a gradient this high, it is possible to have localized pockets of spawning gravel, provided that large woody debris (LWD) creates storage sites for gravel, plunge pools, a more stair-stepped overall channel gradient, and zones of gravel sorting. However, this site as viewed in Figure 80 has very little LWD to create this needed zonation of gradients and spawning gravel storage sites. Site dsgr4-000277 (Figure 78) has a D_{50} of 86 mm, near the upper threshold for suitable spawning gravel in riffles, but has a very high D_{84} value (i.e., 225 mm). Channel gradient in this site was 1.11%, a value that is higher than the 0.5% that seems to be near optimal. When too large a percentage of the substrate surface is comprised of large particles beyond the capability of spring Chinook to move them, the size of potential spawning patches becomes too limiting. For example, the CRITFC protocol for spawning patches requires a minimum area of 1.5 m² (Justice et al. 2012). With a D_{84} as high as 225 mm, the potential for having a large portion of a 1.5-m² patch occupied with large immobile particles becomes so great that spawning opportunities are limited. This site had exceptionally low LWD, low fish cover elements, and marginal water depth (as noted visually from the photo), so redd density was only 5.5 redds/km. A more in-depth quantitative analysis would be instructive in a multiple regression to evaluate the influence of other channel characteristics on redd density.

Site CBW05583-370490 (Figure 76) has a gradient that is slightly less (0.86%) and has a lower D_{50} (i.e., 50 mm) that is within the limits of the CRITFC range for spawning patches, but also has a much smaller D_{84} (i.e., 115 mm). This apparently led to a much greater redd density (i.e., 59.3 redds/km). LWD presence was not visibly greater than at site dsgr4-000277, but it appears that the much lower D_{84} means that potential spawning patches are much less likely to be impaired with too much surface coverage within a 1.5-m² patch by particles that are too large for spring Chinook to move or work around.

Summary

- 1) Timing of peak flow events in relation to the timing of life stage events is capable of influencing survival at either the incubation stage via scouring or the post-emergence stage (downstream displacement of juveniles to the lower Grande Ronde valley) where mortality would be high during summer juvenile rearing stages.

- 2) One streamflow gage is found in each of the two key study basins that is able to represent the streamflows (both peak flow and low flow) affecting primary spawning and rearing sites. These gages include the Grande Ronde below Clear Creek (13317850) and Catherine Creek near Union (13320000). These gages provide a meaningful flow record length as well as covering CHaMP sites through all the years in which monitoring was conducted.
- 3) The timing of average monthly and maximum monthly streamflows in the UGR mainstem varies considerably with position in the watershed. It is important to select gages carefully so that the peak flows with greatest relevance to the timing of incubation and early juvenile rearing life stages can be assessed.
- 4) The OWRD gage on the Grande Ronde near Perry (13318960) is located downstream of the mouth of Five Points Creek and far downstream of extant spring Chinook mainstem spawning. This gage reflects the influence of summertime water withdrawal (see low flow report included in this annual report). This gage also exhibits a peak flow behavior that is very different from the gage below Clear Creek (13317850) in the upper basin. The gage near Perry has produced highest annual peak flows in any month from January through June over the period 1997-2016. The highest annual peak occurred in January of 1997. May of 2011 was the next highest peak flow during this period. In terms of average monthly streamflows, the highest values recorded between 1997 and 2016 were found in March, April, and May.
- 5) Upstream at the OWRD gage (13317850) below Clear Creek on the UGR mainstem, maximum monthly streamflows were found predominantly in May and June, while April had the highest monthly peak flow in 2012. In terms of average monthly flows, the highest values each year from 1993-2016 (data missing in 1998-2000) were recorded predominantly in May, while highest averages were found in June in 2010 and 2011. June 2011 had the highest average monthly value for this period of years.
- 6) Data from the gage 13317850 below Clear Creek on the UGR mainstem show that the peak flows in May and June over the years 1993-2016 are highly related. That is, typically when a monthly maximum is high in May, it is also high in June. This indicates that in years where a high biological impact occurs in the UGR near the primary spawning zone due to a high peak flow, there are associated peak flows in the same year that provide a sequence of disturbance events.
- 7) A comparison of the gage on the UGR near Perry (13318960) with the gage on Catherine Creek near Union (13320000) for the period 1999-2016 shows that streamflow varies by a little more than two orders of magnitude in the UGR mainstem, but not quite two orders in Catherine Creek.
- 8) A scatter plot of mean daily flows between gage 13318960 on the UGR mainstem and gage 13320000 on Catherine Creek reveals a significant regression, but one with a great deal of dispersion. When the mean daily flow data on Catherine Creek was plotted against that of the UGR gage below Clear Creek (13317850), the dispersion is much less. This probably reflects the fact that these two basins are more similar in drainage area and elevation, which would tend to

result in greater alignment in timing of snowmelt. When one gage's data are used as a means of filling in missing data in another gage, it is important to account for the degree of similarity in basin characteristics. Biological response of spring Chinook life stages would be closely linked to timing of peaks, so it is critical that peak flow timing and magnitudes are evaluated in relation to basin characteristics.

- 9) A regression of mean annual flows from gage 13320000 vs those of gage 13318960 reveal a significant relationship.
- 10) A regression of peak annual flows (annual maximum average daily flow) from gage 13320000 vs those of gage 13318960 reveal a significant relationship. Despite the degree of scatter that occurs on the basis of average daily flows, the peak annual flows for each of these two gages maintain a high level of co-linearity.
- 11) Climate change is thought to bring about long-term changes in summer low flows attributable to advanced timing of snowmelt. In terms of long-term trends in annual peak flows (annual maximum of average daily flows) from 1912-2016, no significant trend was detected from data recorded at the Catherine Creek gage near Union, Oregon. This is a preliminary exploration of the data. It is possible that trends might be more apparent in basins of greater size or lower mean elevation. It is possible that peaks localized in tributaries subject to summer thunderstorms could exist and trends related to climate change could be possible. Also, shifts in monthly averages are possible over time. The biological impact of an increase in monthly duration of peak flows above a certain threshold could also be of concern. Trends in these types of events should be evaluated.
- 12) It is possible that the magnitude of biological impact of an annual peak flow is a function of (a) a single annual peak flow per year, (b) a peak monthly flow where the peak has a timing corresponding to either incubation or early juvenile emergence, (c) a summation of monthly flows, (d) a count of flows that are greater in magnitude than a certain statistical flow level (e.g., the 99th percentile high flow). We evaluated for the period of years in which CHaMP surveys were done how these indices would vary and create a physical basis for a biological trend.
- 13) In 2011 there were 26 days with streamflows greater than or equal to the 99th percentile flow on the UGR below Clear Creek and 21 days on the UGR near Perry
- 14) In 2011 Catherine Creek near Union had 15 occurrences of flows exceeding the 99th percentile value.
- 15) The count of exceedances of the 99th percentile threshold indicates similar behavior in the UGR and Catherine Creek for a peak flow year. Given the differences in gradient and channel morphology, it is unknown whether flows exactly equal to the 99th percentile value would generate comparable stream powers or ability to move the bed materials in each location. This can be explored further.

- 16) The sum of monthly mean daily flows for May and June at gage 13317850 (UGR below Clear Creek) for years 1993-2016 (data missing for 1998-2000) reveals the highest cumulative flow total for June 2011. During the years of CHaMP surveys (2011-2016) the highest cumulative total flows occurred in May for 2012-2016.
- 17) It is possible that the magnitude of biological impact of peak flows that can occur at one site supporting spring Chinook vs. another site can be interpreted with respect to the long-term flow duration statistics. This approach does not alone implicate any specific year as one having a high peak, but instead evaluates the long-term tendency (frequency) for flows of a certain magnitude or higher to occur in various months. The months can be considered in relation to timing of life stage events. The magnitudes of flows can be related to stream power development.
- 18) The gage on the UGR near Perry (13318960) has 5% of all daily flows in April and May that exceed 70 m³/s. In June, the 5% flow duration corresponds to flows greater than 47.6 m³/s.
- 19) At gage 13318960 the median flow duration values by month ranked from high to low are April (29.7 m³/s), May and June (21.5 m³/s), February (7.2 m³/s), January (3.8 m³/s), December and July (1.8 m³/s), and November, October, August, and September (0.65 m³/s). August and September are months in which spring Chinook spawning is concluding.
- 20) The gage 13317850 on the UGR below Clear Creek has 5% of all daily flows in May and June that exceed 8 m³/s. April flows were next highest. The 5% flow duration value in April was 3.7 m³/s.
- 21) At gage 13317850 the median flow duration values by month ranked from high to low are May (3.37 m³/s), June (2.44 m³/s), April (1.16 m³/s), July (0.62 m³/s), and the remaining months (0.27-0.37 m³/s).
- 22) The return period for the 2011 peak flow experienced at the UGR gage 13317850 (below Clear Creek) was calculated as 11.51 years based on the USGS program PeakFQ. The return period for the 2011 peak flow experienced at the UGR gage 13318960 (near Perry) was 20.17 years. This calculation was based upon a regression developed from data downloaded from OWRD (2017b). These computations suggest that a peak flow with a given return period would be nearly matched by a peak flow of a similar return period within the same basin. However, as shown elsewhere in this peak flow analysis, the finer level variations in timing of peaks, duration of flows, and cumulative nature of flows exceeding statistical thresholds varies between these gages representing different positions within the UGR basin.
- 23) True annual peak flow values for years 2011-2016 (years in which CHaMP surveys were conducted) measured at the UGR gage 13317850 (below Clear Creek) were extrapolated to 10 nearby CHaMP sites using methodology of Cooper (2006). This requires calculation of annual return period for annual true peak flows and application of an area coefficient at each CHaMP site. The annual peaks flows were used with channel gradient at each CHaMP site to calculate stream power. Next, application of data on channel bankfull width allowed calculation of unit stream power.

- 24) Unit stream power was used as a predictor of apparent juvenile survival. This survival index was the ratio of density (numbers/m) of total juvenile Chinook observed in snorkel surveys in one year to the redd density (number of redds/km) observed in the previous year. It was hypothesized that a high unit stream power generated from a single annual peak flow occurring in May-June in the key spawning zone of the UGR would result in an impact on juvenile survival (or displacement downstream) in proportion to its magnitude. Such a relationship between unit stream power and juvenile survival index seems apparent using data only for the upper two CHaMP sites (i.e., dsgn4-000009 and CBW05583-099818). This relationship becomes degraded with inclusion of additional sites downstream. This suggests that additional factors such as total number of redds upstream of each site that generate juveniles and channel complexity or LWD abundance, factors that could provide shelter for juveniles in peak flows, are influential in determining juvenile survival (or resistance to downstream displacement).
- 25) Next steps in testing this hypothesis might be (a) evaluate data from Catherine Creek, (b) include data on LWD, fish cover, and pool frequency or volume in each site, and number of redds upstream, (c) exploring the utility of measures of annual cumulative peak flows exceeding various thresholds, (d) estimating the ability of various peak flows to move substrate particles in the CHaMP sites.
- 26) D_{50} and D_{84} are highly correlated with and explanatory of the channel gradient found in CHaMP sites.
- 27) Redd densities (redds/km) within CHaMP sites were significantly related, using regression equations, to the CHaMP site channel gradient measured using a Total Station instrument.
- 28) Inspection of the uppermost 10 CHaMP sites provides support for application of the substrate size criteria in Justice et al. (2012) for identification of potential spawning patches. However, it appears that in addition to the application of D_{50} criteria, limiting the D_{84} particle size is also critical in selecting potential spawning patches. If the upper limit of D_{50} is to be taken as about 90 mm, the upper limit of D_{84} should probably be no more than about 120 mm for high quality spawning gravel. Also, D_{50} values more toward the center of the 11-90 mm range suggested in Justice et al. (2012) is likely more optimal but depends upon the size of the fish too. However, the resistance to bed movement in peak flows is also a consideration when balancing the pros and cons of particle size in a life cycle context.
- 29) Peak flow magnitude and seasonality are undoubtedly critical factors with a major influence on survival of spring Chinook in the incubation and early juvenile life stages. Peak flow magnitude has often been linked to depth of scour of spawning gravel. Scour depth in relation to depth of egg deposition is a determining factor on percentage of egg/alevin loss. However, spatial distribution of scour in relation to distribution of substrate size, local stream power, and abundance of bedform protective mechanisms such as LWD, boulders, islands, and meanders determine the percentage of redds that can be destroyed in peak flows. Peaks that occur during post-emergence months have the potential to move young juveniles downstream. The

magnitude of displacement of the juvenile cohort downstream may be a function of the peak annual flow or the cumulative action of peak flows exceeding a certain magnitude.

Displacement downstream might kill juveniles directly by physical impact, but also might kill them indirectly if they end up in stream reaches that become too warm during summer and where these fish cannot re-distribute themselves up the mainstem or into tributaries that have favorable thermal environments. In the Upper Grande Ronde River there are very few known coldwater refuges downstream of Beaver Creek that could act as rearing areas. It is the intent of this initial exploration of peak flows that a linkage might be found between annual peak flows and annual variations in juvenile or smolt numbers reaching Lower Granite Dam or an index of survival at this life stage. This report considers a variety of indices of peak flows and compares what these might look like among streams in the Upper Grande Ronde River and Catherine Creek.

Figures

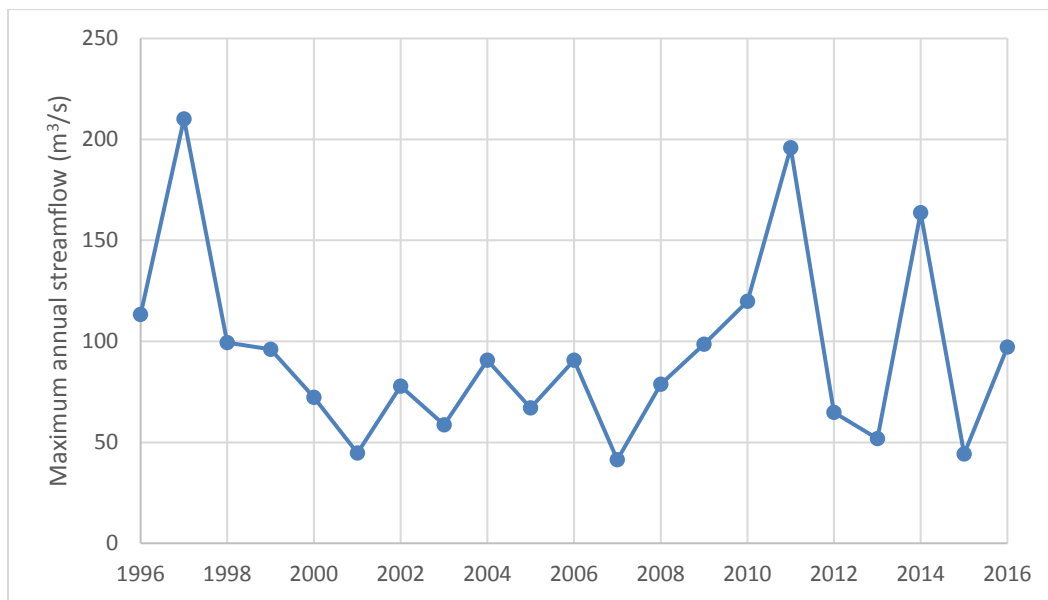


Figure 37. Maximum annual streamflow (m³/s) from 1996-2016 at USGS gage 13318960--Grande Ronde River NR Perry

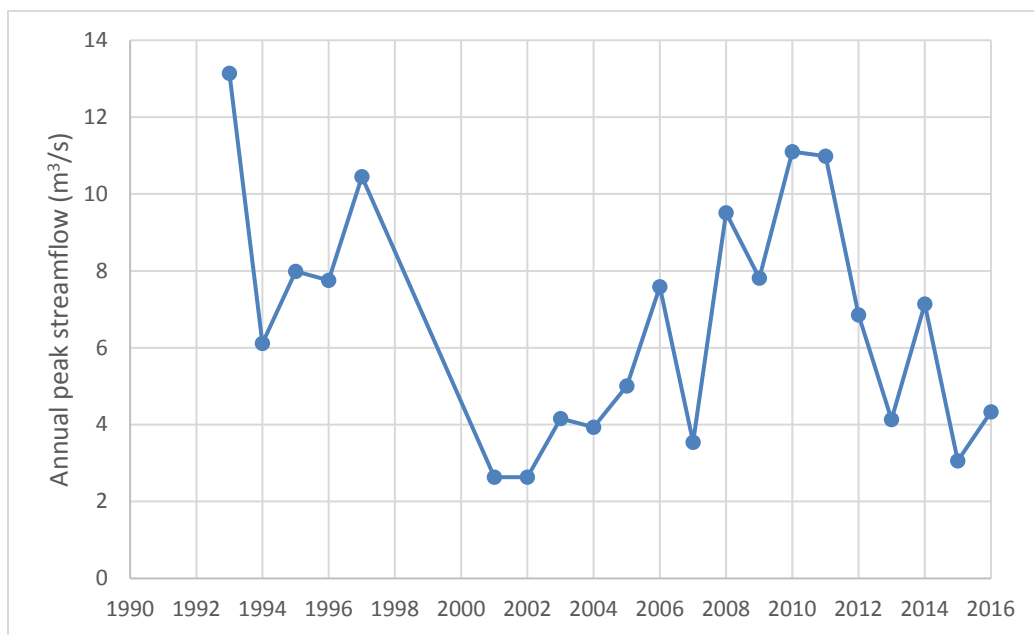


Figure 38. Maximum annual streamflow (m³/s) at USGS gage 13317850--Grande Ronde BL Clear Creek (data missing in 1998-2000).

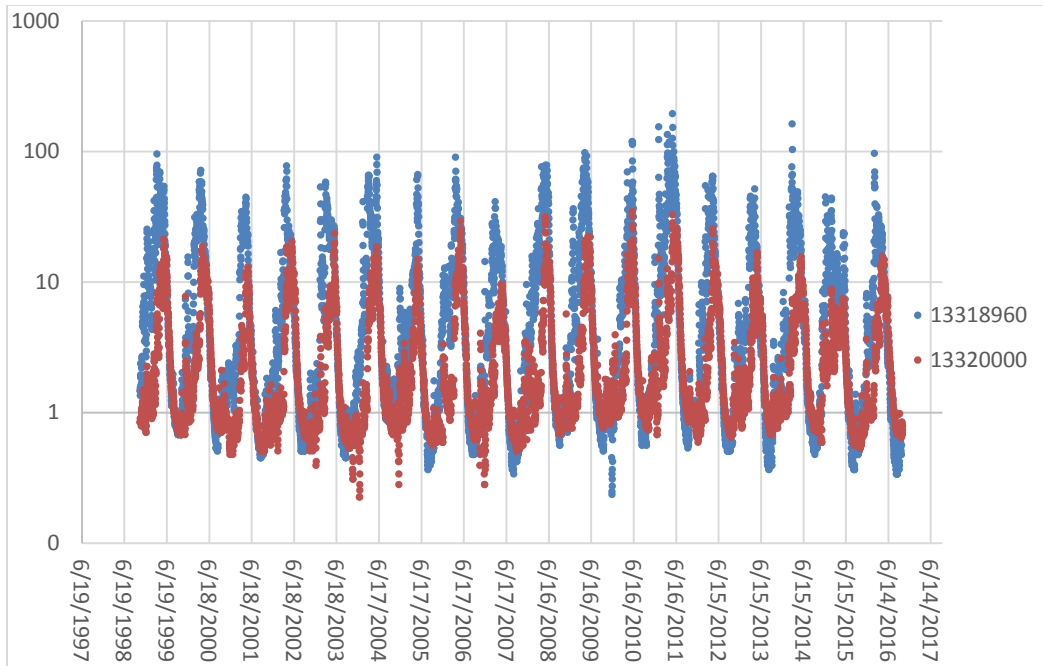


Figure 39. Average daily streamflows for the Grande Ronde mainstem near Perry at gage 13318960 vs. Catherine Creek near Union at gage 13320000.

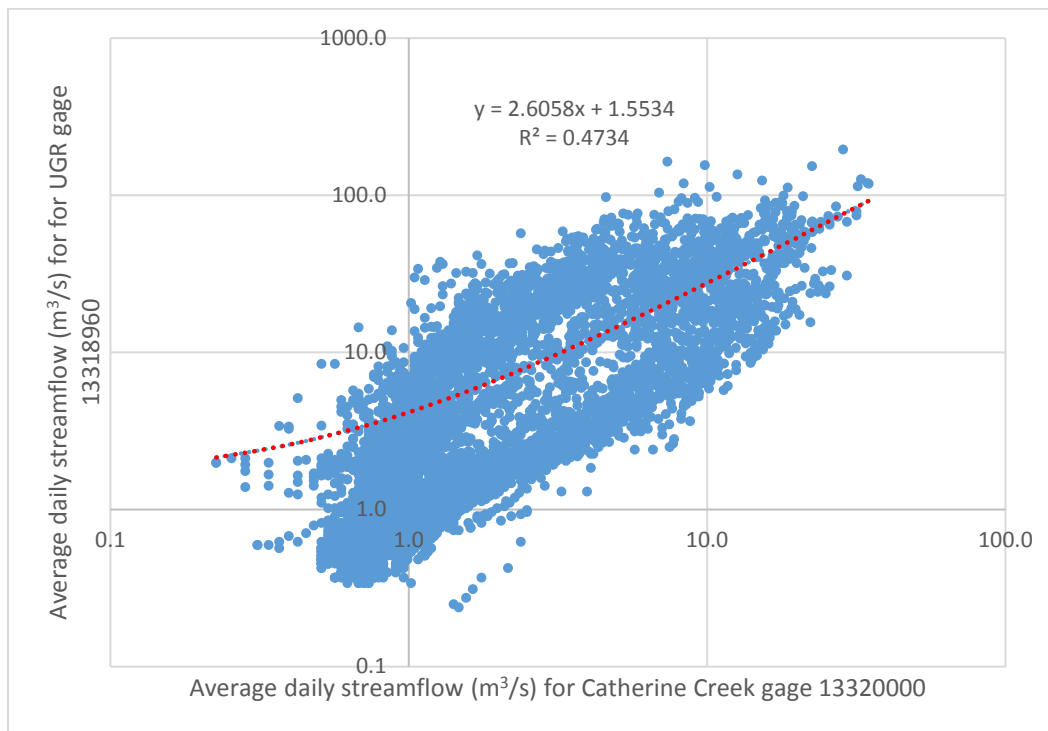


Figure 40. Average daily streamflows (m³/s) for Upper Grande Ronde gage 13318960 vs Catherine Creek gage 13320000 for period 11/1/1998-10/13/2016

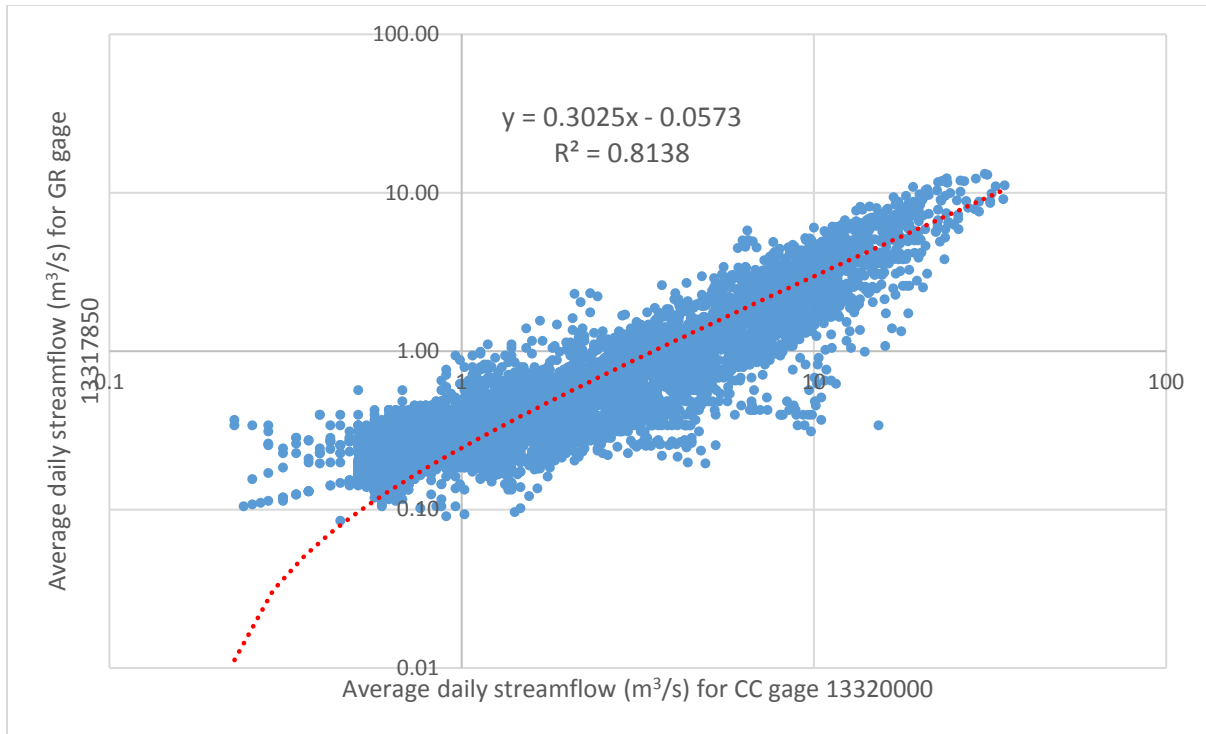


Figure 41. Average daily streamflows (m³/s) for the Grande Ronde gage 13317850 vs Catherine Creek gage 13320000 based on data for October 1, 1992-Nov 22, 2016 (missing data 10/1/1996-7/9/2000).

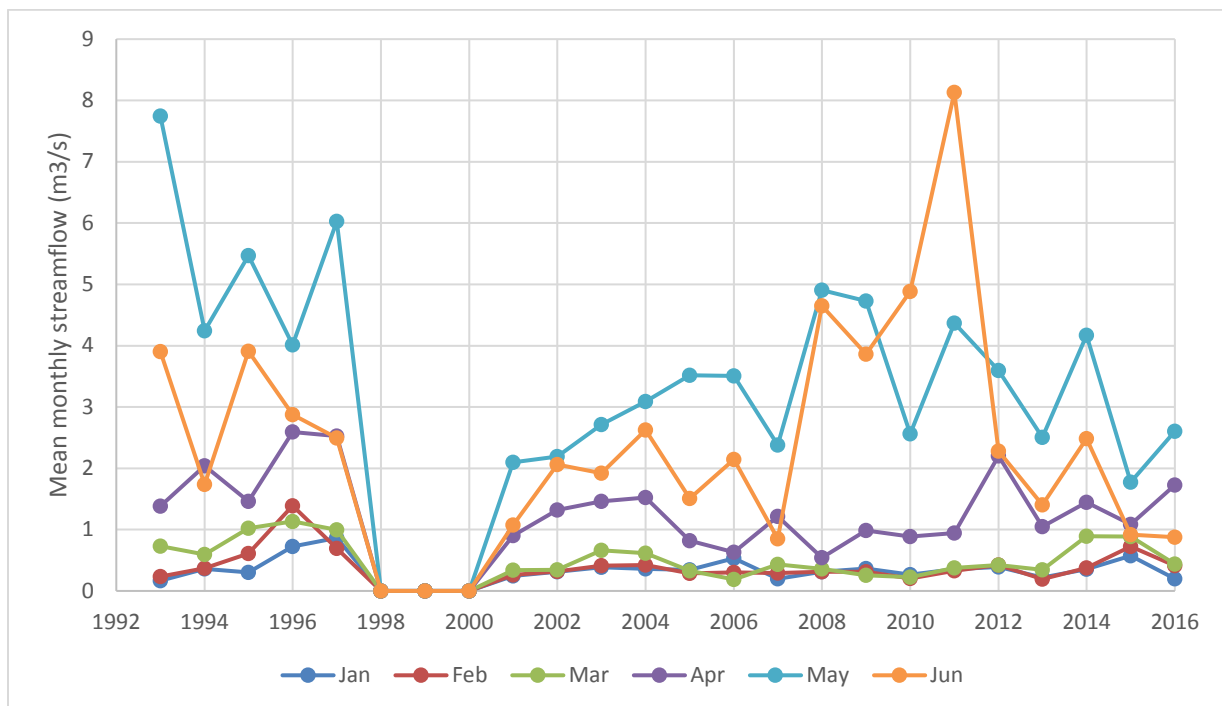


Figure 42. Average monthly streamflow (m³/s) at USGS gage 13317850--Grande Ronde BL Clear Creek (data missing in 1998-2000).

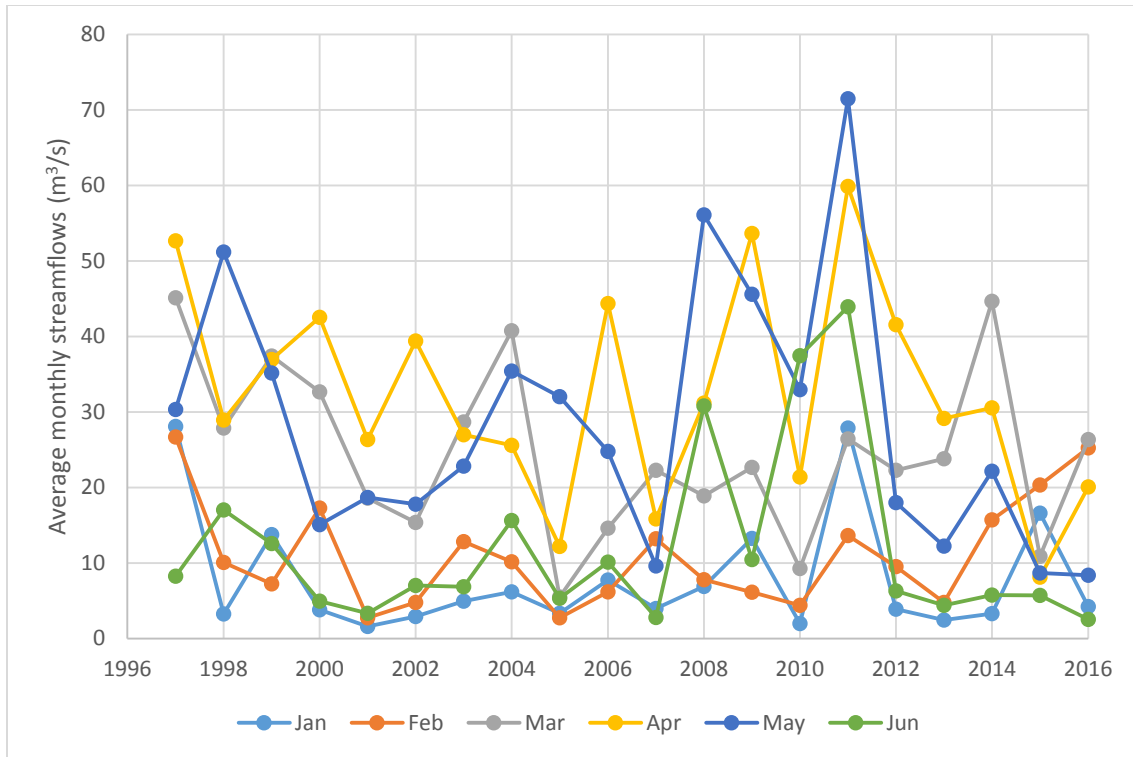


Figure 43. Average monthly (Jan-Jun) streamflows (m³/s) from 1997-2016 at USGS gage 13318960 (Grande Ronde NR Perry).

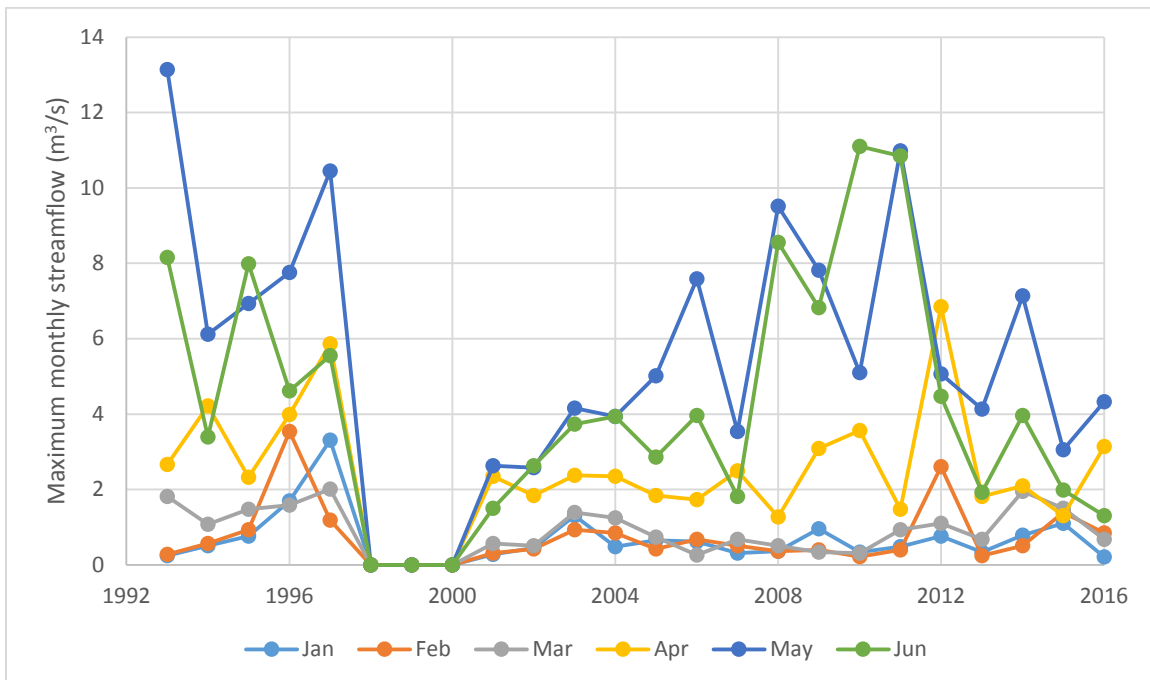


Figure 44. Maximum monthly streamflow (m³/s) at USGS gage 13317850--Grande Ronde BL Clear Creek (data missing in 1998-2000).

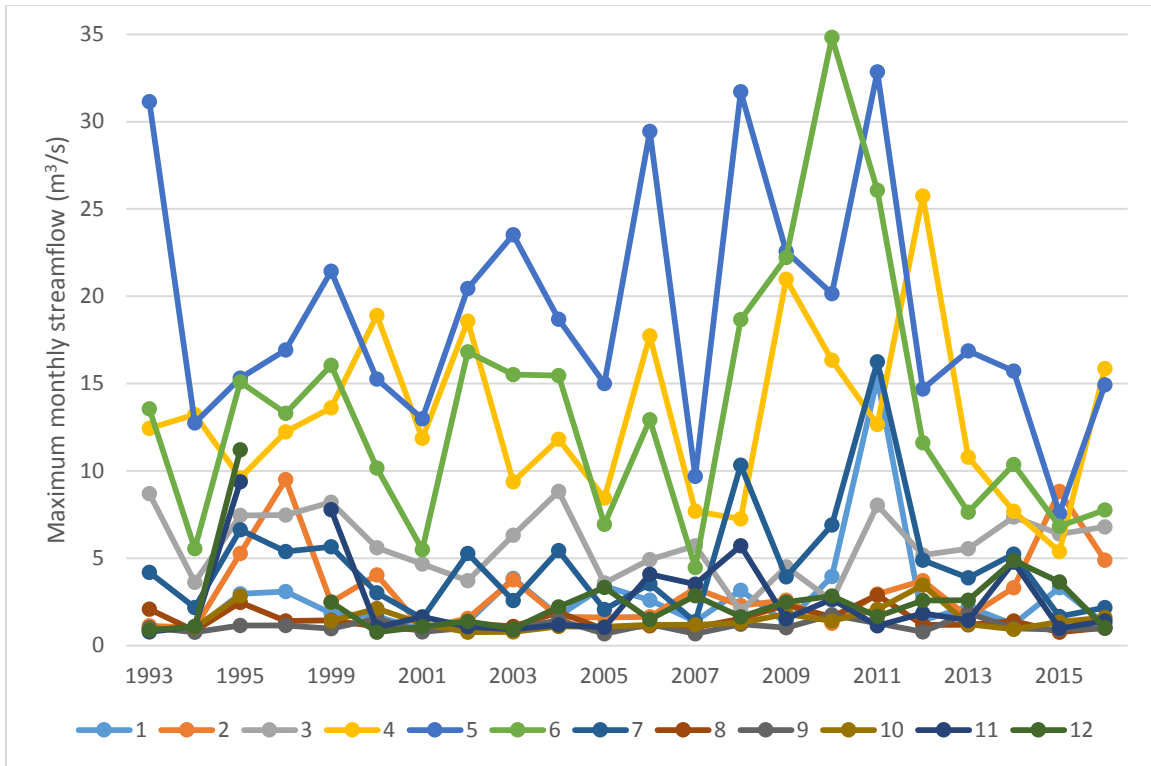


Figure 45. Maximum monthly streamflow (m³/s) at USGS gage 13320000--Catherine Creek near Union, OR (data missing Oct-Dec 1996, and 1997-1998).

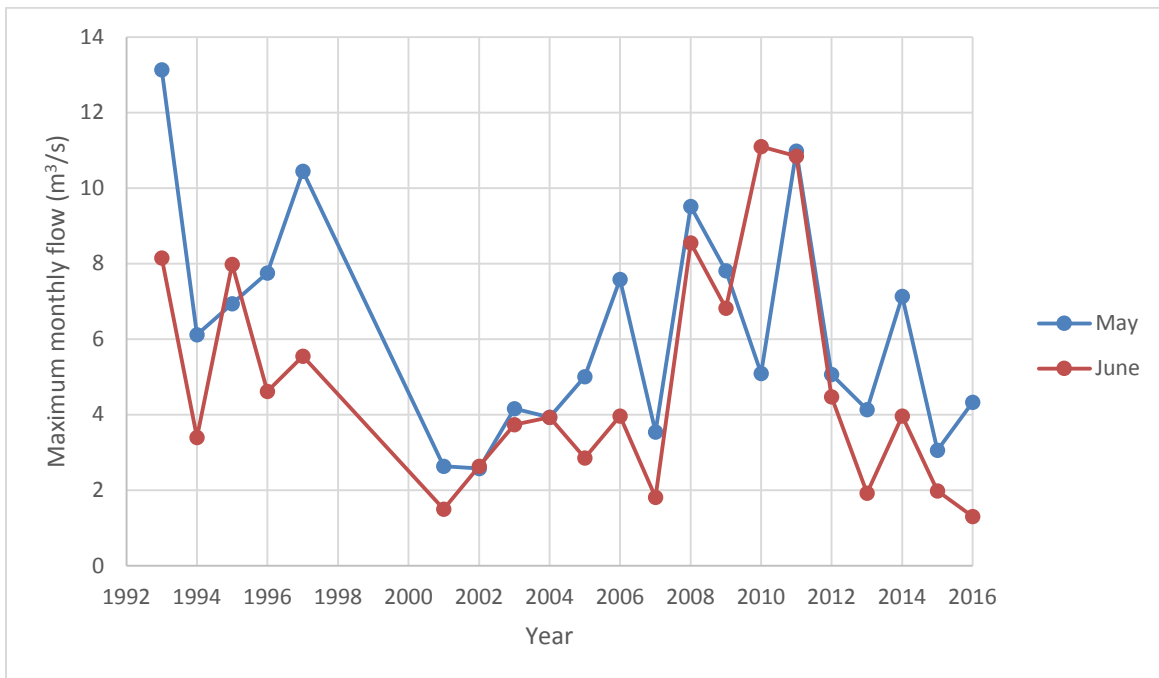


Figure 46. Maximum monthly streamflow (m³/s) at USGS 13317850-Grande Ronde BL Clear Creek (data missing for 1998-2000).

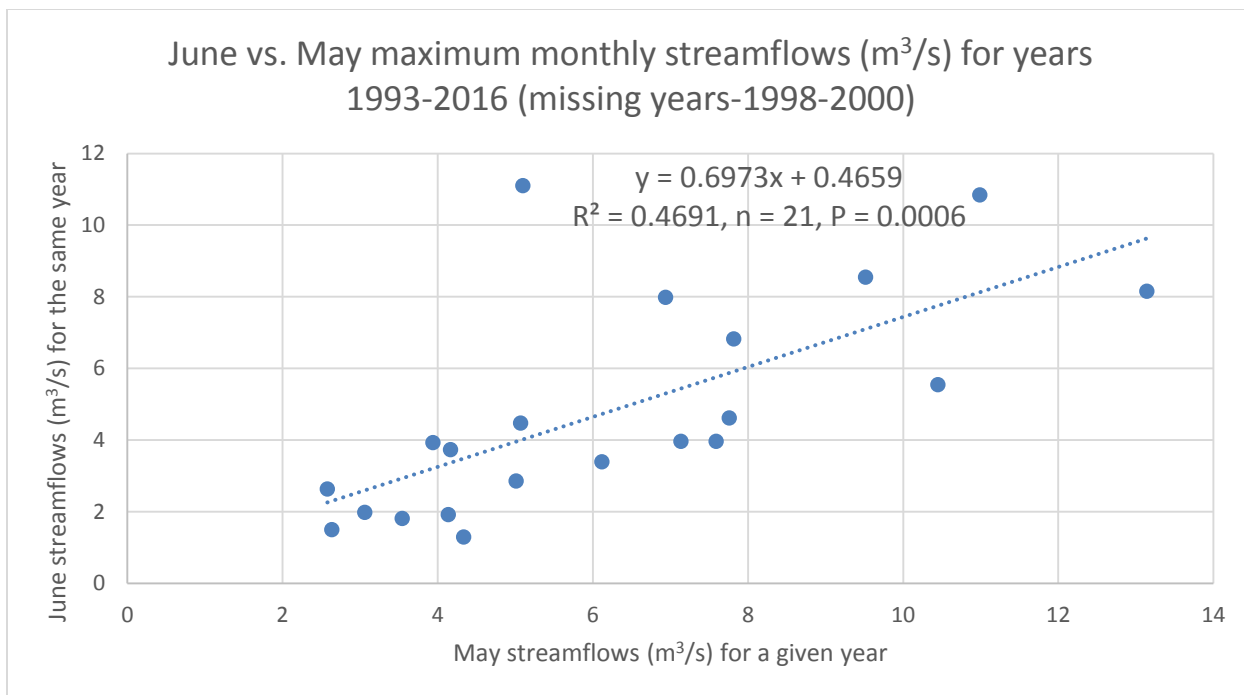


Figure 47. June vs. May maximum monthly streamflows (m^3/s) for years 1993-2016 (missing years-1998-2000).

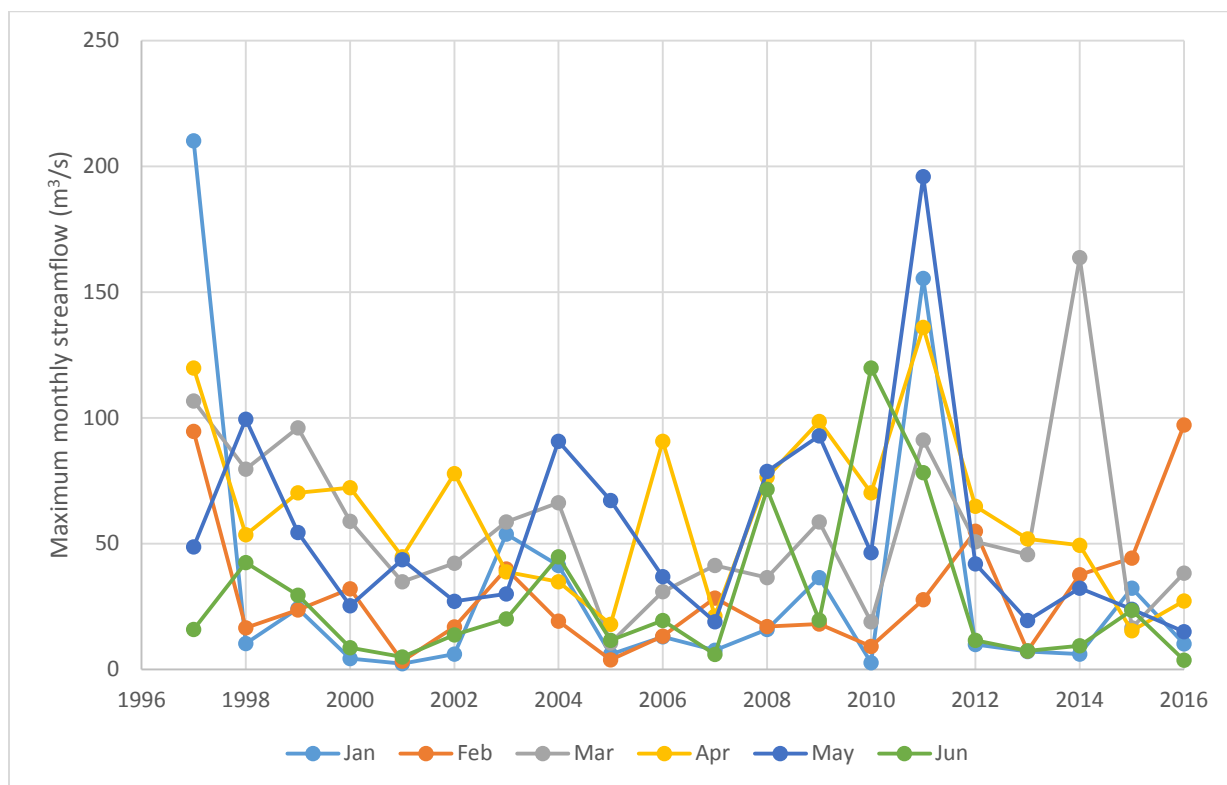


Figure 48. Maximum monthly (Jan-Jun) streamflows (m^3/s) from 1997-2016 at USGS gage 13318960 (Grande Ronde NR Perry).

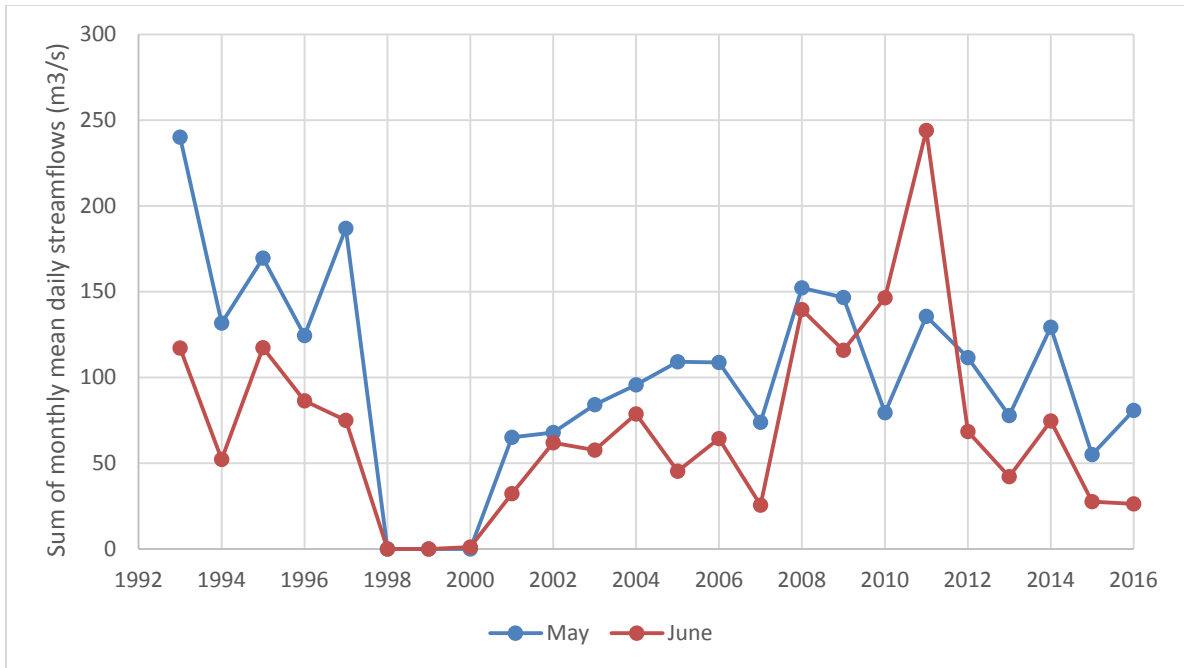


Figure 49. Sum of monthly mean daily streamflows (m³/s) for 1993-2016 at USGS gage 13317850-Grande Ronde BL Clear Creek (data missing for 1998-2000).

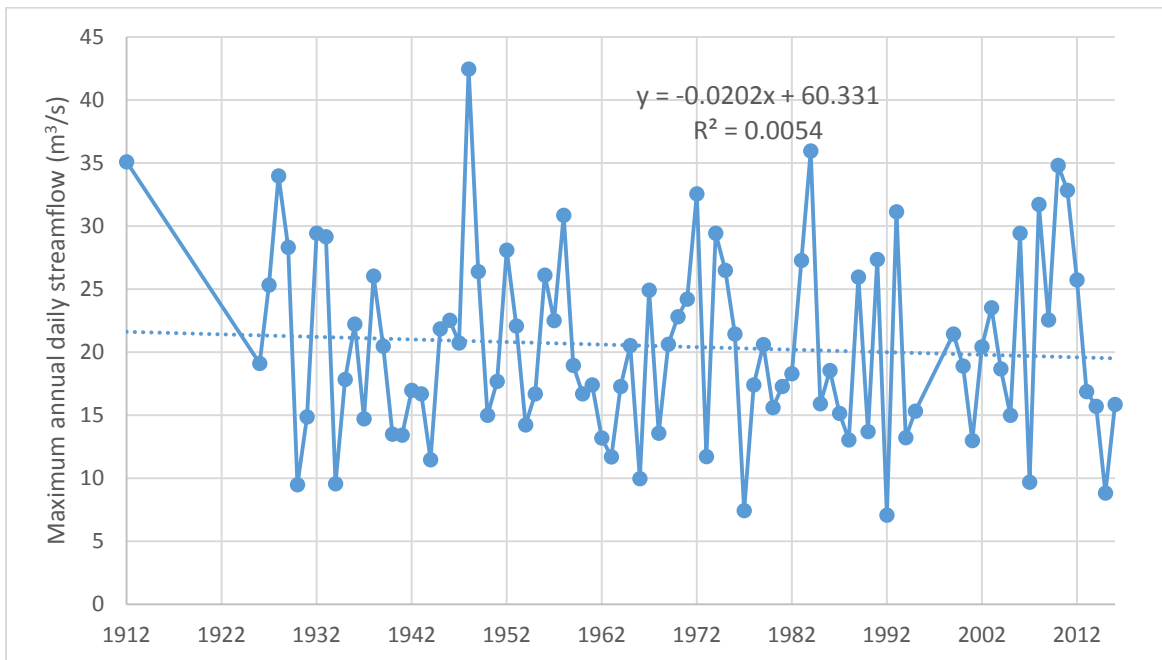


Figure 50. Max annual daily streamflow (m³/s) from 1912 to 2016 (years with missing data (1913-1925, 1996-1998)).

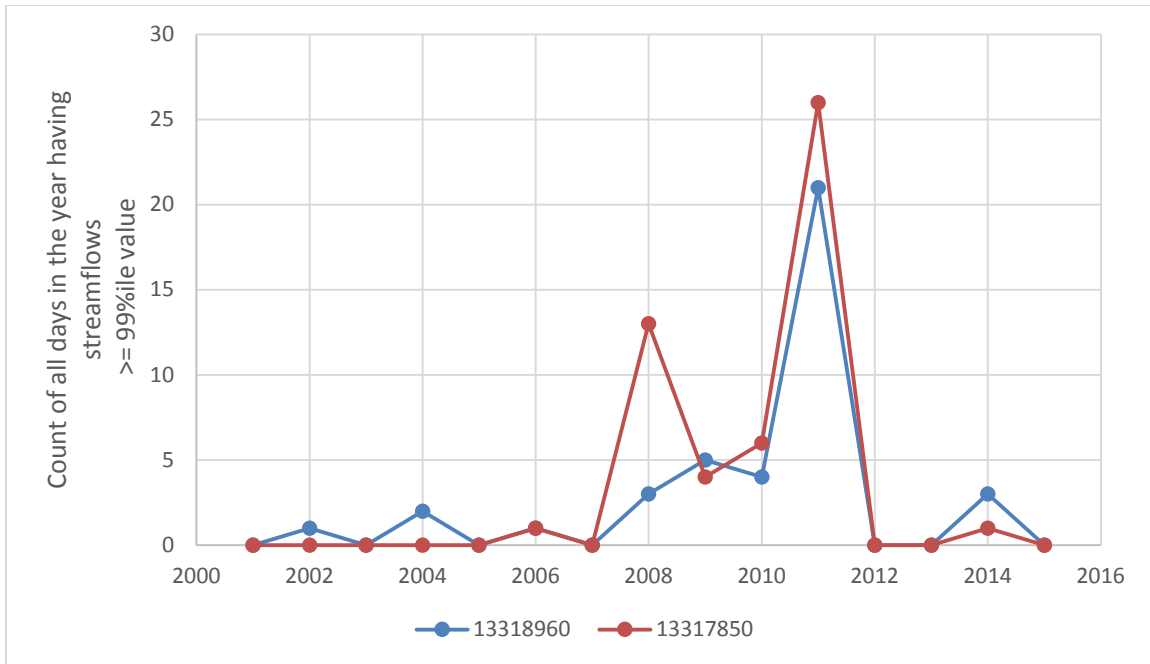


Figure 51. Count of all days in the year having streamflow \geq 99%ile in Upper Grande Ronde River

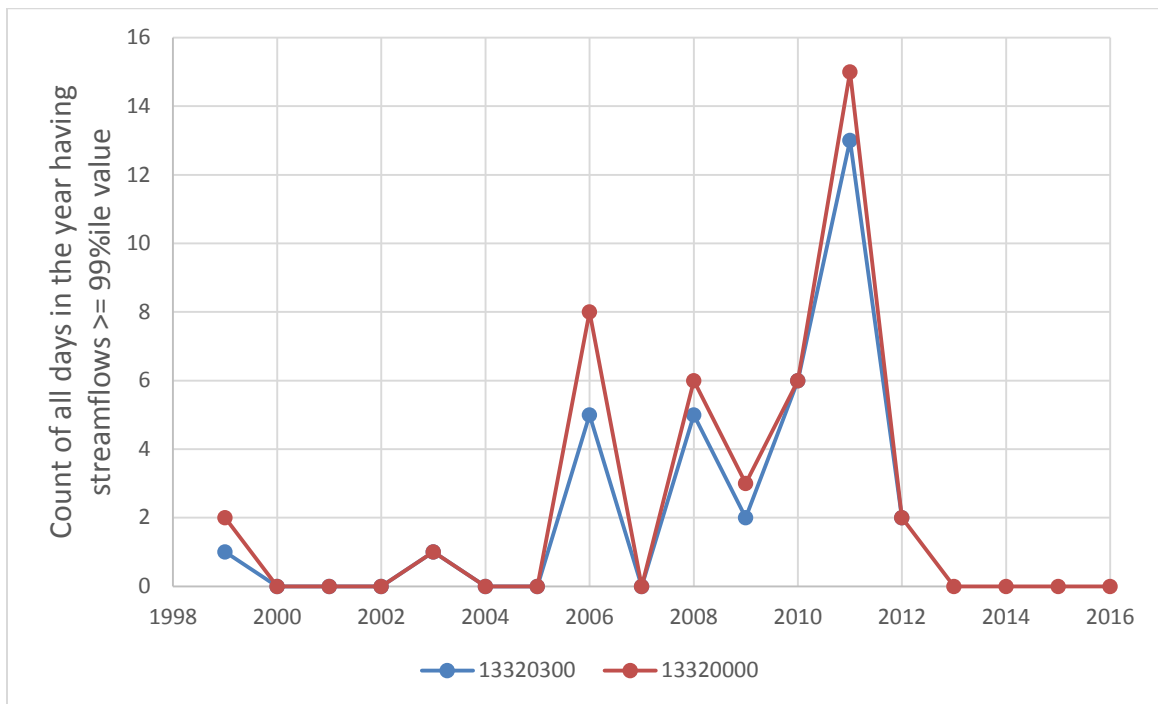


Figure 52. Count of all days in the year having streamflow \geq 99%ile in Catherine Creek.

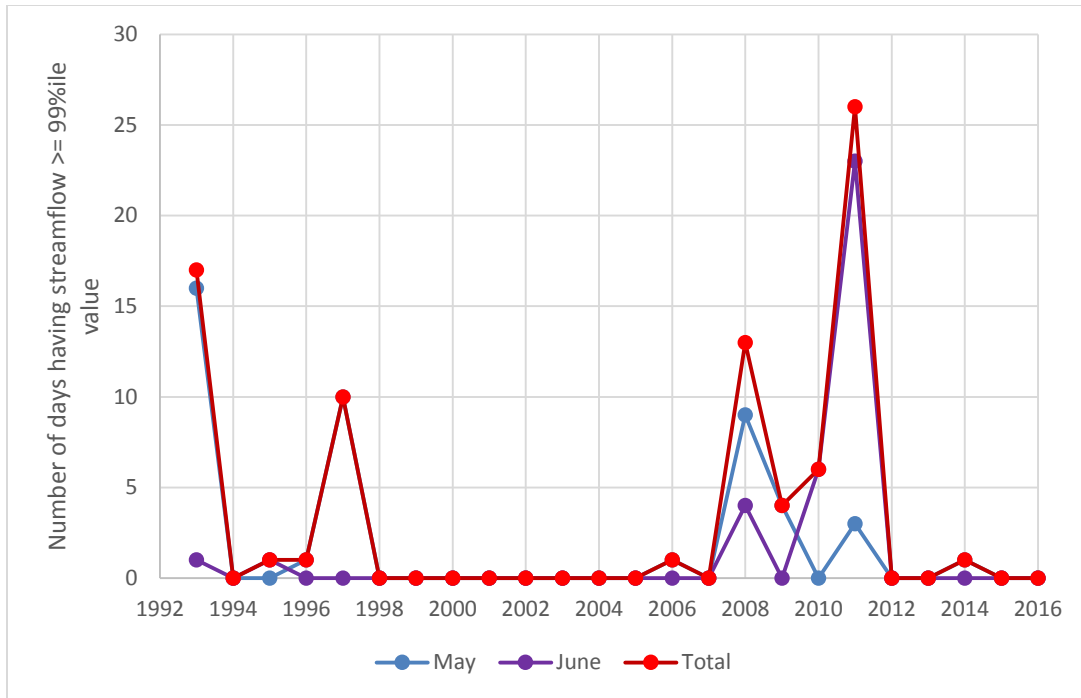


Figure 53. Count of days having peak streamflows $\geq 99\%$ ile value at Grande Ronde BL Clear Creek gage site 13317850.

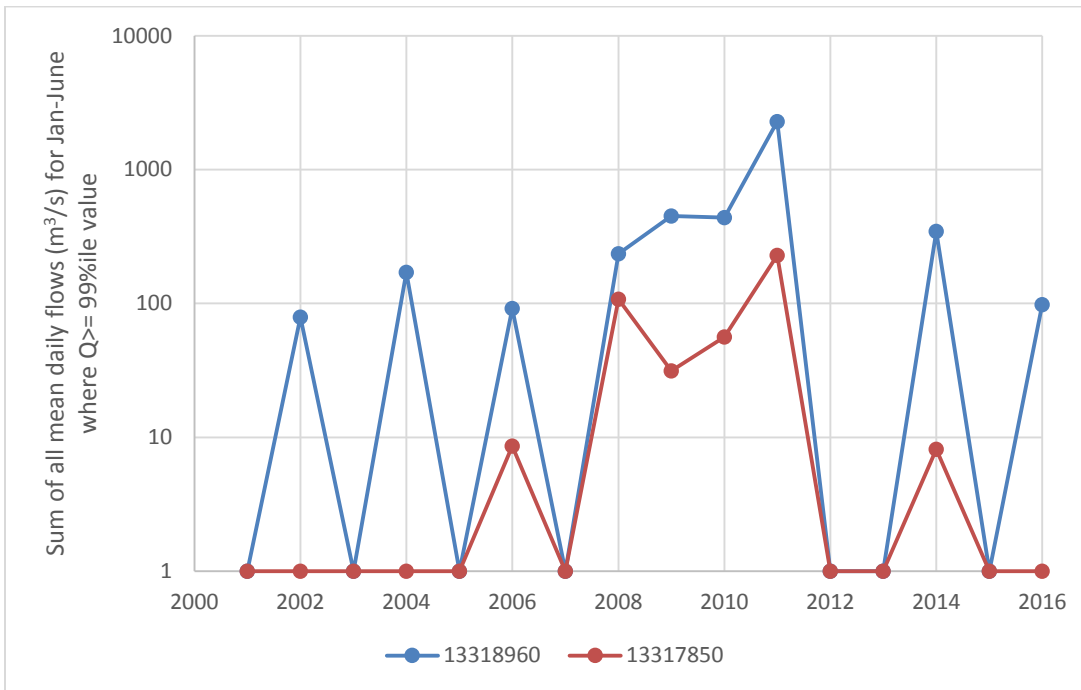


Figure 54. Sum of all mean daily streamflows (m^3/s) for Jan-June where $Q \geq 99\%$ ile value for the Upper Grande Ronde.

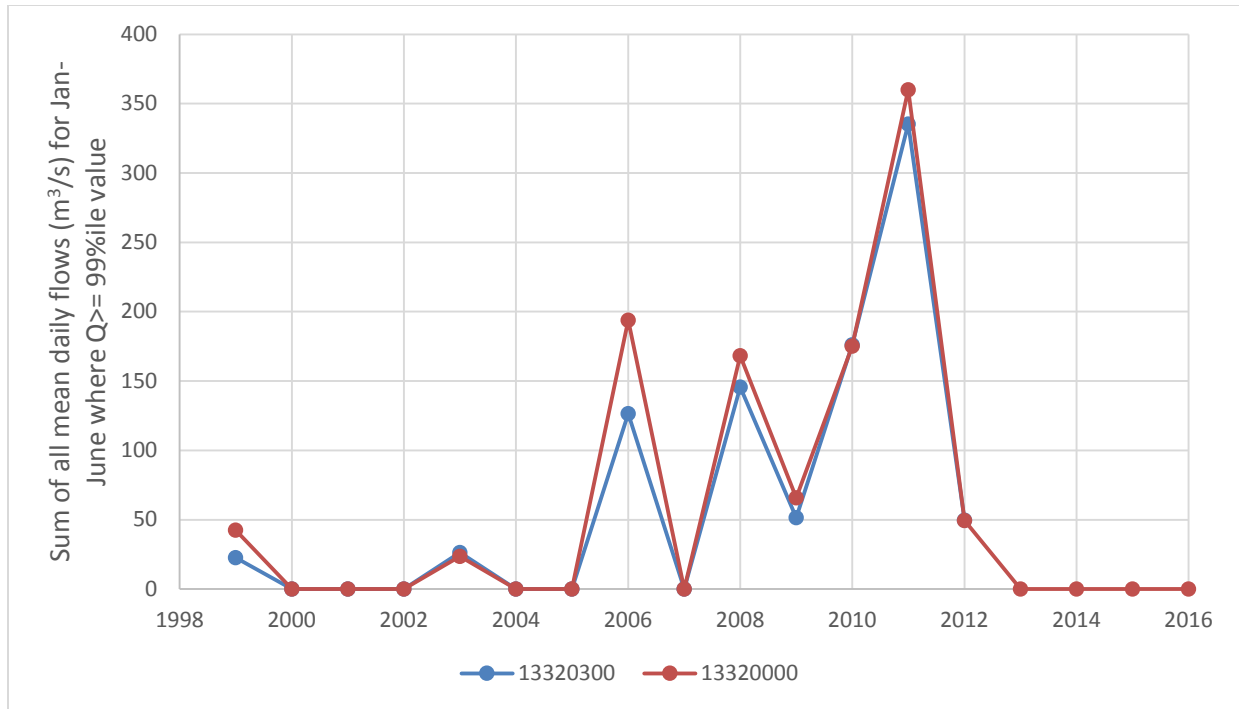


Figure 55. Sum of all mean daily streamflows (m^3/s) for Jan-June where $Q \geq 99\%$ ile value in Catherine Creek.

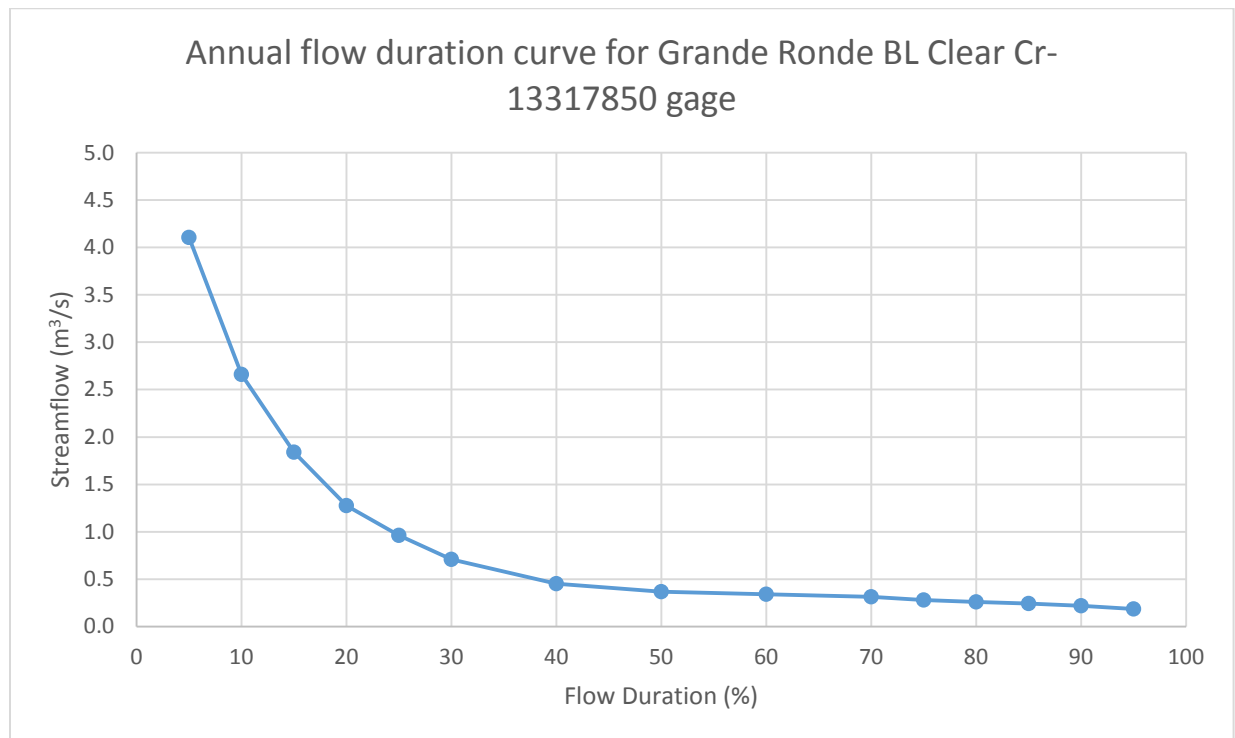


Figure 56. Plot of annual flow duration curve for the Grande Ronde mainstem below Clear Creek (gage 13317850). Data were obtained from OWRD (2017a).

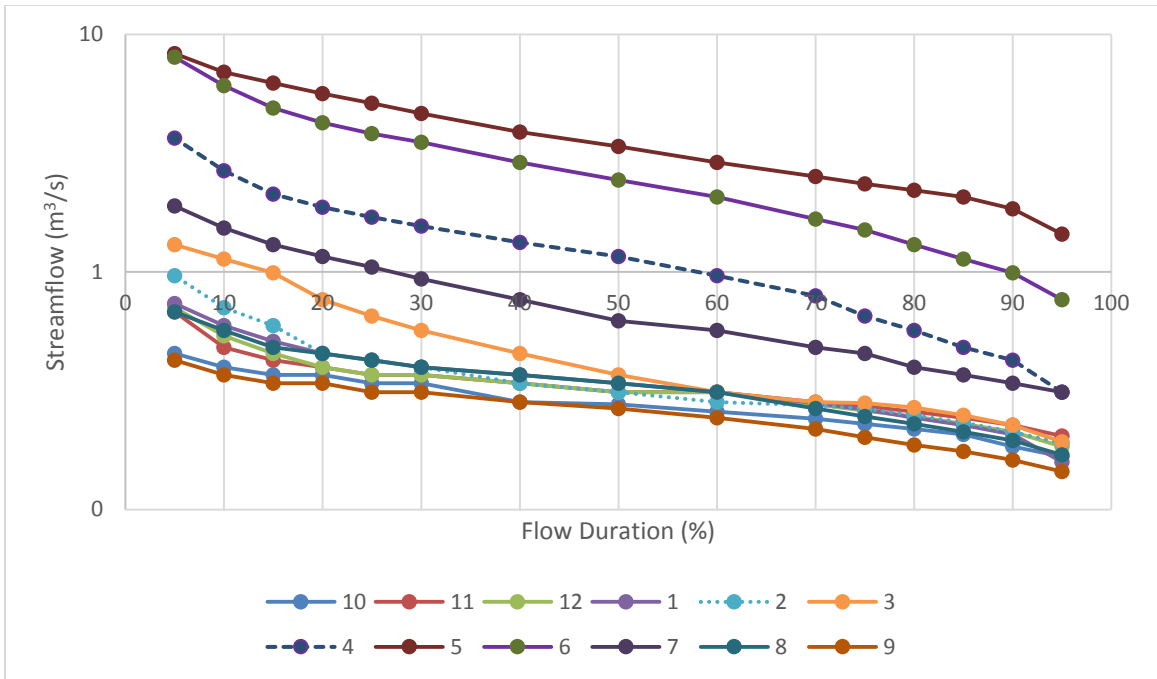


Figure 57. Flow duration curves by month for Grande Ronde BL Clear Cr-13317850 gage.

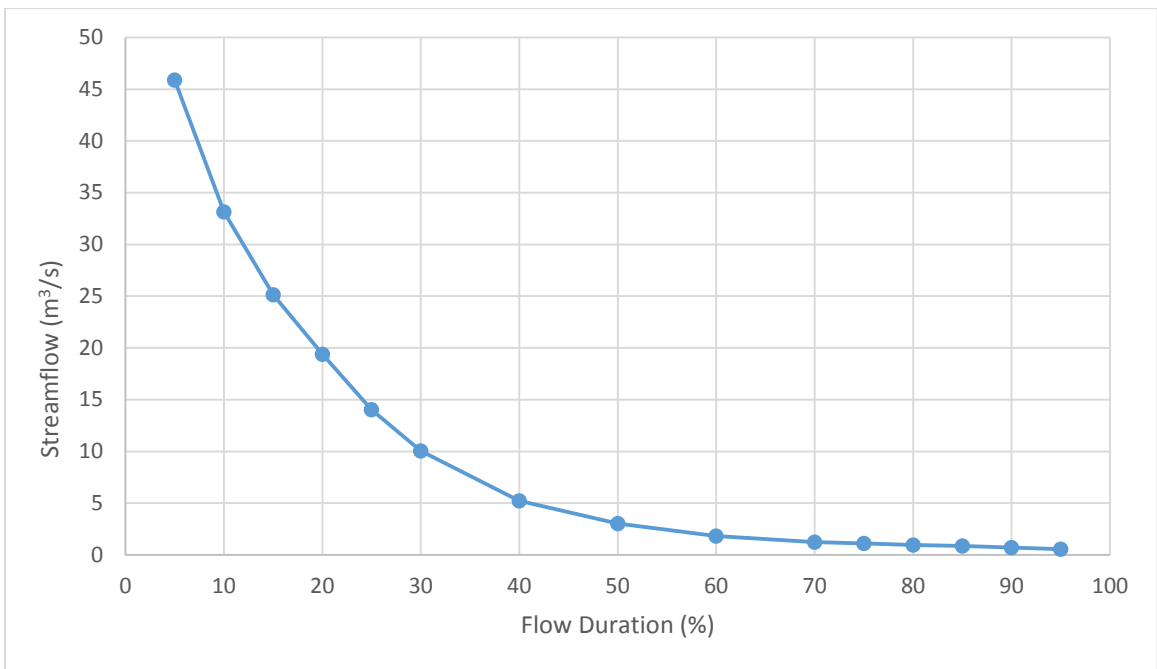


Figure 58. Annual flow duration curve for Grande Ronde R NR Perry-13318960 gage.

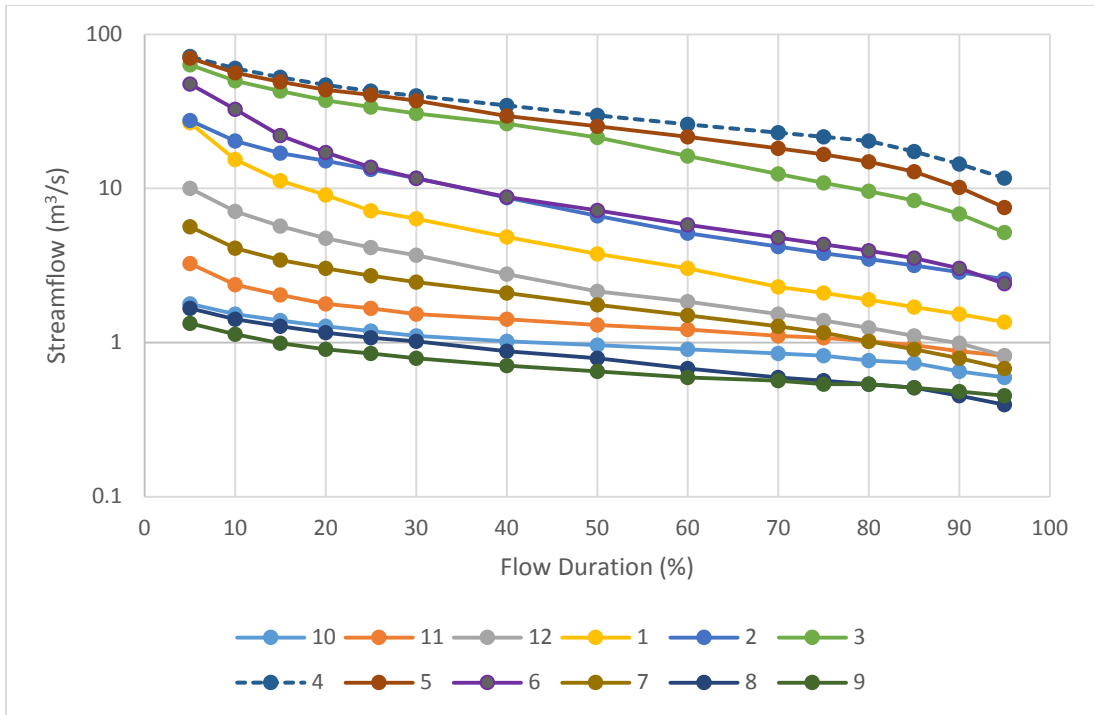


Figure 59. Flow duration curves by month for Grande Ronde NR Perry-13318960 gage.

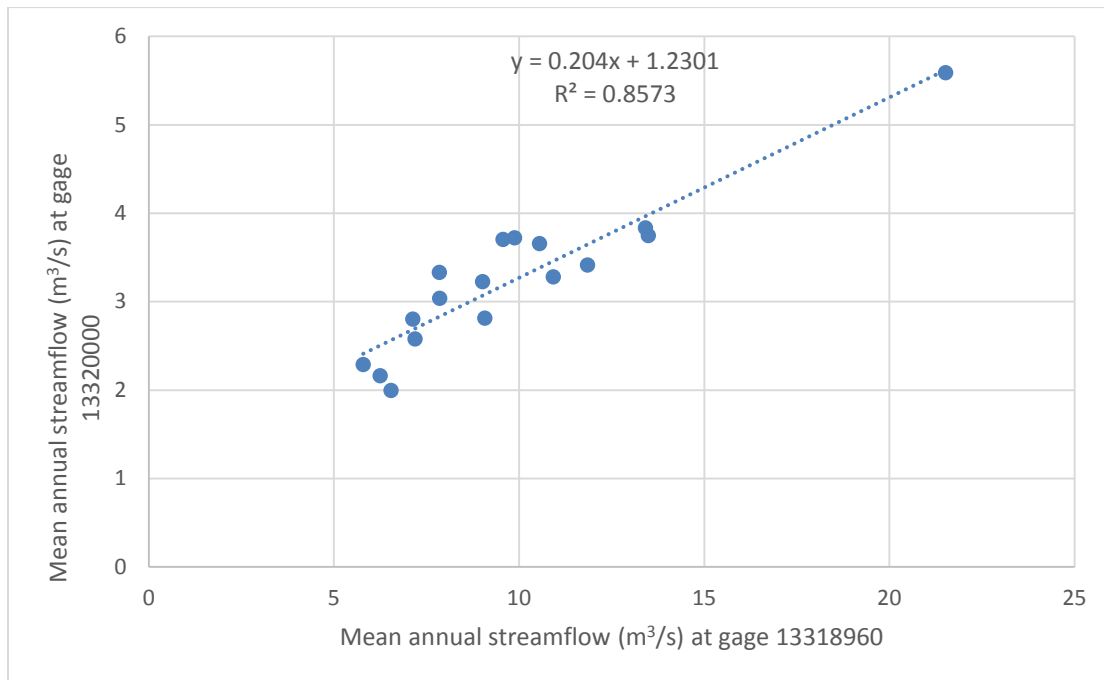


Figure 60. Comparison of mean annual streamflows for Catherine Creek NR Union (gage 13320000) vs Grande Ronde NR Perry (gage 13318960) for water years 1999-2015.

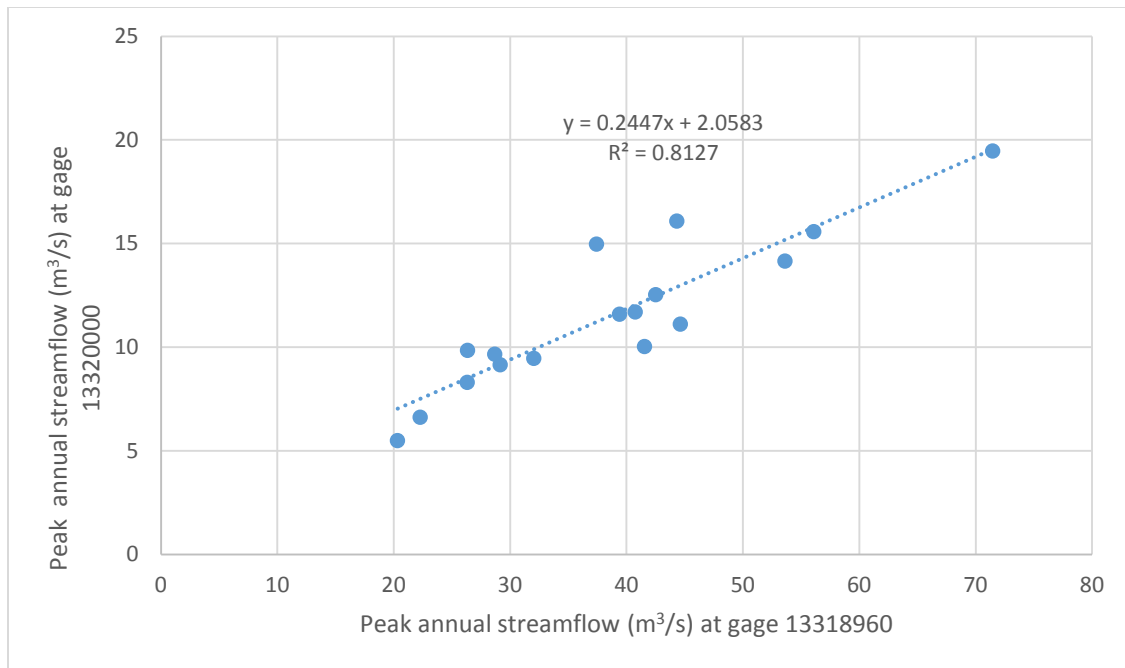


Figure 61. Comparison of peak annual streamflows for Catherine Creek NR Union vs Grande Ronde NR Perry for water years 1999-2015.

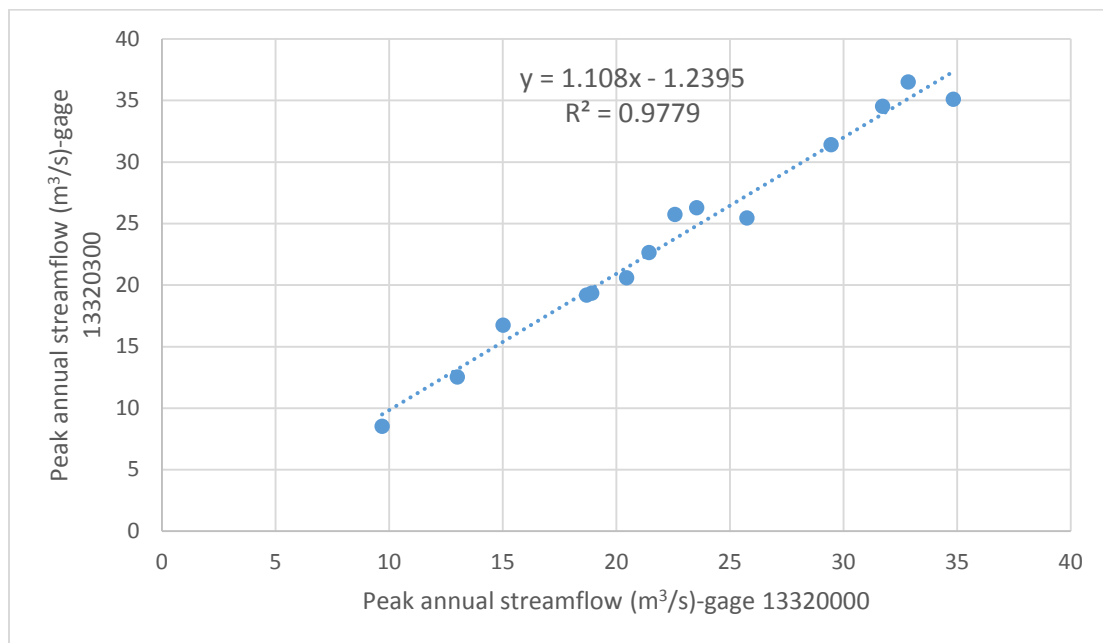


Figure 62. Comparison of peak annual streamflows measured from water years 1996-2011 in two Catherine Creek gaging stations (13320300 and 13320000).

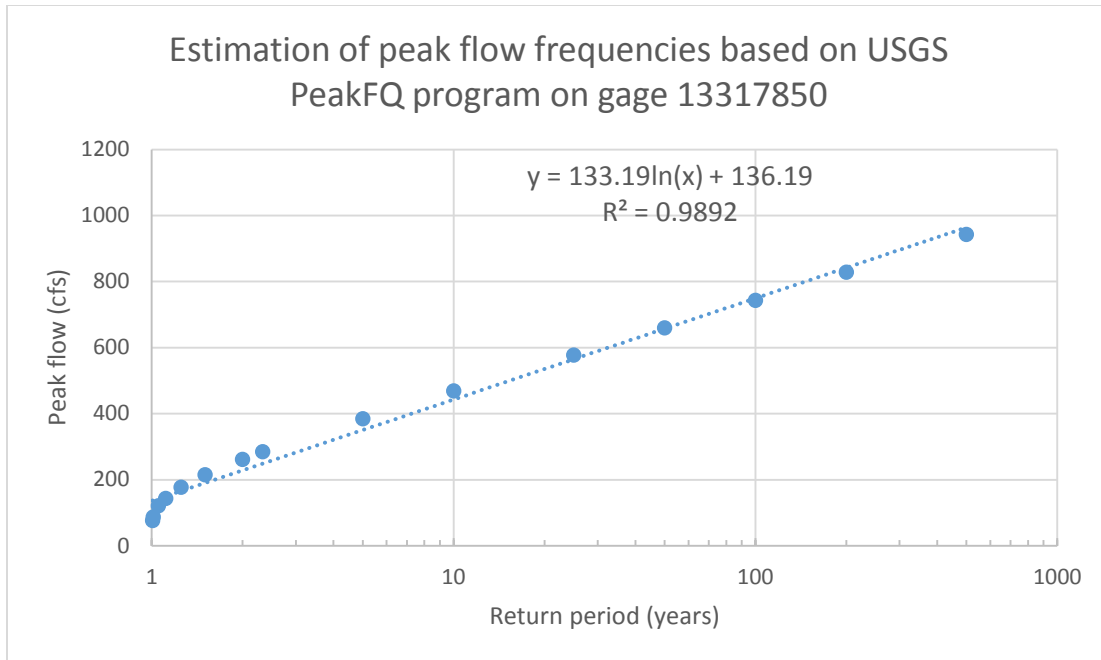


Figure 63. Estimation of peak flow frequencies based on USGS PeakFQ program on gage 13317850.

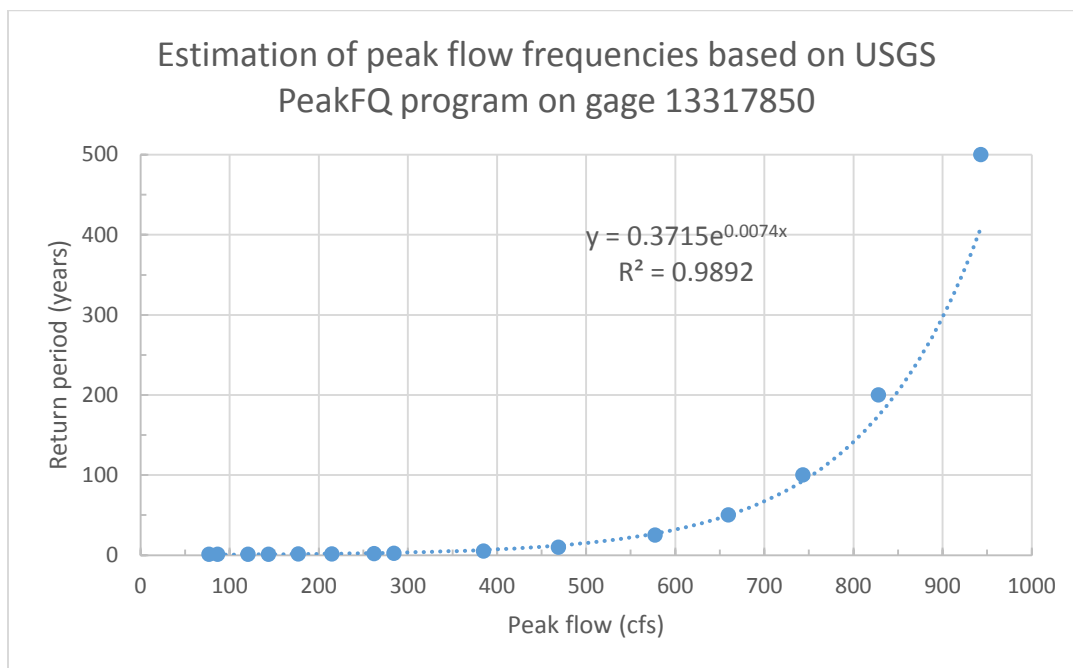


Figure 64. Estimation of peak flow frequencies based on USGS PeakFQ program on gage 13317850.



Figure 65. Geographic location of four CHaMP monitoring sites on the upper Grande Ronde River mainstem downstream from the confluence of the UGR with Sheep Creek and six CHaMP sites above the confluence in relation to the USGS gage (13317850) below Clear Creek on the UGR. These CHaMP sites were used in comparison of measured streamflows against the flow statistics available for the nearby gage site in order to estimate the annual variations in peak flows that could affect scouring of eggs from redds or displace young juveniles.

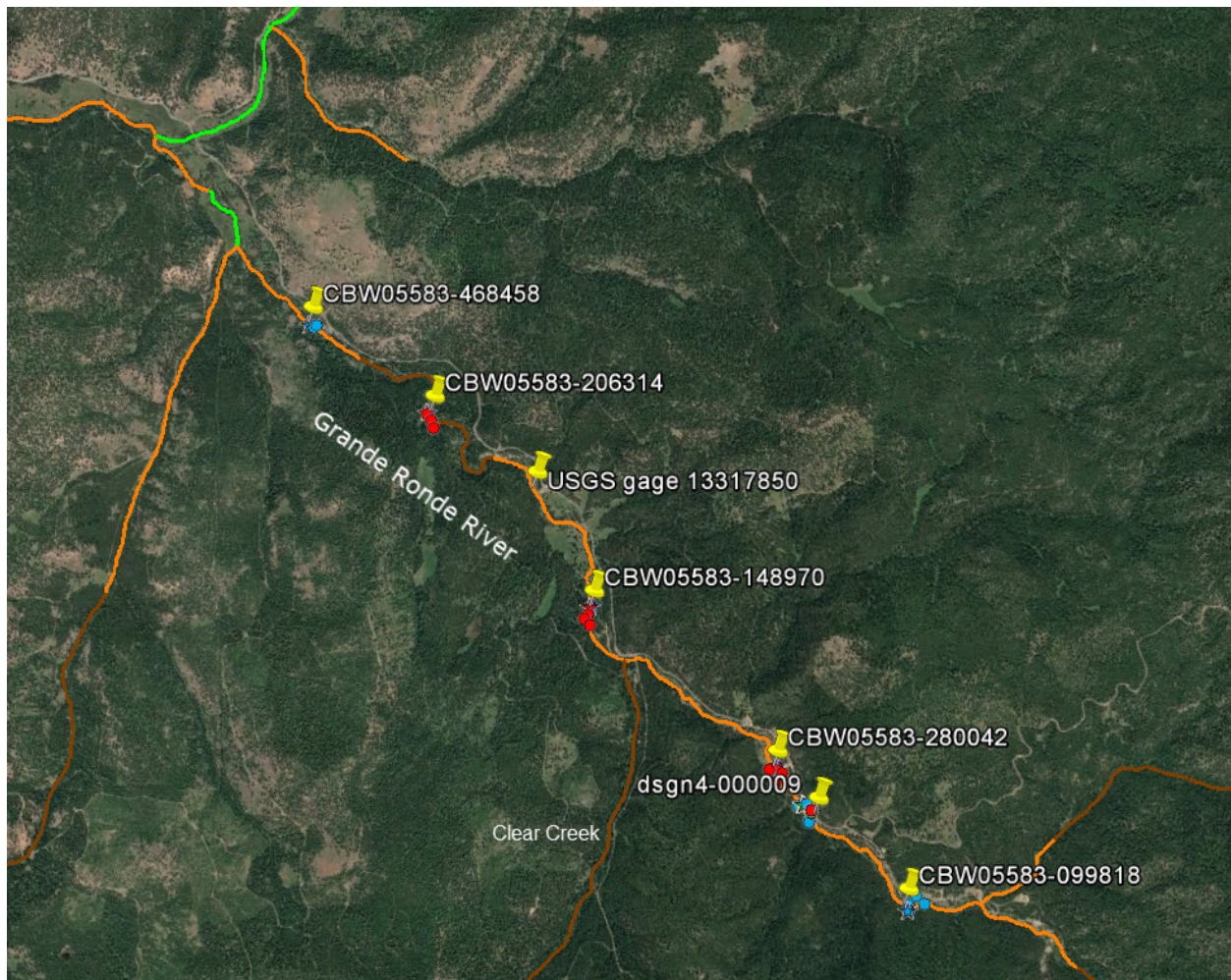


Figure 65 (cont). Geographic location of four CHaMP monitoring sites on the upper Grande Ronde River mainstem downstream from the confluence of the UGR with Sheep Creek and six CHaMP sites above the confluence in relation to the USGS gage (13317850) below Clear Creek on the UGR. These CHaMP sites were used in comparison of measured streamflows against the flow statistics available for the nearby gage site in order to estimate the annual variations in peak flows that could affect scouring of eggs from redds or displace young juveniles.

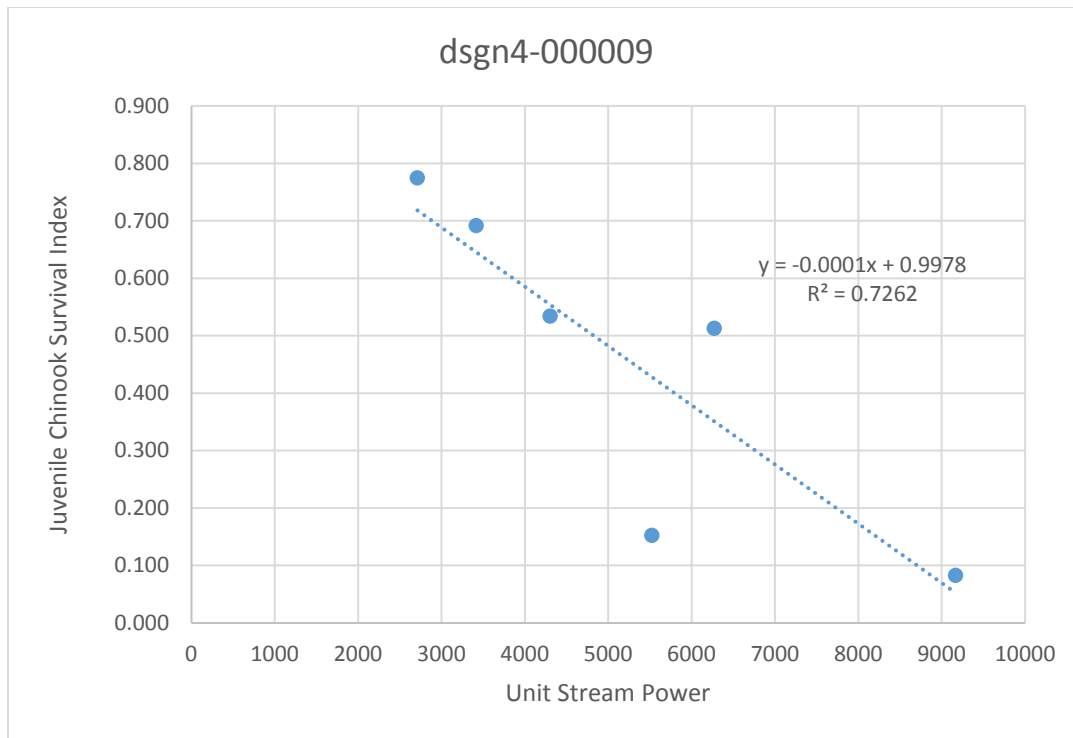


Figure 66. Juvenile Chinook survival index vs. unit stream power plotted for CHaMP site dsgn4-000009.

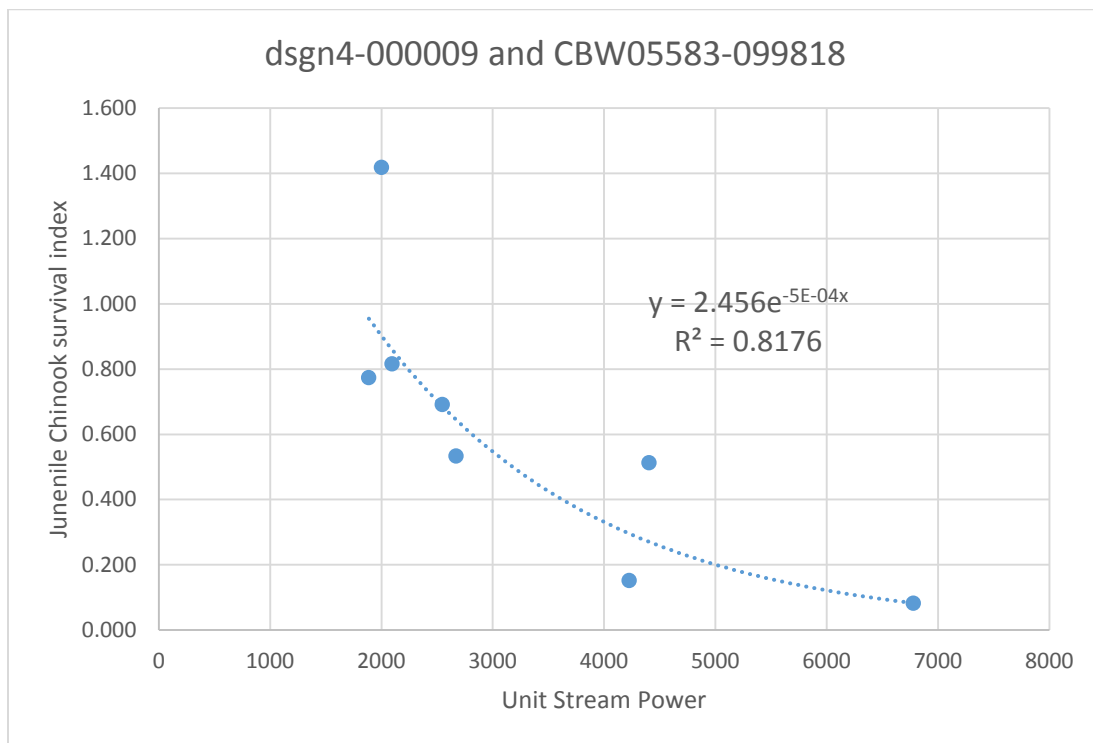


Figure 67. Juvenile Chinook survival index vs. unit stream power plotted for CHaMP sites dsgn4-000009 and CBW05583-099818.

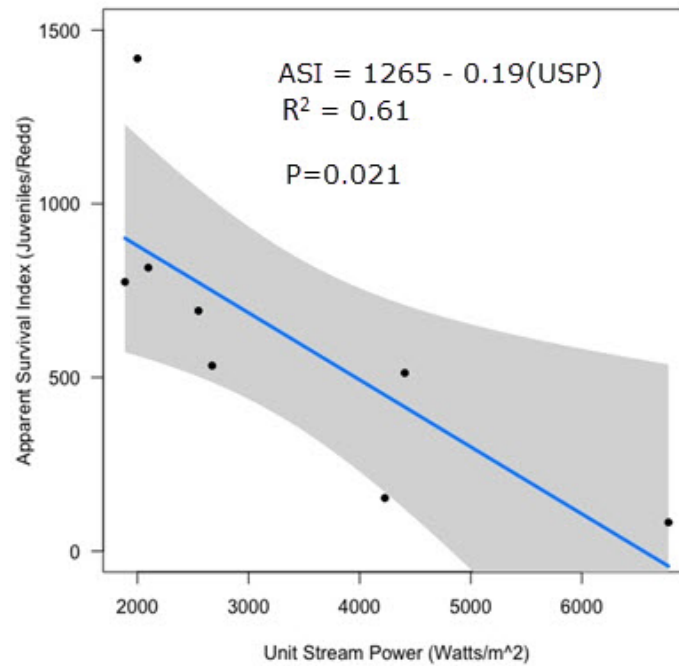


Figure 68. Juvenile Chinook survival index vs. unit stream power plotted for CHaMP sites dsgn4-000009 and CBW05583-099818. Linear plot with 95% confidence intervals.

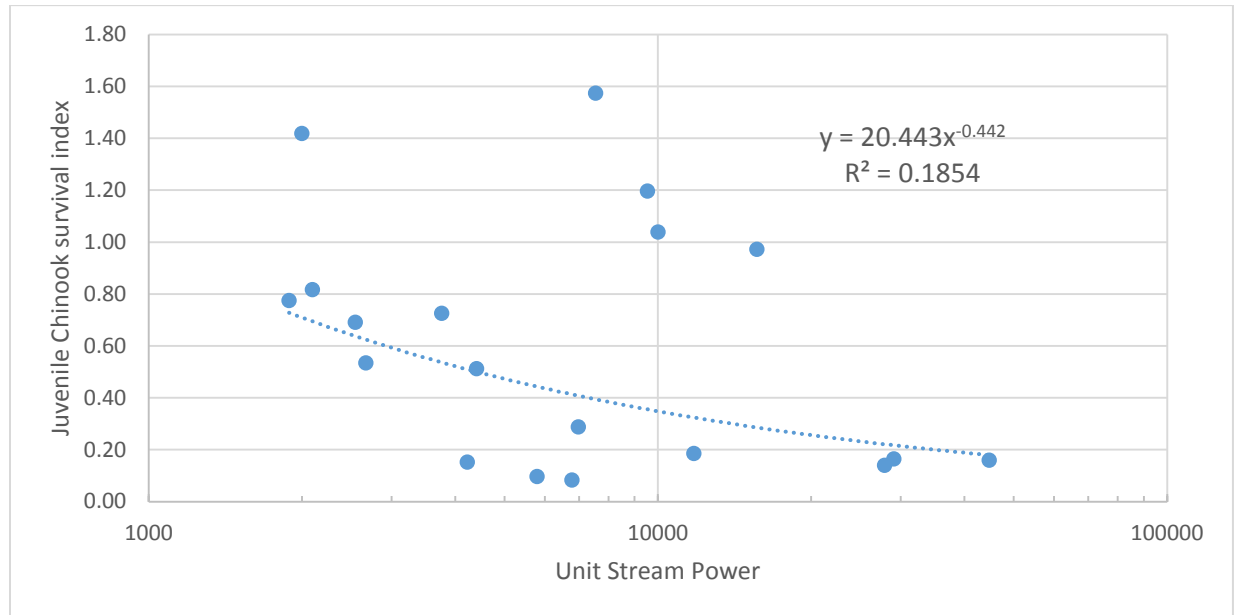


Figure 69. Juvenile Chinook survival index vs. unit stream power plotted for 10 CHaMP sites snorkeled from 2011-2016. This chart deletes data point for CBW05583-148970 (2014) and dsgn4-000277 (2011).

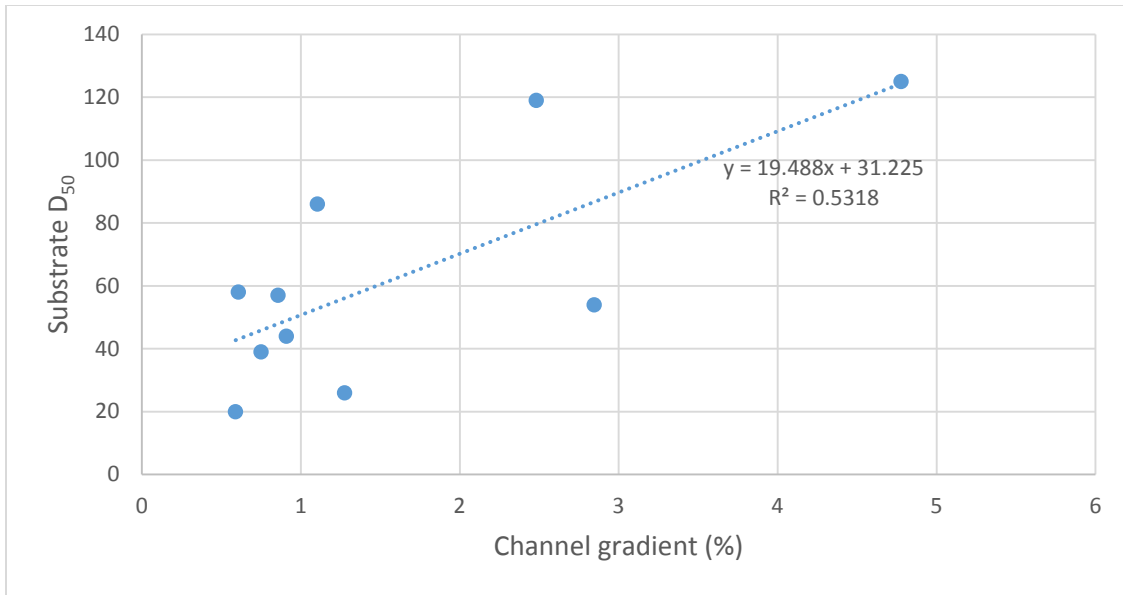


Figure 70. Relationship between riffle particle substrate composition and channel gradient for upper 10 CHaMP sites on Grande Ronde River mainstem

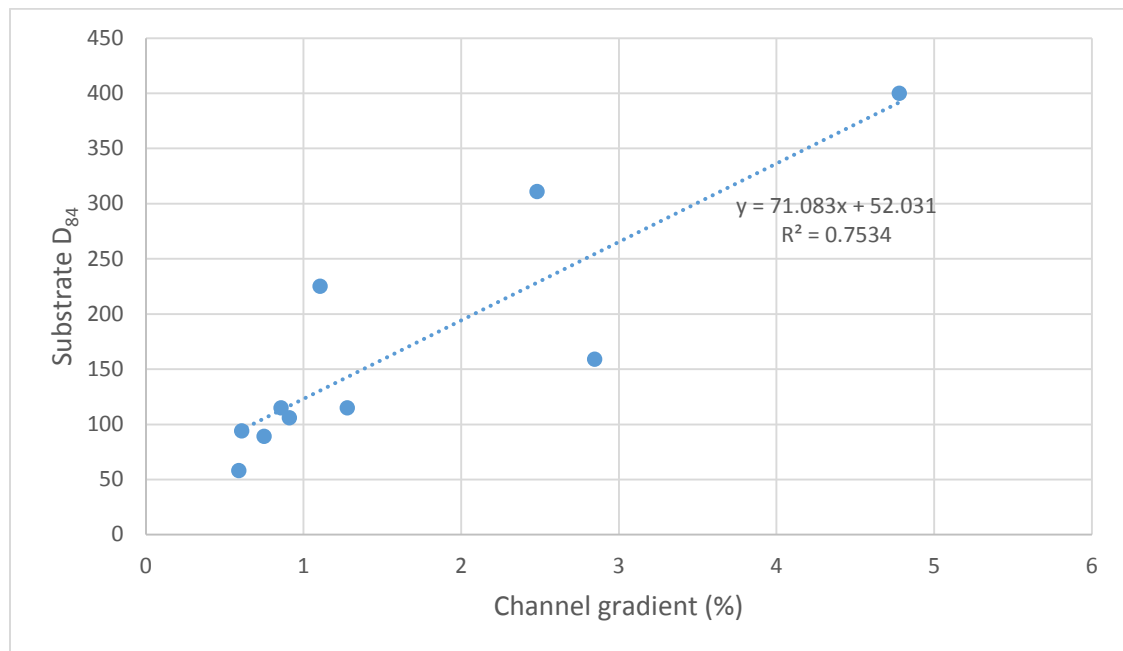


Figure 71. Relationship between riffle particle substrate composition and channel gradient for upper 10 CHaMP sites on Grande Ronde River mainstem.

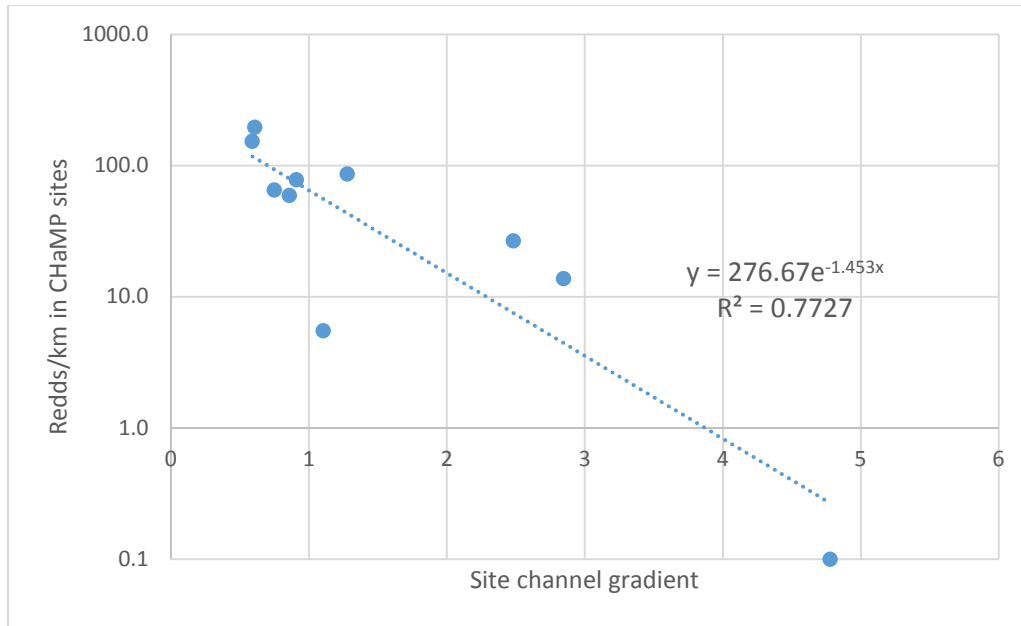


Figure 72. Redd density (no./km) vs. CHaMP site channel gradient (%) for 10 sites in UGR mainstem

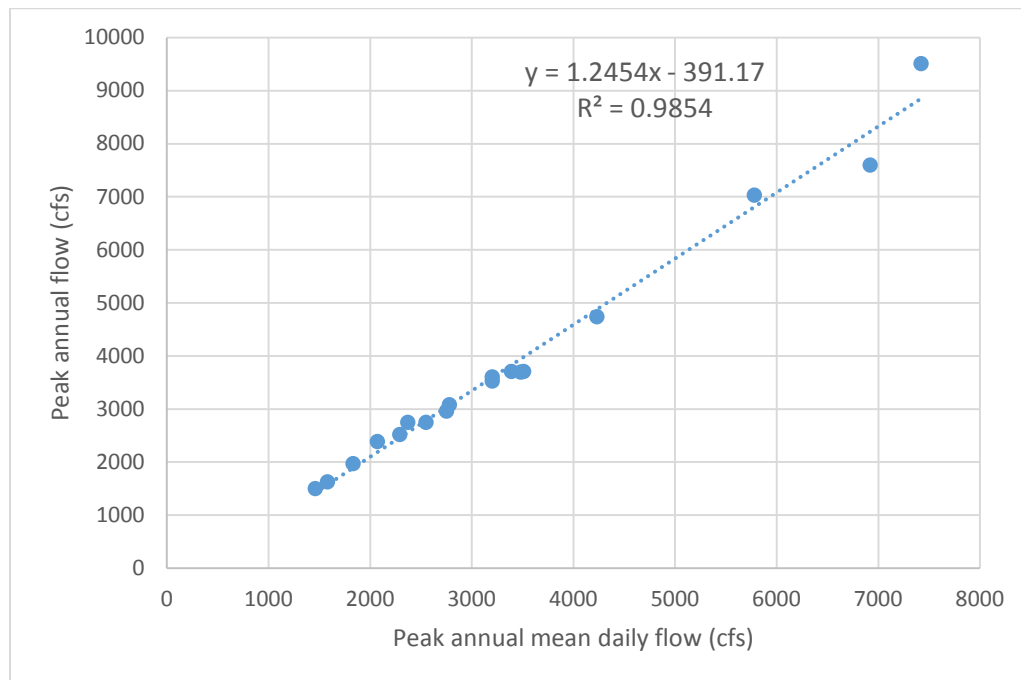


Figure 73. Comparison of true peak annual flow vs maximum annual average daily flow at the OWRD gage 13318960 near Perry (13318960).

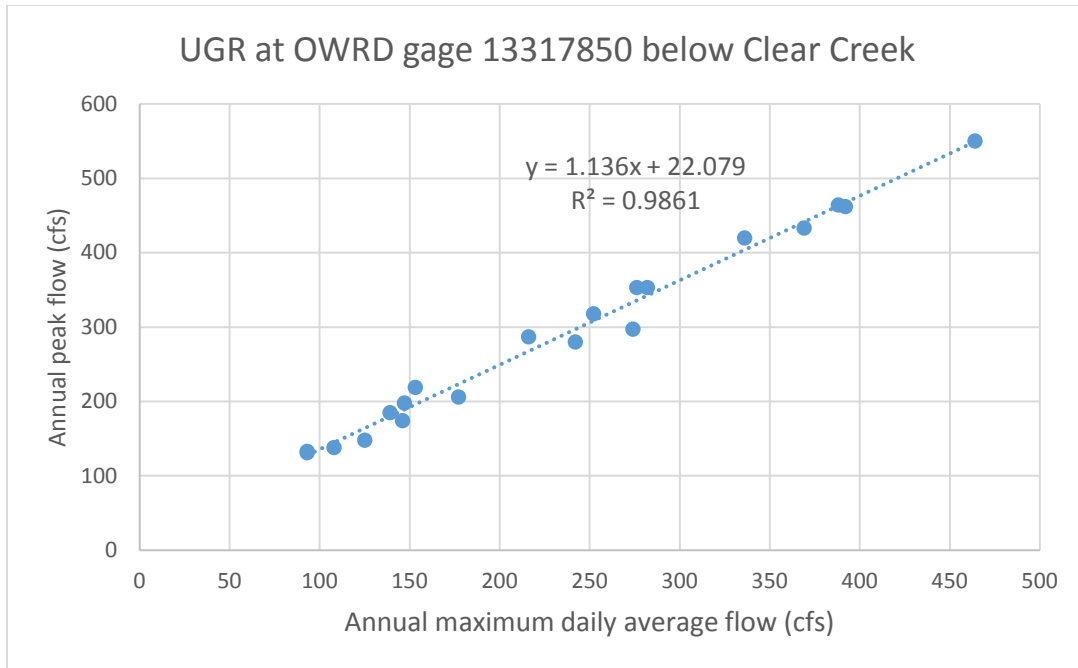


Figure 74. Comparison of true peak annual flow vs maximum annual average daily flow at the OWRD gage on the Grande Ronde River below Clear Creek (13317850).



Figure 75. CHaMP site CBW05583-235322, looking center-up from transect T11. Sub₅₀ = 44 mm; SubD₈₄ = 106 mm. Redd density in CHaMP site = 78.0/km. Gradient = 0.91%.



Figure 76. CHaMP site CBW05583-370490, looking center-up from transect T11. Sub₅₀ = 57 mm; SubD₈₄ = 115 mm. Redd density in CHaMP site = 59.3/km. Gradient = 0.86%.



Figure 77. CHaMP site CBW05583-321338, looking center-up from transect T11. Sub₅₀ = 54 mm; SubD₈₄ = 159 mm. Redd density in CHaMP site = 13.7/km. Gradient = 2.85%.



Figure 78. CHaMP site dsgn4-000277, looking center-up from transect T11. $Sub_{50} = 86$ mm; $SubD_{84} = 225$ mm. Redd density in CHaMP site = 5.5/km. Gradient = 1.11%.



Figure 79. CHaMP site CBW05583-468458, looking center-up from transect T11. $Sub_{50} = 119$ mm; $SubD_{84} = 311$ mm. Redd density in CHaMP site = 26.7/km. Gradient = 2.48%.



Figure 80. CHaMP site CBW05583-206314, looking center-up from transect T11. $Sub_{50} = 125$ mm; $SubD_{84} = 400$ mm. Redd density in CHaMP site = 0.0/km. Gradient = 4.78%.



Figure 81. CHaMP site CBW05583-148970, looking center-up from transect T11. $Sub_{50} = 26$ mm; $SubD_{84} = 115$ mm. Redd density in CHaMP site = 86.4/km. Gradient = 1.28%.



Figure 82. CHaMP site CBW05583-280042, looking center-up from transect T11. Sub₅₀ = 58 mm; SubD₈₄ = 94 mm. Redd density in CHaMP site = 196.2/km. Gradient = 0.61%.



Figure 83. CHaMP site dsgn4-000009, looking center-up from transect T11. Sub₅₀ = 39 mm; SubD₈₄ = 89 mm. Redd density in CHaMP site = 65.2/km. Gradient = 0.75%.



Figure 84. CHaMP site CBW05583-099818, looking center-up from transect T11. $Sub_{50} = 20$ mm; $SubD_{84} = 58$ mm. Redd density in CHaMP site = 153.1/km. Gradient = 0.59%.

Tables

Table 36. Complete listing of all gaging stations in the Grande Ronde or Catherine Creek mainstems and tributaries within the full extent of the Upper Grande Ronde and Catherine Creek Spring Chinook populations having mean daily flows available and greater than or equal to one complete water year, or with peak or low flow records. This list includes both active and discontinued gages and gages with from one to 88 complete years of flow records.

Station ID	Station Name	Status	Mean daily flow available	Complete water years	Peak flow records	Low flow records	Start date	End date
13317850	GRANDE RONDE R BL CLEAR CR, NR STARKEY, OR	Active	Yes	17	17	6	1992	2012
13317900	GRANDE RONDE R NR STARKEY, OR	Discontinued	Yes	1	0	0	1936	1937
13318050	MEADOW CR BL SMITH CR NR STARKEY, OR	Discontinued	Yes	2	1	1	1977	1979
13318060	MEADOW CR AB BEAR CR NR STARKEY, OR	Active	Yes	10	6	5	1977	2012
13318200	MEADOW CR NR STARKEY, OR	Discontinued	Yes	1	4	3	1931	1935
13318210	MEADOW CR BL DARK CANYON CR NR STARKEY, OR	Active	Yes	8	8	5	1992	2012
13318500	GRANDE RONDE R NR HILGARD, OR	Discontinued	Yes	19	19	19	1937	1956
13318800	GRANDE RONDE R AT HILGARD, OR	Discontinued	Yes	15	15	15	1966	1981
13318920	FIVE POINTS CR AT HILGARD, OR	Active	Yes	10	11	7	1992	2012
13318960	GRANDE RONDE R NR PERRY, OR	Active	Yes	18	18	3	1996	2014
13319000	GRANDE RONDE R AT LA GRANDE, OR	Discontinued	Yes	80	81	79	1903	1989
13319700	S CATHERINE CR D NR MEDICAL SPRINGS, OR	Discontinued	Yes	8	0	0	1966	1984
13319800	S FK CATHERINE CR NR MEDICAL SPRINGS, OR	Discontinued	Yes	0	0	0	1926	1927
13319900	N FK CATHERINE CR NR MEDICAL SPRINGS, OR	Active	Yes	9	2	1	1992	2012
13320000	CATHERINE CR NR UNION, OR	Active	Yes	88	90	81	1911	2014
13320300	CATHERINE CR AT UNION, OR	Active	Yes	15	16	11	1996	2012
13323495	GRANDE RONDE R NR IMBLER, OR	Discontinued	Yes	2	3	2	1997	2003
13323500	GRANDE RONDE R NR ELGIN, OR	Discontinued	Yes	26	26	26	1955	1981
13323600	INDIAN CR NR IMBLER, OR	Discontinued	Yes	12	13	12	1938	1950
13323700	N FK CLARKS CR NR ELGIN, OR	Discontinued	Yes	13	18	16	1965	1983

Table 37. Area coefficients selected for hydrologic Region 3 to match the peak flow return period for each year of the CHaMP surveys (see Cooper 2006) for peak flow prediction for ungaged sites.

Year	Peak flow (cfs)	Peak flow (m ³ /s)	Return period (years)	Area coefficient (<i>a</i>)
2011	464	13.14	11.51	0.7431
2012	280	7.93	2.95	0.7459
2013	174	4.93	1.35	0.7546
2014	318	9.01	3.91	0.7459
2015	138	3.91	1.03	0.7546
2016	219	6.20	1.88	0.7546

Table 38. Basin characteristics for 10 CHaMP sites clustered downstream and upstream of OWRD stream gaging station on the Grande Ronde River below Clear Creek (13317850).

Name	Rotating Panel	distance from gage (km)	DA (km ²)	DA (mi ²)	PRECIP (cm)	MINBELEV (m)	ELEVMAX (m)	Grad	DpthBf_ Avg	BfWdth_ Avg	% of DA at gage
CBW05583-235322	1	-15.99	360.18	139.06	73.61174	1156.41	2415.02	0.91	0.34	12.33	351.2%
CBW05583-370490	3	-14.97	357.01	137.84	73.67524	1169.81	2415.02	0.86	0.51	16.76	348.1%
CBW05583-321338	1	-13.78	349.00	134.75	73.79716	1183.85	2415.02	2.85	0.49	11.79	340.3%
dsgn4-000277	annual	-12.8	338.52	130.70	73.91654	1202.84	2415.02	1.11	0.37	15.64	330.1%
CBW05583-468458	3	-1.96	105.02	40.55	82.93	1309.26	2415.02	2.48	0.35	10.77	102.4%
CBW05583-206314	1	-0.97	104.07	40.18	83.08	1339.27	2415.02	4.78	0.49	11.67	101.5%
Grande Ronde R BL Clear Cr, NR Starkey, OR (13317850)		0	102.56	39.60	83.31	1371.60	2414.02				100.0%
CBW05583-148970	1	0.79	101.18	39.07	83.48	1381.36	2415.02	1.28	0.46	11.53	98.7%
CBW05583-280042	1	2.32	63.87	24.66	86.07	1401.61	2415.02	0.61	0.40	7.02	62.3%
dsgn4-000009	annual	2.65	63.65	24.58	86.12	1404.83	2415.02	0.75	0.50	7.39	62.1%
CBW05583-099818	3	3.75	61.87	23.89	86.57	1412.69	2415.02	0.59	0.46	7.20	60.3%

Table 39. True annual peak streamflow (cfs and m³/s) for 10 CHaMP sites clustered downstream and upstream of OWRD stream gaging station on the Grande Ronde River below Clear Creek (13317850).

Name	True Annual Peak Q (cfs)						True Annual Peak Q (m ³ /s)					
	2011	2012	2013	2014	2015	2016	2011	2012	2013	2014	2015	2016
CBW05583-235322	1180.0	714.6	449.0	811.6	356.1	565.1	33.42	20.24	12.71	22.98	10.08	16.00
CBW05583-370490	1172.3	709.9	446.0	806.3	353.7	561.3	33.20	20.10	12.63	22.83	10.02	15.90
CBW05583-321338	1152.7	698.0	438.4	792.7	347.7	551.8	32.65	19.77	12.42	22.45	9.85	15.63
dsgn4-000277	1126.9	682.3	428.4	774.9	339.8	539.2	31.91	19.32	12.13	21.94	9.62	15.27
CBW05583-468458	472.2	285.0	177.1	323.7	140.5	223.0	13.37	8.07	5.02	9.17	3.98	6.31
CBW05583-206314	469.0	283.1	175.9	321.5	139.5	221.4	13.28	8.02	4.98	9.10	3.95	6.27
Grande Ronde R BL Clear Cr, NR Starkey, OR (13317850)	464.0	280.0	174.0	318.0	138.0	219.0	13.14	7.93	4.93	9.01	3.91	6.20
CBW05583-148970	459.3	277.2	172.2	314.8	136.6	216.8	13.01	7.85	4.88	8.92	3.87	6.14
CBW05583-280042	326.3	196.7	121.7	223.4	96.5	153.2	9.24	5.57	3.45	6.33	2.73	4.34
dsgn4-000009	325.5	196.2	121.4	222.8	96.3	152.8	9.22	5.56	3.44	6.31	2.73	4.33
CBW05583-099818	318.7	192.1	118.8	218.1	94.2	149.6	9.03	5.44	3.37	6.18	2.67	4.24

Table 40. Stream power and unit stream power for 10 CHaMP sites clustered downstream and upstream of OWRD stream gaging station on the Grande Ronde River below Clear Creek (13317850).

Name	Stream Power						Unit Stream Power						Site Length (m)
	2011	2012	2013	2014	2015	2016	2011	2012	2013	2014	2015	2016	
CBW05583-235322	298,028	180,478	113,387	204,971	89,927	142,711	24,172	14,638	9,197	16,625	7,294	11,575	333.35
CBW05583-370490	278,836	168,852	106,074	191,767	84,128	133,507	16,638	10,076	6,330	11,443	5,020	7,967	354.05
CBW05583-321338	910,503	551,329	346,281	626,152	274,637	435,837	77,247	46,775	29,379	53,123	23,300	36,977	364.73
dsgn4-000277	345,591	209,244	131,388	237,642	104,205	165,368	22,095	13,378	8,400	15,193	6,662	10,573	364.09
CBW05583-468458	325,304	196,317	122,022	222,960	96,776	153,580	30,192	18,220	11,325	20,693	8,982	14,254	224.46
CBW05583-206314	621,986	375,352	233,284	426,292	185,018	293,616	53,311	32,172	19,995	36,538	15,858	25,166	166.85
Grande Ronde R BL Clear Cr, NR Starkey, OR (13317850)													
CBW05583-148970	162,798	98,237	61,040	111,569	48,411	76,826	14,125	8,523	5,296	9,680	4,200	6,666	196.75
CBW05583-280042	54,977	33,132	20,505	37,628	16,262	25,807	7,830	4,719	2,920	5,359	2,316	3,675	163.12
dsgn4-000009	67,756	40,833	25,270	46,374	20,041	31,805	9,166	5,524	3,419	6,274	2,711	4,303	168.61
CBW05583-099818	52,187	31,448	19,457	35,716	15,431	24,489	7,247	4,367	2,702	4,959	2,143	3,400	169.77

Table 41. Redd density (redds per km) and spring Chinook juvenile density (numbers/m) for 10 CHaMP sites clustered downstream and upstream of OWRD stream gaging station on the Grande Ronde River below Clear Creek (13317850).

Name	Reddspkm						CH_tot_ab_Site (no./m)					
	2011	2012	2013	2014	2015	2016	2011	2012	2013	2014	2015	2016
CBW05583-235322	18.94	6.22	5.99	0.00	12.91	2.05	2.66			2.17		
CBW05583-370490	20.63	6.03	4.42	1.02	16.02	2.04						3.21
CBW05583-321338	4.61	1.91	0.00	0.00	7.20	0.00				1.14		
dsgn4-000277	1.96	1.00	0.00	0.00	2.26	0.00	4.41	0.97	1.05	0.13	0.65	4.40
CBW05583-468458	9.74	10.61	5.35	2.02	11.67	5.01			6.41			5.21
CBW05583-206314	29.82	36.67	14.20	10.95	30.08	34.31	4.77			1.80		
Grande Ronde R BL Clear Cr, NR Starkey, OR (13317850)												
CBW05583-148970	23.92	19.05	6.98	1.83	5.77	15.61	4.43			4.35		
CBW05583-280042	29.33	31.99	15.09	5.14	12.90	11.62	2.83			3.73		
dsgn4-000009	27.13	29.88	13.95	7.90	12.87	10.02	2.25	4.56	9.65	4.05	9.97	5.35
CBW05583-099818	19.33	20.44	6.31	8.82	7.67	6.10			8.95			4.98

Table 42. Snorkel dates and survival index for 10 CHaMP sites clustered downstream and upstream of OWRD stream gaging station on the Grande Ronde River below Clear Creek (13317850).

Name	Snorkel date						Survival Index (total Chinook juveniles per m/total redds per km)					
	2011	2012	2013	2014	2015	2016	2011	2012	2013	2014	2015	2016
CBW05583-235322	8/12/2011			8/7/2014			0.140					
CBW05583-370490						8/6/2016					1.575	
CBW05583-321338				8/8/2014								
dsgn4-000277	8/15/2011	9/26/2012	7/30/2013	8/8/2014	7/30/2015	8/6/2016	2.249	0.973			0.288	
CBW05583-468458			8/21/2013			8/3/2016			1.197			1.039
CBW05583-206314	9/19/2011			8/8/2014			0.160			0.165		
Grande Ronde R BL Clear Cr, NR Starkey, OR (13317850)												
CBW05583-148970	8/9/2011			8/7/2014			0.185			2.377		
CBW05583-280042	8/9/2011			8/7/2014			0.097			0.726		
dsgn4-000009	8/9/2011	8/7/2012	7/30/2013	8/7/2014	7/25/2015	8/3/2016	0.083	0.153	0.692	0.513	0.775	0.534
CBW05583-099818			8/21/2013			8/3/2016			1.418			0.816

References

- Cooper, R.M. 2006. Estimation of peak discharges for rural, unregulated streams in western Oregon. Open File Report SW 06-001. State of Oregon, Water Resources Department.
- Justice, C., S. White, and D. McCullough. 2012. Spawning Gravel Composition Survey Methods. A component of Monitoring Recovery Trends in Key Spring Chinook Habitat Variables and Validation of Population Viability Indicators.
- Justice, C., D. McCullough, R. Lessard, and S. White. 2014. Appendix K. Factors influencing body size and survival of juvenile Chinook salmon migrants in the Upper Grande Ronde River basin. In: D. McCullough, S. White, C. Justice, R. Lessard, L. Hill, N. Tursich, D. Kelsey, D. Graves, and J. Nowinski. Monitoring Recovery Trends in Key Spring Chinook Habitat Variables and Validation of Population Viability Indicators. BPA Project # 2009-004-00. Annual Report 2013. Produced by Columbia River Inter-Tribal Fish Commission for Bonneville Power Administration, Portland, Oregon.
- Justice, C., S.M. White, D.A. McCullough, D.S. Graves, and M.R. Blanchard. 2016. Can stream and riparian restoration offset climate change impacts to salmon populations? J. Environmental Management <http://dx.doi.org/10.1016/j.jenvman.2016.12.005>.
- McCullough, D.A., S. White, C. Justice, M. Blanchard, R. Lessard, D. Kelsey, D. Graves, and J. Nowinski. 2015. Assessing the Status and Trends of Spring Chinook Habitat in the Upper Grande Ronde River and Catherine Creek. BPA Project # 2009-004-00. Annual Report 2014. Produced by Columbia River Inter-Tribal Fish Commission for Bonneville Power Administration, Portland, Oregon.
- McElhaney, P., M. H. Ruckelshaus, M. J. Ford, T. C. Wainwright, and E. P. Bjorkstedt. 2000. Viable salmonid populations and the recovery of evolutionarily significant units. NOAA Technical Memo NMFS–NWFSC–42. U.S. Department of Commerce. 156 pp.
- McIntosh, B.A., J.R. Sedell, J.E. Smith, R.C. Wissmar, S.E. Clarke, G.H. Reeves, and L.A. Brown. 1994. Management history of eastside ecosystems: changes in fish habitat over 50 years, 1935 to 1992. Gen. Tech. Report PNW-GTR-321. USDA Forest Service. Pacific Northwest Forest and Range Experiment Station. Portland, Oregon. 54 p.
- McIntosh, B.A., J.R. Sedell, R.F. Thurow, S.E. Clarke, and G.L. Chandler. 2000. Historical changes in pool habitats in the Columbia River basin. Ecol. Appl. 10(5):1478-1496.
- McIntosh, B.A. 1992. Historical changes in anadromous fish habitat in the Upper Grande Ronde River, Oregon, 1941-1990. Ph.D. thesis. Oregon State University, Corvallis, Oregon.
- McNyset, K.M., C.J. Volk, and C.E. Jordan. 2015. Developing an effective model for predicting spatially and temporally continuous stream temperatures from remotely sensed land surface temperatures. Water 7:6827-6846. doi:10.3390/w7126660.

- OWRD. 2017b. Oregon Water Resources Department Peak Discharge Estimation Mapping Tool. Oregon Water Resources. Salem Oregon. http://apps.wrd.state.or.us/apps/sw/peak_discharge_map/
- OWRD. 2017a. Oregon Water Resources Department Historical Streamflow and Lake Level Data. Oregon Water Resources Department. Salem Oregon. http://apps.wrd.state.or.us/apps/sw/hydro_report/.
- USFS. 2017. NorWeST Stream temp. Regional database and modeled stream temperatures. <https://www.fs.fed.us/rm/boise/AWAE/projects/NorWeST.html>
- USGS. 2017a. Peak streamflow for the nation. US Geological Survey. https://nwis.waterdata.usgs.gov/nwis/peak?search_criteria=search_site_no&submitted_form=introduction.
- USGS. 2017b. PeakFQ. Flood Frequency Analysis Based on Bulletin 17B and recommendations of the Advisory Committee on Water Information (ACWI) Subcommittee on Hydrology (SOH) Hydrologic Frequency Analysis Work Group (HFAWG). US Geological Survey. <https://water.usgs.gov/software/PeakFQ/>.
- USGS. 2017c. Welcome to StreamStats. US Geological Survey. <https://water.usgs.gov/osw/streamstats/>
- White, S.M., C. Justice, D.A. Kelsey, D.A. McCullough, and T. Smith. 2017. Legacies of stream channel modification revealed using General Land Office surveys, with implications for water

Files Involved in Peak Flow Analysis

All stations available from OWRD.xlsx
 Catherine Creek NR Union-OR-13320000-b.xlsx
 Comparison of three gages-peak flows.xlsx
 Compilation of charts for peak flows.pptx
 Grande Ronde BL Clear Cr-13317850-flow duration.xlsx
 Grande Ronde River-nr Perry-13318960.xlsx
 Grande Ronde River-nr Perry-13318960-Summary Statistics-Flow Duration.xlsx
 Redds_by_Site (Recovered).xlsx
 ReddSummary.accdb
 USGS 13317850-Grande Ronde below Clear Creek.xlsx

Toxic Chemicals in the Environment

Full Title: Toxic Chemicals in the Environment of the Upper Grande Ronde and Potential Level of Concern for Aquatic Life

Introduction

In 2016 the Northwest Power and Conservation Council released a report (ISAB/ISRP 2016-1) in which they reviewed the critical uncertainties for the Columbia River basin Fish and Wildlife Program. The current research plan for the Fish and Wildlife Program details 44 critical uncertainties that are considered to be “important knowledge gaps about resources and the functional relationships that determine fish and wildlife productivity in the Columbia River ecosystem.”

A key assumption of the Program is that restoration of tributary habitat is a key means of offsetting the mortalities attributed to the hydrosystem. Uncertainties identified with this assumption are that (1) restoration of tributary habitat can enhance habitat capacity in a way that can mitigate for reduced survival in downstream habitats (mainstem, estuary, ocean), (2) the improvements in tributary habitat would provide benefits for the wild components of populations with impaired habitat, and (3) the improved habitat capacity and survival would increase resilience of the impaired populations that are subject to climate change stress and toxic contaminants (NPCC 2016).

A key concern in implementing restoration actions in tributary habitats and throughout the other habitats supporting the entire life cycle of salmon is that there may be toxic chemicals present in the environment from current applications in agriculture or urban use or from legacy applications that contribute persistent toxics that cycle through the food chain. The presence of these combinations of toxic chemicals confers the potential to negate all benefits of physical or biological habitat restoration and could be significantly reducing salmon productivity and abundance (NPCC 2016). The agricultural, ranching, and timber producing areas have historically caused significant negative impacts to salmon habitat via increased water temperatures and increased sediment delivery. The application of pesticides and herbicides in agriculture, timber production, and urban areas adds to the potential limiting factors to salmon viability.

These chemical effects are uncertain because of a variety of reasons: (1) The number of toxic chemicals applied in the environment can be very large, (2) The ability to measure many toxics is limited, (3) Monitoring programs typically monitor only select chemicals, only select streams are monitored, and funding for monitoring is typically insufficient, (4) Concentrations of any toxicant can vary dramatically seasonally, annually, and in response to rainfall, residence time in the environment and pathways to surface water, and (5) Many toxics can be more lethal when combined with other toxics, or their degradates can be more toxic than their parent chemical, and many toxics become more damaging with increasing temperature, which makes them of greater concern as climate change proceeds.

EPA submitted comments to NPCC concerning its Critical Uncertainties report to emphasize that research is needed to measure and map the spatial and temporal patterns of toxic chemical use, transfer, accumulation and persistence in the Columbia River Basin (Soscia 2016). In addition, these EPA

comments pointed out the great need to understand the extent of impact of toxic chemical concentrations and combinations on growth, migration, maturation, and survival of native fish in all habitats throughout their life cycle so that it can be determined whether the observed population trends in any specific watershed are attributable to measured trends in physical/biological habitat quality or to unseen and largely unmeasured levels of toxics.

The effects of individual chemicals or mixtures of two or more of these compounds are evaluated for risk to salmonids in a variety of ways. Regulators, such as EPA, evaluate the acute exposure to the chemical using LC₅₀ tests. Increased water temperature often has a direct bearing on the acute exposures needed to cause mortality. Chronic exposure evaluates direct impacts to growth via feeding reduction or reduction in swimming speed, which limits prey capture; indirect growth effects due to reduction in prey abundance; inability to avoid predators due to reduced swimming speed and avoidance behavior; reduced spawning success; impaired olfactory behavior that impairs migration success, imprinting, predator avoidance, and kin recognition (NOAA 2008).

Methods

USGS (2006a) recently developed an interactive, web-based mapping tool that provides extensive information by major stream on the predicted concentrations of a 108 pesticides and herbicides in all US waters. Concentrations predicted in this mapping program (Watershed Regressions for Pesticides—WARP) include the 4-, 21-, 30-, 60-, and 90-day moving average concentration (Table 43). This mapping facility also provides the probability of exceeding benchmarks.

Table 43. Benchmarks utilized in the WARP program.

Benchmark	Probability of Exceeding Benchmark
Maximum Contaminant Level	Probability that annual mean exceeds benchmark
Acute Invertebrates	Probability that 4-day moving average exceeds benchmark
Acute Fish	Probability that 4-day moving average exceeds benchmark
Acute Nonvascular Plant	Probability that 4-day moving average exceeds benchmark
Acute Vascular Plant	Probability that 4-day moving average exceeds benchmark
Chronic Invertebrates	Probability that 21-day moving average exceeds benchmark
Chronic Fish	Probability that 60-day moving average exceeds benchmark
Aquatic Community Effects	Probability that 60-day moving average exceeds benchmark
Criterion Continuous Concentration	Probability that 4-day moving average exceeds benchmark
Criterion Maximum Concentration	Probability that 4-day moving average exceeds benchmark

In addition, there are 482 pesticides, herbicides, and fungicides whose intensity of use in pounds/mi² is mapped for the lower 48 states from 1992, annually, to 2013 (USGS 2016b). Maps of use are accompanied by bar charts showing estimated use in million pounds for this span of years by major crop.

USGS (2016b) also provides in its website access to Baker and Stone's (2015) report that details the methodology for estimating annual agricultural pesticide use by county in the conterminous US. This USGS website also provides access to seven text files that provide estimates for 423 compounds by year, state, and county in kilograms applied in the period 2008-2012. Estimates of total of each compound applied was made by multiplying the application rate per crop by harvested-crop acres. The methodology of Baker and Stone (2015) yielded an EPest-low and EPest-high "estimated pesticide use" value. I adopted the EPest-high value, which applied area-wide average application rates for compounds for which a particular CRD (crop reporting district) did not report on use of certain compounds. The EPest-low method assigns zero use to a particular pesticide-crop combination if no use data are available, which seems likely to under-report actual use.

Predictions of the amounts of these toxic compounds traveling from crop land to streams were made based on tables of the Henry's law constant (K_H) and the soil organic carbon-water partition coefficient (K_{OC}) for each toxic compound. The Henry's law constant defines the partitioning between air and water, while the K_{OC} defines partitioning in the soil or sediment between water and organic matter. These coefficients define the affinity of toxics for water and ability to be transported. In addition, toxics have varying levels of persistence and volatility. Degradation by microbes, sunlight, or other processes convert toxic compounds at varying rates to degradates that may have lower, the same, or higher toxicity levels as the parent compounds. Movement of toxics and their degradates to streams or groundwater and the concentrations expected in surface waters is based on knowledge of the affinities for water or other materials, periodicity of rainfall or irrigation, and rates of degradation.

Results and Discussion

In order to evaluate the potential impact of toxic chemicals (pesticides, herbicides, fumigants, and fungicides) on aquatic life, it would be helpful to review the application of toxic compounds at a national scale on agricultural and urban lands. Release of heavy metals, acids, or bases may also be of great concern in either mining areas or in industrial zones, but is an issue needing separate review. Knowledge of the most commonly used toxic compounds and use by crop will help set the foundation for assessing the potential impacts on aquatic resources.

The USGS NAWQA (National Water-Quality Assessment) Program produced a national review of toxics that impair water quality in surface and groundwater (Gilliom et al. 2006) from surveys between 1992 and 2001. This study analyzed 75 compounds and 8 degradates of certain toxic parent compounds. These 75 compounds accounted for 78% of the total weight of agricultural pesticides applied. Of this group studied, 25 compounds were herbicides (accounting for 92% of all herbicide use) and 25 were insecticides (accounting for 91% of all insecticide use). Across the US, sampling indicated that one or more pesticides (or their degradates) were found in 90% of streams on agricultural, urban, or mixed-use

land. Even undeveloped streams had one or more detectable pesticides present 65% of the time, which tend to be associated with forest management.

The Gilliom et al. (2006) study showed that for the 186 streams sampled nationally, the 83 streams in agricultural areas had pesticide levels exceeding aquatic-life benchmarks in 57% of those streams for one or more of the pesticides from 1993 to 2000. These agricultural streams had concentrations of chlorpyrifos exceeding benchmarks in 21% of the sites, aziniphos-methyl in 19%, atrazine in 18%, and alachlor in 15%.

The pesticides detected most frequently in stream water included: (1) five agricultural herbicides that were among the most heavily used during the study period—atrazine (and its degradate deethylatrazine), metolachlor, cyanazine, alachlor, and acetochlor; (2) five herbicides extensively used for nonagricultural purposes, particularly in urban areas—simazine, prometon, tebuthiuron, 2,4-D, and diuron; and (3) three of the most extensively used insecticides during the study period—diazinon, chlorpyrifos, and carbaryl. Simazine, prometon, diuron, 2,4-D, diazinon, and carbaryl, which are commonly used to control weeds, insects, and other pests in urban areas, were frequently found at relatively high levels in urban streams throughout the Nation.

In terms of sheer frequency of detection in streams within agricultural areas, the herbicides atrazine, its primary degradate deethylatrazine, and metolachlor were all found in more than 75% of samples. In agricultural, urban, and mixed land use watersheds, two or more of these toxic compounds were found 90% of the time. Detection of 10 or more compounds were found 20% of the time in these areas.

Herbicides, as opposed to pesticides, are detected at very high rates in agricultural areas in the US. The most commonly detected herbicides (found in combination in 30% of all samples) included atrazine (and its degradate), metochlor, simazine, and premeton. Urban streams commonly carried mixtures of the insecticides diazinon, chlorpyrifos, carbaryl, and malathion.

The NAWQA monitoring program (Gilliom et al. 2006) determined that the top 5 herbicides used by weight were atrazine, metolachlor, 2,4-D, glyphosate, and acetochlor. Among these, only glyphosate was not frequently detected in water. Other herbicides that were frequently detected were cyanazine, 2,4-D, and simazine. The top 5 insecticides used in terms of weight were chlorpyrifos, terbufos, parathion-methyl, malathion, and carbaryl. Terbufos and parathion-methyl were not frequently detected in water. Other insecticides that were frequently detected were diazinon and carbofuran.

Among many of the most commonly used herbicides and insecticides, some of their degradates are more than 10 times more toxic to fish and daphnids than their parent compounds. 2,4-D has several degradates that are 10 times more toxic than the parent compound itself. Diuron and diazinon also have degradates that are 10 times more toxic than the parent. Degradates that are more than 10 times less toxic are also produced from malathion, atrazine, chlorpyrifos, and diazinon. For these compounds the critical issue is the ability to migrate to streams, the rate of degradation or persistence, the timing of application relative to rainfall, and the amounts applied of the parent compounds.

Among these most commonly applied insecticides, chlorpyrifos, diazinon, and malathion (all organophosphorus pesticides) came under scrutiny in a biological opinion (NOAA 2008) prompted by EPA's consideration of registering these insecticides. The BiOp evaluated their potential to affect viability of 28 listed salmonids in the Pacific Northwest. These three pesticides plus carbaryl were commonly detected in urban streams. Diazinon and chlorpyrifos detection rates were 75% and 30%, respectively, in urban streams. Chlorpyrifos is a chlorinated organophosphorus compound used to kill insects, mites, nematodes, and termites.

Malathion is commonly used for mosquito control. Given the increasing concern for mosquito-borne diseases, such as zika, and the influence of a warming climate in extending the northern boundary of mosquito species disease vectors, application of insecticides such as malathion may increase. For spring Chinook in the Snake River basin, the life history of juveniles tends to put them in habitats where exposure to these three insecticides of concern is high and also where elevated water temperatures are common (NOAA 2008). Specifically, downstream migration of juveniles to off-channel rearing areas in the fall prior to smolting puts juveniles in close proximity to agricultural areas where these insecticides are applied. This produces a high potential to impair productivity and abundance.

In USGS NAWQA monitoring studies conducted from 1992 to 2006 in California, IDAHO, Oregon, and Washington, it was found that chlorpyrifos, diazinon, and malathion were detected in 26%, 40%, and 6%, respectively, of all samples tested. The maximum concentrations of these three pesticides in samples were 0.40, 3.8, and 1.35 ug/l, respectively.

Chlorpyrifos

Chlorpyrifos is a chlorinated organophosphorus pesticide that is able to bioaccumulate in fish and aquatic organisms. It is approved for application to over 60 agricultural crops in California alone. Chlorpyrifos binds to soil particles and is not highly soluble in water, but enters water with soil erosion. Its half-life is approximately 72 days (NOAA 2008).

Salmonid LC_{50s} for chlorpyrifos have been reported from < 1.0 to 2200 ug/l. EPA rates this chemical is very highly toxic to moderately toxic. Even a chemical concentration of < 100 ug/l is considered to be "very highly toxic." In a study on rainbow trout the LC₅₀ at 13°C was 7.1 ug/l and was < 1.0 ug/l at 18°C. EPA takes 1.8 ug/l as the effect concentration in its risk analysis and a value of 0.09 ug/l as the concentration that would produce no effects (NOAA 2008). Given the sharp increase in effects with increasing water temperatures, it is not hard to imagine that for salmonids subject to temperatures as high as 25°C in their upper thermal range in the Grande Ronde basin that the limitation to Chinook distribution with temperature may also be significantly controlled by chlorpyrifos concentrations.

In terms of reproductive success, there is concern for the potential impacts of chlorpyrifos on the mean number of eggs produced by females, survival of adults, embryo hatching success, and spawning success. Although the reproductive success studies to date have been carried out on fathead minnows, the concentrations of chlorpyrifos producing negative reproductive effects were relatively low. NOAA summarized the concentrations that produce the range of reproductive impacts listed above as being from 0.12 to 2.68 ug/l. Given that salmonids are two orders of magnitude more sensitive in acute

toxicity tests than fathead minnows, it is likely that reproductive effects of chlorpyrifos on salmonids would occur at even lower levels. Growth of fathead minnows was negatively affected at concentrations of 0.12 ug/l. These concentrations applied during the lifespan of fathead minnows resulted in 9% body weight reduction and 53% reduction in egg biomass. The greater sensitivity of salmonids in acute toxicity tests causes even greater concern for the negative impacts of these low levels of chlorpyrifos.

Impacts of chlorpyrifos on salmonid prey invertebrates are also of great concern. Acute toxicity tests on four prey species eaten by salmonids ranged from 0.1-50 ug/l. LC₅₀ values on caddisflies, mayflies, midges, stoneflies, daphnids, amphipods, and copepods were < 1 ug/l (EPA 2003, as cited by NOAA 2008). A study of a macroinvertebrate assemblage in an artificial stream revealed that a concentration of chlorpyrifos as low as 1.2 ug/l was needed in a 6-h exposure to significantly alter assemblage composition. Concentrations as low as 0.5 ug/l in ponds with native fathead minnows and receiving a single application of chlorpyrifos had significant growth rate reductions in 31 days due to reductions in macroinvertebrate prey abundance and diversity (NOAA 2008).

Fish swimming capacity and swimming behavior are two performances that indicate sublethal effects of pesticides. Swimming activity affects the ability to feed, migrate, avoid predators, and spawn. More subtle swimming behaviors, such as ability to make turns, feeding swimming speed, food strikes, and form and pattern of swimming can determine ability to avoid predators. These swimming behaviors can be impaired significantly at concentrations that are 0.3-5% of LC₅₀ concentrations. For chlorpyrifos, concentrations below 2 ug/l were sufficient to create these impacts. The three acetylcholinesterase (AChE) inhibiting insecticides described here are known to impair swimming capacity and behavior. Swimming rate of coho can be reduced by 10% at chlorpyrifos concentrations of 0.3 ug/l.

Sandahl et al. (2005) found benchmark concentrations producing a 10% reduction in brain AChE activity of 0.6 ug/l in steelhead and 0.4 ug/l in coho. They take this concentration range as reflective of the genus *Oncorhynchus* in general. Sandahl et al. (2005) recommend use of sensitive measures of sublethal biological effect such as AChE inhibition rather than gross measures of acute lethality. Inhibition of AChE activity produce sluggish swimming, impairment in prey capture and predator avoidance, inability to defend territories. Because chlorpyrifos is an insecticide, it also can reduce the availability of prey for salmonid juveniles. It is also of concern that brief (e.g., 8-h) exposure to concentrations of 100 ug/l can impair brain function in mosquitofish (*Gambusia affinis*) enough to require six weeks for brain activity to recovery AChE activity (Sandahl and Jenkins 2002). Brief, high dose impacts or multiple exposure to lower doses whose concentrations and periodicity of entry to aquatic environments are controlled by precipitation events, runoff timing, and spray timing. In addition, Hoffman et al. (2000; as cited by Sandahl et al. (2005) found that >80% of stream water samples in urban areas had three or more pesticides. Mixtures of organophosphates (e.g., chlorpyrifos, diazinon, and malathion) are commonly found together and all (including their oxon derivatives) act additively to produce AChE inhibition.

USGS (2016a) provides EPest-high mapping of chlorpyrifos usage on crops across the conterminous US states. Although usage in the central US is very high, there are portions of Oregon that also have high application rates (pounds/mi²), such as the Willamette Valley and the Blue Mountains (Figure 85). From 1992 to 2013 the use of chlorpyrifos has steadily declined, but as of 2013 there was still about 7 million

pounds applied. Primary crops that have received applications of this pesticide are corn, soybeans, wheat, orchards and grapes, and alfalfa (Figure 86) (USGS 2016a).

The maximum 21-day moving average concentration of chlorpyrifos is available for the upper Grande Ronde River and Catherine Creek, plus major tributaries of these rivers. The estimated concentrations in Catherine Creek downstream of Little Creek and two of its major tributaries (Little Creek and Pyles Creek) is higher (0.001 to 0.01 ug/l) than for the upper Grande Ronde (< 0.001 ug/l) (Figure 87). Also, in 2012 the probability of exceeding the chronic macroinvertebrate benchmark; i.e., 0.04 ug/l) in Catherine Creek was mapped as 5-25% (USGS 2016a). The estimated maximum 4-d moving average concentration was also estimated as 0.001 to 0.01 ug/l.

Data from USGS (2016b) was compiled into an Excel spreadsheet on the county by county total application (kg) of 423 pesticides and herbicides. These data are summarized for selected commonly used pesticides and herbicides for Umatilla, Union, and Wallowa Counties (Table 44). In Union County there was an estimated total application of 288.3 kg of chlorpyrifos in 2012, while in 2009 the total application was 2740.1, nearly 10 times greater. If the estimated range of concentrations found in 2012 provided a 21-day maximum average of 0.001-0.01 ug/l (Figure 87), a 10 times greater application rate might logically provide a 0.01-0.1 ug/l concentration. Also, if there is a 5-25% chance of exceeding the chronic macroinvertebrate standard of 0.04 ug/l with the estimated 21-day maximum moving average chlorpyrifos concentration in 2012 (Figure 88), a 10 times greater application in 2009 of this pesticide could easily exceed this concentration. Consequently, the annual level of fluctuation in application of this chemical has the potential to cause a variety of sublethal impacts, such as reduced growth rates of juvenile Chinook. Also, if the salmonid LC₅₀ at 18°C occurs at concentrations of < 1.0 ug/l and water temperature causes a significant increase in toxicity, the concentrations found in 2009 could easily cause significant sublethal effects (Baldwin et al. 2009).

In summary, NOAA (2008) concludes that with exposure times of 96 h, chlorpyrifos concentrations of > 1 ug/l would be expected to cause substantial juvenile salmon mortality and some mortality in adults. Salmonid prey species are expected to exhibit significant reduction in abundance at concentrations > 0.1 ug/l (NOAA 2008). Increased water temperatures will make these predicted effects greater.

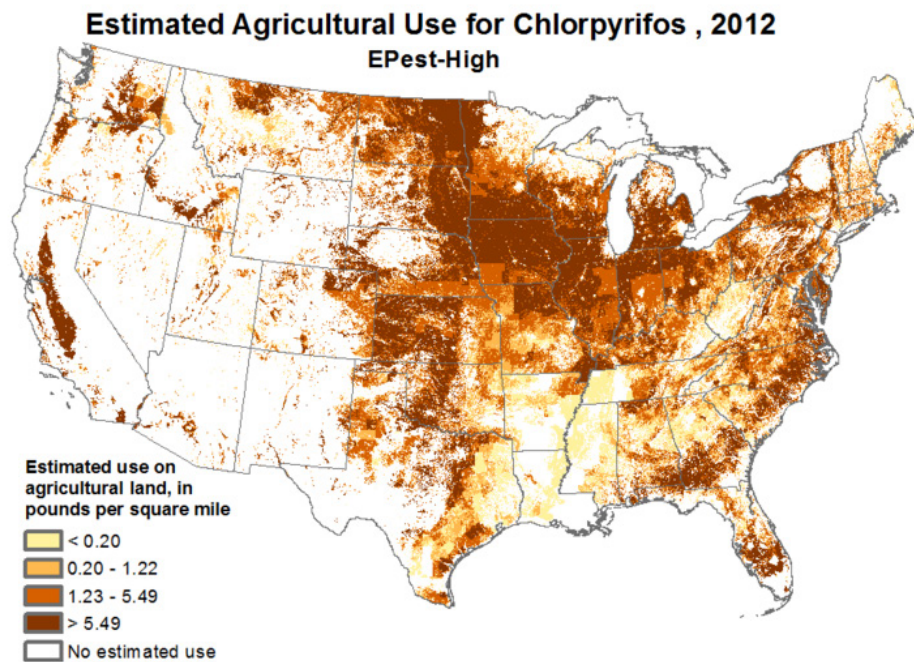


Figure 85. Estimated agricultural use for Chlorpyrifos in 2012 in the US, using the USGS EPest-High process.

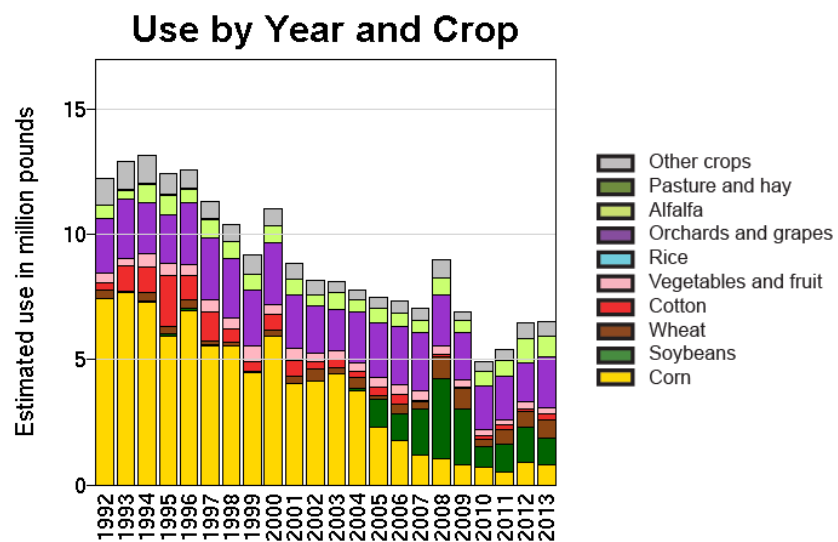


Figure 86. Use of chlorpyrifos by year and crop across the US.

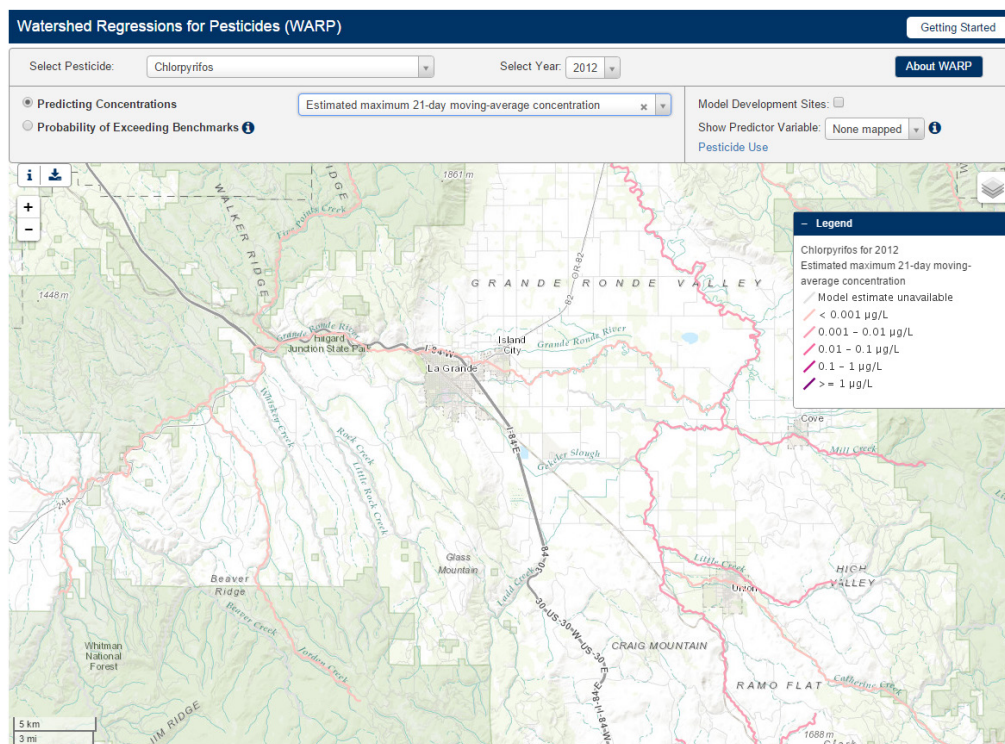


Figure 87. The estimated maximum 21-day moving average concentration of chlorpyrifos in the upper Grande Ronde River and Catherine Creek.

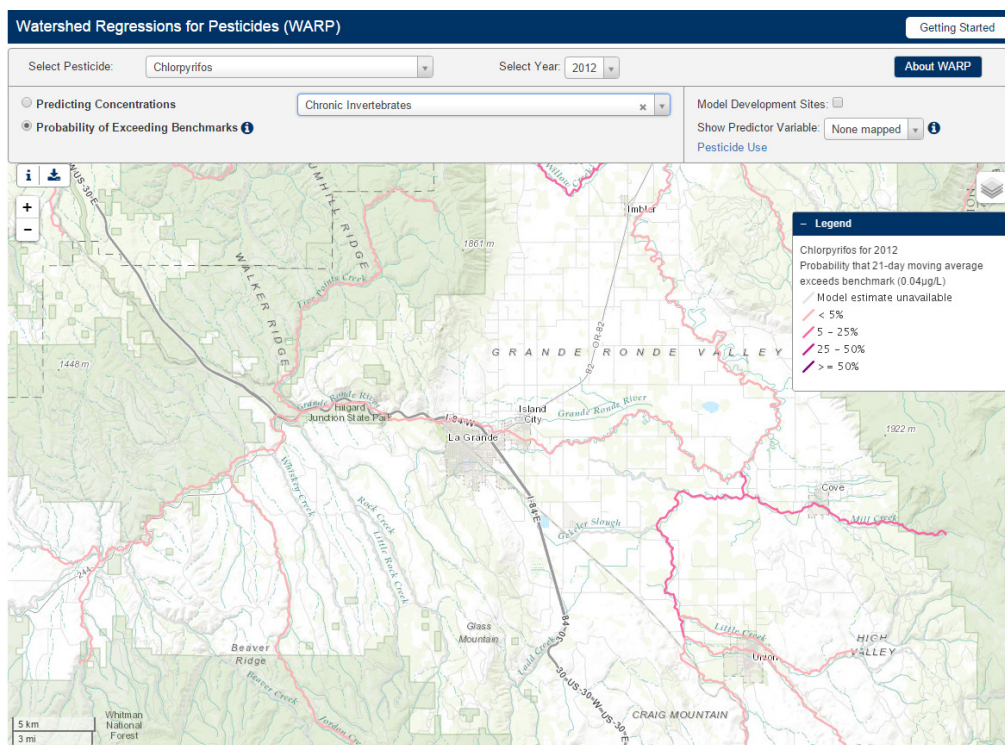


Figure 88. Estimated probability that the 21-day moving average concentration of chlorpyrifos exceeds the chronic macroinvertebrate benchmark of 0.04 µg/l.

Table 44. Total weight (kg) of some commonly used pesticides and herbicides applied in Umatilla County, Union County, and Wallowa County over the years 2008-2012.

County	Year	2,4-D	ATRAZINE	DICHLORO- PROPENE	DIURON	EPTC	GLYPHOSATE
59-Umatilla County (kg)	Average (2008-2012)	20970.5	999.6	225688.6	2007.0	12497.8	52767.5
	2008	15076.9	529.9	193880.5	1271.6	12628.3	51247.6
	2009	12724.0	119.2	216999.3	2445.8	11551.4	74917.1
	2010	50243.6	456.2	56392.7	2996.6	11561.2	55569.4
	2011	12052.5	1106.5	317397.1	387.6	9586.4	33883.7
	2012	14755.3	2786.4	343773.5	2933.4	17161.5	48219.6
61-Union County (kg)	Average (2008-2012)	2816.5	27.0	23577.2	1002.9	1315.5	6320.6
	2008	2916.6	66.8	27723.2	632.3	1856.8	7557.6
	2009	2721.8	0.4	29914.6	820.3	1618.5	8056.7
	2010	4057.4	1.6	6225.6	1691.7	1177.6	5947.9
	2011	1349.3	5.1	40232.6	104.0	1211.8	5492.4
	2012	3037.4	61.1	13789.8	1766.4	712.9	4548.2
63-Wallowa County (kg)	Average (2008-2012)	1531.8	6.8	3389.9	715.8	268.4	2331.9
	2008	1762.4	2.0	5301.9	467.1	311.2	2717.8
	2009	1554.2	0.1	7326.4	515.0	223.5	2706.4
	2010	1216.6	0.5	578.6	1147.5	572.5	1241.1
	2011	561.0	1.7	2652.8	56.9	97.7	1644.9
	2012	2564.9	29.9	1089.9	1392.7	137.0	3349.2

County	Year	HEXAZINONE	METAM	METAM POTASSIUM	METIRAM
59-Umatilla County (kg)	Average (2008-2012)	564.1	413726.5	107098.9	11454.3
	2008	541.7	437183.2	93888.9	9977.6
	2009	570.3	378713.0	98188.2	28314.7
	2010	631.9	205918.9	229644.7	3194.5
	2011	605.1	245948.4		
	2012	471.6	800869.2	6673.8	4330.5
61-Union County (kg)	Average (2008-2012)	466.9	31728.3	14213.7	1580.6
	2008	433.4	61930.1	12769.8	1547.1
	2009	488.9	10581.0	12173.6	4118.5
	2010	526.6	25881.9	31909.7	479.2
	2011	564.8	29808.6		
	2012	320.9	30440.1	1.6	177.5
63-Wallowa County (kg)	Average (2008-2012)	320.2	3606.0	1548.1	188.5
	2008	300.0	9805.5	1840.6	222.9
	2009	346.3	1415.5	1406.3	473.1
	2010	358.1	2413.4	2942.3	44.1
	2011	342.9	1977.5		
	2012	253.5	2418.2	3.1	13.9

County	Year	METOLACHLOR	METOLACHLOR-S	METRIBUZIN	PARAQUAT
59-Umatilla County (kg)	Average (2008-2012)	8300.0	3334.2	4101.1	3950.4
	2008		3634.5	2763.5	3771.3
	2009	14157.2	1018.5	1224.5	3575.7
	2010	8747.4	5134.8	7844.7	7431.8
	2011		3833.5	2211.8	1516.7
	2012	1995.4	3049.6	6460.8	3456.6
61-Union County (kg)	Average (2008-2012)	111.0	308.1	1598.7	1760.2
	2008		583.7	1130.4	1662.5
	2009	111.0	85.6	237.3	2151.0
	2010	87.8	451.6	4951.9	3582.0
	2011		334.1	667.3	502.9
	2012	134.2	85.5	1006.6	902.4
63-Wallowa County (kg)	Average (2008-2012)	92.6	89.0	1006.8	1151.6
	2008		42.4	655.3	1033.0
	2009	21.6	10.1	105.7	1470.5
	2010	57.2	234.4	3272.4	2358.2
	2011		140.6	337.2	249.1
	2012	199.1	17.7	663.6	647.1

County	Year	DIAZINON	MALATHION	CARBARYL	CHLORPYRIFOS
59-Umatilla County (kg)	Average (2008-2012)	360.3	1257.7	755.9	4863.0
	2008	533.2	850.2	545.8	2190.0
	2009	261.0	379.8	427.4	6128.9
	2010	188.7	2084.4	1077.7	4223.2
	2011	131.0	1380.0	1101.9	3062.7
	2012	687.8	1594.0	626.9	8710.4
61-Union County (kg)	Average (2008-2012)	32.2	550.9	116.1	999.4
	2008	22.4	229.5	68.9	483.2
	2009	22.8	146.7	101.9	2740.1
	2010	2.4	1039.5	137.5	925.4
	2011	6.2	904.3	115.8	559.9
	2012	107.0	434.7	156.4	288.3
63-Wallowa County (kg)	Average (2008-2012)	4.7	223.7	6.7	558.2
	2008	8.7	2.9	4.5	76.7
	2009	11.1	41.0	1.5	1782.9
	2010	0.7	572.3	4.2	499.8
	2011	0.5	449.5	4.2	241.4
	2012	2.7	52.8	18.9	190.0

Diazinon

Diazinon is another organophosphorus pesticide of high concern by NOAA (2008) due to its toxicity and widespread, heavy use. In the US there was 1 million pounds applied in agricultural areas, 4 million pounds in nonagricultural areas (NOAA 2008). It is approved for application to 80 crops in California. Urban streams had higher detectable concentrations than in agricultural streams. In Union County in 2012 there was 107.0 kg of diazinon applied (*Table 44*). Estimated application rates were > 0.04 pounds/mi² (*Figure 89*). This was the highest amount applied in the period from 2008-2012. In other years than 2012 the amounts applied were less than about 20% of the 2012 total. Amounts applied in Umatilla County in 2012 were approximately 6 times greater than the 2012 amount in Union County.

Diazinon, on uptake, is converted to diazoxon, which is also a cholinesterase inhibitor. However, its toxicity to fish is 20 times greater than diazinon. The half-life of diazinon varies from 12 to 138 days depending on pH and rate of photolysis and metabolism in water and soil. Diazinon does not significantly bioaccumulate.

Diazinon is less toxic to fish than is chlorpyrifos. LC₅₀ values for salmonids in the literature range from 90 to 1650 ug/l. Exposures of brook trout for a period of 274 d to 0.8 ug/l of diazinon was sufficient to cause significant growth impairment (NOAA 2008). For a wide range of aquatic invertebrates exposed for between 3 and 96 h, LC₅₀ values ranged from 0.03 to 2500 ug/l. Diazinon concentrations of 1.3 ug/l

were sufficient to produce a 96-h LC₅₀ in first instar *Hydropsyche* caddisflies. Older instars required concentrations of 29.4 ug/l for the same impact.

In summary, diazinon produces the greatest impact to salmonids via mortality of prey, which can occur at concentrations of about 0.06 ug/l or greater. Fish reproduction is also impaired at 0.1 to 10 ug/l. Olfactory-mediated behaviors that can aid salmonids in avoiding predators can be impaired at levels of 0.1 ug/l. Given the measured response of chlorpyrifos to increasing water temperature, NOAA (2008) expected diazinon to also become more toxic with increasing temperature.

In Catherine Creek the 21-d concentration of diazinon estimated by USGS is 0.001 to 0.01 ug/l (Figure 91). The probability that the 21-d concentration of diazinon would exceed the chronic macroinvertebrate benchmark of 0.17 ug/l is < 5% (Figure 92). The 21-d concentrations estimated for the Upper Grande Ronde (i.e., < 0.001 ug/l) were considerably less than for Catherine Creek.

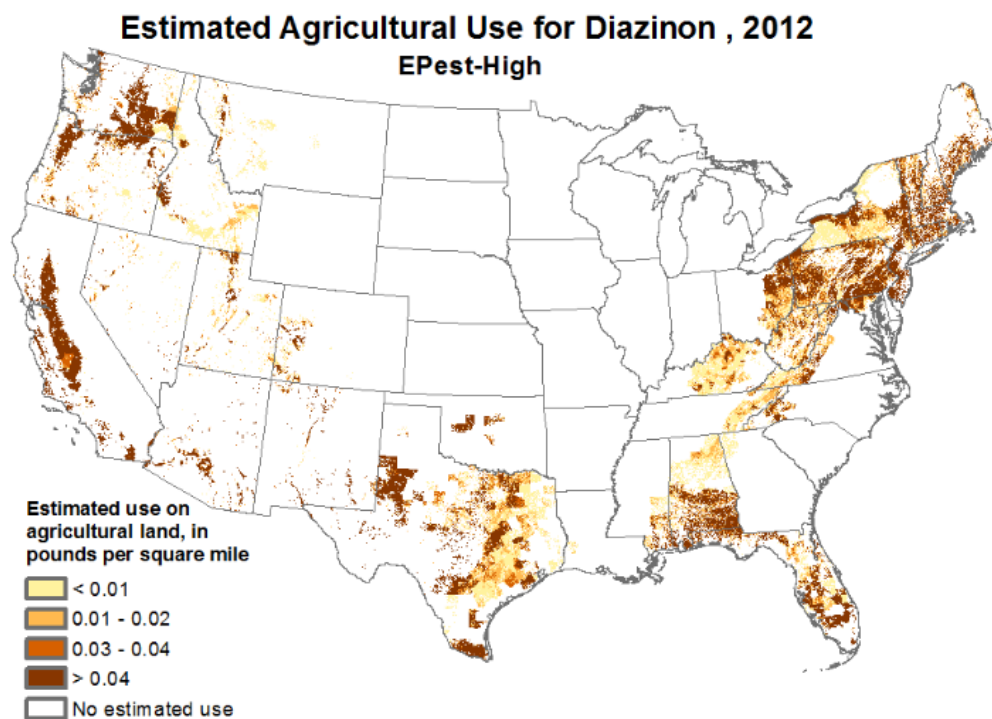


Figure 89. Estimated agricultural use for Diazinon in 2012 in the US, using the USGS EPest-High process.

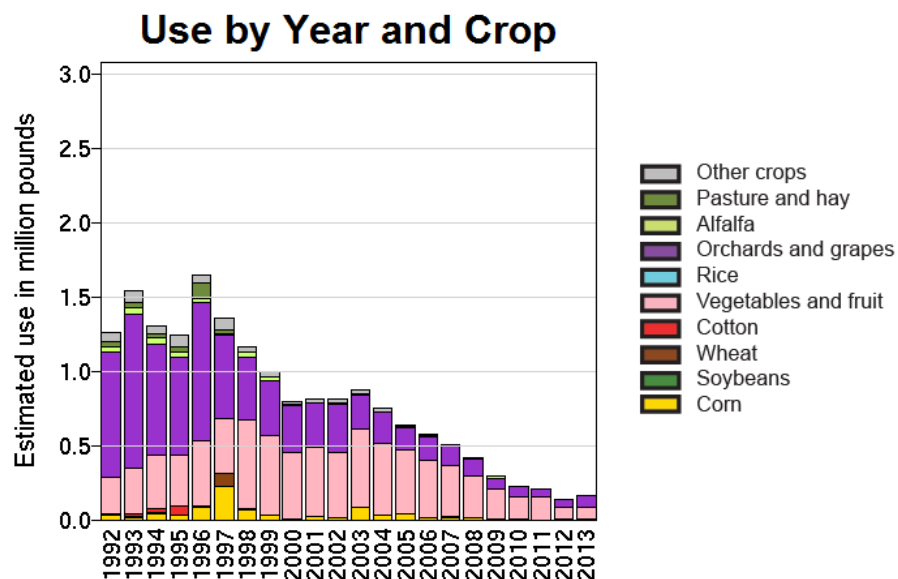


Figure 90. Use of diazinon by year and crop across the US.

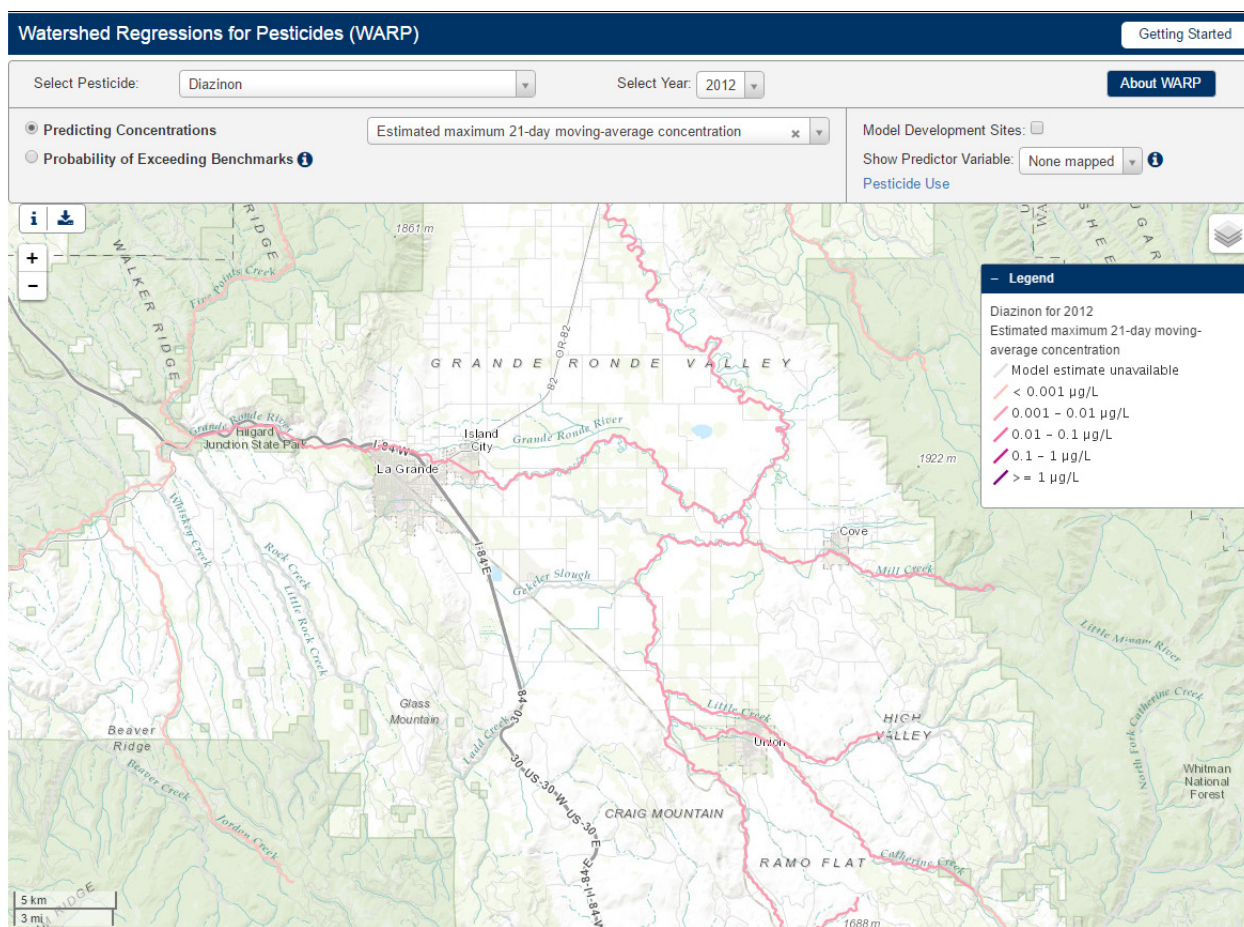


Figure 91. The estimated maximum 21-day moving average concentration of diazinon in the upper Grande Ronde River and Catherine Creek.

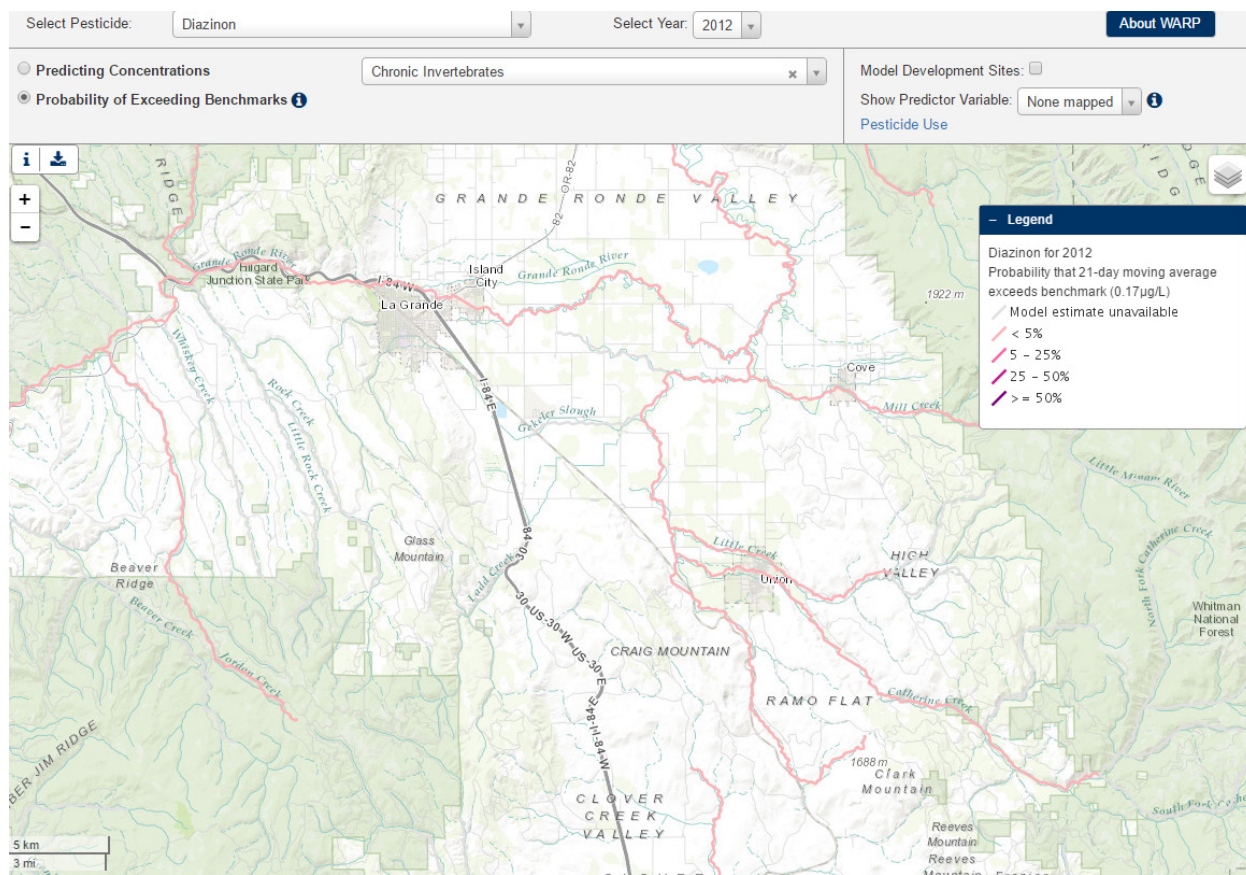


Figure 92. Estimated probability that the 21-day moving average concentration of diazinon exceeds the chronic macroinvertebrate benchmark of 0.17 µg/L.

Malathion

Malathion is an organophosphorus insecticide, similar to chlorpyrifos and diazinon, used commonly to kill sucking and chewing insects affecting a wide variety (over 100) of agricultural crops. All three pesticides are commonly found in surface waters of agricultural, residential, and mixed land use watersheds (NOAA 2008). The mode of action of these pesticides is to inhibit the enzyme acetylcholinesterase (AChE) in brain and muscle tissue of invertebrates and vertebrates.

Malathion has two degradates generated by oxidation whose toxicity level is higher than the parent chemical. Malathion, as well as chlorpyrifos and diazinon, were considered to have a “may affect” and “likely to adversely affect” most of the 26 listed Pacific salmonids. The Snake River spring Chinook are estimated to be subject to effects of these pesticides.

Malathion has a half-life that varies considerably with pH. It also is degraded rapidly in soils with active microbiota. It is generally water soluble, so it moves from soils to streams with runoff.

Although malathion is routinely applied to a large number of crops, it is also a commonly used pesticide used in mosquito control in shallow-water habitats. Malathion is not permitted to be sprayed over commercial fish-rearing surface waters, there are no restrictions to wetlands or backwaters used by

salmonid rearing. Applications to control mosquitos (0.5 lbs. active ingredient/acre) typically results in a concentration in shallow surface waters (i.e., 0.5 m) of approximately 112 ug/l. In waters that are 0.1 m deep, the concentration expected would be 560 ug/l. If application rates are doubled, one would expect the concentrations to double (NOAA 2008). Variation in application rates and water depths then could cause mortalities of rearing salmonids in localized habitats, whereas predictions from average application rates might indicate no problem.

LC₅₀ values for a variety of salmonids studied ranged from 2.8 to 234 ug/l. No information is available on salmonid life stage sensitivity for malathion. Macroinvertebrate prey items are highly sensitive to low levels of malathion. Acute toxicity measured in 48-h and 96-h LC₅₀ tests showed that 0.5 ug/l was sufficient to kill amphipods and 0.69 ug/l for stoneflies. Concentrations of 0.1 ug/l impaired reproduction, growth, and survival of daphnids.

NOAA (2008) judges that malathion would be similar to chlorpyrifos in its increased toxicity to increasing water temperatures.

Malathion is the main ingredient in many pesticide formulations that contain a wide variety of other chemicals. For example malathion formulations are known to contain other ingredients, such as piperonyl butoxide, methoxychlor, remethrin, captan, and carbaryl. These other ingredients often are found in higher concentrations than malathion, making the entire formulation toxic by a variety of modes of action. Piperonyl butoxide is very toxic to aquatic invertebrates and fish. Rainbow trout exposed for 96 h to piperonyl butoxide had LC₅₀s of 2.4 and 6.1 ug/l in two tests. It is also very highly toxic to mussels. LC₅₀ (96-h) of methoxychlor, an organo-chlorine insecticide, for Atlantic salmon was 1.7 ug/l. Resmethrin, a pyrethroid insecticide used to kill flying insects such as mosquitos) has LC₅₀s for salmonids ranging from 0.78 to 1.8 ug/l. Captan is a fungicide used on fruit trees, ornamentals, and vegetables that is highly toxic to fish and aquatic invertebrates. Its acute LC₅₀ (96-h) values are 0.056 ug/l for salmon, which is extreme. Carbaryl is a carbamate insecticide used in agriculture on crops, livestock, poultry, and pets. It bioaccumulates in the environment. Acute toxicity ranges from 0.35 to 7.2 ug/l for freshwater fish (NOAA 2008).

Estimated 21-d concentrations of malathion for the Upper Grande Ronde and Catherine Creek are not available in the USGS WARP program.

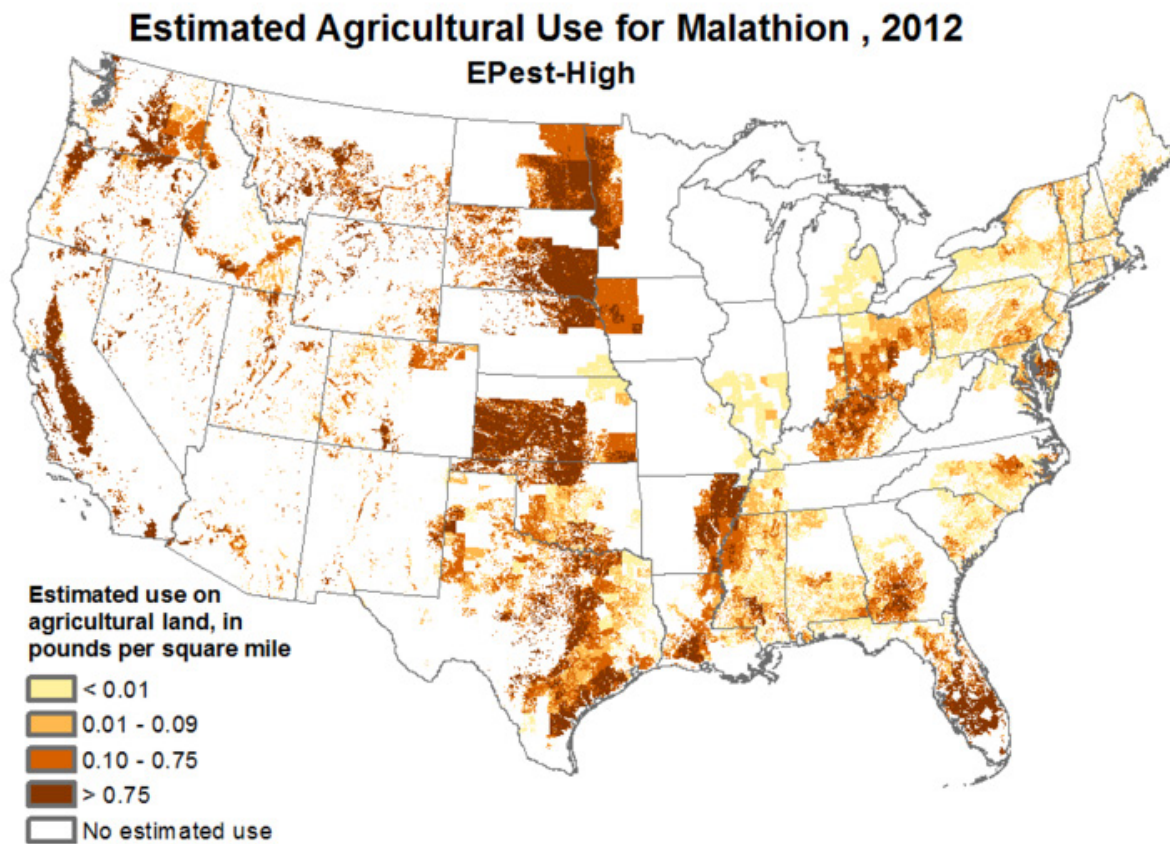


Figure 93. Estimated agricultural use for malathion in 2012 in the US, using the USGS EPest-High process.

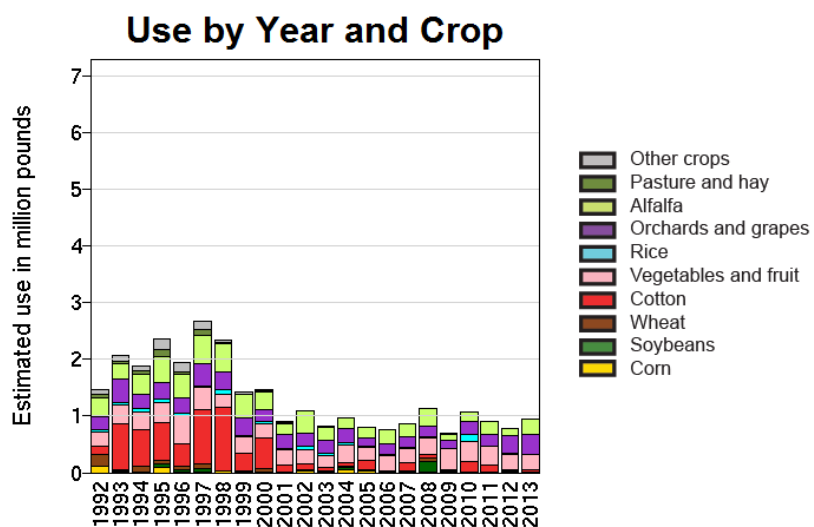


Figure 94.. Use of malathion by year and crop across the US.

Multiple Applications of Pesticides

It is common in environmental sampling of surface waters to find more than one pesticide or herbicide simultaneously. Effects of multiple pesticides on fish or invertebrates can be greater when applied together than would be expected from the combined action of each pesticide. This is a synergistic effect. Also, the conversion of pesticides to their oxon degradative product, which in many cases is even more toxic than the parent product, can result in two chemical forms causing toxic effect to a population.

In addition, pesticides such as chlorpyrifos, diazinon, and malathion, which all have the same mode of operation (i.e., act as a cholinesterase-inhibitor), might be used simultaneously. There are seldom any restrictions placed on joint use of compounds with similar modes of action. This indicates that nervous system impacts to target populations and non-target populations could be greater than expected, given a lack of testing of combinations of pesticides.

Applications of various pesticide formulations, such as malathion, which is combined with a variety of other pesticides, tend to subject aquatic life to multiple modes of lethality or impairment of biological function. Even though the effects of most common ingredients have some degree of testing, there is great difficulty in predicting the acute toxicity of mixtures. Mixtures are presented in the formulations themselves. Also, because the various constituents are adsorbed to sediments or solubilized in water and transported to varying extents, the final concentrations in natural habitats can also vary. Tests on “fish” are frequently only available on taxa such as fathead minnows. When tests are available on salmonids, there is often no detail on impact by age or size class. Toxicity of the oxons (degradate) of parent pesticides is often available only on juvenile survival of a select fish taxon and the various impacts to other biotic functions are not studied. The acute toxicity data available on even salmonid species often exhibit a large range in LC_{50} from approximately 1 $\mu\text{g/l}$ to up to two orders of magnitude higher. This makes the certainty of impact prediction poor. Concentrations from known application rates vary by water depth, and probably by flow rate. The rate of increase in toxicity with increase in water temperature is also critically important information that is often missing in tests with invertebrates and fish.

Test results are also complicated from multiple applications of the same pesticide on a given species. Recovery times from an application of a pesticide, as detected by recovery of AChE function, ranged from 25 to 42 days, depending on salmonid species tested. Time between applications of a single pesticide can be critical to the test result.

Food Chain Effects

Secondary food chain effects on salmonids occur via toxicity to aquatic macroinvertebrates that serve as the prey source. Salmonids typically obtain their prey on insects present in the drift. Macroinvertebrate drift may be termed catastrophic drift when the benthic community is subject to organophosphate pesticides. Drift may occur by individuals attempting to avoid pesticide contamination. It also occurs when dead or moribund individuals enter the drift due to lethal or sublethal impacts. This flux of drifting organisms can act as a direct food chain effect on salmonids that ingest contaminated macroinvertebrates and also are exposed via gill transport.

Land Use Effects

Intensity of agricultural production has been shown to be linked to invertebrate taxa richness from studies in the Yakima River basin (Cuffney et al. 1997, as cited by NOAA 2008). Habitat degradation produced from agricultural impacts, plus the direct correlation between total pesticide/herbicide use and total agricultural activity, are responsible for loss of invertebrate richness.

Chlorpyrifos applications in agricultural sites have been found to cause significant changes in macroinvertebrate community composition between sprayed sites and downstream control sites (references in NOAA 2008). Chlorpyrifos applications resulting in concentrations from 0.032 to 0.183 ug/l for an 8-d period caused marked declines in macroinvertebrate abundance that can be probable cause for salmonid growth decrease. Reduced growth rate is linked to lower size at smolting in juveniles and thereby lower survival (see Appendix 1, NOAA 2008).

The widespread use of the three pesticides that were the subject of the NOAA BiOp (2008) were evaluated as single applications or as combined applications. Formulations that contain any of the three principal pesticides can have other compounds combined as active ingredients, but these formulas often have adjuvants that make the mixtures even more toxic. Also, the oxon degradates can contribute unknown concentrations to aquatic systems due to varying rates of conversion in the environment that can make prediction of additive or synergistic impacts uncertain. Nonetheless, NOAA (2008) estimates that the application of these toxics on a basin scale will likely reduce population viability.

Atrazine

Atrazine is an herbicide that along with glyphosate are the two most commonly used. It is also the most commonly detected pesticide in US drinking water. Atrazine and its degradate (deethylatrazine) are found in agricultural stream water samples between 75 and 85% of the time (Gilliom et al. 2006). Atrazine was banned in the European Union in 2004 due to problems with groundwater contamination that could not be controlled, but is still used in the US despite increasing skepticism of its safety (Wikipedia). Atrazine is applied in agriculture on corn, sugarcane, sorghum, tree plantations, and on turf to control broadleaf plants and grasses. It acts as an endocrine disruptor. Atrazine has a half-life of 13 to 261 days, depending upon microbe activity levels in soil and can be detectable in soil for several years. Consequently, it can build up in surface or groundwater with repeated applications.

A recent critical review of effects of atrazine on fish, amphibians, and aquatic reptiles (Solomon et al. 2008) concluded that a weight of evidence approach indicated that the vast majority of studies show no reproductive effects at the concentrations normally found in agricultural lands. This study was supported by a second study (Van Der Kraak et al. 2014) that promoted a quantitative weight of evidence model for rating the strength of methods used and the strength of the evidence in support of no adverse effect or presence of an adverse effect.

The amount of atrazine applied to Union County in 2012 was approximately 61 kg. By contrast, the amount applied to Umatilla County was 2786 kg (Table 44). The probability that the 21-d moving average concentration in streams of Union County exceed the chronic invertebrate benchmark of 60 ug/l is depicted as <5%. Predicted estimated maximum 21-d moving average concentrations of atrazine

in 2012 were 0.01-0.1 ug/l in Catherine Creek, but 0.001-0.01 ug/l in the upper Grande Ronde (Figure 97). The estimated probability of exceeding the 21-d chronic macroinvertebrate concentration is < 5% (Figure 98). Assuming that 60 ug/l is a safe benchmark that was established by EPA, it would appear there is no likely adverse effect. However, the impact of atrazine to reproductive success in fish has been pointed out recently as an area needing additional study (Tillitt et al. 2010). These authors noted lower total egg production (19-39% lower) in atrazine concentrations ranging from 0.5 to 50 ug/l in 17-20 days of exposure. Exposure was also accompanied by impairment of maturation of oocytes and gonadal abnormalities in males and females. These results were considered weak in the Van der Kraak et al. (2014) weight of evidence procedure because of use of lower than EPA-recommended numbers of males and females per test chamber. However, the lack of extensive information on reproductive performance of salmonids calls for further research. Also, the extensive Van der Kraak et al. (2014) study did not consider the effect of multiple toxics. Anderson and Lydy (2002) found that atrazine concentrations of > 40 ug/l combined with every concentration of chlorpyrifos and diazinon tested (LC1, LC5, LC15, and LC50) produced a significant increase in toxicity for *Hyalella azteca*, a common amphipod. Atrazine, even at concentrations that were lower than the EPA invertebrate benchmark of 60 ug/l, decreased AChE activity and increased the effect of the OP insecticides chlorpyrifos and diazinon.

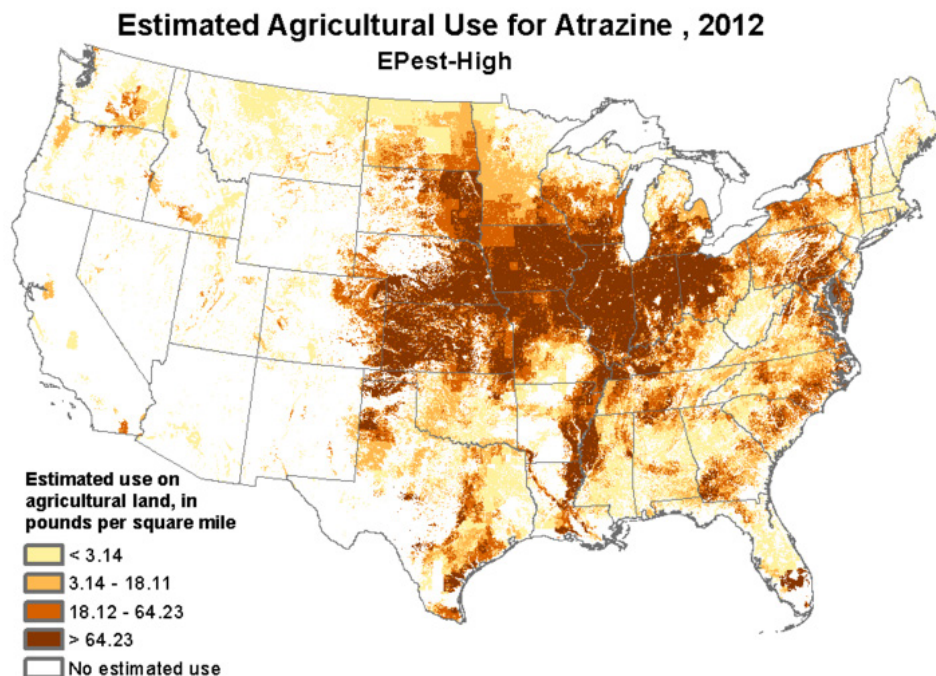


Figure 95. Estimated agricultural use for Atrazine in 2012 in the US, using the USGS EPest-High process.

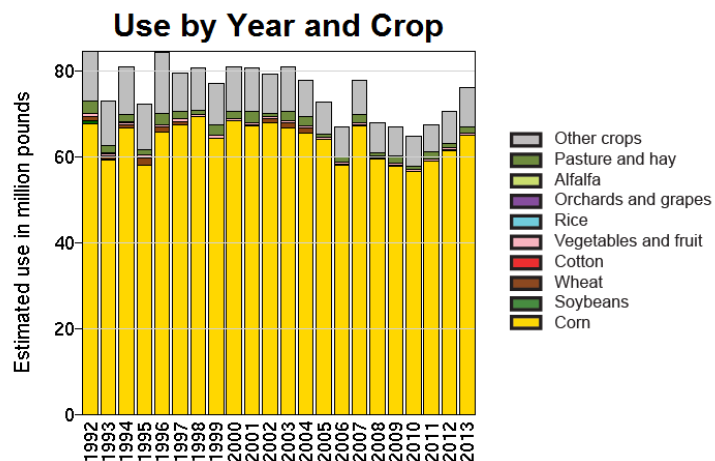


Figure 96. Use of atrazine by year and crop.

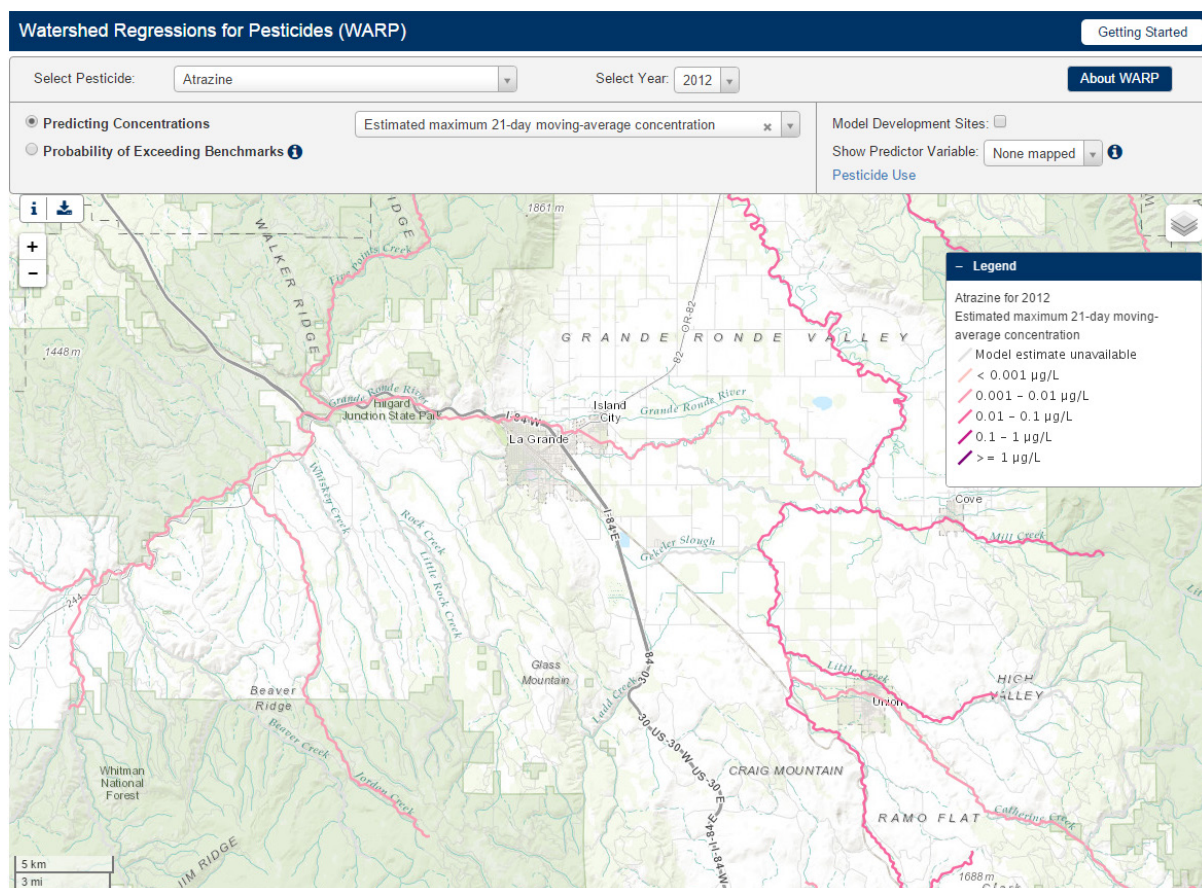


Figure 97. The estimated maximum 21-day moving average concentration of atrazine in the upper Grande Ronde River and Catherine Creek.

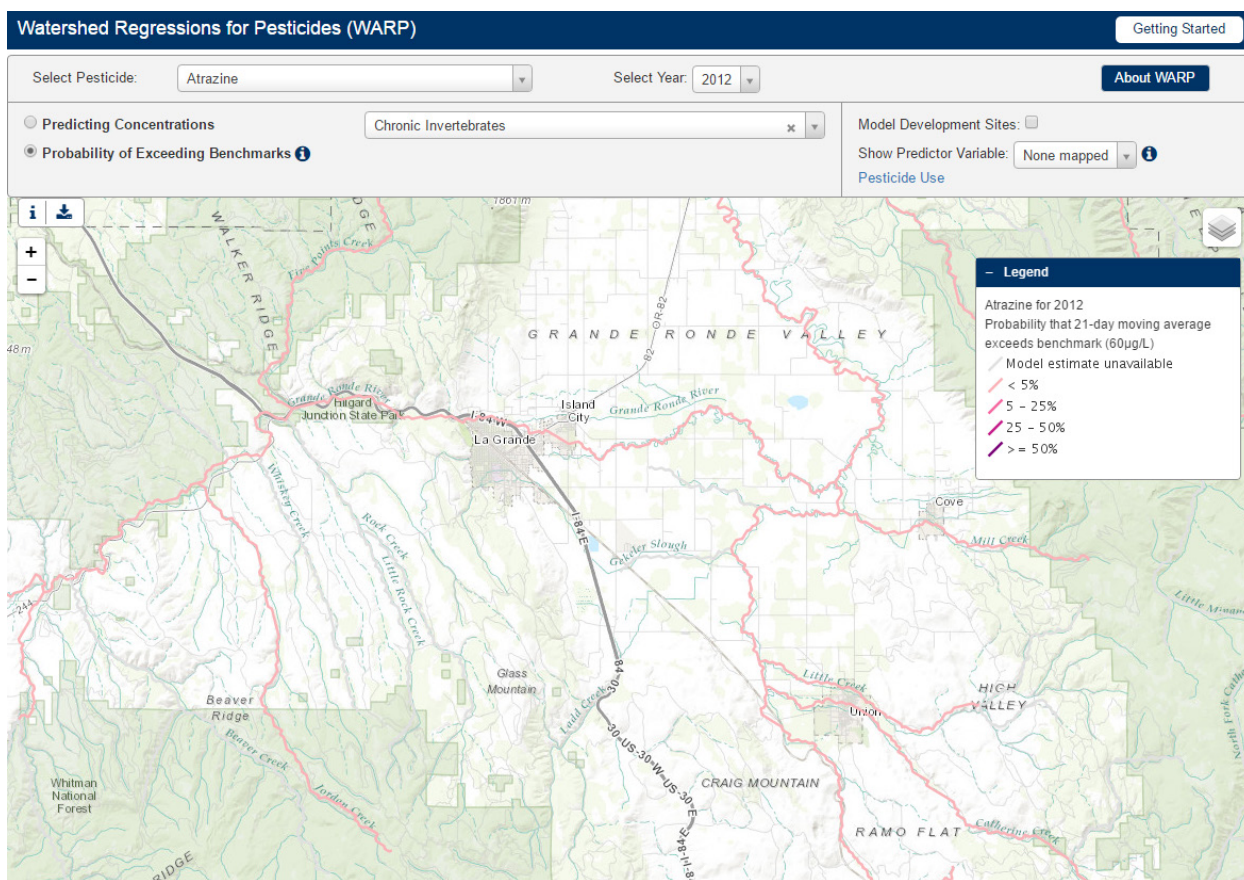


Figure 98. Estimated probability that the 21-day moving average concentration of atrazine exceeds the chronic macroinvertebrate benchmark.

Fumigants

Among the largest quantities of pesticides applied in Union County are fumigants. In Union County between 2009 and 2012 there was an average of 23577 kg of dichloropropene applied and an average of 107099 kg of metam-sodium (Table 1). Application rates for dichloropropene in the vicinity of the Upper Grande Ronde River appear to be high (i.e., > 81.16 pounds/mi²; Figure 99). Dichloropropene is used heavily on potatoes, sugar beets, sweet potatoes, onions, and carrots, all crops that are grown in Union County. It is also applied to many other common vegetable crops. Metam sodium is an organosulfur compound used as a soil fumigant, pesticide, herbicide, and fungicide. This compound is available as a sodium salt of methyl dithiocarbamate (Wikipedia). After its application on soils it decomposes to form methyl isothiocyanate (MITC), a fumigant, whose mode of action is to inactivate certain amino acids (Cox 2006). Application rates for metam-sodium in the vicinity of the Upper Grande Ronde River appear to be high (i.e., > 49.08 pounds/mi²; Figure 101).

1,3-Dichloropropene is an organochlorine pesticide used as a fumigant and nematicide. The threshold limit value is 1 ppm (Wikipedia). This compound is classified by EPA as a probable human carcinogen. The EPA STORET database indicates that of 12673 water samples in the US assayed for dichloropropene,

43% of them had dichloropropene. The mean concentration in these samples was 0.5 ug/l and the maximum concentration was 25 ug/l (USDHHS).

1,3-D volatilizes rapidly (volatilization half-life of about 4 hours), which causes it to leave waterbodies rapidly, but it also biodegrades and is hydrolyzed (hydrolyzation half-life of about 11 days at 20°C). It does not adsorb readily to sediment. Within 2 to 3 weeks after application, approximately 40% of 1,3-D volatilizes in the air, where it is photochemically degraded (7 to 12-hour half-life) (Vidrio 2012).

1,3-D is found minimally in surface runoff after application. Less than 0.005% of the compound applied was detected in runoff water and concentrations were less than 20 ug/l. This level is not considered to be toxic to invertebrates. The acute toxicity in a 48-h study on *Daphnia* was 6150 ug/l (EPA 1980, as cited by Vidrio 2012). The 96-h LC50 on rainbow trout was 3900 ug/l.

Metam sodium is one of the most commonly used pesticides in US agriculture, and the most commonly used soil fumigant. Most (90%) of its use in the US is in Idaho, Washington, Oregon, and California (Cox 2006). It is a soil fumigant used to kill nematodes, weeds, and fungi to protect fruit and vegetables. Exposure of rabbits to doses of > 30 mg/kg causes significant reduction in fetus survival. LD50 values for exposure of mice were 146-280 mg/kg (Beyond Pesticides 2007). In zebrafish, concentrations of as little as 38 ug/l can cause up to 50% of fish to develop malformed notochords and 50% to fail to hatch (Haendel 2004). The 20-h LC50 for sodium metam was 248 ug/l (Haendel 2004).

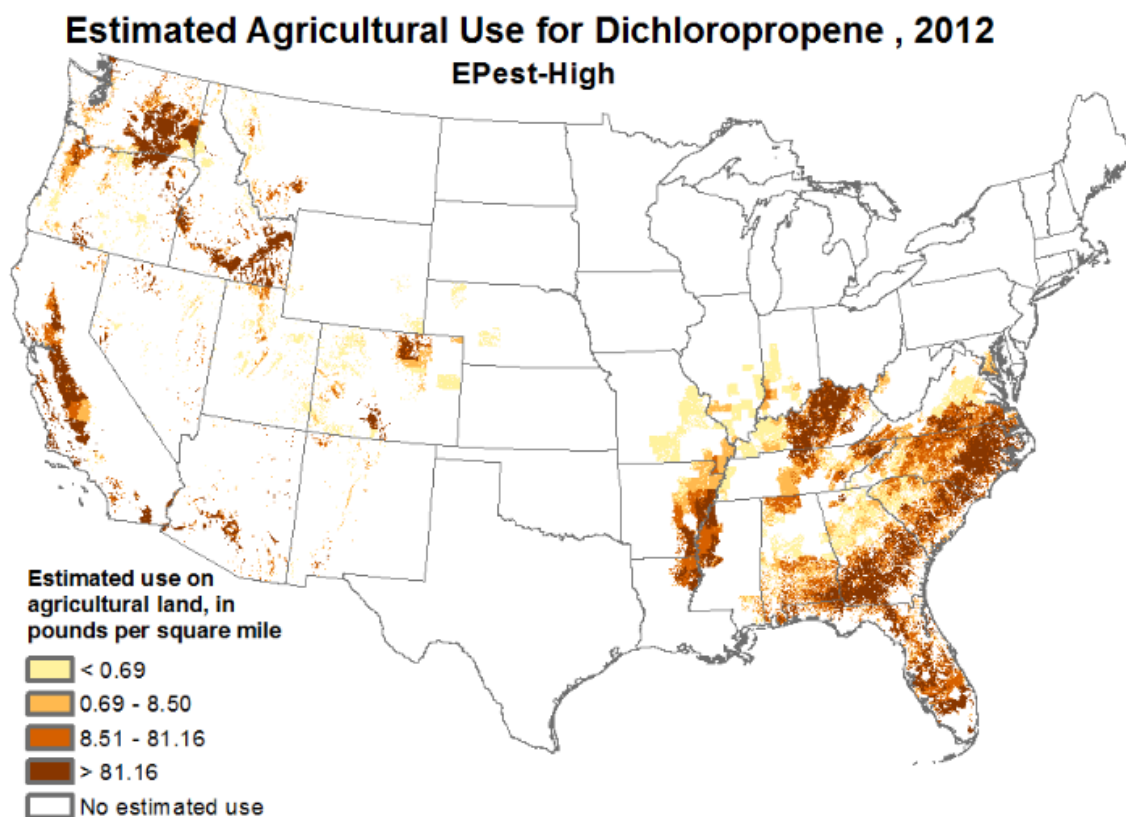


Figure 99. Estimated agricultural use for dichloropropene in 2012 in the US, using the USGS EPest-High process.

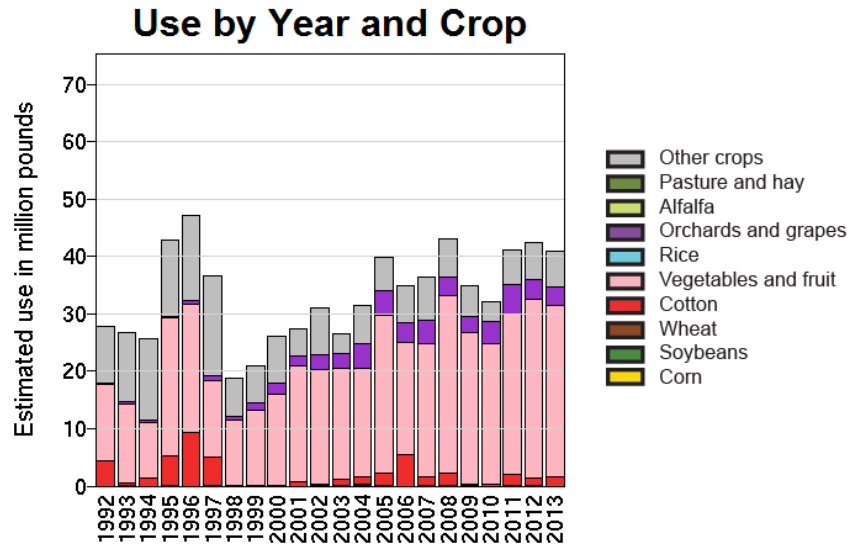


Figure 100. Use of dichloropropene by year and crop across the US.

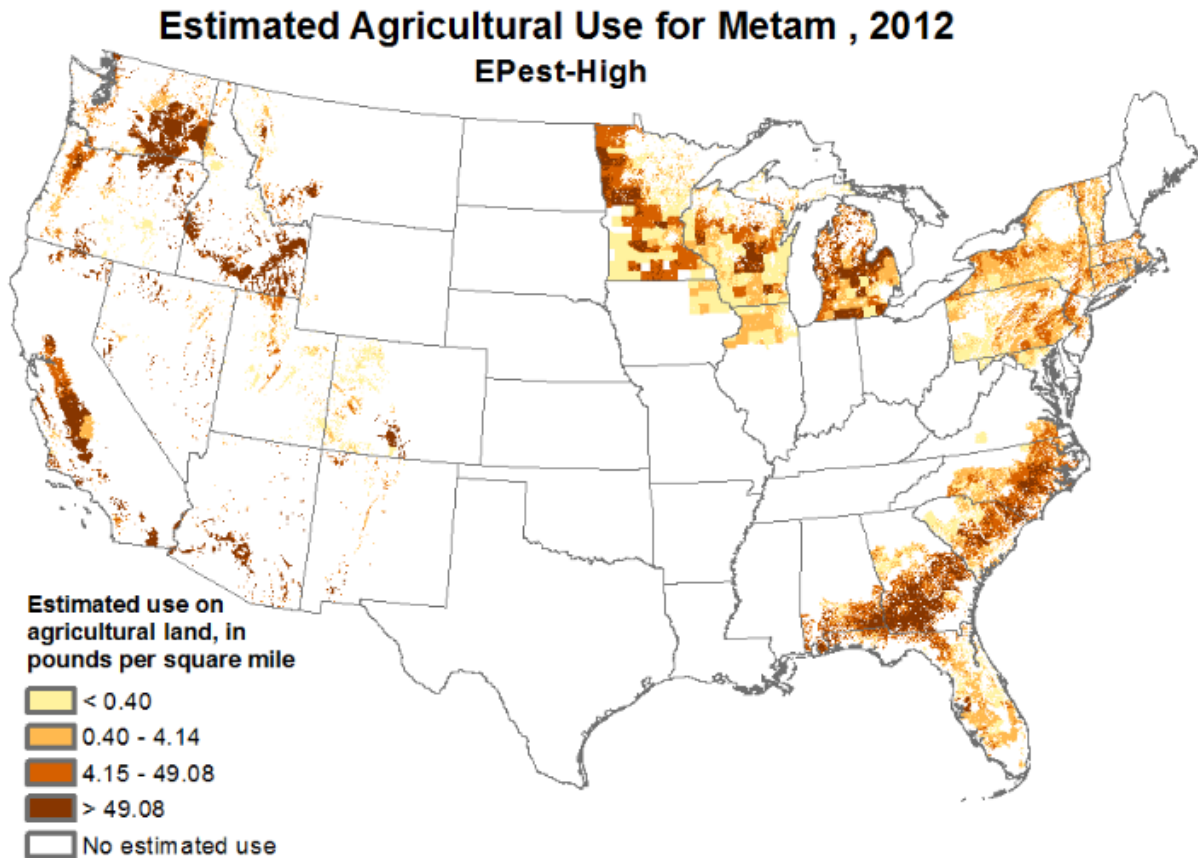


Figure 101. Estimated agricultural use for metam-sodium in 2012 in the US, using the USGS EPest-High process.

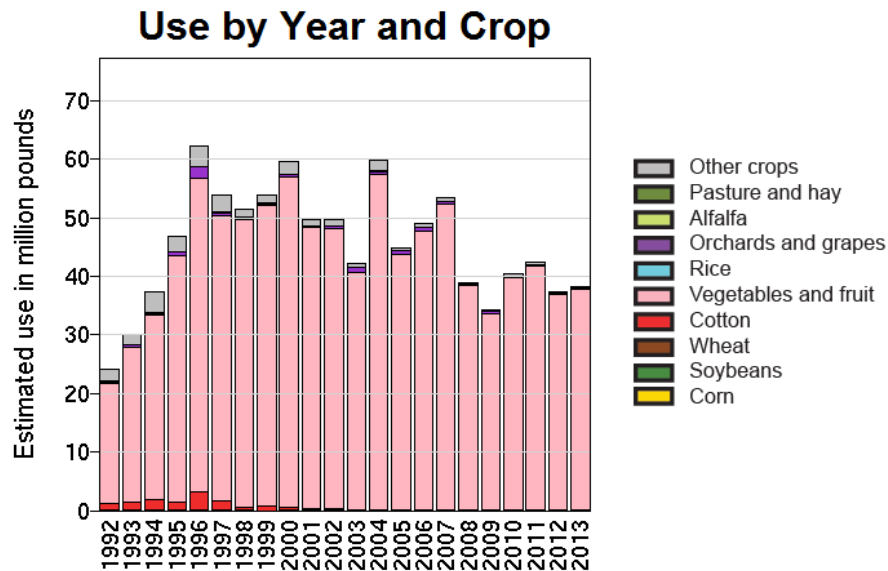


Figure 102. Use of metam sodium by year and crop across the US.

Cropland Subject to Pesticide Us

Union County is 5280 km² in total area (1,300,480 acres) (OSU 2011). Of this total area, 487,584 acres were in farm land in 2011 (OSU 2011). Ownership is 49.7% public and 50.3% private (OSU 2011). In 2011, farms comprised 487,584 acres of the county area (37.5% of the total). Farm acreage was subdivided into cropland (29%), woodland (16%), pasture (53%), and other land (2%). Of the total farm acreage, 13% was irrigated.

Table 45. Apportionment of crops into the total farmland of Union County in 2011 (OSU 2011).

Crop (general)	Crop (specific)	Acres
small grains	wheat	31150
	barley	2300
	oats	200
hay	alfalfa	23000
	other hay	15000
turf grass	Kentucky bluegrass	4550
	fescue	2240
	other hay	210
peppermint		7800
sweet cherries		340
other crops	potato,sugar beet, seed crops	5800
Total Cropland		92590

Table 46. Status of farms in Union County. Data from USDA (2012)

	Year	
	2007	2012
Farms in Union County	880	829
Land in farms (acres)	487584	411671
Average size of farm (acres)	554	497

The total of cropland compiled for Table 45 equals 92590 acres, which is 19% of total farmland (OSU 2011). OSU (2011) also identified cropland to comprise 29% of the total 487,584 acres of farmland, which appears to imply that there are other miscellaneous crops not accounted for by the specific crop tabulation given in the same publication.

The number of farms in Union County declined between 2007 and 2012 from 880 to 829, and the average size per farm declined from 554 to 497 acres per farm (Table 46) (USDA 2012). From 2007 to 2012 there was a 15.6% decline in the total farm acreage (USDA 2012). It is uncertain what uses this farm acreage adopted.

The use of pesticides by year and crop illustrate the typical crops in the entire US that receive various pesticide applications. In Union County, the types of crops grown for which Chlorpyrifos is used include pasture and hay, alfalfa, orchards and grapes, wheat, and vegetables and fruit (Figure 86). Diazinon is applied to orchards and grapes, alfalfa, vegetables and fruit, and wheat (Figure 90). Malathion is applied to alfalfa, orchards and grapes, vegetables and fruit, and other crops (Figure 94). Atrazine is mostly applied to corn, which is not a predominant crop in Union County, but is also applied to other crops (Figure 96). Dichlorpropene is applied to orchards and grapes, vegetables and fruit, and other crops (Figure 100). Metam-sodium is applied to vegetables and fruit and other crops (Figure 102). There is a high likelihood that single crops in field in Union County could be sprayed with pesticide or herbicide formulations that include multiple chemicals in the same dose, or could receive multiple pesticides or herbicides from sequential applications.

2,4-D

2,4-D (also known as 2,4-dichlorophenoxyacetic acid) is a chlorophenoxy herbicide that mimics a class of plant hormone (i.e., auxins). It was developed during World War II in an effort to find a chemical to stop plant growth. 2,4-D is a selective herbicide that controls dicots (broadleaf plants) while not affecting monocots (grass-like crops such as wheat, corn, rice, and other cereals) (Wikipedia, accessed May 2016). It is also used in forest replanting, on pasture and rangeland, in control of roadside and aquatic weeds, on fruit and vegetable crops, and in urban areas on lawns (Gilbert 2007, Beyond Pesticides).

2,4-D was reported by EPA in 2007 to not have the potential to cause cancer in humans, but the IARC's (International Agency for Research on Cancer) World Health Organization in 2015 restated and confirmed its earlier (1987) designation of 2,4-D as a possible carcinogen (Wikipedia, accessed May 2016, Beyond Pesticides). The acid, sodium salt, and the dimethylamine salt forms of 2,4-D are listed by NIOSH as chromosomal mutagens (Gilbert 2007). The hazards associated with 2,4-D are amplified

considerably depending on the amount of contaminants, such as dioxin and 2,4,5-T (2,4,5-trichlorophenoxyacetic acid), in the formula. The percentage of contaminants varies greatly depending upon manufacturer (Wikipedia, accessed May 2016). Current processes for production of 2,4-D in acid form yield a dioxin-free formula, but the amine and ester products have dioxin contamination (Exttoxnet 1993). In general, EPA found that 25% of 2,4-D samples were contaminated with dioxin, a known carcinogen and mutagen at very low doses (CDC NIOSH 2005, as cited by Gilbert 2007). 2,4-D amine products tested had dioxin contamination ranging from 5 to 500 ppb (EPA 1987, as cited by Exttoxnet 1993). Most 2,4-D ester products contain dioxin contamination (Exttoxnet 1993), but since 2000 the chemical manufacturers have made great efforts to reduce dioxin contaminant concentrations (EPA Appendix E). Average levels of dioxin congeners ranged from 0.06 to 2.17 ug/kg (or ppb) in four technical 2,4-D and/or 2,4-D ester products (EPA 2015).

2,4-D, present as either an amine salt or ester form, typically has a relatively short half-life (6.2 d) in aerobic mineral soils where it is chemically degraded by microbes. The half-life is about 15 d in aerobic aquatic environments, but can be extended to nearly a year in anaerobic environments (Wikipedia, accessed May 2016).

2,4-D binds poorly to mineral soils and sediment. Consequently, if it is not chemically degraded by microbes in the soil first, it is readily transported to streams.

Toxicity depends upon the chemical form. 2,4-D comes as either one of eight salts or esters, or in the more common acid form (Gilbert 2007, Beyond Pesticides n.d.). Toxicity of the 2,4-D butoxyethanol ester is very high for fish and other aquatic biota (Beyond Pesticides) but other ester forms may have lower toxicity. 2,4-D generally has moderate toxicity for birds and mammals, and slight toxicity to aquatic invertebrates (Wikipedia, accessed May 2016). The acid and amine salts have very low toxicity to freshwater fish (Beyond Pesticides n.d.). The LC₅₀ of 2,4-D to cutthroat trout ranges from 1.0 mg/l to 100 mg/l. Mortality of channel catfish exposed to 10 mg/l for 48 h was 10%.

Bioconcentration in fish from the 2,4-D acid form is minimal, but the isooctyl ester form does bioconcentrate (Beyond Pesticides n.d.).

2,4-D is applied to lands in the vicinity of the Grande Ronde basin according to USGS mapping (Figure 103). Application rates are high in this vicinity (>25.83 pounds/mi²). This herbicide is used on a variety of crops across the conterminous US, including corn and soybeans, pasture and hay, wheat, and alfalfa (Figure 104). These crops are significant targets in the Upper Grande Ronde and Catherine Creek, except for corn and soybeans.

The estimated maximum 21-d average concentration of 2,4-D in the study area is approximately 0.001 to 0.01 ug/l in the headwaters of the Upper Grande Ronde River and 0.01 to 0.1 ug/l in the Upper Grande Ronde downstream of Hilgard State Park. Most of Catherine Creek has 2,4-D levels of 0.01 to 0.1 ug/l. However, Little Creek has higher concentrations estimated for its waters (0.1 to 1 ug/l) (Figure 105). The probability that concentrations projected for the 21-d moving average would exceed the benchmark value of 200 ug/l are estimated as less than 5%. The lowest level estimated to produce an LC₅₀ for cutthroat, cited above, is 1000 times less than the highest estimated concentrations to be found

as a 21-d moving average. Estimated 4-d moving average concentrations were as high as 1 ug/l for both Pyles Creek (a tributary entering Catherine Creek downstream of Union) and Little Creek.

Because 2,4-D has been known to produce effects on neurotransmitters (Gilbert 2007), it is possible that it may produce biological impacts that are additive to those AChE effects produced by the organophosphate pesticides that are also used in the Upper Grande Ronde. Such effects on fish might contribute to sublethal impacts to behavior and activity levels that could impair survival and growth.

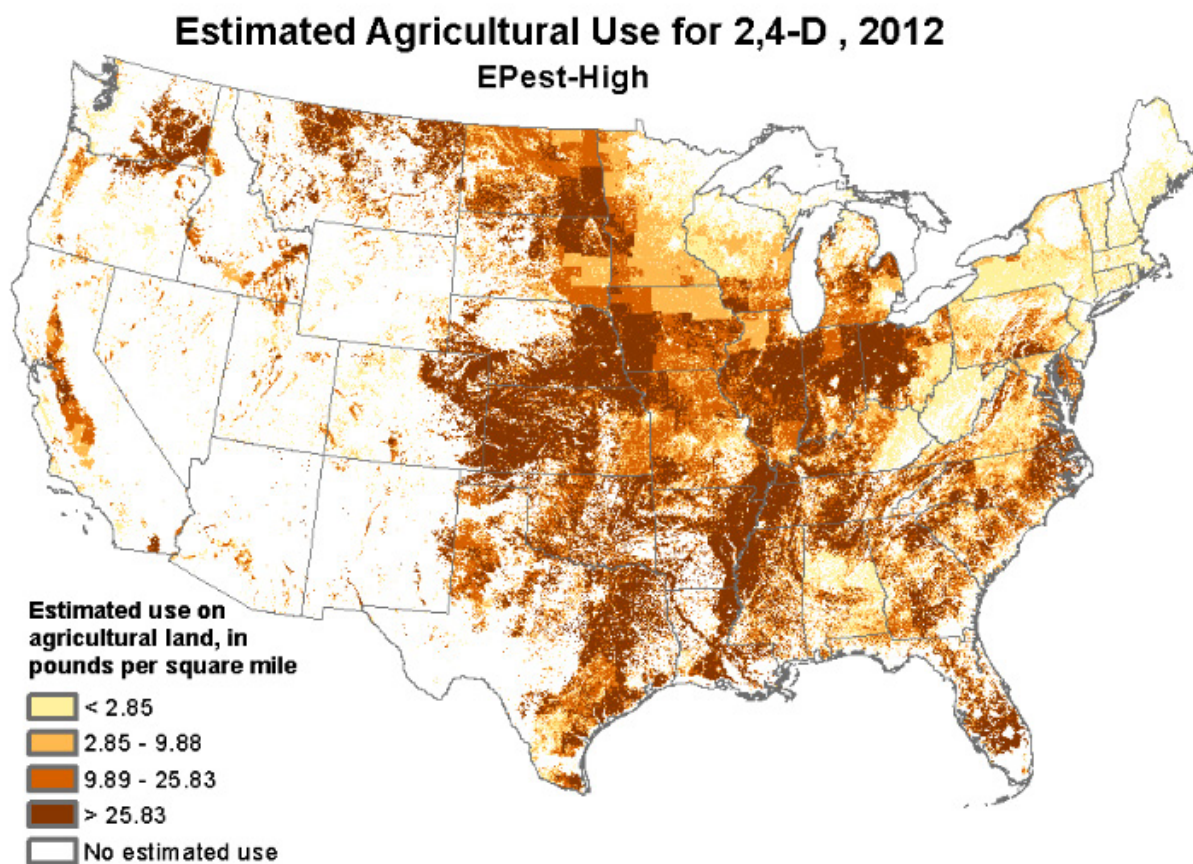


Figure 103. Estimated agricultural use for 2,4-D in 2012 in the US, using the USGS EPest-High process.

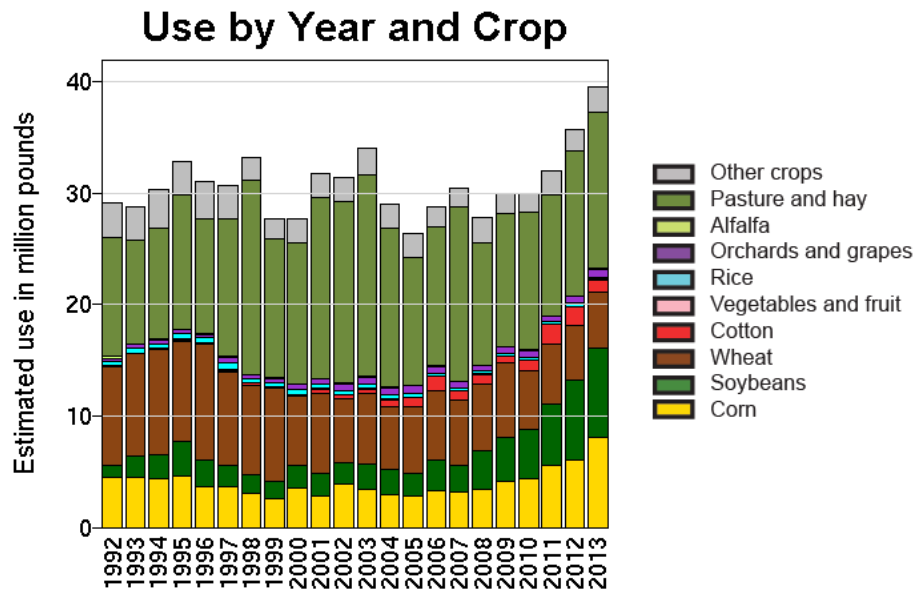


Figure 104. Use of 2,4-D sodium by year and crop across the US.

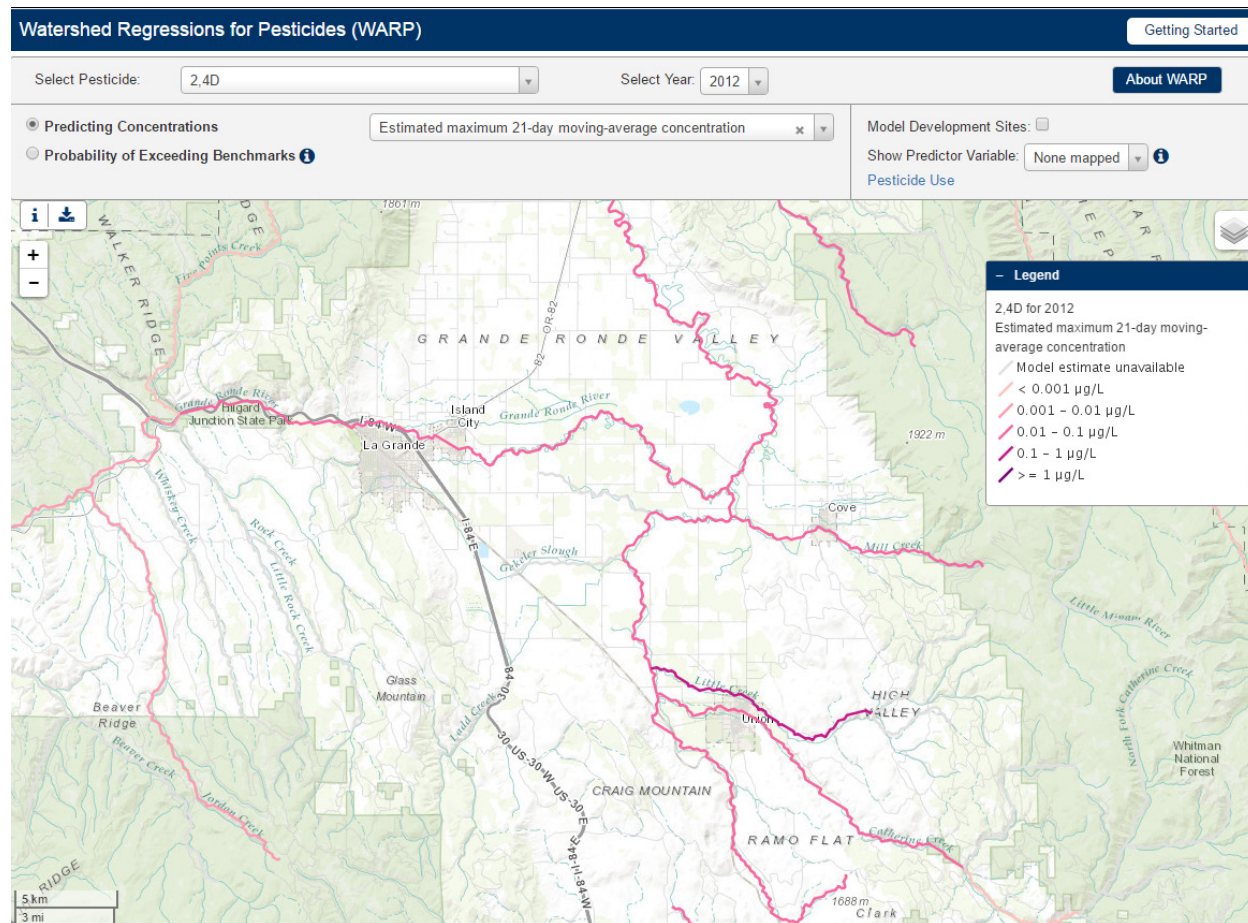


Figure 105. The estimated maximum 21-day moving average concentration of 2,4-D in the upper Grande Ronde River and Catherine Creek.

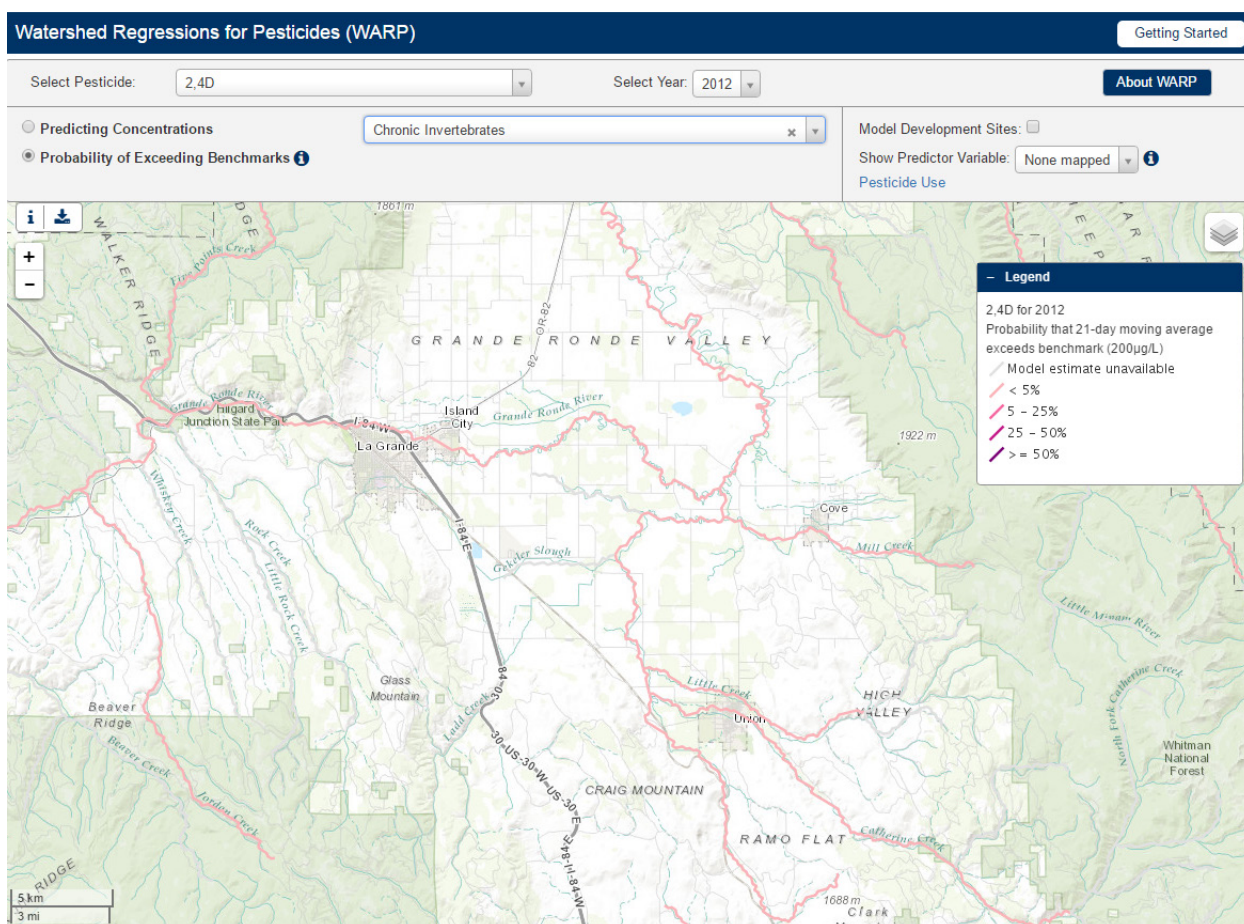


Figure 106. Estimated probability that the 21-day moving average concentration of 2,4-D exceeds the chronic macroinvertebrate benchmark.

Total Application of Pesticides and Herbicides that are AChE Inhibitors

Pesticides that impair the activity of acetylcholinesterase enzyme (AChE) include organophosphate pesticides (OP) and carbamate (CB) pesticides. The organophosphate pesticides that are included in the USGS (2016a) WARP database and are applied in the Grande Ronde basin include: azinphos-methyl, chlorethoxyfos, chlorpyrifos, diazinon, dimethoate, disulfoton, ethoprophos, malathion, methamidophos, methidathion, methyl parathion, oxdemeton-methyl, photate, phosmet, and terbufos. The total amount of these pesticides that were applied annually from 2008-2012 in Umatilla, Union, and Wallowa Counties are presented in Table 47.

Carbamates are also AChE inhibitors (i.e., neurotoxins) and include the following pesticides included in the USGS (2016a) database and found in the Grande Ronde basin: aldicarb, carbaryl, carbofuran, methomyl, and oxamyl. The total amount of these pesticides that were applied annually from 2008-2012 in Umatilla, Union, and Wallowa Counties are presented in Table 48. The average annual carbamate applied in Union County from 2008 to 2012 was 2224.8 kg/yr.

In addition to the organophosphate and carbamate pesticides, some herbicides also are AChE inhibitors. These include dicamba and 2,4-D (Table 49). The average annual phenoxy herbicide applied in Union County from 2008 to 2012 was 3181.1 kg/yr.

The OP pesticides bind the acetylcholinesterase enzyme irreversibly, but the CB pesticides bind the enzyme reversibly. The irreversible binding creates long-term biological problems for fish exposed to OP pesticides because it may require several weeks for a fish to synthesize new enzyme to replace the bound enzyme. As discussed above, enzyme inhibition may yield sublethal effects on individual growth rates due to impairment of swimming rates and reaction times. The lethal effects on the macroinvertebrate food base may also reduce the food availability for fish, resulting in lower growth rates and smaller size at the age for downstream migration. Smaller size (length at age) during migration is linked to reduced survival rates that can be applied in population models (Baldwin et al. 2009).

For OP pesticides that can produce a 50% inhibition in a 4-d exposure, the half-life of the pesticide was taken by Baldwin et al. (2009) to be 0.5 days and the half-life for recovery of the AChE activity level was 26 days. A 4-d exposure under these conditions results in outmigrant Chinook that are about 10% shorter in length. Baldwin et al. (2009) used a length-survival function for Chinook developed by Zabel and Achord (2004) to predict survival relative to unexposed control fish based on the length of fish on reaching the Columbia River estuary. The impact of 50% AChE inhibition on feeding rate was translated to growth rate and length achieved using a growth model. With this level of impact on AChE activity in Chinook, Baldwin et al. (2009) were able to predict that after 20 years of exposure to annual 4-d pulses from an OP source, the spawner abundance was only 27% of that of the unexposed population. The reduction in intrinsic growth rate (λ) was from 1.10 (unexposed control) to 1.03 (exposed population). Even though both populations had λ greater than 1.0, the exposed population had a significant impairment in ability to recover.

In the previous discussion, the significant potential effects on chlorpyrifos in particular were discussed. The annual average application total for chlorpyrifos in Union County was 999.4 kg, based on annual total applications for the county from 2008 to 2012. When all other OP pesticides are included, the average total OP pesticide amounts applied in Union County is 2733.2 kg. The yearly totals vary from 1141.7 to 3695.9 kg in this 5-year period. The predictions for effects on fish and invertebrates from 21-d exposures were based on applications made in 2012. Total OP pesticide applications made in 2009 were over 3 times greater than in 2012. Annual variations in concentrations of total OP pesticides reaching streams in Union County can be dependent upon the coincidence of precipitation events with application, the vagaries of spray drifting into aquatic environments, and the co-occurrence in time or juxtaposition of crops sprayed relative to streams.

Another factor that should be considered is the toxicity of individual pesticides and herbicides. The compounds listed in Table 47-Table 49 all share the same mode of toxicity, but vary in their level of toxicity. For example, Fishel (2014) listed the LC50 toxicity to fish in various categories. Methidathion and aziniphos-ethyl were listed as very highly toxic. Phosmet, malathion, chlorpyrifos, diazinon, and ethoprophos were considered to be highly toxic to fish. InChem (2016) listed the toxicity to rats of OP pesticides. Among the OP pesticides in Table 47, they listed ethoprophos, parathion, phorate, and

turbufos as extremely hazardous. Aziniphos ethyl and aziniphos methyl were listed as highly hazardous, and chlorpyrifos, diazinon, and phosmet were listed as moderately hazardous.

Considering the low levels of chlorpyrifos that can cause significant sublethal effects on fish and macroinvertebrates and the lower hazard level assigned to it compared with some other OP pesticides applied in Union County, there is reason for concern about the combined actions of the OP and CB pesticides and the phenoxy herbicides on fish, and especially salmonids, which tend to be more sensitive than other test fish used in the literature. Further, the increased toxicity of these compounds that is often temperature-dependent is likely to be a significant cause for concern in the Upper Grande Ronde and Catherine Creek basins where elevated water temperature is the key habitat factor limiting productivity and abundance of spring Chinook. In addition to the pesticides and herbicides that act as AChE inhibitors, the combined effects of these with other pesticides, herbicides, fumigants, nematicides, and other compounds applied may produce sub-lethal or lethal effects on the survival, growth, reproduction, or other biological functions of salmonids in the basin. Predictions of concentrations in streams of Union County made by USGS are helpful to gauge the level of concern about toxic impacts on listed fish and their macroinvertebrate food base. However, it would be important to obtain direct measures of concentrations of these probable toxicants in surface waters of Union County. Fortunately, Oregon Department of Environmental Quality is planning to monitor pesticide concentrations in fish during the summer of 2016.

Table 47. Annual use (kg) of organophosphate pesticides in Umatilla, Union, and Wallowa Counties from 2008 to 2012.

County	Year	AZINPHOS-METHYL	CHLORETHOXYFOS	CHLORPYRIFOS	DIAZINON
59-Umatilla County (kg)	Average (2008-2012)	511.3	26.2	4863.0	360.3
	2008	639.0		2190.0	533.2
	2009	347.0	26.2	6128.9	261.0
	2010	989.5		4223.2	188.7
	2011	379.8		3062.7	131.0
	2012	201.2		8710.4	687.8
61-Union County (kg)	Average (2008-2012)	39.4	0.1	999.4	32.2
	2008	65.8		483.2	22.4
	2009	53.0	0.1	2740.1	22.8
	2010	56.5		925.4	2.4
	2011	15.6		559.9	6.2
	2012	6.3		288.3	107.0
63-Wallowa County (kg)	Average (2008-2012)	4.5		558.2	4.7
	2008	5.9		76.7	8.7
	2009	5.1		1782.9	11.1
	2010	5.6		499.8	0.7
	2011	3.7		241.4	0.5
	2012	2.0		190.0	2.7

County	Year	DIMETHOATE	DISULFOTON	ETHOPROPHOS	MALATHION
59-Umatilla County (kg)	Average (2008-2012)	2543.9	70.4	809.0	1257.7
	2008	3223.5	119.0	2642.2	850.2
	2009	2532.3	103.8	197.0	379.8
	2010	2474.8	60.8	575.1	2084.4
	2011	2998.5	49.0	187.8	1380.0
	2012	1490.6	19.4	443.0	1594.0
61-Union County (kg)	Average (2008-2012)	337.5	13.9	116.1	550.9
	2008	460.1	26.6	422.7	229.5
	2009	223.4	18.3	28.7	146.7
	2010	240.2	7.6	86.3	1039.5
	2011	510.1	3.2	24.8	904.3
	2012	253.5		18.2	434.7
63-Wallowa County (kg)	Average (2008-2012)	165.1	0.3	15.0	223.7
	2008	151.0	0.6	60.7	2.9
	2009	91.4	0.4	3.3	41.0
	2010	96.1	0.2	7.9	572.3
	2011	289.5	0.1	1.6	449.5
	2012	197.3		1.4	52.8

County	Year	METHAMIDOPHOS	METHIDATHION	METHYL PARATHION	OXYDEMETON -METHYL
59-Umatilla County (kg)	Average (2008-2012)	1806.6	20.2	348.7	145.1
	2008	2905.3		601.5	248.9
	2009	2221.4	22.8	464.2	183.4
	2010	293.1		368.2	196.8
	2011			135.9	66.2
	2012		17.5	173.8	30.0
61-Union County (kg)	Average (2008-2012)	277.3	1.2	41.7	0.1
	2008	464.8		124.7	0.1
	2009	323.1	0.2	0.2	0.1
	2010	44.0		0.1	0.1
	2011				
	2012		2.2		
63-Wallowa County (kg)	Average (2008-2012)	35.9	0.2	17.4	0.1
	2008	66.7		86.4	0.2
	2009	37.1	0.2	0.3	0.1
	2010	4.0		0.2	0.1
	2011			0.1	
	2012		0.1	0.1	

County	Year	PHORATE	PHOSMET	TERBUFOS	Total OP Pesticides
59-Umatilla County (kg)	Average (2008-2012)	815.5	1445.6		15023.6
	2008	336.1	2098.3		16387.2
	2009	671.9	797.3		14337.0
	2010	737.1	378.0		12569.7
	2011	2103.7	3771.1		14265.7
	2012	228.9	183.2		13779.8
61-Union County (kg)	Average (2008-2012)	109.9	34.9	20.9	2733.2
	2008	53.8	97.6	14.0	2465.3
	2009	97.7	10.0	31.5	3695.9
	2010	110.6	12.1	25.2	2550.0
	2011	277.8	32.5	12.8	2347.2
	2012	9.4	22.1		1141.7
63-Wallowa County (kg)	Average (2008-2012)	9.6	22.5		1075.1
	2008	7.7	58.7		526.2
	2009	11.2	5.4		1989.5
	2010	10.2	10.9		1208.0
	2011	18.3	25.8		1030.5
	2012	0.7	11.9		459.0

Table 48. Annual use (kg) of carbamate pesticides in Umatilla, Union, and Wallowa Counties from 2008 to 2012.

County	Year	ALDICARB	CARBARYL	CARBOFURAN	METHOMYL	OXAMYL	Total
59-Umatilla County (kg)	Average (2008-2012)	4789.9	755.9	455.8	4549.8	5605.1	16156.5
	2008	6214.5	545.8	455.8	5168.0	4966.6	17350.7
	2009	4919.7	427.4		4244.8	3301.1	12893.0
	2010	6696.8	1077.7		7262.2	4021.7	19058.4
	2011	1328.4	1101.9		1832.6	3910.7	8173.6
	2012		626.9		4241.2	11825.5	16693.6
61-Union County (kg)	Average (2008-2012)	852.1	116.1	251.0	460.4	545.1	2224.8
	2008	1161.7	68.9	251.0	811.7	754.9	3048.2
	2009	724.4	101.9		383.8	464.9	1675.0
	2010	1229.3	137.5		786.7	544.5	2698.0
	2011	293.0	115.8		107.7	503.8	1020.3
	2012		156.4		212.3	457.6	826.3
63-Wallowa County (kg)	Average (2008-2012)	125.9	6.7	158.2	87.5	56.4	434.6
	2008	142.7	4.5	158.2	116.5	108.5	530.4
	2009	82.2	1.5		45.0	53.5	182.2
	2010	165.6	4.2		73.4	50.3	293.5
	2011	112.9	4.2		10.9	33.2	161.2
	2012		18.9		191.7	36.3	246.9

Table 49. Annual use (kg) of phenoxy herbicides in Umatilla, Union, and Wallowa Counties from 2008 to 2012.

County	Year	DICAMBA	2,4-D	Total
59-Umatilla County (kg)	Average (2008-2012)	2915.7	20970.5	23886.2
	2008	1890.1	15076.9	16967.0
	2009	1739.9	12724.0	14463.9
	2010	2388.7	50243.6	52632.3
	2011	5237.9	12052.5	17290.4
	2012	3322.1	14755.3	18077.4
61-Union County (kg)	Average (2008-2012)	364.6	2816.5	3181.1
	2008	320.6	2916.6	3237.2
	2009	389.8	2721.8	3111.6
	2010	337.5	4057.4	4394.9
	2011	427.7	1349.3	1777.0
	2012	347.3	3037.4	3384.7
63-Wallowa County (kg)	Average (2008-2012)	170.0	1531.8	1701.8
	2008	137.3	1762.4	1899.7
	2009	205.5	1554.2	1759.7
	2010	203.9	1216.6	1420.5
	2011	164.2	561.0	725.2
	2012	139.2	2564.9	2704.1

ODEQ Pesticide Monitoring Plan for 2016

Oregon Department of Environmental Quality (ODEQ) will be initiating a monitoring program (Table 50) to sample surface water and fish for pesticides in NE Oregon in the summer of 2016. ODEQ technical staff discussed their monitoring plan with CRITFC technical staff on April 25, 2016. Based on this meeting and the preliminary work done working on this report to assess the expected levels of pesticides in the Grande Ronde basin, ODEQ decided to add a site in Catherine Creek to intentionally capture data on what may be a stream reach with higher than average levels of pesticides. CRITFC and ODFW will work with ODEQ in the summer of 2016 to assist in collection of fish that can be processed to detect pesticide contamination levels.

Table 50. ODEQ plan for sampling sites (water, fish, macroinvertebrates) in NE Oregon in the summer of 2016 for toxics.

Group	Basin	Site ID	Site Name	2008-10 repeat/ new for Tox Mon	GPS-LAT	GPS-LONG
B-1	John Day	11386	John Day R at Hwy 206	repeat	45.4767	-120.4716
B-2	John Day	36787	Rock Creek at mouth	new		
B-3	John Day	38510	North Fork John Day River at Hwy 359 bridge river mile 61	new	44.9992	-118.9479
B-4	John Day	31990	John Day River Clyde Holiday park	repeat	44.4155	-119.0887
B-5	John Day	31987	Canyon Creek, John Day City Park	repeat	44.4195	-118.9585
B-6	John Day	24135	Clear Cr near Red Boy mine	repeat	44.7972	-118.4731
B-7	Powder/Burnt	36191	North Powder R at Hwy 30 bridge	new	44.9956	-117.9039
B-8	Powder/Burnt	34438	Powder R Hudspeth Rd near Sumpter	new site	44.6846	-118.0925
B-9	Powder/Burnt	33829	Burnt River 150 feet upstream of Huntington WWTP outcall			
B-10	Powder/Burnt	11857	Powder R at Snake R Rd	repeat	44.7463	-117.1729
B-11	Grande Ronde	11521	Grande Ronde River at Peach Lane (Island City)	repeat	45.3496	-117.9638
B-12	Grande Ronde	11647	Grande ronde River at Lower Cove Rd (Markert Rd)	new		
B-13	Grande Ronde	10719	Grande Ronde River at Hwy 82 (North Elgin)	repeat	45.5660	-117.9111
B-14	Grande Ronde	11457	Minam R at Minam	new	45.6199	-117.7279
B-15	Grande Ronde	10410	Wallowa River at Minam	new	45.6210	-117.7198
B-16	Grande Ronde	34238	Bear Creek at Frontage Road (Wallowa, Grande Ronde)	new	45.8580	-117.5400
B-17	Grande Ronde	24072	Prarie Cr. At Walter St in Enterprise, OR, RM 0.6	new	45.4256	-117.2894
B-18	Walla Walla	10711	Walla Walla at Hwy 11 (Milton-Freewater)	new	46.0126	-118.3891

Group	Basin	Site ID	Site Name	2008-10 repeat/ new for Tox Mon	GPS-LAT	GPS-LONG
B-19	Walla Walla	33084	Little Walla Walla R. West Branch/Crocket	new	45.9694	-118.4098
B-20	Walla Walla	32010	West Prong Little WW south of state line rd	new	46.0008	-118.4358
	John Day	28221	NF John Day upstream of Camas Creek	new		
	Powder/Burnt	11494	Burnt R Huntington	repeat	44.3566	117.2536
	John Day	new	Thirtymile Cr at Hwy 19 bridge south of Condon	new		
	John Day	new	new Thirtymile Cr, or Rock Creek Hwy 206?	new	45.1665	-120.1757
	John Day	new	Rock Creek Hwy 206?	new	45.2657	-120.0271
	Grande Ronde	24072	Prarie Cr. At Holmes St in Enterprise, OR,	new		
	Walla Walla	23503	Pine Creek at State Line Rd	new	46.0011	-118.5906

Summary

1. Restoration of damaged tributary habitat in order to enhance habitat carrying capacity and productivity has been assumed to be a means to recover listed populations of fish in the Columbia Basin.
2. The restoration of habitat requires amelioration of key limiting factors. These factors have typically been considered to include reduction in water temperature and fine sediment concentrations in the stream, recovery of riparian vegetation, increased availability of pool habitats achieved via enhanced large woody debris abundance and distribution, and reduced nutrient inputs.
3. The application of pesticides, herbicides, and fumigants to timberlands and croplands, however, has the potential to be a significant hidden source of mortality of aquatic macroinvertebrates that constitute the food base of the salmonid community. These toxic substances can cause direct mortality of salmonids or provide sublethal impacts to growth rates, reproductive rates, behavior, migration, predator avoidance, etc. that can cause population impairment in a life cycle context and threaten the ability to restore the population.
4. In addition to the lethal or sublethal impacts of individual toxics, the fact that there are as many as 482 pesticides, herbicides, and fungicides used in the US and their interactions or synergistic or additive effects are largely unknown or poorly studied makes the potential for impact to the aquatic populations of great concern. Across the US, one or more pesticides were found in 90% of streams on agricultural, urban, or mixed-use land. A study by Gilliom et al. (2006) showed that in 83 streams sampled in agricultural areas, 57% had one or more pesticides present in levels exceeding aquatic-life benchmarks. Chlorpyrifos exceeded benchmarks in 21% of these streams, while atrazine exceeded benchmarks in 18%.

5. In addition, impacts to the human population in the area of application or from streams draining affected watersheds are known to cause impairment to people. Despite the risks of chlorpyrifos, the EPA recently reversed its proposed ban, citing unresolved uncertainties in the extent of damage caused by normal applications of this pesticide (Lipton 2017). Impacts to people, fish, and macroinvertebrates of this pesticide are neurological impairments.
6. The USGS provides a website that indicates modeled concentrations in rivers of a wide variety of toxics that are applied on watersheds based on knowledge of amounts applied, timing, types of crops present, and ability of the toxic chemical to migrate through soil or air to streams.
7. NOAA (2008) reviewed the known biological literature on impacts of chlorpyrifos, diazinon, and malathion. A wide range of impacts to fish and aquatic macroinvertebrates was described. Among the findings were that four prey species eaten by salmonids had acute toxicity levels of 0.1-50 $\mu\text{g/l}$. LC50 values on a wide range of aquatic macroinvertebrates were less than 1 $\mu\text{g/l}$ (EPA 2003, as cited by NOAA 2008). Diazinon, another organophosphorus pesticide, can cause mortality in macroinvertebrates at concentrations as low as 0.06 $\mu\text{g/l}$, growth impairment at concentrations of 0.8 $\mu\text{g/l}$, and impaired reproduction at concentrations of 0.1-10 $\mu\text{g/l}$, depending upon species and study.
8. USGS data shows that expected concentrations of chlorpyrifos in Catherine Creek downstream of Little Creek ranged from 0.002 to 0.01 $\mu\text{g/l}$. A 21-day maximum moving average of chlorpyrifos estimated for applications made in 2012 in Catherine Creek provided a 5-25% chance that the chronic macroinvertebrate standard of 0.04 $\mu\text{g/l}$ would be exceeded. Higher application rates would be likely to create greater concentrations than those estimated for 2012.
9. In Catherine Creek the 21-d concentration of diazinon is estimated using methods in USGS to be 0.001-0.01 $\mu\text{g/l}$. The probability of 21-d concentrations exceeding the chronic macroinvertebrate benchmark of 0.17 $\mu\text{g/l}$ is <5%.
10. Degradates of applied pesticides and herbicides can often be far more toxic than the primary chemical itself and produce effects that are exceedingly unpredictable and potentially more hazardous. Estimates of impact based solely on the expected concentrations of the primary pesticide may significantly underestimate the actual lethality.
11. Using USGS data on amounts of pesticides applied in Oregon by basin, we compiled the total mass (kg) of pesticides having a common of biological impact applied in the Upper Grande Ronde basin and the Catherine Creek basin. Chlorpyrifos, diazinon, and malathion are all organophosphorus pesticides. Pesticides that impair the activity of acetylcholinesterase enzyme (AChE) include organophosphate pesticides (OP) and carbamate (CB) pesticides. The organophosphate pesticides that are included in the USGS WARP database and are applied in the Grande Ronde basin include: azinphos-methyl, chlorethoxyfos, chlorpyrifos, diazinon, dimethoate, disulfoton, ethoprophos, malathion, methamidophos, methidathion, methyl parathion, oxdemeton-methyl, photate, phosmet, and terbufos. The total amount of these pesticides that were applied annually from 2008-2012 in Umatilla, Union, and Wallowa Counties was compiled. Many of these toxics are listed as highly hazardous (i.e., even more hazardous than chlorpyrifos itself).

12. Although the threat of significant limitation of spring Chinook recovery via direct impact to the fish or their prey base from individual pesticides or herbicides appears to be primarily just at or below the levels known to begin causing measurable impacts, there are several reasons to have concern about these toxic substances in the environment. There are many toxics having similar modes of biological impact that could easily work synergistically or additively to heighten the level of mortality. Variations in the extent of planting of crops that typically are subject to applications of these pesticides can cause unpredictable changes in timing of spread of these toxics in the environment. Weather patterns, such as timing of summer precipitation, can cause intense periods of movement of toxics into surface waters. The chemical degradates of primary forms of pesticides and herbicides can be far more toxic than the primary chemical itself. High water temperatures can increase the lethality of any toxic chemical and the combined action of pesticides and herbicides together with other conventional environmental limiting factors that have increased stress levels on listed fish populations are capable of severely restricting recovery potential.

References

- Baker, N.T., and Stone, W.W. 2015. Estimated annual agricultural pesticide use for counties of the conterminous United States, 2008–12. U.S. Geological Survey Data Series 907, 9 p., <http://dx.doi.org/10.3133/ds907>.
- Baldwin, D.H., J.A. Spromberg, T.K. Collier, and N.L. Scholz. 2009. A fish of many scales: extrapolating sublethal pesticide exposures to the productivity of wild salmon populations. *Ecological Applications* 19(8):2004-2015.
- Beyond Pesticides. 2007. Metam Sodium. Chemical Watch Factsheet. Beyond Pesticides, Washington, D.C. www.beyondpesticides.org.
- Beyond Pesticides. nd. 2,4-D. Chemical Watch Factsheet. Beyond Pesticides, Washington, D.C. www.beyondpesticides.org. 7 p.
- EPA. 2015. Appendix E. Review of Dioxin contamination. United States Environmental Protection Agency. Available at <http://www.epa.gov/espp/litstatus/effects/redleg-frog/2-4-d/appendix-e.pdf>
- Extoxnet. 1993. 2,4-D. Extension Toxicology Network. Cornell University, Michigan State University, Oregon State University, and University of California at Davis. 6 p.
- Fishel, F.M. 2014. Pesticide toxicity profile: organophosphate pesticides. University of Florida, IFAS Extension. PL-50. <http://edis.ifas.ufl.edu>.
- Gilbert, S.G. 2007. 2,4-D. Toxipedia. <http://www.toxipedia.org/display/toxipedia/2,4D>
- Gilliom, R.J., J.E. Barbash, C.G. Crawford, P.A. Hamilton, J.D. Martin, N. Nakagaki, L.H. Nowell, J.C. Scott, P.E. Stackelberg, G.P. Thelin, and D.M. Wolock. 2006. The Quality of Our Nation's Waters—Pesticides in the Nation's Streams and Ground Water, 1992–2001. U.S. Geological Survey Circular 1291. US Geological Survey, Reston, Virginia. 172 p.
- Haendel, M.A., F. Tilton, G.S. Bailey, and R.L. Tanguay. 2004. Developmental toxicity of the dithiocarbamate pesticide sodium metam in zebrafish. *Toxicological Sciences* 81:390-400.
- InChem. 2016. Organophosphorus pesticides. International Programme on Chemical Safety Poisons Information Monograph (Group Monograph). <http://www.inchem.org/documents/pims/chemical/pimg001.htm>
- Lipton, E. 2017. E.P.A. Chief, Rejecting Agency's Science, Chooses Not to Ban Insecticide. *New York Times*, March 29, 2017. https://www.nytimes.com/2017/03/29/us/politics/epa-insecticide-chlorpyrifos.html?_r=0
- NOAA. 2008. National Marine Fisheries Service Endangered Species Act Section 7 Consultation. Biological Opinion Environmental Protection Agency Registration of Pesticides Containing Chlorpyrifos, Diazinon, and Malathion. Endangered Species Division of the Office of Protected Resources, National Marine Fisheries Services. 482 p.

- NPCC. 2016. ISAB/ISRP critical uncertainties for the Columbia River basin Fish and Wildlife Program. ISAB/ISRP 2016-1, January 29, 2016. Northwest Power and Conservation Council. Portland, Oregon.
- OSU. 2011. 2011 Profile of Union County Agriculture. Oregon State University, Extension Economic Information Office. <http://extension.oregonstate.edu/union/index.php>
- Sandahl, J.F. and J.J. Jenkins. 2002. Pacific steelhead (*Oncorhynchus mykiss*) exposed to chlorpyrifos: Benchmark concentration estimates for acetylcholinesterase inhibition. *Environmental Toxicology and Chemistry* 21(11):2452-2458.
- Sandahl, J.F., D.H. Baldwin, J.J. Jenkins, and N.L. Scholz. 2005. Comparative thresholds for acetylcholinesterase inhibition and behavioral impairment in coho salmon exposed to chlorpyrifos. *Environmental Toxicology and Chemistry* 24(1): 136–145.
- Soscia, M.L. 2016. Letter to Northwest Power and Conservation Council. Comments on ISAB/ISRP critical uncertainties for the Columbia River basin Fish and Wildlife Program report (ISAB/ISRP 2016-1). Environmental Protection Agency, Portland, Oregon.
- Stone, W.W. 2013. Estimated annual agricultural pesticide use for counties of the conterminous United States, 1992–2009. U.S. Geological Survey Data Series 752, 1-p. pamphlet, 14 tables.
- Stone, W.W., C.G. Crawford, and R.J. Gilliom. 2013. Watershed Regressions for Pesticides (WARP) Models for predicting stream concentrations of multiple pesticides. *Journal of Environmental Quality* 42.6. <https://dl.sciencesocieties.org/publications/jeq/abstracts/42/6/1838>
- USDA. 2012. Union county Oregon. County profile. US Department of Agriculture, Census of agriculture. www.agcensus.usda.gov.
- USDHHS. 2008. Toxicological profile for dichloropropenes. US Department of Health and Human Services Agency for Toxic Substances and Disease Registry, Division of Toxicology and Environmental Medicine, Atlanta, Georgia.
- USGS. 2016a. Watershed Regressions for Pesticides (WARP). <http://cida.usgs.gov/warp/home/>. Accessed May 2016.
- USGS. 2016b. Pesticide National Synthesis Project. http://water.usgs.gov/nawqa/pnsp/usage/maps/compound_listing.php. Accessed May 2016.
- Vidrio, E. 2012. 1,3-Dichloropropene Risk Characterization Document. Environmental Monitoring Branch Department of Pesticide Regulation, California Environmental Protection Agency.
- Wikipedia. 2016. 2,4-Dichlorophenoxyacetic acid. 8 p.

Stream Biota

Fish-Habitat Relationships

Introduction

A general approach to most fish habitat monitoring programs is to measure a suite of habitat conditions and infer how those conditions change (a) over space and time and (b) in response to alternative management strategies or policies. The importance of habitat condition to fish can either be gleaned from extensive literature on fish-habitat relationships (Jackson et al. 2001) or empirically determined by relating fish response to habitat conditions in a statistical model (Fausch et al. 1988). Most fish habitat monitoring programs occur as observational studies in natural systems rather than as controlled experiments, making it challenging to predict how management decisions directly translate into habitat conditions, or how habitat conditions influence fish response. This exemplifies the “correlation does not imply causation” problem of observational studies, where observed correlations among predictors (e.g., habitat conditions) and responses (e.g., fish performance) cannot be relied upon to infer mechanisms or direct causal effects (Shipley 2002).

Structural equation modeling (SEM) is a multivariate approach that emerged from various scientific disciplines and builds upon numerous statistical techniques such as regression, path analysis, factor analysis, and latent variables (Grace 2006). The SEM approach can help address the problems mentioned above, and is one potential approach to estimating tributary habitat carrying capacity. To our knowledge, SEMs have not been employed to estimate carrying capacity of individual fish species. However, the approach has been used by aquatic ecologists for understanding patterns in biodiversity (Belovsky et al. 2011; Duffy et al. 2016), water quality and temperature (Zou and Yu 1994; Isaak and Hubert 2001), ecosystem indicators (Arhonditsis et al. 2006; Maloney and Weller 2011; Irvine et al. 2015) and fish performance (i.e., growth) (Budy et al. 2011).

The advantages of SEM for observational studies and differences from conventional univariate and multivariate approaches are reviewed in (Grace 2007). SEMs graphically relay complex hypotheses about how system components interrelate in a manner easily comprehended by stakeholders (Figure 107). Theoretical knowledge is typically used to develop models, which represent alternative hypotheses about processes leading to observed patterns in the data. The approach is based on the analysis of covariance relations, with maximum-likelihood estimation being the most common method for obtaining solutions; however numerous procedures can be used including Bayesian estimation. Several recent advances to SEMs make it an ideal approach for non-normal or nonlinear data, categorical responses, and hierarchical data structure. Overall, the approach is well suited to elucidating how different processes work in concert, how effects propagate through a system, and evaluating the relative importance of different stimuli (Figure 107) (Wu and Zumbo 2008; Grace et al. 2010).

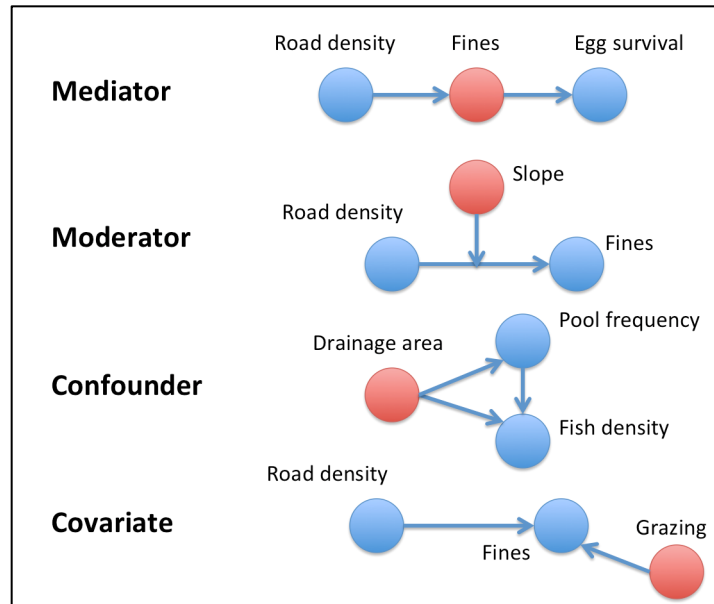


Figure 107. Language for causal models. Paths (arrows) between variables (circles) represent the direction of influence. Mediators influence how an independent variable affects a dependent variable. Moderators alter the direction or strength of an effect of one variable on another. Confounders are associated with both independent and dependent variables. Covariates are associated with a dependent variable only. Structural equation modeling (SEM) is well suited to analysis of these complex relationships.

Methods

We conducted snorkel surveys to quantify juvenile Chinook Salmon and steelhead abundance and size in their summer rearing habitats. These data were used to inform fish assemblage structure and to assess fish-habitat relationships. CRITFC, ODFW, and CTUIR perform snorkel surveys at CHaMP sites where habitat data are collected. These three agencies have recognized the need to use a common snorkel survey protocol so that information collected by individual entities can help managers determine whether aggregate habitat restoration actions will yield a net improvement in basin-wide habitat quality and viability of ESA-listed fish species. To this end, CRITFC developed a snorkeling protocol, drawing heavily from the methods of Thurow (1994) and O’Neal (2007) and integrated with the Pacific Northwest Aquatic Monitoring Program (PNAMP) methods, with the intention that this protocol will be implemented by all agencies responsible for data collection in the Upper Grande Ronde, Catherine Creek, Minam River, and potentially other nearby basins. Details about the snorkel survey methodology can be found in White et al. (2012) (<https://www.monitoringmethods.org/Protocol/Details/499>). Snorkel counts at each CHaMP site are expanded using a correction factor developed from paired mark-recapture to account for fish that were not observed by snorkelers (Jonasson et al. 2015) and screened to include only visits falling within the summer low-flow period of Julian Day 200-260.

We developed a fish-habitat SEM as described in the Introduction using data from the Columbia Habitat Monitoring Program (CHaMP 2016) coupled with snorkel surveys of salmonid densities (McCullough et al. 2015).

Results and Discussion

The 2016 field season marks the completion of three rotating panels and six consecutive visits to annual panels for CHaMP sampling, coupled with associated fish snorkeling and electrofishing to determine late summer rearing capacity. Whereas analyses of fish distribution and its linkages to local and landscape conditions are underway, a cursory look at juvenile Chinook Salmon rearing densities in three ICTRT Chinook Salmon populations (Catherine Creek, upper Grande Ronde, and Minam River) was instructive (Figure 108). Fish densities in the Upper Grand Ronde River are typically lower than other populations, and have substantially decreased since 2011. Catherine Creek densities appeared to decline in 2016, but were highly variable. Juvenile Salmon densities in the Minam River wilderness area tended to be as high or higher than Catherine Creek during the three years of sampling there, with the final year of sampling (2015) exhibiting the most significant difference from other populations.

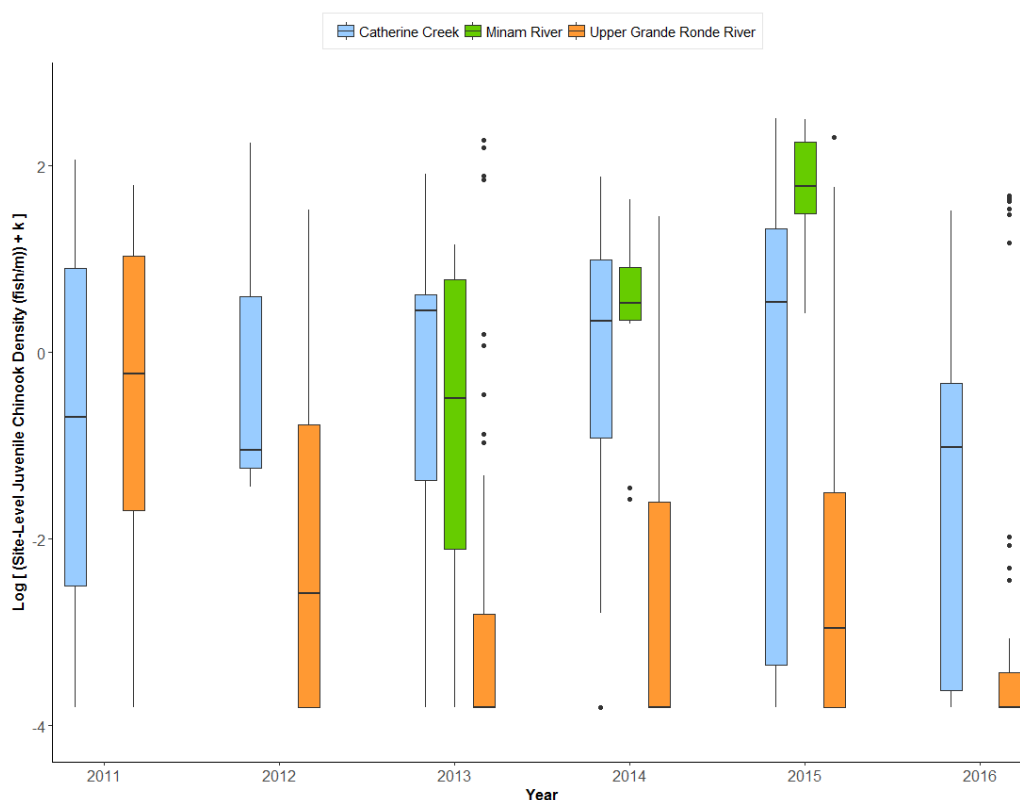


Figure 108. Juvenile spring Chinook Salmon density (fish/m) by ICTRT population from 2011-2016 in Catherine Creek and Upper Grande Ronde River, and from 2013-2015 in the Minam River. Fish density is log + k transformed to better visualize differences, where $k = D_{\min} + D_{\min}/2 = 0.002$ and D_{\min} is the minimum non-zero density value.

The apparent declines in juvenile populations could be due to the recent variations in temperature and stream flow along with other local environmental factors. Alternatively (or additionally), juvenile densities could be responding to shifts in returning spawner abundances or out-of-basin factors including ocean and mainstem Snake and Columbia River conditions. Our work in assigning likely causal factors for the declines is in the preliminary stages. In the face of lower stream flows and higher water temperatures, the Minam, our reference watershed, will continue to be an essential comparison to the

more impacted watersheds of the Grande Ronde and Catherine Creek. Less impacted streams such as wilderness areas or roadless areas have previously been shown to provide a refuge for salmonid populations during droughts even though productivity can be lower overall due to watershed characteristics intrinsic to those areas (higher elevation, simpler riparian communities, colder water temperature, etc.) (White and Rahel 2008).

SEM revealed that higher frequencies of large woody debris and pool availability positively influenced Juvenile Chinook Salmon densities as expected (Figure 109). Large wood had both a *direct* influence on fish density and an *indirect* effect through its positive association with pools. To evaluate the total effect of wood on fish relative to other factors in the model, the sum of the direct standardized path coefficient between wood and fish (0.20) and product of the path of wood on pools (0.47) and pools to fish (0.19) yields a coefficient of 0.29, which is greater than the direct effect of wood on fish, underlining the importance of the indirect role of wood in forming pools used by fish. Landscape context was also an important consideration in this model: reaches with larger cumulative drainage area were strongly associated with higher fish densities, more pools, and lower wood frequency.

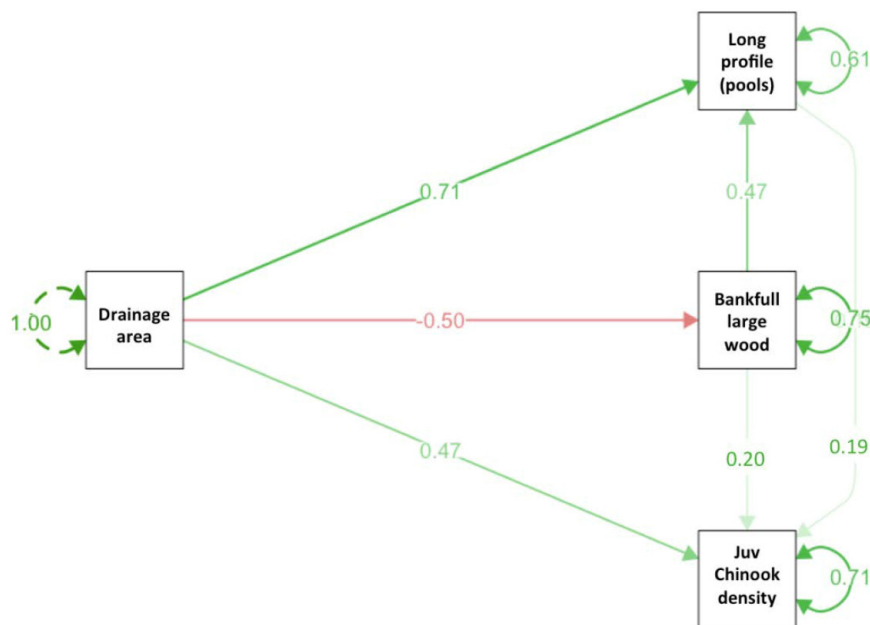


Figure 109. SEM results linking cumulative drainage area with longitudinal thalweg depth profile (a proxy for pool frequency), large wood frequency within the bankfull channel, and juvenile Chinook density (fish/m). Direction of arrows indicates the hypothesized direction of causal effect; whereas the color, shade, sign, and magnitude of the path coefficients indicate the direction and strength of the relationship (green is positive, red is negative, coefficients closer to |1| and darker shade of arrow are stronger). Values in double-headed arrows are amount of variance explained for dependent variables (analogous to R² in linear regression).

The effects of local-scale habitat conditions on fish density would have been obscured without incorporating a variable accounting for the position of reaches in the stream network. Mossop and Bradford (2006) used a similar conceptual model explaining associations among juvenile Chinook salmon density, wood, pools, and reach gradient in small tributaries of the upper Yukon River, Canada. Their study was based on visualizing pairwise correlation coefficients, however, and did not account for the variance-covariance structure inherent in modern SEM.

In the Upper Grande River subbasin, SEMs are one approach to estimating tributary rearing capacity of juvenile Chinook Salmon (*Oncorhynchus tshawytscha*). For this purpose, capacity is defined as the upper limit of abundance or density of a particular life stage under current conditions. As such, approaches that estimate the uppermost distribution of fish density should be used. Traditional SEMs, like most other regression-based approaches, estimate the influence of predictor variables (e.g., habitat condition) on the average value of a response variable (e.g., fish abundance). However, recent advances in 'piecewise SEM' permit non-normal distributions, random effects, and different correlation structures using local estimation (Lefcheck 2016); piecewise SEM could employ quantile regression to estimate the upper 90th percentile of fish density as a proxy for carrying capacity. Alternative proxies for carrying capacity could include modeling the maximum observed fish densities in years with highest previous-year spawner returns, or standardizing fish density estimates by previous-year spawner returns when that information is known. Because aquatic habitats across the Columbia River basin have been in a state of degradation for several decades (McIntosh et al. 2000), and because it is problematic for migratory species to navigate over man-made barriers (Humphries and Winemiller 2009), values of carrying capacity based on contemporary, empirical data should be considered conservative estimates at best.

References

- Arhonditsis, G.B., C.A. Stow, L.J. Steinburg, M.A. Kenney, R.C. Lathrop, S.J. McBride, and K.H. Reckhow. 2006. Exploring Ecological Patterns with Structural Equation Modeling and Bayesian Analysis. *Ecological Modelling* 192: 385–409.
- Belovsky, Gary E., Doyle Stephens, Clay Perschon, Paul Birdsey, Don Paul, David Naftz, Robert Baskin, et al. 2011. The Great Salt Lake Ecosystem (Utah, USA): Long Term Data and a Structural Equation Approach. *Ecosphere* 2 (3): 1–40. doi:10.1890/ES10-00091.1.
- Budy, Phaedra, Matthew Baker, and Samuel K. Dahle. 2011. Predicting Fish Growth Potential and Identifying Water Quality Constraints: A Spatially-Explicit Bioenergetics Approach. *Environmental Management* 48 (4): 691–709. doi:10.1007/s00267-011-9717-1.
- Duffy, J. Emmett, Jonathan S. Lefcheck, Rick D. Stuart-Smith, Sergio A. Navarrete, and Graham J. Edgar. 2016. Biodiversity Enhances Reef Fish Biomass and Resistance to Climate Change. *Proceedings of the National Academy of Sciences* 113 (22): 6230–35. doi:10.1073/pnas.1524465113.
- Fausch, K.D., C.L. Hawkes, and M.G. Parsons. 1988. Models That Predict Standing Crop of Stream Fish from Habitat Variables: 1950-85. General Technical Report PNW-GTR-213. U.S. Department of Agriculture, Forest Service, Pacific Northwest Research Station.
- Grace, James B., T. Michael Anderson, Han Olff, and Samuel M. Scheiner. 2010. On the Specification of Structural Equation Models for Ecological Systems. *Ecological Monographs* 80 (1): 67–87. doi:10.1890/09-0464.1.
- Grace, J.B. 2006. *Structural Equation Modeling and Natural Systems*. Cambridge, NY: Cambridge University Press.
- Grace, J.B. 2007. Structural Equation Modeling for Observational Studies. *The Journal of Wildlife Management* 72 (1): 14–22.
- Humphries, Paul, and Kirk O. Winemiller. 2009. Historical Impacts on River Fauna, Shifting Baselines, and Challenges for Restoration. *BioScience* 59 (8): 673–84. doi:10.1525/bio.2009.59.8.9.
- Irvine, Kathryn M., Scott W. Miller, Robert K. Al-Chokhachy, Eric K. Archer, Brett B. Roper, and Jeffrey L. Kershner. 2015. Empirical Evaluation of the Conceptual Model Underpinning a Regional Aquatic Long-Term Monitoring Program Using Causal Modelling. *Ecological Indicators* 50 (March): 8–23. doi:10.1016/j.ecolind.2014.10.011.
- Isaak, Daniel J., and Wayne A. Hubert. 2001. A Hypothesis About Factors That Affect Maximum Summer Stream Temperatures Across Montane Landscapes. *JAWRA Journal of the American Water Resources Association* 37 (2): 351–66. doi:10.1111/j.1752-1688.2001.tb00974.x.
- Jackson, D.A., P.R. Peres-Neto, and J.D. Olden. 2001. What Controls Who Is Where in Freshwater Fish Communities -- the Roles of Biotic, Abiotic, and Spatial Factors. *Canadian Journal of Fisheries and Aquatic Sciences* 58 (1): 157–70. doi:10.1139/f00-239.

- Jonasson, B., E. Sedell, S. K. Banks, A. B. Garner, C. Horn, K. L. Bliesner, J. W. Dowdy, F. W. Drake, S. D. Favrot, J. M. Hay, N. A. McConnell, J. P. Ophoff, B. C. Power, J. R. Ruzycki, and R. W. Carmichael. 2015. Investigations into the life history of naturally produced spring Chinook Salmon and summer steelhead in the Grande Ronde River Subbasin. Annual Report 2014, BPA Project # 1992-026-04, Oregon Department of Fish and Wildlife, La Grande, Oregon.
- Lefcheck, Jonathan S. 2016. piecewiseSEM: Piecewise Structural Equation Modelling in R for Ecology, Evolution, and Systematics. Edited by Robert Freckleton. *Methods in Ecology and Evolution* 7 (5): 573–79. doi:10.1111/2041-210X.12512.
- Maloney, Kelly O., and Donald E. Weller. 2011. Anthropogenic Disturbance and Streams: Land Use and Land-Use Change Affect Stream Ecosystems via Multiple Pathways. *Freshwater Biology* 56 (3): 611–26. doi:10.1111/j.1365-2427.2010.02522.x.
- McCullough, D.A., S.M White, C. Justice, M. Blanchard, R. Lessard, D. Kelsey, D. Graves, and J. Nowinski. 2015. Assessing the Status and Trends of Spring Chinook Habitat in the Upper Grande Ronde River and Catherine Creek. Annual Report to Bonneville Power Administration. Portland, OR: Columbia River Inter-Tribal Fish Commission.
- McIntosh, B.A., J.R. Sedell, R.F. Thurow, S.E. Clarke, and G.L. Chandler. 2000. Historical Changes in Pool Habitats in the Columbia River Basin. *Ecological Applications* 10 (5): 1478–96. doi:10.1890/1051-0761(2000)010[1478:HCIPHI]2.0.CO;2.
- Mossop, Brent, and Michael J Bradford. 2006. Using Thalweg Profiling to Assess and Monitor Juvenile Salmon (*Oncorhynchus* Spp.) Habitat in Small Streams. *Canadian Journal of Fisheries and Aquatic Sciences* 63 (7): 1515–25. doi:10.1139/f06-060.
- O’Neal, J. 2007. Snorkel surveys. In *Salmonid Field Protocols Handbook*, ed. D.H. Johnson, B.M. Shrier, J. O’Neal, J.A. Knutzen, X. Augerot, T.A. O’Neil, and T.N. Pearsons, 325-339. Bethesda, Maryland: American Fisheries Society. <https://www.monitoringmethods.org/Method/Details/136>.
- Shipley, Bill. 2002. *Cause and Correlation in Biology: A User’s Guide to Path Analysis, Structural Equations and Causal Inference*. 1 edition. Cambridge: Cambridge University Press.
- Thurow, R.F. 1994. Underwater Methods for Study of Salmonids in the Intermountain West. General Technical Report. Ogden, UT: US Department of Agriculture, Forest Service, Intermountain Research Station.
- White, S.M, C. Justice, D. McCullough. 2012. Protocol for snorkel surveys of fish densities. A component of BPA Project 2009-004-00: Monitoring Recovery Trends in Key Spring Chinook Habitat Variables and Validation of Population Viability Indicators. 15 p. <https://www.monitoringmethods.org/Protocol/Details/499>.

White, S.M., and F.J. Rahel. 2008. Complementation of habitats for Bonneville cutthroat trout in watersheds influenced by beavers, livestock, and drought. *Transactions of the American Fisheries Society* 137 (3): 881–94.

Wu, Amery D., and Bruno D. Zumbo. 2008. Understanding and Using Mediators and Moderators. *Social Indicators Research* 87 (3): 367. doi:10.1007/s11205-007-9143-1.

Zou, S., and Y-S. Yu. 1994. A General Structural Equation Model for River Water Quality Data. *Journal of Hydrology* 162: 197–209.

Redd / Stream Gradient Analysis

Introduction

In order to better understand the spawning habitat preferences of Chinook Salmon *Oncorhynchus tshawytscha* in the Upper Grande Ronde River Basin (UGRRB), our project is investigating several different habitat characteristics. A better understanding of these habitat preferences will allow us to estimate the location and amount of suitable habitat that is available throughout this river basin, and elsewhere. Stream gradient is thought to have an important influence on egg survival, and hence is an important habitat characteristic. For this analysis, we calculated the mean stream gradient around each Chinook redd recorded in our study area.

Methods

For this analysis we assessed the stream gradient of Chinook redd locations sampled between 2009 and 2016. Redd locations were previously collected with GPS. by field staff of the Oregon Department of Fish and Wildlife, and these location were used to create a GIS layer. 1-meter resolution LiDAR data were collected by Watershed Sciences, Inc. for select stream corridors of the UGRRB in 2012 and used to create a “bare earth” GIS layer, providing a high-resolution (1-meter pixel) representation of base elevation. A stream channel vector layer was created by Watershed Sciences from this elevation layer, which follows the lowest elevation in the stream corridor.

During 2017, we transferred the redd location coordinates to their corresponding locations on the stream channel vector layer, discarding any coordinates that fell at a distance greater than 10 meters from the stream channel to control for inaccurate coordinates. Of the streams with LiDAR measurements, the redds fell primarily on the Grande Ronde River mainstem but also on the following tributaries: Limber Jim Creek, McCoy Creek, and Sheep Creek. We created linear referenced “routes” along the channel vectors of these streams, in order to measure stream distances along these routes. For each redd on these stream routes, we measured two additional coordinates: (i) a stream position 40 meters upstream of the redd, and (ii) a stream position 40 meters downstream of the redd. We next calculated the base elevation at each of these coordinates with the LiDAR data. Finally, we calculated the mean gradient in the stream segment that each redd is centered on as (upstream elevation – downstream elevation) / stream segment distance (80 meters). We removed 6 outlier records (out of 848 total records) that appeared to be erroneous, and then summarized the rest of the results as shown below in the Results/Discussion section.

Results and Discussion

The redds were grouped into brackets according to their mean stream gradient, and summarized in Figure 110. The largest grouping of redds (387 of 842) occurred at locations with mean gradients between 0.51 and 1.00%, with the next largest grouping (281 of 842) occurring where mean gradients were between 1.00 and 1.51%. Very few redds (43 of 842) occurred in locations where mean gradients exceeded 2%. The mean stream gradient for all redds was 1.09%.

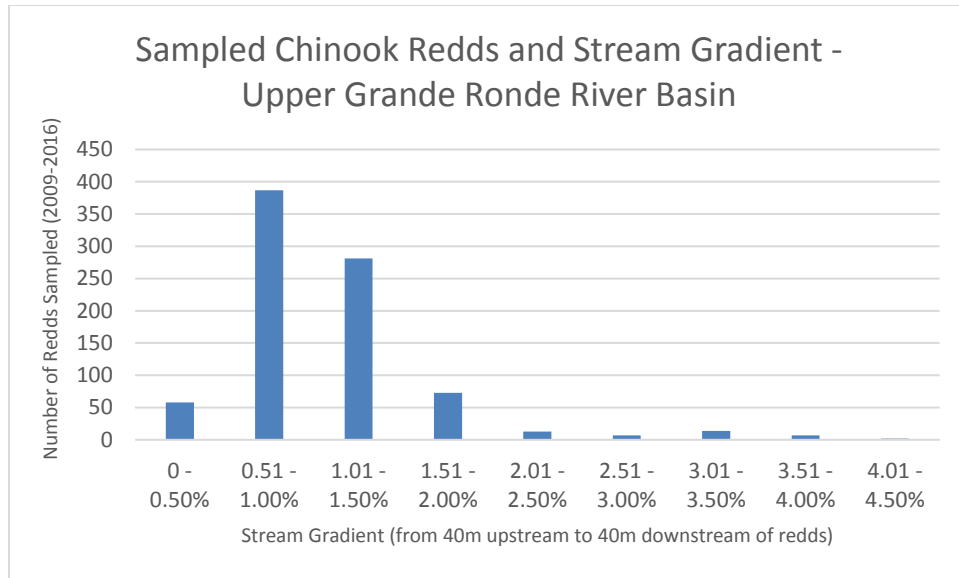


Figure 110. Graph of summary stream gradient results for Chinook redd locations.

The results shown here provide a reasonable estimate of Chinook preference for stream gradient at spawning locations. The stream segment length (80 meters) likely overlooks micro-scale variations in gradient, but provides a general estimate of suitable gradient at an appropriate resolution given by the resolution of the redd data. Cram et al. (2017) studied several Chinook salmon spawning sites in a nearby basin (the Yakima River) to determine which habitat conditions most accurately predicted spawning preference. They found stream power and depth to be the most important predictors of habitat preference, with other secondary and tertiary predictors including bed substrate composition, channel sinuosity and braiding, overhead vegetative cover, thermal variability, and gradient. In general, gradient, when considered in conjunction with stream flow, may be considered a proxy for the primary habitat predictors of flow velocity, depth, and stream power. The finding by Cram et al. (2017) that gradient was a secondary predictor is probably an artifact of the spatial scale of their analysis. They relied on NetMap DEM data to calculate channel gradient. NetMap data had a resolution of 100-1000 m in reach lengths. Also, spatial scales for analysis of redd distributions were 800 m, 3 km, and 6 km, which could easily result in more gross generalizations.

Water temperature is another critical factor that constrains location of Chinook spawning sites and egg survival (McCullough 1999), and suitable temperatures may be considered a consequence of some of the secondary habitat predictors uncovered by Cram et al. (2017) such as riparian cover and stream connections to zones of hyporheic exchange. Additionally, the spatial connectivity of suitable habitat characteristics is an important consideration for Chinook redd occurrence and density (Isaak, et al. 2007).

With the results of this analysis of preferred gradients for spring Chinook Salmon spawning, we plan to proceed to examine stream gradient in other streams within the UGRRB having LiDAR coverage in conjunction with other habitat characteristics. We hypothesize that habitat suitability for Chinook spawning may be assessed on a systematic basis with a knowledge of stream gradient, summer water

temperature, and summer stream discharge, and local migratory barriers. This preliminary study revealed preference for channel gradient on a relatively meso scale, but it will be important to classify all stream reaches according to suitability in terms of water temperature and streamflow in particular. The combination of preference for gradient, summertime water temperature, and streamflow will help identify the availability (e.g., area of stream bottom available) having preferred habitat conditions. Utilization rate and availability together will provide key information in estimating Chinook redd capacity for application in our life cycle model.

References

- Cram, J. M., C. E. Torgersen, R. S. Klett, G. R. Pess, D May, T. N. Pearsons and A. H. Dittman. 2017. Spatial variability of Chinook Salmon Spawning distribution and habitat preferences. *Transactions of the American Fisheries Society* 146(2): 206-221, DOI: 10.1080/00028487.2016.1254112
- Isaak, D. J., R. F. Thurow, B. E. Rieman, and J. B. Dunham. 2007. Chinook Salmon use of spawning patches: relative roles of habitat quality, size, and connectivity. *Ecological Applications* 17:352–364.
- McCullough, D.A. 1999. A review and synthesis of effects of alterations to the water temperature regime on freshwater life stages of salmonids, with special reference to Chinook Salmon. U.S. Environmental Protection Agency, Region 10. Seattle, Washington.
- Torgersen, C. E., D. M. Price, H. W. Li, and B. A. McIntosh. 1999. Multiscale thermal refugia and stream habitat associations of chinook salmon in northeastern Oregon. *Ecological Applications* 9:301–319.

Influence of Water Temperature on Spawning Success

Full Title: Influence of Water Temperature on Spawning Success of Spring Chinook Salmon in the Grande Ronde and Imnaha River Basins, Northeast Oregon.

March 2017

Prepared by:

Casey Justice

Columbia River Inter-Tribal Fish Commission (CRITFC), 700 NE Multnomah St., Suite 1200, Portland OR 97232, jusc@critfc.org

Joseph Feldhaus

Oregon Department of Fish and Wildlife, La Grande Fish Research Office, Badgley 203, One University Boulevard, La Grande, OR 97850

Denise Kelsey (CRITFC)

Abstract

High mortality rates of adult salmon prior to spawning can significantly influence a population's long-term viability, a problem that is likely to be exacerbated by warming stream temperatures associated with climate change. In this study, we used a long time series of salmon carcass recovery data from seven populations of spring- and summer-run Chinook Salmon in the Grande Ronde and Imnaha River basins in Northeast Oregon coupled with water temperature predictions from the NorWeST water temperature model to evaluate the relationship between summer water temperature and spawning success (the complement of pre-spawn mortality). Despite a high degree of spatial and temporal variability in estimates of spawning success, our analysis revealed a significant negative effect of water temperature on the probability of spawning success. Specifically, the predicted proportion spawned for the average river decreased from approximately 1 at 9 °C to about 0.45 at 19 °C, with the proportion spawned decreasing sharply as temperatures exceeded approximately 14-15 °C. These results add to a substantial body of evidence linking high water temperature to reduced spawning success in Pacific Northwest salmon populations and highlight the need for continued habitat restoration or other management actions to improve temperature conditions for fish in temperature-impaired watersheds.

Introduction

Adult Pacific salmon that have successfully migrated to their spawning grounds often die prior to spawning, a process commonly referred to as pre-spawn mortality. High pre-spawn mortality rates observed in salmon populations throughout the Pacific Northwest (up to 90 %; Bowerman et al. 2016) have raised awareness among natural resource managers of the potential threat that pre-spawn mortality poses to population persistence and recovery potential (Keefer et al. 2010, Bowerman et al. 2016) and of need to identify and quantify the environmental and biological factors influencing pre-spawn mortality (Roumasset 2012, King et al. 2013). Some factors that have been associated with pre-spawn mortality include high water temperature (CTUIR and ODFW 2007, Quinn et al. 2007, Keefer et al. 2010, Roumasset 2012), streamflow (Quinn et al. 2007), pollutants (Feist et al. 2011, Scholz et al. 2011), infectious disease (CDFG 2004, Benda et al. 2015), and high fish density (Quinn et al. 2007). Of these factors, high water temperature is most consistently associated with high rates of pre-spawn mortality.

Despite the growing body of evidence linking environmental factors to pre-spawn mortality, recent research has shown a high degree of spatial variability in pre-spawn mortality rates both within and across different geographic areas (Bowerman et al. 2016, Roumasset 2012), suggesting that the environmental or biological factors influencing pre-spawn mortality are likely to be somewhat specific to a given area or fish population. For example, spring and summer-run Chinook Salmon are likely more susceptible to high summer water temperatures than fall Chinook because they typically spawn during August and September when temperatures are at their peak, while fall Chinook enter freshwater and spawn in fall when temperatures are cooler. Thus, the development of predictive models relating environmental factors to pre-spawn mortality should be tailored to the area and population of interest.

Given the increasing threat of climate change and associated warming of streams on fish populations across the Pacific Northwest (Beechie et al. 2013) and North America (Lynch et al. 2016), it is important to understand the extent to which water temperature influences pre-spawn mortality in threatened salmon populations. In this study, we used salmon carcass recovery data on spawning grounds to estimate the probability of spawning success—the complement of pre-spawn mortality—for seven populations of spring- and summer-run Chinook Salmon in the Grande Ronde and Imnaha River basins of NE Oregon. The objective of this research was to evaluate the influence of water temperature on the probability of spawning success. The results from this study were intended to provide managers with the ability to predict how future changes in land management or climate could influence salmon population viability.

Methods

We used water temperature predictions from the NorWeST water temperature model (Isaak et al. 2011) to estimate average water temperatures for each survey reach and year. The NorWeST model provided year-specific predictions of average August water temperature (°C) (*AvgAugTemp*) from 2000 through 2013 for points spaced approximately every kilometer throughout the stream network. This model has been shown to produce robust estimates of water temperature across a large geographic area (Mid-Columbia region model: $R^2 = 0.94$, Root Mean Square Prediction Error = 0.91 °C) (Isaak et al. 2011).

NorWeST prediction points that overlapped spawning reaches were joined to each reach using a spatial join tool in ArcGIS and all prediction points were then averaged by reach and year.

We obtained Chinook Salmon spawning survey data from the Oregon Department of Fish and Wildlife (ODFW) spanning 14 years (2000-2013), 9 different rivers and 112 unique survey reaches within the Grande Ronde and Imnaha River basins (Figure 111). Spawning surveys were conducted within selected reaches in each river ranging in size from 0.3 to 8.5 km (mean = 3.2 km). Surveys were intended to cover the entire spawning extent within each river, with gaps occurring because of landowners permission or other safety or logistical reasons. We used carcass recovery data from female hatchery and natural origin Chinook Salmon to estimate spawning success within each survey reach. For each female salmon carcass observed in a reach, field crews recorded the “percent spawned” based on a visual estimate of the percentage of eggs remaining in each carcass. We designated the spawning outcome for each fish as successful if fewer than 50 % of the eggs were remaining in the carcass (Feldhaus et al. 2017). Percent spawned was not estimated for male fish. Thus, spawning success for each female fish was defined by a binary variable, where 1 = successfully spawned, and 0 = failed to spawn.

Some observations were removed from the dataset prior to analysis because the percent spawned was not recorded or couldn’t be determined in the field, or because fish were outplanted from a hatchery (i.e., captive broodstock) and may consequently have lower spawning success compared with non-transplanted fish (Flagg and Mahnaken 1995, DeWeber et al. 2017). Additionally, data from rivers with fewer than 20 records (i.e., unique combinations of river, reach and year) were excluded from the analysis to ensure sufficient sample size to estimate a temperature effect on the proportion spawned (Bowerman et al. 2016). The final dataset consisted of 8,490 individual female fish carcasses, totaling 739 unique river, reach and year combinations.

We used a generalized linear mixed effects model implemented with the lme4 package in Program R (Bates et al. 2015) to examine the relationship between water temperature and the probability of spawning success (also referred to as “proportion spawned”). Proportion spawned refers to the proportion of fish that successfully released their gametes out of the total number that reached the spawning grounds, the complement of which is pre-spawn mortality (i.e., pre-spawn mortality = 1 – proportion spawned). This metric does not account for the proportion of fish that die during upstream migration (en-route mortality).

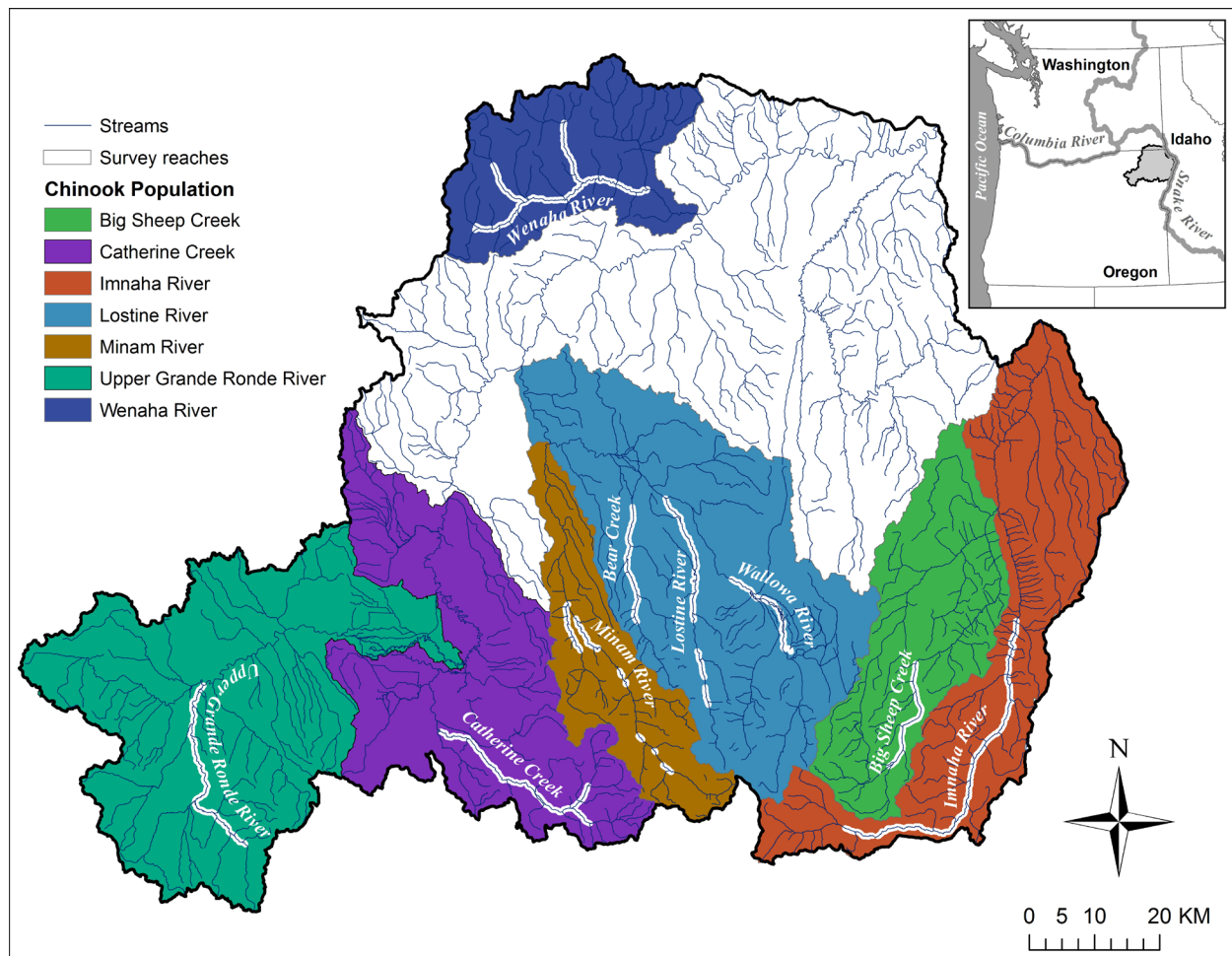


Figure 111. Study area showing locations of spawning survey reaches and spring Chinook Salmon population boundaries in the Grande Ronde and Imnaha River basins in NE Oregon.

Because the spawning survey data was grouped by different rivers and reaches within rivers, it was not appropriate to assume that all observations were statistically independent—a key assumption in general linear modeling. Instead, we assumed that spawning success would vary across rivers because of differences in environmental conditions (Rand et al. 2006, Roumasset 2012), or other population-specific parameters such as run timing (Hinch et al. 2012). In addition, because survey reaches were nested within rivers, estimates of spawning success from reaches within a particular river were likely to be more related than estimates from reaches in a different river. Finally, surveys within each reach were repeated over a number of years (i.e., repeated measures design), resulting in replicates within each reach that were not independent random samples.

We accounted for the lack of statistical independence inherent in this hierarchical repeated measures design by using a mixed-effects model which included *Year*, *River* and *Reach(River)* (i.e., *Reach* nested within *River*) as random grouping effects. *Year* represented the random variation between years, and was intended to capture additional variation in spawner success that was not explained by water temperature. The factor *River* represented the variation between rivers, and *Reach(River)* represented the variation between reaches of the same river. Treating these grouping factors as random effects

rather than fixed effect categorical variables is a more efficient method for analyzing the data because it uses fewer degrees of freedom (Zuur et al. 2009). In addition, treating *River* as a random effect allows us to make general predictions about the influence of water temperature on spawning success in the typical river, including rivers outside of those included in our dataset.

The response variable was proportion spawned (p), defined as the number of female fish that successfully spawned (Y) out of the total number of female carcasses that were recovered and for which spawning success could be estimated (n) for each annual observation in each reach within each river. We assumed Y was binomially distributed ($Y \sim B(n, p)$). A logit link function was used to linearize the relationship between the response and explanatory variables as given by the formula:

$$\text{logit}(p) = \ln\left(\frac{p}{1-p}\right).$$

The final model formula was given by:

$$\text{logit}(p) = \text{AvgAugTemp} + \text{Year} + \text{River} + \text{Reach}(\text{River}),$$

where *AvgAugTemp* is the fixed effect explanatory variable (i.e., average August water temperature), and *Year*, *River* and *Reach(River)* are random effects as described above. This model structure assumed a common slope for the effect of temperature on $\text{logit}(p)$ across all rivers and years, but allowed for differences in the model intercept. We assumed that the slope of the temperature effect was largely driven by physiological tolerance limits to water temperature, and was therefore not likely to differ significantly among rivers within the same general region.

Model assumptions were evaluated using standard diagnostic plots generated with the DHARMA package in R (Hartig 2016) and by computing the dispersion parameter $\hat{\phi}$, which provides an indication of potential overdispersion in the data (Harrison 2014). The proportion of deviance explained by the model (pseudo- R^2) was computed using methods described in Nakagawa and Schielzeth (2013) and implemented in package MuMIn in R.

All model predictions, confidence intervals, and prediction plots were generated using the effects package (Fox 2003, Fox and Hong 2009) and sjPlot package (Lüdtke 2017) in program R. Model predictions were untransformed from the linear logit scale to the non-linear “real” scale using the formula:

$$p = \frac{e^{\text{logit}(p)}}{1 + e^{\text{logit}(p)}}.$$

Results

August water temperatures varied considerably across years and rivers, as well as longitudinally within a river (Figure 112). Mean August water temperatures were highest in the Wallowa River (mean = 16.8 °C) and Upper Grande Ronde River (mean = 15.6 °C) and lowest in the Wenaha River (mean = 11.5 °C), Bear Creek (mean = 12.8 °C), and Minam Rivers (mean = 12.9 °C). Spatial variation in water temperature within a river, as denoted by the spread of the data shown in each of the boxes in Figure 112 was

generally lowest in the Minam River, Big Sheep Creek, Bear Creek, and Lostine River, and highest in the Upper Grande Ronde River, Wenaha River, Imnaha River, and Catherine Creek. Inter-annual variation in water temperature was generally similar across rivers, with the highest water temperatures occurring in 2001, 2005, and 2012, and the lowest in 2002, 2006, and 2010.

The proportion of fish that successfully spawned was highly variable across rivers, years, and along a gradient of water temperature, as determined from preliminary plots of the raw data (Figures 3-6). Reach-specific estimates of proportion spawned in rivers such as the Minam River, Wallowa River, Wenaha River, and to a lesser extent, Catherine Creek, were predominantly close to one, while other rivers such as Bear Creek, Big Sheep Creek, Imnaha River, Lostine River, and Upper Grande Ronde River showed a considerably larger range in proportion spawned (Figure 113). Although median values of proportion spawned tended to be close to one in all years, some years such as 2002, 2009, and 2013 had lower and more variable estimates of proportion spawned compared with other years (Figure 114). The relationship between water temperature and proportion spawned appeared strongest for rivers such as the Imnaha River, Lostine River, and possibly Catherine Creek, but was generally weak or not readily apparent for most of the other rivers (Figure 115). However, bivariate plots of the relationship between water temperature and proportion spawned should be interpreted with caution because some of the variation in proportion spawned was explained by other factors such as *Year* that were not shown in the plots. When the data was grouped by year, the negative relationship between water temperature and proportion spawned was more readily apparent (Figure 116).

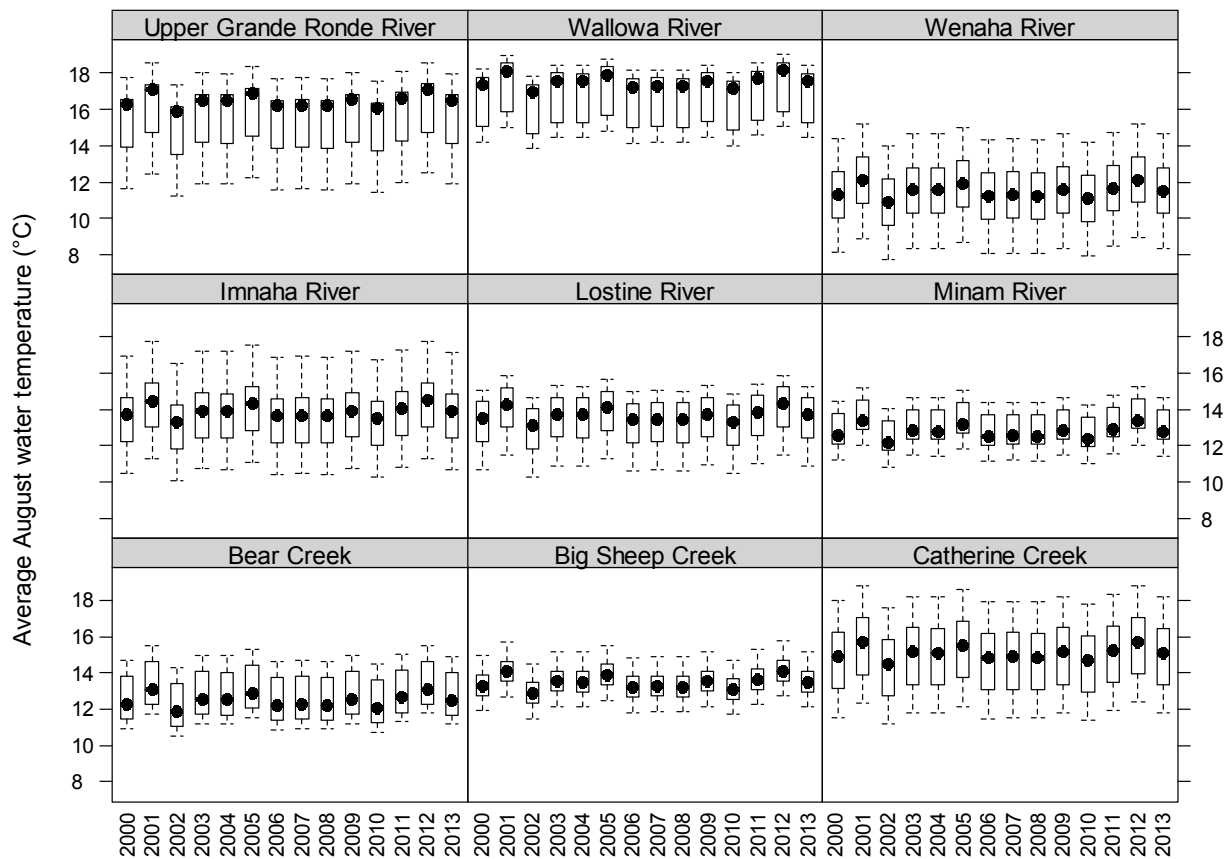


Figure 112. Boxplots of average August water temperature (°C) by year and river. Black dots represent medians, the bottom and top of the boxes show the 25th and 75th percentiles, respectively, and dashed lines show roughly two standard deviations.

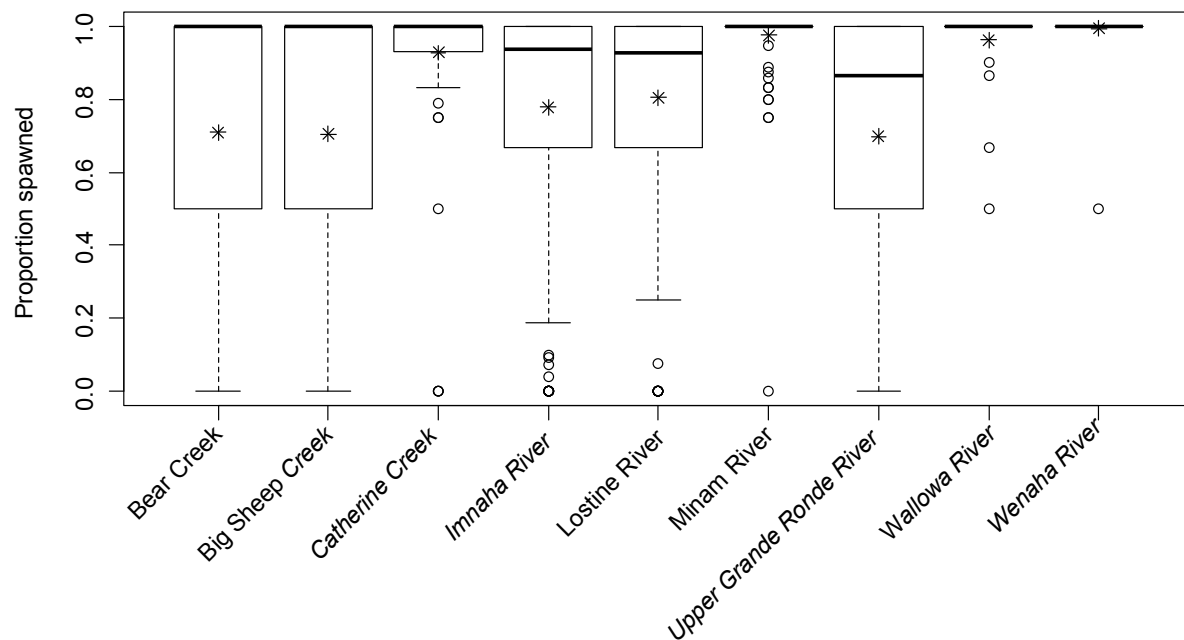


Figure 113. Boxplot of proportion spawned by *River* for all years combined. Horizontal lines represent medians, asterisks represent means, the bottom and top of the boxes show the 25th and 75th percentiles, respectively, vertical dashed lines show roughly 2 standard deviations, and points outside the whiskers are outliers.

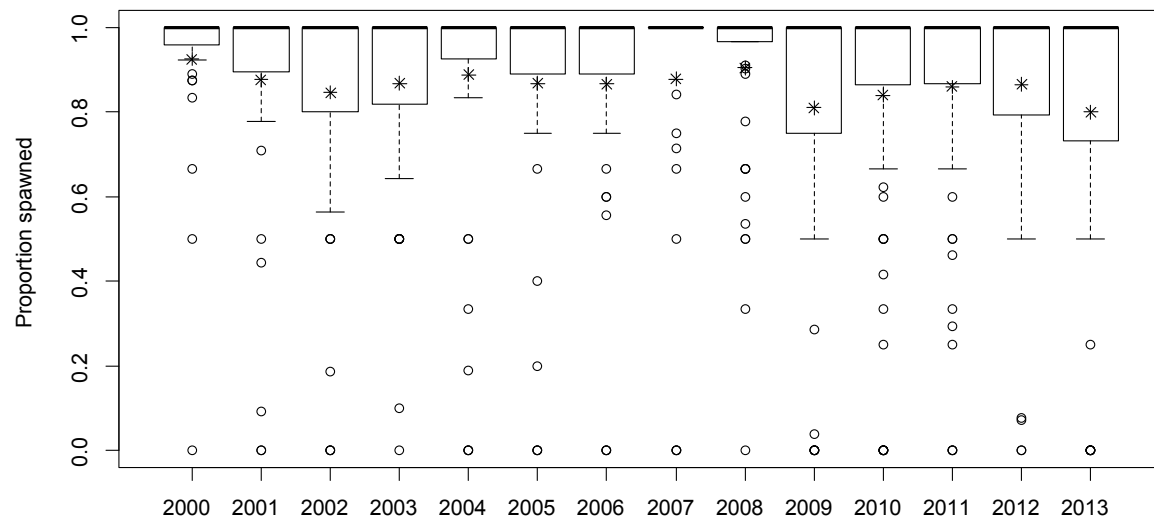


Figure 114. Boxplot of proportion spawned by *Year* for all rivers combined. Bold horizontal lines represent medians, asterisks represent means, the bottom and top of the boxes show the 25th and 75th percentiles, respectively, vertical dashed lines show roughly 2 standard deviations, and points outside the whiskers are outliers.

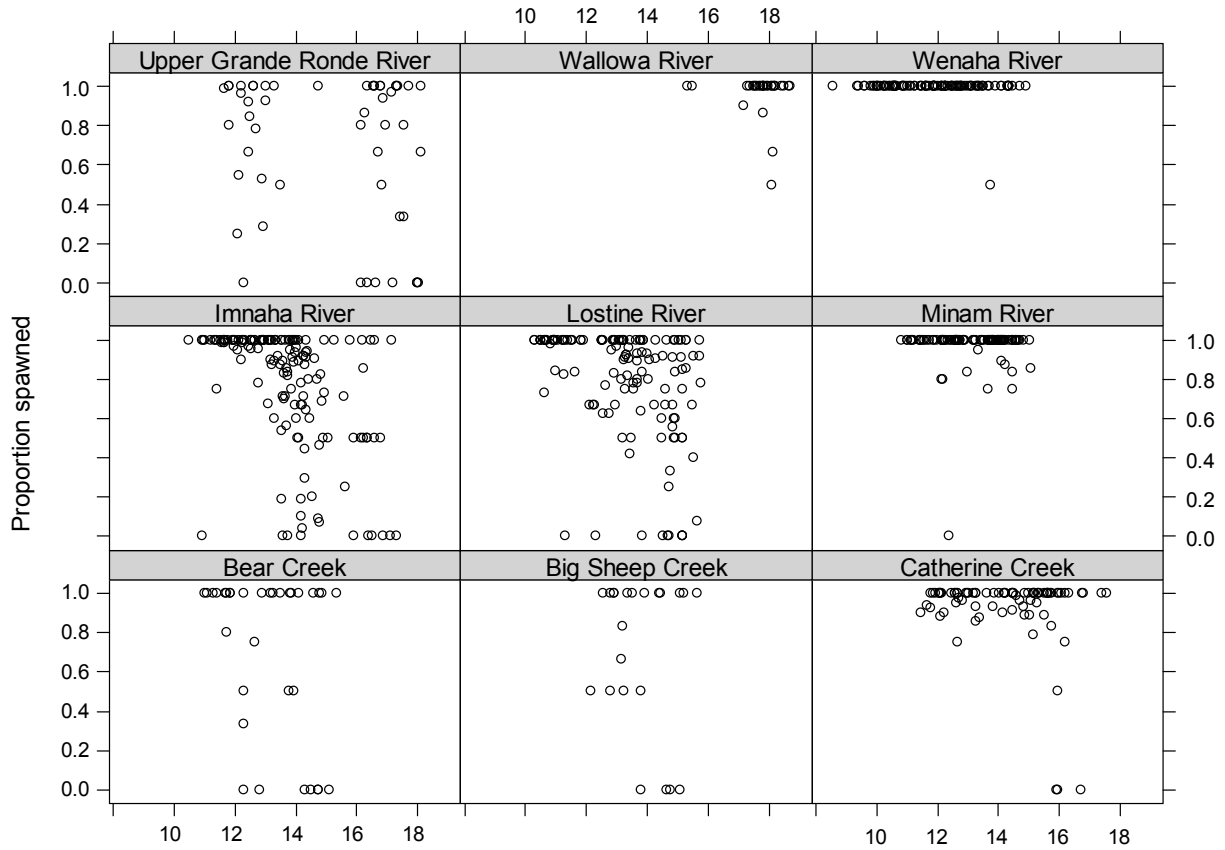


Figure 115. Scatterplots of proportion spawned as a function of average August water temperature (°C) grouped by *River* for all years combined.

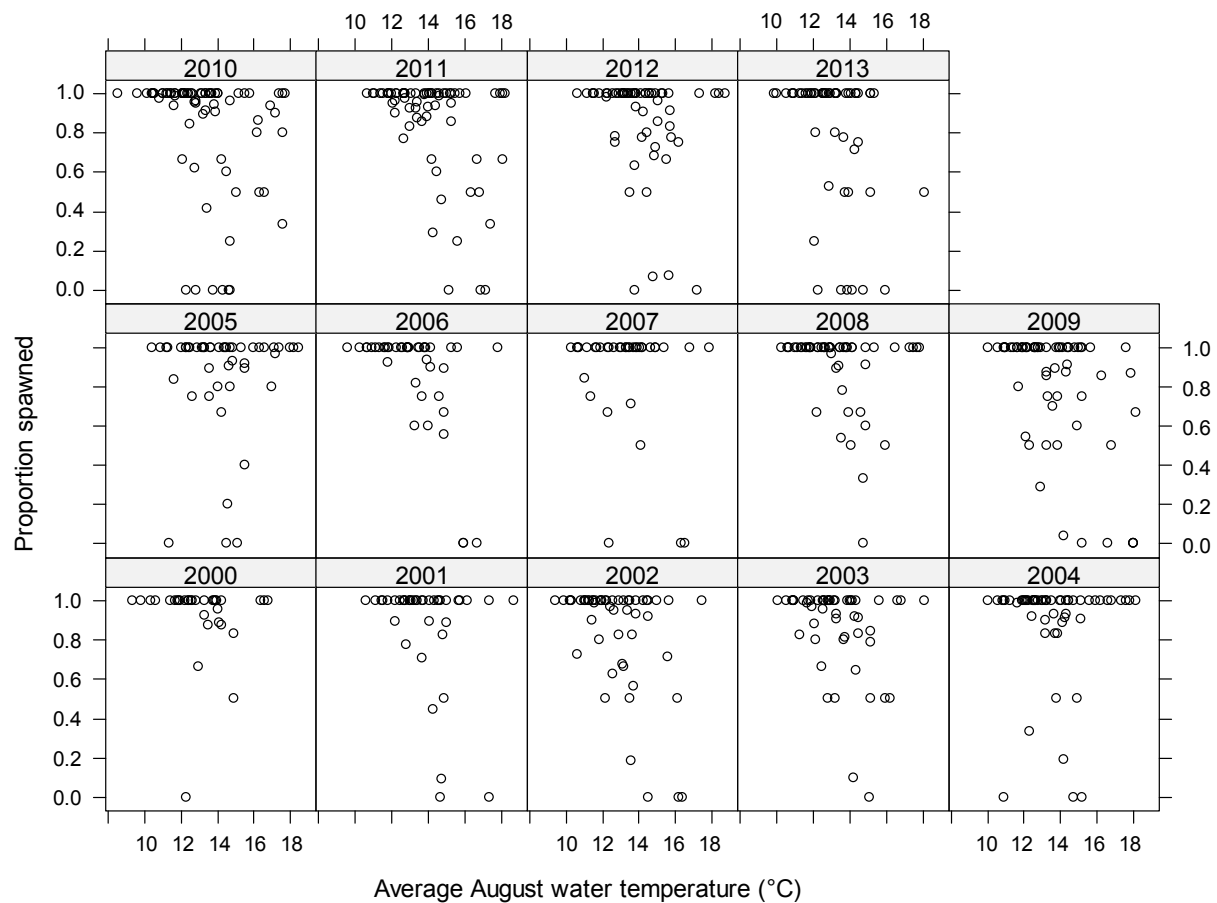


Figure 116. Scatterplots of proportion spawned as a function of average August water temperature (°C) grouped by Year for all rivers combined.

Diagnostic plots indicated that model assumptions of uniformly distributed residuals and homogeneity of variance in the y direction were satisfied. In addition, the dispersion parameter $\hat{\phi}$ was estimated to be 1.34, indicating a minimal amount of overdispersion in the data (Zuur et al. 2009), and therefore additional steps to correct for overdispersion were not merited.

The combination of fixed effects (*AvgAugTemp*) and random effects (*Year*, *River* and *Reach(River)*) explained approximately 56 % of the deviance in the data (conditional quasi- $R^2 = 0.56$), while *AvgAugTemp* alone explained approximately 13 % of the deviance (marginal quasi- $R^2 = 0.13$). A summary of model coefficients are provided in Table 51, and random effect intercepts for each river and year are provided in supplemental materials (Tables 2 and 3). According to this model, average August water temperature had a statistically significant negative effect on the proportion spawned (coefficient for *AvgAugTemp* = -0.58, $p < 0.0001$). The predicted proportion spawned for the average river decreased from approximately 1 at 9 °C to about 0.45 at 19 °C, with the proportion spawned decreasing sharply as temperatures exceeded approximately 14-15 °C (Figure 116). Confidence intervals around this curve were quite wide, indicating a high amount of across-river and -reach variation as well as random noise in the data.

This model implies one average curve for the effect of water temperature on proportion spawned (the thick black line shown in Figure 116) that is allowed to be shifted up or down for each river, year and reach. The magnitude of the vertical shift is defined by the standard deviation (Std. Dev.) for each random effect. For example, *River* explained the largest amount of the variation in proportion spawned (Std. Dev. = 1.66), followed by *Reach(River)* (Std. Dev. = 1.24), and finally by *Year* (Std. Dev. = 0.54) (Table 51).

Although the model structure assumed a common slope parameter for all rivers, the inclusion of a random intercept for *River* resulted in very different predictions of proportion spawned across rivers for a given value of water temperature (Figure 117). Consistent with plots of the raw data (Figure 115), rivers such as the Minam River, Wallowa River, and Wenaha River showed consistently high predicted values for proportion spawned across the range of temperatures sampled, while other rivers such as Bear Creek, Big Sheep Creek, Imnaha River, and Lostine River showed a more substantial decrease in proportion spawned with increased water temperature. The Upper Grande Ronde River, which showed no apparent relationship between proportion spawned and water temperature in plots of the raw data, was predicted to have a negative relationship with water temperature as a result of pooling the data from all rivers and assuming a common slope across rivers.

Table 51. Summary of model coefficients for global model (m1).

Random effects	Name	Variance	Std. Dev.	
<i>Reach(River)</i>	(Intercept)	1.549	1.244	
<i>Year</i>	(Intercept)	0.296	0.544	
<i>River</i>	(Intercept)	2.748	1.658	
Number of obs: 739, groups: Reach(River), 112; Year, 14; River, 9				
Fixed effects	Estimate	Std. Error	z	p-value
(Intercept)	10.852	1.495	7.260	3.86E-13
<i>AvgAugTemp</i>	-0.583	0.096	-6.067	1.30E-09

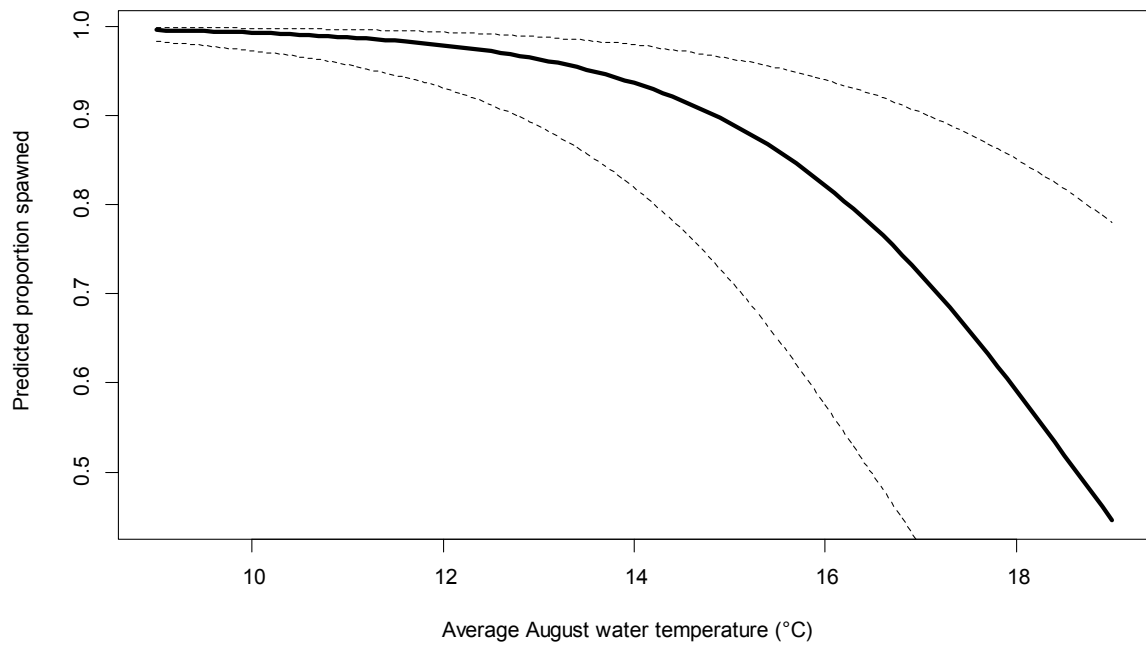


Figure 117. Predicted proportion spawned as a function of Average August water temperature (°C) for the average river (i.e., marginal effect of *AvgAugTemp*) from model m1. The dashed lines represent 95% confidence intervals.

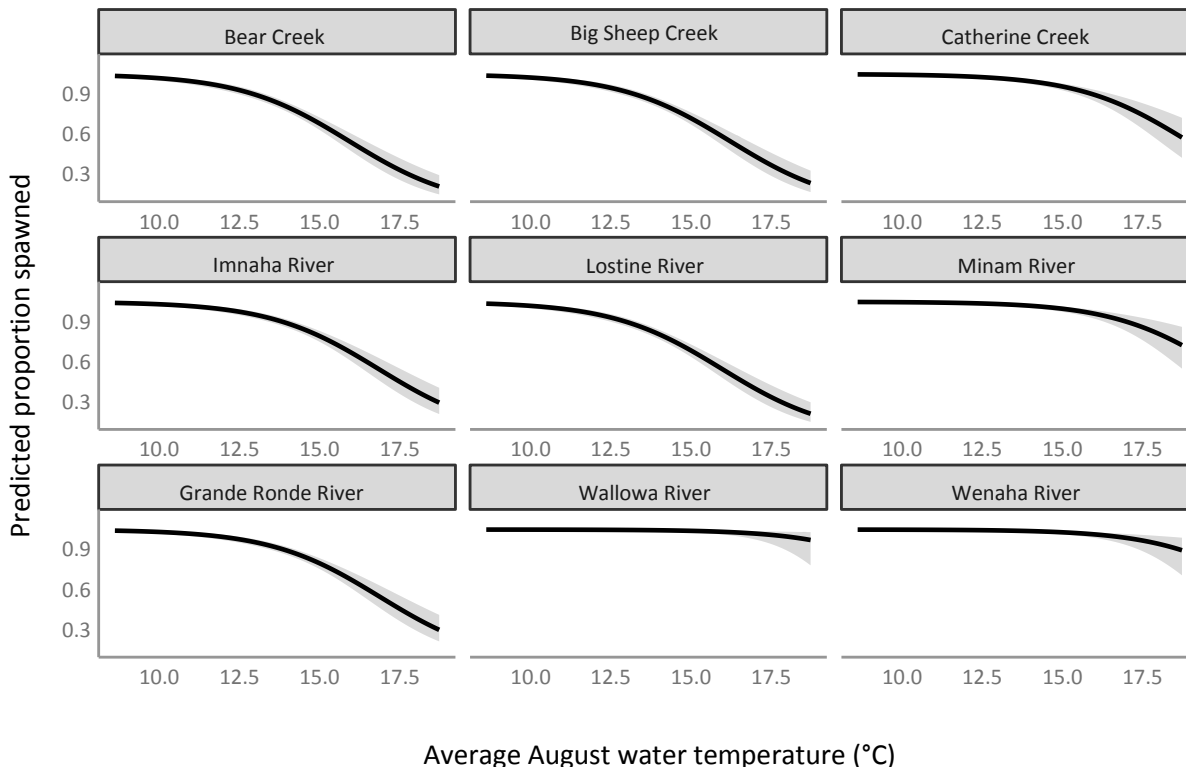


Figure 118. Predicted proportion spawned as a function of average August water temperature (°C) grouped by the random effect *River* from model m1. Shading around each bold line represents 95% confidence intervals.

Discussion

The probability of Grande Ronde/Imnaha Chinook Salmon spawning success declined significantly with increasing average August water temperature. Similar effects of water temperature on the probability of spawning success have been documented in other salmon populations in the Columbia and Willamette River basins (CTUIR and ODFW 2007, Keefer et al. 2010, Roumasset 2012) and elsewhere in the Pacific Northwest (Heard 1991, Hinch et al. 2012). To gain a better understanding of how the predicted temperature relationship with proportion spawned compared with other similar studies, we compared our results with the temperature/pre-spawn mortality curve presented in CTUIR and ODFW (2007) for spring Chinook Salmon in the Umatilla River (Figure 119), a nearby Eastern Oregon river with similar hydrologic and climatic characteristics. Because the Umatilla River study used maximum stream temperature as the predictor variable instead of average August temperature, we converted our predictor variable to maximum water temperature (*MaxTemp*) using a linear regression model developed from Columbia Habitat Monitoring Program (CHaMP) data at 574 sites over 9 years ($MaxTemp = 2.188 + 1.246 * AvgAugTemp$; $R^2 = 0.72$). Additionally, we converted our predicted values of proportion spawned to percentage pre-spawn mortality by simply subtracting each value from one and multiplying by 100. The converted prediction curve is shown in Figure 120.

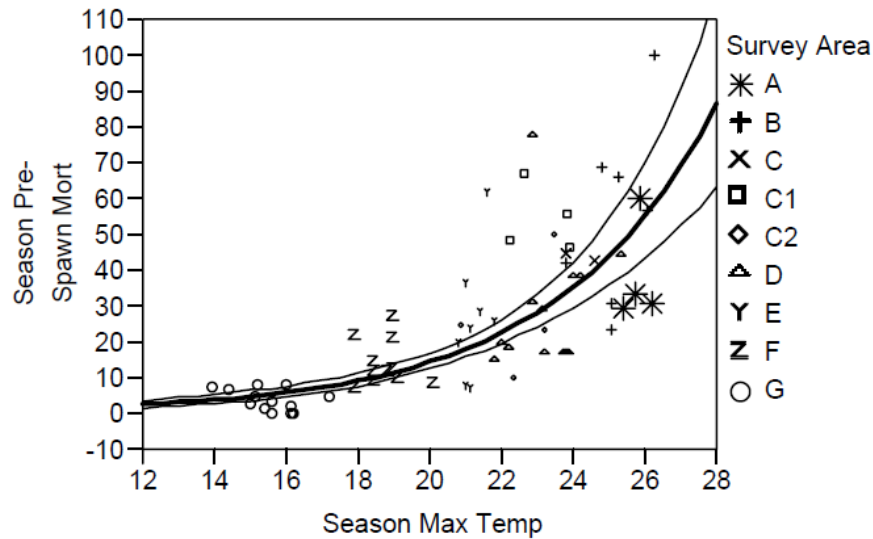


Figure 119. Relationship between seasonal maximum stream temperature (°C) and pre-spawning mortality (%) for spring Chinook in the Umatilla River (from CTUIR and ODFW 2007).

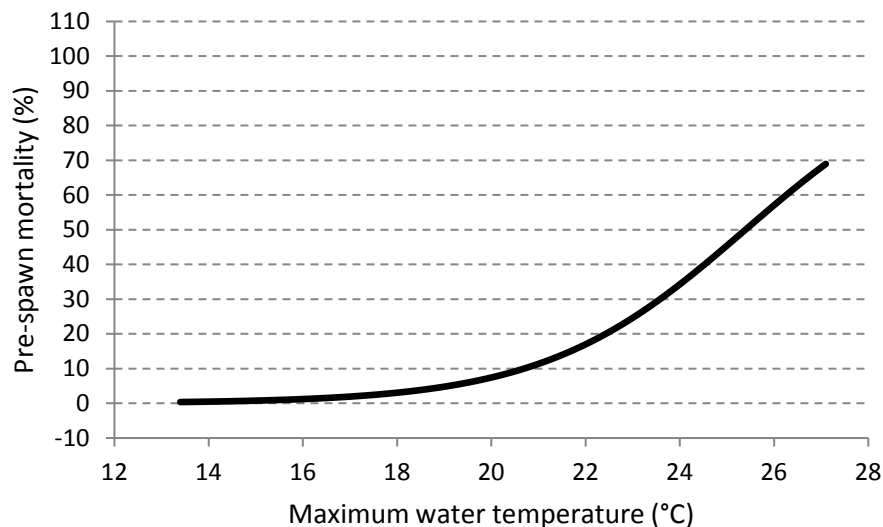


Figure 120. Predicted relationship between seasonal maximum water temperature (°C) and pre-spawning mortality (%) for spring Chinook Salmon in the Grande Ronde and Imnaha River basins.

A comparison of the two prediction curves showed that the effect of water temperature on pre-spawn mortality was remarkably similar between the Umatilla and Grande Ronde/Imnaha basins. For instance, both curves predicted an average pre-spawn mortality of approximately 55 % at a maximum water temperature of 26 °C. For a water temperature of 22 °C, the Umatilla curve predicted a pre-spawn mortality rate of about 20 %, compared with about 17 % for the Grande Ronde/Imnaha curve. One caveat to consider with this comparison is that the shape of the relationship might change somewhat if the model had actually been fit to maximum water temperature rather than simply transforming the x-

axis as we did here. However, the similarity in prediction values using this simplistic comparison is still compelling and lends credibility to the broader applicability of our model results.

We used NorWeST predictions of average August water temperature instead of field-based water temperature measurements because field measurements were not consistently available at the reach-scale, a requirement for evaluating how the proportion spawned would vary in response to longitudinal differences in stream temperature. One potential drawback of using the NorWeST data was that temperature predictions were only available as August means. It's possible that alternative temperature metrics such as cumulative degree days or maximum annual water temperature would provide more precise or informative relationships with proportion spawned. For example, fish that spawn in cooler headwater reaches of the Upper Grande Ronde River may still exhibit lower spawning success due to cumulative exposure to high temperatures during holding or migration in warmer downstream reaches. Unfortunately, the requisite data on holding locations and migration timing for this type of analysis were not available. In addition, Isaak et al. (2011) found that several commonly used metrics used to describe water temperatures during the low flow summer period were highly correlated, suggesting that alternative temperature metrics would show a similar relationship with spawning success. Furthermore, the potential drawbacks of the NorWeST data are potentially outweighed by its broad availability throughout the Pacific Northwest and Mountain West regions, opening up the possibility for similar analyses investigating temperature impacts to salmon populations across a much larger geographic range.

Although the relationship between proportion spawned and water temperature was statistically significant, there was a substantial amount of uncertainty in the relationship due in part to random variation among rivers (Figures 116 and 117). Some variation among rivers may have been due to differences in the range of temperatures over which spawning surveys occurred or because of differences in cumulative temperature exposure. For example, most of the survey reaches in the Wallowa River were narrowly clustered in the high range of observed water temperatures (Figure 115; temperature range = 15.3 - 18.7 °C), while reaches in the Minam River were clustered near the cooler end of the spectrum (range = 10.8 – 15.0 °C). Other rivers such as the Imnaha River spanned a much broader range of temperatures (range = 10.5 – 17.3 °C). In addition, sample size differed considerably across rivers due in part to differences in the spatial coverage of spawning surveys over time and to low spawner returns to certain rivers. For example, the Upper Grande Ronde River has had very low average spawner returns between 2000 and 2013 (total spawners excluding jacks: range = 14 – 2,043; median = 119), resulting in lower detection probability for carcasses and an associated reduced precision in estimates of proportion spawned. Given these factors, we have more confidence in the average relationship between water temperature and the probability of spawning success (i.e., marginal effect of temperature for all rivers combined; Figure 117) for predictive purposes than in the river-specific curves (Figure 118) per se.

Most of the rivers included in this analysis have weirs installed during the spawning season, while some (Minam and Wenaha) do not. Weirs are used to capture migrating adult salmon for purposes of obtaining brood stock for hatcheries, estimating abundance, and sampling biological attributes. It is possible that weirs could impact survival of salmon through handling stress or by impeding upstream

passage, thereby forcing fish to spend longer amounts of time in lower river reaches where water temperatures are warmer and spawning habitat may be less suitable. While it would be tempting to include a weir factor in the model to test the hypothesis that fish spawning in reaches above a weir or with no weir exhibited higher spawning success compared with fish spawning below a weir, we maintain that the correlative modeling analysis used here which pools data from a variety of rivers is not an appropriate analytical method for detecting a weir effect. One reason for this is that a weir effect would be potentially confounded with water temperature. Since weirs are typically located near the downstream extent of the spawning area where water temperatures are warmer, it's unclear whether pre-spawn mortalities found below a weir perished because of migration blockage or water temperature or a combination of both. Additionally, fish spawning above a weir may have experienced similar handling stress or delayed migration as compared to fish spawning below a weir, but this is not readily apparent from the final location that their carcass was recovered. Finally, rivers with no weir (Minam and Wenaha) are wilderness streams with generally cooler water temperatures, so the probability of spawning success would be expected to be higher regardless of the presence of a weir. A more robust method for evaluating a weir effect would be a before and after control impact (BACI) design or similar control/treatment design in which the proportion spawned is estimated before and after the installation of a weir, and is compared with a control stream or set of streams in which no weirs were installed.

Estimates of pre-spawn mortality based on carcass recoveries can be influenced significantly by variation in detection probability of fish carcasses (DeWeber et al. 2017). Factors such as stream size, discharge and water clarity, observer effort and experience, fish behavior, fish sex, size-selective predation, and the timing and frequency of spawning surveys can all affect detection probability (Bowerman et al. 2016). Among these factors, the timing of spawning surveys relative to when fish arrive at the spawning grounds has been shown to be one of the biggest contributors to bias in estimates of pre-spawn mortality (Bowerman et al. 2016). Using a detailed dataset of Chinook Salmon carcass recovery data from central Idaho, Bowerman et al. (2016) found that spawning surveys conducted over a limited time window (i.e., during the spawning period only) accounted for only 12.8 % on average of the total pre-spawn mortality that was observed over the entire sampling period (i.e., surveys starting 4-5 weeks prior to spawning and ending 1 week after last spawner observed). Given that spawning surveys in the Grande Ronde/Imnaha River basins were generally conducted during the spawning period only (mid July – mid September), we assumed that estimates of total pre-spawn mortality were substantially negatively biased (i.e., proportion spawned was biased high). That said, it's unclear how this potential bias would influence the relative effect of water temperature on proportion spawned as described by the model. Given that surveys were conducted during the middle of the summer when water temperatures are most likely to influence fish survival, we assumed that our model captured the majority of the temperature effect on proportion spawned and that the slope of this relationship would not change significantly as a result of the truncated timing of the spawning surveys. Additional work is needed in the Grande Ronde basin to evaluate the magnitude of bias in pre-spawn mortality estimates resulting from timing of spawning surveys.

This study focused on factors influencing the probability of spawning success for fish that reached the spawning grounds, but did not account for mortality of fish occurring during migration to the spawning

grounds (termed en-route mortality). En-route mortality can account for a significant portion of the total mortality experienced by a salmon population throughout its life cycle and is often associated with high water temperatures (Rand et al. 2006, Crossin et al. 2007, Macdonald et al. 2010), infectious disease (CDFG 2004, Benda et al. 2015), or depleted energy reserves (Rand et al. 2006, Cooke et al. 2006). While en-route mortality is an important metric to consider for overall management of salmon populations, it was not included in this analysis because accurate estimates of en-route mortality were not available. Additionally, characterizing the effects of environmental factors on en-route mortality would require detailed information about migration timing, holding locations, and temperature exposure along the migration route (Cooke et al. 2006). A radio-telemetry study focusing on the causes and overall rates of en-route mortality of Grande Ronde/Imnaha salmon populations could help identify important survival bottlenecks and lead to improvements in future management and recovery strategies.

Summary

Describing how environmental conditions such as water temperature influence the probability spawning success of ESA-listed salmon populations will become increasingly important as water temperatures rise in response to climate change (Bowerman et al. 2016). Despite considerable spatial and temporal variability in the effect of water temperature on the proportion spawned, these results add to a substantial body of evidence linking high water temperature to reduced spawning success in Pacific Northwest salmon populations and highlight the need for continued habitat restoration or other management actions to improve temperature conditions for fish in temperature-impaired watersheds. In addition, the functional relationship between water temperature and probability of spawning success described here could be useful in salmon life cycle models to predict how future changes in water temperature could influence salmon population viability parameters.

References

- Bates, D., M. Maechler, B. Bolker, and S. Walker. 2015. Fitting Linear Mixed-Effects Models Using lme4. *Journal of Statistical Software*, 67(1), 1-48. doi:10.18637/jss.v067.i01.
- Beechie, T., H. Imaki, J. Greene, A. Wade, H. Wu, G. Pess, P. Roni, J. Kimball, J. Stanford, P. Kiffney, and N. Mantua. 2013. Restoring salmon habitat for a changing climate. *River Research and Applications* 29:939–960.
- Benda, S. E., G. P. Naughton, C. C. Caudill, M. L. Kent, and C. B. Schreck. 2015. Cool, Pathogen-Free Refuge Lowers Pathogen-Associated Pre-spawn Mortality of Willamette River Chinook Salmon. *Transactions of the American Fisheries Society* 144(6):1159–1172.
- Bowerman, T., M. L. Keefer, and C. C. Caudill. 2016. Pacific Salmon Pre-spawn Mortality: Patterns, Methods, and Study Design Considerations. *Fisheries* 41(12):738–749.
- CDFG (California Department of Fish and Game). 2004. September 2002 Klamath River fish-kill: final analysis of contributing factors and impacts. CDFG, Sacramento.
- Cooke, S. J., S. G. Hinch, G. T. Crossin, D. A. Patterson, K. K. English, M. C. Healey, J. M. Shrimpton, G. Van Der Kraak, and A. P. Farrell. 2006. Mechanistic basis of individual mortality in Pacific Salmon during spawning migrations. *Ecology* 87(6):1575–1586.
- CTUIR (Confederated Tribes of the Umatilla Indian Reservation), and ODFW (Oregon Department of Fish and Wildlife). 2007. Umatilla projects review. A presentation of the multiple-component Umatilla Basin Fisheries Restoration Program. Page 87.
- DeWeber, J. T., J. T. Peterson, C. Sharpe, M. L. Kent, M. E. Colvin, and C. B. Schreck. 2017. A Hidden-Process Model for Estimating Pre-spawn Mortality Using Carcass Survey Data. *North American Journal of Fisheries Management* 37(1):162–175.
- Feist, B. E., E. R. Buhle, P. Arnold, J. W. Davis, and N. L. Scholz. 2011. Landscape Ecotoxicology of Coho Salmon Spawner Mortality in Urban Streams. *PLoS ONE* 6(8):e23424.
- Feldhaus, J. W., T. L. Hoffnagle, D. L. Eddy, and K. N. Ressel. 2017. Lower Snake River compensation plan: Oregon spring Chinook Salmon evaluation studies 2014 annual progress report. Page 68. Oregon Department of Fish and Wildlife, Salem, OR.
- Flagg, T. A., and C. V. W. Mahnaken. 1995. An assessment of the status of captive broodstock technology for Pacific Salmon. Page 298. Funded by National Oceanic and Atmospheric Administration and Bonneville Power Administration, Project No. 93-56, Contract No. DE-AI79-93BP55064, Seattle, WA.
- Fox, J. 2003. Effect Displays in R for Generalised Linear Models. *Journal of Statistical Software*, 8(15), 1-27. URL <http://www.jstatsoft.org/v08/i15/>.

- Fox, J., J. Hong. 2009. Effect displays in R for multinomial and proportional-odds logit models: extensions to the effects package. *Journal of Statistical Software*, 32(1), 1-24. URL <http://www.jstatsoft.org/v32/i01/>.
- Harrison, X. A. 2014. Using observation-level random effects to model overdispersion in count data in ecology and evolution. *PeerJ* 2:e616.
- Hartig, F. 2016. DHARMA: Residual Diagnostics for Hierarchical (Multi-Level / Mixed) Regression Models. R package version 0.1.3. <https://CRAN.R-project.org/package=DHARMA>
- Heard, W. R. 1991. Life history of Pink Salmon (*Oncorhynchus gorbuscha*). Pages 119–230 in C. Groot and L. Margolis, editors. *Pacific salmon life histories*. University of British Columbia Press, Vancouver, British Columbia, Canada.
- Hinch, S. G., S. J. Cooke, A. P. Farrell, K. M. Miller, M. Lapointe, and D. A. Patterson. 2012. Dead fish swimming: a review of research on the early migration and high premature mortality in adult Fraser River sockeye salmon *Oncorhynchus nerka*. *Journal of Fish Biology* 81(2):576–599.
- Isaak, D. J., S. J. Wenger, E. E. Peterson, J. M. Ver Hoef, S. Hostetler, C. H. Luce, J. B. Dunham, J. Kershner, B. B. Roper, D. Nagel, D. Horan, G. Chandler, S. Parkes, S. Wollrab. 2011. NorWeST: an interagency stream temperature database and model for the Northwest United States. U.S. Fish and Wildlife Service, Great Northern Landscape Conservation Cooperative Grant. www.fs.fed.us/rm/boise/AWAE/projects/NorWeST.html.
- Keefer, M. L., G. A. Taylor, D. F. Garletts, G. A. Gauthier, T. M. Pierce, and C. C. Caudill. 2010. Pre-spawn mortality in adult spring Chinook salmon outplanted above barrier dams: Chinook salmon pre-spawn mortality. *Ecology of Freshwater Fish* 19(3):361–372.
- King, K. A., C. E. Grue, J. M. Grassley, and J. W. Hearsey. 2013. Pesticides in Urban Streams and Pre-spawn Mortality of Pacific Coho Salmon. *Archives of Environmental Contamination and Toxicology* 65(3):546–554.
- Lüdecke, D. 2017. *_sjPlot: Data Visualization for Statistics in Social Science_*. R package version 2.2.1, <URL: <https://CRAN.R-project.org/package=sjPlot>>.
- Lynch, A. J., B. J. E. Myers, C. Chu, L. A. Eby, J. A. Falke, R. P. Kovach, T. J. Krabbenhoft, T. J. Kwak, J. Lyons, C. P. Paukert, and J. E. Whitney. 2016. Climate Change Effects on North American Inland Fish Populations and Assemblages. *Fisheries* 41(7):346–361.
- Macdonald, J. S., D. A. Patterson, M. J. Hague, and I. C. Guthrie. 2010. Modeling the Influence of Environmental Factors on Spawning Migration Mortality for Sockeye Salmon Fisheries Management in the Fraser River, British Columbia. *Transactions of the American Fisheries Society* 139(3):768–782.

- Nakagawa, S., and H. Schielzeth. 2013. A general and simple method for obtaining R^2 from generalized linear mixed-effects models. *Methods in Ecology and Evolution* 4(2):133–142.
- Quinn, T. P., D. M. Eggers, J. H. Clark, and H. B. Rich, Jr. 2007. Density, climate, and the processes of pre-spawning mortality and egg retention in Pacific salmon (*Oncorhynchus* spp.). *Canadian Journal of Fisheries and Aquatic Sciences* 64(3):574–582.
- Rand, P. S., S. G. Hinch, J. Morrison, M. G. G. Foreman, M. J. MacNutt, J. S. Macdonald, M. C. Healey, A. P. Farrell, and D. A. Higgs. 2006. Effects of River Discharge, Temperature, and Future Climates on Energetics and Mortality of Adult Migrating Fraser River Sockeye Salmon. *Transactions of the American Fisheries Society* 135(3):655–667.
- Roumasset, A. G. 2012. Pre-spawn mortality of upper Willamette River spring Chinook Salmon: associations with stream temperature, watershed attributes, and environmental conditions on the spawning grounds. Master's thesis. University of Idaho, Moscow.
- Scholz, N. L., M. S. Myers, S. G. McCarthy, J. S. Labenia, J. K. McIntyre, G. M. Ylitalo, L. D. Rhodes, C. A. Laetz, C. M. Stehr, B. L. French, B. McMillan, D. Wilson, L. Reed, K. D. Lynch, S. Damm, J. W. Davis, and T. K. Collier. 2011. Recurrent Die-Offs of Adult Coho Salmon Returning to Spawn in Puget Sound Lowland Urban Streams. *PLoS ONE* 6(12):e28013.
- Zuur, A., E. N. Ieno, N. J. Walker, A. A. Saveliev, and G. M. Smith. 2009. Mixed effects models and extensions in ecology with R. Springer Science+Business Media, LLC, New York, NY.

Supplemental Material

Table 52. Random effect intercepts by year for model m1.

<i>Year</i>	(Intercept)
2000	0.426
2001	-0.571
2002	-0.626
2003	-0.322
2004	0.293
2005	0.413
2006	0.030
2007	-0.001
2008	0.182
2009	-0.686
2010	0.194
2011	0.942
2012	0.319
2013	-0.756

Table 53. Random effect intercepts by river for model m1.

<i>River</i>	(Intercept)
Bear Creek	-1.596
Big Sheep Creek	-1.423
Catherine Creek	0.149
Imnaha River	-1.064
Lostine River	-1.571
Minam River	0.779
Upper Grande Ronde River	-1.043
Wallowa River	2.512
Wenaha River	1.740

Development of Food Web Metrics

Full Title: Development of Food Web Metrics from Benthic Macroinvertebrate Data

Introduction

Food webs for rearing juvenile fish in tributaries have been identified as a potential bottleneck for fish populations in the Columbia River basin (Independent Scientific Advisory Board 2011). Benthic macroinvertebrate (BMI) communities represent an important component of aquatic food webs, and are highly sensitive to environmental variability including streamflow and water temperature, which are expected to adjust based on climate change scenarios. Many regional fish habitat programs (including CRITFC and its member tribes) collect BMIs as part of ongoing habitat monitoring (Table 54), yet analyses are typically limited to evaluating standard water quality metrics such as indices of biotic integrity (IBIs) and other derived indicators. However, BMI data can also be leveraged to provide information about the salmonid food base using descriptive metrics of food webs (Cohen et al. 2003); and availability to food for salmonids based on life history characteristics, propensity to enter the water column, palatability to salmonids, and other characteristics (Rader 1997). By establishing statistical relationships between BMIs and the streamflow and temperature regimes expected to adjust with climate change, we aim to characterize streamflow- and temperature-mediated threats to salmonid food webs in the present and future climate change scenarios. We anticipate that a vulnerability assessment of salmonid food webs will be useful for advancing tribal climate adaptation strategies (Halofsky et al. 2015).

Table 54. Type of macroinvertebrate samples collected in common fish-habitat programs of the Pacific Northwest.

Program	Abbreviation	Targeted riffle	Reach-wide	Multi-habitat	Drift
USFS-BLM Aquatic and Riparian Effectiveness Monitoring Program	AREMP ¹	X			
California Department of Fish and Game	CDFG ¹	X			
EPA Environmental Monitoring Assessment Program	EMAP ¹	X	X		
National Aquatic Resource Surveys	NARS ²		X		
USFS-BLM Biological Opinion Effectiveness Monitoring Program	PIBO ¹	X			
Upper Columbia Monitoring Strategy	UC ¹	X			
Columbia Habitat Monitoring Program	CHaMP ³				X
BPA Action Effectiveness Monitoring	AEM ²	X		X	
BLM AIM-National Aquatic Monitoring Framework	AIM-NAMF ²	X	X		
USGS National Water-Quality Assessment	NAWQA ²	X			
Status and Trends Monitoring for Watershed Health and Salmon Recovery	WA ²		X		
Oregon Department of Environmental Quality	ODEQ ²	X			

¹ Reviewed in (Roper et al. 2010)

² Pers. comm. (various sources)

³ CHaMP 2016

This document describes the field, laboratory, and analytical methods employed to generate food web metrics from ongoing BMI data collected in the upper Grande Ronde River, Catherine Creek, and Minam River of Northeast Oregon as part of a spring Chinook Salmon habitat monitoring program led by CRITFC (McCullough 2009) at annual fish habitat monitoring sites selected as part of the Columbia Habitat Monitoring Program (CHaMP 2016).

Methods

Field and laboratory procedures

Using a standard regional protocol for targeted riffle samples (Hayslip 2007), a total of 361 benthic macroinvertebrate samples were obtained between 2011 and 2016 at CHaMP sites, using either a D-framed kick net or a Hess sampler. Eight approx. 1 ft² samples of substrate were disturbed to dislodge benthic organisms from the substrate and combined to create one composite sample totaling ~8 ft² (~0.742 m²) per site. Samples were preserved in 80% ethanol and delivered to the labs for subsampling and taxonomic analysis. Composite samples were rinsed of excess ethanol and distributed evenly in a subsampling device for a quantitative random selection of individuals (Caton 1991). Stream debris was subsampled until a target count of 500 individuals (+/- 10%) was obtained. Specimens obtained in the subsampling process were then identified to the lowest practical taxonomic resolution, consistent with PNAMP PNW-STE level II (Wisseman et al. 2016). Ten percent of the samples identified were re-identified by a second taxonomist to ensure the accuracy and precision of specimen identification and

enumeration (Stribling et al. 2003; Stribling et al. 2008). Whole body length measurements to the nearest 0.1 mm were made on each individual and recorded to obtain biomass estimates using published length-weight regressions (Eckblad et al. 1971; Dumont et al. 1975; Rogers et al. 1977; Smock 1980; Meyer 1989; Theiling 1990; Burgherr and Meyer 1997; Benke et al. 1999; Miserendino 2001). If a particular taxon did not have an associated length-weight regression formula, a closely related taxon's formula was used. If no closely related taxon was available a minimum of 10 organisms, or the maximum obtained, were dried at 105°C and weighed to the nearest 0.0001 g to obtain the taxon's mean gravimetric dry mass. The mean dry mass value was then applied to the individual taxon.

Throughout the 5-year period of collection and sample processing, species concepts and taxonomic resolution changed for certain taxa. To ensure consistency throughout the project period, data were evaluated for taxonomic nomenclature changes and reduced to genus or higher-level identifications for data analysis. This resulted in 295 distinct operational taxonomic units being identified for the project period (Appendix 1). Although taxonomists initially identified all taxa to the taxonomic levels prescribed by the PNAMP STE Level II (Wisseman et al. 2016), the ability to effectively create a resource-consumer matrix was limited to the literature information on dietary habits. Due to the condition of specimens in the gut of predators, gut content analysis data are often left at family or higher. A family level resource-consumer pair matrix was initially tested to match the majority of data from diet habits to the consumer and was found to contain too little food web information and overgeneralized the feeding habits of individual taxa from within a family. A compromise was made to reduce the taxonomic data to genus in an attempt to capture some within family feeding differences, while not over generalizing the resources (taxa) consumed. Data were also manipulated to reduce the number of non-unique and non-target taxa. Non-target taxa occur when specimens of a particular taxon are too immature or damaged to identify to the taxonomic targets. The reduction of non-target taxa places non-unique coarser level identifications into the closest related target parent taxon, if in the case that a coarse level taxon has two closely related parent taxa the non-target taxa were equally divided into the two possible parent taxa. For example, if data for a given sample was reported to have 5 *Calineuria*, 4 *Doroneuria*, and 10 non-unique Perlidae the final data would appear as 10 *Calineuria* and 9 *Doroneuria*.

Food web metrics

In order to calculate the suite of food web metrics desired (Table 55), we utilized two published R packages with some modification: CHEDDAR (Hudson et al. 2013; Hudson et al. 2014) and FOODWEB (Perdomo et al.). Each community (sample) requires the total estimated number of individuals, their associated biomass and a table of food web linkages. Food web linkages are defined here as matrix of taxa (consumers) and the resources they consume (periphyton, other taxa, bacteria, etc.) (e.g. Table 56). Density and estimated biomass were derived from the data collected in the subsampling process. Linkages were determined using a tiered systematic approach. First, taxa were assigned a functional feeding groups based on available literature (Merritt et al. 2008; Fore and Wisseman 2012). Non-predator functional feeding groups (e.g. shredder and scraper) were assigned similar resources (e.g. shredder=CPOM and scraper=Periphyton). Non-predator resource assignments were evaluated by external reviewers and improvements made resulting in 12 non-predator resource assignments (dead fish, detritus, diatoms, fish, FPOM, fungi, CPOM, macrophytes, microbes, periphyton, and vascular

plants). Predator assignments were evaluated using two approaches: first a literature search for predator-prey relationships of each taxon; if no available literature was found, taxa were assigned prey based on literature citing a similar taxon or gut content analysis. Due to the resolution of taxonomy in prey items for invertebrate predators, family level identifications were the predominant resolution of prey. The coarse resolution of the prey items resulted in all members of a particular 'known' prey item's family becoming available as prey to the predator. For example, *Skwala* was shown to consume Chironomidae and Simuliidae (Fuller and Stewart 1977), and therefore all members of Chironomidae and Simuliidae in a given sample were designated as available resources for the *Skwala* in a given sample. Feeding assignments for all taxa and literature resources are found in Appendix 2.

Table 55. Food web metrics generated by FOODWEB and CHEDDAR packages in R. NA designates no corresponding metric for that given R package.

FOODWEB Metric	CHEDDAR Metric	Description
Species richness	Taxa richness	Number of taxa in the community
Total links	Number of links	Number of feeding connections among nodes, including cannibalism
Connectance	Connectance	Proportion of links (L) relative to nodes (S) ($C = L/S^2$)
Link density	Link density	The average number of feeding links per taxa (L/S)
Fraction top	Percent top level	Proportion of top level consumers in taxa list
Fraction basal	Percent basal	Proportion of basal prey items in taxa list
Fraction herbivorous	Percent intermediate	Proportion of herbivores in taxa list
Fraction omnivorous	NA	Proportion of omnivores in taxa list
Fraction cannibal	NA	Proportion of cannibals in taxa list
Fraction intermediate	NA	Proportion of intermediate-level consumers in taxa list
Prey:predator	NA	Predator to prey ratio
Total trophic positions	NA	Calculated trophic positions based on feeding associations
NA	Percent isolated	Proportion of taxa list without any linkages within community
NA	Slope (mass~n)	Slope of relationship between log biomass and log abundance for taxa in a community

Table 56. Simplified example of a community resource-consumer pair matrix used to derive food web metrics.

Consumer	Resources Consumed				
<i>Skwala</i>	<i>Glyptotendipes</i>	<i>Chironomus</i>	<i>Baetis</i>	<i>Drunella</i>	
<i>Amiocentrus</i>	FPOM	Diatoms			
<i>Arctopsyche</i>	FPOM	<i>Glyptotendipes</i>	<i>Chironomus</i>		
<i>Baetis</i>	Periphyton				
<i>Chironomus</i>	Periphyton	Diatoms			
<i>Drunella</i>	Periphyton	<i>Baetis</i>	<i>Chironomus</i>		
<i>Rhyacophila</i>	<i>Drunella</i>	<i>Baetis</i>	<i>Chironomus</i>	<i>Glyptotendipes</i>	
<i>Glyptotendipes</i>	Diatoms	FPOM	Microbes	Periphyton	

Propensity to drift

A total of 137 taxa were found in the project that were not contained in the original Rader (1997) manuscript designating life history and ecology traits related to propensity to drift. Taxa missing drift attributes were evaluated for the 11 traits described, using the same criteria as Rader (1997). Again, as in the development of the food web community metric development, a systematic approach was used to assign traits to each taxon. First, primary literature was consulted for attribute affinities. Secondly, if no literature was available, the most closely related taxon's values were used as a surrogate. Finally, if no literature or closely related taxa were available then empirical measurements were made, most

commonly for ‘drag index’ and ‘size’ traits. Attributes were assigned and improved through a peer review process (Robert Wisseman, pers. comm.). Literature sources for the drift attributes are found in Appendix 2 and a complete listing of the Rader score assignments is referenced in Appendix 3

Rader’s (1997) manuscript suggested the use of an “aquatic species composition” (ASC) score incorporating the expected or actual abundance of taxa for each site, weighted to account for each taxon’s potential contribution to the salmonid prey base:

$$ASC_{TotAdj} = \sum_{i=1}^n (St_i \cdot A_i)$$

where, n is the number of taxa in availability guilds, St is the subtotal score (sum of the subcategory scores for each taxon), and A is the abundance adjusted score of the i^{th} taxon from Appendix 3.

Due to the abundance adjustment of the Rader scores the original ASC is a richness based calculation at the sample level. In order to better explore the relationship between drift availability metrics and benthic taxonomic composition, three additional ASC metrics were synthesized; two which incorporate site specific taxon abundances (ASC_{Raw} and ASC_{Rel}) and one additional richness based metric (ASC_{SubTot}):

$$ASC_{Raw} = \sum_{i=1}^n (St_i \cdot C_i)$$

$$ASC_{Rel} = \sum_{i=1}^n (St_i \cdot PRA_i)$$

$$ASC_{SubTot} = \sum_{i=1}^n (St_i)$$

where, St_i is equal to the subtotal of the 11 Rader traits of the i^{th} taxon, C_i is the count in a given sample of the i^{th} taxon, PRA_i is the percent relative abundance of the i^{th} taxon in a given sample.

A hierarchical cluster analysis was completed on the trait scores assigned to these data to create guilds of drift availability. Three guild associations were classified using a Ward cluster analysis with a Euclidean distance measure (Ward 1963), and correspond to highly drift availability, medium drift availability and low drift availability (Figure 121). The dendrogram was cut off at 3 guilds to avoid overclassifying the drift propensity of any given taxa. The 93 low drift available taxa correspond to the taxa primarily occurring in depositional or hyporheic habitats that do not score several of the Rader (1997) metrics due to habitat associations. The low drift availability taxa are excluded from the ASC values as recommended by Rader (1997).

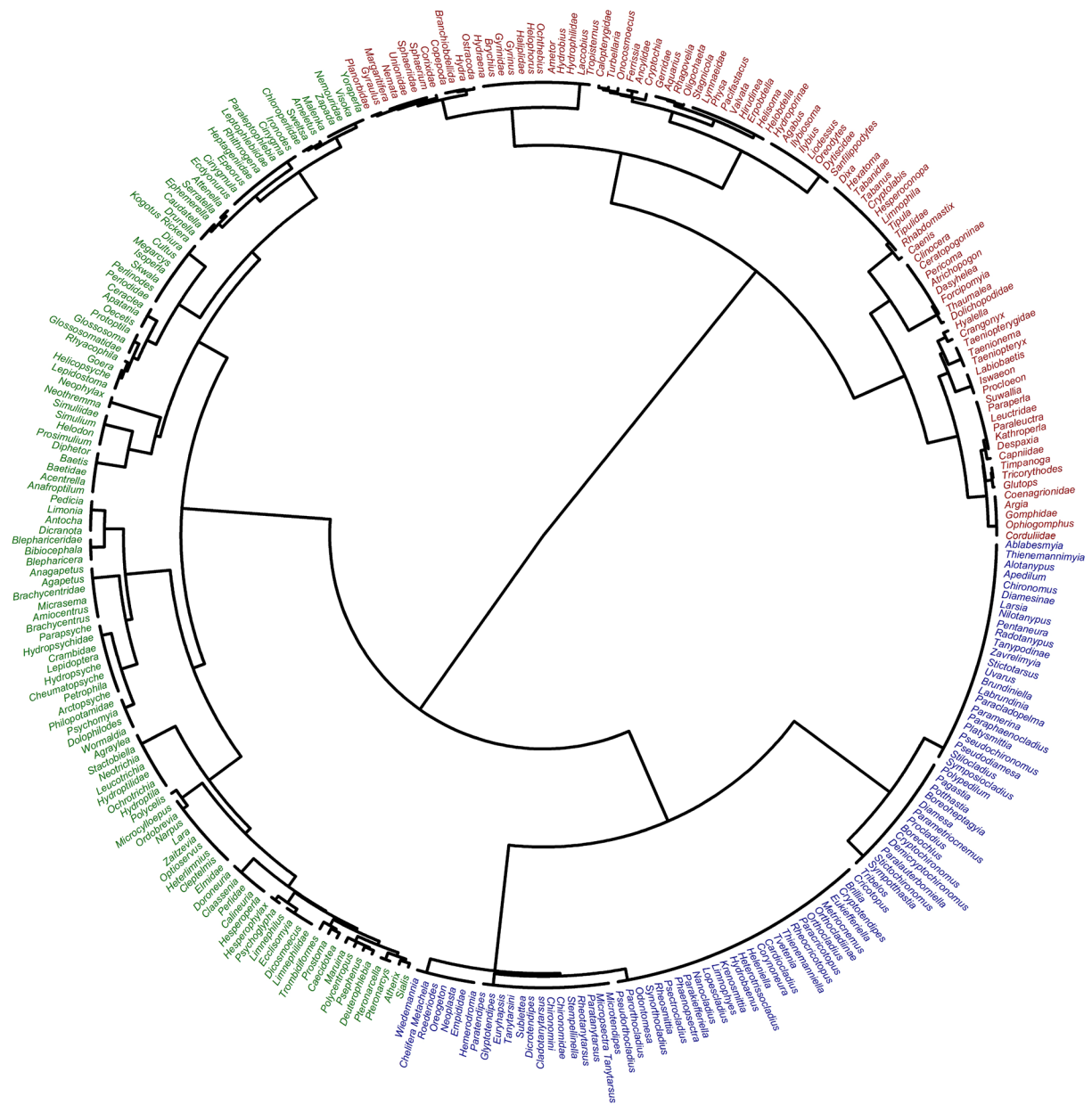


Figure 121. Hierarchical Ward cluster analysis detailing taxa memberships in three drift availability guilds. Taxa names in green, blue, and red correspond to high, medium, and low drift availability guilds, respectively.

Discussion

The methods described in this paper allow for invertebrate food web metrics, prey availability, and traditional community characteristics to be calculated using standard benthic invertebrate sample data. The results of these methods add a layer of analysis to the growing body of information relating the community composition of stream benthos to what is found in the drift and in fish diet studies. Moving beyond traditional benthic community metrics will allow researchers to associate habitat characteristics to food web characteristics and estimate prey availability of a given stream reach without the additional costs of drift or diet sampling and analysis. The methods described in this paper are not novel, but have now been adapted for use in stream reaches of the Upper Columbia River basin, and could be considered as part of any standard benthic analysis. The geographic scope is limited to the Upper Grande Ronde and Minam River basins, undoubtedly as these tools become more widespread in use additional taxa will need to be added, traits evaluated, and feeding associations documented. Additionally, as more work is done on invertebrate food resources further refinement in taxonomic resolution of both consumers and resources may become evident and would greatly improve the accuracy of these tools.

For the Rader (1997) approach, next steps for validation of these methods involve comparing empirical observations of benthic and drift frequencies according to propensity to drift ranking. For both the Rader (1997) and topological food web (Cohen et al. 2003) approaches, further validation will additionally involve determining if food web metrics explain a significant portion of variation in salmonid abundance, growth, or survival. These validation approaches are currently underway and will be documented in an upcoming report.

Acknowledgments

This work was co-sponsored by a Bureau of Indian Affairs Rights Protection Implementation Climate Change contract. Sean Sullivan of Rhithron Associates, Inc. contributed substantially to analysis and reporting. We thank Laura Gephart of Columbia River Inter-Tribal Fish Commission for providing guidance. Bob Wisseman of Aquatic Biology Associates, Inc. provided reviews and valued advice for the foodweb linkages and Rader trait assessments. Nick Weber of Eco Logical Research, Inc. shared a draft table of Rader traits for PNW taxa. Lawrence Hudson of the Natural History Museum, London, provided invaluable assistance adapting the CHEDDAR package in R to our dataset.

References

- Benke AC, Huryn AD, Smock L a, Wallace JB. 1999. Length-mass relationships for freshwater macroinvertebrates in North America with particular reference to the southeastern United States. *J. North Am. Benthol. Soc.* 18:308–343.
- Betts BJ, Wisseman RW. 1995. Geographic range and habitat characteristics of the caddisfly *Cryptochia neosa*. *Northwest Sci.* 69:46–51.
- Blinn DW, Ruiter DE. 2013. Tolerance values and effects of selected environmental determinants on caddisfly (Trichoptera) distribution in northwest and north central Washington, USA. *West. North Am. Nat.* 72:2.
- Burgherr P, Meyer EI. 1997. Regression analysis of linear body dimensions vs. dry mass in stream macroinvertebrates. *Arch. fur Hydrobiol.* 139:101–112.
- Caton LW. 1991. Improved subsampling methods for the EPA Rapid Bioassessment benthic protocols. *Bull. North Am. Benthol. Soc.* 8:317–319.
- Cohen JE, Jonsson T, Carpenter SR. 2003. Ecological community description using the food web, species abundance, and body size. *PNAS* 100:1781–1786.
- Cowan CA., Peckarsky BL. 1990. Feeding by a lotic mayfly grazer as quantified by gut fluorescence. *J. North Am. Benthol. Soc.* 9:368–378.
- Danehy RJ, Langshaw RB, Duke SD, Bilby RE. 2011. Drift distance of macroinvertebrates throughout summer in headwater tributaries of the Calapooia River. *Fundam. Appl. Limnol. Artic. Stuttgart* 1782:111–120.
- Dumont HJ, Van de Velde I, Dumont S. 1975. The dry weight estimate of biomass in a selection of Cladocera, Copepoda and Rotifera from the plankton , periphyton and benthos of continental waters. *Oecologia* 19:75–97.
- Eckblad JW, American S, Naturalist M, Jan N. 1971. Weight-Length regression models for three aquatic gastropod populations. *Am. Midl. Nat.* 85:271–274.
- Elliott JM. 1983. Life cycle and growth of *Dicranota maculata* (Schummel) (Diptera:Tipulidae). *Entomologist's Gaz.* 34:291–296.
- Ferrington LC. 1984. Drift dynamics of Chironomidae larvae: I. Preliminary results and discussion of importance of mesh size and level of taxonomic identification in resolving Chironomidae diel drift patterns. *Hydrobiologia* 114:217–227.
- Fore L, Wisseman RW. 2012. Pacific Northwest benthic invertebrate taxa attribute list.
- Fuller RL, Stewart KW. 1977. The food habits of stoneflies in the upper Gunnison river, Colorado. *Environ. Entomol.* 6:293–302.

- Gilpin BR, Brusven MA. 1970. Food habits and ecology of mayflies of the St. Maries River in Idaho. *Melanderia* 4:20–40.
- Gray LJ, Ward J V. 1979. Food habits of stream benthos at sites of differing food availability. *Source Am. Midl. Nat.* 102:157–167.
- Grzybkowska M, Dukowska M, Figiel K, Szczerkowska E, Tszydel M. 2004. Dynamics of macroinvertebrate drift in a lowland river. *Zool. Pol.* 494:111–127.
- Hall RJ, Waters TF, Cook EF. 1980. The role of drift dispersal in production ecology of a stream mayfly. *Ecology* 61:37–43.
- Halofsky JE, Peterson DL, Marcinkowski KW. 2015. Climate Change Adaptation in United States Federal Natural Resource Science and Management Agencies: A Synthesis.
- Hauer FR, Stanford JA. 1981. Larval specialization and phenotypic variation in *Arctopsyche grandis* (Trichoptera: Hydropsychidae). *Ecology* 62:645–653.
- Hauer FR, Stanford JA. 1982. Ecological responses of hydropsychid caddisflies to stream regulation. *Can. J. Fish. Aquat. Sci.* 39:1235–1242.
- Hawkins CP. 1990. Relationship between habitat dynamics , food availability, and growth patterns of ephemereid mayflies from western North America. In: Cambell I, editor. *Mayflies and Stoneflies: biology and life histories*. Kluwer Academic Publishers. p. 269–274.
- Hemsworth RJ, Brooker MP. 1981. Macroinvertebrate drift in the upper Wye catchment, Wales. *Hydrobiologia* 85:145–155.
- Hudson L, Reuman D, Emerson R. 2014. Cheddar: analysis and visualisation of ecological communities in R.
- Hudson LN, Emerson R, Jenkins GB, Layer K, Ledger ME, Pichler DE, Thompson MSA, O’Gorman EJ, Woodward G, Reuman DC. 2013. Cheddar: analysis and visualisation of ecological communities in R. *Methods Ecol. Evol.* 4:99–104.
- Independent Scientific Advisory Board. 2011. *Columbia River Food Webs: Developing a broader scientific foundation for fish and wildlife restoration*. Portland, Oregon.
- Koslucher DG, Minshall WG. 1973. Food habits of some benthic invertebrates in a northern cool-desert stream (Deep Creek ,Curlew Valley, Idaho-Utah). *Trans. Am. Microsc. Soc.* 92:441–452.
- Larimore WR. 1974. Stream drift as an indication of water quality. *Trans. Am. Fish. Soc.* 103:507–517.
- Larson DJ, Alarie Y, Roughley RE. 2000. *Predaceous diving beetles (Coleoptera: Dytiscidae) of the Nearctic region, with emphasis on the fauna of Canada and Alaska*. Ottawa: National Research Council of Canada.

- López-Rodríguez MJ, Tierno De Figueroa JM, Alba-Tercedor J. 2008. Life history and larval feeding of some species of Ephemeroptera and Plecoptera (Insecta) in the Sierra Nevada (Southern Iberian Peninsula). *Hydrobiologia* 610:277–295.
- McCullough DA. 2009. Proposal: monitoring recovery trends in key Spring Chinook habitat variables and validation of population viability indicators.
- Merritt RW, Cummins KW, Berg MB. 2008. An introduction to the Aquatic insects of North America. Kendall/Hunt Pub. Co.
- Meyer EI. 1989. The relationship between body length parameters and dry mass in running water. *Fundam. Appl. Limnol.* 117:191–203.
- Minakawa N, Gara RI, Honea JM. 2002. Increased individual growth rate and community biomass of stream insects associated with salmon carcasses. *J. North Am. Benthol. Soc.* 21:651–659.
- Miserendino ML. 2001. Length-mass relationships for macroinvertebrates in freshwater environments of Patagonia (Argentina). *Ecol. Austral* 11:3–8.
- Monakov AV. 1972. Review of Studies on Feeding of Aquatic Invertebrates Conducted at the Institute of Biology of Inland Waters, Academy of Science USSR. *J. Fish. Res. Board Canada* 29:363–383.
- Pennak RW. 1989. Fresh-water invertebrates of the United States : protozoa to mollusca. 3rd ed. New York: Wiley.
- Perdomo G, Thompson R, Sunnucks P. food web: an open-source program for the visualisation and analysis of compilations of complex food webs. *Environ. Model. Softw.*
- Perkins PD. 1980. Aquatic beetles of the family Hydraenidae in the Western Hemisphere: classification, biogeography and inferred phylogeny (Insecta: Coleoptera). *Quaest. Entomol.* 16:3–554.
- Provonsa A V. 1990. A revision of the genus *Caenis* in North America (Ephemeroptera: Caenidae). *Trans. Am. Entomol. Soc.* 116:801–884.
- Rader RB. 1997. A functional classification of the drift: traits that influence invertebrate availability to salmonids. *Can. J. Fish. Aquat. Sci.* 54:1211–1234.
- Rader RB, McArthur J V. 1995. The relative importance of refugia in determining the drift and habitat selection of predaceous stoneflies in a sandy-bottomed stream. *Oecologia.*
- Richardson JW, Gauvin AR. 1971. Food habits of some western stonefly nymphs. *Trans. Am. Entomol. Soc.* 97:91–121.
- Roback SS. 1969. Notes on the food of Tanyptodinae larvae. *Entomological News* 80:13–18.
- Rogers LE, Buschbom RL, Watson CR. 1977. Length-weight relationships of shrub-steppe invertebrates. *Ann. Entomol. Soc. Am.* 70:51–53.

- Roper BB, Buffington JM, Bennett S, Lanigan SH, Archer E, Downie ST, Faustini J, Hillman TW, Hubler S, Jones K, et al. 2010. A comparison of the performance and compatibility of protocols used by seven monitoring groups to measure stream habitat in the Pacific Northwest. *North Am. J. Fish. Manag.* 30:565–587.
- Di Sabatino A, Gerecke R, Martin P. 2000. The biology and ecology of lotic water mites (Hydrachnidia). *Freshw. Biol.* 44:47–62.
- Shapas TJ, Hilsenhoff WL. 1976. Feeding habits of Wisconsin's predominant lotic Plecoptera, Ephemeroptera, and Trichoptera. *Gt. Lakes Entomol.* 9:175–188.
- Sheldon AL. 1969. Size relationships of *Acroneuria californica* (Perlidae:Plecoptera) and its prey. *Hydrobiologia* 34:85–94.
- Smock LA. 1980. Relationships between body size and biomass of aquatic insects. *Freshw. Biol.* 10:375–383.
- Smock LA, Roeding CE. 1986. The trophic basis of production of the macroinvertebrate community of a southeastern U.S. blackwater stream. *Holarct. Ecol* 9:165–174.
- Steedman RJ, Anderson NH. 1985. Life history and ecological role of the xylophagous aquatic beetle, *Lara avara* LeConte (Dryopoidea: Elmidae). *Freshw. Biol.* 15:535–546.
- Steine I. 1972. The number and size of drifting nymphs of Ephemeroptera, Chironomidae and Simuliidae by day and night in the River Stranda, western Norway. *Nor. J. Entomol.* 19:127–131.
- Stewart KW, Stark BP. 2002. Nymphs of North American stonefly genera (Plecoptera). 2nd ed. Columbus: The Caddis Press.
- Strand RM, Spangler PJ. 1994. The natural history, distribution, and larval description of *Brychius hungerfordi* Spangler (Coleoptera: Haliplidae). *Proc. Entomol. Soc. Washingt.* 96:208–213.
- Stribling JB, Moulton II SR, Lester GT. 2003. Determining the quality of taxonomic data. *J. North Am. Benthol. Soc.* 22:621–631.
- Stribling JB, Pavlik KL, Holdsworth SM, Leppo EW. 2008. Data quality, performance, and uncertainty in taxonomic identification for biological assessments. *J. North Am. Benthol. Soc.* 27:906–919.
- Theiling CH. 1990. The relationships between several limnological factors and bluegill growth in Michigan lakes. The University of Michigan.
- Thorp JH, Rogers DC. 2015. Ecology and General Biology. Academic Press.
- Turcotte P, Harper PP. 1982. Drift patterns in a high Andean stream. *Hydrobiologia* 89:141–151.
- Walshe BM. 1951. The feeding habits of certain chironomid larvae (subfamily Tendipedinae). *Proc. Zool. Soc. London* 121:63–79.

- Ward JHJ. 1963. Hierarchical grouping to optimize an objective function. Source J. Am. Stat. Assoc. 58:236–244.
- Waringer JA. 1992. The drifting of invertebrates and particulate organic matter in an Austrian mountain brook. Freshw. Biol. 27:367–378.
- Wiggins GB. 2009. Larvae of the North American caddisfly genera (Trichoptera). University of Toronto Press.
- Wisseman RW, Anderson NH. 1987. Recovery of the Trichoptera fauna near Mt. St. Helens five years after the 1980 eruption. In: Bournaud H, Tachet H, editors. Proceedings of the 5th International Symposium on Trichoptera. Dordrecht: Dr. W. Junk. p. 373–376.
- Wisseman RW, Sullivan SP, Pfeiffer J, Salter S, Puls A. 2016. Northwest standard taxonomic effort.
- Wye U, Author W, Hemsworth RJ, Brooker MP. 1979. Nordic Society Oikos The Rate of Downstream Displacement of Macroinvertebrates in the The rate of downstream displacement of macroinvertebrates in the upper Wye, Wales. Source Holarct. Ecol. 278108:130–136.

Appendices

Appendix 1: Taxonomic hierarchy of data used in food web analyses

Phylum	Class	Order	Family	Taxon
Annelida	Clitellata	Arhynchobdellida	Erpobdellidae	Erpobdella
Annelida	Clitellata	Rhynchobdellida	Glossiphoniidae	Helobdella
Annelida	Clitellata			Hirudinea
Annelida	Clitellata			Oligochaeta
Annelida	Clitellata	Branchiobdellida		Branchiobdellida
Arthropoda	Arachnida	Trombidiformes		Trombidiformes
Arthropoda	Malacostraca	Amphipoda	Crangonyctidae	Crangonyx
Arthropoda	Malacostraca	Amphipoda	Hyaellidae	Hyaella
Arthropoda	Malacostraca	Decapoda	Astacidae	Pacifastacus
Arthropoda	Malacostraca	Isopoda	Asellidae	Caecidotea
Arthropoda	Maxillopoda			Copepoda
Arthropoda	Ostracoda			Ostracoda
Arthropoda	Insecta	Coleoptera	Dytiscidae	Stictotarsus
Arthropoda	Insecta	Coleoptera	Dytiscidae	Uvarus
Arthropoda	Insecta	Coleoptera	Dytiscidae	Agabus
Arthropoda	Insecta	Coleoptera	Dytiscidae	Hydroporinae
Arthropoda	Insecta	Coleoptera	Dytiscidae	Ilybiosoma
Arthropoda	Insecta	Coleoptera	Dytiscidae	Ilybius
Arthropoda	Insecta	Coleoptera	Dytiscidae	Liodessus
Arthropoda	Insecta	Coleoptera	Dytiscidae	Oreodytes
Arthropoda	Insecta	Coleoptera	Dytiscidae	Dytiscidae
Arthropoda	Insecta	Coleoptera	Dytiscidae	Sanfilippodytes
Arthropoda	Insecta	Coleoptera	Elmidae	Cleptelmis
Arthropoda	Insecta	Coleoptera	Elmidae	Elmidae
Arthropoda	Insecta	Coleoptera	Elmidae	Heterolimnius
Arthropoda	Insecta	Coleoptera	Elmidae	Optioservus
Arthropoda	Insecta	Coleoptera	Elmidae	Zaitzevia
Arthropoda	Insecta	Coleoptera	Elmidae	Lara
Arthropoda	Insecta	Coleoptera	Elmidae	Narpus
Arthropoda	Insecta	Coleoptera	Elmidae	Ordobrevia
Arthropoda	Insecta	Coleoptera	Elmidae	Microcylloepus
Arthropoda	Insecta	Coleoptera	Gyrinidae	Gyrinidae
Arthropoda	Insecta	Coleoptera	Gyrinidae	Gyrinus
Arthropoda	Insecta	Coleoptera	Halipidae	Brychius
Arthropoda	Insecta	Coleoptera	Halipidae	Halipidae
Arthropoda	Insecta	Coleoptera	Helophoridae	Helophorus
Arthropoda	Insecta	Coleoptera	Hydraenidae	Hydraena
Arthropoda	Insecta	Coleoptera	Hydraenidae	Ochthebius

Phylum	Class	Order	Family	Taxon
Arthropoda	Insecta	Coleoptera	Hydrophilidae	Ametor
Arthropoda	Insecta	Coleoptera	Hydrophilidae	Hydrobius
Arthropoda	Insecta	Coleoptera	Hydrophilidae	Hydrophilidae
Arthropoda	Insecta	Coleoptera	Hydrophilidae	Laccobius
Arthropoda	Insecta	Coleoptera	Hydrophilidae	Tropisternus
Arthropoda	Insecta	Coleoptera	Psephenidae	Psephenus
Arthropoda	Insecta	Diptera	Athericidae	Atherix
Arthropoda	Insecta	Diptera	Blephariceridae	Bibiocephala
Arthropoda	Insecta	Diptera	Blephariceridae	Blepharicera
Arthropoda	Insecta	Diptera	Blephariceridae	Blephariceridae
Arthropoda	Insecta	Diptera	Ceratopogonidae	Ceratopogoninae
Arthropoda	Insecta	Diptera	Ceratopogonidae	Atrichopogon
Arthropoda	Insecta	Diptera	Ceratopogonidae	Dasyhelea
Arthropoda	Insecta	Diptera	Ceratopogonidae	Forcipomyia
Arthropoda	Insecta	Diptera	Chironomidae	Thienemannimyia
Arthropoda	Insecta	Diptera	Chironomidae	Ablabesmyia
Arthropoda	Insecta	Diptera	Chironomidae	Alotanypus
Arthropoda	Insecta	Diptera	Chironomidae	Apedilum
Arthropoda	Insecta	Diptera	Chironomidae	Chironomus
Arthropoda	Insecta	Diptera	Chironomidae	Diamesinae
Arthropoda	Insecta	Diptera	Chironomidae	Larsia
Arthropoda	Insecta	Diptera	Chironomidae	Nilotanypus
Arthropoda	Insecta	Diptera	Chironomidae	Pentaneura
Arthropoda	Insecta	Diptera	Chironomidae	Radotanypus
Arthropoda	Insecta	Diptera	Chironomidae	Tanypodinae
Arthropoda	Insecta	Diptera	Chironomidae	Zavreliomyia
Arthropoda	Insecta	Diptera	Chironomidae	Brundiniella
Arthropoda	Insecta	Diptera	Chironomidae	Labrundinia
Arthropoda	Insecta	Diptera	Chironomidae	Paracladopelma
Arthropoda	Insecta	Diptera	Chironomidae	Paramerina
Arthropoda	Insecta	Diptera	Chironomidae	Paraphaenocladus
Arthropoda	Insecta	Diptera	Chironomidae	Platysmittia
Arthropoda	Insecta	Diptera	Chironomidae	Pseudochironomus
Arthropoda	Insecta	Diptera	Chironomidae	Pseudodiamesa
Arthropoda	Insecta	Diptera	Chironomidae	Stilocladius
Arthropoda	Insecta	Diptera	Chironomidae	Symposiocladius
Arthropoda	Insecta	Diptera	Chironomidae	Pagastia
Arthropoda	Insecta	Diptera	Chironomidae	Polypedilum
Arthropoda	Insecta	Diptera	Chironomidae	Potthastia
Arthropoda	Insecta	Diptera	Chironomidae	Boreoheptagyia

Phylum	Class	Order	Family	Taxon
Arthropoda	Insecta	Diptera	Chironomidae	Diamesa
Arthropoda	Insecta	Diptera	Chironomidae	Parametriocnemus
Arthropoda	Insecta	Diptera	Chironomidae	Procladius
Arthropoda	Insecta	Diptera	Chironomidae	Boreochlus
Arthropoda	Insecta	Diptera	Chironomidae	Cryptochironomus
Arthropoda	Insecta	Diptera	Chironomidae	Demicryptochironomus
Arthropoda	Insecta	Diptera	Chironomidae	Paralauterborniella
Arthropoda	Insecta	Diptera	Chironomidae	Stictochironomus
Arthropoda	Insecta	Diptera	Chironomidae	Sympotthastia
Arthropoda	Insecta	Diptera	Chironomidae	Tribelos
Arthropoda	Insecta	Diptera	Chironomidae	Brillia
Arthropoda	Insecta	Diptera	Chironomidae	Cricotopus
Arthropoda	Insecta	Diptera	Chironomidae	Cryptotendipes
Arthropoda	Insecta	Diptera	Chironomidae	Eukiefferiella
Arthropoda	Insecta	Diptera	Chironomidae	Metriocnemus
Arthropoda	Insecta	Diptera	Chironomidae	Orthoclaadiinae
Arthropoda	Insecta	Diptera	Chironomidae	Orthocladus
Arthropoda	Insecta	Diptera	Chironomidae	Paracricotopus
Arthropoda	Insecta	Diptera	Chironomidae	Rheocricotopus
Arthropoda	Insecta	Diptera	Chironomidae	Thienemanniella
Arthropoda	Insecta	Diptera	Chironomidae	Tvetenia
Arthropoda	Insecta	Diptera	Chironomidae	Cardiocladius
Arthropoda	Insecta	Diptera	Chironomidae	Corynoneura
Arthropoda	Insecta	Diptera	Chironomidae	Heleniella
Arthropoda	Insecta	Diptera	Chironomidae	Heterotrissocladius
Arthropoda	Insecta	Diptera	Chironomidae	Hydrobaenus
Arthropoda	Insecta	Diptera	Chironomidae	Krenosmittia
Arthropoda	Insecta	Diptera	Chironomidae	Limnophyes
Arthropoda	Insecta	Diptera	Chironomidae	Lopescladius
Arthropoda	Insecta	Diptera	Chironomidae	Nanocladius
Arthropoda	Insecta	Diptera	Chironomidae	Parakiefferiella
Arthropoda	Insecta	Diptera	Chironomidae	Phaenopsectra
Arthropoda	Insecta	Diptera	Chironomidae	Psectrocladius
Arthropoda	Insecta	Diptera	Chironomidae	Rheosmittia
Arthropoda	Insecta	Diptera	Chironomidae	Synorthocladus
Arthropoda	Insecta	Diptera	Chironomidae	Odontomesa
Arthropoda	Insecta	Diptera	Chironomidae	Parorthocladus
Arthropoda	Insecta	Diptera	Chironomidae	Pseudorthocladus
Arthropoda	Insecta	Diptera	Chironomidae	Micropsectra_Tanytarsus
Arthropoda	Insecta	Diptera	Chironomidae	Microtendipes

Phylum	Class	Order	Family	Taxon
Arthropoda	Insecta	Diptera	Chironomidae	Paratanytarsus
Arthropoda	Insecta	Diptera	Chironomidae	Rheotanytarsus
Arthropoda	Insecta	Diptera	Chironomidae	Stempellinella
Arthropoda	Insecta	Diptera	Chironomidae	Chironomidae
Arthropoda	Insecta	Diptera	Chironomidae	Chironomini
Arthropoda	Insecta	Diptera	Chironomidae	Cladotanytarsus
Arthropoda	Insecta	Diptera	Chironomidae	Dicrotendipes
Arthropoda	Insecta	Diptera	Chironomidae	Sublettea
Arthropoda	Insecta	Diptera	Chironomidae	Tanytarsini
Arthropoda	Insecta	Diptera	Chironomidae	Euryhopsis
Arthropoda	Insecta	Diptera	Chironomidae	Glyptotendipes
Arthropoda	Insecta	Diptera	Chironomidae	Paratendipes
Arthropoda	Insecta	Diptera	Deuterophlebiidae	Deuterophlebia
Arthropoda	Insecta	Diptera	Dixidae	Dixa
Arthropoda	Insecta	Diptera	Dolichopodidae	Dolichopodidae
Arthropoda	Insecta	Diptera	Empididae	Empididae
Arthropoda	Insecta	Diptera	Empididae	Hemerodromia
Arthropoda	Insecta	Diptera	Empididae	Neoplasia
Arthropoda	Insecta	Diptera	Empididae	Oreogeton
Arthropoda	Insecta	Diptera	Empididae	Roederiodes
Arthropoda	Insecta	Diptera	Empididae	Chelifera_Metachela
Arthropoda	Insecta	Diptera	Empididae	Wiedemannia
Arthropoda	Insecta	Diptera	Empididae	Clinocera
Arthropoda	Insecta	Diptera	Pelecophychidae	Glutops
Arthropoda	Insecta	Diptera	Psychodidae	Maruina
Arthropoda	Insecta	Diptera	Psychodidae	Pericoma
Arthropoda	Insecta	Diptera	Simuliidae	Helodon
Arthropoda	Insecta	Diptera	Simuliidae	Prosimulium
Arthropoda	Insecta	Diptera	Simuliidae	Simulium
Arthropoda	Insecta	Diptera	Simuliidae	Simuliidae
Arthropoda	Insecta	Diptera	Tabanidae	Tabanidae
Arthropoda	Insecta	Diptera	Tabanidae	Tabanus
Arthropoda	Insecta	Diptera	Thaumaleidae	Thaumalea
Arthropoda	Insecta	Diptera	Tipulidae	Antocha
Arthropoda	Insecta	Diptera	Tipulidae	Dicranota
Arthropoda	Insecta	Diptera	Tipulidae	Limonia
Arthropoda	Insecta	Diptera	Tipulidae	Pedicia
Arthropoda	Insecta	Diptera	Tipulidae	Hexatoma
Arthropoda	Insecta	Diptera	Tipulidae	Cryptolabis
Arthropoda	Insecta	Diptera	Tipulidae	Hesperoconopa

Phylum	Class	Order	Family	Taxon
Arthropoda	Insecta	Diptera	Tipulidae	Limnophila
Arthropoda	Insecta	Diptera	Tipulidae	Tipula
Arthropoda	Insecta	Diptera	Tipulidae	Tipulidae
Arthropoda	Insecta	Diptera	Tipulidae	Rhabdomastix
Arthropoda	Insecta	Ephemeroptera	Ameletidae	Ameletus
Arthropoda	Insecta	Ephemeroptera	Baetidae	Acentrella
Arthropoda	Insecta	Ephemeroptera	Baetidae	Anafroptilum
Arthropoda	Insecta	Ephemeroptera	Baetidae	Baetidae
Arthropoda	Insecta	Ephemeroptera	Baetidae	Baetis
Arthropoda	Insecta	Ephemeroptera	Baetidae	Dipheter
Arthropoda	Insecta	Ephemeroptera	Baetidae	Isxaeon
Arthropoda	Insecta	Ephemeroptera	Baetidae	Labiobaetis
Arthropoda	Insecta	Ephemeroptera	Baetidae	Proclaeon
Arthropoda	Insecta	Ephemeroptera	Caenidae	Caenis
Arthropoda	Insecta	Ephemeroptera	Ephemerellidae	Caudatella
Arthropoda	Insecta	Ephemeroptera	Ephemerellidae	Drunella
Arthropoda	Insecta	Ephemeroptera	Ephemerellidae	Ephemerella
Arthropoda	Insecta	Ephemeroptera	Ephemerellidae	Attenella
Arthropoda	Insecta	Ephemeroptera	Ephemerellidae	Serratella
Arthropoda	Insecta	Ephemeroptera	Ephemerellidae	Timpanoga
Arthropoda	Insecta	Ephemeroptera	Heptageniidae	Cinygmula
Arthropoda	Insecta	Ephemeroptera	Heptageniidae	Ecdyonurus
Arthropoda	Insecta	Ephemeroptera	Heptageniidae	Epeorus
Arthropoda	Insecta	Ephemeroptera	Heptageniidae	Heptageniidae
Arthropoda	Insecta	Ephemeroptera	Heptageniidae	Rhithrogena
Arthropoda	Insecta	Ephemeroptera	Heptageniidae	Cinygma
Arthropoda	Insecta	Ephemeroptera	Heptageniidae	Ironodes
Arthropoda	Insecta	Ephemeroptera	Leptohyphidae	Tricorythodes
Arthropoda	Insecta	Ephemeroptera	Leptophlebiidae	Leptophlebiidae
Arthropoda	Insecta	Ephemeroptera	Leptophlebiidae	Paraleptophlebia
Arthropoda	Insecta	Hemiptera	Corixidae	Corixidae
Arthropoda	Insecta	Hemiptera	Gerridae	Aquarius
Arthropoda	Insecta	Hemiptera	Gerridae	Gerridae
Arthropoda	Insecta	Hemiptera	Veliidae	Rhagovelia
Arthropoda	Insecta	Lepidoptera	Crambidae	Petrophila
Arthropoda	Insecta	Lepidoptera	Crambidae	Crambidae
Arthropoda	Insecta	Lepidoptera		Lepidoptera
Arthropoda	Insecta	Megaloptera	Sialidae	Sialis
Arthropoda	Insecta	Odonata	Calopterygidae	Calopterygidae
Arthropoda	Insecta	Odonata	Coenagrionidae	Argia

Phylum	Class	Order	Family	Taxon
Arthropoda	Insecta	Odonata	Coenagrionidae	Coenagrionidae
Arthropoda	Insecta	Odonata	Corduliidae	Corduliidae
Arthropoda	Insecta	Odonata	Gomphidae	Gomphidae
Arthropoda	Insecta	Odonata	Gomphidae	Ophiogomphus
Arthropoda	Insecta	Plecoptera	Capniidae	Capniidae
Arthropoda	Insecta	Plecoptera	Chloroperlidae	Sweltsa
Arthropoda	Insecta	Plecoptera	Chloroperlidae	Chloroperlidae
Arthropoda	Insecta	Plecoptera	Chloroperlidae	Paraperla
Arthropoda	Insecta	Plecoptera	Chloroperlidae	Suwallia
Arthropoda	Insecta	Plecoptera	Chloroperlidae	Kathroperla
Arthropoda	Insecta	Plecoptera	Leuctridae	Leuctridae
Arthropoda	Insecta	Plecoptera	Leuctridae	Paraleuctra
Arthropoda	Insecta	Plecoptera	Leuctridae	Despaxia
Arthropoda	Insecta	Plecoptera	Nemouridae	Zapada
Arthropoda	Insecta	Plecoptera	Nemouridae	Malenka
Arthropoda	Insecta	Plecoptera	Nemouridae	Nemouridae
Arthropoda	Insecta	Plecoptera	Nemouridae	Visoka
Arthropoda	Insecta	Plecoptera	Peltoperlidae	Yoraperla
Arthropoda	Insecta	Plecoptera	Perlidae	Calineuria
Arthropoda	Insecta	Plecoptera	Perlidae	Hesperoperla
Arthropoda	Insecta	Plecoptera	Perlidae	Perlidae
Arthropoda	Insecta	Plecoptera	Perlidae	Claassenia
Arthropoda	Insecta	Plecoptera	Perlidae	Doroneuria
Arthropoda	Insecta	Plecoptera	Perlodidae	Perlinodes
Arthropoda	Insecta	Plecoptera	Perlodidae	Perlodidae
Arthropoda	Insecta	Plecoptera	Perlodidae	Skwala
Arthropoda	Insecta	Plecoptera	Perlodidae	Isoperla
Arthropoda	Insecta	Plecoptera	Perlodidae	Megarcys
Arthropoda	Insecta	Plecoptera	Perlodidae	Cultus
Arthropoda	Insecta	Plecoptera	Perlodidae	Diura
Arthropoda	Insecta	Plecoptera	Perlodidae	Kogotus_Rickera
Arthropoda	Insecta	Plecoptera	Pteronarcyidae	Pteronarcella
Arthropoda	Insecta	Plecoptera	Pteronarcyidae	Pteronarcys
Arthropoda	Insecta	Plecoptera	Taeniopterygidae	Taenionema
Arthropoda	Insecta	Plecoptera	Taeniopterygidae	Taeniopterygidae
Arthropoda	Insecta	Plecoptera	Taeniopterygidae	Taeniopteryx
Arthropoda	Insecta	Trichoptera	Apataniidae	Apatania
Arthropoda	Insecta	Trichoptera	Brachycentridae	Amiocentrus
Arthropoda	Insecta	Trichoptera	Brachycentridae	Brachycentrus
Arthropoda	Insecta	Trichoptera	Brachycentridae	Micrasema

Phylum	Class	Order	Family	Taxon
Arthropoda	Insecta	Trichoptera	Brachycentridae	Brachycentridae
Arthropoda	Insecta	Trichoptera	Glossosomatidae	Agapetus
Arthropoda	Insecta	Trichoptera	Glossosomatidae	Anagapetus
Arthropoda	Insecta	Trichoptera	Glossosomatidae	Glossosoma
Arthropoda	Insecta	Trichoptera	Glossosomatidae	Glossosomatidae
Arthropoda	Insecta	Trichoptera	Glossosomatidae	Protoptila
Arthropoda	Insecta	Trichoptera	Goeridae	Goera
Arthropoda	Insecta	Trichoptera	Helicopsychidae	Helicopsyche
Arthropoda	Insecta	Trichoptera	Hydropsychidae	Arctopsyche
Arthropoda	Insecta	Trichoptera	Hydropsychidae	Cheumatopsyche
Arthropoda	Insecta	Trichoptera	Hydropsychidae	Hydropsyche
Arthropoda	Insecta	Trichoptera	Hydropsychidae	Hydropsychidae
Arthropoda	Insecta	Trichoptera	Hydropsychidae	Parapsyche
Arthropoda	Insecta	Trichoptera	Hydroptilidae	Ochrotrichia
Arthropoda	Insecta	Trichoptera	Hydroptilidae	Hydroptila
Arthropoda	Insecta	Trichoptera	Hydroptilidae	Hydroptilidae
Arthropoda	Insecta	Trichoptera	Hydroptilidae	Leucotrichia
Arthropoda	Insecta	Trichoptera	Hydroptilidae	Neotrichia
Arthropoda	Insecta	Trichoptera	Hydroptilidae	Stactobiella
Arthropoda	Insecta	Trichoptera	Hydroptilidae	Agraylea
Arthropoda	Insecta	Trichoptera	Lepidostomatidae	Lepidostoma
Arthropoda	Insecta	Trichoptera	Leptoceridae	Oecetis
Arthropoda	Insecta	Trichoptera	Leptoceridae	Ceraclea
Arthropoda	Insecta	Trichoptera	Limnephilidae	Dicosmoecus
Arthropoda	Insecta	Trichoptera	Limnephilidae	Limnephilidae
Arthropoda	Insecta	Trichoptera	Limnephilidae	Ecclisomyia
Arthropoda	Insecta	Trichoptera	Limnephilidae	Limnephilus
Arthropoda	Insecta	Trichoptera	Limnephilidae	Hesperophylax
Arthropoda	Insecta	Trichoptera	Limnephilidae	Psychoglypha
Arthropoda	Insecta	Trichoptera	Limnephilidae	Onocosmoecus
Arthropoda	Insecta	Trichoptera	Limnephilidae	Cryptochia
Arthropoda	Insecta	Trichoptera	Philopotamidae	Dolophilodes
Arthropoda	Insecta	Trichoptera	Philopotamidae	Wormaldia
Arthropoda	Insecta	Trichoptera	Philopotamidae	Philopotamidae
Arthropoda	Insecta	Trichoptera	Polycentropodidae	Polycentropus
Arthropoda	Insecta	Trichoptera	Psychomyiidae	Psychomyia
Arthropoda	Insecta	Trichoptera	Rhyacophilidae	Rhyacophila
Arthropoda	Insecta	Trichoptera	Uenoidae	Neophylax
Arthropoda	Insecta	Trichoptera	Uenoidae	Neothremma
Cnidaria	Hydrozoa	Hydroida	Hydridae	Hydra

Phylum	Class	Order	Family	Taxon
Mollusca	Bivalvia	Veneroida	Sphaeriidae	Sphaeriidae
Mollusca	Bivalvia	Veneroida	Sphaeriidae	Sphaerium
Mollusca	Bivalvia	Unionoida	Margaritiferidae	Margaritifera
Mollusca	Bivalvia	Unionoida	Unionidae	Unionidae
Mollusca	Gastropoda	Basommatophora	Ancylidae	Ancylidae
Mollusca	Gastropoda	Basommatophora	Ancylidae	Ferrissia
Mollusca	Gastropoda	Basommatophora	Lymnaeidae	Lymnaeidae
Mollusca	Gastropoda	Basommatophora	Lymnaeidae	Stagnicola
Mollusca	Gastropoda	Basommatophora	Physidae	Physa
Mollusca	Gastropoda	Basommatophora	Planorbidae	Helisoma
Mollusca	Gastropoda	Basommatophora	Planorbidae	Gyraulus
Mollusca	Gastropoda	Basommatophora	Planorbidae	Planorbidae
Mollusca	Gastropoda	Heterostrophia	Valvatidae	Valvata
Nemata				Nemata
Nemertea	Enopla	Hoplonemertea	Tetrastemmatidae	Prostoma
Platyhelminthes	Turbellaria	Tricladida	Planariidae	Polycelis
Platyhelminthes	Turbellaria			Turbellaria

Appendix 2: Consumer assignments with sources and sources for drift propensity scoring for each taxa

Taxon	Consumer	Sources (food web)	Sources (drift)
Ablabesmyia	Predator, FPOM, Periphyton	(Roback 1969)	(Steine 1972; Ferrington 1984; Waringer 1992; Rader 1997)
Acentrella	Diatoms, FPOM, Periphyton	(Merritt et al. 2008)	(Rader 1997)
Agabus	Predator	(Larson et al. 2000)	(Larson et al. 2000)
Agapetus	Periphyton	(Merritt et al. 2008)	(Rader 1997)
Agraylea	Vascular, Plants	(Shapas and Hilsenhoff 1976)	(Rader 1997)
Alotanypus	Periphyton	(Merritt et al. 2008)	(Steine 1972; Ferrington 1984; Waringer 1992; Rader 1997)
Ameletus	Periphyton, FPOM	(Shapas and Hilsenhoff 1976; Merritt et al. 2008)	(Rader 1997)
Ametor	Predator	(Merritt et al. 2008)	(Larimore 1974)
Amiocentrus	Diatoms, FPOM	(Merritt et al. 2008; Wiggins 2009)	(Rader 1997)
Anafroptilum	FPOM, Periphyton	(Gilpin and Brusven 1970; Merritt et al. 2008)	(Rader 1997)
Anagapetus	Periphyton	(Merritt et al. 2008; Wiggins 2009)	(Rader 1997)
Ancylidae	Periphyton	(Pennak 1989; Thorp and Rogers 2015)	(Rader 1997)
Antocha	Predator	(Merritt et al. 2008)	(Rader 1997)
Apatania	Periphyton	(Merritt et al. 2008; Wiggins 2009)	(Rader 1997)
Apedilum	Periphyton	(Merritt et al. 2008)	(Steine 1972; Ferrington 1984; Waringer 1992; Rader 1997)
Aquarius	Predator	(Merritt et al. 2008)	(Larimore 1974)
Arctopsyche	Predator, FPOM	(Hauer and Stanford 1981; Hauer and Stanford 1982; Merritt et al. 2008)	(Rader 1997)
Argia	Predator	(Merritt et al. 2008)	(Rader 1997)*
Atherix	Predator	(Merritt et al. 2008)	(Rader 1997)
Atrichopogon	Predator	(Merritt et al. 2008)	(Rader 1997)
Attenella	Periphyton	(Hawkins 1990; Merritt et al. 2008)	(Rader 1997)
Baetidae	Periphyton	(Cowan and Peckarsky 1990; Merritt et al. 2008)	(Rader 1997)
Baetis	Periphyton	(Cowan and Peckarsky 1990; Merritt et al. 2008)	(Rader 1997)
Bibiocephala	Periphyton	(Merritt et al. 2008)	(Rader 1997)

Taxon	Consumer	Sources (food web)	Sources (drift)
Blepharicera	Periphyton	(Merritt et al. 2008)	(Rader 1997)
Blephariceridae	Periphyton	(Merritt et al. 2008)	(Rader 1997)
Boreochlus	Diatoms, FPOM, CPOM, Microbes, Periphyton	(Merritt et al. 2008)	(Steine 1972; Ferrington 1984; Waringer 1992; Rader 1997)
Boreoheptagyia	Periphyton	(Merritt et al. 2008)	(Steine 1972; Ferrington 1984; Waringer 1992; Rader 1997)
Brachycentridae	Diatoms, FPOM, CPOM, Microbes, Periphyton	(Koslucher and Minshall 1973; Merritt et al. 2008; Wiggins 2009)	(Rader 1997)
Brachycentrus	Diatoms, FPOM, CPOM, Microbes, Periphyton	(Koslucher and Minshall 1973; Merritt et al. 2008; Wiggins 2009)	(Rader 1997)
Branchiobdellida	Predator, Detritus	(Pennak 1989; Thorp and Rogers 2015)	(Thorp and Rogers 2015)
Brillia	Detritus	(Merritt et al. 2008)	(Steine 1972; Ferrington 1984; Waringer 1992; Rader 1997)
Brundiniella	Diatoms, FPOM, CPOM, Microbes, Periphyton	(Merritt et al. 2008)	(Steine 1972; Ferrington 1984; Waringer 1992; Rader 1997)
Brychius	Macrophytes	(Strand and Spangler 1994; Merritt et al. 2008)	(Larimore 1974)
Caecidotea	Diatoms, FPOM, CPOM, Microbes, Periphyton	(Pennak 1989; Thorp and Rogers 2015)	(Grzybkowska et al. 2004)
Caenis	Detritus, FPOM, Fungi, CPOM, Microbes, Periphyton	(Provonsa 1990; Merritt et al. 2008)	(Rader 1997)
Calineuria	Predator	(Sheldon 1969; Merritt et al. 2008)	(Rader 1997)
Calopterygidae	Predator	(Merritt et al. 2008)	(Rader 1997)
Capniidae	Detritus	(Stewart and Stark 2002; Merritt et al. 2008)	(Rader 1997)
Cardiocladius	Predator	(Merritt et al. 2008)	(Rader 1997)
Caudatella	Periphyton	(Hawkins 1990; Merritt et al. 2008)	(Rader 1997)
Ceraclea	Predator, Detritus, Periphyton	(Merritt et al. 2008; Wiggins 2009)	(Rader 1997)
Ceratopogoninae	Predator	(Merritt et al. 2008)	(Rader 1997)
Chelifera_Metachela	Predator	(Merritt et al. 2008)	(Rader 1997)
Cheumatopsyche	Diatoms, FPOM, CPOM, Microbes	(Merritt et al. 2008; Wiggins 2009)	(Rader 1997)
Chironomidae	Diatoms, FPOM,	(Merritt et al. 2008)	(Rader 1997)

Taxon	Consumer	Sources (food web)	Sources (drift)
	CPOM, Microbes		
Chironomini	Periphyton	(Merritt et al. 2008)	(Rader 1997)
Chironomus	Periphyton	(Merritt et al. 2008)	(Steine 1972; Ferrington 1984; Waringer 1992; Rader 1997)
Chloroperlidae	Predator	(Fuller and Stewart 1977; Stewart and Stark 2002; Merritt et al. 2008)	(Rader 1997)
Cinygma	Periphyton	(Merritt et al. 2008)	(Rader 1997)
Cinygmula	Periphyton	(Gilpin and Brusven 1970; Merritt et al. 2008)	(Rader 1997)
Claassenia	Predator	(Fuller and Stewart 1977; Stewart and Stark 2002; Merritt et al. 2008)	(Rader 1997)
Cladotanytarsus	Periphyton	(Merritt et al. 2008)	(Steine 1972; Ferrington 1984; Waringer 1992; Rader 1997)
Cleptelmis	FPOM, Periphyton	(Merritt et al. 2008)	(Rader 1997)
Clinocera	Predator	(Merritt et al. 2008)	(Rader 1997)
Coenagrionidae	Predator	(Smock and Roeding 1986; Merritt et al. 2008)	(Rader 1997)
Copepoda	Predator, Periphyton	(Pennak 1989; Thorp and Rogers 2015)	(Rader 1997)
Corduliidae	Predator	(Smock and Roeding 1986; Merritt et al. 2008)	(Turcotte and Harper 1982)
Corixidae	Predator, Macrophytes	(Merritt et al. 2008)	(Larimore 1974; Hemsworth and Brooker 1981)
Corynoneura	Periphyton	(Merritt et al. 2008)	(Steine 1972; Ferrington 1984; Waringer 1992; Rader 1997)
Crambidae	Periphyton	(Merritt et al. 2008)	(Rader 1997)
Crangonyx	FPOM	(Pennak 1989; Thorp and Rogers 2015)	(Larimore 1974)
Cricotopus	Periphyton, Macroalgae	(Merritt et al. 2008)	(Rader 1997)
Cryptochia	Detritus	(Wisseman and Anderson 1987; Merritt et al. 2008)	(Betts and Wisseman 1995)
Cryptochironomus	Predator	(Merritt et al. 2008)	(Steine 1972; Ferrington 1984; Waringer 1992; Rader 1997)
Cryptolabis	Predator, Periphyton	(Merritt et al. 2008)	(Rader 1997)
Cryptotendipes	Detritus, FPOM, Fungi, CPOM, Microbes	(Merritt et al. 2008)	(Rader 1997)

Taxon	Consumer	Sources (food web)	Sources (drift)
Cultus	Predator	(Fuller and Stewart 1977; Stewart and Stark 2002; Merritt et al. 2008)	(Rader 1997)
Dasyhelea	Predator	(Merritt et al. 2008)	(Rader 1997)
Demicryptochironomus	Periphyton	(Merritt et al. 2008)	(Steine 1972; Ferrington 1984; Waringer 1992; Rader 1997)
Despaxia	Detritus	(Stewart and Stark 2002; Merritt et al. 2008)	(Rader 1997)
Deuterophlebia	Periphyton	(Merritt et al. 2008)	(Rader 1997)
Diamesa	Periphyton	(Merritt et al. 2008)	(Steine 1972; Ferrington 1984; Waringer 1992; Rader 1997)
Diamesinae	Diatoms, FPOM, CPOM, Microbes, Periphyton	(Merritt et al. 2008)	(Steine 1972; Ferrington 1984; Waringer 1992; Rader 1997)
Dicosmoecus	Dead Fish, Periphyton, Vascular Plants	(Merritt et al. 2008)	(Rader 1997)
Dicranota	Predator	(Elliott 1983)	(Rader 1997)
Dicrotendipes	Periphyton	(Merritt et al. 2008)	(Steine 1972; Ferrington 1984; Waringer 1992; Rader 1997)
Dipheter	Periphyton	(Gilpin and Brusven 1970; Merritt et al. 2008)	(Rader 1997)
Diura	Predator	(Fuller and Stewart 1977; Stewart and Stark 2002; Merritt et al. 2008)	(Rader 1997)
Dixa	Periphyton	(Merritt et al. 2008)	(Rader 1997)
Dolichopodidae	Predator	(Merritt et al. 2008)	(Rader 1997)
Dolophilodes	Diatoms, FPOM, CPOM, Microbes	(Shapas and Hilsenhoff 1976)	(Rader 1997)
Doroneuria	Predator	(Stewart and Stark 2002)	(Rader 1997)
Drunella	Predator, Periphyton	(Gilpin and Brusven 1970; Hawkins 1990; Merritt et al. 2008)	(Rader 1997)
Dytiscidae	Predator	(Larson et al. 2000)	(Larson et al. 2000)
Ecclisomyia	Dead fish, Detritus, Periphyton	(Minakawa et al. 2002; Merritt et al. 2008; Wiggins 2009)	(Rader 1997)
Ecdyonurus	Periphyton	(Gilpin and Brusven 1970; Merritt et al. 2008)	(Rader 1997)
Elmidae	Periphyton	(Smock and Roeding 1986;	(Rader 1997)

Taxon	Consumer	Sources (food web)	Sources (drift)
		Merritt et al. 2008)	
Empididae	Predator	(Merritt et al. 2008)	(Rader 1997)
Epeorus	Periphyton	(Gilpin and Brusven 1970; Merritt et al. 2008)	(Rader 1997)
Ephemerella	Periphyton	(Hawkins 1990; Merritt et al. 2008)	(Rader 1997)
Erpobdella	Predator	(Pennak 1989; Thorp and Rogers 2015)	(Hemsworth and Brooker 1981; Turcotte and Harper 1982)
Eukiefferiella	Diatoms, FPOM, CPOM, Microbes	(Merritt et al. 2008)	(Steine 1972; Ferrington 1984; Waringer 1992; Rader 1997)
Euryhopsis	Periphyton	(Merritt et al. 2008)	(Steine 1972; Ferrington 1984; Waringer 1992; Rader 1997)
Ferrissia	Periphyton	(Thorp and Rogers 2015)	(Rader 1997)
Forcipomyia	Predator	(Merritt et al. 2008)	(Rader 1997)
Gerridae	Predator	(Merritt et al. 2008)	
Glossosoma	Periphyton	(Shapas and Hilsenhoff 1976; Wiggins 2009)	(Rader 1997)
Glossosomatidae	Periphyton	(Shapas and Hilsenhoff 1976; Merritt et al. 2008; Wiggins 2009)	(Rader 1997)
Glutops	Predator	(Merritt et al. 2008)	(Rader 1997)
Glyptotendipes	Diatoms, FPOM, CPOM, Microbes, Periphyton	(Monakov 1972; Merritt et al. 2008)	(Steine 1972; Ferrington 1984; Waringer 1992; Rader 1997)
Goera	Periphyton	(Merritt et al. 2008)	(Rader 1997; Wiggins 2009; Blinn and Ruiters 2013)
Gomphidae	Predator	(Merritt et al. 2008)	(Rader 1997)
Gyraulid	Periphyton	(Thorp and Rogers 2015)	(Rader 1997)
Gyrinidae	Predator	(Merritt et al. 2008)	(Larimore 1974)
Gyrinus	Predator	(Merritt et al. 2008)	(Larimore 1974)
Halipididae	Macrophytes	(Merritt et al. 2008)	(Larimore 1974)
Heleniella	Diatoms, FPOM, CPOM, Microbes	(Merritt et al. 2008)	(Steine 1972; Ferrington 1984; Waringer 1992; Rader 1997)
Helicopsyche	Periphyton	(Shapas and Hilsenhoff 1976)	(Rader 1997)
Helisoma	Periphyton	(Pennak 1989)	(Rader 1997)
Helobdella	Predator	(Thorp and Rogers 2015)	(Larimore 1974; Turcotte and Harper

Taxon	Consumer	Sources (food web)	Sources (drift)
			1982)
Helodon	FPOM	(Merritt et al. 2008)	(Rader 1997)
Helophorus	Predator, Detritus, Diatoms, FPOM, CPOM, Microbes, Periphyton	(Merritt et al. 2008)	(Larimore 1974)
Hemerodromia	Predator	(Merritt et al. 2008)	(Rader 1997)
Heptageniidae	Periphyton	(Shapas and Hilsenhoff 1976)	(Rader 1997)
Hesperoconopa	Predator	(Merritt et al. 2008)	(Rader 1997)
Hesperoperla	Predator	(Merritt et al. 2008)	(Rader 1997)
Hesperophylax	Diatoms, FPOM, CPOM, Microbes, Periphyton	(Shapas and Hilsenhoff 1976; Merritt et al. 2008)	(Rader 1997)
Heterolimnius	Periphyton	(Merritt et al. 2008)	(Rader 1997)
Heterotrissocladius	Periphyton	(Merritt et al. 2008)	(Steine 1972; Ferrington 1984; Waringer 1992; Rader 1997)
Hexatoma	Predator	(Merritt et al. 2008)	(Rader 1997)
Hirudinea	Predator	(Pennak 1989; Thorp and Rogers 2015)	(Hemsworth and Brooker 1981; Turcotte and Harper 1982)
Hyaella	FPOM	(Pennak 1989; Thorp and Rogers 2015)	(Rader 1997)
Hydra	Diatoms, FPOM, CPOM, Microbes, Periphyton	(Thorp and Rogers 2015)	(Pennak 1989)
Hydraena	Periphyton	(Merritt et al. 2008)	(Perkins 1980)
Hydrobaenus	Diatoms, FPOM, CPOM, Microbes, Periphyton	(Smock and Roeding 1986; Merritt et al. 2008)	(Steine 1972; Ferrington 1984; Waringer 1992; Rader 1997)
Hydrobius	Predator	(Merritt et al. 2008)	(Wye et al. 1979)
Hydrophilidae	Predator	(Merritt et al. 2008)	(Wye et al. 1979)
Hydroporinae	Predator	(Larson et al. 2000)	(Larson et al. 2000)
Hydropsyche	Diatoms, FPOM, CPOM, Microbes, Periphyton	(Shapas and Hilsenhoff 1976; Merritt et al. 2008)	(Rader 1997)
Hydropsychidae	Diatoms, FPOM, CPOM, Microbes	(Merritt et al. 2008; Wiggins 2009)	(Rader 1997)
Hydroptila	Vascular Plants	(Merritt et al. 2008)	(Rader 1997)
Hydroptilidae	Vascular Plants	(Merritt et al. 2008)	(Rader 1997)
Ilybiosoma	Predator	(Larson et al. 2000)	(Larson et al. 2000)
Ilybius	Predator	(Larson et al. 2000)	(Larson et al. 2000)
Ironodes	Periphyton	(Gilpin and Brusven 1970; Merritt et al. 2008)	(Rader 1997)

Taxon	Consumer	Sources (food web)	Sources (drift)
Isoperla	Predator	(Shapas and Hilsenhoff 1976; Fuller and Stewart 1977; Merritt et al. 2008)	(Rader 1997)
Iswaeon	Periphyton	(Gilpin and Brusven 1970; Merritt et al. 2008)	(Rader 1997)
Kathroperla	Predator	(Stewart and Stark 2002; Merritt et al. 2008)	(Rader 1997)
Kogotus_Rickera	Predator	(Merritt et al. 2008)	(Rader 1997)
Krenosmittia	Periphyton	(Merritt et al. 2008)	(Steine 1972; Ferrington 1984; Waringer 1992; Rader 1997)
Labiobaetis	Detritus, Periphyton	(Gilpin and Brusven 1970; Shapas and Hilsenhoff 1976; Merritt et al. 2008)	(Rader 1997)
Labrundinia	Diatoms, FPOM, CPOM, Microbes	(Merritt et al. 2008)	(Steine 1972; Ferrington 1984; Waringer 1992; Rader 1997)
Laccobius	Predator	(Merritt et al. 2008)	(Perkins 1980)
Lara	Detritus	(Steedman and Anderson 1985; Merritt et al. 2008)	(Rader 1997)
Larsia	Predator	(Merritt et al. 2008)	(Steine 1972; Ferrington 1984; Waringer 1992; Rader 1997)
Lepidoptera	Vascular Plants	(Merritt et al. 2008)	(Rader 1997)
Lepidostoma	Dead, fish, Detritus	(Shapas and Hilsenhoff 1976; Merritt et al. 2008)	(Rader 1997)
Leptophlebiidae	Diatoms, FPOM, Periphyton	(Gilpin and Brusven 1970; Merritt et al. 2008)	(Rader 1997)
Leucotrichia	Periphyton	(Merritt et al. 2008)	(Rader 1997)
Leuctridae	Detritus	(Merritt et al. 2008)	(Rader 1997)
Limnephilidae	Diatoms, FPOM, CPOM, Microbes, Vascular, Plants	(Shapas and Hilsenhoff 1976; Merritt et al. 2008)	(Rader 1997)
Limnephilus	Detritus, Macrophytes	(Shapas and Hilsenhoff 1976; Merritt et al. 2008)	(Rader 1997)
Limnophila	Predator	(Merritt et al. 2008)	(Rader 1997)
Limnophyes	Periphyton	(Merritt et al. 2008)	(Steine 1972; Ferrington 1984; Waringer 1992; Rader 1997)
Limonia	Macrophytes	(Merritt et al. 2008)	(Rader 1997)
Liodessus	Predator	(Larson et al. 2000)	(Larson et al. 2000)
Lopescladius	Periphyton	(Merritt et al. 2008)	(Steine 1972; Ferrington 1984; Waringer 1992; Rader 1997)

Taxon	Consumer	Sources (food web)	Sources (drift)
Lymnaeidae	Periphyton	(Pennak 1989; Thorp and Rogers 2015)	(Rader 1997)
Malenka	Detritus	(Merritt et al. 2008)	(Rader 1997)
Margaritifera	Diatoms, FPOM, CPOM, Microbes, Periphyton	(Thorp and Rogers 2015)	(Thorp and Rogers 2015)
Maruina	Periphyton	(Merritt et al. 2008)	(Rader 1997)
Megarcys	Predator	(Richardson and Gaufin 1971; Merritt et al. 2008)	(Rader 1997)
Metriocnemus	Diatoms, FPOM, CPOM, Microbes, Periphyton	(Merritt et al. 2008)	(Steine 1972; Ferrington 1984; Waringer 1992; Rader 1997)
Micrasema	Macrophytes	(Shapas and Hilsenhoff 1976; Merritt et al. 2008)	(Rader 1997)
Microcylloepus	Periphyton	(Merritt et al. 2008)	(Rader 1997)
Micropsectra_Tanytarsus	Diatoms, FPOM, CPOM, Microbes	(Walshe 1951; Merritt et al. 2008)	(Rader 1997)
Microtendipes	Periphyton	(Walshe 1951; Merritt et al. 2008)	(Steine 1972; Ferrington 1984; Waringer 1992; Rader 1997)
Nanocladius	Periphyton	(Merritt et al. 2008)	(Steine 1972; Ferrington 1984; Waringer 1992; Rader 1997)
Narpus	Periphyton	(Merritt et al. 2008)	(Rader 1997)
Nemata	Predator	(Pennak 1989; Thorp and Rogers 2015)	(Rader 1997; Thorp and Rogers 2015)
Nemouridae	Detritus	(Shapas and Hilsenhoff 1976; Merritt et al. 2008)	(Rader 1997)
Neophylax	Periphyton	(Shapas and Hilsenhoff 1976; Merritt et al. 2008; Wiggins 2009)	(Rader 1997)
Neoplasta	Predator	(Merritt et al. 2008)	(Rader 1997)
Neothremma	Diatoms, Periphyton	(Shapas and Hilsenhoff 1976; Merritt et al. 2008)	(Rader 1997; Blinn and Ruiter 2013)
Neotrichia	Periphyton	(Merritt et al. 2008)	(Rader 1997)
Nilotanypus	Predator	(Merritt et al. 2008)	(Steine 1972; Ferrington 1984; Waringer 1992; Rader 1997)
Ochrotrichia	Vascular, Plants	(Merritt et al. 2008)	(Rader 1997; Blinn and Ruiter 2013)
Ochthebius	Periphyton	(Merritt et al. 2008)	(Perkins 1980)
Odontomesa	Periphyton	(Smock and Roeding 1986; Merritt et al. 2008)	(Steine 1972; Ferrington 1984; Waringer 1992; Rader 1997)

Taxon	Consumer	Sources (food web)	Sources (drift)
Oecetis	Diatoms, FPOM, CPOM, Microbes, Periphyton	(Shapas and Hilsenhoff 1976; Smock and Roeding 1986)	(Rader 1997)
Oligochaeta	FPOM	(Monakov 1972)	(Rader 1997)
Onocosmoecus	Diatoms, Fish, FPOM, CPOM, Microbes, Periphyton	(Wisseman and Anderson 1987)	(Rader 1997)
Ophiogomphus	Predator	(Merritt et al. 2008)	(Rader 1997)
Optioservus	Periphyton	(Merritt et al. 2008)	(Rader 1997)
Ordobrevia	Periphyton	(Merritt et al. 2008)	(Rader 1997)
Oreodytes	Predator	(Larson et al. 2000)	(Larimore 1974; Larson et al. 2000)
Oreogeton	Predator	(Merritt et al. 2008)	(Rader 1997)
Orthoclaadiinae	Periphyton	(Smock and Roeding 1986; Merritt et al. 2008)	(Steine 1972; Ferrington 1984; Waringer 1992; Rader 1997)
Orthocladius	Fungi	(Monakov 1972; Smock and Roeding 1986; Merritt et al. 2008)	(Steine 1972; Ferrington 1984; Waringer 1992; Rader 1997)
Ostracoda	Fungi	(Monakov 1972; Thorp and Rogers 2015)	(Rader 1997)
Pacifastacus	Predator	(Thorp and Rogers 2015)	(Thorp and Rogers 2015)
Pagastia	Fungi	(Merritt et al. 2008)	(Steine 1972; Ferrington 1984; Waringer 1992; Rader 1997)
Paracladopelma	Diatoms, FPOM, CPOM, Microbes, Periphyton	(Monakov 1972; Merritt et al. 2008)	(Steine 1972; Ferrington 1984; Waringer 1992; Rader 1997)
Paracricotopus	Fungi, Periphyton	(Merritt et al. 2008)	(Steine 1972; Ferrington 1984; Waringer 1992; Rader 1997)
Parakiefferiella	Fungi	(Merritt et al. 2008)	(Steine 1972; Ferrington 1984; Waringer 1992; Rader 1997)
Paralauterborniella	Fungi	(Merritt et al. 2008)	(Steine 1972; Ferrington 1984; Waringer 1992; Rader 1997)
Paraleptophlebia	Fungi	(Gilpin and Brusven 1970; Merritt et al. 2008)	(Rader 1997)
Paraleuctra	Detritus	(Merritt et al. 2008)	(Rader 1997)
Paramerina	Predator, Diatoms,	(Merritt et al. 2008)	(Steine 1972;

Taxon	Consumer	Sources (food web)	Sources (drift)
	FPOM, CPOM, Microbes, Periphyton		Ferrington 1984; Waringer 1992; Rader 1997)
Parametrioconemus	Fungi	(Merritt et al. 2008)	(Steine 1972; Ferrington 1984; Waringer 1992; Rader 1997)
Paraperla	Predator, FPOM	(Merritt et al. 2008)	(Rader 1997)
Paraphaenocladus	Diatoms, FPOM, CPOM, Microbes, Periphyton	(Merritt et al. 2008)	(Steine 1972; Ferrington 1984; Waringer 1992; Rader 1997)
Parapsyche	Predator	(Shapas and Hilsenhoff 1976; Merritt et al. 2008)	(Rader 1997)
Paratanytarsus	Diatoms, FPOM, CPOM, Microbes	(Merritt et al. 2008)	(Steine 1972; Ferrington 1984; Waringer 1992; Rader 1997)
Paratendipes	Fungi	(Merritt et al. 2008)	(Steine 1972; Ferrington 1984; Waringer 1992; Rader 1997)
Parorthocladus	Fungi	(Monakov 1972; Merritt et al. 2008)	(Steine 1972; Ferrington 1984; Waringer 1992; Rader 1997)
Pedicia	Predator	(Merritt et al. 2008)	(Rader 1997)
Pentaneura	Diatoms, FPOM, CPOM, Microbes, Periphyton	(Monakov 1972)	(Steine 1972; Ferrington 1984; Waringer 1992; Rader 1997)
Pericoma	Fungi	(Merritt et al. 2008)	(Rader and McArthur 1995)
Perlidae	Predator	(Shapas and Hilsenhoff 1976; Fuller and Stewart 1977)	(Rader 1997)
Perlinodes	Predator	(Stewart and Stark 2002; Merritt et al. 2008)	(Rader 1997)
Perlodidae	Predator	(Merritt et al. 2008)	(Rader 1997)
Petrophila	Periphyton	(Merritt et al. 2008)	(Rader 1997; Merritt et al. 2008)
Phaenopsectra	Periphyton	(Merritt et al. 2008)	(Steine 1972; Ferrington 1984; Waringer 1992; Rader 1997)
Philopotamidae	Diatoms, FPOM, CPOM, Microbes	(Merritt et al. 2008)	(Rader 1997)
Physa	Periphyton, FPOM, Diatoms, CPOM	(Pennak 1989)	(Rader 1997)
Planorbidae	Periphyton	(Monakov 1972; Thorp	(Rader 1997)

Taxon	Consumer	Sources (food web)	Sources (drift)
		and Rogers 2015)	
Platysmittia	Diatoms, FPOM, CPOM, Microbes, Periphyton	(Merritt et al. 2008)	(Steine 1972; Ferrington 1984; Waringer 1992; Rader 1997)
Polycelis	Dead fish, Fungi	(Pennak 1989; Thorp and Rogers 2015)	(Rader 1997)
Polycentropus	Predator	(Shapas and Hilsenhoff 1976; Merritt et al. 2008)	(Rader 1997)
Polypedilum	Diatoms, FPOM, CPOM, Microbes	(Merritt et al. 2008)	(Steine 1972; Ferrington 1984; Waringer 1992; Rader 1997)
Potthastia	Fungi	(Monakov 1972)	(Steine 1972; Ferrington 1984; Waringer 1992; Rader 1997)
Procladius	Predator	(Monakov 1972; Merritt et al. 2008)	(Steine 1972; Ferrington 1984; Waringer 1992; Rader 1997)
Procloeon	Fungi	(Merritt et al. 2008)	(Waringer 1992; Rader 1997)
Prosimulium	Diatoms, FPOM, CPOM, Microbes	(Merritt et al. 2008)	(Rader 1997)
Prostoma	Predator	(Pennak 1989; Thorp and Rogers 2015)	(Pennak 1989; Thorp and Rogers 2015)
Protoptila	Periphyton	(Shapas and Hilsenhoff 1976; Merritt et al. 2008)	(Rader 1997)
Psectrocladius	Periphyton	(Merritt et al. 2008)	(Steine 1972; Ferrington 1984; Waringer 1992; Rader 1997)
Psephenus	Periphyton	(Merritt et al. 2008)	(Rader 1997)
Pseudochironomus	Diatoms, FPOM, CPOM, Microbes, Periphyton	(Merritt et al. 2008)	(Steine 1972; Ferrington 1984; Waringer 1992; Rader 1997)
Pseudodiamesa	Diatoms, FPOM, CPOM, Microbes, Periphyton	(Gray and Ward 1979)	(Steine 1972; Ferrington 1984; Waringer 1992; Rader 1997)
Pseudorthocladius	Fungi	(Merritt et al. 2008)	(Steine 1972; Ferrington 1984; Waringer 1992; Rader 1997)
Psychoglypha	Diatoms, FPOM, CPOM, Microbes, Periphyton	(Merritt et al. 2008)	(Rader 1997)
Psychomyia	Periphyton	(Merritt et al. 2008)	(Larimore 1974;

Taxon	Consumer	Sources (food web)	Sources (drift)
			Turcotte and Harper 1982)
Pteronarca	Detritus	(Richardson and Gaufin 1971; Stewart and Stark 2002)	(Rader 1997)
Pteronarcys	Detritus	(Richardson and Gaufin 1971; Stewart and Stark 2002)	(Rader 1997)
Radotanypus	Diatoms, FPOM, CPOM, Microbes, Periphyton	(Merritt et al. 2008)	(Steine 1972; Ferrington 1984; Waringer 1992; Rader 1997)
Rhabdomastix	Predator	(Merritt et al. 2008)	(Rader 1997)
Rhagovelia	Predator	(Merritt et al. 2008)	(Larimore 1974)
Rheocricotopus	Diatoms, FPOM, CPOM, Microbes	(Merritt et al. 2008)	(Steine 1972; Ferrington 1984; Waringer 1992; Rader 1997)
Rheosmittia	Diatoms, FPOM, CPOM, Microbes	(Merritt et al. 2008)	(Steine 1972; Ferrington 1984; Waringer 1992; Rader 1997)
Rheotanytarsus	Diatoms, FPOM, CPOM, Microbes	(Merritt et al. 2008)	(Steine 1972; Ferrington 1984; Waringer 1992; Rader 1997)
Rhithrogena	Periphyton	(Gilpin and Brusven 1970; Merritt et al. 2008)	(Rader 1997)
Rhyacophila	Predator	(Merritt et al. 2008)	(Rader 1997)
Roederiodes	Predator	(Merritt et al. 2008)	(Rader 1997)
Sanfilippodytes	Predator	(Larson et al. 2000)	(Larson et al. 2000)
Serratella	Detritus, Diatoms, Fungi	(López-Rodríguez et al. 2008)	(Rader 1997)
Sialis	Predator	(Smock and Roeding 1986)	(Rader 1997)
Simuliidae	Diatoms, FPOM, CPOM, Microbes	(Merritt et al. 2008)	(Rader 1997)
Simulium	Diatoms, FPOM, CPOM, Microbes, Periphyton	(Merritt et al. 2008)	(Rader 1997)
Skwala	Predator	(Richardson and Gaufin 1971; Fuller and Stewart 1977)	(Rader 1997)
Sphaeriidae	Fungi	(Monakov 1972)	(Rader 1997)
Sphaerium	Diatoms, FPOM, CPOM, Microbes	(Monakov 1972)	(Rader 1997)
Stactobiella	Detritus	(Merritt et al. 2008)	(Rader 1997)
Stagnicola	Periphyton	(Walshe 1951)	(Rader 1997)
Stempellina	Diatoms, FPOM, CPOM, Microbes,	(Merritt et al. 2008)	(Steine 1972; Ferrington 1984;

Taxon	Consumer	Sources (food web)	Sources (drift)
	Periphyton		Waringer 1992; Rader 1997)
Stempellinella	Diatoms, FPOM, CPOM, Microbes	(Merritt et al. 2008)	(Steine 1972; Ferrington 1984; Waringer 1992; Rader 1997)
Stictochironomus	Fungi	(Merritt et al. 2008)	(Steine 1972; Ferrington 1984; Waringer 1992; Rader 1997)
Stictotarsus	Predator	(Larson et al. 2000)	(Larson et al. 2000)
Stilocladius	Diatoms, FPOM, CPOM, Microbes, Periphyton	(Merritt et al. 2008)	(Steine 1972; Ferrington 1984; Waringer 1992; Rader 1997)
Sublettea	Diatoms, FPOM, CPOM, Microbes	(Merritt et al. 2008)	(Steine 1972; Ferrington 1984; Waringer 1992; Rader 1997)
Suwallia	Predator	(Stewart and Stark 2002; Merritt et al. 2008)	(Rader 1997)
Sweltsa	Predator	(Stewart and Stark 2002)	(Rader 1997)
Symposiocladius	Diatoms, FPOM, CPOM, Microbes, Periphyton	(Merritt et al. 2008)	(Steine 1972; Ferrington 1984; Waringer 1992; Rader 1997)
Sympotthastia	Fungi	(Merritt et al. 2008)	(Steine 1972; Ferrington 1984; Waringer 1992; Rader 1997)
Synorthocladius	Fungi	(Merritt et al. 2008)	(Steine 1972; Ferrington 1984; Waringer 1992; Rader 1997)
Tabanidae	Predator	(Merritt et al. 2008)	(Rader 1997)
Tabanus	Predator	(Merritt et al. 2008)	(Rader 1997)
Taenionema	Detritus, Fungi, Macrophytes, Periphyton	(Richardson and Gaufin 1971; Stewart and Stark 2002)	(Rader 1997)
Taeniopterygidae	Detritus, Fungi, Macrophytes, Periphyton	(Richardson and Gaufin 1971; Stewart and Stark 2002)	(Rader 1997)
Taeniopteryx	Detritus	(Richardson and Gaufin 1971; Stewart and Stark 2002)	(Rader 1997)
Tanypodinae	Predator, Diatoms	(Roback 1969; Smock and Roeding 1986)	(Steine 1972; Ferrington 1984; Waringer 1992; Rader 1997)
Tanytarsini	Fungi	(Smock and Roeding 1986)	(Rader 1997)

Taxon	Consumer	Sources (food web)	Sources (drift)
Thaumalea	Fungi, Periphyton	(Merritt et al. 2008)	(Rader 1997; Merritt et al. 2008)
Thienemanniella	Fungi	(Merritt et al. 2008)	(Steine 1972; Ferrington 1984; Waringer 1992; Rader 1997)
Thienemannimyia	Predator	(Merritt et al. 2008)	(Steine 1972; Ferrington 1984; Waringer 1992; Rader 1997)
Timpanoga	FPOM, Diatoms	(Gilpin and Brusven 1970)	(Rader 1997)
Tipula	Predator, Detritus, CPOM, FPOM	(Smock and Roeding 1986)	(Rader 1997)
Tipulidae	Predator	(Merritt et al. 2008)	(Rader 1997)
Tribelos	Periphyton	(Merritt et al. 2008)	(Steine 1972; Ferrington 1984; Waringer 1992; Rader 1997)
Tricorythodes	Fungi	(Shapas and Hilsenhoff 1976)	(Larimore 1974; Hall et al. 1980)
Trombidiformes	Predator	(Di Sabatino et al. 2000)	(Di Sabatino et al. 2000)
Tropisternus	Predator	(Merritt et al. 2008)	(Rader 1997; Merritt et al. 2008)
Turbellaria	Predator, Dead, fish, periphyton	(Pennak 1989)	(Rader 1997)
Tvetenia	Fungi	(Merritt et al. 2008)	(Steine 1972; Ferrington 1984; Waringer 1992; Rader 1997)
Unionidae	Diatoms, FPOM, CPOM, Microbes, Periphyton	(Pennak 1989; Thorp and Rogers 2015)	(Thorp and Rogers 2015)
Uvarus	Predator	(Larson et al. 2000)	(Larson et al. 2000)
Valvata	Periphyton	(Thorp and Rogers 2015)	(Rader 1997)
Visoka	Detritus	(Merritt et al. 2008)	(Rader 1997)
Wiedemannia	Predator	(Merritt et al. 2008)	(Rader 1997)
Wormaldia	Diatoms, FPOM, CPOM, Microbes	(Merritt et al. 2008)	(Rader 1997)
Yoraperla	Detritus	(Stewart and Stark 2002)	(Danehy et al. 2011)
Zaitzevia	Fungi	(Merritt et al. 2008)	(Rader 1997)
Zapada	Detritus	(Stewart and Stark 2002)	(Rader 1997)
Zavrelimyia	Predator, Diatoms	(Roback 1969)	(Steine 1972; Ferrington 1984; Waringer 1992; Rader 1997)

Appendix 3: Table of traits, scores, total adjusted scores of 295 individual taxa found during the project period

List is in order of the taxonomic hierarchy presented in Appendix 1. Group 1 associated taxa are low drift available taxa and are excluded from the ASC calculations. Group 2 taxa are highly available in the drift. Group 3 taxa are only moderately available in the drift.

Taxon	Active Drift	Habitat	Flow Exposure	Mobility	Drag Index	Drift Distance	Emergence Behavior	Oviposit Behavior	Diel Activity	Benthic Exposure	Size Scores	Abundance	Total	Tot Adj	Rank	Group
Erpobdella	0	1	0	0	0	0	0	0	0	1	9	R	11	5.5	257	1
Helobdella	0	1	0	0	0	0	0	0	0	1	9	R	11	5.5	257	1
Hirudinea	0	1	0	0	0	0	0	0	0	1	9	R	11	5.5	257	1
Oligochaeta	0	1	0	0	0	0	0	0	0	0	9	A	10	10	266	1
Branchiobdellida	0	0	0	0	0	0	0	0	0	0	1	C	1	1	293	1
Trombidiformes	9	9	6	9	3	1	0	0	0	1	1	A	39	39	162	2
Crangonyx	9	1	0	0	0	0	0	0	0	3	9	C	22	22	228	1
Hyaella	9	9	0	0	0	0	0	0	0	3	9	C	30	30	196	1
Pacifastacus	0	1	0	0	0	0	0	0	0	1	9	C	11	11	257	1
Caecidotea	0	9	0	9	3	1	0	0	0	1	3	R	26	13	214	2
Copepoda	0	0	0	0	0	0	0	0	0	0	1	C	1	1	293	1
Ostracoda	0	1	0	0	0	0	0	0	0	1	1	C	3	3	292	1
Stictotarsus	0	9	0	3	1	6	6	6	6	1	9	R	47	23.5	33	3
Uvarus	0	9	0	3	1	6	6	6	6	1	9	R	47	23.5	33	3
Agabus	0	1	0	0	0	0	0	3	0	3	9	C	16	16	237	1
Hydroporinae	0	1	0	0	0	0	0	3	0	3	9	C	16	16	237	1
Ilybiosoma	0	1	0	0	0	0	0	3	0	3	9	C	16	16	237	1
Ilybius	0	1	0	0	0	0	0	3	0	3	9	C	16	16	237	1
Liodessus	0	1	0	0	0	0	0	3	0	3	9	C	16	16	237	1
Oreodytes	0	1	0	0	0	0	0	3	0	3	9	C	16	16	237	1
Dytiscidae	0	1	0	0	0	0	0	3	0	3	9	R	16	8	237	1
Sanfilippodytes	0	1	0	0	0	0	0	3	0	3	9	R	16	8	237	1

Taxon	Active Drift	Habitat	Flow Exposure	Mobility	Drag Index	Drift Distance	Emergence Behavior	Oviposit Behavior	Diel Activity	Benthic Exposure	Size Scores	Abundance	Total	Tot Adj	Rank	Group
Cleptelmis	0	9	6	3	1	3	3	3	0	1	3	A	32	32	187	2
Elmidae	0	9	6	3	1	3	3	3	0	1	3	A	32	32	187	2
Heterolimnius	0	9	6	3	1	3	3	3	0	1	3	A	32	32	187	2
Optioservus	0	9	6	3	1	3	3	3	0	1	3	A	32	32	187	2
Zaitzevia	0	9	6	3	1	3	3	3	0	1	3	A	32	32	187	2
Lara	0	9	6	3	1	3	3	3	0	1	3	C	32	32	187	2
Narpus	0	9	6	3	1	3	3	3	0	1	3	C	32	32	187	2
Ordobrevia	0	9	6	3	1	3	3	3	0	1	3	C	32	32	187	2
Microcylloepus	0	9	6	3	1	3	3	3	0	1	3	R	32	16	187	2
Gyrinidae	0	1	0	0	0	0	0	3	0	3	3	R	10	5	266	1
Gyrinus	0	1	0	0	0	0	0	3	0	3	3	R	10	5	266	1
Brychius	0	1	0	0	0	0	0	3	0	3	3	C	10	10	266	1
Haliplidae	0	1	0	0	0	0	0	3	0	3	3	R	10	5	266	1
Helophorus	0	1	0	0	0	0	0	3	0	3	3	R	10	5	266	1
Hydraena	0	1	0	0	0	0	0	3	0	3	3	C	10	10	266	1
Ochthebius	0	1	0	0	0	0	0	3	0	3	3	R	10	5	266	1
Ametor	0	1	0	0	0	0	0	3	0	3	3	R	10	5	266	1
Hydrobius	0	1	0	0	0	0	0	3	0	3	3	R	10	5	266	1
Hydrophilidae	0	1	0	0	0	0	0	3	0	3	3	R	10	5	266	1
Laccobius	0	1	0	0	0	0	0	3	0	3	3	R	10	5	266	1
Tropisternus	0	1	0	0	0	0	0	3	0	3	3	R	10	5	266	1
Psephenus	0	9	1	1	1	6	3	3	1	1	3	A	29	29	197	2
Atherix	0	9	6	3	6	6	3	0	6	1	9	A	49	73.5	27	2
Bibiocephala	0	9	1	1	1	6	6	0	6	3	9	C	42	50.4	102	2
Blepharicera	0	9	1	1	1	6	6	0	6	3	9	R	42	21	102	2
Blephariceridae	0	9	1	1	1	6	6	0	6	3	9	R	42	21	102	2

Taxon	Active Drift	Habitat	Flow Exposure	Mobility	Drag Index	Drift Distance	Emergence Behavior	Oviposit Behavior	Diel Activity	Benthic Exposure	Size Scores	Abundance	Total	Tot Adj	Rank	Group
Ceratopogoninae	0	1	0	0	0	0	6	6	6	1	3	C	23	23	221	1
Atrichopogon	0	1	0	0	0	0	6	6	6	1	3	R	23	11.5	221	1
Dasyhelea	0	1	0	0	0	0	6	6	6	1	3	R	23	11.5	221	1
Forcipomyia	0	1	0	0	0	0	6	6	6	1	3	R	23	11.5	221	1
Thienemannimyia	0	9	0	3	1	6	6	6	6	1	9	A	47	70.5	33	3
Ablabesmyia	0	9	0	3	1	6	6	6	6	1	9	C	47	56.4	33	3
Alotanypus	0	9	0	3	1	6	6	6	6	1	9	C	47	56.4	33	3
Apedilum	0	9	0	3	1	6	6	6	6	1	9	C	47	56.4	33	3
Chironomus	0	9	0	3	1	6	6	6	6	1	9	C	47	56.4	33	3
Diamesinae	0	9	0	3	1	6	6	6	6	1	9	C	47	56.4	33	3
Larsia	0	9	0	3	1	6	6	6	6	1	9	C	47	56.4	33	3
Nilotanypus	0	9	0	3	1	6	6	6	6	1	9	C	47	56.4	33	3
Pentaneura	0	9	0	3	1	6	6	6	6	1	9	C	47	56.4	33	3
Radotanypus	0	9	0	3	1	6	6	6	6	1	9	C	47	56.4	33	3
Tanypodinae	0	9	0	3	1	6	6	6	6	1	9	C	47	56.4	33	3
Zavreliomyia	0	9	0	3	1	6	6	6	6	1	9	C	47	56.4	33	3
Brundiniella	0	9	0	3	1	6	6	6	6	1	9	R	47	23.5	33	3
Labrundinia	0	9	0	3	1	6	6	6	6	1	9	R	47	23.5	33	3
Paracladopelma	0	9	0	3	1	6	6	6	6	1	9	R	47	23.5	33	3
Paramerina	0	9	0	3	1	6	6	6	6	1	9	R	47	23.5	33	3
Paraphaenocladus	0	9	0	3	1	6	6	6	6	1	9	R	47	23.5	33	3
Platysmittia	0	9	0	3	1	6	6	6	6	1	9	R	47	23.5	33	3
Pseudochironomus	0	9	0	3	1	6	6	6	6	1	9	R	47	23.5	33	3
Pseudodiamesa	0	9	0	3	1	6	6	6	6	1	9	R	47	23.5	33	3
Stilocladus	0	9	0	3	1	6	6	6	6	1	9	R	47	23.5	33	3
Symposiocladius	0	9	0	3	1	6	6	6	6	1	9	R	47	23.5	33	3

Taxon	Active Drift	Habitat	Flow Exposure	Mobility	Drag Index	Drift Distance	Emergence Behavior	Oviposit Behavior	Diel Activity	Benthic Exposure	Size Scores	Abundance	Total	Tot Adj	Rank	Group
Pagastia	0	9	0	1	1	6	6	6	6	1	9	A	45	67.5	60	3
Polypedilum	0	9	0	1	1	6	6	6	6	1	9	A	45	67.5	60	3
Potthastia	0	9	0	1	1	6	6	6	6	1	9	A	45	67.5	60	3
Boreoheptagyia	0	9	0	1	1	6	6	6	6	1	9	C	45	54	60	3
Diamesa	0	9	0	1	1	6	6	6	6	1	9	C	45	54	60	3
Parametriochnemus	0	9	0	1	1	6	6	6	6	1	9	C	45	54	60	3
Procladius	0	9	0	1	1	6	6	6	6	1	9	C	45	54	60	3
Boreochlus	0	9	0	1	1	6	6	6	6	1	9	R	45	22.5	60	3
Cryptochironomus	0	9	0	1	1	6	6	6	6	1	9	R	45	22.5	60	3
Demicryptochironomus	0	9	0	1	1	6	6	6	6	1	9	R	45	22.5	60	3
Paralauterborniella	0	9	0	1	1	6	6	6	6	1	9	R	45	22.5	60	3
Stictochironomus	0	9	0	1	1	6	6	6	6	1	9	R	45	22.5	60	3
Sympotthastia	0	9	0	1	1	6	6	6	6	1	9	R	45	22.5	60	3
Tribelos	0	9	0	1	1	6	6	6	6	1	9	R	45	22.5	60	3
Brillia	0	9	1	1	1	6	6	6	6	1	3	A	40	40	126	3
Cricotopus	0	9	1	1	1	6	6	6	6	1	3	A	40	40	126	3
Cryptotendipes	0	9	1	1	1	6	6	6	6	1	3	A	40	40	126	3
Eukiefferiella	0	9	1	1	1	6	6	6	6	1	3	A	40	40	126	3
Metriochnemus	0	9	1	1	1	6	6	6	6	1	3	A	40	40	126	3
Orthoclaadiinae	0	9	1	1	1	6	6	6	6	1	3	A	40	40	126	3
Orthocladus	0	9	1	1	1	6	6	6	6	1	3	A	40	40	126	3
Paracricotopus	0	9	1	1	1	6	6	6	6	1	3	A	40	40	126	3
Rheocricotopus	0	9	1	1	1	6	6	6	6	1	3	A	40	40	126	3
Thienemanniella	0	9	1	1	1	6	6	6	6	1	3	A	40	40	126	3
Tvetenia	0	9	1	1	1	6	6	6	6	1	3	A	40	40	126	3
Cardiocladius	0	9	1	1	1	6	6	6	6	1	3	C	40	48	126	3

Taxon	Active Drift	Habitat	Flow Exposure	Mobility	Drag Index	Drift Distance	Emergence Behavior	Oviposit Behavior	Diel Activity	Benthic Exposure	Size Scores	Abundance	Total	Tot Adj	Rank	Group
Corynoneura	0	9	1	1	1	6	6	6	6	1	3	C	40	48	126	3
Heleniella	0	9	1	1	1	6	6	6	6	1	3	C	40	48	126	3
Heterotrissocladius	0	9	1	1	1	6	6	6	6	1	3	C	40	48	126	3
Hydrobaenus	0	9	1	1	1	6	6	6	6	1	3	C	40	48	126	3
Krenosmittia	0	9	1	1	1	6	6	6	6	1	3	C	40	48	126	3
Limnophyes	0	9	1	1	1	6	6	6	6	1	3	C	40	48	126	3
Lopescladius	0	9	1	1	1	6	6	6	6	1	3	C	40	48	126	3
Nanocladius	0	9	1	1	1	6	6	6	6	1	3	C	40	48	126	3
Parakiefferiella	0	9	1	1	1	6	6	6	6	1	3	C	40	48	126	3
Phaenopsectra	0	9	1	1	1	6	6	6	6	1	3	C	40	48	126	3
Psectrocladius	0	9	1	1	1	6	6	6	6	1	3	C	40	48	126	3
Rheosmittia	0	9	1	1	1	6	6	6	6	1	3	C	40	48	126	3
Synorthocladius	0	9	1	1	1	6	6	6	6	1	3	C	40	48	126	3
Odontomesa	0	9	1	1	1	6	6	6	6	1	3	R	40	20	126	3
Parorthocladius	0	9	1	1	1	6	6	6	6	1	3	R	40	20	126	3
Pseudorthocladius	0	9	1	1	1	6	6	6	6	1	3	R	40	20	126	3
Micropsectra_Tanytarsus	0	9	0	1	1	6	6	6	6	1	3	A	39	39	162	3
Microtendipes	0	9	0	1	1	6	6	6	6	1	3	A	39	39	162	3
Paratanytarsus	0	9	0	1	1	6	6	6	6	1	3	A	39	39	162	3
Rheotanytarsus	0	9	0	1	1	6	6	6	6	1	3	A	39	39	162	3
Stempellinella	0	9	0	1	1	6	6	6	6	1	3	A	39	39	162	3
Chironomidae	0	9	0	1	1	6	6	6	6	1	3	C	39	46.8	162	3
Chironomini	0	9	0	1	1	6	6	6	6	1	3	C	39	46.8	162	3
Cladotanytarsus	0	9	0	1	1	6	6	6	6	1	3	C	39	46.8	162	3
Dicrotendipes	0	9	0	1	1	6	6	6	6	1	3	C	39	46.8	162	3
Sublettea	0	9	0	1	1	6	6	6	6	1	3	C	39	46.8	162	3

Taxon	Active Drift	Habitat	Flow Exposure	Mobility	Drag Index	Drift Distance	Emergence Behavior	Oviposit Behavior	Diel Activity	Benthic Exposure	Size Scores	Abundance	Total	Tot Adj	Rank	Group
Tanytarsini	0	9	0	1	1	6	6	6	6	1	3	C	39	46.8	162	3
Euryhopsis	0	9	0	1	1	6	6	6	6	1	3	R	39	19.5	162	3
Glyptotendipes	0	9	0	1	1	6	6	6	6	1	3	R	39	19.5	162	3
Paratendipes	0	9	0	1	1	6	6	6	6	1	3	R	39	19.5	162	3
Deuterophlebia	0	9	1	3	1	6	6	3	6	3	3	R	41	20.5	110	2
Dixa	0	1	0	0	0	0	3	0	6	1	3	C	14	14	246	1
Dolichopodidae	0	1	0	0	0	0	6	6	6	1	1	R	21	10.5	230	1
Empididae	0	9	0	3	1	6	6	6	6	1	3	C	41	49.2	110	3
Hemerodromia	0	9	0	3	1	6	6	6	6	1	3	C	41	49.2	110	3
Neoplasta	0	9	0	3	1	6	6	6	6	1	3	C	41	49.2	110	3
Oreogeton	0	9	0	3	1	6	6	6	6	1	3	C	41	49.2	110	3
Roederiodes	0	9	0	3	1	6	6	6	6	1	3	C	41	49.2	110	3
Chelifera_Metachela	0	9	0	3	1	6	6	6	6	1	3	R	41	20.5	110	3
Wiedemannia	0	9	0	3	1	6	6	6	6	1	3	R	41	20.5	110	3
Clinocera	0	1	0	0	0	0	6	6	6	1	3	C	23	23	221	1
Glutops	0	1	0	0	0	0	6	6	6	1	9	C	29	29	197	1
Maruina	1	9	1	1	1	0	6	6	6	1	3	R	35	17.5	184	2
Pericoma	0	1	0	0	0	0	6	6	6	1	3	C	23	23	221	1
Helodon	9	9	6	1	1	3	6	6	6	3	3	A	53	79.5	6	2
Prosimulium	9	9	6	1	1	3	6	6	6	3	3	A	53	79.5	6	2
Simulium	9	9	6	1	1	3	6	6	6	3	3	A	53	79.5	6	2
Simuliidae	9	9	6	1	1	3	6	6	6	3	3	C	53	63.6	6	2
Tabanidae	0	1	0	0	0	0	3	0	6	1	3	C	14	14	246	1
Tabanus	0	1	0	0	0	0	3	0	6	1	3	C	14	14	246	1
Thaumalea	0	1	0	0	0	0	6	6	6	1	3	R	23	11.5	221	1
Antocha	0	9	0	3	6	6	3	0	6	1	9	A	43	43	89	2

Taxon	Active Drift	Habitat	Flow Exposure	Mobility	Drag Index	Drift Distance	Emergence Behavior	Oviposit Behavior	Diel Activity	Benthic Exposure	Size Scores	Abundance	Total	Tot Adj	Rank	Group
Dicranota	0	9	0	3	6	6	3	0	6	1	9	C	43	51.6	89	2
Limonia	0	9	0	3	6	6	3	0	6	1	9	R	43	21.5	89	2
Pedicia	0	9	0	3	6	6	3	0	6	1	9	R	43	21.5	89	2
Hexatoma	0	1	0	0	0	0	3	0	6	1	3	A	14	14	246	1
Cryptolabis	0	1	0	0	0	0	3	0	6	1	3	C	14	14	246	1
Hesperoconopa	0	1	0	0	0	0	3	0	6	1	3	C	14	14	246	1
Limnophila	0	1	0	0	0	0	3	0	6	1	3	C	14	14	246	1
Tipula	0	1	0	0	0	0	3	0	6	1	3	C	14	14	246	1
Tipulidae	0	1	0	0	0	0	3	0	6	1	3	C	14	14	246	1
Rhabdomastix	0	1	0	0	0	0	3	0	6	1	3	R	14	7	246	1
Ameletus	3	9	6	3	3	3	3	6	6	1	9	A	52	78	22	2
Acentrella	9	9	6	9	1	1	6	3	6	3	9	A	62	93	1	2
Anafrptilum	9	9	6	9	1	1	6	3	6	3	9	A	62	93	1	2
Baetidae	9	9	6	9	1	1	6	3	6	3	9	A	62	93	1	2
Baetis	9	9	6	9	1	1	6	3	6	3	9	A	62	93	1	2
Diphetor	9	9	6	9	1	1	6	3	6	3	9	A	62	93	1	2
Iswaeon	9	1	0	0	0	0	6	6	6	3	9	C	40	48	126	1
Labiobaetis	9	1	0	0	0	0	6	6	6	3	9	R	40	20	126	1
Procloeon	9	1	0	0	0	0	6	6	6	3	9	R	40	20	126	1
Caenis	1	1	0	0	0	0	3	3	6	1	3	R	18	9	234	1
Caudatella	1	9	6	3	3	3	6	6	6	1	9	A	53	79.5	6	2
Drunella	1	9	6	3	3	3	6	6	6	1	9	A	53	79.5	6	2
Ephemerella	1	9	6	3	3	3	6	6	6	1	9	A	53	79.5	6	2
Attenella	1	9	6	3	1	3	6	6	6	1	9	A	51	76.5	23	2
Serratella	1	9	6	3	1	3	6	6	6	1	9	A	51	76.5	23	2
Timpanoga	1	1	0	0	0	0	6	6	6	0	9	C	29	29	197	1

Taxon	Active Drift	Habitat	Flow Exposure	Mobility	Drag Index	Drift Distance	Emergence Behavior	Oviposit Behavior	Diel Activity	Benthic Exposure	Size Scores	Abundance	Total	Tot Adj	Rank	Group
Cinygmula	3	9	6	3	1	3	6	6	6	1	9	A	53	79.5	6	2
Ecdyonurus	3	9	6	3	1	3	6	6	6	1	9	A	53	79.5	6	2
Epeorus	3	9	6	3	1	3	6	6	6	1	9	A	53	79.5	6	2
Heptageniidae	3	9	6	3	1	3	6	6	6	1	9	A	53	79.5	6	2
Rhithrogena	3	9	6	3	1	3	6	6	6	1	9	A	53	79.5	6	2
Cinygma	3	9	6	3	1	3	6	6	6	1	9	C	53	63.6	6	2
Ironodes	3	9	6	3	1	3	6	6	6	1	9	C	53	63.6	6	2
Tricorythodes	1	1	0	0	0	0	6	6	6	0	9	A	29	29	197	1
Leptophlebiidae	3	9	6	3	1	3	6	6	6	1	9	A	53	79.5	6	2
Paraleptophlebia	3	9	6	3	1	3	6	6	6	1	9	A	53	79.5	6	2
Corixidae	0	1	0	0	0	0	0	0	1	3	3	R	8	4	282	1
Aquarius	0	0	0	0	0	0	0	0	0	0	9	R	9	4.5	279	1
Gerridae	0	0	0	0	0	0	0	0	0	0	9	R	9	4.5	279	1
Rhagovelia	0	0	0	0	0	0	0	0	0	0	9	R	9	4.5	279	1
Petrophila	3	9	1	1	6	3	6	3	1	1	9	A	43	43	89	2
Crambidae	3	9	1	1	6	3	6	3	1	1	9	C	43	51.6	89	2
Lepidoptera	3	9	1	1	6	3	6	3	1	1	9	C	43	51.6	89	2
Sialis	0	9	6	3	6	3	3	0	6	1	3	C	40	48	126	2
Calopterygidae	1	1	0	0	0	0	3	0	0	3	9	R	17	8.5	236	1
Argia	3	1	0	0	0	0	3	6	6	1	9	C	29	29	197	1
Coenagrionidae	3	1	0	0	0	0	3	6	6	1	9	C	29	29	197	1
Corduliidae	3	1	0	0	0	0	3	6	6	1	9	R	29	14.5	197	1
Gomphidae	3	1	0	0	0	0	3	6	6	1	9	C	29	29	197	1
Ophiogomphus	3	1	0	0	0	0	3	6	6	1	9	C	29	29	197	1
Capniidae	1	0	0	0	0	0	0	6	6	0	9	C	22	22	228	1
Sweltsa	1	9	6	3	3	3	3	6	6	1	9	A	50	75	25	2

Taxon	Active Drift	Habitat	Flow Exposure	Mobility	Drag Index	Drift Distance	Emergence Behavior	Oviposit Behavior	Diel Activity	Benthic Exposure	Size Scores	Abundance	Total	Tot Adj	Rank	Group
Chloroperlidae	1	9	6	3	3	3	3	6	6	1	9	C	50	60	25	2
Paraperla	1	0	0	0	0	0	3	6	6	0	9	C	25	25	215	1
Suwallia	1	0	0	0	0	0	3	6	6	0	9	C	25	25	215	1
Kathroperla	1	0	0	0	0	0	3	6	6	0	9	R	25	12.5	215	1
Leuctridae	1	0	0	0	0	0	3	6	6	0	9	C	25	25	215	1
Paraleuctra	1	0	0	0	0	0	3	6	6	0	9	C	25	25	215	1
Despaxia	1	0	0	0	0	0	3	6	6	0	9	R	25	12.5	215	1
Zapada	1	9	6	3	1	3	3	6	6	1	9	A	48	72	28	2
Malenka	1	9	6	3	1	3	3	6	6	1	9	C	48	57.6	28	2
Nemouridae	1	9	6	3	1	3	3	6	6	1	9	C	48	57.6	28	2
Visoka	1	9	6	3	1	3	3	6	6	1	9	C	48	57.6	28	2
Yoraperla	1	9	6	3	1	3	3	6	6	1	9	C	48	57.6	28	2
Calineuria	3	9	6	3	6	1	3	6	1	1	3	A	42	42	102	2
Hesperoperla	3	9	6	3	6	1	3	6	1	1	3	A	42	42	102	2
Perlidae	3	9	6	3	6	1	3	6	1	1	3	A	42	42	102	2
Claassenia	3	9	6	3	6	1	3	6	1	1	3	C	42	50.4	102	2
Doroneuria	3	9	6	3	6	1	3	6	1	1	3	C	42	50.4	102	2
Perlinodes	1	9	6	3	3	3	3	6	1	1	9	A	45	67.5	60	2
Perlodidae	1	9	6	3	3	3	3	6	1	1	9	A	45	67.5	60	2
Skwala	1	9	6	3	3	3	3	6	1	1	9	A	45	67.5	60	2
Isoperla	1	9	6	3	3	3	3	6	1	1	9	C	45	54	60	2
Megarcys	1	9	6	3	3	3	3	6	1	1	9	C	45	54	60	2
Cultus	1	9	6	3	3	3	3	6	1	1	9	R	45	22.5	60	2
Diura	1	9	6	3	3	3	3	6	1	1	9	R	45	22.5	60	2
Kogotus_Rickera	1	9	6	3	3	3	3	6	1	1	9	R	45	22.5	60	2
Pteronarcella	1	9	6	3	6	3	3	3	1	1	3	C	39	46.8	162	2

Taxon	Active Drift	Habitat	Flow Exposure	Mobility	Drag Index	Drift Distance	Emergence Behavior	Oviposit Behavior	Diel Activity	Benthic Exposure	Size Scores	Abundance	Total	Tot Adj	Rank	Group
Pteronarcys	1	9	6	3	6	3	3	3	1	1	3	C	39	46.8	162	2
Taenionema	3	0	0	0	0	0	3	0	6	0	9	R	21	10.5	230	1
Taeniopterygidae	3	0	0	0	0	0	3	0	6	0	9	R	21	10.5	230	1
Taeniopteryx	3	0	0	0	0	0	3	0	6	0	9	R	21	10.5	230	1
Apatania	0	9	6	3	6	0	6	6	1	1	9	C	47	56.4	33	2
Amiocentrus	0	9	1	1	3	6	6	6	1	3	9	A	45	67.5	60	2
Brachycentrus	0	9	1	1	3	6	6	6	1	3	9	A	45	67.5	60	2
Micrasema	0	9	1	1	3	6	6	6	1	3	9	A	45	67.5	60	2
Brachycentridae	0	9	1	1	3	6	6	6	1	3	9	C	45	54	60	2
Agapetus	0	9	1	1	3	6	6	6	1	3	9	C	45	54	60	2
Anagapetus	0	9	1	1	3	6	6	6	1	3	9	C	45	54	60	2
Glossosoma	0	9	6	3	1	0	6	3	1	3	9	A	41	41	110	2
Glossosomatidae	0	9	6	3	1	0	6	3	1	3	9	C	41	49.2	110	2
Protoptila	0	9	6	3	1	0	6	3	1	3	9	C	41	49.2	110	2
Goera	0	9	6	3	3	0	6	3	1	1	9	R	41	20.5	110	2
Helicopsyche	0	9	6	3	3	0	6	3	1	1	9	A	41	41	110	2
Arctopsyche	3	9	1	1	6	3	6	3	1	1	9	A	43	43	89	2
Cheumatopsyche	3	9	1	1	6	3	6	3	1	1	9	A	43	43	89	2
Hydropsyche	3	9	1	1	6	3	6	3	1	1	9	A	43	43	89	2
Hydropsychidae	3	9	1	1	6	3	6	3	1	1	9	C	43	51.6	89	2
Parapsyche	3	9	1	1	6	3	6	3	1	1	9	C	43	51.6	89	2
Ochrotrichia	0	9	1	0	1	0	6	3	1	3	3	A	27	27	207	2
Hydroptila	0	9	1	0	1	0	6	3	1	3	3	C	27	27	207	2
Hydroptilidae	0	9	1	0	1	0	6	3	1	3	3	C	27	27	207	2
Leucotrichia	0	9	1	0	1	0	6	3	1	3	3	C	27	27	207	2
Neotrichia	0	9	1	0	1	0	6	3	1	3	3	C	27	27	207	2

Taxon	Active Drift	Habitat	Flow Exposure	Mobility	Drag Index	Drift Distance	Emergence Behavior	Oviposit Behavior	Diel Activity	Benthic Exposure	Size Scores	Abundance	Total	Tot Adj	Rank	Group
Stactobiella	0	9	1	0	1	0	6	3	1	3	3	C	27	27	207	2
Agraylea	0	9	1	0	1	0	6	3	1	3	3	R	27	13.5	207	2
Lepidostoma	0	9	6	3	3	0	6	3	1	1	9	A	41	41	110	2
Oecetis	0	9	6	3	6	0	6	6	1	1	9	C	47	56.4	33	2
Ceraclea	0	9	6	3	6	0	6	6	1	1	9	R	47	23.5	33	2
Dicosmoecus	0	9	6	3	6	0	6	3	1	1	3	C	38	45.6	179	2
Limnephilidae	0	9	6	3	6	0	6	3	1	1	3	C	38	45.6	179	2
Ecclisomyia	0	9	6	3	6	0	6	3	1	1	3	R	38	19	179	2
Limnephilus	0	9	6	3	6	0	6	3	1	1	3	R	38	19	179	2
Hesperophylax	0	9	6	3	6	0	6	0	1	1	3	C	35	42	184	2
Psychoglypha	0	9	6	3	6	0	6	0	1	1	3	C	35	42	184	2
Onocosmoecus	0	1	0	0	0	0	6	0	1	1	9	C	18	18	234	1
Cryptochia	0	1	0	0	0	0	6	3	1	1	3	C	15	15	245	1
Dolophilodes	3	9	1	1	3	3	6	3	1	1	9	C	40	48	126	2
Wormaldia	3	9	1	1	3	3	6	3	1	1	9	C	40	48	126	2
Philopotamidae	3	9	1	1	3	3	6	3	1	1	9	R	40	20	126	2
Polycentropus	3	9	1	1	6	3	6	3	1	1	3	C	37	44.4	183	2
Psychomyia	3	9	1	1	3	3	6	3	1	1	9	C	40	48	126	2
Rhyacophila	0	9	6	3	3	3	6	3	1	1	9	A	44	66	88	2
Neophylax	0	9	6	3	3	0	6	3	1	1	9	C	41	49.2	110	2
Neothremma	0	9	6	3	3	0	6	3	1	1	9	C	41	49.2	110	2
Hydra	0	0	0	0	0	0	0	0	0	0	1	R	1	0.5	293	1
Sphaeriidae	0	1	0	0	0	0	0	0	0	0	3	R	4	2	287	1
Sphaerium	0	1	0	0	0	0	0	0	0	0	3	R	4	2	287	1
Margaritifera	0	1	0	0	0	0	0	0	0	0	3	R	4	2	287	1
Unionidae	0	1	0	0	0	0	0	0	0	0	3	R	4	2	287	1

Taxon	Active Drift	Habitat	Flow Exposure	Mobility	Drag Index	Drift Distance	Emergence Behavior	Oviposit Behavior	Diel Activity	Benthic Exposure	Size Scores	Abundance	Total	Tot Adj	Rank	Group
Ancylidae	0	1	0	0	0	0	0	0	0	1	6	C	8	8	282	1
Ferrissia	0	1	0	0	0	0	0	0	0	1	6	C	8	8	282	1
Lymnaeidae	0	1	0	0	0	0	0	0	0	1	9	C	11	11	257	1
Stagnicola	0	1	0	0	0	0	0	0	0	1	9	C	11	11	257	1
Physa	0	1	0	0	0	0	0	0	0	1	9	C	11	11	257	1
Helisoma	0	1	0	0	0	0	0	0	0	1	9	R	11	5.5	257	1
Gyraulus	0	1	0	0	0	0	0	0	0	1	3	C	5	5	285	1
Planorbidae	0	1	0	0	0	0	0	0	0	1	3	C	5	5	285	1
Valvata	0	1	0	0	0	0	0	0	0	1	9	C	11	11	257	1
Nemata	0	1	0	0	0	0	0	0	0	0	3	C	4	4	287	1
Prostoma	0	9	6	9	6	1	0	0	0	3	9	C	43	51.6	89	2
Polycelis	0	9	6	3	1	6	0	0	0	1	3	C	29	29	197	2
Turbellaria	0	1	0	0	0	0	0	0	0	3	9	C	13	13	256	1

Benthic and Drift Macroinvertebrates

Full Title: Benthic and Drift Macroinvertebrate Data and Contrasts for 2011 – 2016

Introduction

CRITFC has collected benthic macroinvertebrate samples from 2011 through 2016 from CHaMP sites. Annual CHaMP sites were sampled every year in general, except when a new annual site was designated as a replacement for one that was discontinued due to landowner access issues. Rotating panel sites were sampled every three years. For these sites, an individual site would be sampled in 2011 and 2014, 2012 and 2015, or 2013 and 2016 within the period 2011-2016. For the coming field season, macroinvertebrate samples will be taken that complete three cycles in the series 2011, 2014, and 2017.

Our objective in collecting benthic macroinvertebrate samples has been to characterize the capacity of the stream site to generate a food base for the fish communities and to link the macroinvertebrate communities with current conditions and trends in water quality, habitat characteristics, and position in the stream network (e.g., River Continuum). Although benthic macroinvertebrate community composition varies with time (seasonally, annually), it is not likely to vary on a diurnal basis as is the drifting portion of the community. Also, indices such as taxa richness are likely to remain stable in benthic samples in a CHaMP site during the summer survey period provided that individuals per species are simply increasing in size through the summer.

Collections of benthic macroinvertebrates were taken in riffles, whereas drift collections reflect both the riffle where nets were installed as well as upstream habitats. Even though drift nets were installed near the downstream end of riffles of average length and at the upstream end of study sites, which were 20 times bankfull width in length, the tendency of drifting organisms to move downstream with the currents ensures that many specimens collected in nets represent upstream pools, glides (fast non-turbulent), or side channels in addition to riffles. Comparisons of the macroinvertebrate communities in benthic samples to drift samples depend upon an assumption that instream and riparian habitat conditions experienced by the benthic community is the same as that experienced by the drift community. This may not be totally accurate because the drift nets are stationed at the upstream end of the study area. Consequently, the riparian conditions, in particular those adjoining upstream sources of drifting organisms, may well be different than those in the study site. Also, the distance that drifting organisms travel could be considerable and may vary depending upon size and density in relation to current velocity and water depth. Drifting macroinvertebrates travel in a saltatory manner, entering the drift and then reattaching to the substrate in hops.

The objective of collecting drifting macroinvertebrate samples is to assess the abundance and biomass density (number or biomass per m³) within CHaMP sites to gage the ability of the site to support salmonid feeding, where feeding mode is primarily based upon drifting organisms. Drift is comprised of macroinvertebrates whose origin is from the stream bottom (termed Aquatic and AquaticTerrestrial) as well as macroinvertebrates whose origin is from the riparian vegetation (Terrestrial). Our project also has additional objectives: (1) to explore the linkages between the benthic and the drift communities, (2) assess the propensity of various taxa to drift and whether the relative abundance of drift is related to

the relative abundance of the taxon in the benthos, (3) and to determine whether sites with high riparian vegetative cover produce greater amounts of terrestrial drift.

There were 54 benthic samples collected in the Upper Grande Ronde and Catherine Creek by the combined work of CRITFC and ODFW in 2016. There were also 38 drift samples collected in 2016 by these two monitoring teams. Samples were collected by CTUIR but these results were not available to us yet.

Methods

Benthic samples were collected with either a Hess sampler or a kick net, depending upon the depth, water velocity, or substrate size at riffles being sampled. Care was taken to sample an area defined by the dimensions set by the sampling device. The Hess sampler had an inside bottom area of 0.086 m². The kick net has a frame width of 1 ft. If a kick net was the sampler of preference given the conditions (e.g., either low or high water depth, high current velocity, large substrate), care was taken to ensure a quantitative sample by gathering all substrate within the 1 ft² area upstream of the net mouth. With the kick net, cobbles were sequentially moved to a position in front of the net so that attached organisms could be directed into the net. Substrate was excavated as deep as feasible, disturbed with a small hand rake, and brushed thoroughly. With both samplers all cobbles and pebbles were brushed with a kitchen brush to dislodge macroinvertebrates that were then directed by current flow or forcible current movements made by hand into the net. The mesh size of the collection nets on both sampler types was 500 µm, which ensures capture of the majority of small size classes. A total of 8 component samples from randomly selected positions in a sequence of riffles within the study site were composited to form a total sample per CHaMP site, which then represented 8 ft² (0.7432 m² with the kick net or 0.688 m² with the Hess sampler) of streambed. The 8 component samples were taken at randomly selected positions on a 3 x 3 grid overlaid on each riffle. Center points of each of 9 grid cells occurred at the 25%, 50%, and 75% position longitudinally and on channel cross sections. If there were 10 riffles in a study site, samples were collected from randomly selected cells in each of the first 8 riffles. When there were fewer than 8 riffles per study site, samples were distributed according to proportional area of riffles within the site. Composited samples were held in a screen-bottomed pail, transferred to bottles, preserved in 100% ethanol, labeled, and sent to Rhithron Associates, Inc. for sorting, identification, and analysis of basic community metrics. More details on sampling protocol can be found in Hayslip (2007).

Drift samples were collected using two custom-made nets, each of 60 cm vertical height by 40 cm width. Nets were placed at the downstream end of a riffle which was located at the upstream end of each CHaMP study site (or immediately above the upstream end so as not to interfere with co-occurring topographic and auxiliary habitat surveys). Net mesh size was 500 µm. Nets were typically installed at 9 am to 10:30 am and collected drift for a minimum of 3 hours and up to about 5 hours. Current velocity and water depth were measured at the beginning and end of net deployments to allow calculation of total volume filtered. Nets were not touched during filtration so that it could be inferred that average current velocity in the center of the net mouth would decline linearly throughout the entire deployment period. Attempts were made to retrieve samples before final current velocities declined significantly (e.g., more than 20%). Efforts were made to set up nets at sites where currents were relatively laminar

approaching the net rather than exhibiting strong directional shifts or velocity strength gradients across the face of the net. If velocity variation appeared unavoidable at the net mouth, then three uniformly spaced velocities were averaged to generate initial and final average velocities.

Drift samples were collected at each CHaMP site on the date of conducting the total site survey (topographic and auxiliary data collection). This produces a data set of drift community data that are distributed throughout the summer field period from approximately June 15-October 1. This is contrasted with the benthic sample collection that is made within a 2-week period that is focused in the period of July 15-August 15 in most years that coincides with fish snorkel counting. It would be preferable to have drift sample collection also fall within this same period and to move the drift collection stations to the bottom-of-site of each CHaMP site. However, for logistical reasons this has not been feasible. It would also be desirable to collect drift samples at all sites with repeated samples spaced out in time intervals through the season to better represent temporal variation in drift rates and drift community composition.

There were 54 benthic community samples taken by CRITFC and ODFW in 2016 throughout the Upper Grande Ronde River basin and Catherine Creek basin. CRITFC took 25 samples from 26 total sites surveyed in 2016. The West Fork Chicken Creek site had such low stream flow that benthic samples and snorkeling were not conducted.

Benthic community metrics computed for each sample included:

(1) standard BCI indices

(2) functional feeding group composition, namely, collector-filterer, macrophyte herbivore, omnivore, parasite, piercing herbivore, predator, scraper, shredder.

(3) Hilsenhoff metrics

(4) tolerant/intolerant species based on fine sediment and temperature (using, in part, indicator taxa by Huff et al. 2006)

(5) PREDATOR (Western Cordillera and Columbia Plateau model) (Hubler 2008). This model is a RIVPACS-type model that calculates observed/expected ratios, where the expected taxa are those that are expected to be found in a reference site for the region having characteristics similar to those found in the study area. The O/E ratio based on taxa with a greater than 50% likelihood of being captured at a reference site is the preferred O/E for site evaluation (Hubler 2008).

(6) total taxa densities (no. individuals/m²)

(7) biomass per taxon (mg/m²) and total sample biomass/m²

(8) Eastern Oregon multimetric index (Hubler 2006), including component metrics of mayfly, stonefly, and caddisfly richness, number of sensitive taxa, number of sediment-sensitive taxa, modified HBI, percentage of tolerant taxa, percentage of sediment tolerant taxa, and community dominance by the

single most abundant taxon. Each of these metrics was also given ratings of 1, 3, or 5 related to the magnitude of the individual measurements. These scores by component of the Eastern Oregon IBI were summed to produce a total score. The maximum IBI score (sum of all 10 individual metrics) is 50 and the minimum is 10. Ratings were assigned categories of Severe impairment (<27), High impairment (27-34), Moderate impairment (35-41), and No impairment (>41) (Hubler 2006). This total score has been found to vary with respect to study site elevation and water temperature in the Upper Grande Ronde River and Catherine Creek (McCullough et al. 2016).

(9) DEQ temperature and fine sediment stressor models. These stressor models identify number of temperature sensitive indicator taxa, number of temperature tolerant indicator taxa, number of fine sediment sensitive indicator taxa, number of fine sediment tolerant indicator taxa (Huff et al. 2006). This sensitivity classification of all regional taxa according to optima and tolerances was based on a set of previous regional studies (Huff et al. 2006). The taxa optima and tolerances were estimated using abundance of taxa at sites by water temperature and fine sediment condition. This weighted average inference model is essentially a method of using the weighted abundance of indicator taxa to identify the water temperature or fine sediment conditions that would need to be found at the site to produce that relative abundance for all indicator taxa. If taxa are good indicators of water temperature or fine sediment levels in the stream, the benthic community composition evaluated by these metrics will be a good integrator of these conditions.

Any aspect of drift methodology not fully described here is available either in CHaMP protocol documents (available at www.champmonitoring.org) or at www.monitoringmethods.org (hosted by PNAMP).

Benthic data are stored in CRITFC's data storage facility in Portland, Oregon. Drift data from Cole Ecological and Rhithron Associates, Inc. are stored by the CHaMP data management team. Habitat data collected in CHaMP are available via champmonitoring.org under the export tab.

Total sample biomass (mg) and total density (no./m²) were calculated from summation of all biomass for benthic Coleoptera, Diptera, Ephemeroptera, Plecoptera, and Trichoptera. All taxonomic identification from finest levels of differentiation were summed at the Order level for each CHaMP site on the mainstem of the Upper Grande Ronde River and Catherine Creek. Sheep Creek sites were not included in the Upper Grande Ronde River continuum. However, for Catherine Creek the sites in the NF Catherine, SF Catherine, and MF Catherine Creek were ordered by elevation, followed by the sites down the mainstem sampled in 2016. This was done because the NF Catherine and SF Catherine Creek in particular are about the same size and can each be considered as an extension of the mainstem. Lepidoptera and Odonata were included in evaluations of the total biomass by Order and percentage of total biomass by Order only for the Upper Grande Ronde River.

Total sample biomass was selected for contrasting biomass among sites. Because sites were sampled using either a Hess sampler or a kick net, the total area sampled with 8 composite benthic collections should be identical. Using a mg/m² conversion would have been ideal instead of assuming the samplers sampled identical areas. In fact, the Hess composite samples covered 0.688 m² and the kick net 0.743

m². This means that the kick net samples are 8.0% larger than the Hess samples. This affects only what is reported as total sample biomass and not relative percentages of biomass by Order or density of individuals per Order by site.

Benthic samples by site were analyzed according to the taxa that were classified as aquatic, aquatic-terrestrial, and terrestrial. It has been a key assumption when surveying benthic and drift community composition that these communities reflect the riparian communities that are adjacent to or upstream of each study site. For drift organisms, the terrestrial macroinvertebrates that fall into the stream and are transported have been hypothesized as being related in magnitude to the percentage cover by riparian vegetation or by the total cover for the individual layers of vegetation (overstory, understory, and ground cover). These data were not currently available in the champmonitoring.org database although they were collected. These data will be used when they become available. Instead, the solar access by CHaMP site was used as a measure of riparian cover that could influence the ability of riparian vegetation to produce terrestrial macroinvertebrates that contribute to total drift. To make this calculation most meaningful, the biomass of *Pacifasticus* (crayfish) and *Margaritifera* (mussels) were filtered out of the aquatic taxa because their presence can add such large amounts of biomass that they detract from estimation of amounts of biomass that could more readily provide a food source to salmonids. The percentage of sample total biomass that was composed of terrestrial macroinvertebrates was then computed without the presence of these two heavy-bodied taxa.

Results and Discussion

Benthic samples are comprised principally by macroinvertebrate orders Coleoptera, Diptera, Ephemeroptera, Plecoptera, and Trichoptera by biomass (mg/m²) and density (indiv/m²). Other general taxa that contribute less biomass and individuals include Trombidiformes, Veneroida, Podocopa, Sarcophagidae, Basommatophora, Lepidoptera, Odonata, Arhynchobdellida, Megaloptera, Hemiptera, and Oligochaeta. *Pacifasticus* and *Margaritifera* were eliminated from this summation of benthic macroinvertebrate biomass because their presence would frequently add such large amounts of biomass that it would skew the results. Among these broad taxonomic groups aside from the five principal orders, the Odonata and Arhynchobdellida (leech) were the only taxa that contributed large biomasses relative to other orders within a CHaMP site, although their occurrences were sparse.

The orders Coleoptera, Diptera, Ephemeroptera, Plecoptera, and Trichoptera are comprised by many taxa that were identified in samples processed by Rhithron Associates and previously by Cole Ecological. Summation of the biomass at the order level for these five orders plus Lepidoptera and Odonata is shown in Figure 122. The Diptera as an order maintain approximately a constant biomass per sample among sites arrayed along the Upper Grande Ronde mainstem. Two samples (dsgn4-000205 and CBW05583-099818) had surprisingly low total biomasses of these seven orders relative to the other sites on the mainstem. Plecoptera in general comprised a greater percentage of the total sample biomass (based on a sum of strictly these seven orders) toward the upstream end of the Upper Grande Ronde. Trichoptera comprised a significant percentage of the total biomass in all samples, but this relative biomass appeared to increase in a downstream direction. Ephemeroptera were relatively abundant at site dsgn4-000245 (Upper Grande Ronde above Beaver Creek) and were present in all sites,

but the relative abundance was sometimes very small. Odonata were relatively prominent in terms of relative biomass in two sites, but otherwise were totally absent in six of 11 mainstem sites.

Benthic Sample Biomass and Density along Mainstem of Catherine Creek and Upper Grande River in 2016

In Catherine Creek along the mainstem, Diptera again comprised a very uniform absolute biomass per sample except at the upper two sites out of 15 (Figure 123). Coleoptera also were relatively constant in absolute biomass per sample in the lower 10 of 15 sites. Ephemeroptera had relatively constant absolute biomass per sample in the upper 8 of 15 sites, were found in all sites, but were present in greater biomass per sample toward the upper half of the continuum. Trichoptera, like with the Upper Grande Ronde increased in absolute abundance toward the lower half of the continuum. Plecoptera contributed the greatest amount to variation in absolute biomass per sample and had their greatest absolute biomass per sample in the lower half of the continuum.

In terms of percentage of total sample biomass (based on biomass of 7 orders) in the Upper Grande Ronde River, Ephemeroptera comprised more than 5% of total biomass in only two of 11 sites (Figure 124). Diptera comprised about 5 to 40% of total sample biomass, but predominantly were 5-15%. Trichoptera ranged from about 9 to 72% of total sample biomass and Plecoptera ranged from 2 to 81%. The highest relative biomass for Trichoptera was found in the lower half of the sites, while the highest relative biomass per sample for Plecoptera were found in the higher elevation sites. The highest elevation site was somewhat of an anomaly in having no Odonata or Lepidoptera, a small representation by Plecoptera, but large proportions of Coleoptera, Diptera, and Trichoptera. Definitely further work remains to be done in exploring the distribution of taxa within each of these principal orders with elevation or water temperature along the mainstem. This type of analysis was begun in McCullough et al. (2016).

In Catherine Creek along the mainstem continuum (Figure 125), Ephemeroptera comprised significant percentages (>7%) of the total sample biomass in the upper 9 of 15 sites. The highest relative percentage of mayflies among this set was 48%. Plecoptera comprised 32-77% of total sample biomass for a middle group of 6 sites. Diptera comprised from 7-44% of total biomass, but the highest relative percentages (23-44%) were found in the three sites of lowest elevation.

Benthic macroinvertebrate samples were also evaluated in terms of density (numbers of individuals/m²). Again, considering only the five principal orders of macroinvertebrates, high densities of Diptera, Ephemeroptera, and Trichoptera were found in two of the upper three sites in the Upper Grande Ronde River mainstem (Figure 126). Plecoptera were found in high density primarily in one site (dsgn4-000245 or the UGR above Beaver Creek). This site also had the highest density of Ephemeroptera among the 11 UGR sites. Coleoptera were found in densities ranging from 356-1991 indiv/m² among these 11 sites, which appears to be relatively stable.

Catherine Creek had Trichoptera in all 15 sites but the highest densities were found in the lowest four of 15 sites (Figure 127). Plecoptera were found in densities ranging from 38-458 indiv/m² but appeared to be stable along the continuum. Ephemeroptera were in very high abundance in one site in the middle of

this continuum (2116 indiv/m²), but had a more stable presence (183-928 indiv/m²) that had no apparent longitudinal pattern along the continuum. Coleoptera, on the other hand had its highest densities in the lower 10 of 15 sites. Diptera were found in stable densities in the lower five sites (735-1393 indiv/m²), but appeared in densities as high as 2220 indiv/m² toward the upstream portion of this distribution.

Drift in 2016 related to Riparian Vegetation

Drifting macroinvertebrates were collected in a total of 36 sites (CRITFC and ODFW) within the UGR and Catherine Creek. The percentage of total drift macroinvertebrate biomass (mg/m³/s) that was of terrestrial origin was plotted against percentage solar access (Figure 128). Although the regression line has a low R² and non-significant P value (0.156), elimination of 7 of the 36 points leaves the remainder densely clustered along the regression line. A high solar access indicates a high percentage of potential solar radiation reaching the stream surface, which would also be reflective of low riparian canopy cover. Riparian canopy is measured with a Solmetric Suneye instrument on 11 transects uniformly distributed in each CHaMP site. It is possible that this level of data capture is occasionally not sufficient to accurately indicate average cover for the entire site. Also, in cases where the riparian canopy upstream of a CHaMP site is significantly different from the canopy cover within the site, the composition of the drift could be attributable to conditions different from those recorded in the study site itself. We would have used the CHaMP data collection of riparian canopy cover by overstory, understory, and ground layers, but they were not currently available in a form suitable for this analysis. It would be useful to correlate solar access and riparian canopy cover metrics, and then to use each of these to relate to the percentage terrestrial organisms within the drift.

Despite the weak statistical significance level, it does appear that a relationship exists between terrestrial drift and solar access. The higher the total average light level on the study reach, the greater the input of terrestrial biomass. Obviously, more work needs to be done to investigate this relationship. A large terrestrial macroinvertebrate such as a grasshopper could significantly influence the percentage of terrestrial organisms by biomass (mg/m³) in the drift. The analysis reported here was based upon the drift without inclusion of “large/rare” individuals. However, exclusion of the L/R applies to a search for those individuals in the Caton tray cells that are not part of the subsample counted. Large or rare individuals that are counted in the subsample of Caton tray cells are included in what is termed “drift with L/R.” A true estimation of whole sample biomass is best made with inclusion of L/R individuals identified in the entire sample. Anomalous large individuals are expected primarily in the terrestrial component of the drift. A re-analysis of these data would be useful after exclusion of terrestrial drift larger than a certain threshold size (e.g., a size beyond that suitable for the largest juvenile Chinook).

Based on these 36 drift samples from the UGR and Catherine Creek, the mean percentage of all samples that was comprised by terrestrial origin biomass was 69.3% and the median was 76.4%. Minimum and maximum values were 0.6 and 98.9% terrestrial. It is clear that in certain sites, terrestrial contribution to overall drift biomass in transport can be very high. It is not likely that this would always be the case at these sites due to phenology of terrestrial invertebrates. Greater understanding is needed on the temporal trends of terrestrial macroinvertebrate delivery to transport in the drift. Given the possibility that terrestrial macroinvertebrate activity and entry into the drift could be timed according to air

temperature, which can vary with elevation and month of collection of the drift, the percentage of terrestrial biomass in the drift could vary throughout the monitoring season. This is another reason why the regression in Figure 128 has outliers.

Benthic Average Biomass per Individual by Insect Orders and Site

Average biomass per individual (mg/indiv) in benthic samples was calculated for the five major insect orders (Coleoptera, Diptera, Ephemeroptera, Plecoptera, and Trichoptera) for the 15 sites in Catherine Creek (Table 57) and the 11 sites in the Upper Grande River mainstems (Table 58). Biomass and number of individuals for all individual taxa within each order were summed and the total biomass was then divided by the total number of individuals for all taxa in each order. Coleoptera in Catherine Creek had a very narrow range and variation in biomass/individual. The other orders had significantly more variation. For example, Plecoptera that were 11.2 to 42.4 mg/indiv were found in three CHaMP sites in succession, but elsewhere the biomass per individual ranged from 0.36-8.0 mg/indiv. Among these 15 sites, Trichoptera had biomass/indiv values ranging from 2.2-3.2 mg/indiv in 6 sites, while the remainder of the sites ranged from 0.38-0.996 mg/indiv. No longitudinal trend appeared to be present. Diptera in two sites were 1.27-1.41 mg/indiv, but in all other sites the range expressed was 0.11-0.86. With Diptera the 7 downstream sites had large bodied individuals. Ephemeroptera ranged in size from 0.15-0.89 mg/indiv among sites. It remains to be determined on closer inspection of distribution of individual taxa within each order how the variations in average biomass/indiv occur. For example, a predominance of Plecoptera taxa having large bodies in certain sites and minor representation by smaller bodied taxa could explain why certain sites have such large average sizes.

In the Upper Grande Ronde River the Coleoptera again had a very narrow range in biomass per individual (0.18-0.35 mg/indiv). With Plecoptera, 5 sites had values ranging from 7.4-14.9 mg/indiv, while the remainder of sites ranged from 0.17-4.6 mg/indiv. The average Plecoptera biomass in the UGR was not as great as in Catherine Creek, but this might be attributable to a greater representation by stonefly taxa with smaller body size. With Trichoptera, 4 sites had values ranging from 1.3-2.2 mg/indiv, while the remainder ranged from 0.22-0.60 mg/indiv. This distribution of values was similar to Catherine Creek, but in neither stream was there an apparent longitudinal trend. Diptera ranged in size from 0.08-0.76 mg/indiv, while Ephemeroptera ranged from 0.09-0.77 mg/indiv. This size range for Diptera was less in the UGR than in Catherine Creek, but the Ephemeroptera biomass/indiv values were similar in each stream, with no apparent longitudinal trend.

Drift Rates (mg/m³) of Aquatic Insect Orders by Site

Drift rates of Aquatic + AquaticTerrestrial members of the 5 major insect orders were evaluated for longitudinal trends and consistency among sites within streams and between streams. For Coleoptera the highest three sites in terms of drift rate (mg/m³) was 2.16-8.72 in Catherine Creek (CC) (

Table 59) but 0.71-1.43 for the UGR (Table 60). Other values for each stream were approximately in the range 0.02-0.5 mg/m³. For Diptera Catherine Creek had 7 sites with values of about 1.87-4.88, while the UGR had 5 sites with values of 1.39-4.37. Other sites had lower values, extending to about 0.02. For Ephemeroptera, the highest six values in CC were 1.02-3.05 and the highest two in the UGR were 1.02-1.06. Other values in each stream ranged to lows of about 0.01 mg/m³. The highest Plecoptera drift

rates in CC was 3.08 mg/m³ while that in the UGR was 0.37 mg/m³. Highest Trichoptera drift rates in the two sites were 2.7 and 2.3 mg/m³, respectively.

An attempt was made to relate drift rate (mg/m³) at the taxonomic order level to benthic total sample biomass of each order. For example, the total drift rate for all Coleoptera taxa were summed for each drift sample and plotted against the total sample biomass (mg) of all benthic Coleoptera taxa for each CHaMP site. This process revealed no apparent relationship between drift rate at the order level and benthic biomass at the order level (Figure 129-Figure 133). It is possible that a clearer relationship exists at the level of individual taxa. That is, if *Baetis* is especially prone to drift, it may well be related to the total biomass of *Baetis* in the benthos. The addition of the drift rate of other mayflies when compared to the benthic biomass of *Baetis* plus other mayflies likely obscures the linkage between the drift rate (mg/m³) of those that drift and the benthic biomass (mg/m²) of those same taxa. It is clear that presence in the drift of an insect order is not simply a function of the biomass of that order in the benthos of specific taxa. It might be worth exploring the relationship between the numbers in the drift (no./m³) and density (no./m²) in the benthos. If large bodied individuals are less likely to drift or to drift significant distances, high numbers of small individuals of an order of insects could be produced from high numbers of the same order in the benthos. This remains to be determined.

Trends in Benthic Community Metrics along Catherine Creek and the Upper Grande Ronde River Mainstems for 2011-2016

Benthic samples were evaluated with various metrics of community composition for samples collected from 2011-2016. The full list of annual sites across both Catherine Creek and the Upper Grande Ronde River was evaluated for taxa richness (Table 61) and Total Score (Table 62). Annual sites provide the ability to look for annual trends. Also, because most of these annual sites have complete data for all years, it is possible to evaluate average basin trends through the years of study.

In terms of taxa richness, some of the highest values (e.g., values >60) were found in sites in 2014 and 2015. At all sites except one, values declined substantially the next year when values of >60 occurred in either 2014 or 2015. The exception was site dsgn4-000009, where taxa richness was 65 in 2014 but declined only to 64 in 2015. For 23 CHaMP sites, the average value by site ranged from 31 to 59. Within a site, taxa richness values ranged from 10 to 27 between the minimum and the maximum values. Among years, 2014 and 2015 had the highest average taxa richness values. Average values for all sites combined had a maximum range of 9 points (i.e., average taxa richness of 52 in 2015 and 43 in 2013).

The same type of analysis done using Total Score revealed a much higher level of inter-annual consistency on average among all 23 CHaMP sites. From 2011 to 2015 the average Total Score ranged from 39 to 42. In 2016 that value dropped to 35. Average values (6-year averages) for each of the 23 sites ranged from 31 to 49.

Select macroinvertebrate metrics were evaluated for the ten CHaMP sites on the Upper Grande Ronde mainstem that are in the prime spawning area and were the subject of analysis of low flow impacts on salmon spawning and rearing. Because they include a combination of annual and rotating panel sites, each site does not have a value in all years. These sites were evaluated as a group with the idea that

they represent conditions that are most favorable during the summer period for spawning and rearing of spring Chinook. If salmon are able to reflect the suitability of the habitat for coldwater species, it is possible that the macroinvertebrate community in this section of the river known to be heavily used may also be relatively homogeneous.

Trends in Benthic Community Metrics for Prime Spawning and Rearing Zones in the Upper Grande Ronde River and Catherine Creek (2011-2016)

In terms of taxa richness (Table 63) this set of ten sites in the uppermost end of the UGR mainstem had values that ranged from about 42 to 65. There was no apparent trend from downstream to upstream in taxa richness. In site dsgn4-000009, high values of taxa richness were observed in 2014 and 2015 (65 and 64, respectively), but this pattern was not reflected in annual site dsgn4-000277 (46 and 61, respectively). Several richness values greater than 60 were found in sites in 2014, but 2011 had lower values (44-56). Because 2011 was a very high flow year (peaks occurring in May-June), it is possible that the lower taxa richness across these sites in 2011 was attributable to peak flows prior to macroinvertebrate sampling. However, it is also possible that given the limited number of individuals identified per sample that the probability of revealing high taxa richness can vary. Taxa richness values might vary due to the influence of equitability (evenness). That is, in the event that species diversity is high, but the large number of taxa are relatively evenly represented numerically, and only 550 individuals are counted per sample, the probability of missing species that are present could be different than in sites where there is a high taxa richness, some species are in high abundance, but most are in low abundance. If taxa richness is related to annual variation in relative abundance of individual taxa more than it is to absolute presence or absence of the taxa, and if variation in sampling date is able to cause these differences, trends might not be revealed with great sensitivity using taxa richness alone.

Sensitive taxa (Table 64) appear to be a much better metric for revealing differences among CHaMP sites, even among the ten sites in the upper mainstem reach of the UGR. Site dsgn4-000009 had 10 to 13 sensitive taxa in samples from 2011-2015. The other annual site (dsgn4-000277) had from 4 to 6 sensitive taxa among the six years of sampling. For some reason, 2016 had lower sensitive taxa values in the uppermost two sites that in all other years in those sites. In all years (2011-2016) sensitive taxa were more abundant in general in an upstream direction.

The metric sediment sensitive taxa (Table 65) appears to have no longitudinal pattern, indicated by the downstream to upstream series of values in 2011 and 2014. All values in 2016 appear to be lower than those from 2011. If 2011 was a high flow year, it might be that fine sediment was moved out of this section of the mainstem. No trends were detectable in the two annual sites (dsgn4-000277 and dsgn4-000009). More evaluation is needed to assess whether there were measured differences in fine sediment in riffles or pool tails between 2011 and 2016.

The metric percentage tolerant taxa (Table 66) decreased from downstream to upstream in all years. Annual site dsgn4-000277 was relatively constant in this metric across all six years and had values that were relatively high for this set of ten CHaMP sites in the UGR mainstem. Also, annual site dsgn4-000009, which is near the upper end of the mainstem, was also relatively constant in percentage tolerant taxa through the years and was much lower than the downstream annual site.

Total Score values for this set of ten sites in the UGR mainstem were very similar among sites and years (Table 67). However, despite the small absolute differences to Total Score values, the value in each year from 2011-2016 was greater for dsgn4-000009 than in dsgn4-000277. Differences between these two sites ranged from 6 to 12 among the six individual years.

Macroinvertebrate density (indiv/m²) values (Table 68) were relatively stable at annual site dsgn4-000277 through the years 2011-2016. The values for this site in these years were also higher than in most other sites in years 2011-2014. In 2015 and 2016, sites dsgn4-000009 and CBW05583-468458 had very high values (approximately 2-3 times greater than the high values of site dsgn4-000277). Missing values in various years due to the rotating panel design make some contrasts difficult to discern. It appears that 2011 high flows might have had something to do with the low densities in the upper half of the distribution in the UGR mainstem but the sites from dsgn4-000277 downstream were not especially low density sites.

Trends in Benthic Community Metrics for Mainstem of Upper Grande Ronde and Catherine Creek in 2016

Trends in benthic macroinvertebrate metrics were also evaluated for all CHaMP sites on the Catherine Creek mainstem and the UGR mainstem, downstream to upstream, for 2016 alone. Site elevations ranged from 871 to 1398 m on Catherine Creek (Table 69) and 910 to 1413 m on the UGR mainstem (Table 70). Total Scores tended to increase from downstream to upstream in both Catherine Creek and the UGR mainstems, although the patterns of increases were irregular. The overall increase in Catherine Creek was from about 32 to 50, while in the UGR the trend was from 22 to 44. The UGR is a significantly more damaged stream than Catherine Creek, even in its headwaters.

Some other trends were quite clear for these two mainstem reaches. In Catherine Creek (Table 69) there was a dramatic trend in numbers of temperature sensitive taxa (from 0 to 11) and fine sediment sensitive taxa (3 to 11). The weighted average temperature inference metric revealed from the macroinvertebrate samples collected that the highest 7-day average of the daily maximum value (Huff et al. 2006) would range from about 22.5°C at 871 m elevation to 13.2°C at 1398 m in Catherine Creek. The weighted average inference model for fine sediment less than 0.06 mm estimates fine sediment percentages of 8.4-11% in the lower two sites, 2.2-4.8% in the middle 12 sites, and 0.9% in the upper site on Catherine Creek. Temperature tolerant taxa were high in the lower seven sites, but low in the upper eight sites. O/E (<0.5) reached values as high as 1.27, but in the lower six sites values less than 1.0 were common. Lower elevation sites in Catherine Creek become visibly degraded from Union, Oregon downstream. But, interestingly the six sites on the mainstem from Hall Ranch to the farmland upstream of Union all had O/E scores of 0.74-1.04. It is somewhat surprising that the lower sites in this series are as high as they were given the magnitude of land use along the stream. This warrants further evaluation of the suitability of reference samples for the region that represent potential condition of these streams.

The series of 11 sites on the UGR mainstem runs from an elevation of 910 m just above Hilgard State Park to the upper end of the mine tailings area at 1413 m. Total Scores ranged from 22 at the downstream end of this series to a maximum in the mine tailings zone of 44. As with Catherine Creek, the increase in scores with elevation was not uniform. However, a comparison of Catherine Creek with

the UGR using a linear regression of Total Score vs. elevation reveals two linear relationships with nearly identical slopes (Figure 134. Relationship between Total Score (Oregon Multimetric Index) to elevation at the bottom of site for CHaMP sites on the mainstem of the Upper Grande Ronde River and Catherine Creek. There was a distinct trend in temperature sensitive indicator taxa from 0 to 5 in the UGR mainstem series of sites with increasing elevation. Catherine Creek had twice as many temperature sensitive taxa at high elevations. There were approximately 5-6 temperature tolerant taxa in the lower sites and 3-4 in the upper sites. Fine sediment sensitive taxa were 0-2 in lower sites and 3-5 in upper sites in this series. Fine sediment tolerant taxa numbered 3 in the upper half of this series and were as high as 7 in the lower portion. The weighted average inference model was very sensitive in predicting the maximum 7-day average of the daily maximum temperature. The value predicted for the upper site was 17.6°C, while the lowest site had a value of 25.6°C. This prediction should be related to measured water temperatures from CHaMP surveys. This is a task for future work. The weighted average inference model for fine sediment based on community composition provided estimates of 5.5% to 8.8% in the lower river, with one value of 13.2% at dsgr4-000245 (UGR above Beaver Creek). The fine sediment values inferred for the UGR were about twice as high as those for Catherine Creek.

Summary

1. Benthic and drift macroinvertebrate samples were collected in all CHaMP sites designated each year from 2011-2016 for sampling according to the annual and rotating panel schedules.
2. Benthic samples provide a means of identifying water quality and channel conditions, such as water temperature, water chemistry, and fine sediment impacts on macroinvertebrate community composition. Factors that influence benthic macroinvertebrate community composition are expected to, in turn, influence the potential for drift macroinvertebrate community composition.
3. Drift density (numbers/m³, biomass/m³) and composition were hypothesized as being related to the density (numbers/m², biomass/m²) of taxa in the benthos. This analysis was conducted at the insect order level. More refined evaluation at the family, genus, or species level is needed to adequately understand this relationship.
4. Benthic biomass of five principal insect orders vary with position on the mainstem continuum. Plecoptera decline in biomass in a downstream direction in the Upper Grande Ronde River. This river increases significantly in water temperature over the continuum expressed in samples collected in 2016. Trichoptera appear to increase in a downstream direction. Diptera and Coleoptera are relatively stable along this path, but Ephemeroptera are not present in significant biomass and appear to be extinguished toward the downstream end of this series.
5. Catherine Creek mainstem provides a much different environmental gradient to that in the Upper Grande Ronde. Plecoptera becomes much greater in abundance with distance downstream. Diptera is present in greater biomass than in the UGR and increases downstream. Ephemeroptera was present in greater biomass upstream, but remains as a more significant component of the community at all sites along its continuum. Water temperatures are not as warm toward the downstream end of this continuum as in the UGR. Trichoptera were a significant component by biomass in all sites and appeared to increase toward the lower extent

of this continuum. Future analyses should explore whether this trajectory is characterized by greater presence of filter feeding Trichoptera.

6. Total benthic biomass of the primary insect orders decreased in the UGR in a downstream direction but increased downstream in Catherine Creek.
7. The ranges in total benthic biomass values were approximately equal in Catherine Creek and the UGR although the longitudinal trends were different.
8. In the UGR, densities of Coleoptera were significant but stable over the entire continuum evaluated. Densities of Diptera were highest toward the headwaters as were the Trichoptera. Plecoptera were present in low densities in all except one site.
9. In Catherine Creek, densities of Coleoptera were significant at all sites except one high elevation site, and increased steadily downstream. Diptera were present in high density in most sites. Trichoptera densities increased in a downstream direction. Plecoptera densities were significant in all sites, but were relatively uniform along the entire continuum.
10. In the UGR, insect densities appeared to decline with distance downstream, while they increased downstream in Catherine Creek. Six of 11 sites in the UGR had densities of 3000-5000 indiv/m², while 8 of 15 sites in Catherine Creek had densities in this range.
11. Although the regression equation is considered non-significant statistically ($P=0.156$), there still appears to be a predominant relationship between percentage drift of terrestrial origin and solar access (%). This would indicate that the greater the access of sunlight to the stream, the lower the percentage of drift biomass that comes from the riparian vegetation cover. Future analysis will attempt to also relate terrestrial drift biomass to auxiliary data on riparian cover.
12. In Catherine Creek along the mainstem, drift biomass (mg/m³) by Plecoptera is predominantly of minor importance compared with the other four primary aquatic insect orders. Diptera, Ephemeroptera, and Trichoptera frequently provide drift biomass rates of 0.3-2.5 mg/m³. Diptera were the predominant source of aquatic-origin drift biomass. In three sites of 15, Coleoptera provided drift biomass of 2.2-8.7 mg/m³.
13. In the UGR among the 11 sites surveyed, the number of sites having aquatic drift biomass exceeding 1 mg/m³ among the five insect orders were: Coleoptera 2, Diptera 5, Ephemeroptera 2, Plecoptera 0, and Trichoptera 1. Plecoptera were not present in 3 of 11 sites and were in very low biomass density in the drift in 4 of the other sites and moderate (0.12-0.37) in the rest. Drift rates in Diptera had 5 sites with rates of 1.3-4.4 mg/m³.
14. No apparent relationship existed at the order level of the primary aquatic insect orders between the drift biomass density and the density in the benthos. This suggests that relationships that do exist occur at finer taxonomic levels.
15. Taxonomic richness is an important ecological concern, but this metric alone does not appear to be useful as a means to show environmental trends given the changes from 2011 through 2016. It seems more likely that annual shifts in specific taxa that are abundant but reflective of key environmental trends would be more important. For example, if the abundance of macroinvertebrate taxa that were an index of cold water expanded downstream, this would be a sensitive index of improvement. Because the richness itself does not indicate whether

sensitive species are lost and replaced by tolerant species, trends in richness alone are probably of limited use. Shifts in evenness that accompany richness need to be explored.

16. Benthic data collected from CHaMP sites in 2016 revealed that metrics that can effectively show environmental trends (longitudinally and at a site over time) include Total Score, O/E (0.5), weighted area inference for water temperature and fine sediment, water temperature sensitive and tolerant taxa, fine sediment sensitive and tolerant taxa, and weighted area inverse method for estimating fine sediment percentage.
17. Total Scores for benthic samples taken along the Catherine Creek and UGR mainstems increased with elevation. Regressions of Total Score on elevation were parallel for both mainstem continua, but scores at the same elevation for the UGR were significantly lower than those for Catherine Creek.

Figures

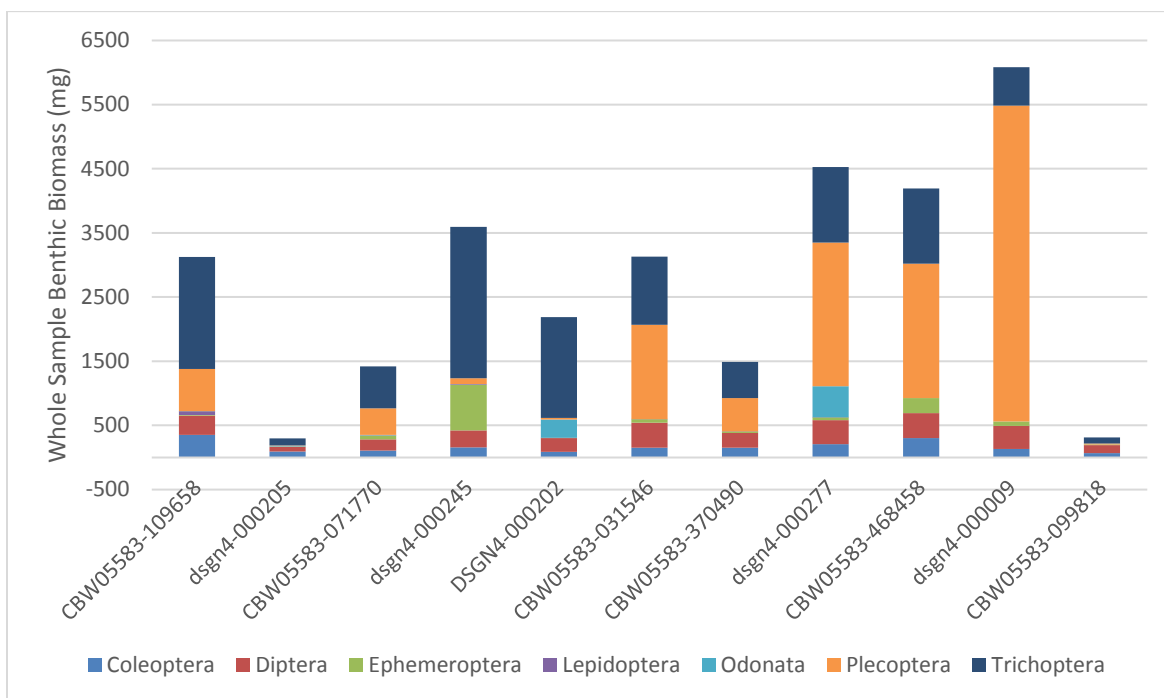


Figure 122. Whole sample biomass (mg) contributed by seven major macroinvertebrate orders for benthic samples collected in 2016 in the Upper Grande River. Only mainstem sites are shown from lowest elevation sites on the left to highest elevation on the right.

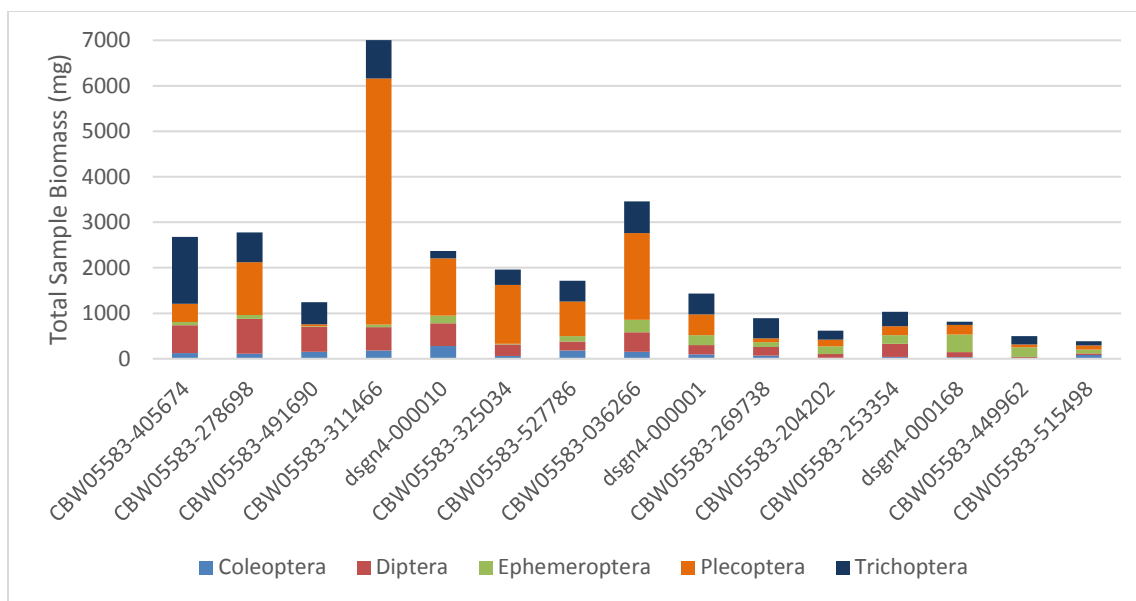


Figure 123. Whole sample biomass (mg) contributed by five major macroinvertebrate orders for benthic samples collected in 2016 in Catherine Creek. Only mainstem sites are shown from lowest elevation sites on the left to highest elevation on the right.

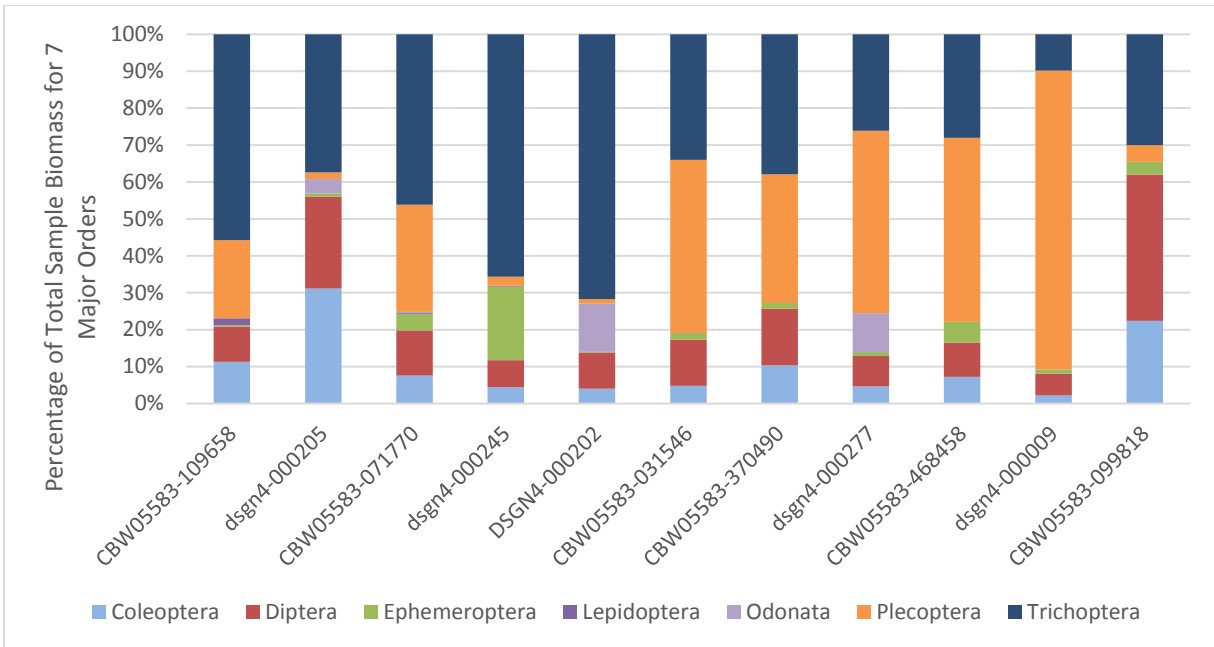


Figure 124. Whole sample biomass contributed by seven major macroinvertebrate orders as a percentage of the total for these orders for benthic samples collected in 2016 in the Upper Grande River. Only mainstem sites are shown from lowest elevation sites on the left to highest elevation on the right.

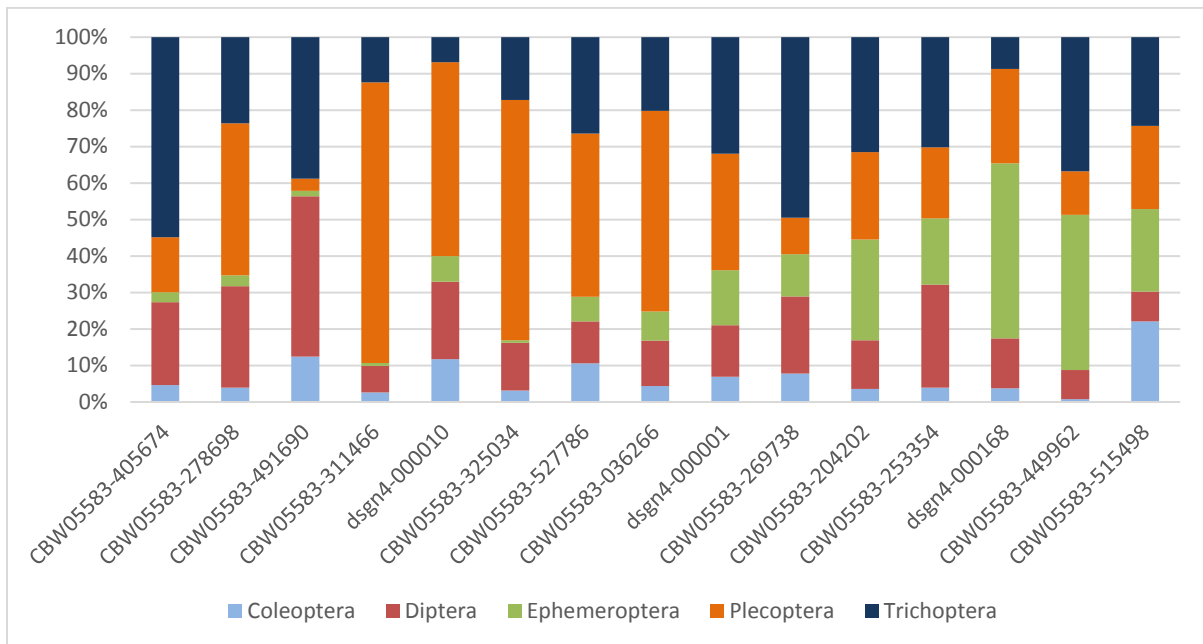


Figure 125. Whole sample biomass contributed by five major macroinvertebrate orders as a percentage of the total for these orders for benthic samples collected in 2016 in the Catherine Creek. Only mainstem sites are shown from lowest elevation sites on the left to highest elevation on the right.

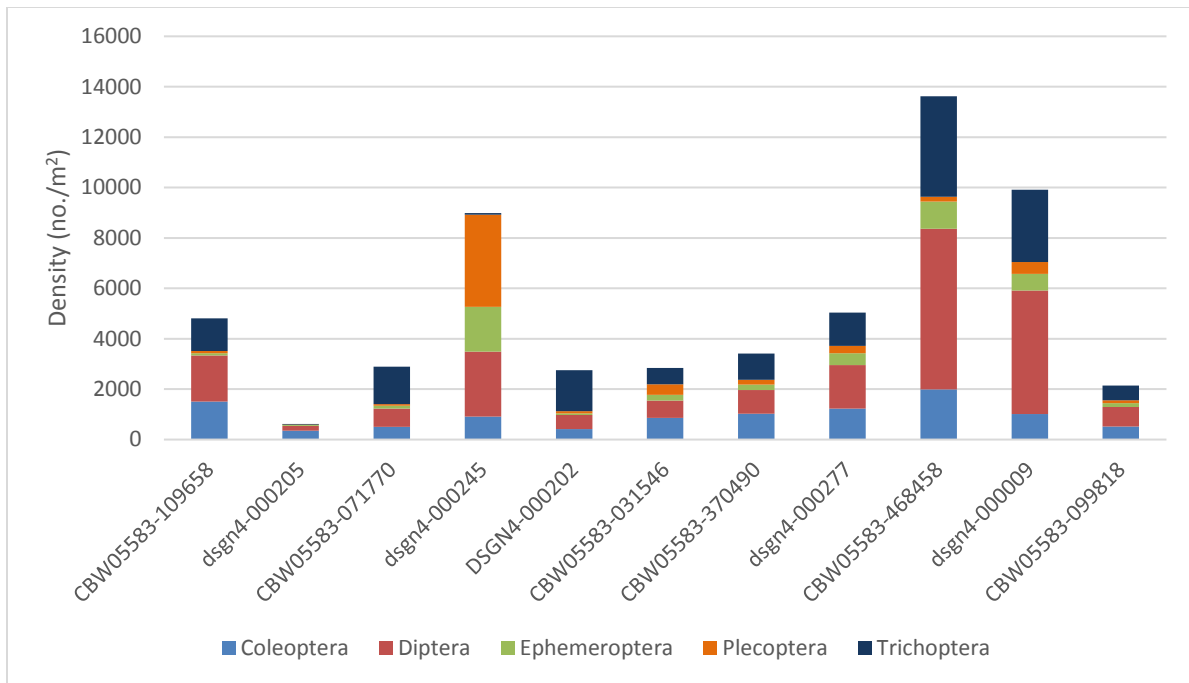


Figure 126. Total density (no./m²) in CHaMP sites contributed by five major macroinvertebrate orders collected in 2016 in the Upper Grande Ronde River. Only mainstem sites are shown from lowest elevation sites on the left to highest elevation on the right.

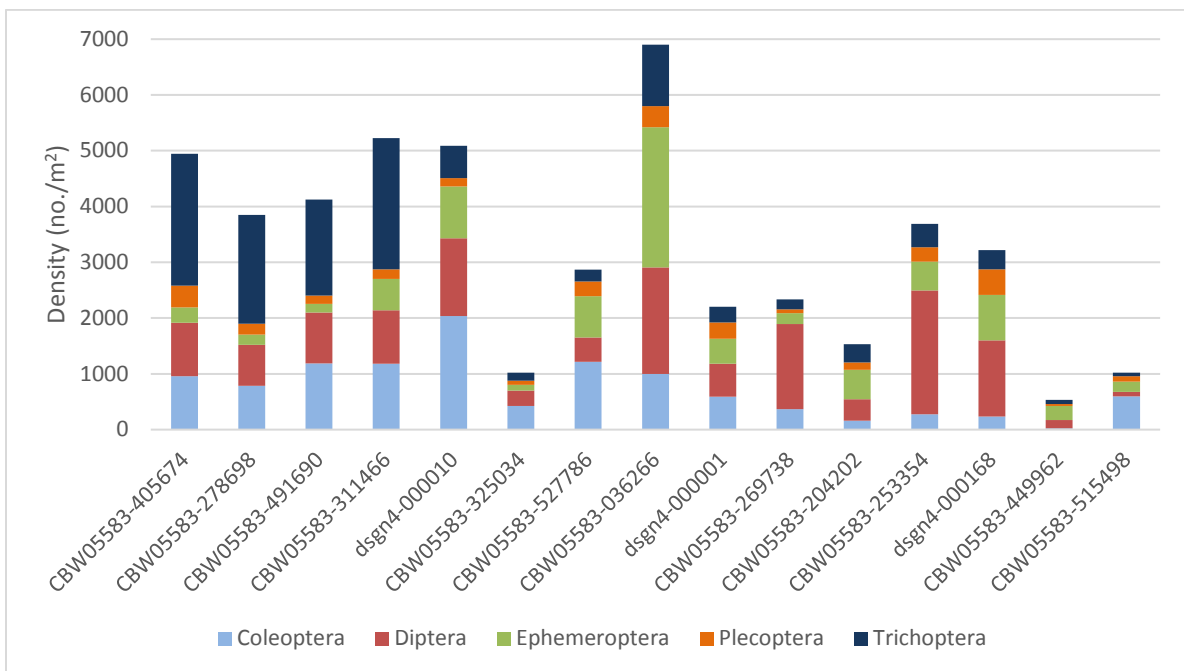


Figure 127. Total density (no./m²) in CHaMP sites contributed by five major macroinvertebrate orders collected in 2016 in Catherine Creek. Only mainstem sites are shown from lowest elevation sites on the left to highest elevation on the right.

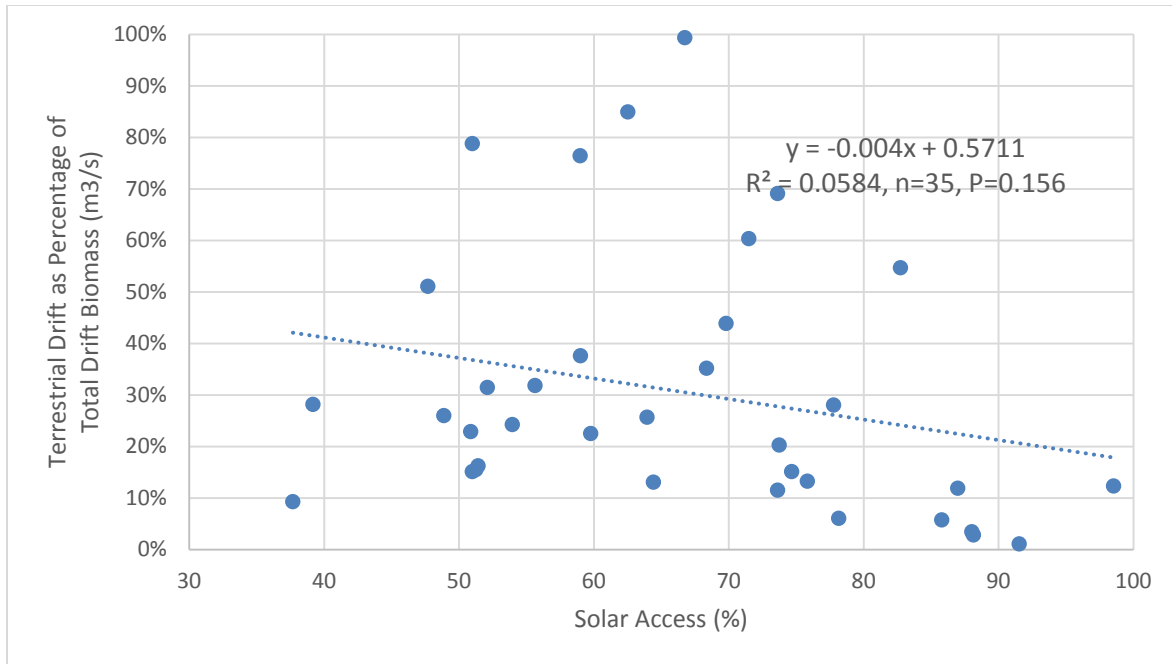


Figure 128. Percentage of total drift biomass that is of terrestrial origin for CHaMP sites in the Upper Grande Ronde River and Catherine Creek in relation to solar access (%).

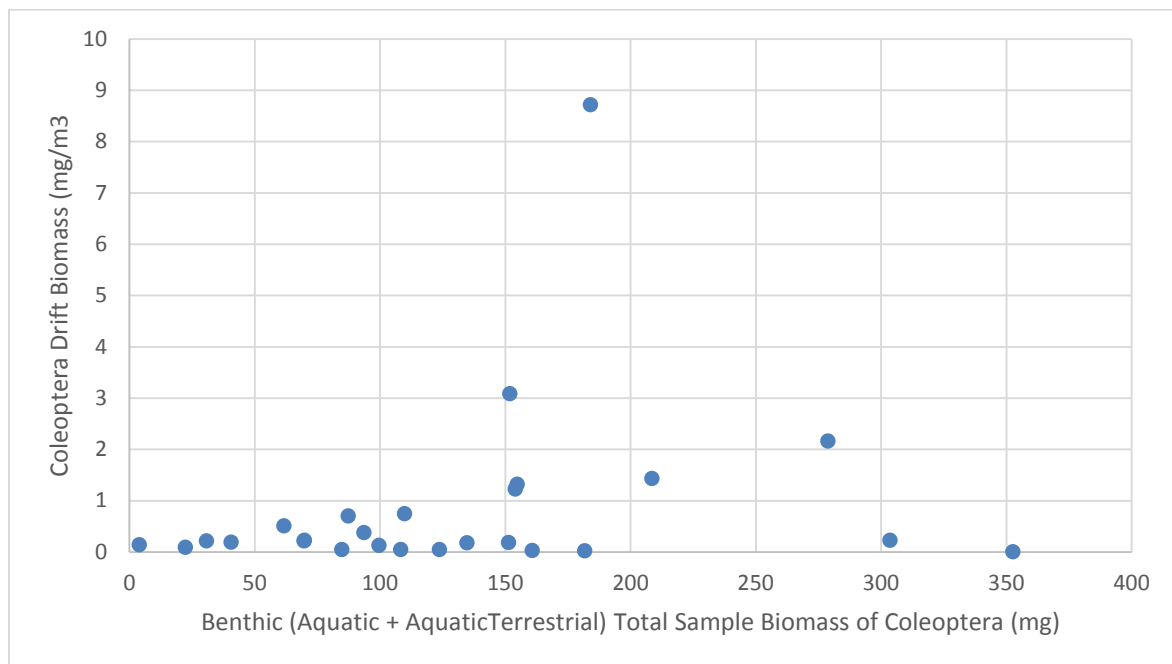


Figure 129. The relationship between Coleoptera drift biomass (mg/m³) to total benthic sample biomass (mg) of Coleoptera.

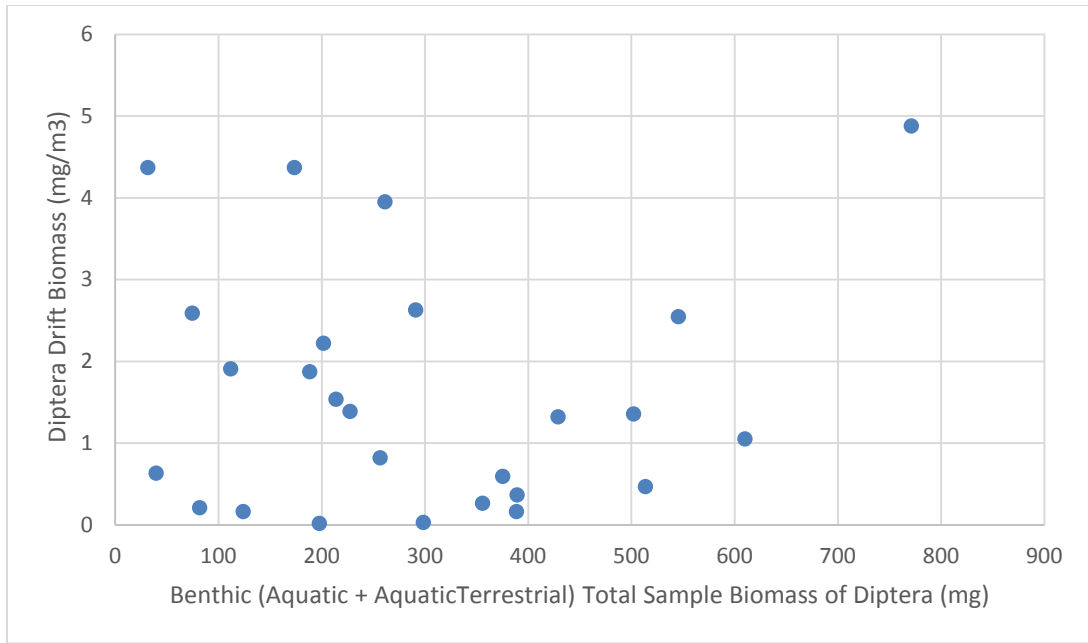


Figure 130. The relationship between Diptera drift biomass (mg/m³) to total benthic sample biomass (mg) of Diptera.

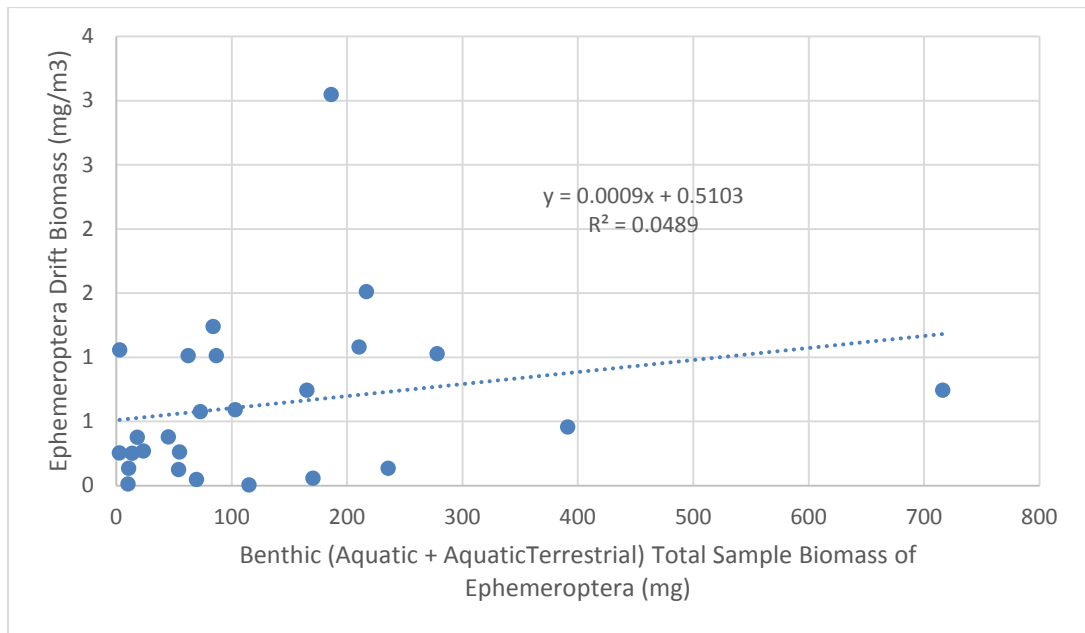


Figure 131. The relationship between Ephemeroptera drift biomass (mg/m³) to total benthic sample biomass (mg) of Ephemeroptera.

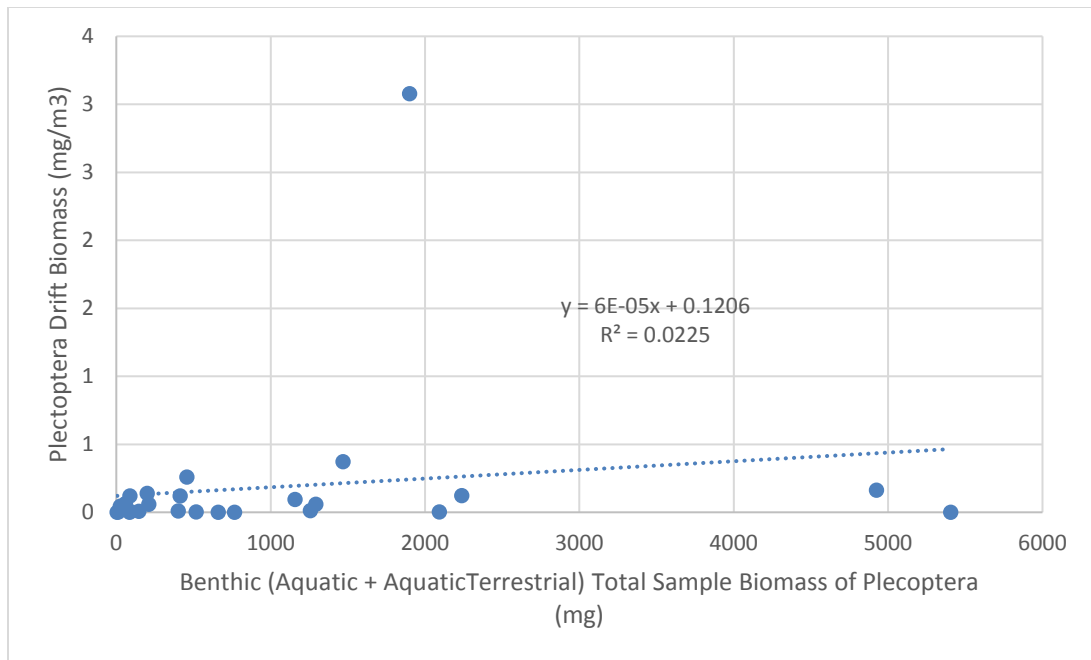


Figure 132. The relationship between Plecoptera drift biomass (mg/m³) to total benthic sample biomass (mg) of Plecoptera.

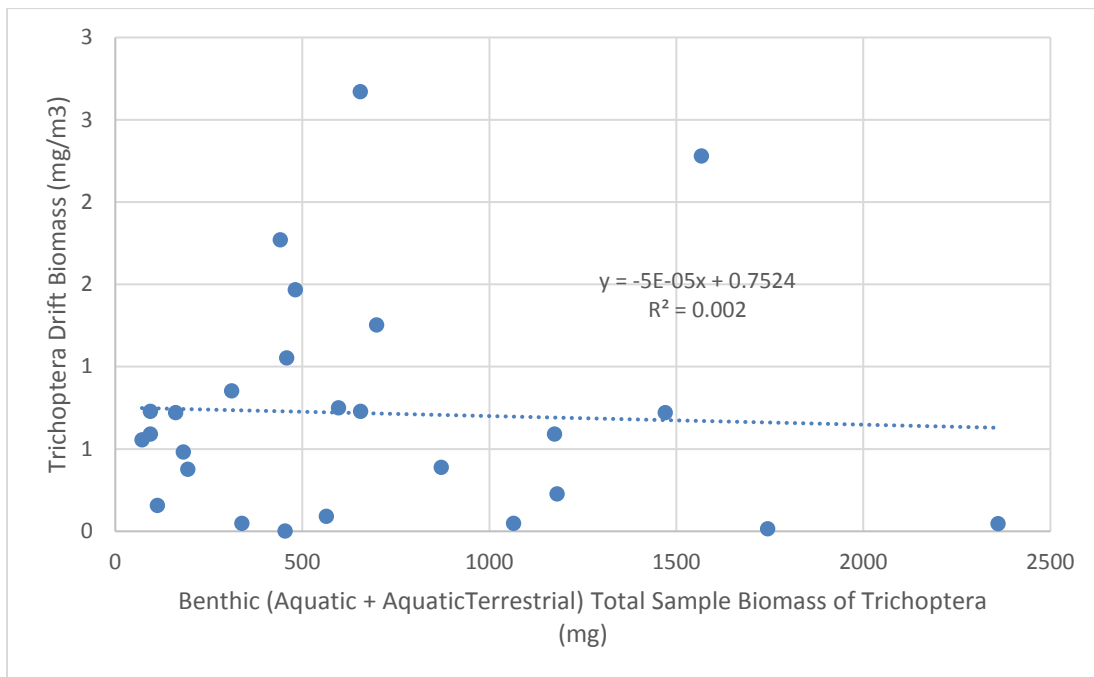


Figure 133. The relationship between Trichoptera drift biomass (mg/m³) to total benthic sample biomass (mg) of Trichoptera.

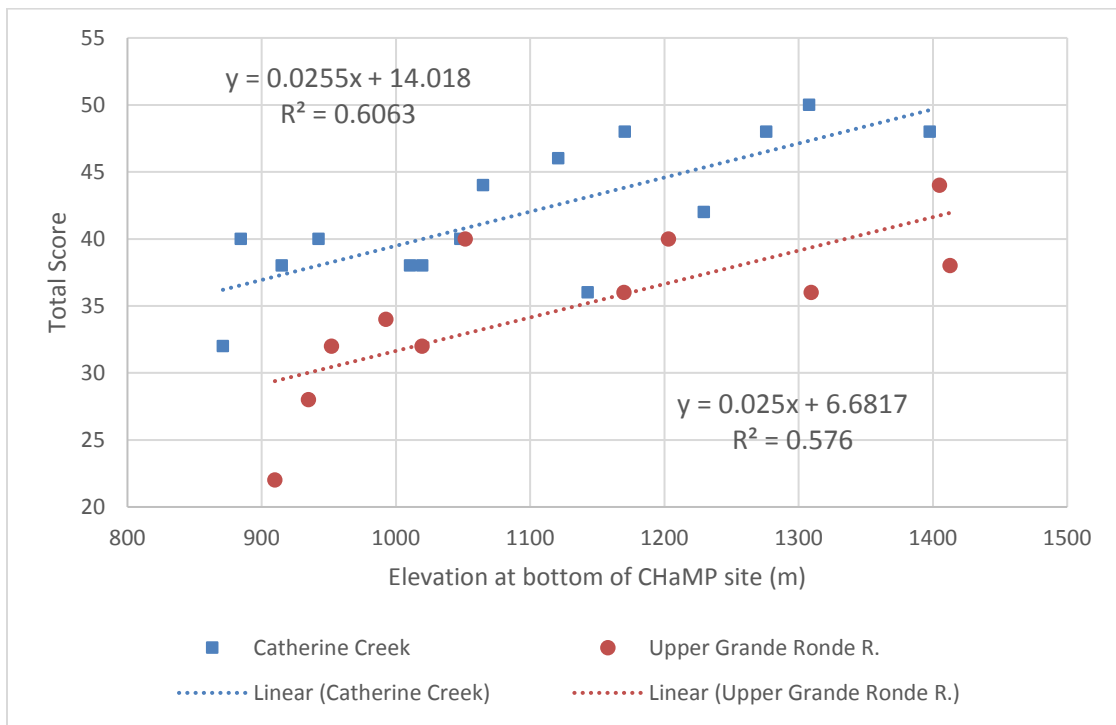


Figure 134. Relationship between Total Score (Oregon Multimetric Index) to elevation at the bottom of site for CHaMP sites on the mainstem of the Upper Grande Ronde River and Catherine Creek.

Tables

Table 57. Average biomass per individual (mg/indiv) of benthic samples for sites along the Catherine Creek mainstem for five major macroinvertebrate orders. Sites are arranged from downstream to upstream.

CHaMP Site	Coleoptera	Diptera	Ephemeroptera	Plecoptera	Trichoptera
CBW05583-405674	0.174	0.856	0.360	1.377	0.838
CBW05583-278698	0.189	1.412	0.610	8.040	0.451
CBW05583-491690	0.175	0.804	0.162	0.359	0.377
CBW05583-311466	0.210	0.721	0.129	42.397	0.498
dsgn4-000010	0.184	0.485	0.240	11.185	0.378
CBW05583-325034	0.195	1.269	0.173	23.400	3.199
CBW05583-527786	0.201	0.615	0.208	3.888	2.939
CBW05583-036266	0.205	0.302	0.149	6.790	0.851
dsgn4-000001	0.227	0.460	0.650	2.108	2.221
CBW05583-269738	0.255	0.166	0.720	1.677	3.391
CBW05583-204202	0.186	0.286	0.435	1.521	0.792
CBW05583-253354	0.199	0.176	0.485	1.045	0.996
dsgn4-000168	0.176	0.110	0.647	0.619	0.279
CBW05583-449962	0.179	0.109	0.217	1.002	2.195
CBW05583-515498	0.193	0.287	0.888	1.781	2.622

Table 58. Average biomass per individual (mg/indiv) of benthic samples for sites along the Upper Grande Ronde River mainstem for five major macroinvertebrate orders. Sites are arranged from downstream to upstream.

CHaMP Site	Coleoptera	Diptera	Ephemeroptera	Plecoptera	Trichoptera
CBW05583-109658	0.315	0.220	0.153	9.797	1.802
dsgn4-000205	0.354	0.521	0.085	0.312	0.491
CBW05583-071770	0.287	0.324	0.766	7.418	0.595
dsgn4-000245	0.238	0.136	0.543	0.953	0.869
dsgn4-000202	0.279	0.520	0.063	0.409	1.292
CBW05583-031546	0.237	0.763	0.329	4.631	2.237
CBW05583-370490	0.204	0.323	0.147	3.840	0.727
dsgn4-000277	0.228	0.293	0.131	10.291	1.202
CBW05583-468458	0.205	0.082	0.295	14.948	0.397
dsgn4-000009	0.180	0.098	0.141	14.275	0.280
CBW05583-099818	0.182	0.216	0.093	0.169	0.215

Table 59. Drift biomass density (mg/m³) of Aquatic + AquaticTerrestrial macroinvertebrates in sites along the Catherine Creek mainstem for five major macroinvertebrate orders. Sites are arranged from downstream to upstream. Drifting macroinvertebrates of Terrestrial origin are eliminated.

Catherine Creek	Coleoptera	Diptera	Ephemeroptera	Plecoptera	Trichoptera
CBW05583-405674	0.0468	1.0512	0.5785	0.0089	0.7210
CBW05583-278698	0.7487	4.8802	1.2407	0.0943	2.6708
CBW05583-491690	1.2297	2.5470	0.3773	0.0457	1.4673
CBW05583-311466	8.7193	0.4691	0.1256	<>	0.3879
dsgn4-000010	2.1620	1.3569	0.7453	0.0120	0.7217
CBW05583-325034	0.5109	0.8225	0.2536	0.0595	0.0483
CBW05583-527786	0.0219	0.0194	0.0063	<>	0.0017
CBW05583-036266	3.0848	1.3243	1.0300	3.0786	1.2529
dsgn4-000001	0.1291	2.2213	1.5130	0.2601	1.0528
CBW05583-269738	0.2193	1.8738	0.5935	0.0068	1.7703
CBW05583-204202	0.0920	0.2121	0.0604	0.0079	0.3778
CBW05583-253354	0.1953	2.6311	3.0495	0.1382	0.8537
dsgn4-000168	0.2193	1.9108	0.4581	0.0589	0.5567
CBW05583-449962	0.1443	0.6346	1.0815	0.0647	0.4824
CBW05583-515498	0.0481	4.3714	1.0150	0.1207	0.7291

Table 60. Drift biomass density (mg/m³) of Aquatic + AquaticTerrestrial macroinvertebrates in sites along the Upper Grande Ronde River mainstem for five major macroinvertebrate orders. Sites are arranged from downstream to upstream. Drifting macroinvertebrates of Terrestrial origin are eliminated.

UGR	Coleoptera	Diptera	Ephemeroptera	Plecoptera	Trichoptera
CBW05583-109658	0.0077	0.0300	0.0146	0.0000	0.0162
dsgn4-000205	0.3811	2.5919	0.2556	0.0000	0.1573
CBW05583-071770	0.0481	4.3714	1.0150	0.1207	0.7291
dsgn4-000245	0.0318	3.9524	0.7462	0.0000	0.0465
dsgn4-000202	0.7067	1.5389	1.0580	0.0453	2.2805
CBW05583-031546	0.1878	0.3695	0.2637	0.3711	0.0486
CBW05583-370490	1.3231	1.3903	0.2706	0.0023	0.0905
dsgn4-000277	1.4347	0.5938	0.3799	0.1236	0.2279
CBW05583-468458	0.2324	0.1625	0.1370	0.0021	0.5910
dsgn4-000009	0.1813	0.2666	0.0504	0.1634	0.7496
CBW05583-099818	0.2324	0.1625	0.1370	0.0021	0.5910

Table 61. Taxa richness by CHaMP site and by year for annual sites alone for display of trends in benthic macroinvertebrate data from 2011-2016.

CHaMP Site	2011	2012	2013	2014	2015	2016	Average	Min	Max
CBW05583-013882			41	53	38	54	47	38	54
CBW05583-095642		26	36	48	48	45	41	26	48
CBW05583-135615		54	44	49	51	48	49	44	54
CBW05583-142490	42	32	43	46	37	47	41	32	47
CBW05583-228666	58	53	50	57	65	50	56	50	65
CBW05583-240730	41	45	40	46		35	41	35	46
CBW05583-252730	44	42	46	47	56	47	47	42	56
CBW05583-382778	56	43	40	44	54		47	40	56
CBW05583-405674	44	46	41	47	64	45	48	41	64
dsgn4-000001	43	48	45	64	50	51	50	43	64
dsgn4-000006	50	41	38	35	51	27	40	27	51
dsgn4-000009	55	51	49	65	64	46	55	46	65
dsgn4-000010	47	52	41	57	53		50	41	57
dsgn4-000092	52	26	50	45	25	44	40	25	52
dsgn4-000094	42	57	41	48	47	47	47	41	57
dsgn4-000161	37	43	41	59	61		48	37	61
dsgn4-000168	39	44	43	55	58	59	50	39	59
dsgn4-000202	46	46	38	49	54	41	46	38	54
dsgn4-000204	44	39	46	54			46	39	54
dsgn4-000205	56	42	43	50	45	38	46	38	56
dsgn4-000213	50	45	45	47	58	51	49	45	58
dsgn4-000245	51	50	46	58	48	49	50	46	58
dsgn4-000277	52	44	42	46	61	49	49	42	61
Average	47	44	43	51	52	46	47	43	52
Min	37	26	36	35	25	27	31	25	37
Max	58	57	50	65	65	59	59	50	65

Table 62. Total Score for Eastern Oregon Multimetric Index by CHaMP site and by year for annual sites alone for display of trends in benthic macroinvertebrate data from 2011-2016.

CHaMP Site	2011	2012	2013	2014	2015	2016	Average	Min	Max
CBW05583-013882			46	44	38	44	43	38	46
CBW05583-095642		20	36	40	32	26	31	20	40
CBW05583-135615		48	46	44	44	44	45	44	48
CBW05583-142490	42	28	44	40	34	32	37	28	44
CBW05583-228666	48	46	46	48	48	46	47	46	48
CBW05583-240730	30	34	32	34		26	31	26	34
CBW05583-252730	32	30	28	34	44	28	33	28	44
CBW05583-382778	46	42	46	40	40		43	40	46
CBW05583-405674	42	42	44	42	44	32	41	32	44
dsgn4-000001	48	48	46	50	48	46	48	46	50
dsgn4-000006	42	42	36	40	40	26	38	26	42
dsgn4-000009	48	50	49	50	48	44	48	44	50
dsgn4-000010	50	46	46	46	46	38	45	38	50
dsgn4-000092	40	32	40	38	16	18	31	16	40
dsgn4-000094	42	42	37	42	28	34	37	28	42
dsgn4-000161	46	44	50	48	50		48	44	50
dsgn4-000168	50	50	44	50	50	48	49	44	50
dsgn4-000202	42	34	35	44	36	32	37	32	44
dsgn4-000204	44	42	44	40			43	40	44
dsgn4-000205	32	30	38	40	36	28	34	28	40
dsgn4-000213	32	28	29	32	32	32	31	28	32
dsgn4-000245	38	38	40	40	38	34	38	34	40
dsgn4-000277	42	42	37	38	40	40	40	37	42
Average	42	39	41	42	40	35	40	34	44
Min	30	20	28	32	16	18	31	16	32
Max	50	50	50	50	50	48	49	46	50

Table 63. Taxa richness of benthic samples for the 10 mainstem sites along the Upper Grande Ronde River described in the low flow analysis in this annual report.

Site Name	Taxa.Richness					
	2011	2012	2013	2014	2015	2016
CBW05583-235322	48			61		
CBW05583-370490			42			50
CBW05583-321338	44			58		
dsgn4-000277	52	44	42	46	61	49
CBW05583-468458			49			40
CBW05583-206314	45			59		
CBW05583-148970	48			61		
CBW05583-280042	56			63		
dsgn4-000009	55	51	49	65	64	46
CBW05583-099818			46			41

Table 64. Numbers of sensitive taxa in benthic samples for the 10 mainstem sites along the Upper Grande Ronde River described in the low flow analysis in this annual report.

Site Name	Sensitive Taxa					
	2011	2012	2013	2014	2015	2016
CBW05583-235322	4			5		
CBW05583-370490			5			4
CBW05583-321338	4			4		
dsgn4-000277	5	6	5	4	6	6
CBW05583-468458			11			6
CBW05583-206314	9			8		
CBW05583-148970	10			11		
CBW05583-280042	8			11		
dsgn4-000009	11	12	10	13	11	7
CBW05583-099818			10			7

Table 65. Numbers of sediment sensitive taxa in benthic samples for the 10 mainstem sites along the Upper Grande Ronde River described in the low flow analysis in this annual report.

Site Name	Sediment Sensitive Taxa					
	2011	2012	2013	2014	2015	2016
CBW05583-235322	5			5		
CBW05583-370490			3			3
CBW05583-321338	4			5		
dsgn4-000277	5	3	3	3	4	3
CBW05583-468458			4			3
CBW05583-206314	4			5		
CBW05583-148970	3			4		
CBW05583-280042	4			5		
dsgn4-000009	4	2	3	4	3	2
CBW05583-099818			1			1

Table 66. Percentage of tolerant taxa in benthic samples for the 10 mainstem sites along the Upper Grande Ronde River described in the low flow analysis in this annual report.

Site Name	Pct. Tolerant Taxa					
	2011	2012	2013	2014	2015	2016
CBW05583-235322	41.7			19.0		
CBW05583-370490			39.9			35.0
CBW05583-321338	18.5			23.4		
dsgn4-000277	33.8	39.3	29.6	36.1	31.8	38.7
CBW05583-468458			18.8			21.3
CBW05583-206314	12.9			23.4		
CBW05583-148970	10.3			14.3		
CBW05583-280042	12.0			12.5		
dsgn4-000009	7.2	3.7	9.7	7.1	8.5	7.3
CBW05583-099818			9.6			18.0

Table 67. Total Score (Oregon Multimetric Index) for benthic samples for the 10 mainstem sites along the Upper Grande Ronde River described in the low flow analysis in this annual report.

Site Name	Total Score					
	2011	2012	2013	2014	2015	2016
CBW05583-235322	42			42		
CBW05583-370490			40			36
CBW05583-321338	42			40		
dsgn4-000277	42	42	37	38	40	40
CBW05583-468458			46			36
CBW05583-206314	42			46		
CBW05583-148970	48			48		
CBW05583-280042	48			46		
dsgn4-000009	48	50	49	50	48	44
CBW05583-099818			48			38

Table 68. Total density (indiv/m²) in benthic samples for the 10 mainstem sites along the Upper Grande Ronde River described in the low flow analysis in this annual report.

Site Name	Density_indiv_m ²					
	2011	2012	2013	2014	2015	2016
CBW05583-235322	2589.7			3113.7		
CBW05583-370490			4182.2			3848.0
CBW05583-321338	3261.4			1952.7		
dsgn4-000277	5901.2	6448.9	6506.3	7782.2	5178.5	5901.3
CBW05583-468458			1360.1			15219.9
CBW05583-206314	825.4			1182.4		
CBW05583-148970	458.0			1394.5		
CBW05583-280042	538.4			4703.8		
dsgn4-000009	982.9	3033.7	7305.8	2295.9	15133.6	11393.4
CBW05583-099818			1547.8			2527.1

Table 69. Select summary statistics for benthic macroinvertebrate samples taken in sites along the Catherine Creek mainstem for five major macroinvertebrate orders. Sites are arranged from downstream to upstream.

Catherine Creek	Elevation (m)	Total Score	O_E_P0.5	O_E_P0.0	WA_inv_Temp.C (°C)	n.Temp.Sens. Indicator. Taxa	n.Temp.Tol. Indicator. Taxa	n.FS.Sens. Indicator. Taxa	n.FS.Tol. Indicator. Taxa	Untrans.WA _Inv._Pct. Fine. Sediment (%)
CBW05583-405674	871.1	32	1.02	1.14	22.48	0	6	3	3	8.44
CBW05583-278698	884.5	40	0.90	1.19	22.85	0	5	3	4	11.05
CBW05583-491690	915.0	38	0.74	1.00	19.42	1	3	3	2	4.56
CBW05583-311466	942.5	40	0.81	1.05	20.33	1	5	5	2	2.42
dsgn4-000010	1010.4	38	1.04	1.26	19.34	2	5	6	3	2.19
CBW05583-325034	1019.5	38	0.84	1.26	19.92	3	4	5	4	2.63
CBW05583-527786	1048.0	40	1.12	1.45	17.98	4	5	6	5	4.20
CBW05583-036266	1065.0	44	1.02	1.24	17.73	4	3	6	3	2.16
dsgn4-000001	1120.9	46	1.21	1.12	15.72	7	2	8	3	4.78
CBW05583-269738	1142.8	36	0.96	0.78	16.13	5	2	8	3	4.44
CBW05583-204202	1170.5	48	1.21	1.21	15.28	8	2	9	2	2.92
CBW05583-253354	1229.4	42	1.10	1.22	14.31	8	2	7	2	3.89
dsgn4-000168	1275.8	48	1.27	1.26	13.40	11	2	9	3	3.42
CBW05583-449962	1307.8	50	1.14	1.08	12.88	10	2	9	3	2.54
CBW05583-515498	1397.7	48	1.06	1.16	13.21	10	2	11	3	0.94

Table 70. Select summary statistics for benthic macroinvertebrate samples taken in sites along the Upper Grande Ronde River mainstem for five major macroinvertebrate orders. Sites are arranged from downstream to upstream.

UGR	Elevation	Total Score	O_E_P0.5	O_E_P0.0	WA_inv_Temp.C (°C)	n.Temp.Sens . Indicator. Taxa	n.Temp.Tol. Indicator. Taxa	n.FS.Sens. Indicator. Taxa	n.FS.Tol. Indicator. Taxa	Untrans.WA _Inv._Pct. Fine. Sediment (%)
CBW05583-109658	909.8	22	0.86	0.92	25.60	0	5	1	4	7.08
dsgn4-000205	934.6	28	1.05	1.05	22.39	1	5	2	3	8.78
CBW05583-071770	952.0	32	0.70	0.87	25.81	0	6	0	3	7.44
dsgn4-000245	992.5	34	0.96	1.05	25.91	1	6	2	7	13.17
dsgn4-000202	1019.4	32	0.89	0.97	24.61	0	5	1	5	8.37
CBW05583-031546	1051.6	40	0.92	1.14	21.74	1	6	2	3	6.94
CBW05583-370490	1169.8	36	0.86	1.09	21.87	1	5	3	3	6.25
dsgn4-000277	1202.8	40	0.99	0.99	21.01	1	5	4	3	8.49
CBW05583-468458	1309.3	36	0.67	0.90	18.60	4	4	5	3	5.94
dsgn4-000009	1404.8	44	1.10	1.07	17.36	5	3	4	3	6.96
CBW05583-099818	1412.7	38	1.06	1.01	17.62	4	4	4	3	5.52

References

- Hayslip, G. (editor). 2007. Methods for the collection and analysis of benthic macroinvertebrate assemblages in wadeable streams of the Pacific Northwest. Pacific Northwest Aquatic Monitoring Partnership, Cook, Washington.
- Hubler, S. 2006. Pine Creek (Wheeler County) Stream Condition Assessment. Oregon Department of Environmental Quality, Watershed Assessment Section, Portland, Oregon.
- Hubler, S. 2008. PREDATOR: Development and use of RIVPACS-type macroinvertebrate models to assess the biotic condition of wadeable Oregon streams. DEQ Report DEQ08-LAB-0048-TR. 51 pp.
- Huff, D.L., S.L. Hubler, Y. Pan, and D. L. Drake. 2006. Detecting Shifts in Macroinvertebrate Assemblage Requirements: Implicating Causes of Impairment in Streams. Unpublished report prepared by Oregon Department of Environmental Quality, Portland, Oregon.

Files included in analysis

Macro results-Annual Report-2016-dm.pptx
CRITFC ALL samples 2016 - Data-dm.xlsx
Analysis of 2011-2016 bugs.xlsx
SiteIDs for samples-2016-dm.xlsx

Dissemination of Project Findings

Presentations

- Justice, C., S. White, D. McCullough, M. Blanchard. February 2016. Influence of riparian restoration and climate change on stream temperature and fish abundance in the Upper Grande Ronde River. Presentation to the Grande Ronde Atlas Group, State of the Science Meeting, La Grande, Oregon.
- Justice, C., S. White, D. McCullough, M. Blanchard. March 2016. Watershed restoration in the Upper Grande Ronde River. Presentation to the Columbia River Inter-Tribal Fish Commission, Commission Meeting, Mission, Oregon.
- Justice, C., S. White, D. McCullough. November 2016. Influence of riparian restoration and climate change on stream temperature and fish abundance in the Upper Grande Ronde River. Presentation to the Upper Salmon Basin Watershed Program, Technical Team Meeting, Coeur d'Alene, Idaho.
- Justice, C., S. M. White, D. A. McCullough, D. S. Graves, M. R. Blanchard. February 2017. Can stream and riparian restoration offset climate change impacts to salmon populations. Presentation to the Sandy River Basin Watershed Council, Climate Adaptations Workshop, Troutdale, Oregon.
- White, S.M. and Sullivan, S.P. 2016. Using standard benthic macroinvertebrate sampling for food web metrics in salmon-bearing streams. Society for Freshwater Science (PNW Chapter). Astoria, Oregon.
- White, S.M. 2016. Historical ecology of the Grande Ronde River with implications for salmon restoration. Upper Grande Ronde/Catherine Creek Atlas. 1st Annual State of the Science Meeting. La Grange, Oregon.
- White, S.M. 2016. Documenting historical trends in fish habitat conditions using CHaMP and other stream surveys. Advanced Trainer Workshop, Columbia River Habitat Monitoring Program, Cove, Oregon.
- White, S.M., Justice, C., McCullough, D., Kelsey, D., Sedell, T. 2017. Using historical ecology to guide stream habitat restoration. River Restoration in Eastern Oregon and Eastern Washington Session, Oregon Chapter of the American Fisheries Society, Bend, Oregon.

Publications

- CHaMP (Columbia Habitat Monitoring Program) (multiple contributing authors). 2016. Scientific protocol for salmonid habitat surveys within the Columbia Habitat Monitoring Program. Prepared by CHaMP for the Bonneville Power Administration.
- Justice, C. 2016. In hot water: Can habitat restoration improve water temperatures for salmon in the Upper Grande Ronde River? Ripples in the Grande Ronde, Fall Edition.
<http://www.grmw.org/ripples/2016/>
- Justice, C., S. M. White, D. A. McCullough, D. S. Graves, and M. R. Blanchard. 2017. Can stream and riparian restoration offset climate change impacts to salmon populations? Journal of Environmental Management 188:212–227.

- Kelly, V.J. and White, S.M. 2016. A method for characterizing late-season low-flow regime in the Upper Grande Ronde basin. U.S. Geological Survey, Water Science Center Report, Portland, Oregon.
- Sullivan S.P, White S.M. 2017. Methods supporting the development of food web metrics from benthic macroinvertebrate data. Report prepared for the Bureau of Indian Affairs Rights Implementation Climate Change Contract AO9AV00480 by Rhithron Associates, Inc., Missoula, MT, and Columbia River Inter-Tribal Fish Commission, Portland, OR.
- White, S.M., C. Justice, D.A. Kelsey, D.A. McCullough, T. Smith. 2017. Legacies of Stream Channel Modification Revealed Using General Land Office Surveys, with Implications for Water Temperature and Aquatic Life. *Elem Sci Anth* 5(3):1-18. doi:10.1525/elementa.192.

Draft journal articles

- Justice, C., J. Feldhaus, D. Kelsey. (to be submitted in spring 2017). Influence of water temperature on spawning success of spring Chinook Salmon in the Grande Ronde and Imnaha River basins, northeast Oregon. Intended for *North American Journal of Fisheries Management*.
- Kaylor, M.J., A. Argerich, B. VerWey, I. Arismendi, and S.M. White (to be submitted in spring 2017) Light conditions and periphyton biomass influence in situ measurements of stream benthic chlorophyll a. Intended for *Freshwater Science*.
- White, S.M., McHugh, P., Naman, S., Baxter, C., Bellmore, R., Naiman. R., and Danehy, R. A practical guide to food web perspectives and methods for riverine fish conservation. Intended for *Fisheries*.

Appendix 1 – Life Cycle Model

Catherine Creek spring Chinook Life Cycle Model

December 2016-March 2017 Progress Report

Eco Logical Research



Contents

1. Introduction.....	3
1.1. Report overview	3
2. Modeling framework	3
2.1. Life cycle modeling framework.....	3
2.2. Study system overview	5
2.3. Base model parameterization.....	5
2.4. Management scenarios.....	6
2.5. Simulation specifications and performance metrics.....	7
2.6. Assumptions, limitations, and uncertainties	8
3. Results and discussion.....	8
4. Future considerations & next steps.....	15
Acknowledgements.....	16
References	17
Appendix A. Base parameterization and references for Catherine Creek spring Chinook salmon.	18
Appendix B. Overview of the approach taken to model hatchery supplementation programs.....	19

1. Introduction

1.1. Report overview

This document provides an overview of Eco Logical Research's progress towards a life cycle model (LCM) based assessment of restoration opportunities within the Catherine Creek (CC) and Upper Grande Ronde River (UGR) watersheds. The specific goals of our project were to (1) parameterize two Chinook salmon (*Oncorhynchus tshawytscha*) LCMs, one for Catherine Creek and the other for the Upper Grande Ronde River (UGR) and (2) extend UGR and CC LCMs to assess the effects of several different habitat restoration treatments, varying in specificity, on the performance of model populations. Between December 2016 and March 2017, we made progress in several areas:

- (1) We reviewed available demographic data for the UGR and CC populations and successfully parameterized LCMs for both populations. However, due to (a) the time required to incorporate item 2 (below) into the project, (b) staffing changes within Eco Logical Research, and (c) data uncertainties for UGR Chinook, we present only CC results here.
- (2) We made LCM code modifications to support the modeling of the hatchery supplementation strategies currently in place for CC and UGR Chinook salmon. We initially hoped to avoid modeling hatchery programs; however, doing so was necessary because preliminary analyses projected rapid extinction with only natural production regardless of initial abundance conditions. Additionally, while our LCM allowed for the modeling of simple supplementation scenarios, Catherine Creek's 'sliding scale' style supplementation management necessitated coding changes.
- (3) We simulated population performance under seven different scenarios that consider alternative future temperature, habitat, and climate conditions, adapted from the abundance projections of Justice et al. (2017).

In the following pages, we review progress on items 1-3 in detail, summarize findings in general terms, and end with several suggestions for further developing this work.

2. Modeling framework

2.1. Life cycle modeling framework

Chinook salmon population performance under alternative habitat scenarios was assessed using a life cycle modelling framework. A life cycle model (LCM) is simply a mathematical representation of a Pacific salmon's life history (**Figure 1**) that, given relevant inputs (e.g., stage-specific productivity, capacity), can be used to simulate population dynamics. LCMs are particularly well suited for addressing habitat scenarios because they can simulate population trajectories as a function of the same demographic parameters that management aims to modify (e.g., summer rearing capacity, overwinter survival, etc.), all while considering uncertainty in model inputs. More specifically, the LCM used here (i.e., McHugh et al. In Press) is a stage-structured, stochastic projection model, adapted from Sharma et al. (2005) and implemented in the R statistical computing language (R Core Team 2014). This LCM propagates cohorts across a complete life cycle according to a series of stage-specific Beverton-Holt 'spawner' (N_i) and 'recruit' (N_{i+1}) relationships (after Moussalli and Hilborn 1986), each of which is governed by stage-specific capacity (c_i) and productivity (p_i , maximum recruits per spawner) parameters,

Equation 1.
$$N_{i+1} = \frac{N_i}{\frac{1}{p_i} + \frac{1}{c_i} N_i}$$

Although this functional form implies that density dependence occurs at all life stage transitions, density independent assumptions can also be modeled here simply by setting capacity to an infinitely large value and using empirical estimates of survival (S_i) as the productivity input (p_i). Otherwise, realized survival ($S_i = N_{i+1} / N_i$) is a function of both the capacity and productivity for a given population or segment thereof. Note that these parameters form the basis for representing management scenarios; we discuss parameter sourcing in further detail below under 2.3. *Base model parameterization*.

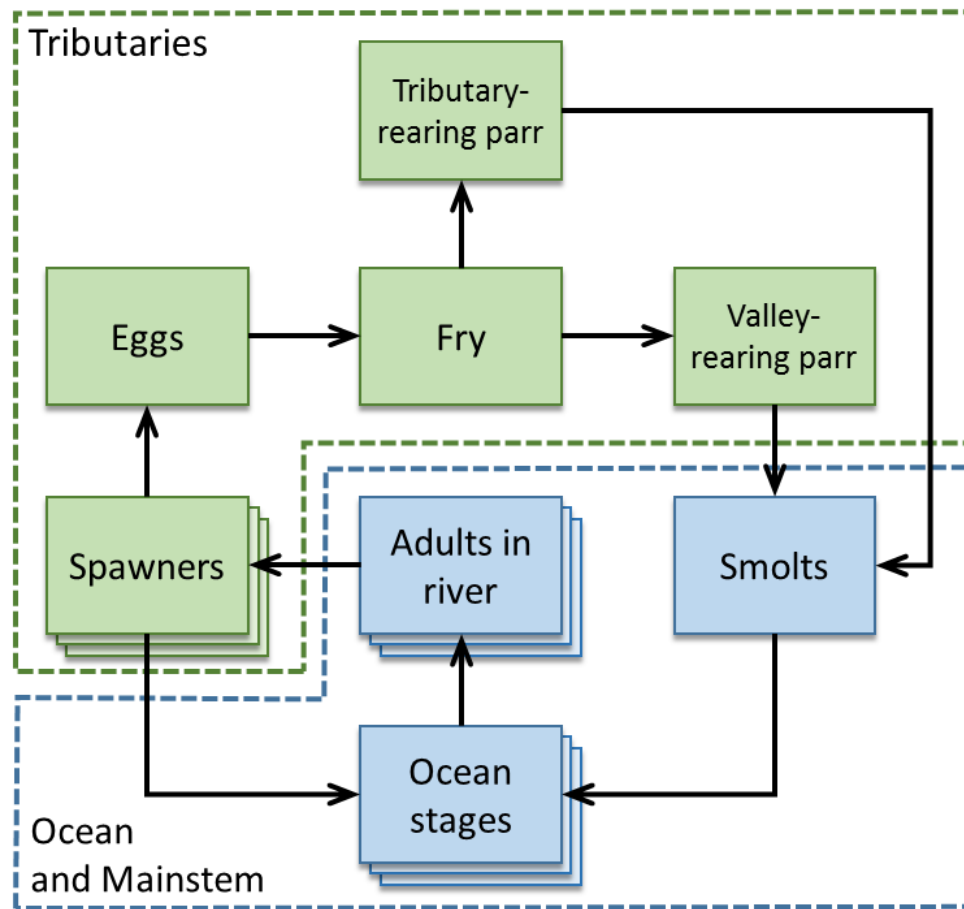


Figure 1. Conceptual diagram of the life cycle model (LCM) framework used to assess restoration scenarios in Catherine Creek. Stacked boxes represent life stages for which multiple ages exist and are tracked accordingly. In our LCM, parr can ‘choose’ to migrate downstream and overwinter in the Grande Ronde Valley (‘Valley’) or remain in the upper mainstem and tributaries of Catherine Creek (‘Tributary’). Otherwise, the LCM’s smolts are enumerated at Lower Granite Dam (LGD), where ‘ocean stages’ begin and are modeled via LGD-to-LGD smolt-to-adult return rates.

2.2. Study system overview

For modeling purposes, Catherine Creek Chinook salmon express two life history trajectories which occur over three different spatial strata (**Figure 1**). All fish spawn in late summer, hatch in spring, and rear through the bulk of their first summer out of the gravel within the upper mainstem and tributaries of Catherine Creek, above the primary location at which state and tribal agencies enumerate abundance via ‘fish in-fish out’ sampling (i.e., juvenile trap, adult weir). In the autumn of their first year, parr diverge into one of two life histories: parr either (a) move down river and overwinter in the Grande Ronde Valley (‘Valley’ life history), before moving downstream towards Lower Granite Dam (LGD) as smolts in the spring, or (b) remain in the upper mainstem/tributaries of Catherine Creek (‘Tributary’ life history) for the winter, and migrate to LGD as smolts in the subsequent spring. Thereafter, both life history pathways begin the mainstem–ocean segment of their life cycle before returning in 1 to 3 years to the upper mainstem/tributary stratum as prespawners/spawners.

2.3. Base model parameterization

In most LCM applications, capacity and productivity parameters appropriate for the species or system of interest are difficult to obtain, as these parameters are rarely estimated as part of routine monitoring programs. Here, however, a combination of entities monitors populations and habitats in such a way that estimating these parameters using population-specific data or models is possible; the Oregon Department of Fish and Wildlife (ODFW), Confederated Tribes of Umatilla Reservation (CTUIR), Columbia River Inter-Tribal Fish Commission (CRITFC), and other parties, collect the data needed to estimate spawner, parr, and smolt abundance and/or survival each year. Additionally, as part of the Columbia Habitat Monitoring Program (CHaMP) and Integrated Status and Effectiveness Monitoring Program (ISEMP), population-specific habitat data are collected and analyzed in such a way that permits the estimation of adult and juvenile carrying capacities as a function of current habitat conditions. More specifically, both egg-to-parr (late summer) and parr-to-smolt (at Lower Granite Dam, LGD) survival inputs were based on estimates generated by ODFW’s ‘Early Life Histories’ monitoring program. ‘Ocean’ (i.e., smolts passing LGD downstream to adults passing LGD upstream) survival and adult maturation schedules were estimated using age-specific smolt-to-adult return rate estimates (SARs) generated by the Fish Passage Center (McCann et al. 2016), similar to those used in B. Lessard’s LCM (McCann et al. 2016)¹. We additionally included carrying capacity terms for two freshwater tributary life stages, summer parr and adult spawners (expressed in terms of eggs), respectively: (a) juvenile capacity was estimated using an empirical model that predicts parr carrying capacity as a function of habitat variables (i.e., a quantile random forest model; K. See, unpublished manuscript), and (b) adult carrying capacity was predicted using habitat suitability index models after McHugh et al. (In Press). Where necessary, other LCM parameters were informed by literature values where necessary. Complete details on our base/status quo (scenario ‘Curr’ in **Table 1**) Catherine Creek LCM parameterization, including assumptions about stochasticity, are presented in **Appendix A**.

Beyond the basic numerical and life history parameter details associated with our LCM, other parameterization decisions were made to represent population dynamics as accurately as possible in space and time given the data available, including:

¹ Note that here we model SARs assuming a single ‘average’ outmigrant experience and make no attempt to distinguish transported vs. in-river migrants; thus, our assumption is that conditions during the 2001-2014 smolt migration years provide reasonable insight on average future mainstem/ocean conditions.

- (1) Although the LCM allows fish to exhibit separate Tributary and Valley life history trajectories, and at the frequency with which they occur in sampling data, the current model implementation assumes they share a similar overwinter survival in both places. In other words, the current life history trajectory construct is simply a placeholder for future evaluation and comparisons of spatially distinct scenarios affecting overwintering survival, and the LCM preserves total survival from the summer parr stage to LGD smolts in a manner consistent with available data.
- (2) Upon return, adults are recognized perfectly by production type and passed over the weir or taken to the hatchery according to the Catherine Creek supplementation program's sliding scale rule set (**See Appendix B**). In practice, weir management is more difficult due to the fact that collection decisions are made in real time with imperfect knowledge about the total run size. Note additionally that supplementation is handled in the model through the annual release of 150,000 smolts (less if broodstock needs are not met in year $y - 2$, **See Appendix B**) and it is assumed that supplementation fish home perfectly back to the natal basin.

2.4. Management scenarios

We modeled several scenarios for Catherine Creek Chinook (**Table 1**). First, we modeled the population under 'current conditions', i.e., based on recent averages for demographic parameters (**Appendix A**). This scenario provides insight on performance under a 'do nothing' case and also provides an opportunity to verify that population dynamics are consistent with those of the actual CC Chinook population. In addition to the base case ('Curr'), we considered six different scenarios based on the recent temperature modeling work of Justice et al. (2017). Specifically, we modeled the population-level effects of alternative temperature/habitat futures ranging from a scenario that considered the effects of global warming, manifested as increased water temperature and decreased streamflow, in the absence and presence of habitat restoration (i.e., scenarios 'Clim', 'ClimVeg', 'Clim...', etc.) to scenarios that considered the effects of riparian restoration under current thermal conditions (e.g., scenario 'PNV'). Benefits/changes were expressed via a simple proportional change in summer parr rearing capacity, based on the abundance changes that Justice et al. (2017) predicted under each scenario. Note also that changes are imposed at the outset of simulations; thus scenarios/results do not account for the differing time scales required for changes to be realized in practice.

Beyond habitat restoration, we explicitly modeled the CC hatchery supplementation strategy according to the 'sliding scale' weir management system described in Carmichael et al. (2011) and in **Appendix B**. In brief, the passage (to spawning grounds) or collection (for spawning in hatchery) of hatchery (i.e., adult returns from releases of supplementation smolts) and natural adults reaching the CC weir are managed to maintain the overall genetic integrity of the population while offering the abundance-boosting benefits of hatchery spawning. Thus, the adult trap is used to manage three aspects of escapement that are pertinent to supplementation goals: (i) P_{NOS-R} (i.e., the proportion of the total natural-origin returns that is retained for the hatchery), (ii) P_{HOS} (i.e., the proportion of natural spawners that is of hatchery origin), and (iii) P_{NOB} (i.e., the proportion of hatchery broodstock/egg-take that is of natural origin). Although our LCM could be used to look at the effects of varying supplementation strategies, here we modeled all scenarios assuming the same operation, which is described in **Appendix B**. Thus, although it is embedded herein as a 'management strategy,' it is consistent across each of the seven scenarios described in Table 1.

Lastly, although harvest scenarios can also be addressed using our model, we do not explicitly model harvest management here. This modeling decision is reasonable for ocean fisheries because they minimally affect interior Columbia Basin spring Chinook stocks. However, future analyses should consider whether the differential impact of mark-selective freshwater sport and net fisheries on hatchery (i.e., the basis for SAR estimation; **Appendix A**) relative to natural fish affects the relative performance of model populations across habitat and/or supplementation scenarios.

Table 1. Scenarios modeled using the CC LCM, after Justice et al. (2017). For LCM inputs, each scenario is represented as a proportional increase or decrease in summer parr rearing capacity.

Scenario Abbreviation	Description	Proportional Δ in Capacity
Curr	Baseline model calibrated using 2010 temperature, climate, vegetation, and hydrologic conditions	0.00
PNV	Vegetation across the entire model extent set to potential natural vegetation (PNV) cover and height, assuming climax conditions (i.e., 300-year cover and height).	0.61
HiPr	Vegetation in high priority areas set to PNV and other areas set to current conditions.	0.30
WidPNV	Channel width set to historic conditions and vegetation set to PNV.	0.67
Clim	Air temperature and streamflow set to 2080s climate projections.	-0.36
ClimVeg	2080s climate projections and vegetation set to potential cover and height at 75 years.	0.20
ClimVegWid	2080s climate projections, vegetation set to potential cover and height at 75 years, and channel width set to historic conditions.	0.37

2.5. Simulation specifications and performance metrics

To evaluate population performance across different scenarios (**Table 1**), we simulated dynamics for a 30-year period (i.e., 40 years, less a 10-year burn-in period) for $N = 100$ separate Monte Carlo iterations for each of the seven habitat scenarios. All models were initialized with 1,000,000 natural-origin fry and 150,000 hatchery-origin smolts. Supplementation releases were tracked as hatchery (H1) fish until their death; all progeny spawned in the wild were tracked and treated as being ‘natural’, regardless of parentage (e.g., $H1 \times H1 = \text{natural}$, $\text{natural} \times H1 = \text{natural}$, ...). Although LCM results can be summarized in innumerable ways, here we focus on one metric, the natural-origin adult run size (‘abundance’) returning to CC. More specifically, abundance for each Monte Carlo trial in terms of the geometric mean natural-origin run size returning to the adult trap (i.e., pre-sliding scale management) for the modeled 30-year time horizon. Although we considered other summary metrics, such as quasi-extinction risk, we determined that this metric is less relevant here due to the continuously bolstering effect of the heavy supplementation component that was modeled for CC. Additionally, although a metric such as the proportion of fish spawning naturally that is of natural origin (i.e., P_{NOS} , or its corollary P_{HOS}) may be informative, in this case it is simply a mathematical rearrangement of our abundance metric given the consistent release of 150,000 hatchery-reared smolts. Beyond abundance, we conducted initial simulations using base model (scenario ‘Curr’) parameters to verify that the overall LCM properly

captured freshwater productivity (i.e., smolts/spawner and its dependence on adult density), age structure (returning adult), SARs, and life history expression (i.e., Tributary vs. Valley) as intended.

2.6. Assumptions, limitations, and uncertainties

Although the CC and UGR population and habitat monitoring cases are perhaps best-case scenarios for LCM development (i.e., in temporal and stage coverage), simplifying assumptions were nonetheless made in order to make LCM-based scenario evaluations tractable. Perhaps the most noteworthy of these are the following:

1. First-generation hatchery fish and subsequently produced natural fish (and back-crosses thereof) have similar fitness. Although studies show fitness differences for wild- and hatchery-origin fish, as well as captive-reared fish and parent wild populations spawning naturally, little information exists for representing these effects numerically in a LCM for spring Chinook in the Grande Ronde Basin in particular. Further, previous analyses suggest that where differences may exist, they are either inconsistent and on average compensating (e.g., the larger size of hatchery smolts offsets the acclimatization advantage held by natural fish). For these reasons, we used the same (species-specific) survival, fecundity, and maturation inputs for all fish, regardless of origin.
2. Habitat benefits are realized instantaneously. Whereas riparian revegetation and associated thermal benefits may take decades to centuries to be realized, here scenarios assume that they are realized at the outset of model runs. Thus, we provide a comparative view of population performance that has inherent uncertainty regarding if/how other pertinent factors might change in the future. At a minimum, future phases of modeling may wish to consider phasing in restoration-related benefits over appropriate time scales and perhaps consider alternative population metrics (e.g., does the population ‘wink out’ before benefits are established?).

3. Results and discussion

Overall, our base parameterization (i.e., ‘Curr’) appeared to accurately capture both the stage-specific (i.e., freshwater vs. marine) and total life cycle productivity of spring Chinook salmon in Catherine Creek—despite being developed from disparate and somewhat independent datasets in a piecewise fashion (e.g., freshwater survivals from long-term monitoring datasets vs. a habitat-based parr capacity model that predicts how many fish a basin can produce). For example, the relationships between smolts per female spawner in our modeled dataset closely mirrors the relationship evident in ODFW’s 20-year sampling dataset (**Figure 1**). Similarly, natural-origin fish reaching CC were well within recent average values (i.e., those summarized in Carmichael et al. 2011). Given these patterns, we believe that our base LCM parameterization (‘Curr’) reasonably captured the demographics of the intended composite hatchery–natural population. Accordingly, we used this model, with the capacity modifications described in **Table 1** to assess the effects of the Justice et al. (2017) scenarios on total spawner abundance. While no attempt is made to infer meaning here, LCM simulation results (summarized in **Table 2** and **Figures 3-5**) illustrate the following:

- The proportional changes in juvenile carrying capacity reflecting the Justice et al. (2017) habitat scenarios translated into a natural origin adult abundance response that was similar on a rank-order basis. However, the magnitude of adult increase/decrease, while proportional to the juvenile capacity manipulation, was approximately 25-40% lower in magnitude. In other words, adult abundance did not respond on a one-to-one basis.
- Overall, the 'PNV' and 'WidPNV' scenarios, which assume maximum cooling of stream temperatures in the absence of climate change effects, showed the greatest response, with an approximate 30-40% increase in spawner abundance. On the other hand, 'doing nothing' vegetation/restoration wise in the face of the anticipated effects of climate change on conditions in CC (scenario 'Clim') translated into a 30% reduction in spawner abundance. Scenarios considering the positive effects of restoration and negative effects of climate change showed an intermediate response.
- Finally, a scenario testing the effects of ceasing all supplementation efforts after 20 years (all other inputs set to 'Curr' values), illustrated that natural origin extinction was a virtual certainty under current freshwater and marine capacity/productivity assumptions in the absence of hatchery support.

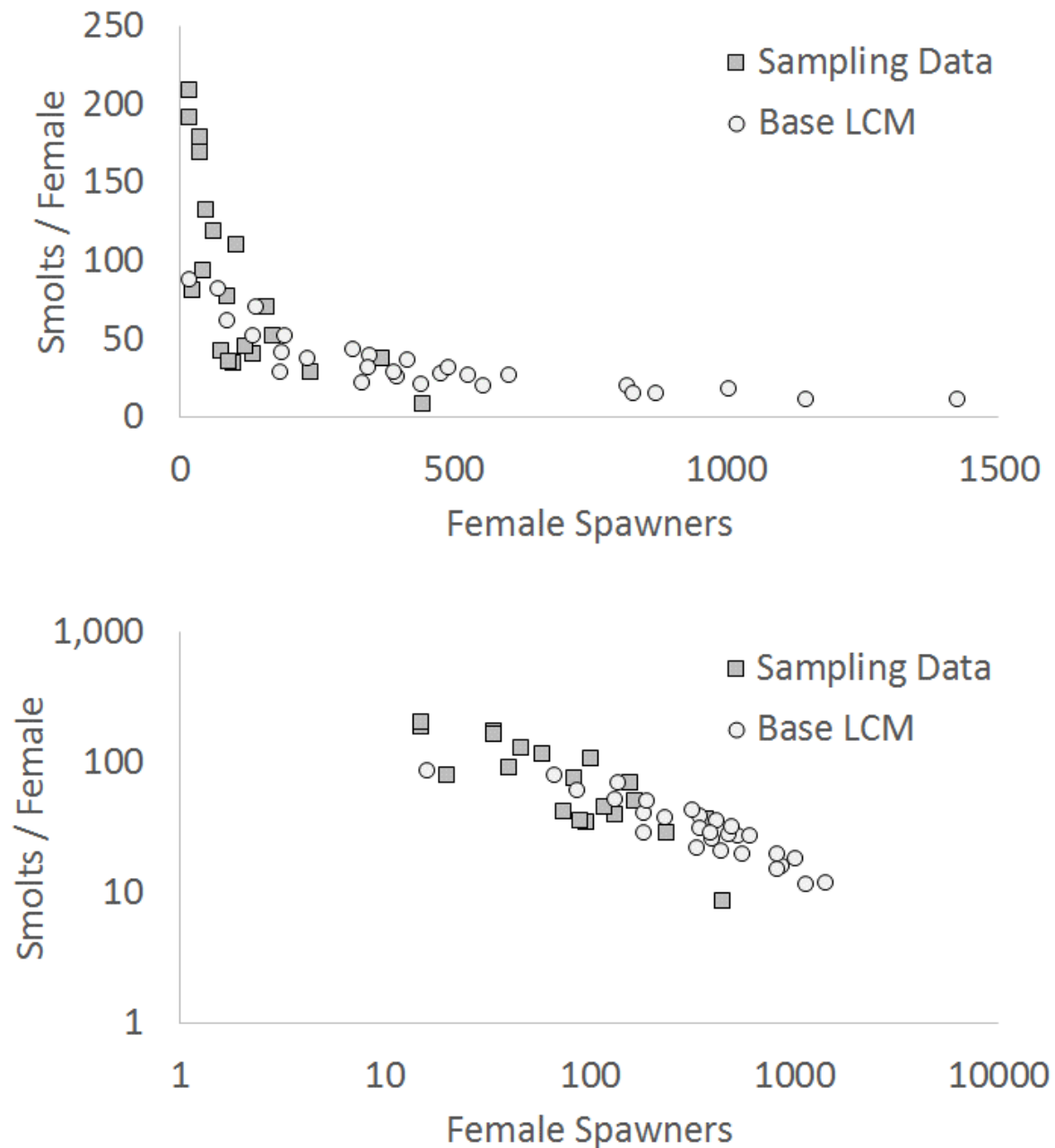


Figure 2. Comparison of simulated ('Base LCM') and observed ('Sampling Data') estimates of freshwater productivity relative to spawner abundance, plotted on untransformed (upper panel) and \log_{10} (lower panel) axes. Sampling data are brood year 1993-2012 estimates of smolts per female, where smolts are in LGD equivalents and a "female spawner" assumes one female per redd, whereas LCM data are one realization of smolts and females from a 30-year simulation period given (a) sampling estimates of freshwater productivity, (b) Habitat model-based estimates of spawner and juvenile carrying capacities, and (c) Beverton-Holt-type density dependence (See **Appendix A** for further details on all).

Table 2. Summary statistics for natural-origin adult returns to the Catherine Creek adult trap from N = 100 Monte Carlo trials, by scenario. See Table 1 for scenario descriptions. Values represent summary statistics on the trial-level abundance metric (i.e., geometric mean abundance from each 30-year simulation).

Scenario Abbreviation	Mean	Median	SD	Range	Proportional Δ rel. to 'Curr'
Curr	81	95	21	42-125	0.00
PNV	114	133	26	68-233	0.39
HiPr	104	119	22	51-159	0.25
WidPNV	112	124	27	45-204	0.30
Clim	57	70	14	32-101	-0.27
ClimVeg	95	108	24	34-172	0.13
ClimVegWid	97	116	27	51-193	0.21

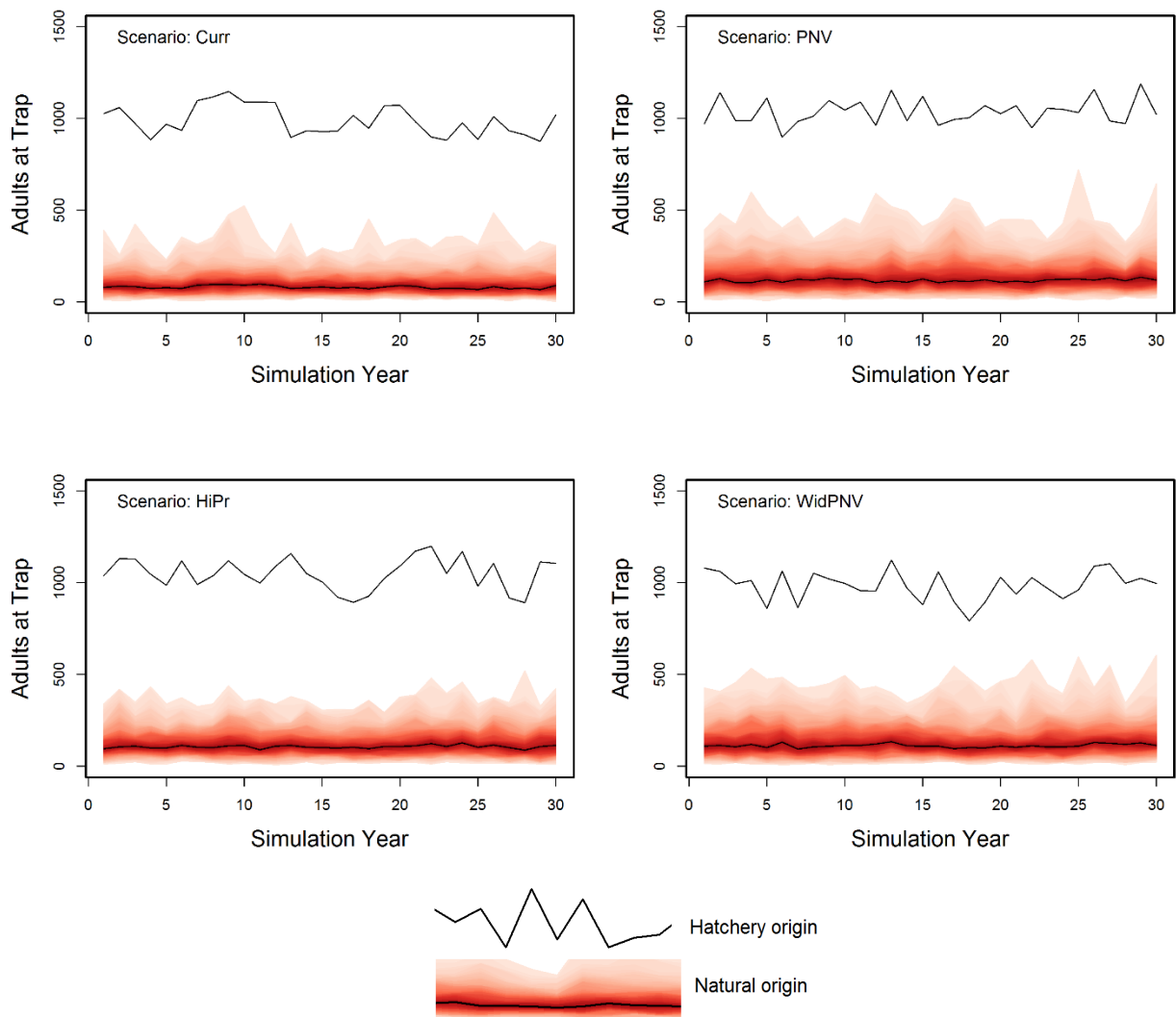


Figure 3. Time series density plots of natural-origin Chinook salmon returns to the Catherine Creek adult trap over a 30-year simulation for each of seven scenarios. In each plot, the higher thin black line is the median abundance of hatchery-origin returns whereas the second black line (flanked by red shading) represents the median abundance of natural-origin returns (i.e., natural-origin fish or progeny of H1 [or otherwise] spawning in wild); shading reflects the density of abundance observations across the N = 100 Monte Carlo trials.

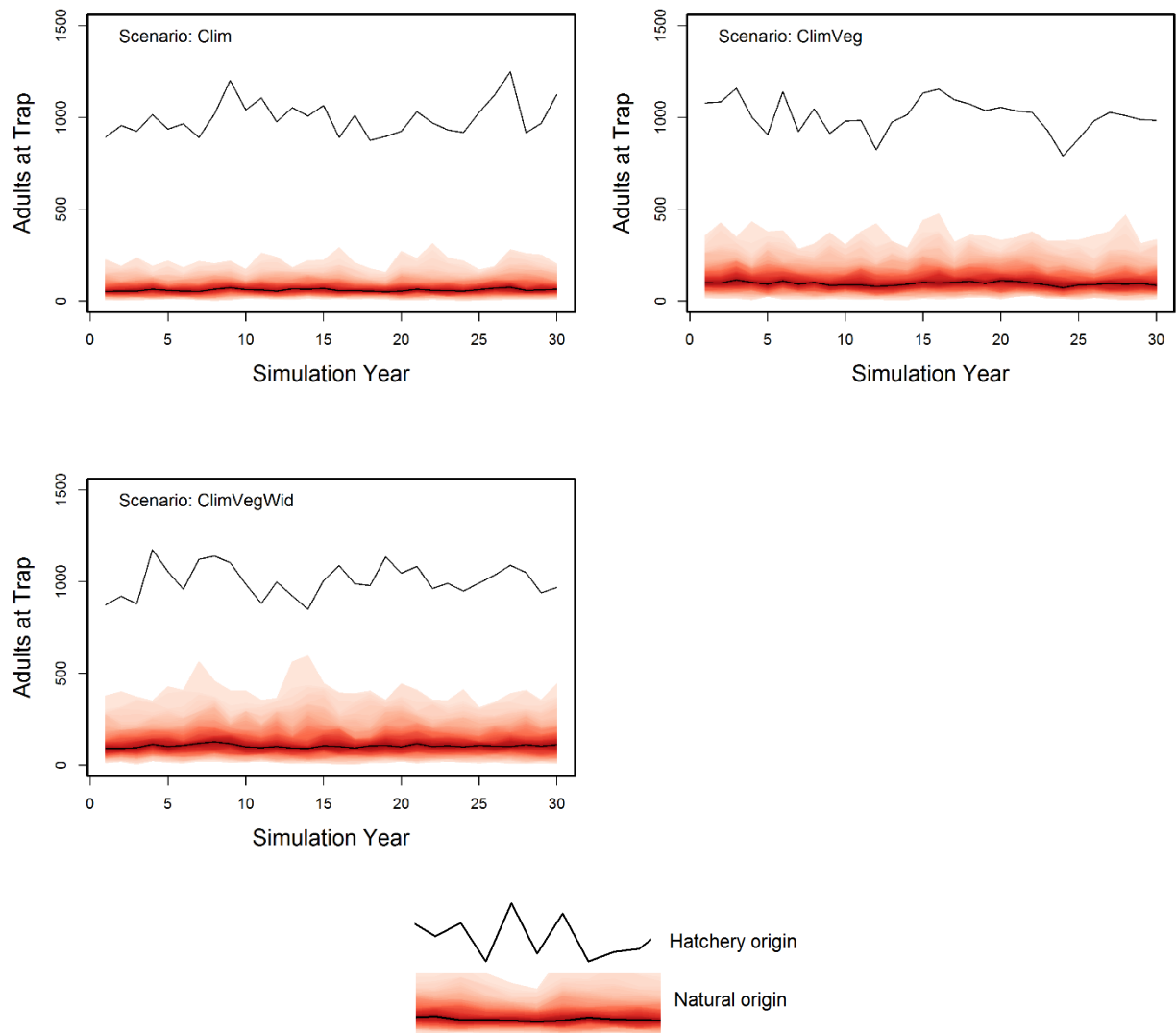


Figure 3. Continued.

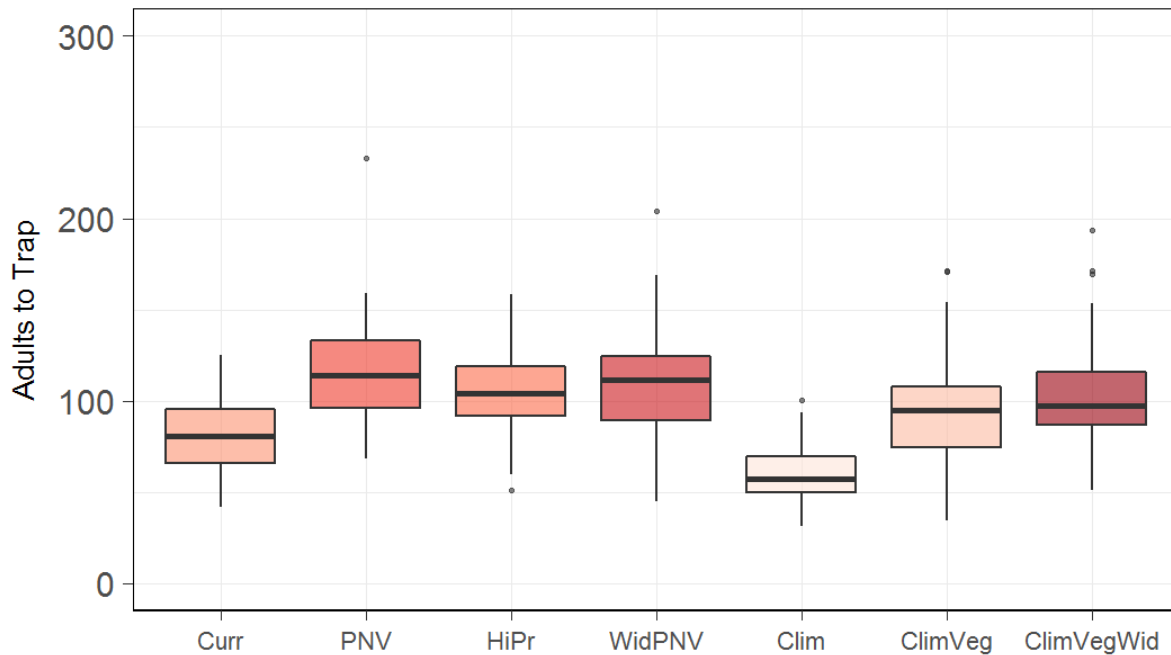


Figure 4. Box-and-whisker plots of natural-origin adult returns to the Catherine Creek adult trap, by scenario (based on N = 100 Monte Carlo trials). See Table 1 for scenario definitions.

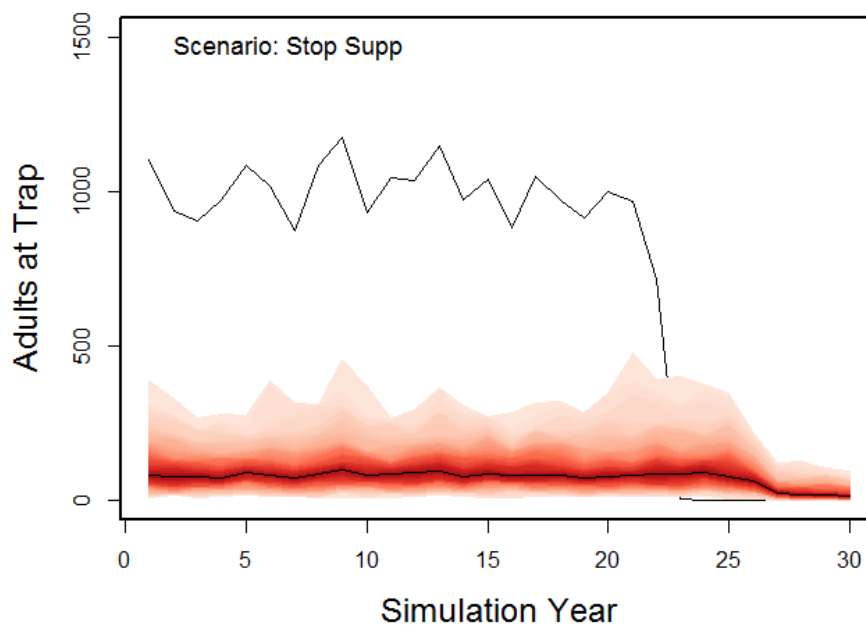


Figure 5. Time series density plots of natural-origin Chinook salmon returns to the Catherine Creek adult trap over a 30-year simulation for a scenario considering the effects of ceasing supplementation activities after 20 years under the base model parameterization (i.e., ‘Curr’ scenario). The higher thin black line is the median abundance of hatchery-origin returns whereas the second black line (flanked by red shading) represents the median abundance of natural-origin returns (i.e., natural-origin fish or progeny of H1 [or otherwise] spawning in wild); shading reflects the density of abundance observations across the N = 100 Monte Carlo trials.

4. Future considerations & next steps

Although the preceding analyses lend insight of immediate relevance, scenario inputs can be further refined and so that the LCM framework's utility is maximized relative to the needs of stakeholders working to recover spring Chinook in the Grande Ronde Basin. Based on the work summarized here, future analyses and model updates might consider any of the following:

- (1) *Revisit the demographic parameters used to model tributary life stages.* Additional data sources may improve the accuracy of our base model parameterization. Additionally, although inputs selected here yielded results with qualitative similarities to monitoring data collected for the actual CC population, reviewing model inputs in collaboration with other basin partners will help achieve buy-in/agreement on future modelling results.
- (2) *Expand the analysis to include the Upper Grande Ronde spring Chinook population.* As noted in the introduction, we had hoped to include UGR Chinook here and thus view this as a top priority for future phases of modeling. Thus, in concert with pursuing item 1 for CC Chinook, the data review associated with an updated/final parameterization should be pursued simultaneously for both the UGR and CC populations.
- (3) *Consider alternative parameterizations for modeling the Justice et al. (2017) scenarios.* For example, here we represent scenarios via proportional changes in juvenile carrying capacity. Perhaps there is a basis for inferring a parr productivity benefit as well, or even a response for other life stages.
- (4) *Consider modeling alternative supplementation scenarios.* For example, although this work includes a feedback between adult run sizes and the availability of smolts for release in subsequent years, no attempt was made to model a life span for supplementation programs (e.g., phasing it out based on some time or abundance threshold).
- (5) *As new data become available, consider modeling hatchery vs. natural survival differentials for various life stages.* Due to the highly integrated status of the supplementation programs, and due to other considerations (noted above), we assumed similar survival/fitness for hatchery and natural fish in the wild.
- (6) *Integrate habitat modeling scenarios/hypotheses with model runs that address management actions affecting other life stages and or habitat effects that influence survival beyond spawning/rearing streams.* For instance, downstream passage scenarios could be developed to represent different smolt transportation, embodied in different SAR inputs (e.g., results of B. Lessard's chapter in McCann et al. 2016). Alternatively, temperature projections associated with different scenarios could be used to inform growth predictions that shape smolt survival or SARs given size–survival linkages.
- (7) *Do more MC trials.* While the relative findings here are adequate to gauge inter-scenario differences, additional MC iterations will minimize the influence of random variation on general patterns.

- (8) *Consider other performance metrics, in addition to abundance, that are relevant to heavily supplemented populations and reassess LCM results.* Although natural-origin spawner abundance is the perhaps the most relevant response, there are likely other metrics that will be useful to managers for assessing inter-scenario differences. Additionally, evaluations that consider how supplementation programs interact with other actions to shape spawner abundance (e.g., by turning hatchery programs ‘on’ or ‘off’, as in **Figure 5**)

Acknowledgements

We thank Casey Justice, Seth White, Dale McCullough, Rishi Sharma, and Gene Shippentower for their direction and support for this work. Additionally, we thank Bob Lessard, CRITFC, as well as Joseph Feldhaus, Chris Horn, and Ted Sedell, ODFW, for sharing insights on population monitoring and demographic data for spring Chinook in the Grande Ronde Basin. Lastly, support from CHaMP and ISEMP program partners, particularly Matt Nahorniak, Carol Volk, Kevin See, and Matt Reimer, was instrumental in developing habitat model-based estimates of habitat capacity and variability.

References

- Carmichael and coauthors. 2011. Catherine Creek spring Chinook salmon hatchery program review. Oregon Department of Fish and Wildlife report to Lower Snake Comp. Program.
<https://www.fws.gov/lsnakecomplan/Reports/ODFW/Eval/CatherineCreekSpringChinookSalmonHatcheryReviewFINAL.pdf>
- Justice, C., White, S.M., McCullough, D.A., Graves, D.S., Blanchard, M.R., 2017. Can stream and riparian restoration offset climate change impacts to salmon populations? *Journal of Environmental Management* 188, 212-227.
- Kareiva, P., Marvier, M., McClure, M., 2000. Recovery and management options for spring/summer chinook salmon in the Columbia River Basin. *Science* 290, 977-979.
- McCann, J., and coauthors. 2016. Comparative Survival Study of PIT-tagged Spring/Summer/Fall Chinook, Summer Steelhead, and Sockeye. 2015 Annual Report BPA Contract # 19960200.
http://www.fpc.org/documents/CSS/CSS_2016_Final.pdf
- McHugh, P., and coauthors. In Press. Linking models across scales to assess the viability and restoration potential of a threatened population of steelhead (*Oncorhynchus mykiss*) in the Middle Fork John Day River, Oregon, USA. Submitted to *Ecological Modelling*.
- Moussalli, E., and R. Hilborn. 1986. Optimal stock size and harvest rate in multistage life-history models. *Canadian Journal of Fisheries and Aquatic Sciences* 43(1):135-141.
- R Core Team, 2014. R: A language and environment for statistical computing. R Foundation for Statistical Computing, Vienna, Austria.
- Sharma, R., A. B. Cooper, and R. Hilborn. 2005. A quantitative framework for the analysis of habitat and hatchery practices on Pacific salmon. *Ecological Modelling* 183(2-3):231-250.

Appendix A. Base parameterization and references for Catherine Creek spring Chinook salmon.

Input category	Life stage(s)	Parameter	Value(s)	Stochasticity	Source(s)	Comments
survival/ productivity	egg-to-parr	egg-to-summer parr productivity	0.26	target CV: 40%	B. Jonasson, ODFW, monitoring spreadsheet	Computed from ODFW estimates of late summer parr, relative to ODFW's redd counts (above trap), assuming 1 female/redd and average fecundity; modeled using 75th% value to reflect productivity (rather than survival) model usage
	summer parr-to-smolt	summer parr-to-smolt survival	0.12	target CV: 70%	B. Jonasson, ODFW, monitoring spreadsheet	survival from fall to LGD as a smolt; computed for entire cohort of summer parr rather than via separate Tributary vs. Valley overwintering component
	ocean rearing stages [by ocean age (oa)]	survival by ocean age, Soa1, Soa2, Soa3, ...	Soa1 = 0.02, Soa2 = 0.32, Soa3 = 0.56	target CV: 50, 30, 30%, respectively	Based on CSS age-specific smolt-to-adult return rates (McCann et al. 2016)	Survival inputs & maturation probabilities (below) yield adult return age composition of Catherine Creek Acclimation Pond releases oa1 = 23%, oa2 = 75%, oa3 = 3%
	spawners	prespawn survival (on spawning grounds)	0.97	target CV < 10%	J. Feldhaus, ODFW, and T. Bowerman prespawn mort summaries	Because this is a pre-spawn 'productivity' in Beverton-Holt sense, used higher value. Note also that losses between LGD and the spawning grounds are assumed to be negligible; violation of this assumption introduces a positive bias in adult survival
capacity	summer parr	total capacity	159,708	n/a (static)	K. See (2016), unpublished	Quantile random-forest carrying capacity prediction for CC.
	adult (spawners)	total capacity	12,578	n/a (static)	Habitat suitability index model-based female spawner (redd) capacity, CHaMP	Modeled in units of eggs assuming average spawner age structure and age-specific fecundity [~48M eggs]
other life history or mgmt parameters	fall/early winter parr	probability of moving downstream to overwinter	e = 0.76	n/a (static)	B. Jonasson, ODFW, monitoring spreadsheet	Allows for spatial redistribution of fish in fall, in manner reflective of obs'd fall vs. spring migrant abundance
	ocean rearing stages [by ocean age (oa)]	maturation probability, Moa1, Moa2, Moa3, ...	Moa1 = 0.11, Moa2 = 0.95, Moa3 = 1.00	target CV: 80, 15, 0, respectively	Estimated from SARs data (see note for marine survival above)	see McHugh et al. (In Press) appendix for details estimation approach
	fecundity, by total age	f3, f4, f5, ...	f3 = 3,257, f4 = 4,095, f5 = 5,149	n/a (static)	Kareiva et al. (2000) values as preliminary input	Replace with basin-specific values; note, however, that these yield average fec (age-weighted) within 100 eggs of CC-specific means
	smolts	supplementation releases	150,000	n/a (static)	n/a	Current management target; varies in LCM as f(run size) if hatchery broodstock req's aren't met.

Appendix B. Overview of the approach taken to model hatchery supplementation programs.

The Catherine Creek (CC) and the Upper Grande Ronde River (UGR) populations of spring Chinook are presently supplemented by the annual release of approximately 150K (CC) and 250K (UGR) hatchery-reared smolts (N_{sm-sup}), which are released into acclimation ponds near the spawning grounds in both systems. As surplus production permits, additionally, modest numbers of eyed eggs are occasionally released into specific tributaries (UGR = Meadow and Sheep creeks; Catherine = Indian Creek). Adults returning from supplementation releases (HOR) are meant to home to the spawning grounds and spawn naturally, in tandem with natural-origin (NOR) fish. Similarly, a fraction of the natural-origin fish returning to spawn in the wild are retained for spawning in the hatchery to support an integrated hatchery program. To help maintain genetic integrity while offering abundance benefits, weirs and adult traps situated in both streams are used to manage three aspects of escapement that are pertinent to supplementation goals: (i) P_{NOS-R} (i.e., the proportion of the total natural-origin returns that's retained for the hatchery), (ii) P_{HOS} (i.e., the proportion of natural spawners that is of hatchery origin), and (iii) P_{NOB} (i.e., the proportion of hatchery broodstock/egg-take that's of natural origin). Because supplementation efforts influence abundance dynamics in both CC and UGR populations, measures were taken to accurately represent this management strategy in life cycle model (LCM) simulations, which we describe here.

Several simplifying assumptions were made in order to represent a mixed, supplemented hatchery-natural population for each the CC and UGR case:

1. Beyond hatchery-reared stages (i.e., smolt+), we assume that survival and life history differences for natural and supplementation (i.e., hatchery) fish are negligible. This means that common rates were used, regardless of fish origin, including (i) survival rates from tributaries to Lower Granite Dam (LGD), (ii) LGD-to-LGD smolt-to-adult return rates (SARs), and (iii) adult maturation schedules. [*Note, this can be revised using tributary-to-LGD outmigrant survival and/or LGD-to-LGD SAR differentials, e.g., based on C. Justice's survival analyses, etc.*].
2. We assume that all hatchery-reared fish are produced from supplementation fish captured in the wild and reared according to conventional hatchery practices; thus, we do not model a captive broodstock component, due to its discontinued status and previously documented life history differences.
3. To model a feedback between total (HOR+NOR) adult returns ($N_{AD-tot} = N_{AD-h} + N_{AD-N}$, adults eligible for retention as broodstock (N_{BS}), and N_{sm-sup} in year $y+2$, we assumed an egg take requirement of 85 females to produce 250K smolts (M. McLean, CTUIR, pers. comm.); or an equivalency of 1,470 smolts per adult, assuming a 50:50 sex ratio. Thus, N_{sm-sup} in year $y+2$ is determined as noted below, where N_{BS} is determined according to stream-specific rules below. Hatchery broodstock goals for UGR and CC are 170 and 103 adults (fem+male), respectively.

If N_{BS} in year $y \geq$ hatch. Goal { N_{sm-sup} in $y+2$ = smolt goal (i.e., 150K CC, 250K UGR) }
Else { $N_{sm-sup} = N_{BS}$ in year $y+2 = N_{BS} * 1,470$ }

Catherine Creek. In CC (rule type = 4 in input files), where adult trapping operations span the entire run, the management of hatchery and natural fish on the spawning grounds and in hatchery broodstock follows a 'sliding scale' framework under which target levels for P_{NOS-R} , P_{HOS} , and P_{NOB} vary across three levels of run size (N_{AD-tot}), <250, 250-500, and >500 (Carmichael et al. 2011). At low abundance, P_{NOS-R} is capped at 40% and there are no constraints on P_{HOS} , and P_{NOB} , and hatchery fish are otherwise retained to meet egg-take requirements. At high abundance, P_{HOS} is minimized (max allowed = 50%), P_{NOB} is maximized (target \geq 30%), and is P_{NOS-R} more tightly constrained (max allowed = 20%). At moderate abundance, P_{NOS-R} is similarly constrained (20%

cap) and there is tolerance for higher P_{HOS} (max allowed = 70%) and lower P_{NOB} (target $\geq 20\%$). While this rule set is straightforward, there are cases for which it is impossible to meet all constraints simultaneously, which made implementing it in code somewhat complicated. Consider for example a case in which returns fall between 250 and 500, but are almost exclusively (say 80+%) of hatchery origin. In this case, it's quite likely that egg take needs will not be met if weir management strictly follows the sliding scale's P_{NOB} and P_{NOS-R} constraints; nor is it clear what passage goals (to spawning grounds) should be in cases for which returns exceed the scale's upper abundance threshold but are based predominantly on hatchery origin returns. Thus, to operationalize the CC sliding scale, several additional 'rules' were imposed, via the following pseudo-code:

Case 1 (in the low abundance tier)

```

If  $N_{AD-tot} < \text{lower threshold}$  (i.e., <250 adults, H+N) then ... {
  If  $N_{AD-N} > 0$  ... {
    Retain up to 40% of the natural run for hatchery broodstock
    Make up the balance of broodstock needs with hatchery fish
  } Else (i.e., case for which  $N_{AD-N}$  is 0, but  $N_{AD-h}$  is  $> 0$ ) ... {
    Collect hatchery fish up to the broodstock goal
  }
  Rescale H and N run sizes to account for fish taken to hatchery
  Pass everything that wasn't collected to the spawning grounds
  If adult collections < broodstock goals {
    Recompute smolt releases for year y+2 as function of fish retained (i.e., per #3 above)
  }
}

```

Case 2 (in the mid abundance tier)

```

If lower threshold <  $N_{AD-tot}$  < upper threshold (i.e., 250-500 adults) then ... {
  If  $N_{AD-N} > 0$  ... {
    Retain up to 20% of the natural run for hatchery broodstock
    Make up the balance of broodstock needs with hatchery fish
  } Else (i.e., case for which  $N_{AD-N}$  is 0, but  $N_{AD-h}$  is  $> 0$ ) ... {
    Collect hatchery fish up to the broodstock goal
  }
  Rescale H and N run sizes to account for fish taken to hatchery
  Determine  $P_{HOS}$  would be if remaining fish were allowed to spawn
  If  $P_{HOS} > 70\%$  {
    If you can meet  $P_{HOS}$  goal without dropping into lower abundance tier {
      Remove hatchery fish until you meet  $P_{HOS}$  goal
    } Else { Don't worry about it }
  }
  Rescale H run size to account for removals
  Pass remaining fish to spawning grounds
  If adult collections < broodstock goals {
    Recompute smolt releases for year y+2 as function of fish retained (i.e., per #3 above)
  }
}

```

Case 3 (in the high abundance tier)

```

If  $N_{AD-tot} > \text{upper threshold}$  (i.e., 500 adults) then ... {
  If  $N_{AD-N} > 0$  ... {
    Retain up to 20% of the natural run for hatchery broodstock
    Make up the balance of broodstock needs with hatchery fish
  } Else (i.e., case for which  $N_{AD-N}$  is 0, but  $N_{AD-h}$  is  $> 0$ ) ... {

```

```

    Collect hatchery fish up to the broodstock goal
  }
  Rescale  $N_{AD-H}$  and  $N_{AD-N}$  run sizes to account for fish taken to hatchery
  Determine  $P_{HOS}$  would be if remaining fish were allowed to spawn
  If  $P_{HOS} > 50\%$  {
    If you can meet the system total escapement goal with natural fish alone {
      Pass only natural fish to the spawning grounds ( $P_{HOS} = 0$ )
    } Else If  $N_{AD-N} / \text{upper threshold} \geq 50\%$  {
      Remove hatchery fish until you're at or under  $P_{HOS} = 50\%$ 
    }
  }
  Rescale H run size to account for removals
  Pass remaining fish to spawning grounds
  If adult collections < broodstock goals {
    Recompute smolt releases for year  $y+2$  as function of fish retained (i.e., per #3 above)
  }
}

```

As the above pseudo-code illustrates, we made no attempt to constrain the modeled supplementation program based on the stated hatchery P_{NOB} goals, because (a) as doing so introduced additional coding complications (i.e., due to exceptions and circular dependencies), and (b) was virtually impossible to meet under the natural population's current life cycle productivity/capacity assumptions.

Upper Grande Ronde River. In the Upper Grande Ronde (rule type = 5 in input files), the management of HOS/NOS on the spawning grounds and HOB/NOB at the hatchery is less formalized than in Catherine Creek, due to the fact that the weir is typically pulled before the majority of the run makes its way through to the spawning grounds and because its supplementation program is generally less restrictive regarding target P_{NOS-R} , P_{HOS} , and P_{NOB} values. In brief, the main constraint imposed on weir/program management is that no more than 50% of the natural run can be retained for hatchery broodstock. This is executed in code according to the following pseudo-code:

```

If  $N_{AD-N} > 0$  ... {
  Retain up to 50% of the natural run for hatchery broodstock
  Make up the balance of broodstock needs with hatchery fish
} Else (i.e., case for which  $N_{AD-N}$  is 0, but  $N_{AD-H}$  is > 0) ... {
  Collect hatchery fish up to the broodstock goal
}
Rescale H and N run sizes to account for fish taken to hatchery
Pass everything that wasn't collected to the spawning grounds
If adult collections < broodstock goals {
  Recompute smolt releases for year  $y+2$  as function of fish retained (i.e., per #3 above)
}

```